

**INCIDENT-RESPONSE MONITORING TECHNOLOGIES  
FOR AIRCRAFT-CABIN AIR QUALITY**

by

**PAUL W. MAGOHA**

M.S., Lvov Polytechnic Institute, Ukraine, 1984

**AN ABSTRACT OF A DISSERTATION**

submitted in partial fulfillment of the requirements for the degree

**DOCTOR OF PHILOSOPHY**

Department of Mechanical Engineering  
College of Engineering

**KANSAS STATE UNIVERSITY**  
Manhattan, Kansas

2012

## Abstract

Poor air quality in commercial aircraft cabins can be caused by volatile organophosphorus (OP) compounds emitted from the jet engine bleed air system during smoke/fume incidents. Tri-cresyl phosphate (TCP), a common anti-wear additive in turbine engine oils, is an important component in today's global aircraft operations. However, exposure to TCP increases risks of certain adverse health effects. This research analyzed used aircraft cabin air filters for jet engine oil contaminants and designed a jet engine bleed air simulator (BAS) to replicate smoke/fume incidents caused by pyrolysis of jet engine oil. Field emission scanning electron microscopy (FESEM) with X-ray energy dispersive spectroscopy (EDS) and neutron activation analysis (NAA) were used for elemental analysis of filters, and gas chromatography interfaced with mass spectrometry (GC/MS) was used to analyze used filters to determine TCP isomers. The filter analysis study involved 110 used and 74 incident filters. Clean air filter samples exposed to different bleed air conditions simulating cabin air contamination incidents were also analyzed by FESEM/EDS, NAA, and GC/MS. Experiments were conducted on a BAS at various bleed air conditions typical of an operating jet engine so that the effects of temperature and pressure variations on jet engine oil aerosol formation could be determined. The GC/MS analysis of both used and incident filters characterized tri-*m*-cresyl phosphate (TmCP) and tri-*p*-cresyl phosphate (TpCP) by a base peak of an  $m/z = 368$ , with corresponding retention times of 21.9 and 23.4 minutes. The hydrocarbons in jet oil were characterized in the filters by a base peak pattern of an  $m/z = 85, 113$ . Using retention times and hydrocarbon thermal conductivity peak (TCP) pattern obtained from jet engine oil standards, five out of 110 used filters tested had oil markers. Meanwhile 22 out of 74 incident filters tested positive for oil fingerprints. Probit analysis of jet engine oil aerosols obtained from BAS tests by optical particle counter (OPC) revealed lognormal distributions with the mean (range) of geometric mass mean diameter (GMMD) = 0.41 (0.39, 0.45)  $\mu\text{m}$  and geometric standard deviation (GSD),  $\sigma_g = 1.92$  (1.87, 1.98). FESEM/EDS and NAA techniques found a wide range of elements on filters, and further investigations of used filters are recommended using these techniques. The protocols for air and filter sampling and GC/MS analysis used in this study will increase the options available for detecting jet engine oil on cabin air filters. Such criteria could support policy development for compliance with cabin air quality standards during incidents.



**INCIDENT-RESPONSE MONITORING TECHNOLOGIES  
FOR AIRCRAFT-CABIN AIR QUALITY**

by

PAUL W. MAGOHA

M.S., Lvov Polytechnic Institute, Ukraine, 1984

A DISSERTATION

submitted in partial fulfillment of the requirements for the degree

DOCTOR OF PHILOSOPHY

Department of Mechanical Engineering  
College of Engineering

KANSAS STATE UNIVERSITY  
Manhattan, Kansas

2012

Approved by:

Co-Major Professor  
Steven J. Eckels

Approved by:

Co-Major Professor  
Byron W. Jones

# **Copyright**

PAUL W. MAGOHA

2012

## Abstract

Poor air quality in commercial aircraft cabins can be caused by volatile organophosphorus (OP) compounds emitted from the jet engine bleed air system during smoke/fume incidents. Tri-cresyl phosphate (TCP), a common anti-wear additive in turbine engine oils, is an important component in today's global aircraft operations. However, exposure to TCP increases risks of certain adverse health effects. This research analyzed used aircraft cabin air filters for jet engine oil contaminants and designed a jet engine bleed air simulator (BAS) to replicate smoke/fume incidents caused by pyrolysis of jet engine oil. Field emission scanning electron microscopy (FESEM) with X-ray energy dispersive spectroscopy (EDS) and neutron activation analysis (NAA) were used for elemental analysis of filters, and gas chromatography interfaced with mass spectrometry (GC/MS) was used to analyze used filters to determine TCP isomers. The filter analysis study involved 110 used and 90 incident filters. Clean air filter samples exposed to different bleed air conditions simulating cabin air contamination incidents were also analyzed by FESEM/EDS, NAA, and GC/MS. Experiments were conducted on a BAS at various bleed air conditions typical of an operating jet engine so that the effects of temperature and pressure variations on jet engine oil aerosol formation could be determined. The GC/MS analysis of both used and incident filters characterized tri-m-cresyl phosphate (TmCP) and tri-p-cresyl phosphate (TpCP) by a base peak of an  $m/z = 368$ , with corresponding retention times of 21.9 and 23.4 minutes. The hydrocarbons in jet oil were characterized in the filters by a base peak pattern of an  $m/z = 85, 113$ . Using retention times and hydrocarbon thermal conductivity peak (TCP) pattern obtained from jet engine oil standards, five out of 110 used filters tested had oil markers. Meanwhile 22 out of 77 incident filters tested positive for oil fingerprints. Probit analysis of jet engine oil aerosols obtained from BAS tests by optical particle counter (OPC) revealed lognormal distributions with the mean (range) of geometric mass mean diameter (GMMD) = 0.41 (0.39, 0.45)  $\mu\text{m}$  and geometric standard deviation (GSD),  $\sigma_g = 1.92$  (1.87, 1.98). FESEM/EDS and NAA techniques found a wide range of elements on filters, and further investigations of used filters are recommended using these techniques. The protocols for air and filter sampling and GC/MS analysis used in this study will increase the options available for detecting jet engine oil on cabin air filters. Such criteria could support policy development for compliance with cabin air quality standards during incidents.

# Table of Contents

List of Figures .....	ix
List of Tables .....	xiv
Acknowledgements .....	xvi
Dedication .....	xvii
Preface .....	xviii
Acronyms .....	xix
CHAPTER 1 - INTRODUCTION .....	1
1.1 Background .....	1
1.1.1 Defining aircraft cabin air quality incidents .....	1
1.2 Literature Review .....	2
1.2.1 Commercial aircraft environmental control system (ECS) .....	2
1.2.2 Air filtration in commercial aircraft cabins .....	4
1.2.3 Aircraft cabin air quality and standards .....	4
1.2.4 Commercial aircraft bleed air system .....	7
1.2.5 Mobil Jet Oil II: A synthetic jet engine lubricating oil .....	10
1.3 Problem Identification and Description .....	13
1.4 Justification for the Study .....	15
1.5 Objectives of the Study .....	19
1.6 Research Methodology .....	20
1.7 Scope of the Study .....	21
1.8 References .....	21
CHAPTER 2 - ANALYSIS OF USED AIRCRAFT CABIN AIR FILTERS BY FIELD EMISSION SCANNING ELECTRON MICROSCOPY (FESEM) WITH ENERGY DISPERSIVE X-RAY SPECTROSCOPY (EDS) .....	26
2.1 Abstract .....	26
2.2 Introduction .....	27
2.2.1 Aircraft cabin air recirculation filters .....	29
2.2.2 The standards for aircraft cabin air filters .....	31
2.3 Materials and Methods .....	33

2.3.1 Filter sampling .....	33
2.3.2 Experimental protocol.....	34
2.4 Analysis, Results and Discussion .....	37
2.4.1 Data analysis .....	37
2.4.2 Results and discussion .....	41
2.5 Conclusions.....	71
2.6 References.....	72
<b>CHAPTER 3 - USING GAS CHROMATOGRAPHY AND MASS SPECTROMETRY TO</b>	
<b>DETERMINE JET ENGINE OIL MARKERS IN AIRCRAFT CABIN AIR FILTERS.....</b>	
3.1 Abstract.....	75
3.2 Introduction.....	76
3.3 Materials and Methods.....	81
3.3.1 Filter sampling .....	81
3.3.1 Principle operation of GC/MS .....	83
3.3.1 Analysis of used aircraft filters by Agilent Series 6890 GC with 5973 MSD .....	83
3.3.2 Procedures for preparation of standard solution for GC/MS analysis .....	84
3.4 Analysis, Results and Discussion .....	85
3.4.1 Data analysis .....	85
3.4.2 Results and discussion .....	86
3.5 Conclusions.....	92
3.6 References.....	92
<b>CHAPTER 4 - NEUTRON ACTIVATION ANALYSIS (NAA) OF COMMERCIAL</b>	
<b>AIRCRAFT CABIN AIR RECIRCULATION FILTERS .....</b>	
4.1 Abstract.....	96
4.2 Introduction.....	97
4.2.1 Principles of neutron activation analysis (NAA) .....	98
4.3 Materials and methods .....	100
4.4 Analysis, Results and Discussion .....	114
4.4.1 Data analysis .....	114
4.4.2 Results and discussion .....	115
4.5 Recommendations.....	120

4.5.1 Statistical analysis .....	120
4.6 Conclusions .....	130
4.7 References .....	131
CHAPTER 5 - MONITORING SIMULATED COMMERCIAL AIRCRAFT CABIN AIR	
QUALITY INCIDENTS USING BLEED AIR SIMULATOR (BAS).....	133
5.1 Abstract .....	133
5.2 Introduction.....	133
5.2.1 Trends in development of aircraft engine bleed air monitor.....	136
5.3 Materials and Methods.....	140
5.3.1 Experimental setup.....	140
5.3.2 Process control and monitoring.....	152
5.4 Analysis, Results and Discussion .....	161
5.4.1 Data analysis and results .....	161
5.4.2 Discussion .....	180
5.5 Recommendations.....	182
5.6 Conclusions.....	183
5.7 References.....	185
CHAPTER 6 - CONCLUSIONS AND FUTURE WORK .....	
6.1 Conclusions and contributions of the study .....	190
6.1.1 Significance and impact of the study .....	192
6.1.2 Limitations of the study .....	193
6.2 Recommendations and future work .....	194
Appendix A - FESEM/EDS: Raw Data on Distribution of Atomic Weight Percentage of	
Elements in Aircraft Cabin Air Recirculation Filters .....	196
Appendix B - Summarized GC/MS Analytical Report on Used Aircraft Cabin Air Recirculation	
Filters .....	259
Appendix C - Summarized NAA Data on Used HEPA Cabin Air Recirculation Filters .....	
Appendix D - Operating procedures for BAS.....	
Appendix E - Simulated Operational Conditions of Bleed Air Simulator and Aerosol Data.....	
E.1 Temperature and pressure trends in aircraft engine BAS and duct system.....	371

## List of Figures

Figure 1.1 A schematic of typical aircraft air-conditioning system.....	3
Figure 1.2 Pattern of air circulation inside aircraft cabin .....	3
Figure 1.3 Schematic of typical commercial aircraft bleed air system.....	8
Figure 1.4 Typical bleed air system in commercial transport aircraft .....	10
Figure 2.1 Some HEPA cabin air recirculation filters approved by FAA for installation on various commercial aircrafts.....	30
Figure 2.2 (a) Filter sampling process (b) Filter panel (c) Filter sample for FESEM/EDS analysis .....	34
Figure 2.3 Nova™ NanoSEM model 430 FESEM/EDS System .....	36
Figure 2.4 Top row – Atomic adsorption spectrum (EDS) of clean HEPA filter media manufactured by (a) Pall Aerospace Co., (b) Keddeg Co., and (c) Donaldson and bottom row – their corresponding qualitative composition of elements shown as (d), (e) and (f) respectively .....	44
Figure 2.5 (a) EDS spectrum (b) Elemental distribution of clean filter spiked with Mobil Jet Oil II .....	46
Figure 2.6 Variability of phosphorus, sulfur and bromine in used filters.....	47
Figure 2.7 Variability of phosphorus, sulfur and bromine in incident filters .....	48
Figure 2.8 (a) EDS Spectrum and (b) elemental composition of used filter ID-9RZMC2.....	49
Figure 2.9 Box plots showing variability of mean atomic weight percent of phosphorus in (a) used and (b) incident filters from different aircraft types .....	55
Figure 2.10 Box plots showing variability of mean atomic weight percent of sulfur in (a) used and (b) incident filters from different aircraft types .....	56
Figure 2.11 Box plots showing variability of mean atomic weight percent of bromine in (a) used and (b) incident filters from different aircraft types .....	57
Figure 2.12 Scatter plots of mean atomic weight percent of phosphorus in used and incident filters from different aircraft types.....	58
Figure 2.13 Scatter plots of mean atomic weight percent of sulfur in used and incident filters from different aircraft types .....	58

Figure 2.14 Scatter plots of mean atomic weight percent of bromine in used and incident filters from different aircraft types .....	59
Figure 2.15 Comparison of Sulfur and phosphorus in used filters .....	60
Figure 2.16 Comparison of sulfur and phosphorus in incident filters .....	60
Figure 2.17 Comparison of bromine and sulfur in used filters .....	61
Figure 2.18 Comparison of bromine and sulfur in incident filters .....	61
Figure 2.19 Comparison of bromine and phosphorus in used filters .....	62
Figure 2.20 Comparison of bromine and phosphorus in incident filters .....	62
Figure 2.21 Decrease in silicon with increasing carbon in used filters .....	63
Figure 2.22 Decrease in oxygen with increasing carbon in used filters .....	64
Figure 2.23 Relationship of phosphorus with carbon in used filters .....	64
Figure 2.24 Relationship of sulfur with carbon in used filters .....	65
Figure 2.25 Relationship of bromine with carbon in used filters .....	65
Figure 2.26 Electron micrograph of clean HEPA filter manufactured by Keddeg Co. ....	66
Figure 2.27 Mixed elemental maps for P, S and Br in used filter samples.....	67
Figure 2.28 Composite image of electron micrographs for (a) used filters ID 3Q5J9L and 9RZMC2 and (b) incident filters ID 163B4J and 23937 .....	68
Figure 3.1 The chemical structure of TCP and its three main isomers.....	77
Figure 3.2 (a) Filter sampling process (b) Filter panel (c) Filter sample for GC/MS analysis.....	82
Figure 3.3 Hewlett Packard (HP) Agilent series 6890 GC/MS system with 5973 MSD .....	83
Figure 3.4 GC/MS spectrum of standard solution .....	87
Figure 3.5 Spectra of used filters: (a) ID E63JVE (b) ID GF68X3 and (c) ID SJA33J with peaks below detection levels.....	88
Figure 3.6 Spectra of incident filters (a) ID A22609HC and (b) A24246HC.....	89
Figure 3.7 Histograms of mean concentration of TCP isomers detected in used filters.....	90
Figure 3.8 Histograms of mean concentrations of TCP isomers detected in incident filters.....	90
Figure 4.1 Schematic illustrating neutron activation process and emission of gamma rays .....	99
Figure 4.2 Filter sampling preparation for NAA .....	101
Figure 4.3 Top view of TRIGA MARK II Reactor at Kansas State University .....	102
Figure 4.4 Net peak area calculation for different background continuum counts.....	104
Figure 4.5 Energy calibration using the MGS-1 certificate file.....	108



Figure 4.6 Efficiency calibration curve fitting using MGS-1 certificate file.....	110
Figure 4.7 Basic steps in gamma ray data acquisition flow chart.....	113
Figure 4.8 Gamma ray spectra showing the elements photo peaks of filter samples from Donaldson, Keddeg and Pall companies irradiated for 8 hours and counted for 1 hour with an HPGe detector after 7-10 days decay time.....	116
Figure 4.9 Gamma ray spectra showing the elements photo peaks from jet engine oil samples irradiated for 8 hours and counted for 1 hour with an HPGe detector after 7-10 days decay time .....	117
Figure 4.10 Gamma ray spectra showing the elements photo peaks from used filter samples irradiated for 8 hours and counted for 1 hour with an HPGe detector after 7-10 days decay time .....	118
Figure 4.11 Gamma ray spectra showing the elements photo peaks from incident filter samples irradiated for 8 hours and counted for 1 hour with an HPGe detector after 7-10 days decay time .....	119
Figure 4.12 Comparison of isotopes with mean concentrations found to be statistically significantly different in used and incident filters .....	126
Figure 4.13 Process flow chart of aircraft cabin air filter analysis by NAA .....	129
Figure 5.1 Schematic diagram for aircraft bleed air simulation (BAS) system.....	141
Figure 5.2 Schematic of pyrolytic reactor for jet engine oil.....	144
Figure 5.3 Calculation of dilution factor.....	150
Figure 5.4 LabVIEW function converting counts to mass deposited on filter .....	151
Figure 5.5 Schematic diagram of the BAS and data acquisition system .....	153
Figure 5.6 Aerosol sampling device assembly .....	157
Figure 5.7 A 25-mm Air sampling filter cassette holder .....	158
Figure 5.8 Comparison of particulate distribution at cruise test 1 and top climb test 1 conditions .....	162
Figure 5.9 Histogram of particle count distribution at simulated ground operations test 1 (14.1 PSI, 170.4°C) .....	163
Figure 5.10 Histogram of particle count distribution at top climb (take-off) condition test 1 (103.2 PSI, 308.0°C).....	163

Figure 5.11 Histogram of particle count distribution at simulate cruise speed test 1: (50.7 PSI, 249.7°C) .....	164
Figure 5.12 Flowchart for calculation of Mobil Jet Oil II aerosol characteristics: Probit analysis .....	165
Figure 5.13 Histogram of aerosol concentration distribution at simulated ground operations test 1 (14.1 PSI, 170.4°C) .....	167
Figure 5.14 Histogram of aerosol concentration distribution at simulated top climb (Hot test 1: 102.2 PSI, 308.0°C) .....	167
Figure 5.15 Histogram of aerosol concentration distribution at simulated cruise speed conditions test 1 (50.7 PSI, 149.7°C).....	168
Figure 5.16 Histogram of aerosol concentration distribution at simulated initial descent from cruise test 1 (29.7 PSI, 185.2°C).....	168
Figure 5.17 Histogram of aerosol concentration distribution at simulated end of descent test 1 (66.9 PSI, 230.7°C).....	169
Figure 5.18 Histogram of aerosol concentration distribution at simulated high pressure to low pressure switch-over (Hot test 1: 70.9 PSI, 280.5°C).....	169
Figure 5.19 Comparison of Mobil Jet Oil II aerosol concentrations generated from different simulated bleed air conditions.....	170
Figure 5.20 Cumulative mass distribution curves for Mobil Jet Oil II aerosols at different simulated bleed air conditions.....	171
Figure 5.21 Probits versus $\ln(d_p)$ at cruise test 1 (50.7 PSI, 249.7°C).....	172
Figure 5.22 Probits versus $\ln(d_p)$ at ground operations test 1 (14.1 PSI, 170.4°C).....	172
Figure 5.23 Probits versus $\ln(d_p)$ at top climb test 1 (103.2 PSI, 308.0°C) .....	173
Figure 5.24 Variability of MMAD of Mobil Jet Oil II aerosols with temperature in bleed air simulator .....	175
Figure 5.25 Variability of GSD of Mobil Jet Oil II aerosols with temperature in bleed air simulator .....	176
Figure 5.26 Variability of MMAD of Mobil Jet Oil II aerosols with pressure in bleed air simulator .....	176
Figure 5.27 Variability of GSD of Mobil Jet Oil II aerosols with pressure in bleed air simulator .....	177

Figure 5.28 Logarithmic scale for cumulative mass percent curves vs aerodynamic diameter for simulated bleed air conditions.....	178
Figure 5.29 Comparative analysis of the effect of temperature on concentrations of TCP isomers on clean filters exposed in BAS at varied durations .....	179
Figure D.1 Pop-up menu from the LabVIEW software at the start of experiment.....	324
Figure D.2 Control panel pop-up menu from LabVIEW system software.....	325
Figure D.3 User interface for aerosol particle counting and CO monitoring .....	326
Figure E.1 Block diagram showing VI in LabVIEW program.....	370
Figure E.2 Block showing VI in LabVIEW Program.....	370
Figure E.3 Temperature profiles in BAS during modeling pyrolysis of Mobil Jet Oil II at top climb and cruise speed conditions (OPC: One nozzle open) .....	371
Figure E.4 BAS temperature profiles during modeling of pyrolysis of Mobil Jet Oil II at initial descent and end of descent from cruise conditions (OPC: One nozzle open) .....	372
Figure E.5 BAS temperature profiles during modeling of pyrolysis of Mobil Jet Oil II at high pressure to low pressure switch-over and ground operations (OPC: One nozzle open).....	373
Figure E.6 Trends in pressure profiles of pyrolysis of Mobil Jet Oil II at simulated top climb, cruise and initial descent from cruise.....	374
Figure E.7 Trends in pressure profiles of pyrolysis of Mobil Jet Oil II at simulated high pressure to low pressure switch over and ground operations (cold tests) .....	375

## List of Tables

Table 1-1 Typical temperatures and pressures of an operating aircraft engine .....	9
Table 1-2 Key features and benefits of jet engine lubricating oils .....	11
Table 1-3 Additives to jet engine oils and possible health effects on exposure to humans.....	12
Table 2-1 Distribution of used and incident filters by manufacturer and type of aircraft .....	37
Table 2-2 Elements identified in clean filter samples from (a) Pall Aerospace Inc., (b) Keddeg Co. and (c) Donaldson Co.....	43
Table 2-3 Elements identified in clean filter media spiked with Mobil Jet Oil II .....	45
Table 2-4 Summarized descriptive statistics of normality test results for elemental contaminants from Mobil Jet Oil II identified in used and incident filters .....	50
Table 2-5 ANOVA – Test for homogeneity of jet engine oil contaminants variance in used and incident filters .....	53
Table 3-1 Health symptoms of long and short-term exposure to smoke/fume incidents .....	80
Table 3-2 Descriptive statistics for TmCP and TpCP in used and incident filters .....	90
Table 4-1 Energy calibration data.....	108
Table 4-2 Efficiency calibration data.....	109
Table 4-3 Elements detected in background, clean, used, incidents filters and jet engine oil....	115
Table 4-4 Isotopes with statistically significant concentration differences in used and incident filters .....	125
Table 4-5 Cost evaluation chart and comparison guide for analysis of used aircraft cabin air filters by NAA.....	130
Table 5-1 Air quality parameters measured in commercial airliner cabin environment .....	135
Table 5-2 The OSHA and ACGIH standards for ToCP .....	136
Table 5-3 Thermal-physical properties of air at 477.59 K.....	144
Table 5-4 Calculated reactor parameters .....	146
Table 5-5 Calculation of dilution factor.....	149
Table 5-6 Distribution of aerosol particulates in percentages from various size ranges at different simulated bleed air operations.....	162
Table 5-7 Key steps in Probit analysis: Cruise speed (Test 1: 50.7 PSI, 249.7°C).....	166

Table 5-8 Summarized results of probit analysis parameters for simulated aircraft bleed air operations .....	173
Table 5-9 Results of simulated experimental conditions for aircraft bleed air operations .....	174
Table 5-10 Mean aerosol characteristics and simulated bleed air conditions.....	175
Table 5-11 Cumulative mass percentage and aerodynamic diameter for simulated bleed air conditions .....	177
Table 5-12 Exposure tests.....	178
Table 5-13 Pattern of Mobil Jet Oil II markers on clean filters exposed in BAS.....	179
Table A-1 FESEM/EDS Data for Used Filters .....	196
Table A-2 FESEM/EDS Data for Incident Filters .....	208
Table A-3 SAS OUTPUT .....	222
Table A-4 ANALYSIS OF VARIANCE (ANOVA) USING PROC GML and PROC MIXED PROCEDURES.....	227
Table B-1: GC/MS results for used filters .....	259
Table B-2: GC/MS results for incident filters.....	262
Table C-1: NAA data on used filters .....	264
Table C-2 NAA data on clean filters .....	318
Table C-3 NAA data for jet engine lubricating oil (Mobil Jet Oil II).....	323
Table E-1 Aerosol counts at simulated ground operations (Test 1: 14.1 PSI, 170.4°C).....	328
Table E-2 Aerosol counts at simulated top climb (take-off) conditions (Test 1: 103.2 PSI, 308.0°C) .....	335
Table E-3 Aerosol counts at simulated cruise speed conditions (Test 1: 50.8 PSI, 249.7°C) ....	342
Table E-4 Aerosol counts at simulated initial descent from cruise conditions (Test 1: 29.7 PSI, 185.1°C) .....	349
Table E-5 Aerosol counts at simulated end of descent conditions (Test 1: 66.1 PSI, 230.9°C). 356	
Table E-6 Aerosol counts at simulated high pressure to low pressure conditions (Test 1: 70.9 PSI, 279.5°C) .....	363

## **Acknowledgements**

I would like to express my sincere appreciation to my supervisors, Professor Steven J. Eckels and Professor Byron W. Jones of Mechanical Engineering at Kansas State University, for their guidance, encouragement, and advice in the course of my studies and the preparation of this dissertation. I would like to thank also all the examiners: Professor B. Terry Beck, and Professor Ronaldo G. Maghirang for their time and effort in serving on the advisory committee and for helpful discussions that led to various suggestions and amendments to the dissertation. I am also grateful to Professor Oliver L. Weaver, for kindly agreeing to be the outside chair. I wish also to acknowledge the assistance from Professor Clifford Weisel with GC/MS analysis, Dr. Dan Boyle for assisting with FESEM/EDS analysis and Dr. Jeffrey Geuther for assisting with NAA analysis, and Professor James Higgins for advising on interpretation of statistics. Finally, I wish to thank my family and friends for their support and encouragement throughout the years of study. I gratefully acknowledge the Federal Aviation Administration (FAA) of USA for their financial support of this work which was made possible through a grant number 04-ACE-KSU. Although the FAA sponsored this study, it neither endorses nor rejects the findings of this research.

## **Dedication**

To my grandson Mikel Braden Magoha

## **Preface**

During the last five decades, unprecedented global demand for travel and international business requirements and ever expanding manufacture of different aircraft models have created the modern global civil aviation industry. On the cusp of this century's second decade, the global civil aviation finds itself balancing efficiency and availability while safety demands and energy costs increase. In particular, in response to growing demands for a more controlled aircraft cabin environment, scientific research on aircraft cabin air supply have gained ground over the past decade. Looking ahead to the next 10 years, aircraft manufacturers will emerge as leaders that augment airlines' business alignment and performance while implementing technologies and services that reduce costs by improving design, management, and operating efficiency, including cabin air quality. While many nations worldwide still rely on aircrafts with bleed air technology, new solutions are emerging that will deliver significant improvements in cabin air quality supply operations. The use of aircraft cabin air quality monitoring technologies combined with filter analysis techniques in a strategic blended implementation could help airlines address many of their objectives including aircraft environmental control system performance, compliance and safety. This study presents some critical technological trends that will drive improvements in aircraft cabin air quality in the next decade and beyond. The research focuses on presenting analytical techniques that may improve understanding of cabin air quality by analyzing used cabin air-recirculating filters. The aim is to find technological solutions in aircraft cabin air supply operations; an airline's success may thus depend on implementing effective technological changes whilst, at the same time, avoiding significant harmful side effects to humankind.



## Acronyms

AChE	Acetylcholinesterase
ACGIH	American Conference of Governmental Industrial Hygienists
ANSI	American National Standards Institute
APU	Auxiliary Power Unit
ASHRAE	American Society of Heating, Refrigerating and Air-Conditioning Engineers
ASME	American Society of Mechanical Engineers
BAe	British Aerospace
BALPA	British Airline Pilot Association
BAS	Bleed Air Simulator
BChE	Butyrylcholinesterase
BEI	Biological Exposure Indices
BSE	Back Scattered Electron
Bq	Becquerel
CASA	Australian Civil Aviation Safety Authority
CEN	European Comite de Normalization
Ci	Curie
CO <sub>2</sub>	Carbon dioxide
CO	Carbon monoxide
COT	Committee on toxicity
°C	degrees Celsius
cm <sup>3</sup>	cubic centimeter(s)
CFM	cubic foot per min.
cm	centimeter(s)
CNS	Central Nervous System
DBPP	Dibutyl phenyl phosphate
DOP	Di-octyl phthalate
DOT	U.S. Department of Transportation
DSA	Digital Spectrum Analyzer
°F	degrees Fahrenheit

EASA	European Aviation Safety Agency
EDS	Electron dispersive spectroscopy
EOHSI	Environmental and Occupational Health Sciences Institute
EPA	US Environmental Protection Agency
EPAAQ	Expert Panel on Aircraft Air Quality
ECS	Environmental Control System
FAA	US Federal Aviation Administration
FESEM	Field emission scanning electron microscopy
FWHM	Full width at half maximum
GC/MS	Gas Chromatography-Mass Spectrometry
g	gram(s)
GSD	Geometric Standard Deviation
HEPA	High Efficiency Particulate Air (Filter)
HPGe	High Purity Germanium
ICAO	International Civil Aviation Organization
IER	Institute of Environmental Research
IEST	US Institute of Environmental Science and Technology
in.	inches
IPCS	International Programme on Chemical Safety
kcps	Kilocounts per second
kN	Kilonewton(s)
LabVIEW	Laboratory Virtual Instrumentation Engineering Workbench
lbf	Pound-force
L	Liter(s)
m	meter(s)
MAK	Maximale Arbeitsplatz-Konzentration (German Maximum Workplace Concentrations)
μg	microgram(s)
μm	micrometer(s)
mm <sup>2</sup>	Square millimeter(s)
m <sup>3</sup>	cubic meter(s)

mbar	millibar
min.	minute(s)
μCi/mg	Micro-Curie per milligram
μg/m <sup>3</sup>	Microgram per cubic meter
MMAD	Mass Median Aerodynamic Diameter
MERV	Minimum Efficiency Reporting Value
MIL-STD	Military Standard
mL	milliliter(s)
MPPS	Most Penetrating Particle Size
mR/hr	milliRontgen per hour
MSDS	Material Safety Data Sheet
nA	nanoamperes
NAA	Irradiation Neutron Activation Analysis
NASA	US National Aeronautics and Space Administration
nm	nanometer
NRC	US National Research Council
OP	Organophosphates
OPC	Optical Particle Counter
OPICN	Organophosphate ester induced chronic neurotoxicity
OSHA	US Occupational Safety and Health Administration
O <sub>3</sub>	Ozone
Pa	Pascal
PAN	N-phenyl-1-naphthylamine
pg	Picograms
PEL	Permissible exposure limits
ppm	parts per million
ppb	parts per billion
PSD	Particle size distribution
psi	pounds per square inch
PSID	Pounds per square inch differential
RSP	Respirable suspended particulates

s	Second(s)
SAS	Statistical application software
SAE	Society of Automotive Engineers
SBO	Smoke and burning odor
SCFH	Standard cubic foot per hour
SDD	Silicon drift detector
SIM	Single Ion Monitoring
SVOC	Semi Volatile Organic Compounds
TBP	Tri-butyl phosphate
TCP	Tricresyl phosphate
TMPP	Trimethylyolpropane phosphate
TMPE	Trimethylyolpropane ester
TmCP	Tri- <i>meta</i> -cresyl phosphate
ToCP	Tri- <i>ortho</i> -cresyl phosphate
TpCP	Tri- <i>para</i> -cresyl phosphate
TPP	Tri-phenyl phosphate
TVOC	Total volatile organic compounds
TLVs	Threshold limit values
TWA	Time weighted average
ULPA	Ultra low penetration air
VOC	Volatile organic compounds
WHO	World Health Organization

### Notations

$C_m$ = Mass concentration (mg/m <sup>3</sup> )	$Nu$ = Nusselt number
$m$ = Net mass increase of the filter after sampling (mg)	$Re$ = Reynolds number
$Q$ = Flow rate (m <sup>3</sup> /s)	$Pr$ = Prandtl number
$Q_s$ = Sampling rate of each filter (m <sup>3</sup> /s)	$T_l$ = Absolute temperature of air (K)
$R$ = Gas constant (Pa·m <sup>3</sup> /kg·K)	$\gamma$ = Specific heat ratio
$t$ = Sampling period (s)	$D$ = Tube diameter (m)
	$A$ = Surface area (m <sup>2</sup> )

$L$	=	Length of the tube reactor (m)	$\mu_x$	=	Weight fraction of element $x$ in the sample
$h$	=	Heat transfer coefficient ( $\text{W}/\text{m}^2 \cdot \text{K}$ )	$p_{i'}$	=	Abundance of precursor isotope $i$ in the element of interest
$c_p$	=	Specific heat capacity of the fluid $\text{J}/(\text{kg} \cdot \text{K})^{-1}$	$f_j$	=	Branching ratio of the gamma $j$ in the radioisotope of interest
$k$	=	Thermal conductivity of the fluid ( $\text{W}/\text{m} \cdot \text{K}$ )	$\eta_j$	=	Overall detection efficiency, including intrinsic efficiency and geometry
$R$	=	$\text{kJ}/(\text{kmol} \cdot \text{K})^{-1}$	$A_x$	=	Atomic mass of the element $x$
$\dot{q}$	=	Wall heat flux ( $\text{W}/\text{m}^2$ )	$\lambda_i$	=	Decay constant of the isotope of interest ( $\text{s}^{-1}$ )
$\dot{m}_{air}$	=	Flow rate of air ( $\text{kg}/\text{s}$ )	$t_o$	=	Irradiation time (s)
$C_j(\mu_x)$	=	Total number of counts under the peak associated with gamma ray energy $E_j$ from radionuclide $I$ (counts)	$t_w$	=	Waiting time between the end of irradiation and the start of counting (s)
$N_a$	=	Avogadro's number ( $\text{mol}^{-1}$ )	$t_c$	=	Counting time of the detector (s)
$\bar{\sigma}_a$	=	Average thermal absorption cross section of precursor isotope $i$ ( $\text{cm}^2$ )			
$\phi$	=	Thermal flux density ( $\text{cm}^{-2} \text{s}^{-1}$ )			
$m$	=	Sample mass (micrograms)			

# CHAPTER 1 - INTRODUCTION

## 1.1 Background

Modern commercial aircraft display impressive technology that highlights advances in global air transportation. That success ensures safe and efficient air travel. However, scrutiny of the air quality in commercial aircraft reveals some technical challenges that must still be overcome. The quality of aircraft cabin air depends both on the quality of the bleed air, sources outside the cabin and the strength and nature of the emissions from cabin sources. Without effective ventilation systems in aircraft cabins, passengers and crew may suffer from the effects of poor air quality. In fact, concerns about the potential hazards of cabin air have motivated most studies performed to date on the quality of the air being supplied to aircraft cabins. These studies have led to technologies that have minimized the impact of air pollution in aircraft cabins. The air-filtration and air-cleaning systems used in aircraft reduce the effects of pollutants in the cabin by removing the air contaminants from the cabin air supply. The contaminants emanating within the cabin that are of greatest concern and most need to be controlled include human body odors, microbial aerosols, volatile organic compounds (VOCs), carbon dioxide (CO<sub>2</sub>), and carbon monoxide (CO). The large quantity of outside airflow supplied to the cabin helps maintain low levels of gaseous and VOCs not removed by the filtration system (Hunt and Space, 1994). Historically, air quality standards for commercial aircraft cabins have been met by complying with reasonable safety and health requirements established by codes and guidelines. These regulations typically address the threats associated with emissions from cabin sources, fire, and weather changes, but not aircraft cabin air quality incidents.

### 1.1.1 Defining aircraft cabin air quality incidents

An aircraft cabin air quality incident, which is often referred to as cabin air contamination event or simply as a smoke/fume incident, is a very complex phenomenon, whose symptoms often mimic smoke generation in a closed environment. A smoke/fume incident is also sometimes called an incident-occurrence or simply an incident or episodic event (ANSI/ASHRAE Standard 161-2007, 2007). The BALPA report submitted to the COT committee refers to a smoke/fume incident as a contaminated air event (BALPA, 2006). An “incident” is not a technical term. Rather it is an informal way of referring to a potentially

serious process that occurs in the aircraft bleed air system and culminates in contaminating the cabin's air supply. An incident poses a serious threat to safety of aircraft cabin occupants. The smell resulting from smoke/fume incidents is based on the perceptions and experiences of airline crew and maintenance staff across the airline industry. Different words have been used worldwide to describe the odor coming from incidents, but the most commonly used words are “dirty socks” or “oil smell.”

## **1.2 Literature Review**

### **1.2.1 Commercial aircraft environmental control system (ECS)**

The conditions in the aircraft cabin, including the temperature, relative humidity (RH), cabin pressure, and cabin air quality, all affect the comfort, productivity, and well-being of cabin occupants. The type of ECS design as well as the air-exchange rate determines the quality and quantity of air supplied to aircraft cabins. Air is supplied and exhausted from the cabin continuously. The outside air supplied to the cabin is provided by the engine compressors and cooled by air-conditioning packs. The conditioned air from the packs flows into a common mix manifold, where it is mixed with recirculated cabin air. The mixed air is then supplied to the passenger cabin. The air enters the passenger cabin from overhead distribution outlets that run the length of the cabin. These outlets are designed to create carefully controlled circular airflow patterns in the cabin. The exhaust air is extracted from the cabin through return air grilles in the sidewalls near the floor, running the length of the cabin on both sides.

In most airplanes, the cabin exhaust passes into the “cheek” area below the cabin floor alongside the cargo hold. Recirculation fans may draw air from this area; one or more outflow valves, which control the cabin pressure, also draw air from this area. Approximately 20 CFM of a mixture of fresh and recirculated air is provided per passenger. This leads to a complete cabin air exchange every two to three minutes: 20 to 30 air changes per hour (Hunt and Space, 1994). On a typical passenger jet, the ratio of fresh to recycled air is about 50-50 (ASHRAE, 1999). But, depending on the design requirements, all modern commercial aircrafts recirculate from 10 to 50 percent of the cabin air. According to Hocking (2000), outside air provided to aircraft passengers is at least close to the 7.0 – 9.4 L/s (15 – 20 cfm) per person. Figure 1.1 shows the various components of a typical aircraft air-conditioning system in a modern airplane (ASHRAE, 1999). Figure 1.2 shows the pattern of air circulation inside aircraft cabins.

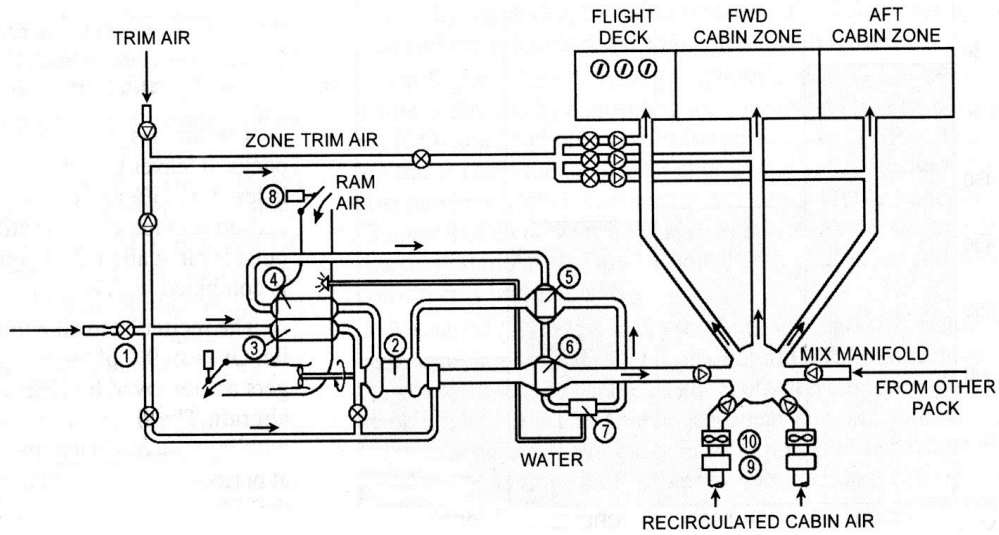


**Figure 1.1 A schematic of typical aircraft air-conditioning system**

Source: ASHRAE Handbook, 1999, ©ASHRAE, www.ashrae.org

- |                             |                    |                         |
|-----------------------------|--------------------|-------------------------|
| 1. Flow control valve       | 5. Reheater        | 9. Recirculating filter |
| 2. Air cycle machine        | 6. Condenser       | 10. Recirculating fan   |
| 3. Primary heat exchanger   | 7. Water collector |                         |
| 4. Secondary heat exchanger | 8. Ram air         |                         |

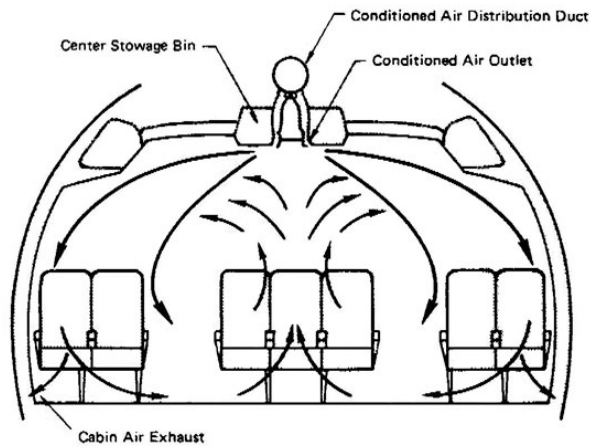


**Figure 1.2 Pattern of air circulation inside aircraft cabin**

(Source: The Committee on Airliner Cabin Air Quality, 1986).

In modern building environmental control systems, the recirculation systems are commonly designed and operated with up to 90 percent recirculated air with the flow rates of



outside air provided at about 0.5 kg/min. (1.1 lb/min) (ASHRAE 1999). Meanwhile, in modern aircrafts, the amount of outside air used for ventilation varies from one model to another, ranging from 10 to 50 percent of the total air supply (ASHRAE, 1999). The high air exchange rate controls temperature gradients, prevents stagnant hot or cold areas, maintains air quality, and dissipates odors in the cabin. The outside airflow maintains cabin pressurization within the pressure hull of the aircraft, a critical function of the environmental control system. Moreover, this fresh air supply should have acceptable quality and should not contain pollutants in quantities that would be considered harmful if introduced to the cabin. Besides exchanging air between the inside and outside of the cabin, the ventilation system decreases cabin air pollutant concentrations by diluting cabin airborne pollutants, thereby improving cabin air quality.

### **1.2.2 Air filtration in commercial aircraft cabins**

The aircraft's ventilation system and cabin air recirculation filters are both very important safety components. The aircraft's ventilation system is designed to remove particles in the recirculated air and reduce bio-effluent levels including toxic gases, VOCs, and any hazardous chemical substances present in cabin environment. HEPA filters are important to the ECS and help maintain a healthy environment in the cabin. The HEPA filters are used for two important reasons: to prevent the spread of pathogens through the cabin with recirculated air and to protect ECS components, fans in particular, from dust and lint.

### **1.2.3 Aircraft cabin air quality and standards**

Previous studies by Spengler et al. (1997) and Nagda and Rector (2003) reported a wide range of VOCs and SVOCs in aircraft cabin air during aircraft operations. These studies could not conclusively trace VOCs to specific sources. However, potential sources for these pollutants are hydraulic fluid, engine and APU lubricants, jet fuels, de-icing fluids, pesticides (in aircraft flying from mosquito-infected parts of the world), cleaning chemicals and disinfectants, perfume worn by cabin occupants (air fresheners and cosmetics), outgassing of cabin materials and furnishings, in-flight catering (particularly vapors from distilled spirits), and human bio-effluents coming from human metabolic processes. The bio-burden in an aircraft cabin depends primarily on the amount of ventilation per person and not on the occupant density. Viable and non-viable particulates on passengers' clothing, may also contribute to contamination of cabin air although the total air volume on airplanes is exchanged every two to three minutes, far more frequently

than the exchange rate in a typical air-conditioned building (Walkinshaw, 2010). The recirculated air poses little or no threat to the health of the cabin occupants as long as the aircraft is equipped with a HEPA filter. In an aircraft ECS, air filtration has been a key process guaranteeing desirable air quality and is vital in meeting air quality standards in the aircraft cabin environment.

### ***1.2.3.1 Aircraft cabin air quality standards***

The U.S. FAA has issued several guidelines and regulations for air in aircraft cabins. However, these guidelines are not specific. Nonetheless, since 1943, the Society of Automotive Engineers (SAE) International has been developing and updating standards on air quality and safety within commercial aircrafts; each standard has a primary feature. The first SAE standard publication released in 1943 contained general requirements for control of air temperature, cabin air pressure, and humidity. An approach to air purity-dilution with outside or recirculated air was also included (SAE ARP85E, 1943). In 1978, SAE published an updated diagram of the typical bleed air system and considerations addressing bleed air duct sizing, materials, acoustics, failure protocols, and proof and burst test conditions (SAE ARP1796A, 1978). The SAE International publication, ARP1539B, issued in 1981 and reaffirmed in 2003, was the first document to provide information on aircraft ECS particulate contamination (SAE ARP1539B, 1981). The SAE ARP4418A published in 1995 provided a table of marker compounds to be sampled for and analyzed during bleed air quality tests. It used prN4618 limits as reference limits for all constituents except particulates, which use a NIOSH limit. Testing techniques were also identified in the publication. The standard defined engine-generated concentrations as measurements of engine bleed air minus air supply inlet (SAE ARP4418A, 1995).

Historically, the first aircraft air quality standards originated because of military safety and health specifications (Fox, 2009). The ASHRAE review process for air quality within commercial aircraft has evolved over the past two decades. The actual development of the ASHRAE standard for airliners started in June 1994, when ASHRAE TC 9.3, Transportation Air-conditioning, made a formal recommendation to ASHRAE to form a Standards Project Committee (SPC) with a charter to derive air quality standards specific to commercial aircrafts. The result was the formation of ASHRAE SPC 161, Air Quality within Commercial Aircraft, which began developing a new standard. In 2007 ASHRAE Standard 161-2007 was issued and approved by ANSI in May 2008. In addition to continuing to update the standard, the committee

is developing a companion guideline, Guideline 28, which provides additional detail, background information, and additional recommendations on the standard. A draft version of the guideline was released for public review and comments, but the final guideline has not yet been published. The ASHRAE Standard 161 (2007) provides minimum criteria for air quality in commercial aircraft. It defines the requirements for air quality in an airliner and specifies methods for measuring and testing for compliance. Further, the standard addresses the unique characteristics of an aircraft cabin environment: the high occupant density, occupant activity levels that range from completely sedentary (passengers) to very active (flight attendants), classification as a public place (passengers) and a workplace (crew), and comparatively low pressure and relative humidity. The standard also covers the chemical, physical, and biological contaminants that may affect air quality as well as the physical cabin environment parameters, such as the temperature, relative humidity, and pressure, and measures to address these parameters (ANSI/ASHRAE Standard 161-2007). The document lays a solid groundwork for upcoming standards on establishing and operating air quality programs in commercial airplanes. Although the standard serves as a reference guideline for airline operators, it is a work in progress. The research presented in this dissertation is a part of that progress. The European Aviation Safety Agency (EASA, 2009); World Health Organization (WHO, 1990), and International Civil Aviation Organization (ICAO, 2001) have also published standards or codes for operating commercial aircraft.

Past studies of cabin air quality standards have focused largely on prevention and establishing rules and regulations based on experience. This conventional approach to establishing standards and codes for air quality within commercial aircraft uses a prescriptive approach. The major drawback to the prescriptive approach is the assumption that all air entering the aircraft ECS is pristine at high altitude (Fox, 2009). While many aspects of ANSI/ASHRAE Standard 161-2007 apply to the operational characteristics of commercial aircraft air quality, it does not cover bleed air quality monitoring in detail or have protocols for monitoring bleed air system operations.

Modern airplanes have technological innovations that allow room for improvement and replacement of individual components or systems. However, since scientific innovations in commercial aerospace industry have been driven by business mindset, standards do not have regulatory force in aircraft manufacturing. Airlines are beginning to assume more responsibility

as good stewards, in part due to public awareness and in part to research. In future, standards may become mandatory for the aircraft cabin environment. At present, an aggressive profile of a commercial jet operation reveals high performance characteristics, including an ECS that will adjust itself to perfectly adapt to changing flight conditions. This means that an ECS in a modern jetliner operates in continually and rapidly evolving environmental conditions in which air quality provision is given a high priority.

#### **1.2.4 Commercial aircraft bleed air system**

Aircraft engine bleed air is defined as the air extracted from compressor stages of gas turbine propulsion engines and auxiliary power units (ANSI/ASHRAE Standard 161-2007; Shang et al., 2010). Aircraft cabin air recirculation systems with bleed air technology were first developed in the wake of studies conducted by the National Aeronautics and Space Administration (NASA) and McDonnell Douglas Corporation. Those studies indicated that substantial fuel savings could be realized without compromising cabin air quality by using a bleed air system, and, today, most modern aircraft use this technology. Bleed air technology has been used in commercial aircraft engines since 1963. Its use has marked a significant turnaround for aircraft operations. Bleed air applications include ECS use, fuel tank pressurization, anti-icing systems, aerodynamic blowing, and driving compressors and suction pumps (Evans, 1991). As a primary source of air for the ECS, the bleed air system provides high pressure, high temperature air bled from the engines and routed throughout the airframe to secondary systems responsible for air conditioning in the aircraft cabin and keeps critical parts of the aircraft, like the leading edge of the wing, ice-free (SAE ARP 1796, 2007).

Bleed air is bled from the engine into a complex system that conditions the air before it is delivered into the cabin. Typically, the bleed air supply to the aircraft cabin environment is drawn from certain compressor stages of the jet propulsion engines at high pressure and temperatures ranging from 170°C (340°F) during ground operations to as high as 350°C (670°F) at take-off depending on the mode of operation, the stage of the compressor used for the extraction, and the speed of the engine (NRC Report, 2002). The outside air enters the engine compressor at atmospheric conditions and is compressed in several stages, raising its pressure up to 650 kPa (100 psi) (about five times atmospheric pressure) with higher temperatures usually topping 310°C (590°F) during top climb (NRC Report, 2002). A small portion of this air is then

extracted from the engine through one or more bleed port openings on the “dry” side of the engine, cooled, compressed, cooled again, expanded for further cooling, and then routed into the passenger compartment. Turbine jet engines also have a “wet” side that comes in contact with engine oil. While the dry side of the engine is intended to remain oil free, in certain conditions it can be contaminated with engine oil.

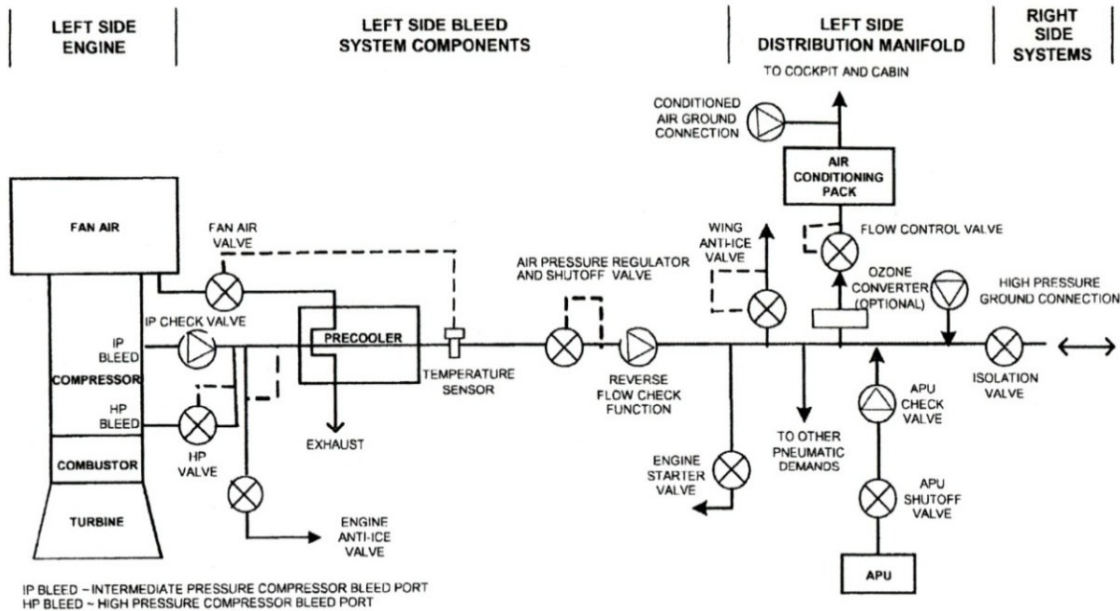


**Figure 1.3 Schematic of typical commercial aircraft bleed air system**

(Source: Standards ARP 1796, SAE International, 1987)

Figure 1.3 shows a schematic of a typical commercial aircraft bleed air system (Standards ARP 1796, SAE International, 1987). Most engines have two bleed air ports: high pressure and low pressure. The pressure at a given location within the compressor depends primarily on the power level at which the engine is operating. The bleed air systems automatically switch between the high and low ports choosing the low pressure port whenever pressure is adequate and switching to the high pressure port when the engine is operating at lower power levels and, consequently, generating lower pressures in the compressor. The hot, high-pressure air coming from the engine compressor is cooled by the pre-cooler to safer temperatures before it is distributed through the ducts to pneumatic aircraft systems. The pre-cooler automatically discharges excess energy back into the atmosphere as waste heat. The pre-cooler ensures that the

temperature of the pneumatic duct line is always well below the ignition temperature of fuel and/or below the critical level for surrounding equipment. The air is then ducted into the aircraft air-conditioning packs, where it is mixed with recirculated air before going to the cabin. In addition to the engines, the auxiliary power unit (APU) on the aircraft provides bleed air for use on the ground and, for some aircraft, in flight usually until just after take-off and just before landing. Table 1.1 shows typical conditions for the bleed air from a jet engine.

**Table 1-1 Typical temperatures and pressures of an operating aircraft engine**

<b>Mode of Operation</b>	<b>Temperature °C (°F)</b>	<b>Absolute Pressure kPa (PSI)</b>	<b>Extraction Stage</b>
Top of climb	310 (590)	690 (100)	Low pressure
Cruise	250 (490)	340 (50)	Low pressure
Initial descent from cruise	185 (365)	200 (29)	High pressure
End of descent (ground level)	230 (445)	460 (67)	High pressure
High pressure to low pressure switch-over	280 (535)	80 (70)	High pressure
Ground operations	170 (340)	-	APU

(Source: NRC, 2002)

The bleed air, which is tapped from a compressor stage of the aircraft engines, is used to pressurize aircraft cabins. The air tapped from an engine increases the fuel consumption of the engine since the tapped air is no longer available to the engine to generate thrust; consequently, the engine compressor must be larger than what is actually required to generate thrust alone (Evans, 1991). To reduce the requirement for bleed air, a certain proportion of the siphoned air is cooled, conditioned to comfortable levels, and mixed with recirculated filtered cabin air before it is introduced to the passenger cabin, instead of having outside air produced from bleed air supplied constantly to the passenger cabin (Markwart, 2009).

With this design, a balance between recirculated air and fresh air is achieved so that a high level of cabin air quality is maintained, fuel efficiency is improved, and the environment is less affected (ANSI/ASHRAE 2007, Ensign and Gallman 2006, NRC 2002). The use of bleed

air from the jet engines may account for the largest operating cost in providing necessary secondary power and environmental control functions for the aircraft (US Patent 5956960, 1999). Figure 1.4 shows a bleed air duct used in most of commercial transport aircraft manufactured by Airbus Industries.



**Figure 1.4 Typical bleed air system in commercial transport aircraft**

(Source: [http://www.liebherr.com/AE/en-GB/products\\_ae.wfw/id-160-0](http://www.liebherr.com/AE/en-GB/products_ae.wfw/id-160-0))

### **1.2.5 Mobil Jet Oil II: A synthetic jet engine lubricating oil**

Jet engine lubricating oils are specialized synthetic oils with a formulation designed specifically for use in high-performance jet engines. The oils have unique physical and chemical properties for lubricating jet engines. According to Winder and Balouet (2002), in jet oil, TCP is used in the formulation of lubricants as an anti-wear additive to enhance load bearing properties and improve tolerance to increasing speed of rotating or sliding motion. It also has flame-retardant properties. Their high performance as lubricants in gas turbine propelled aircrafts

means they offer remarkable advantages over petroleum-based lubricating oils. The multifaceted functions of the jet engine oils have contributed to their popularity in the market. This study focused on Mobil Jet Oil II, which has a molecular weight of 368.37 and a maximum viscosity of 380 cSt at 50°C (Streicher, 1994). Its melting point is 11°C and boiling point 410°C at 1.20 g/mL. Mobil Jet Oil II has a vapor density of 1.1 kg/m<sup>3</sup> at 15°C and a flash point of 270°C (518°F) (Streicher, 1994; MSDS, 2010). The important features and benefits Mobil Jet Oil II as a jet engine lubricant are summarized in Table 1-2.

**Table 1-2 Key features and benefits of jet engine lubricating oils**

<b>Feature</b>	<b>Advantages and Potential Benefits</b>
Excellent thermal and oxidation stability	Reduces the formation of carbon and sludge deposits; Maintains engine efficiency and extends engine life; Reduces bulk oil oxidation and increases deposit control by 50°F
Excellent wear and corrosion protection	Extends seal, gear and bearing life; Reduces engine maintenance
Viscosity and shear stability across wide temperature range	Provides effective lubrication at high operating temperatures
Chemically stable at high operating temperature	Reduces evaporation losses and oil consumption
Excellent resistance to foaming	Maintains film strength under rigorous operating conditions
Good low temperature	Permits start-up and ensures effective lubrication of critical components at temperatures as low as – 40°F

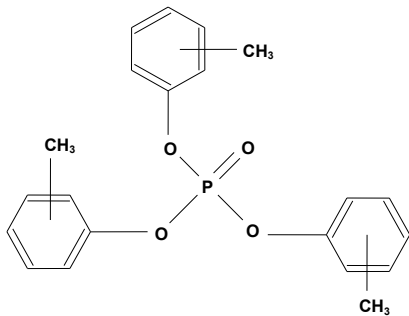
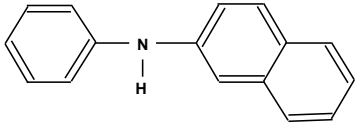
(Source: MSD. [http://www.exxonmobil.com/UKEnglish/Aviation/PDS/GLXXENAVIEMMobil\\_Jet\\_Oil\\_II.asp](http://www.exxonmobil.com/UKEnglish/Aviation/PDS/GLXXENAVIEMMobil_Jet_Oil_II.asp))

The jet engine oils are a combination of a highly stable synthetic base fluid and a unique chemical additive package, providing outstanding thermal and oxidative stability that resists deterioration and deposit formation in both the liquid and vapor phases as well as excellent resistance to foaming. The load-carrying ability of the oil comes from its synthetic base stock viscosity and, therefore, is not subject to loss from viscosity index additive shear (Rudnick, 2003). Additionally, jet engine oils are formulated to meet the demanding requirements of aircraft with gas turbine engines that must perform well over a wide range of severe operating conditions. The closely controlled, low-temperature viscosity of the oil, along with its low pour point, ensure good low-temperature fluidity to permit an effective operating range between – 40°C (– 49°F) and 204°C (400°F). The product has a high specific heat to ensure good heat



transfer from oil-cooled engine parts. Laboratory testing and in-flight performance have shown that the oil has excellent bulk oil stability at temperatures up to 204°C (400°F) for extended periods. The evaporative rate at this temperature is low enough to prevent excessive loss of volume. The ingredients that have been commonly added to jet engine lubricating oils are listed in Table 1-3.

**Table 1-3 Additives to jet engine oils and possible health effects on exposure to humans**

Ingredients	Concentration (% by weight)	Effects of exposure on human health
Tricresyl phosphate (TCP) $(\text{CH}_3\text{C}_6\text{H}_4\text{O})_3\text{P}=\text{O}$ 	1 – 5.0%	Neurotoxin
N-Phenyl-1-Naphthylamine (PAN) $\text{C}_{16}\text{H}_{13}\text{N}$ 	0.1 – 1.0%	Skin sensitizer
Akylated-diphenylamines	< 2.0%	None

(Source: ACGIH 2001; MSDS, 2010)

Jet engine lubricating oils are supplied in many (intermediate) grades classified by viscosity. Type II oils are required for the main engines, while Type I oils are recommended for APU use by some engine manufacturers for its cold-start properties. One of the constituents of interest in jet engine oils in this study are TCP isomers because they are organophosphates and known to have adverse effects on human health. The TCP isomers could as well serve as oil markers on filters. TCP exists in ten isomeric forms, but three isomers, ortho-, meta- and para-, are the most common forms. The ortho-isomer is highly toxic; its presence should be minimized as much as possible. The meta- and para-isomers of TCP are relatively inactive (Winder and

Balouet, 2002). The TCP boiling point is about 200°C, so that under typical domestic conditions it would not vaporize (Holt, 2011). Jet turbine lubricating oils are formulated to operate efficiently at higher temperature conditions and allow longer operation. Jet engines require oils with a lower pour point, or better viscosity temperature characteristics, and a higher degree of resistance to oxidation or thermal decomposition than petroleum derived oils. Therefore, synthetic lubricants are not made from natural crude oils, which would breakdown under high temperatures. They are made from a highly stable polyol ester basestock and can handle high temperatures without breaking down or forming carbonaceous deposits. The presence of polyol ester base stock in jet engine oil implies that in any chemical analysis of oil, the substance could also serve as oil marker on used filters. Because of the high temperatures that develop in turbine engines, the synthetic lubricating oils are formulated to dissipate heat quickly and provide a cushioning effect. In addition to being able to handle high temperatures, lubricants for modern jet engines must be able to handle extreme speed and structural stress conditions without breaking down or forming deposits. Thus, the addition of TCPs to jet engine oils might be viewed as a “potentially fatal poison or as unpleasant but necessary economic benefits.”

### **1.3 Problem Identification and Description**

During a flight, the aircraft engine experiences a wide range of temperatures and pressures. These changes depend strongly on flight conditions (weather, including wind speeds), payload, and length of the flight. Most of these variations are non-critical and may be simply described as aircraft system reactions to flight conditions. At lower temperatures, the formation of jet engine oil mist in the bleed air may result in an incident. Additionally pyrolysis of jet engine oil can also result in incidents. Addressing the pollutant emissions from a rare event such as smoke/fume incident caused by pyrolysis of lubricating jet engine oil has been a really significant challenge. The unpredictability of smoke/fume incidents is compounded by the constantly changing temperatures associated with processes occurring in the aircraft engine.

During pyrolysis, the jet engine lubricating oil, and specifically some of the synthetic anti-wear oil additives, which include the toxic organophosphate TCP, can undergo thermal decomposition into a range of substances: VOCs of low molecular weight; organic acids; esters; ketones; TCP isomers, including neurotoxin ToCP; and carbon monoxide (CO) (van Netten, 2000; MSDS, 2008). Therefore, even though jet engine oils are excellent for lubricating aircraft

engine parts, they can degrade cabin air quality. The AAIB bulletin describes how jet engine oil leaks into an aircraft's ECS: The engine lubrication system supplies pressurized oil to the main shaft bearings. Various devices are in place to ensure that the air pressure external to the bearing chambers exceeds the local oil pressure to prevent engine oil from escaping and contaminating the compressor airflow. The forward bearing on the low pressure shaft uses a continuous cast iron seal ring as part of its sealing arrangement. Its purpose is to ensure that a positive air pressure gradient is maintained to prevent oil from escaping from the bearing housing.

However, when the bearing floating seal ring fails or is worn out, the engine fuel or lubricant fumes and gases can leak into the compressor airflow path and be ingested into the bleed air system. The quality of the provided air to the cabin air conditioning system becomes degraded (van Netten and Leung, 2000; AAIB Bulletin, 2009). When this happens, an incident is said to have occurred. Such seal failures have occurred in Boeing 757-204 powered by Rolls-Royce engine model RB211-535E4-37 (AAIB Bulletin, 2009). According to an AAIB report, the cause of the malfunctioning of a compressor seal for a known and investigated case of a smoke/fume incident was tensile fracture, with a possible fatigue mechanism as the origin. In this case, the compressor seal fracture may have been caused by the drag between the static seal ring carrier plates and the rotating lower pressure shaft. Another cause of smoke/fume incidents problem is the overfilling of jet engine lubricating oil (maintenance irregularities) by the aircraft's maintenance staff (Harrison et al. 2008; Murawski and Hecker, 2011).

The frequency and intensity of smoke/fume incidents are, in fact unknown. Every smoke/fume incident is different, but there is a growing scientific awareness that all of these disparate incidents have a common result: the occasional contamination of cabin air supply while the aircraft is in flight. Consequently, incidents are potential problems for airlines' crews and air travelers. Incidents can create high anxiety among cabin occupants, disrupt the comfort of air travelers during flight, and threaten their health and safety. For the cockpit crew, an incident can escalate into a crisis threatening the crews' ability to control an aircraft. Generally, smoke/fume incidents can tarnish an airliner's reputation as a safe mode of travel by risking the lives of passengers and crew. Besides smoke/fume incidents, electrical arcing has caused fire and smoke in aircrafts. Modern large transport aircraft have more than 500,000 ft. of wire, and electrical arcing has caused fire and smoke in airliners (Cox, 2006). Therefore, burning wire

insulation is also a potential source of smoke/fume in aircraft cabin environment. This study did not address this issue.

#### **1.4 Justification for the Study**

Following the introduction of bleed air technology, the overall aircraft engine efficiency improved, but the technology also introduced the possibility of engine oil contaminants (gases and particulates) leaking into the cabin air supply. This means that although the bleed air system conserves energy in the aircraft, it cannot provide the level of safety required for critical ECS applications during smoke/fume incidents. According to BALPA report (2006) submitted to COT Secretariat, acute and chronic illnesses may be induced in pilots and cabin crew who inhale smoke/fumes from engine oil and hydraulic fluid, additives present in these products, and pyrolysis products that may be emitted from the engines and auxiliary power unit (APU) into the air conditioning system of certain aircraft types during air contamination incidents (BALPA Report, 2006). The air supplied to the cabin occupants include recirculated air which has passed through cabin air filters. In the face of the risks associated with the human intake of airborne particulates formed during smoke/fume incidents, analyses of used and incident filters and monitoring simulated bleed air, is an important step in a strategy to address smoke/fume incidents problem. This implies that the recirculation filters can be an effective sampling mechanism for assessing cabin air quality and investigating air quality incidents.

The primary purpose of the cabin air recirculation filter is to remove particulate matter from recirculation air system. The impact of the filter on air quality may, however, extend far beyond just removing particulate matter. After many hours of operation, the filter media becomes highly loaded with a variety of matter and may actually serve as a source of some contaminants. Since approximately 50% of air supplied to the cabin passes through these filters, out-gassing from this matter in the filter may result in contaminants being introduced into the supply air stream, which may adversely affect air quality. Also, the heavily loaded filter media can serve as a reactive bed where particulate contaminants, both solid and liquid, have collected; gasses passing through the filter media may react with them. In this way, secondary contaminants may then be introduced into the cabin supply air.

Tens of thousands of liters of air pass through cabin air recirculation filters on a typical flight. In fact, what is collected on the filters is not really a sample, but effectively a global

collection of the suspended particulate matter in the cabin air during the flight. Because large quantities of air pass through recirculation filters in the ECS, the filters may also serve as a useful diagnostic tool for assessing the air quality in general and smoke/fume incidents in particular through analysis of materials collected on the filters. This large sampling volume is both an advantage and a challenge in using cabin air recirculation filters for diagnostic purposes. The large and comprehensive sample of air passing through the filter means that whatever particulate matter which was in the air will show up on the filters and in large quantities, compared to that which can be collected with air sampling devices. However, aircraft HEPA cabin air recirculation filters are non-specific and will have not only an integrated sample for the entire flight but also the material collected from many other flights as well. Thus, pinpointing which sample came from a particular contamination event may be difficult. While HEPA cabin air recirculation filters may be useful diagnostic tools, the most useful results come when they are used in conjunction with other sampling methods.

The concentration levels of some airborne aerosol particulates and gases from aircraft engine bleed air during normal operations have been reported in the scientific literature (Crump et al. 2011; De Nola et al. 2011). Scientists have yet, however, to investigate both the fate of aerosols with different pressure and temperature in an aircraft's bleed air system and how varied conditions in the bleed air system alter aerosol formation during pyrolysis of jet engine oils. While much research has focused on the toxicology of TCP and its isomers in workplaces, relatively few studies have examined how these pollutant emissions are generated in an aircraft bleed air system and transported in the aircraft environmental control systems (ECS). The dangers posed by smoke/fume incidents are hard to measure, and practical ways to remove contaminants generated by smoke/fumes incidents when they occur are lacking. The toxicity levels of the constituents or degradation products of jet engine oils and the relationships between exposures and reported health effects on cabin crews have not been established. Scientists have compiled information about toxicity levels for the amounts of TCPs and ToCP found in workplaces. But much still remains unknown about the effect of TCPs in aircraft cabin environment.

Both animal studies and those conducted in workplaces have shown that high levels of ToCP are hazardous to human health. In particular, ToCP has been linked to cancer (Winder and Balouet, 2002). Somkuti et al. (1988) and Baron et al. (1962) have shown that ToCP is a

powerfully neuropathic substance. The risks of cabin fume exposure include both short-term health problems and long-term illness, disease and disability (Vakas, 2007). According to the Occupational Safety and Health Administration (OSHA) the lethal human oral dose of ToCP is about 1 g/kg and doses of 6 to 7 mg/kg have produced serious paralysis (OSHA, 1978, Kelso et al. 1988; MSDS, 2011). The American Conference of Governmental Industrial Hygienists' (ACGIH) standard for ToCP is 0.1 mg/m<sup>3</sup> of air averaged over an eight-hour work shift (ACGIH, 2001). Some evidence links exposure to smoke/fumes produced during incident-occurrences to serious health risks to passengers and crew (van Netten, 1998; Michaelis, 2003; Bobb, 2003; Swedish Statens Haverkommission, 2003; Mangili and Gendreau, 2005).

Additional evidence exists of some significant flight safety concerns, indicated by incidents reported by United Kingdom Civil Aviation Authority (CAA) (BALPA Report, 2005), and by an investigation of the Swedish Board of Accidents into a 1999 incident in which pilots became incapacitated (Swedish Statens Haverkommission, 2003). The NRC Committee has also described a number of case studies and anecdotal reports that available from other reporting systems (NRC Report, 2002). A definitive understanding of bleed air composition during smoke/fume incidents can only be achieved by a scientific study that facilitates real-time monitoring of the quality of the air passing through the bleed air system. Jet engine lubricating oils have not been exhaustively studied and their use remains largely unregulated. The amount of smoke/fumes from jet engine oil needed to pose a risk has not been quantified because the exact amount of airborne aerosol particulates released during various incidents remains unknown. Scientists have yet to establish acceptable limits for the amount of aerosol particles emitted during smoke/fume incidents: that is the concentration levels of TCP isomers that would be considered a safe threshold. So far, no study has made any attempt at quantifying the particulate size distribution of these compounds from aircraft bleed air systems either. Yet the bleed air system is a conduit for air going into the aircraft cabin.

Reference criteria, such as OSHA's permissible exposure limits (PELs), the ACGIH's threshold limit values (TLVs), and MAK's for the TCP isomers in an aircraft cabin environment have not been developed. The existing industrial exposure standards for TCP and ToCP were not developed for aircraft cabins (Rayman, 2002; and Fox, 2000), and little is known about the health effects of exposures to mixtures of airborne particulate contaminants from jet engine lubricating oil. This makes providing proper aircraft cabin air quality an occupational health and

safety issue. Airborne byproducts of the pyrolysis of jet engine oils in the aircraft bleed air system are not covered by the standards currently applied to pollutant emissions in cabin air.

Furthermore, airborne Mobil Jet Oil II aerosol particulate emissions from the aircraft bleed air system during incidents have not been characterized. The characteristic differences in the size and composition of aerosol particles formed in bleed air systems during smoke/fume incidents have yet to be scientifically examined. Considerably more monitoring of bleed air systems is necessary to establish the factual information needed to make these determinations. Currently, automated real-time data acquisition systems that can generate these data are not available. Nor do means of forewarning of smoke/fume incidents in commercial aircrafts exist. Yet passengers and crew may suffer discomfort and adverse health effects if the quality of air from engine bleed air is poor. In addition to the chemical constituents of pyrolyzed jet engine oil, contaminated bleed air may also contain CO as a byproduct of incomplete combustion of phosphate esters. Acute exposure to CO may cause nausea, headaches, dizziness, and drowsiness. Moreover, chronic neurological sequelae have been reported after acute high-level exposure to CO (Prockop and Chichkova, 2007). Although a better understanding of the levels of TCP and other contaminants during incidents is necessary, methodologies do not currently exist for sampling, analyzing, and displaying instantaneous readings of both particulate and gaseous concentration levels of these compounds in aircraft engine bleed air systems, particularly during smoke/fume incidents.

To begin to explain the relationship between exposure to particulates and health problems, used aircraft cabin air filters and sampling simulated bleed air could be analyzed. Developing testing protocols for monitoring engine bleed air in commercial transport aircrafts will pave the way for risk control and for helping maintain cabins as safe working environments. Performance-based regulations in conjunction with monitoring bleed air system parameters can ensure that the health, safety, and comfort objectives in the aircraft cabin are met. Whether based or expressed on the basis of the number of flights or the number of hours flown, a study by expert panel on aircraft air quality (EPAAQ) established by the Australian Civil Aviation Safety Authority (CASA) reported that fume events are quite rare (CASA Report, 2009). Although considered rare, smoke/fume incidents are shrouded in uncertainty and have become a public health issue in international air travel. No matter how rare these events are, human safety is at stake during such incidents, and the risks of exposure to aerosols from aircraft bleed air during

smoke/fume incidents must be understood better (U.S. GAO, 2004). Even the magnitude of the problem is not known, yet global air travel may be affected. The level of impact of bleed air emissions on cabin air quality is also not known. According Winder and Balouet, immune-suppression is one of the health symptoms of long-term exposure to smoke/fume incidents (Winder and Balouet, 2001). Therefore, learning how aerosol emissions from jet engine oils containing TCPs can affect the most vulnerable is necessary, particularly for travelers with underlying medical conditions such as diabetes, lung disease or heart disease, as well as young children, the elderly, pregnant women, and those with weakened immune systems, who are at highest risk.

## **1.5 Objectives of the Study**

The objective of this study was to determine if aircraft cabin air recirculation filters can be analyzed to determine the source contaminants involved in air quality incidents. Specifically, the study examined aircraft cabin filters by various methods to determine whether jet engine lubricating oil is the source of contaminants in an air quality incident. The focus was on finding markers for the presence of engine oil on used and incident filters using three analytical techniques: FESEM/EDS, GC/MS, and NAA. The analyses of incident and used filters by these methods allowed assessment of whether or not jet engine lubricating oil marker(s) can be detected and quantified in used and incident cabin air recirculation filters. FESEM/EDS analysis identified filters contaminant elements from jet oil, and GC/MS was performed to specifically investigate filters for TCPs and other compounds found in jet engine oils. This study was undertaken to identify acceptable best practices for investigating cabin air quality in commercial aircraft through analysis of cabin air recirculation filters and the development of aircraft bleed air simulator (BAS). The research delivers unique perspectives and advice to airlines on how they can leverage novel analytical techniques to identify smoke/fume incidents to solve air quality problems in aircraft cabins.

Consequently, this research aimed to provide the most effective and meaningful metrics and tools for investigating cabin air quality in commercial aircraft during smoke/fume incidents. Using cabin air recirculation filters as a diagnostic tool for cabin air quality assessment was critical, and the goal was to determine the ability of the analytical methods to establish fingerprints of aircraft engine lubricating oil on dirty and incident filters. The study established a



firm specific link (tracer) between smoke/fume incident and possible detection method and used the outcome to develop practical tools for examining aerosol particulates in cabin air recirculation filters. Another objective of this study was to develop the BAS system.

The specific objectives of the study were:

- To develop techniques for analyzing used cabin air recirculation filters. This included developing procedures for sampling HEPA cabin air recirculation filters.
- To develop an aircraft BAS system to simulate bleed air during different flight phases and investigate air quality breaches in those simulated flight conditions. This involved conducting real-time monitoring of aerosol particles formed during pyrolysis of engine oil at micron levels. The experimental work also included sampling simulated bleed air and loading it onto clean cut samples of cabin air recirculation filter media with known concentrations of engine oil aerosols generated by BAS.
- To measure gaseous products, in particular, CO, as a characteristic determinant or marker for the incident-occurrence process.

With the above objectives in mind, the study expects (a) to advance the understanding of air quality science and the challenges and opportunities in identifying the contaminant so that the source can be eliminated and (b) to develop the best engineering practices for implementing an experimental setup for investigating air quality breaches in the aircraft bleed air system. The aim of developing the BAS was to provide a way to create simulated oil contamination under controlled conditions over a range of temperatures, pressures, and transit times in typical bleed air systems. The practical demonstration of the applied engineering techniques used to arrive at the results was also a strategic goal in this study.

## **1.6 Research Methodology**

FESEM/EDS, GC/MS, and NAA were used to assess whether or not jet oil marker(s) can be detected and quantified in used and incident cabin air recirculation filters. This research was designed to analyze used and incident filters and develop an aircraft bleed air simulator. The study implemented experimental protocols for monitoring simulated bleed air and profiles clean, used, and incident HEPA cabin air recirculation filters to model responses to aircraft bleed air contamination events. Filter samples from the used and incident filters were collected both prior to and following exposure to known concentrations of engine oil contaminants. Detailed

chemical and elemental analysis of the filter samples were conducted using FESEM/EDS, GC/MS, and NAA. In addition to filter analyses, the bleed air simulator (BAS) was developed to model smoke/fume incidents to determine the feasibility of using both analytical techniques and to detect sampled air of aerosols of Mobil Jet Oil II. BAS development also allowed us to determine the size distribution and composition of aerosols in a simulated bleed air. Practical studies and statistical models were used to evaluate data from used and incident filters.

## **1.7 Scope of the Study**

The scope of this study is confined to examining used HEPA filters from commercial aircraft ventilation and air conditioning systems. The methods and procedures used for analyzing TCPs and elements on the filter surface are focused on determining jet engine oil contamination on filters. The BAS was developed and used to simulate smoke/fume incidents caused by jet engine lubricating oil.

## **1.8 References**

- AAIB Bulletin 6/2009, (2009). G-BYAO EW/C2006/10/108. [http://www.aaib.gov.uk/cms\\_resources.cfm?file=/Bulletin%206-2009.pdf](http://www.aaib.gov.uk/cms_resources.cfm?file=/Bulletin%206-2009.pdf) (Cited May 5<sup>th</sup>, 2010).
- ACGIH, 2001. Threshold Limit Values and Biological Exposure Indices (TLVs and BEIs). Cincinnati: American Conference of Governmental Industrial Hygienists. ISBN: 1-882417-40-2, pp. 58.
- ASHRAE, (1999). ASHRAE Handbook – HVAC Applications, Chapter 9, Aircraft. American Society of Heating, Refrigerating and Air-Conditioning. Atlanta, GA.
- ASHRAE, (2007). ANSI/ASHRAE Standard 161-2007, Air Quality within Commercial Aircrafts. 20 pp. Product code: 86493. ISBN: 1041-2336. Atlanta, GA: American Society of Heating, Refrigerating and Air-conditioning Engineers, Inc.
- ASHRAE, (1999). ANSI/ASHRAE Standard 52.2-1999. Method of Testing General Ventilation Air-Cleaning Devices for Removal Efficiency by Particle Size. Atlanta, GA: American Society of Heating, Refrigerating and Air-conditioning Engineers, Inc.
- Australian Civil Aviation Safety Authority (CASA). Expert Panel on Aircraft Air Quality (EPAAQ), Contamination of aircraft cabin air by bleed air – a review of the evidence. September 2009. [http://www.casa.gov.au/wcmswr/\\_assets/main/cabin/epaaq/epaaq-entire-report.pdf](http://www.casa.gov.au/wcmswr/_assets/main/cabin/epaaq/epaaq-entire-report.pdf)

- Baron, R. L., Bennett, D. R. and Casida, J. E., (1962). Neurotoxic syndrome produced in chickens by a cyclic phosphate metabolite of Tri-o-cresyl phosphate – A clinical and pathological study. *Brit. J. Pharmacol.* (1962), 18, 465 – 473).
- British Airline Pilot Association (BALPA) Report, (2005). U.K. Civil Aviation Authority (CAA). [http://www.rsc.org/images/balpa\\_tcm18-99526.pdf](http://www.rsc.org/images/balpa_tcm18-99526.pdf) (Cited: January 7, 2012).
- British Airline Pilot Association (BALPA) Report, (2006). U.K. Civil Aviation Authority (CAA). <http://cot.food.gov.uk/pdfs/cot-laystatementbalpa200706.pdf> (Cited: November 20<sup>th</sup>, 2011).
- Bobb, A. J., (2003). Known harmful effects of constituents of jet oil smoke. TOXDET-03-04. Ohio: U.S. Naval Health Research Center Detachment (Toxicology), 2003.
- Cox, J. M., (2006). Reducing the Risk of Smoke, fire and Fumes in transport Aircraft. Past History, Current Risks and Recommended Mitigations. Cockpit Smoke Solution Report. [http://www.safeopsys.com/docs/SOS\\_SAFITA.pdf](http://www.safeopsys.com/docs/SOS_SAFITA.pdf) (Cited: Nov. 20<sup>th</sup>, 2010).
- Crump, D., Harrison, P. and Walton, C., (2011). Aircraft Cabin Air Sampling Study; Part 2 of the Final Report, Institute of Environment and Health, Cranfield University, April 2011. <https://dspace.lib.cranfield.ac.uk/handle/1826/5306> (Cited: November 24<sup>th</sup>, 2011).
- De Nola, G., Hanhela, P. J. and Mazurek, W. (2011). Determination of Tricresyl Phosphate Air Contamination in Aircraft. *Ann. Occup. Hyg.* Vol. 55. No. 7, pp. 710-722, 2011. Oxford University Press on behalf of the British Occupational Hygiene Society doi:10.109/annhyg/mer040.
- European Aviation Safety Agency (EASA). <http://www.easa.eu.int/rulemaking/technical-publications.php>.
- Evans, A. B. (1991). The Effects of Compressor Seventh-Stage Bleed Air Extraction on Performance of the F100-PW-200 Afterburning Turbofan Engine. NASA Contract Report 179447. February 1991.
- Ensign, T. R. and Gallman, J. W., (2006). Energy optimized equipment systems for general Aviation Jets. 44<sup>th</sup> AIAA Aerospace Sciences Meeting and Exhibit. Reno: 9 – 12 January 2006, Nevada.
- Fox, R. B., (2009). A US Perspective on Cabin Air Quality Standard Development. ICE International Aviation Conference. Munich, 9-10 March 2009.
- Harrison, R., Murawski, J., McNeely, E., Guerriero, J., Milton, D., (2008). Bleed-Air Contaminant Exposure Management Guide. Management of Exposure to Aircraft Bleed-air Contaminants among Airline Workers: A guide for health care providers. August 2008.

- Hocking, M. B., (2000). Passenger aircraft cabin air quality: trends, effects, societal costs, proposals. *Chemosphere* 41 (2000) 603 – 615. Pergamon Press.
- Holt, G. C., (2011). A conference most revealing: aircraft cabin air quality. *Journal of Biological Physics and Chemistry* 11 (2011) 216–220 © 2011. Collegium Basilea & AMSI doi: 10.4024/22HO11A.jbpc.11.04.
- Hunt, E. H. and Space, D. R., (1994). The Airplane Cabin Environment: Issues Pertaining to Flight Attendant Comfort. International In-flight Service Management Organization Conference, Montreal, Canada, November 1994.
- ICAO, (2001). Aircraft disinfection practices survey. FALP/3-IP/1 International Civil Aviation Organization, Montreal, Canada.
- Kelso, A. G., Charlesworth, J. M. Mcvea, G. G., (1988). Contamination of Environmental Control Systems in Hercules Aircraft. Australian Government Department of Defence Materials Research Laboratory. Report MRL-R-1116.
- Liebherr Aerospace Product. [http://www.liebherr.com/AE/en-GB/products\\_ae.wfw/id-160-0](http://www.liebherr.com/AE/en-GB/products_ae.wfw/id-160-0). (Cited: May. 15<sup>th</sup>, 2011).
- Mangili, A. and Gendreau, M. A., (2005). Transmission of infectious disease during commercial air travel. *Lancet* 2005, 365: 989 – 996.
- Markwart, M., (2009). System For Improving Air Quality In An Aircraft Pressure Cabin. Patent application number: 20090277445. AIRBUS DEUTSCHLAND GMBH\ CINCINNATI, OH US IPC8 Class: AA61M1600FI. USPC Class: 12820312.
- Material Safety Data Sheet (MSDS) for Tricresyl Phosphate. Issued: 05/18/2008. <http://mobiljet2.com/msds.pdf>
- Michaelis, S., (2003). A survey of health symptoms in BALPA Boeing 757 pilots. *J. Occup Health Safety - Aust NZ* 2003, 19(3): 253 – 261.
- Murawski, J. and Hecker, S., (2011). Exposure to oil fumes on aircraft: necessary to regulate? *Occupational Health & Safety, Australian & New Zealand Journal of Health, Safety and Environment* 2011 Volume 27(2).
- Nagda, N. L. and Rector, H. E., (2003). A critical review of reported air concentrations of organic compounds in aircraft cabins. *Indoor Air* 2003; 13: 292 – 301. Copyright Blackwell Munksgaard. ISSN 0905-6947.
- National Research Council (NRC) Report, (2002). The Airliner Cabin Environment and the Health of Passengers and Crew Committee on Air Quality in Passenger Cabins of Commercial Aircraft., Washington DC: National Academy Press. ISBN 0-309-17023-0 e-pub.

- OSHA, (1978). Occupational Health Guideline for Tri-ortho-cresyl Phosphate. Occupational Safety and Health Administration, U.S. Department of Labor, September 1978.
- Prockop, L. D. and Chichkova, R. I., (2007). Carbon monoxide intoxication: an updated review. *J. Neurol. Sci.* 262(1-2):122 – 30.
- Rudnick, L. R., (2003). *Lubricant Additives: Chemistry and Applications*. CRC Press ISBN: 978-0-8247-0857-3.
- Ryman, R. B., (2002). Cabin air quality: an overview. *Aviat Space Environ Med*, 73(3): 211-5.
- SAE ARP-85E, (1943). Reaffirmed 1991. *Air Conditioning Systems for Subsonic Airplanes* Society of Automotive Engineers International, Warrendale, PA.
- SAE ARP-1539B, (1981). *Aerospace Recommended Practice: Environmental Control System Contamination*. Society of Automotive Engineers International, Warrendale, PA.
- SAE ARP-1796A, (1978). *Engine Bleed Air System for Aircraft*. Society of Automotive Engineers International, Warrendale, PA.
- SAE ARP-4418A, (1995). *Procedures for Sampling and Measurements of Engine and APU Generated Contaminants in Bleed Air Supplies from Aircraft Engines*. Society of Automotive Engineers International, Warrendale, PA.
- SAE ARP 1976, (2007). *Aerospace Recommended Practice: Engine bleed air system for aircraft*. Society of Automotive Engineers International, Warrendale, PA.
- Shang, L., Liu, G., Hodal, P. (2010). Development of High Performance Aircraft Bleed Air Temperature Control System With Reduced Ram Air Usage, *IEEE Transactions on Control Systems Technology*, Vol. 18, No. 2, March 2010.
- Somkuti, S. G., Tilson, H. A., Brown, H. R., Campbell, G. A., Lapadula, D. M. Abou-Donia, M. B., (1988). Lack of Delayed Neurotoxic Effect after Tri-o-cresyl Phosphate Treatment in Male Fischer 344 Rats: Biochemical, Neurobehavioral and Neuropathological Studies. *Fundam. Appl. Toxicol.* 10, 199 – 205.
- Spengler, J., Burge, H., Dumyahn, T., Muilenberg, M. and Forester, D., (1997). *Environmental Survey on Aircraft and Ground-Based Commercial Transportation Vehicles*. Prepared by Department of Environmental Health, Harvard University School of Public Health, Boston, MA, for Commercial Airplane Group, The Boeing Company, Seattle, WA. May 31, 1997.
- Streicher, R. P., (1994). *NIOSH/DPPSE. NIOSH Manual of Analytical Methods (NMAM) 4<sup>th</sup> edition*. 1994.

- Swedish Statens Haverkommission (Swedish Board of Accident Investigation). Incident onboard aircraft SE-DRE during flight between Stockholm and Malmo M County, Sweden on 12 November 1999, Report RL 2001:41E. Stockholm: Statens Haverkommission, 2003.
- The Committee on Airliner Cabin Air Quality, (1986). *The Airliner Cabin Environment: Air Quality and safety*. The National Academies Press 1986. Copyright National Academy of Sciences.
- U.S. GAO, (2004). *AVIATION SAFETY More research needed on the effects of air quality on airliner cabin occupants*. U.S. General Accounting Office. Report to the ranking Democratic Member, Subcommittee on Aviation Committee on Transportation and Infrastructure, House of Representatives January, 2004.
- US Patent 5956960, (1999). Multiple mode environmental control system for pressurized aircraft cabin
- Vakas, N., (2007). *Interests and the shaping of an occupational health and safety controversy: the BAe 146 case*, Ph.D. Thesis, University of Wollongong, 2007.
- van Netten, C., (1998). Air quality and health effects associated with the operation of the BAe 146-200 aircraft. *Appl Occup Environ Hyg* 1998, 13(10): 733-739.
- van Netten, C., (2000). Analysis of two jet engine lubricating oils and a hydraulic fluid: their pyrolytic breakdown products and their implication on aircraft air quality In: Nagda, NL (eds). *Air Quality and Comfort In Airliner Cabins*. pp. 61-75 ASTM STP 1393. American Society for Testing and Materials, West Conshohocken, PA
- van Netten, C, Leung, V., (2000). Comparison of the constituents of two jet engine lubricating oils and their volatile pyrolytic degradation products. *Applied Occupational and Environmental Hygiene* (2000). Volume: 15, Issue: 3, Pages: 277 – 283
- Walkinshaw, D. S., (2010). Germs flying and the truth. *ASHRAE Journal*. Volume 52. April 2010.
- Winder, C. and Balouet, J. C., (2002). *The Toxicity of Commercial Jet Oils*. Environmental Research Section A. Vol. 89. No. 2: 146 – 164. Publisher Academic Press.
- Winder, C., and Balouet, J. C., (2001). Aircrew Exposure to Chemicals in Aircraft: Symptoms of Irritation and Toxicity. *Journal of Occupational Health and Safety – Australia and New Zealand* 17: 471 – 483, 2001.
- WHO, (1990). Tricresyl phosphate. (Environmental health criteria; 110) ISBN 92 4 157110 1. <http://www.inchem.org/documents/ehc/ehc/ehc110.htm>

# CHAPTER 2 - ANALYSIS OF USED AIRCRAFT CABIN AIR FILTERS BY FIELD EMISSION SCANNING ELECTRON MICROSCOPY (FESEM) WITH ENERGY DISPERSIVE X-RAY SPECTROSCOPY (EDS)

## 2.1 Abstract

Most jet turbine engine oils contain the additive tricresyl phosphate (TCP), an organophosphorus (OP) compound; it offers excellent lubricating properties but is hazardous to human health. Rising concern about the toxicity of TCPs is the principal motivation for smoke/fume incidents research. The objective of the study was to identify jet engine oil markers on used aircraft cabin air recirculation filters that could point to jet engine oil as the source contaminant in bleed air incidents. The Nova<sup>TM</sup> Nano field emission scanning electron microscopy (FESEM) model 430 with energy dispersive X-ray spectroscopy (EDS) equipped with 80mm<sup>2</sup> X-Max silicon drift detector (SDD) was used to determine the composition of elements on the surface of used filters. The filter analysis study involved 99 *used*, non-incident filters and 34 *incident* filters. The term “used” filter refers to filters that were removed from aircraft during normal servicing, normally at the end of a service period. While detailed records were not available for these aircraft for the service period of the filters, they were not reported as problem aircraft. “Incident” filters refer to filters that were removed from aircraft that had air quality issues. The nature of the issues was not reported. In at least some cases, filters were removed for analysis before their normal service period of replacement. Clean, *unused* filters were also examined as controls. The analysis identified phosphorus (P), sulfur (S), and bromine (Br) elements as potential markers for jet engine oil contamination in used filters. The mean (range) atomic weight % of P concentrations for used filters was 0.052 (0.007, 0.144) and for incident filters 0.032 (0.005, 0.080). The statistical analysis suggest a normal distribution as a good fit model for P on used filters (p-values for normality test are greater than 0.05). Statistical analysis also suggests that P is correlated to S ( $r = 0.6$ ;  $p\text{-value} = 0.0001$ ). The analysis of variance of means of P for used filters obtained from different aircraft types revealed that p-values of pair-wise comparisons of aircraft models with Bonferroni adjustment at  $\alpha = 0.05$  were statistically significantly different for A320-B777 ( $p = 0.0298$ ) and B737-747 ( $p = 0.0002$ ) but not significant for other pair-wise

comparisons. The electron micrographs and associated elemental maps revealed a diverse morphology of particulate deposition on used filter surfaces. Phosphorus, sulfur, and bromine were found on nearly all filters. In the second approach of analysis where every point was considered, no strong correlation between the amounts was found, so the substantial difference between the ratios of these elements found on filters and in oil-spiked filter samples, and lack of differences in patterns between used and incident filters, leads to the conclusion that non-oil sources of these elements are ubiquitous in aircraft cabins and, thus, they might not be used as unique indicators of the presence of jet engine oil in the cabin air.

## **2.2 Introduction**

Commercial aircraft are the workhorses of global air transportation. Because of increased air travel and challenging environmental regulations, aircrafts must operate at their best. Efficiency must be maximized across the entire spectrum of an aircraft's operation, and cabin air quality must be maintained at all times during flight. Technology must be leveraged to the highest degree possible in every aspect of aircraft operation, including aircraft cabin air quality to respond to changing human health requirements. In any built environment meant for human occupation, clean air supply is necessary to health. Aircraft cabin occupants need a continuous air supply that does not pose hazards to safety, comfort, and health. Providing good air quality in aircraft cabins, however, requires accurate and effective control of a variety of contaminants within the cabin and from outside air. These contaminants include volatile organic compounds (VOCs) and gaseous byproducts from reactions taking place in aircraft engine bleed air system during smoke/fume incidents. The major sources of air pollution from the cabin include bio-effluents, disinfectants, carpets, paints, and furnishings treated with flame-retardant chemicals, such as upholstery, drapes, and curtains. According to Pall Corporation, there is no definite time interval for replacing a cabin air filter element. Airlines often choose to replace cabin air filter elements at regular intervals to fit in with routine scheduled maintenance periods, such as a C-check. The definition of a C-check varies between aircraft models and operators (Pall Corporation).

During past decades, smoke/fume incidents may have been underreported, so these incidents may not have received the attention they deserve. Shortfalls in accounting for incidents have been reported in Britain and Australia. The expert panel on aircraft air quality (EPAAQ)



established by the Australian Civil Aviation Safety Authority (CASA) reported that throughout the world there is no consistency in the collection of data on contaminated cabin air events. According to Winder and Michaelis, the Australian Senate inquiry into the BAe 146 cabin air quality and the UK CAA database on Boeing 757 incident reports over the same period showed cases of underreporting (Winder and Michaelis, 2005, Michaelis, 2007). Recent reports from U.S. FAA indicate that US airlines have reported significant increases in smoke/fume incidents. Such incidents have been reported fleet-wide across a wide range of aircraft types (Murawski and Supplee, 2008). From January to December 2010, US Airways documented 87 air supply contamination events that involved engine oil or hydraulic fluids (ISP, CWA, AFL-CIO, 2011). An October 2010 circular released to airline operators states that more than 900 cases of smoke/fume incidents occur annually (U.S. DOT FAA InFO 10019, 2010). Increases in reporting of incidents suggest that airlines are becoming more responsive to incident-occurrences. Additionally, airlines may now be recognizing that smoke/fume incidents are challenges worth tackling. In addition, the increased number of incident reports puts new pressure on airlines to provide appropriate safety and security on aircraft without discouraging passengers and crew.

Rising concern about the toxicity of TCPs as well as public concern about aircraft air quality has motivated research into smoke/fumes incidents. Commensurately, advances in these scientific studies have also created increased public awareness of airborne contaminants in aircraft and in particular the adverse health effects of airborne pollutants on humans. In addition, technological advances have also made available a range of innovative tools for testing cabin air quality. Whenever a smoke/fume incident occurs, it significantly undermines an airline's efforts to provide quality air to the passengers and crew because of airborne particulates (BALPA Report, 2005). As a result, an incident can disturb cabin occupants, both passengers and crew, which can adversely affect cabin crew morale and their motivation to work. The substances of interest are jet engine oils, hydraulic fluids and deicing fluids (NRC, 2002; Solbu et al. 2007; De Nola et al. 2008). In the case of jet engine oils, the airborne aerosols produced from either mists of oil or the pyrolyzed products of jet engine oil can cause a range of health problems for cabin occupants (Michaelis, 2003; Winder and Michaelis, 2005).

According to various scientific reports, a wide variety of chemical compounds have been found in aircraft cabin air (Hunt and Space, 1994; Spengler et al. 1997). While studies have shown chemical pollutants in aircraft cabin air, only recently have a few studies identified TCPs

in cabin air during normal aircraft operations. Crump et al. (2011) and De Nola et al. (2011) both identified ToCP and CO in the cabin air supply during normal operations. Van Netten and Leung (2000) also identified TCPs and CO in cabin air during normal aircraft operations. In the civil aviation industry, synthetic jet engine oils contain additives that offer the best lubrication properties for jet engines. However, the usage of these oils may pose potential safety and health risks to air passengers and cabin crew.

### **2.2.1 Aircraft cabin air recirculation filters**

Technological advances in air filtration materials and design have ensured that aircraft cabin air recirculation filters maintain desirable air quality in aircraft cabins. Regardless, air passengers and crew are still exposed to many cabin contaminants and probably other unknown contaminants. An aircraft cabin air filter helps mitigate the health effects of airborne particulate pollutants by eliminating particulate pollutants from the recirculation air returned to the cabin environment, thereby improve the air quality in the cabin. According to Molhave (1991), exposure to VOCs, even at very low concentrations has been linked to a number of health problems, including upper respiratory irritation, neurological symptoms, and cancer. Thus, in aircraft cabins, air filtration reduces the environmental burden caused by airborne pollutant emissions from the cabin and outside air supply. To make sure the air supply in the aircraft cabin is safe, every filter is tested and rated when manufactured according to strict specifications. Aircraft cabin air filters remove bacteria and viruses at an efficiency greater than 99.999% (Harding, 1994). This means that the filters can protect the passengers and crew against the spread of microbes and viruses during flight. It also means that air purity, particularly for particulates, is high when air is supplied to cabin occupants.

The aircraft cabin air recirculation filters generally are made of fibrous materials, usually randomly arranged synthetic glass fibers that capture particulate matter or respirable aerosols using a combination of four filtration mechanisms, namely, inertial impaction, diffusion, interception, and sieving (Cooper and Alley, 2002; Michaelis and Loraine, 2005). The filters are manufactured in a variety of sizes and shapes to fit aircraft's ECS retrofit needs. Figure 2.1 shows some typical cabin air recirculation filters and the aircraft frame model in which they are used. Donaldson's HEPA cabin air recirculation filter for the Boeing 767-300 series has a label

containing important technical information including (a) a maximum resistance of 250 Pa (1.20 in. W.G) at 1500 CFM and (b) a maximum penetration of 0.10 % at 1500 CFM.



**Figure 2.1 Some HEPA cabin air recirculation filters approved by FAA for installation on various commercial aircrafts**

(a) Airbus: A318/A319/A320/A321 (b) Boeing 777-200, 777-300, 777-300ER (c) Boeing 737 and Boeing 757 models. (d) Boeing 767 models (e) Boeing 747-400 and (f) Charcoal filter: Boeing 767-model.

The filter medium is constructed from ultra-fine glass fibers intertwined to form a mesh structure held together with an organic binder. The filters are pleated to increase the surface area available for capturing particulates and to reduce the face velocity. The characteristics of the pleating are the length of pleat, distance between two pleats, and filtration area. Corrugated separators strengthen the filter pack and prevent the media from collapsing. The filter media is sealed to a rigid aluminum frame using an adhesive.

### **2.2.2 The standards for aircraft cabin air filters**

The performance of HEPA filters or their ability to reduce exposure to airborne particulate matter is defined by their efficiency. Every aircraft cabin air recirculation filter is tested and rated, so it delivers certifiable performance according to certain air quality standards. The Military Standard-282 Method 102.9.1 (1965) was the initial standard efficiency specification adopted by HEPA filter manufacturers for commercial aircraft, requiring the filters to capture 99.97% of 0.3  $\mu\text{m}$  particles. HEPA filters are also usually rated at 99.99% sodium flame test efficiency or the equivalent efficiency of 99.97% DOP (di-octyl phthalate) efficiency (Bull, 2008). The criterion that aerosol penetration for the HEPA filters should not exceed 0.03% (0.0003) for 0.3  $\mu\text{m}$  diameter particles represents the most difficult particle size to capture, i.e., the most penetrating particle size (MPPS) for a HEPA filter (Hinds, 2000). The diameter specification of 0.3  $\mu\text{m}$  corresponds to the MPPS. For aircraft cabin air recirculation filters, ASHRAE Standard 161 (2007) recommends a HEPA filter that meets or exceeds the requirements of Institute of Environmental Science and Technology IEST-RP-CC001.5 Filter Type "A", with a minimum efficiency of at least 99.97% on 0.30  $\mu\text{m}$  size particles. ASHRAE Standard 52.2-2007 recommends evaluating HEPA filters according to a minimum efficiency reporting value (MERV). A MERV is a rating for describing filter performance. For example, a filter MERV rating of 17 has an efficiency of nearly 100% when particles of 0.3  $\mu\text{m}$  size are considered. The European Comite de Normalization (CEN) has developed Standard EN 1822.1 (2009) for the classification and testing of HEPA and ultra-low penetration air (ULPA) filters, based on particle counting at the MPPS, which provides a minimum of 99.95% penetration efficiency for 0.4  $\mu\text{m}$  particles. To meet the U.S. EPA definition, HEPA cabin air recirculation filters must be 99.97% effective in capturing dust, vapors, bacteria, fungi and some viruses. A

study by Korves et al. (2011) has demonstrated that analysis of filters could characterize viruses in aircraft cabin air.

Filter manufacturers use HEPA filtration technology because of high air quality, capacity, and ability to satisfy aircraft cabin air supply requirements. However, stricter legislation has increased the demand for techniques to monitor bleed air. The concerns stem in part from unknown threshold levels of airborne particulate emissions formed from jet engine lubricating oils during smoke/fume incidents. These threats loom while regulations, standards, and procedures to manage them remain unspecific. Currently, the airline industry worldwide is actively seeking to develop innovative air quality monitoring techniques that would minimize the burden of smoke/fume incidents on cabin air quality. In fact, the impact of bleed air on cabin air quality depends on many variables: namely the conditions that promote incidents and the amount of aerosol emissions produced from the process. This means airlines need air quality monitoring solutions that meet stricter requirements of the air quality in cabin environment. To implement requirements for safety measures that can reduce the risk of smoke/fume incidents and enhance the level of protection for cabin occupants, it is necessary to understand the threshold levels for jet engine oil contaminants in cabin air supply. Screening techniques like analysis of cabin air recirculation filters could be indispensable in detecting jet engine oil contaminants in cabin air if they can produce reliable results. Currently, no standard method exists for assessing cabin air quality using analysis of cabin air filters installed in aircrafts, and no information has been published on the effectiveness of such analysis in detecting sources of air contamination. With cabin air recirculation filters as the only air-cleaning device fitted to an aircraft's ECS, these filters are therefore the focus for investigation of air quality in airplane cabins. Analyses of used cabin recirculation filters may answer questions about how the cabin air quality parameters change during smoke/fume incidents.

In this study, samples of clean and used cabin air recirculation filters were characterized by FESEM, Nova<sup>TM</sup> NanoSEM model 430 equipped with EDS, Oxford Instruments INCA 350 with 80 mm<sup>2</sup> X-Max SDD detector. The FESEM/EDS is a high powered microscope with an emission spectrometer, both of which are useful for an investigation of surface phenomena (Nadeau and Herguth, 2004). The FESEM/EDS technique can also provide high-quality morphological images showing the features of contaminants and the spectra of the elemental constituents present on the surface of a sample (Stellmack, 2010). In this study, used and incident

aircraft cabin air recirculation filters were examined to determine if jet engine oil contamination signatures could be identified. The study also addressed effective filter analytical options for monitoring incidents by testing clean cabin filters exposed to Mobil Jet Oil II. Mobil Jet Oil II was used in the laboratory tests because it is the most widely used jet engine oil (B. W. Jones, personal communication). The aim was to determine whether elements in jet engine lubricating oil and deposits on used filters could be linked.

## **2.3 Materials and Methods**

### **2.3.1 Filter sampling**

Filter sample preparation was a very important step in analyzing aircraft cabin air recirculation filters because it could affect the accuracy of the data gathered during analysis. All the necessary steps for the preparation of the filter samples were conducted in the clean room at the KSU Institute for Environmental Research (IER). The air circulation system for this room is fitted with both HEPA and electrostatic filters that keep concentrations of airborne particulate to below 2648 counts/m<sup>3</sup>. Before the filter sample preparation began, the air-circulation system in the room was turned on and left running for about 10 minutes to reach a steady state. The boxes containing the filters were moved from the closet into the clean room one at a time. After a box containing a filter was moved into the clean room, it was cut open to remove a filter, which was always wrapped in a plastic bag. The filter was then placed on a table covered with aluminum foil. At this point, the person performing the sampling put on sterilized plastic gloves and a dust mask. All the tools used in disassembling the filters and cutting out specimens were wiped with isopropyl alcohol. This sterilization step was included because filter specimens were also collected for biological analysis (Korves et al. 2011). The outer aluminum casing was cut with a sheet metal snip to separate it from the filter. The use of the clean room and sterilized equipment throughout the sampling process ensured that cross-contamination was highly unlikely. The sequence of operations used for preparing filter samples by FESEM/EDS analysis is shown in Figure 2.2 below. For the FESEM/EDS measurements, approximately two 2.5 cm square samples were cut from each filter and placed in a zip-lock plastic bag measuring 18 × 24 in. Each zip-lock bag was labeled with a filter ID for future identification.

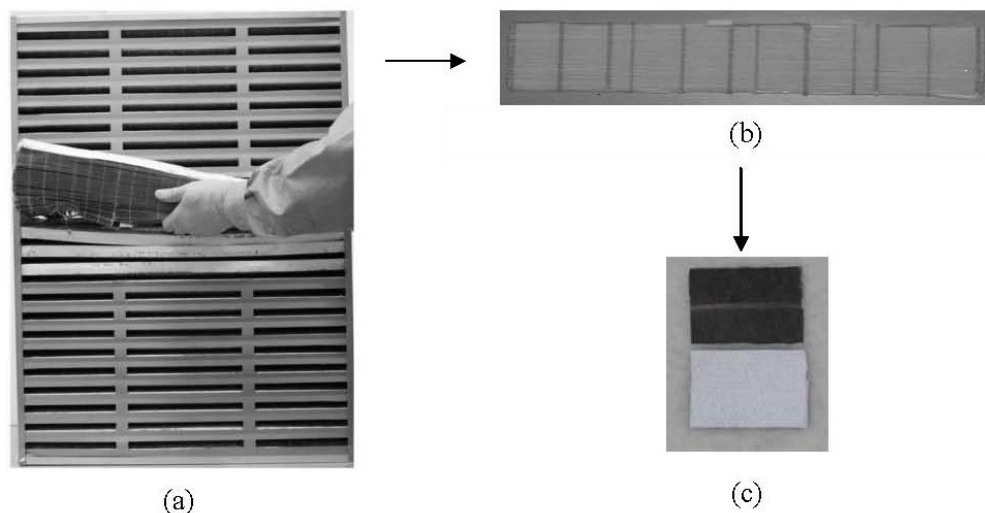


**Figure 2.2 (a) Filter sampling process (b) Filter panel (c) Filter sample for FESEM/EDS analysis**

The zip-lock bags containing the filter samples were then shipped for FESEM/EDS analysis. Samples from clean filters and clean filter samples spiked with Mobil Jet Oil II were also analyzed with the FESEM/EDS method and their spectra examined. The clean filters used in the study were acquired from three major aircraft cabin air recirculation filter manufacturers: Keddeg, Pall, and Donaldson. The study used aircraft cabin air recirculation filters came from several major US airlines and were collected over two years. Some of the filters were provided directly by airlines, and some were received via third parties without the source airline being identified. In total, 110 used and 90 incident filters were analyzed.

### **2.3.2 Experimental protocol**

From each specimen, a 2.0-mm diameter trephine was used to cut filter samples, which were then placed on an aluminum stub with carbon adhesive to hold samples on the stage and help ground them. A Nova<sup>TM</sup> NanoSEM model 430 from FEI Company, FESEM equipped with an Oxford X-Max large area analytical EDS silicon drift detector (SDD) 80 mm<sup>2</sup> was used to determine the elemental composition of filter samples. Standardized operating conditions were set at 18 kV accelerating voltage, spot size 4.5 (0.74 nA beam current), 5.0 – 6.5 mm working distance, and the sample chamber under vacuum ( $10^{-4}$  –  $10^{-5}$  torr). Quant optimization was performed on the EDS system using copper (Cu) as standard. These parameters were determined to produce accuracy of quantification of lighter and heavier elements of interest. In addition,

these parameters did not require extensive sample preparation or preparatory procedures that might have damaged the sample or altered the spectra.

The area to be analyzed had a horizontal field width (HFW) = 149  $\mu\text{m}$  square fields ( $22,201 \mu\text{m}^2$ ) at  $\times 1000$  magnification. Standard operating conditions produced X-ray count rates between 1–3 kcps and dead times less than 3%. The scanning duration was 2 minutes. The FESEM/EDS was also used to investigate the changes induced in clean filter surfaces by sampling air containing pyrolyzed Mobil Jet Oil II using a bleed air simulator. Clean filters spiked with Mobil Jet Oil II and dried under vacuum at  $40^\circ\text{C}$  (to possibly make volatile components evaporate) were also subjected to detailed FESEM/EDS analysis to identify contaminants from jet oil. The filter surface microstructure and microelement analysis of clean, dirty, and incident aircraft HEPA cabin air recirculation filters also were all analyzed by this methodology. The filter surface characterization, quantitative results were obtained using virtual pack standards supplied with the INCA 350 software. A spectrum of the energy versus relative counts of the detected X-rays was obtained and evaluated for qualitative and quantitative determinations of the elements present on the sample.

The phasemap tool in the INCA 350 software system was used to identify elemental phases with ternary element plots of specific pixel information from montaged X-ray maps. The procedure for element map acquisition involved the use of so-called ternary phase diagrams. The software generated elemental maps of relative concentrations for the elements specified by the user. The element information embedded in each image pixel was rearranged so that regions of similar (ternary) composition could be determined in the phase diagram. Superposition of images obtained from different ternary phase diagrams were represented as a false color map that yielded a phase map. Thus, a realistic reconstruction of elemental distribution in the cross-sectioned sample could be achieved, and the obtained elemental map was mixed into the scanning electron image. Each filter was given a unique, specific identification. The images of the surface characteristics of used filters with magnifications of 500, 1000, and 4000 were acquired by FESEM for comparative analysis. Figure 2.3 shows a picture of Nova<sup>TM</sup> NanoSEM model 430 used in this study.





**Figure 2.3 Nova™ NanoSEM model 430 FESEM/EDS System**

Aside from obtaining atomic weight percentages and elemental distributions, filter samples were also viewed under the FESEM at 500x, 1000x, and 5000x magnifications. Excel software was used to calculate the mean atomic weight percentage levels by averaging the values obtained from six different square fields ( $22,201 \mu\text{m}^2$ ) analyzed.

### ***2.3.3 Statistical procedures used in data analysis to identify filter contaminant elements***

The data obtained from analyzing both used and incident filters were subjected to statistical analysis using SAS Procedures. All analyses were done with the SAS system for Windows (release 9.2; SAS Institute, Cary, NC). This study analyzed data from a total of 200 cabin air recirculation filters considered a representative sample of HEPA filters used in commercial aircrafts. The analysis considered 99 used and 34 incident filters. Using various SAS codes, descriptive statistics of identified jet engine oil contaminant elements on both groups of filters were calculated with PROC UNIVARIATE and PROC CORR procedures. The PROC TTEST procedure was used to test for the difference between the two categories of filters. Meanwhile, both PROC GLM and PROC MIXED procedures were used for analysis of variance (ANOVA). The study analyzed samples from used and incident filters that fit seven different aircraft models as shown in Table 2-1.

**Table 2-1 Distribution of used and incident filters by manufacturer and type of aircraft**

Filter manufacturer	Used filters							
	Type of aircraft							
	A320	MD-80	A340	B737	B767	B777	B747	Total
Donaldson	0	0	0	0	0	10	9	110
Keddeg	12	0	0	8	1	17	2	
Pall	0	0	0	4	7	21	2	
Puralator	0	0	0	0	0	17	0	
Filter manufacturer	Incident filters							
	Type of aircraft							
	A320	MD-80	A330	B737	B767	B777	B747	Total
Donaldson	0	0	0	0	0	3	0	90
Keddeg	28	0	0	15	0	0	0	
Pall	2	4	2	16	16	4	0	
Puralator	0	0	0	0	0	0	0	

N.B. Only 133 filters tabulated in appendix A4 (pp. 228 – 231): SAS output were considered in this study.

## 2.4 Analysis, Results and Discussion

### 2.4.1 Data analysis

The analysis of the FESEM/EDS data involved examining distribution patterns of jet engine oil contaminant elements and analyzing photomicrographs to determine the unique features caused by jet engine oil contamination on filters. The EDS analysis provided results in units of weight percent for the atomic elements present on the surface of filter debris. The data in appendices A1 and A2 include the atomic percentage values of elements detected by EDS analysis for every spot analyzed on used and incident the filters. In both the used and incident filters, more than 20 elements were present in a wide variety of atomic weight percentage levels. The PROC UNIVARIATE procedure was used to test normality for distribution of jet engine oil contaminant elements in used and incident filters. The SAS PROC UNIVARIATE code used to

determine both the descriptive statistics and distribution of phosphorus (P) was written as follows:

```

data pdata;
  label conc = 'Phosphorus % atomic weight';
  input conc @@;
  Phosphorus = log(conc);
  datalines;

(data arranged in 9 rows and 11 columns)
;
run;
title 'Distribution of Phosphorus in Used Aircraft Filters';
proc univariate data=pdata normal cbasic alpha = 0.05;
  var Phosphorus;
  probplot Phosphorus;
  Histogram / Normal (COLOR=red FILL)
    vaxis = axis1
    name = 'phist';
  inset n mean(5.3) std = 'Std Dev' (5.3) skewness(5.3)
    / pos = ne header = 'Summary Statistics';
  axis label = (a=90 r=0);
run;

```

The phosphorus data were converted to log by program command on the fourth line in the above program. The p-values for the four methods (Shapiro-Wilk, Kolmogorov-Smirnov, Cramer-von Mises, and Anderson-Darling) were calculated by the program. Meanwhile the distributions of S and Br were determined without log conversion.

The SAS PROC CORR procedure (Pearson Correlation) tested for the probability of observing a correlation coefficient or one more extreme under the null hypothesis so that the correlation ( $\rho$ ) is 0. The SAS code for the correlation of jet engine oil contaminant elements on filters was written as follows with the appropriate data for used and incident filters:

```

data corrpsb;
  input Phosphorus Sulfur Bromine;
  datalines;
(data arranged in columns)
;
run;
title 'Calculation and Test of Correlations, 95% CI for Used Filters';
ods output FisherPearsonCorr=corr;
proc corr data=corrpsb Fisher (biasadj=no);
  var Phosphorus Sulfur Bromine;
run;
ods html;
ods graphics on;
proc corr data=corrpsb plots=scatter(alpha=.2 0.3);
  var Phosphorus Sulfur Bromine;
run;

```

```
ods graphics off;
ods html close;
```

The PROC TTEST procedure was used to test for the equality of means of two sets of the same variable from used and incident filters.

```
Options nodate;
data filter (drop=Used);
input Category$ @;
do used=1 to 99;
input Phosphorus @;
output;
end;
datalines;
.....
;
run;
proc ttest data=filter Alpha=.05;
class category;
var Phosphorus;
run;
```

The PROC GML and PROC MIXED procedures were used for the analysis of variance (ANOVA) of mean values of identified contaminant elements from jet engine oil. The PROC GML procedure tested whether the set of data subjected to analysis had the same variability, i.e., whether the variance in the observation was the same. The PROC MIXED procedure was used with a repeated statement so that separate variance for each aircraft model could be calculated. The procedure included a Satterthwaite denominator degree of freedom adjustment. Appropriate SAS procedures were also used to graphically represent variances and spread of the data by box plots and scatter plots.

```
options nodate;
data filter;
input Filter_ID $ Aircraft $ Phosphorus Sulfur Bromine Category $;
datalines;
. . . . .(data in appendix A1)
;
run;
proc print data=filter;
run;
proc sort data=filter;
by category aircraft;
proc boxplot data=filter;
by category;

plot Phosphorus*aircraft;
run;
proc boxplot data=filter;
```

```

    by category;
    plot Sulfur*aircraft;
run;
proc boxplot data=filter;
    by category;
    plot Bromine*aircraft;
run;
proc sort;
    by category;
run;
*Comparison of Used vs Incident;
proc glm data=filter;
    class category;
    model Phosphorus Sulfur Bromine = category/solution ss3;
    lsmeans category/pdiff stderr cl adjust=bon;
run;
quit;
proc sort data=filter;
    by category;
run;
proc glm data=filter;
    by category;
    class aircraft;
    model Phosphorus Sulfur Bromine = Aircraft/solution ss3;
    means aircraft/hovtest=bartlett hovtest=levene(type=abs)
        hovtest=BF hovtest=obrien(w=0.5) Welch;
    lsmeans Aircraft/pdiff stderr cl adjust=bon;
run;
quit;
symbol color=red value=circle;
symbol2 color=black;

*scatterplots to visualize variability of aircraft;
proc gplot data=filter;
    plot Phosphorus*aircraft=category;
run;
proc gplot data=filter;
    plot Sulfur*aircraft=category;
run;
proc gplot data=filter;
    plot Bromine*aircraft=category;
run;
proc MIXED data=filter;
    by category;
    class aircraft;
    model Phosphorus = Aircraft/ddfm=satterth;
    repeated/group=aircraft;
    lsmeans aircraft/pdiff cl adjust=bon;
run;
quit;
proc MIXED data=filter;
    by category;
    class aircraft;
    model Sulfur = Aircraft/ddfm=satterth;
    repeated/group=aircraft;
    lsmeans aircraft/pdiff cl adjust=bon;
run;

```

```

quit;
proc MIXED data=filter;
  by category;
  class aircraft;
  model Bromine = Aircraft/ddfm=satterth;
  repeated/group=aircraft;
  lsmeans aircraft/pdiff cl adjust=bon;
run;
quit;

```

The following statement in the SAS code PROC GLM procedure:

```

model Phosphorus Sulfur Bromine = Aircraft/solution ss3;
means aircraft/hovtest=bartlett hovtest=levene(type=abs)
      hovtest=BF hovtest=obrien(w=0.5) Welch;

```

enables the program to perform four tests of homogeneity for each identified contaminant element: Levene's, O'Brien's, Brown and Forsythe's, Bartlett's and Welch's tests. The procedure tested for equal variances, i.e., whether the variances of means of one type of contaminant in different aircrafts were equal. In pairwise comparisons, the "adjust=bon" in the code accounted for the differences in sample sizes and produced Bonferroni adjusted p-values (Adj P).

The statement "model Phosphorus=Aircraft/ddfm=satterth; model Phosphorus = Aircraft/ddfm=satterth;" in PROC MIXED procedure allowed the program to calculate lsmeans and standard error for each aircraft model and adjusted for unequal variances. This approach averaged data points obtained from each filter and focused mainly on three identified contaminants: phosphorous, bromine, and sulfur.

## 2.4.2 Results and discussion

### 2.4.2.1 EDS assessment

The data revealed that all of the filters, regardless of manufacturer, clean, spiked with oil, or only used had common elements in different proportions. Each filter set produced different results, and the analyses of spots yielded different results with varying atomic weight of elements. The common elements are oxygen (O<sub>2</sub>), sodium (Na), magnesium (Mg), aluminum (Al), silicon (Si), chlorine (Cl), potassium (K), calcium (Ca), zinc (Zn), and barium (Ba). The identified elements in clean, clean oil-spiked, used, and incident filters are listed in Tables 2.3, 2.4, 2.5, and 2.6 and as a combined used and incident filter listing in Appendix A1. The units are given in percentage of atomic weight values for each element. Although more than 20 elements

were identified in both used and incident filters, only three were identified as markers for jet engine oil contamination analysis after comparison with elements obtained from clean filters.

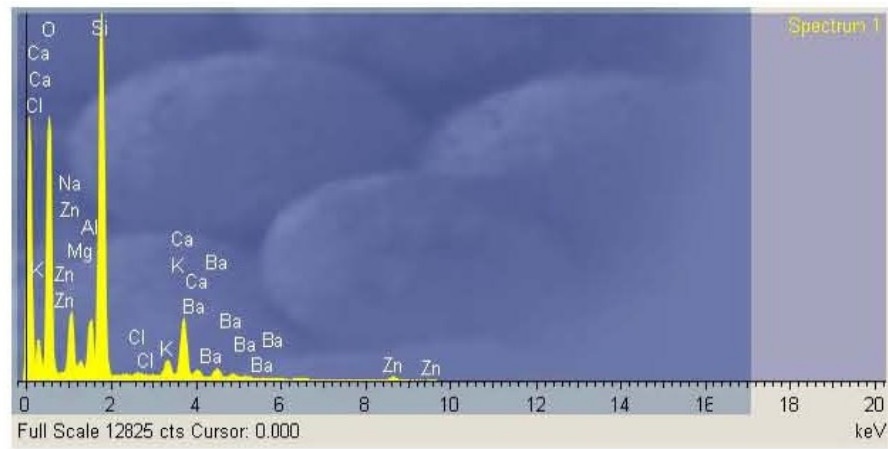
#### 2.4.2.1.1 *Distribution of elements in clean filters*

Table 2-2 shows variation of mean, standard variation of elements in clean filters samples from three filter manufacturers. The elemental composition of clean filters was computed from six different observations or spots analyzed from two samples obtained from a clean filter set. The elements observed in different proportions were O<sub>2</sub>, Na, Mg, Al, Si, Cl, K, Ca, Zn, and Ba. The top row in Figure 2.4 shows elements present in the clean filters from Pall Aerospace Co., Keddeg Co., and Donaldson, and the bottom row shows corresponding elemental distributions. From Figure 2.4 it is evident that the EDS and qualitative analyses of clean filters had higher percentages of O<sub>2</sub> and Si, respectively. The EDS results are convincing evidence that Si and O<sub>2</sub> are the main elements in clean filters. The finding suggests that clean filters are mainly manufactured from silica (SiO<sub>2</sub>). The spectra data show high oxygen content, which is most likely from SiO<sub>2</sub>.

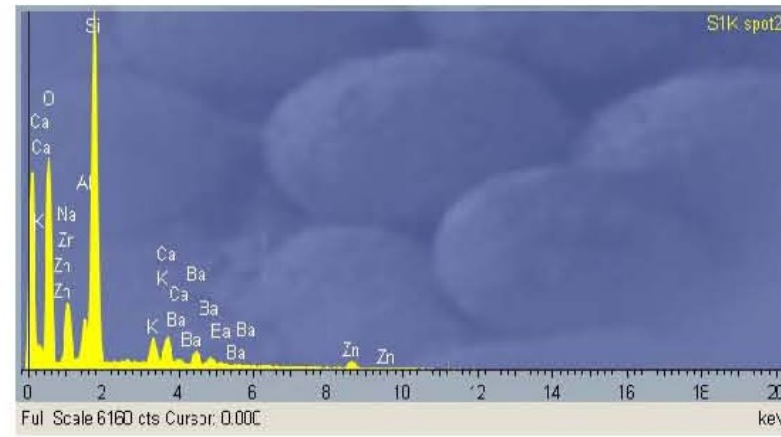
**Table 2-2 Elements identified in clean filter samples from (a) Pall Aerospace Inc., (b) Keddeg Co. and (c) Donaldson Co.**

(a) Filter from Pall Aerospace Corporation					
Element	Number of observations	Mean atomic Weight %	Std. Dev.	Minimum	Maximum
Oxygen	6	69.9467	1.0550	67.8900	70.9300
Sodium	6	5.2400	0.6490	4.3800	5.9200
Magnesium	6	0.6750	0.0675	0.6200	0.7900
Aluminum	6	2.18500	0.2236	1.9600	2.5200
Silica	6	17.1750	0.4547	16.5400	17.8200
Chlorine	6	0.0750	0.0867	0.0000	0.2000
Potassium	6	0.8900	0.0919	0.7900	1.0500
Calcium	6	2.4083	0.5222	1.7700	2.9600
Zinc	6	0.8567	0.3058	0.6300	1.4700
Barium	6	0.5500	0.1101	0.4700	0.7700
(b) Filter from Keddeg Company					
Element	Number of observations	Mean atomic Weight %	Std. Dev	Minimum	Maximum
Oxygen	6	68.2000	0.6348	67.3800	69.3100
Sodium	6	5.6917	0.3394	5.1200	6.0300
Magnesium	6	0.0767	0.1878	0.0000	0.4600
Aluminum	6	2.2917	0.1619	2.1200	2.5400
Silica	6	19.0167	0.5260	18.1800	19.5900
Potassium	6	1.1133	0.1021	0.9700	1.2300
Calcium	6	1.6650	0.3473	1.3500	2.2100
Zinc	6	1.2083	0.1292	1.0300	1.3300
Barium	6	0.7350	0.0950	0.6300	0.8600
(c) Filter from Donaldson Company					
Element	Number of observations	Mean atomic Weight %	Std. Dev.	Minimum	Maximum
Oxygen	6	68.2217	1.4584	65.9400	70.1200
Sodium	6	5.8433	0.2041	5.6400	6.1600
Aluminum	6	2.2917	0.1270	2.1100	2.4700
Silica	6	18.9033	0.9346	17.7600	20.4000
Potassium	6	1.1717	0.1470	0.9800	1.4000
Calcium	6	1.5633	0.1711	1.3600	1.7800
Zinc	6	1.2283	0.2038	0.9900	1.5700
Barium	6	0.7767	0.1011	0.6700	0.9300

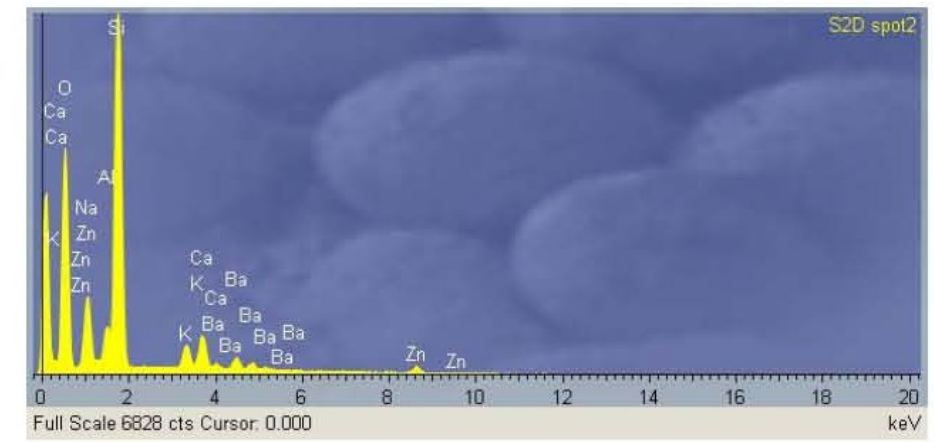




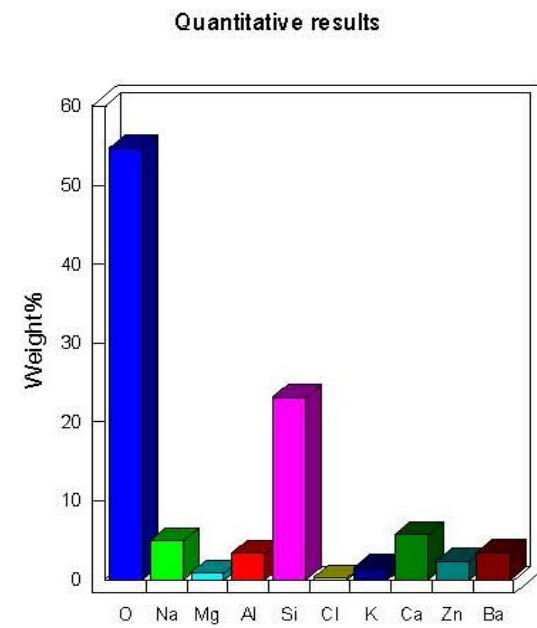
(a)



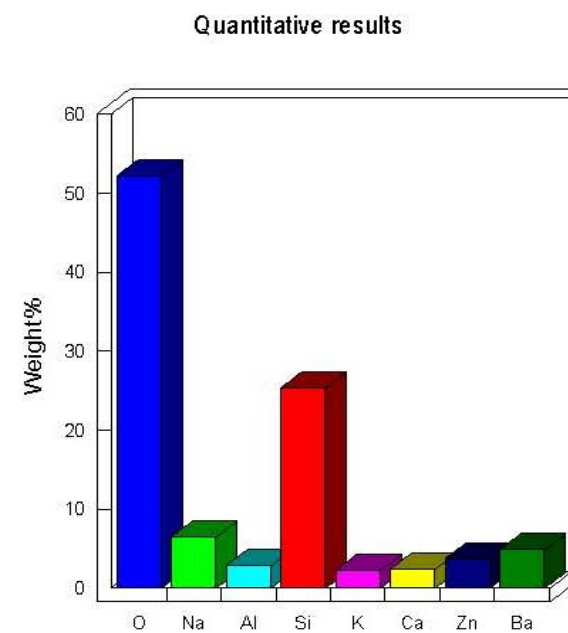
(b)



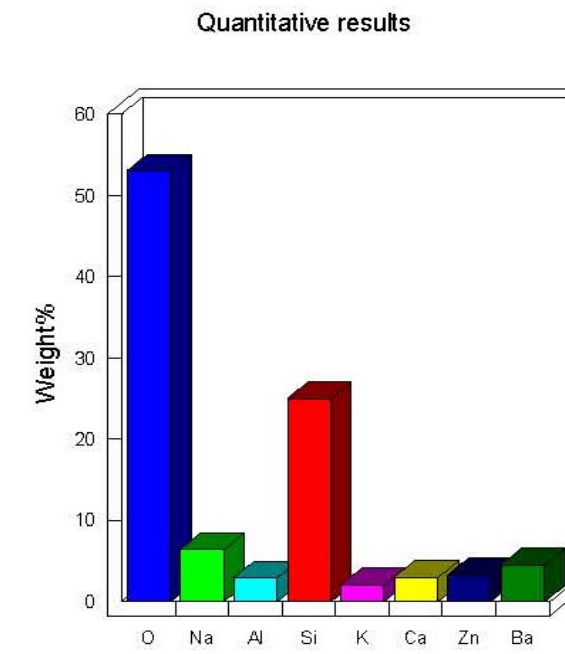
(c)



(d)



(e)



(f)

Figure 2.4 Top row – Atomic adsorption spectrum (EDS) of clean HEPA filter media manufactured by (a) Pall Aerospace Co., (b) Keddeg Co., and (c) Donaldson and bottom row – their corresponding qualitative composition of elements shown as (d), (e) and (f) respectively

#### 2.4.2.1.2 *Distribution of elements in clean filters spiked with Mobil Jet Oil II*

An analysis of the clean filter spiked with Mobil Jet Oil II showed that carbon (C), sulfur (S), phosphorus (P), and bromine (Br) were introduced by adding oil to the filter. The mean atomic weight percentage values for other elements decreased compared to clean filters. The elemental distribution in clean filter spiked with jet engine oil indicates that the elements were present in both the filter and Mobil Jet Oil II. The new elements that altered the elemental distribution are P, S, and Br. Table 2-3 shows the distribution of elements in clean filters spiked with Mobil Jet Oil II. When the clean filter and spiked filter samples are compared, the trails left by Mobil Jet Oil II on cabin air filters are clear and consists of C, P, S, and Br. Carbon with a mean atomic weight percentage value of 60.4% is the main constituent element in the clean filter samples that were spiked with jet oil.

**Table 2-3 Elements identified in clean filter media spiked with Mobil Jet Oil II**

Element	Number of observations	Mean atomic weight %	Std. Dev.	Minimum	Maximum
Carbon	6	60.4233	7.9906	44.8400	65.3700
Oxygen	6	33.7533	5.5572	30.0500	44.5400
Sodium	6	1.0283	0.4372	0.6800	1.8500
Aluminum	6	0.3600	0.1728	0.1900	0.6700
Silica	6	3.5117	1.4797	2.5200	6.3900
Phosphorus	6	0.0467	0.0121	0.0300	0.0600
Sulfur	6	0.0150	0.0084	0.0100	0.0300
Potassium	6	0.2200	0.0121	0.1500	0.3900
Calcium	6	0.2650	0.1537	0.1300	0.1500
Zinc	6	0.1783	0.0924	0.1000	0.5300
Bromine	6	0.0850	0.0517	0.0000	0.1500
Barium	6	0.1233	0.0532	0.0800	0.2200

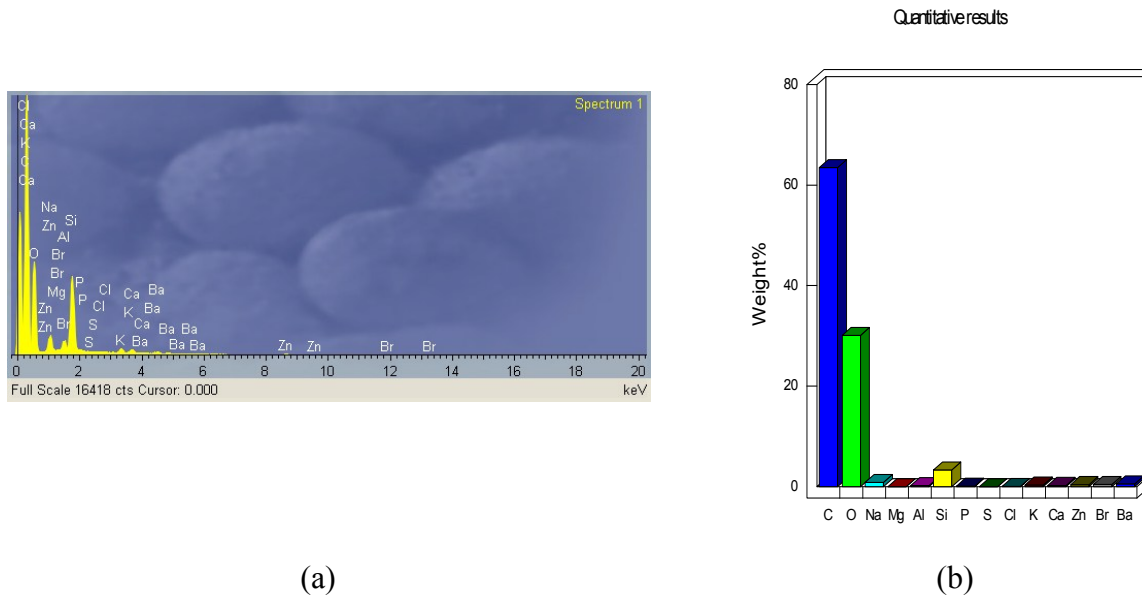


**Figure 2.5 (a) EDS spectrum (b) Elemental distribution of clean filter spiked with Mobil Jet Oil II**

#### 2.4.2.1.3 *The distribution of elements in used and incident filters*

Based on the above results, C, P, S, and Br are potential markers for oil on the cabin filters. Carbon was not considered further because it is known to have multiple, significant sources otherwise present on aircraft filters (e.g., lint, human skin flakes, etc.). This leaves P, S, and Br as potential markers. Based on the investigation of the 110 used filters across seven aircraft models, the study showed that 100 percent of filters had traces of these three elements. Likewise, nearly 100 percent of the incident filters also have these elements present. The mean (range) atomic weight percent of P concentrations for used filters was 0.052 (0.007, 0.144) and for incident filters 0.032 (0.005, 0.080). Figures 2.6 and 2.7 depict the variability of filter contaminant elements from jet engine oil. In contrast, the average P levels were slightly lower in incident filters. The differences in variability could be due to the short periods that incident filters might have remained installed in the aircraft because incident filters were removed from the aircraft soon after an incident was suspected to have occurred.

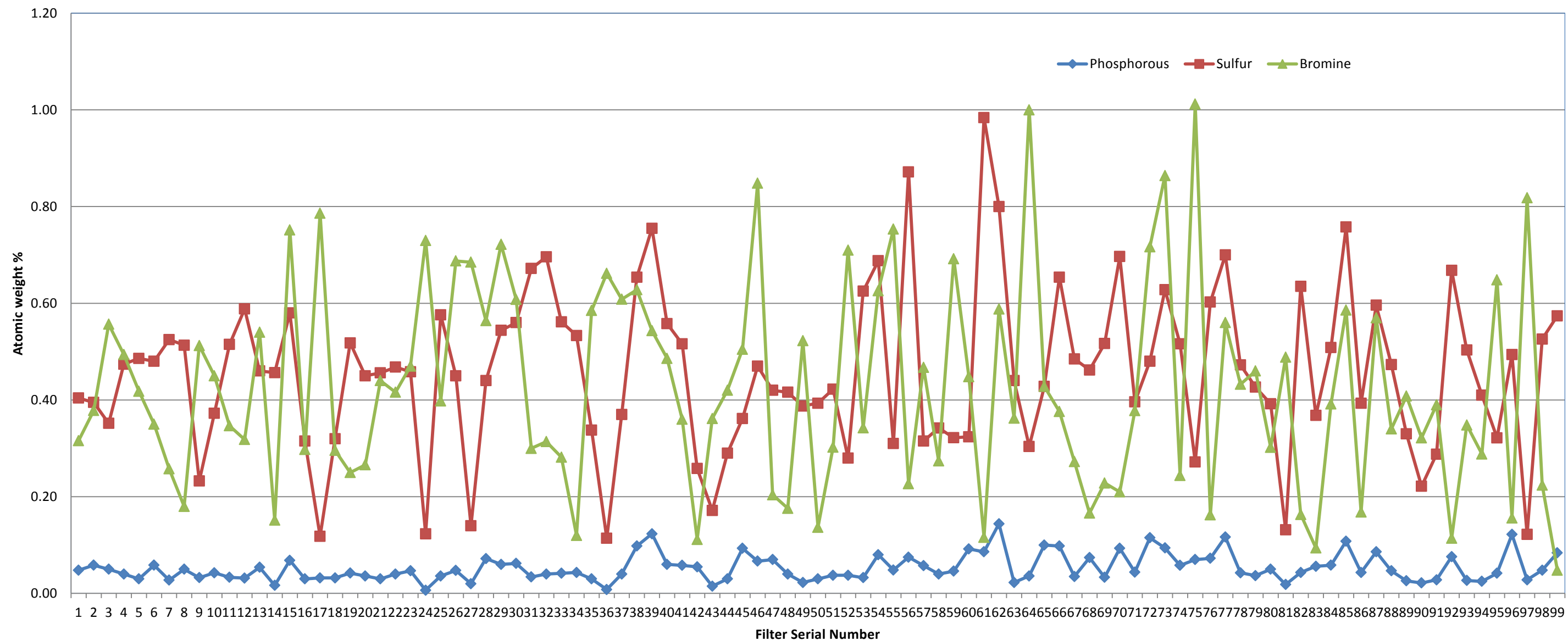


Figure 2.6 Variability of phosphorus, sulfur and bromine in used filters

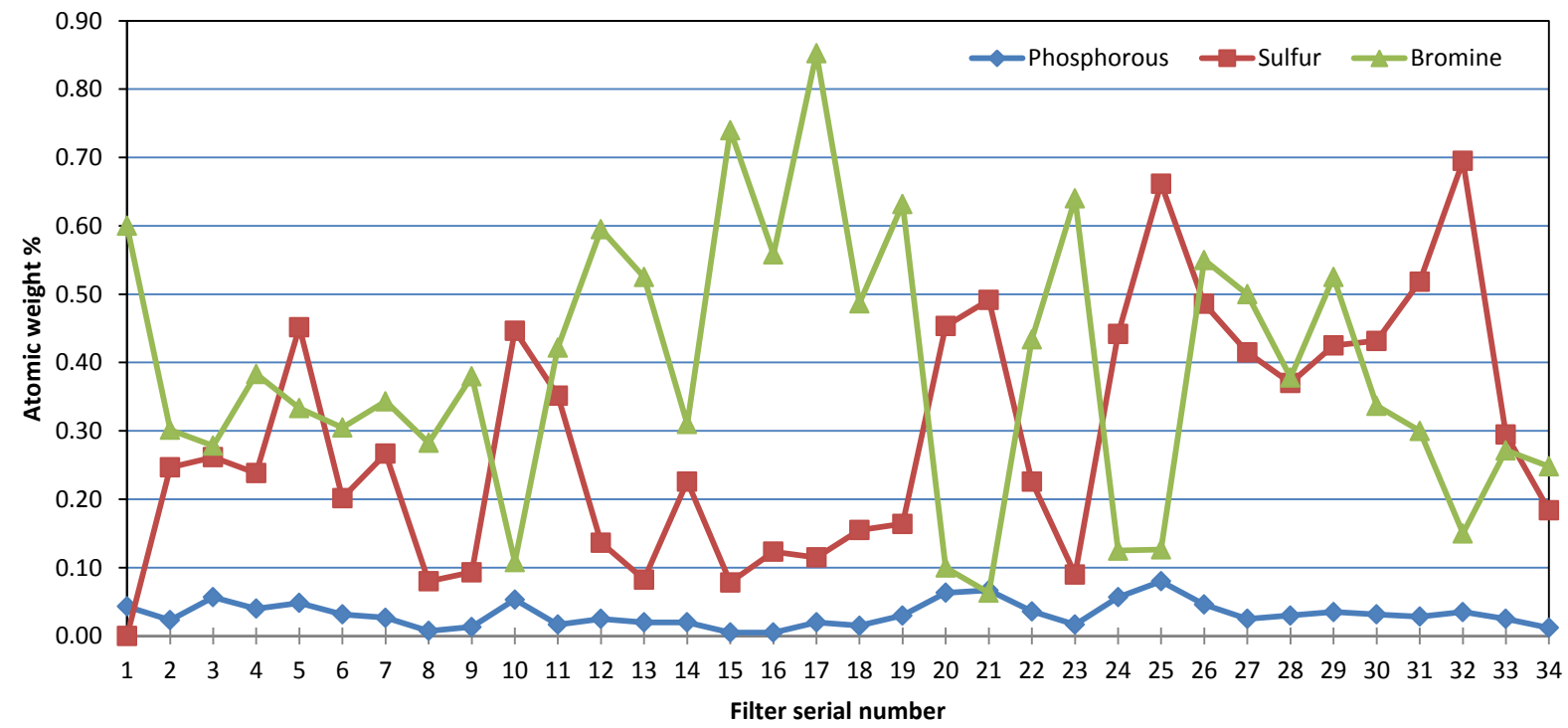
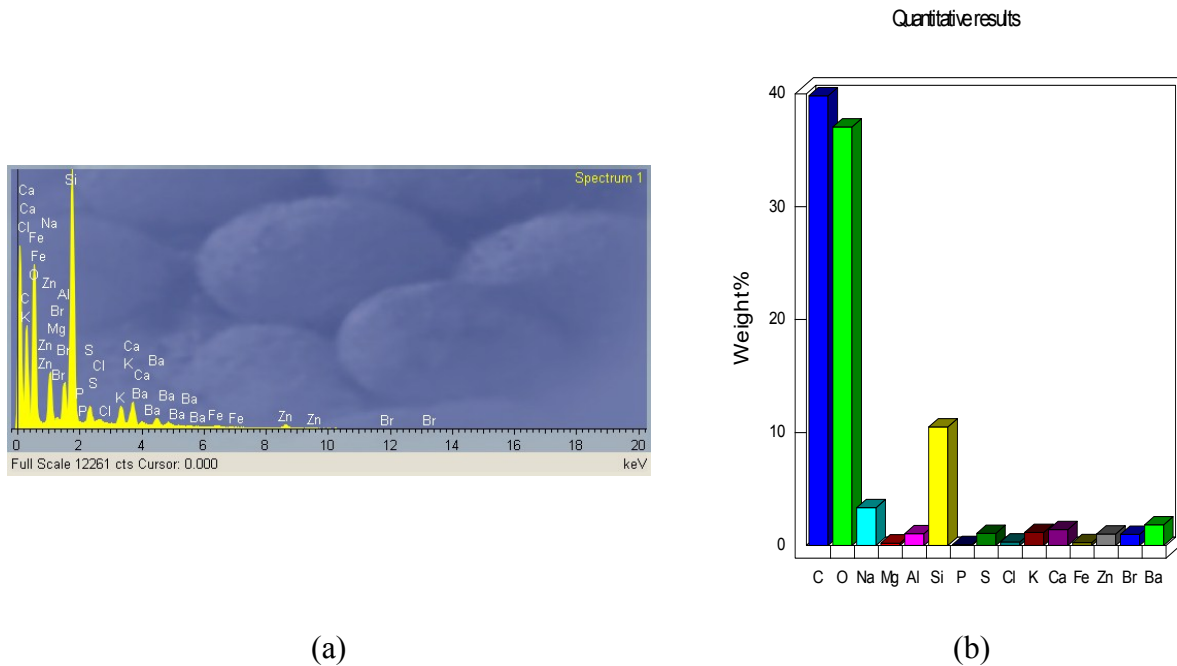


Figure 2.7 Variability of phosphorus, sulfur and bromine in incident filters



**Figure 2.8 (a) EDS Spectrum and (b) elemental composition of used filter ID-9RZMC2**

Figures 2.8 (a) and (b) above and the data in appendices A1 and A2 show that C and O<sub>2</sub> make up more than 94.0% of the elements present in the used and incident filters. Of the 99 used filters investigated, one filter had traces of arsenic. Other elements that showed up as traces in some filters included: cesium, titanium, lead, and chromium. However, data sets for the clean, spiked, used, and incident filters clearly identified P, S, and Br as potential markers for jet engine oil contamination and showed that their levels were detectable.

2.4.2.1.4 *Statistical analysis of identified contaminant elements in used and incident filters:*  
*Results of first approach*

**Table 2-4 Summarized descriptive statistics of normality test results for elemental contaminants from Mobil Jet Oil II identified in used and incident filters**

<b>Used Filters (99)</b>						
Element	Method of Test for Normality	p-value	Mean weight %	Std. Dev.	Maximum	Minimum
Phosphorus	Shapiro-Wilk	0.5193	-3.0885 (0.0524)	0.5517 (0.02778)	(0.0067)	(0.1440)
	Kolmogorov-Smirnov	> 0.1500				
	Cramer-von Mises	0.2500				
	Anderson-Darling	0.2500				
Sulfur	Shapiro-Wilk	0.2933	0.4564	0.1663	0.1140	0.9840
	Kolmogorov-Smirnov	> 0.1500				
	Cramer-von Mises	0.2500				
	Anderson-Darling	0.2500				
Bromine	Shapiro-Wilk	0.0246	0.4253	0.2127	0.4800	1.0120
	Kolmogorov-Smirnov	0.1500				
	Cramer-von Mises	0.0792				
	Anderson-Darling	0.0628				
<b>Incident Filters (34)</b>						
Phosphorus	Shapiro-Wilk	0.0936	-1.3921 (0.0320)	0.6580 (0.0184)	(0.0500)	(0.0800)
	Kolmogorov-Smirnov	0.1500				
	Cramer-von Mises	0.2500				
	Anderson-Darling	0.2118				
Sulfur	Shapiro-Wilk	0.1129	0.2913	0.1777	0.0000	0.6950
	Kolmogorov-Smirnov	> 0.1500				
	Cramer-von Mises	0.0985				
	Anderson-Darling	0.0948				
Bromine	Shapiro-Wilk	0.5309	0.3878	0.1924	0.0633	0.8525
	Kolmogorov-Smirnov	0.5309				
	Cramer-von Mises	>0.1500				
	Anderson-Darling	>0.2500				

N.B: Minus numbers are log<sub>10</sub> of values of P.

The p-values for normality test from the SAS code PROC UNIVARIATE were used to determine the distribution of P on used and incident filters as shown in Table 2-4. All the p-values for normality tests are greater than 0.05. There was no significant evidence for rejecting the assumption of normality. Therefore, the computed test statistic for distribution of P supported the hypothesis of normality. However two outliers in data distribution were omitted.

The output of PROC CORR procedure:

Calculation and Test of Correlations, 95% CI for Used Filters

The CORR Procedure

Pearson Correlation Coefficients, N = 99

Prob > |r| under H0: Rho=0

	Phosphorus	Sulfur	Bromine
Phosphorus	1.00000	0.58591	0.07262
Sulfur	0.58591	1.00000	-0.28531
Bromine	0.07262	-0.28531	1.00000
		<.0001	0.4750
		<.0001	0.0042
		0.4750	0.0042

Calculation and Test of Correlations, 95% CI for Incident Filters

The CORR Procedure

Pearson Correlation Coefficients, N = 34

Prob > |r| under H0: Rho=0

	Phosphorus	Sulfur	Bromine
Phosphorus	1.00000	0.65239	-0.56459
Sulfur	0.65239	1.00000	-0.62509
Bromine	-0.56459	-0.62509	1.00000
		<.0001	0.0005
		<.0001	<.0001
		0.0005	<.0001

The Pearson correlation procedure was used to calculate the correlation coefficients and prints the entire correlation matrix, which includes p-values as well as descriptive statistics. The p-values obtained by running SAS code PROC CORR procedure for used filters showed some significant levels of correlation between potential marker elements. They were as follows: P versus S is significant ( $r = 0.65239$ ;  $p\text{-value} < 0.0001$ ); S versus Br is significant ( $r = 0.63509$ ;  $p\text{-value} < 0.0001$ ). But the correlation for P versus Br was not significant ( $r = -0.56459$ , and  $p\text{-value} < 0.0005$ ). On the other hand, for incident filters, P versus S was significant ( $r = 0.58591$ , and  $p\text{-value} < 0.0001$ ), and S versus Br was significantly correlated ( $r = -0.28531$ , and  $p\text{-value} = 0.0042$ ). However, P versus Br was not significantly correlated ( $r = 0.07262$ , and  $p\text{-value} = 0.4750$ ). A comparison of the p-values for used and incident filters suggested that contaminant elements in the used filters were more highly correlated than were in the incident filters.



The output of the PROC TTEST procedure is shown below:

Variable: Phosphorus						
Category	N	Mean	Std Dev	Std Err	Minimum	Maximum
Incident	34	0.0320	0.0184	0.00315	0.00500	0.0800
Used	99	0.0524	0.0278	0.00280	0.00670	0.1440
Diff (1-2)		-0.0204	0.0258	0.00512		

Category	Method	Mean	95% CL Mean		Std Dev	95% CL Std Dev	
Incident		0.0320	0.0256	0.0384	0.0184	0.0148	0.0242
Used		0.0524	0.0469	0.0579	0.0278	0.0244	0.0323
Diff (1-2)	Pooled	-0.0204	-0.0305	-0.0103	0.0258	0.0230	0.0293
Diff (1-2)	Satterthwaite	-0.0204	-0.0288	-0.0120			

Method	Variances	DF	t Value	Pr >  t
Pooled	Equal	131	-3.98	0.0001
Satterthwaite	Unequal	87.29	-4.84	<.0001

Equality of Variances				
Method	Num DF	Den DF	F Value	Pr > F
Folded F	98	33	2.30	0.0080

The SAS code for PROC TTEST procedure above shows that the means of used and incident filters are not equal (p-value = 0.0001). Therefore, the Satterthwaite method for testing of inequality was considered. The Folded F test had a p-value = 0.0080, suggesting that the inequality of variances in means for the used and incident filters is statistically significant at the 10% level. The PROC GLM procedure was used to perform ANOVA by using a pairwise comparison of means, standard deviations, and confidence intervals of phosphorus data from used and incident filters.

Table 2-5 shows the homogeneity tests. The homogeneity tests for all p-values were less than 0.1, indicating that unequal variances for P and Br were statistically significant. For S, all p-values were greater than 0.1, suggesting that the variability of means of S was not significant in used filters. For incident filters, the p-values for all the tests of homogeneity for P and S were greater than 0.1, suggesting that the unequal variances were not statistically significant, whereas for Br, unequal variance was statistically significant.

**Table 2-5 ANOVA – Test for homogeneity of jet engine oil contaminants variance in used and incident filters**

ANOVA for jet engine oil contaminant elements in used filters			
Test method	p-value for P	p-value for S	p-value for Br
Levene's test	0.0026	0.3062	0.0066
O'Brien's test	0.0810	0.4683	0.0192
Brown and Forsythe's test	0.0192	0.3214	0.0100
Bartlett's test	0.0002	0.2079	0.0106
Welch's test	0.0006	0.0478	0.0626
ANOVA for jet engine oil contaminant elements in incident filters			
Levene's test	0.1311	0.0833	0.0169
O'Brien's test	0.3384	0.4007	0.0535
Brown and Forsythe's test	0.1400	0.2132	0.0154
Bartlett's test	0.2548	0.0892	0.0349
Welch's test	0.4063	0.0075	0.0065

-----Category=Used -----

The Mixed Procedure

Type 3 Tests of Fixed Effects (Response = P)

Effect	Num		Den		F Value	Pr > F
	DF	DF	DF	DF		
Aircraft	4	15.8	3.18	0.0003		

Least Squares Means

Effect	Aircraft	Standard			t Value	Pr >  t	Alpha	Lower	Upper
		Estimate	Error	DF					
Aircraft	A320	0.03964	0.004042	10	9.81	<.0001	0.05	0.03063	0.04864
Aircraft	B737	0.05534	0.009072	10	6.10	0.0001	0.05	0.03512	0.07555
Aircraft	B747	0.03263	0.002634	10	2.39	<.0001	0.05	0.02676	0.03850
Aircraft	B767	0.04792	0.008214	5	5.83	0.0021	0.05	0.02680	0.06903
Aircraft	B777	0.05828	0.003899	59	14.95	<.0001	0.05	0.05047	0.06608

Differences of Least Squares Means

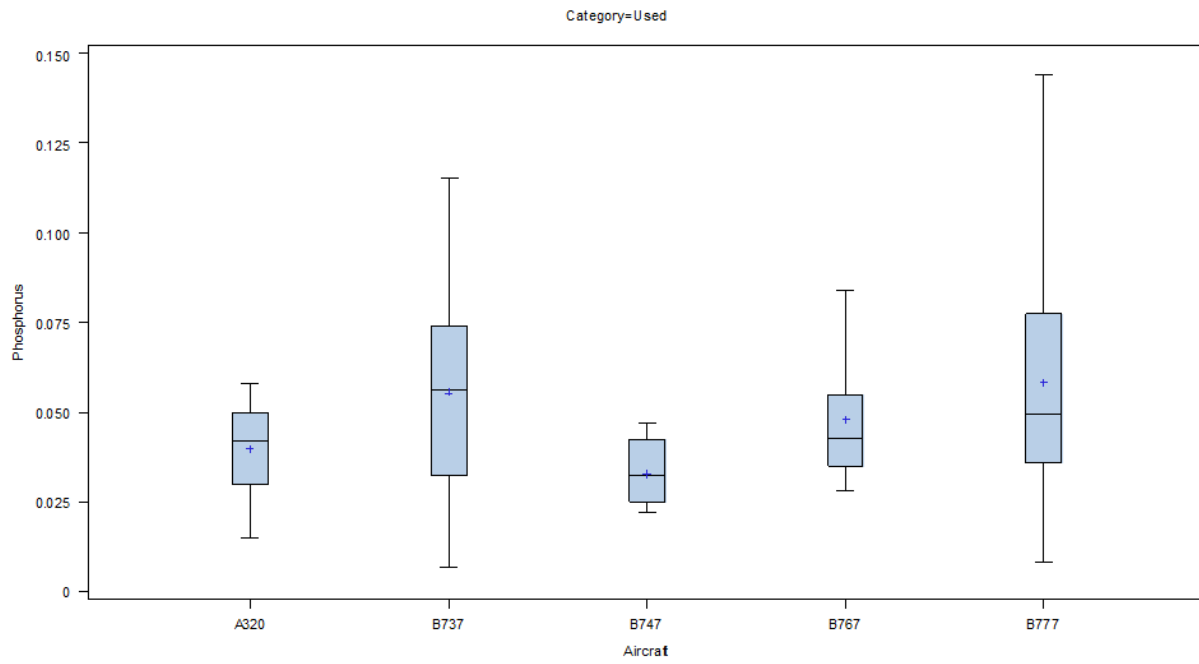
Effect	Aircraft-Aircraft	Standard			t Value	Pr >  t	Adjustment	Adj P
		Estimate	Error	DF				
Aircraft	A320 B737	-0.01570	0.009932	13.8	-1.58	0.1365	Bonferroni	1.0000
Aircraft	A320 B747	0.007009	0.004825	17.2	1.45	0.1643	Bonferroni	1.0000
Aircraft	A320 B767	-0.00828	0.009155	7.5	-0.90	0.3939	Bonferroni	1.0000

Aircraft	A320	B777	-0.01864	0.005616	32.5	-3.32	0.0022	Bonferroni	0.0298
Aircraft	B737	B747	0.02271	0.009447	11.7	2.40	0.0338	Bonferroni	0.2465
Aircraft	B737	B767	0.007420	0.01224	14.1	0.61	0.5540	Bonferroni	1.0000
Aircraft	B737	B777	-0.00294	0.009874	14	-0.30	0.7704	Bonferroni	1.0000
Aircraft	B747	B767	-0.01529	0.008626	6.05	-1.77	0.1263	Bonferroni	0.8953
Aircraft	B747	B777	-0.02565	0.004705	56.1	-5.45	<.0001	Bonferroni	0.0002
Aircraft	B767	B777	-0.01036	0.009092	7.47	-1.14	0.2898	Bonferroni	1.0000

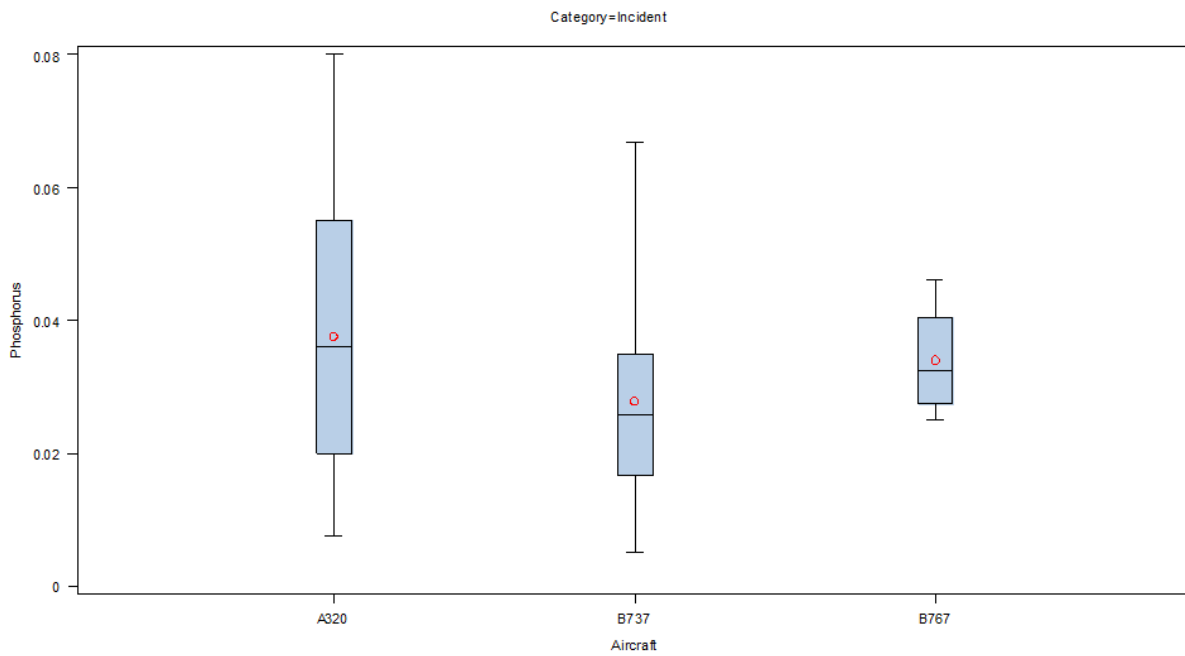
The results for the PROC MIXED procedure for used filters suggests that the pair-wise comparison between the means of A320 versus B777 and B747 versus B777 were statistically significantly different ( $p = 0.0298$  and  $0.0002$ , respectively). This could be due to disproportionately high filter sample size for the affected aircrafts (Refer to Table 2.1). Otherwise, the overall p-values of pair-wise comparisons of aircraft models with Bonferroni adjustment at  $\alpha = 0.05$  were not significant for other pairwise comparisons, suggesting that aircraft model has no role in P concentrations.

```
----- Category=Incident -----
                        The Mixed Procedure
                    Type 3 Tests of Fixed Effects (Response = P)
                        Num      Den
Effect                DF      DF   F Value   Pr > F
Aircraft              2      13.6    1.02    0.3865
```

The output of PROC MIXED procedure for incident filters had p-value = 0.3865, suggesting that the aircraft type has no effect on phosphorus concentration. The effect of aircraft model was not significant in average concentration levels of phosphorus found in filters. Figures 2.9 (a) and (b); 2.10 (a) and (b); and 2.11 (a) and (b) show the box plots of mean percent atomic weights of P, S, and Br in both used and incident filters for different aircraft frame models covered by the study. Meanwhile, Figures 2.12 through 2.14 show the scatter plots for P, S, and Br in different aircrafts. These scatter plots show the spread of mean atomic weight percent of P, S, and Br and the outliers.

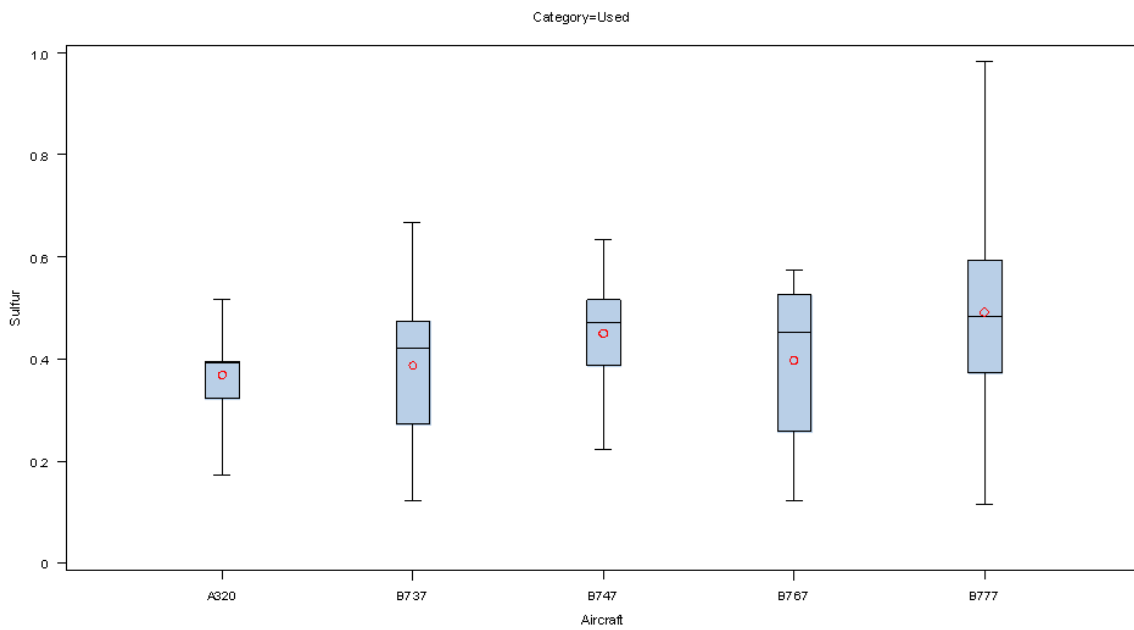


(a)

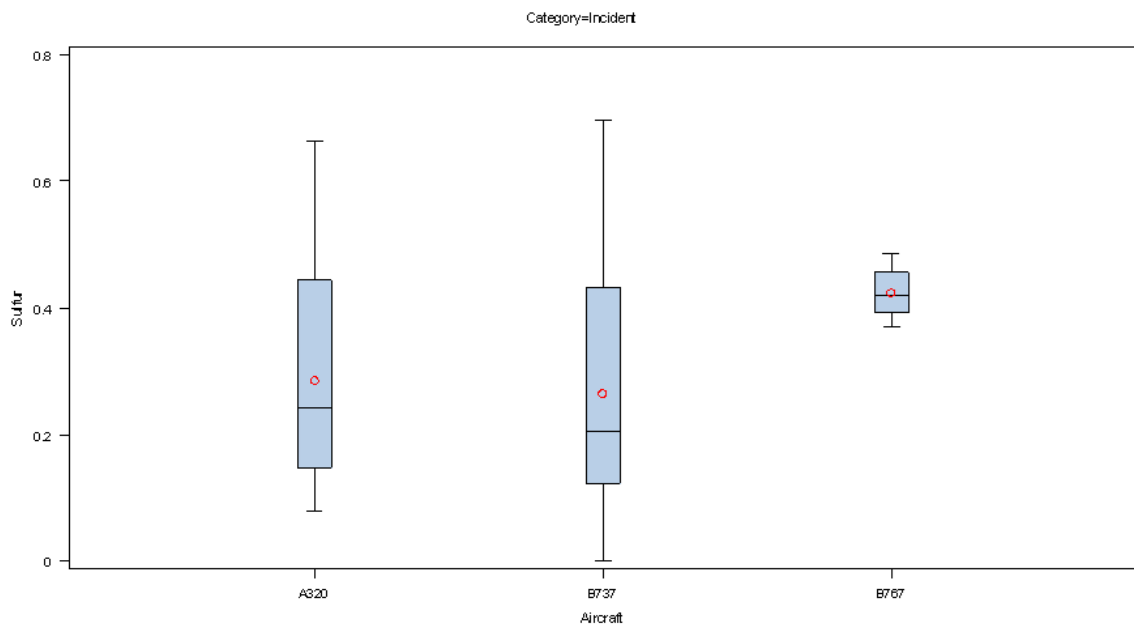


(b)

**Figure 2.9** Box plots showing variability of mean atomic weight percent of phosphorus in (a) used and (b) incident filters from different aircraft types

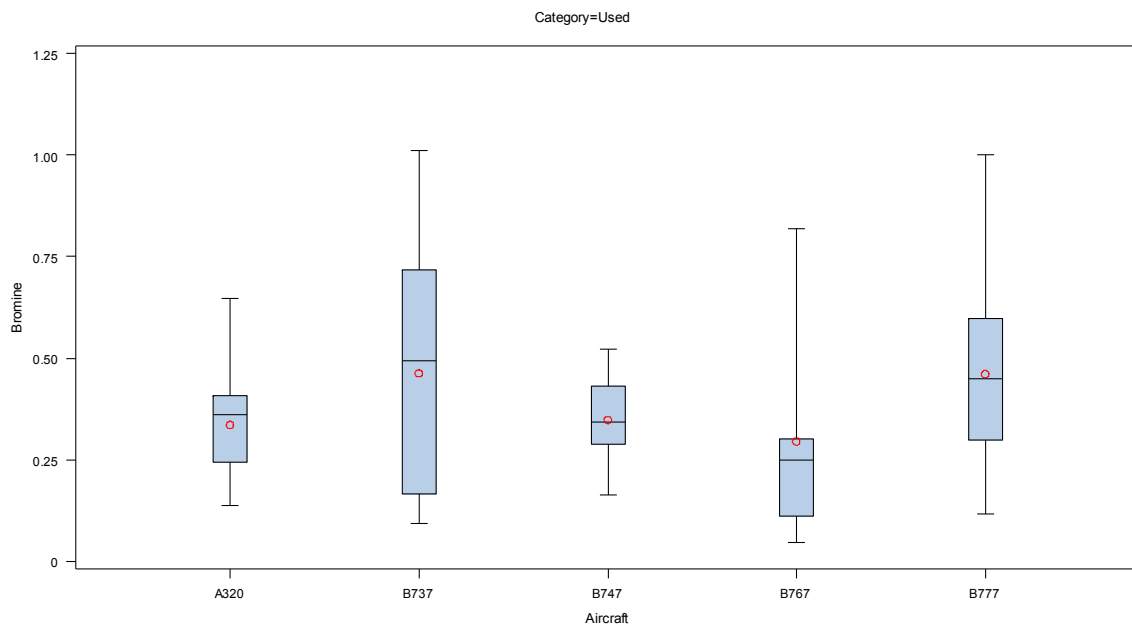


(a)

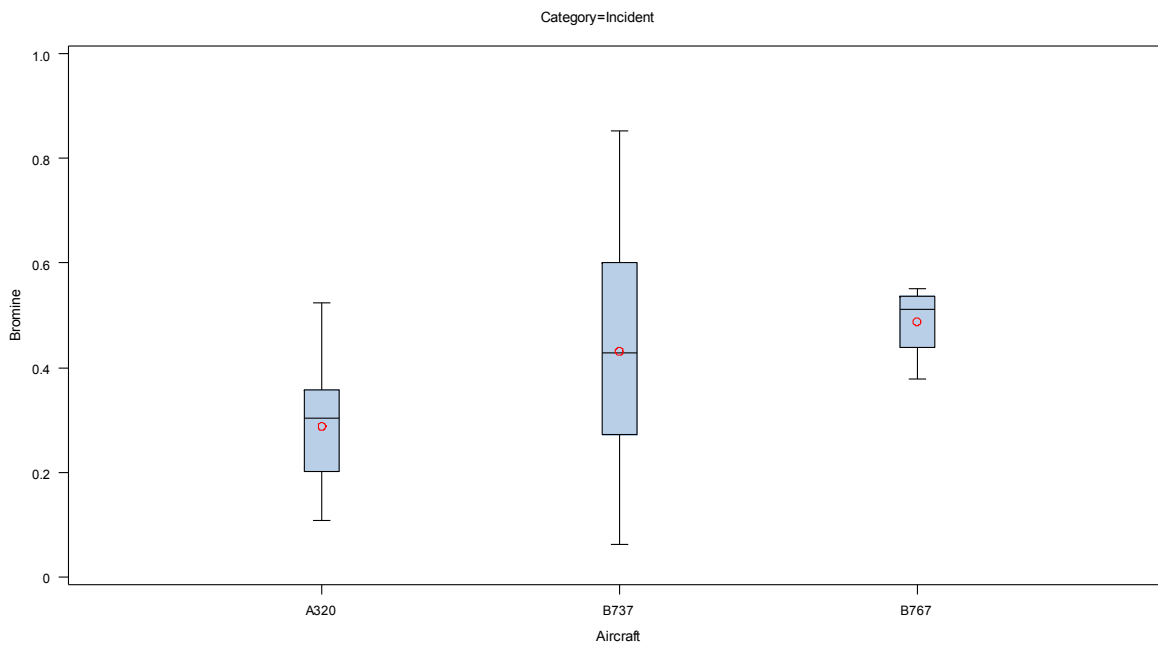


(b)

**Figure 2.10** Box plots showing variability of mean atomic weight percent of sulfur in (a) used and (b) incident filters from different aircraft types



(a)



(b)

**Figure 2.11** Box plots showing variability of mean atomic weight percent of bromine in (a) used and (b) incident filters from different aircraft types

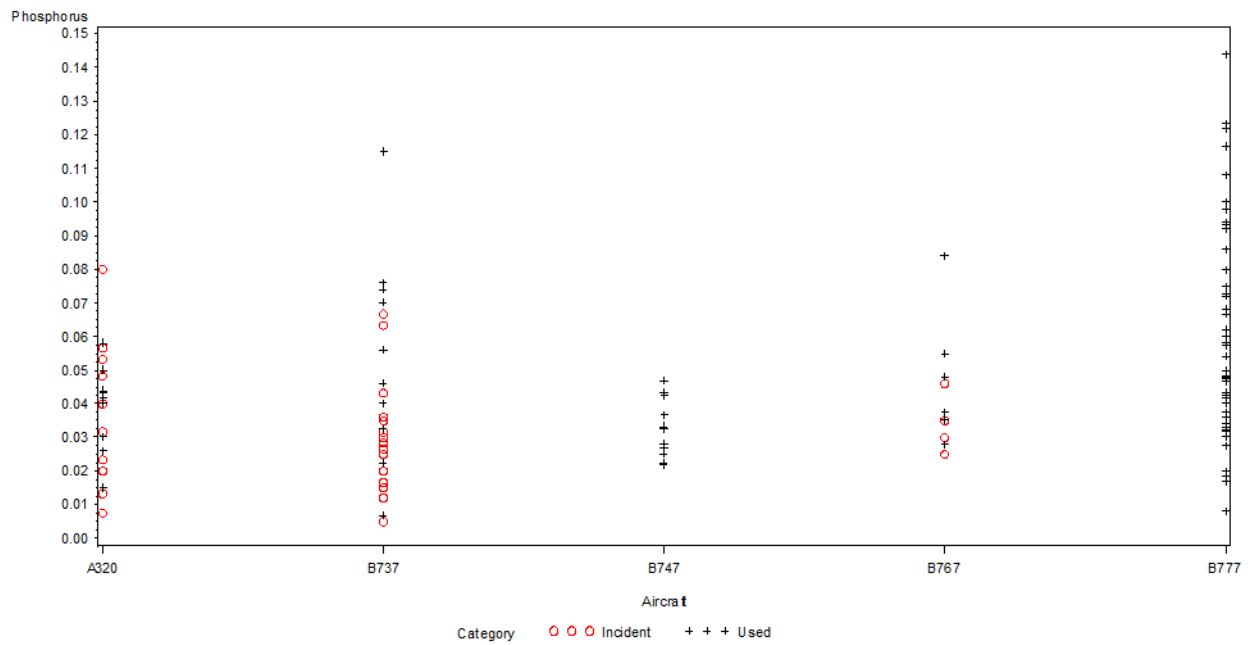


**Figure 2.12 Scatter plots of mean atomic weight percent of phosphorus in used and incident filters from different aircraft types**

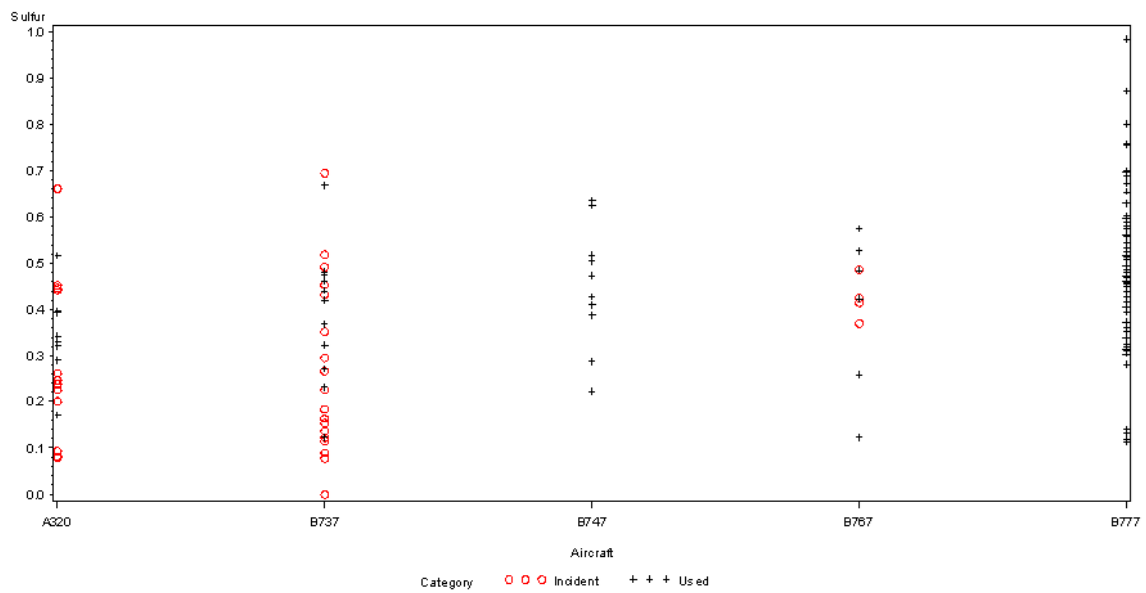


**Figure 2.13 Scatter plots of mean atomic weight percent of sulfur in used and incident filters from different aircraft types**

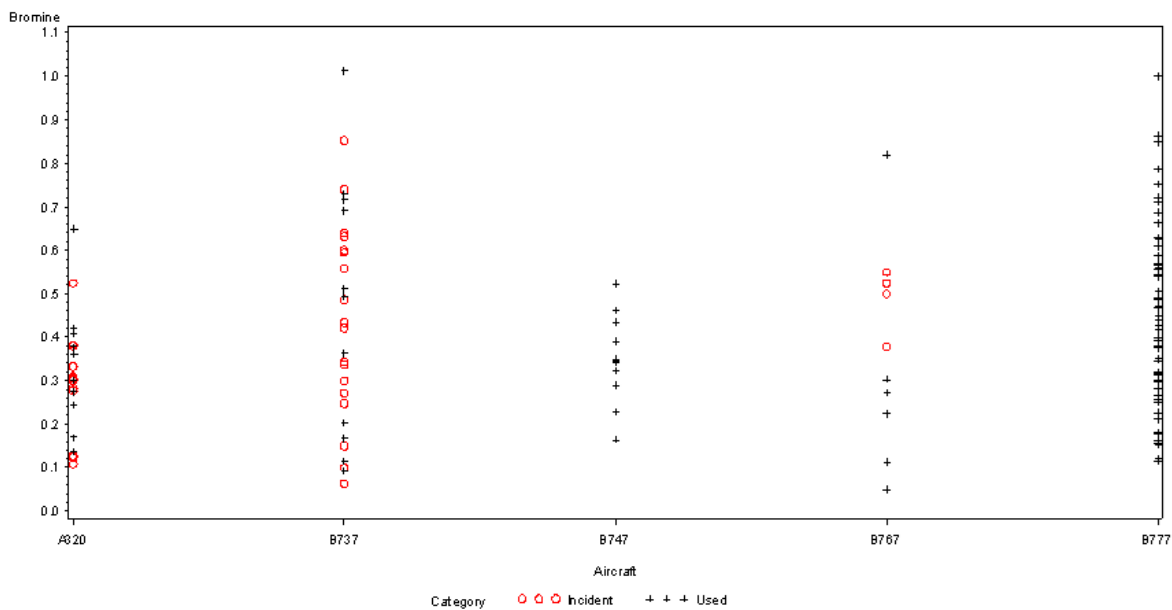


**Figure 2.14 Scatter plots of mean atomic weight percent of bromine in used and incident filters from different aircraft types**

#### ***2.4.2.2 Further assessment of P, S, and Br as markers for jet engine oil on aircraft filters***

In additional analyses, all filters and every measured data point (not averaged spot values) were used in Excel to compute the correlations of P, Br, S, C, O<sub>2</sub>, and Si. The nearly ubiquitous presence of P, S, and Br on used filters made it difficult to attribute their presence uniquely to oil. While the statistical analysis indicated some significant correlations, the strength of the correlations also was not enough to make a convincing argument that the presence of these elements was uniquely due to jet engine oil. To better understand the nature of these deposits, the individual specimen data presented in Appendices A.1 and A.2 were plotted in pair-wise combinations in Figures 2.15 through 20. Consistent with the statistical analysis, P and S were correlated suggesting some commonality of source, but the wide scatter indicates multiple, independent sources as well. Bromine shows no or negative correlation with P and S, again consistent with the statistical analysis, which indicates no commonality of source.



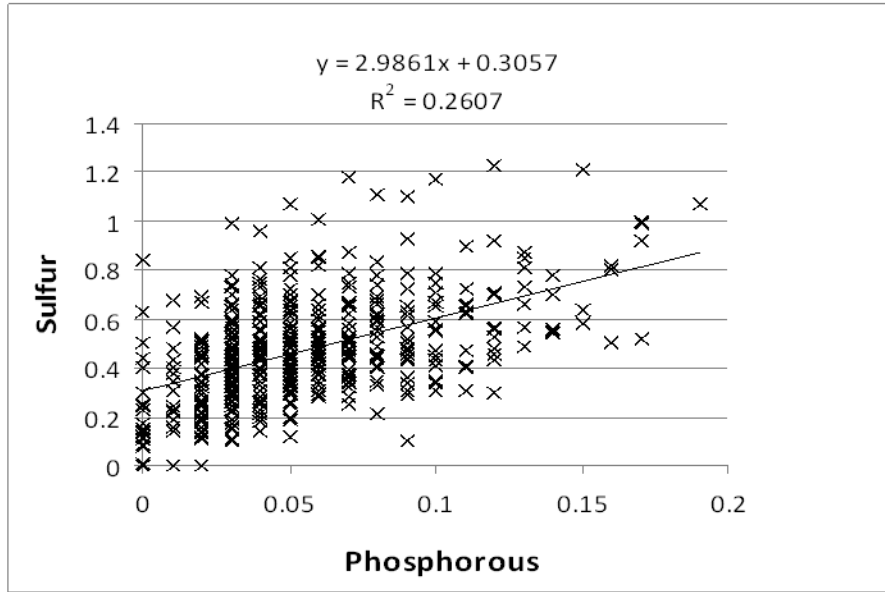


Figure 2.15 Comparison of Sulfur and phosphorus in used filters

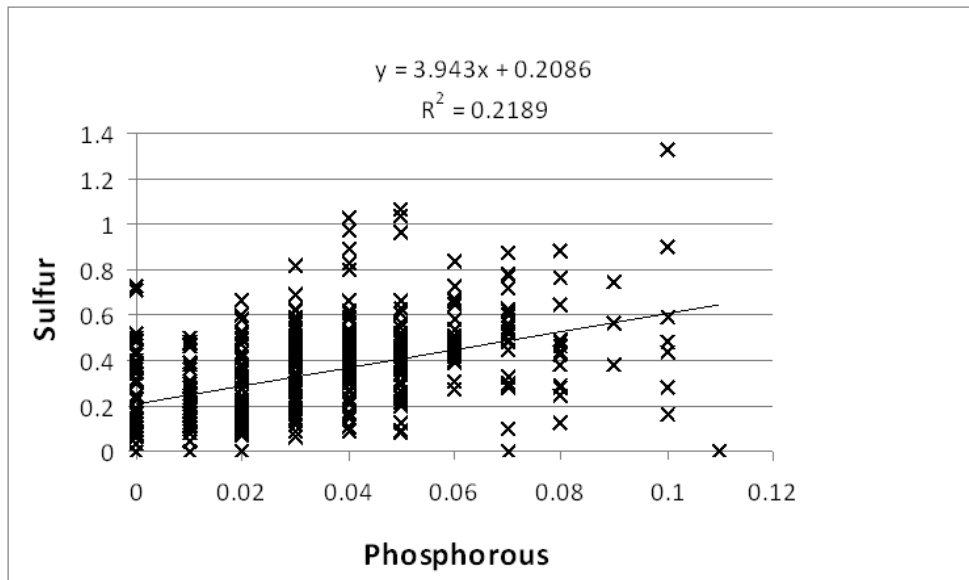
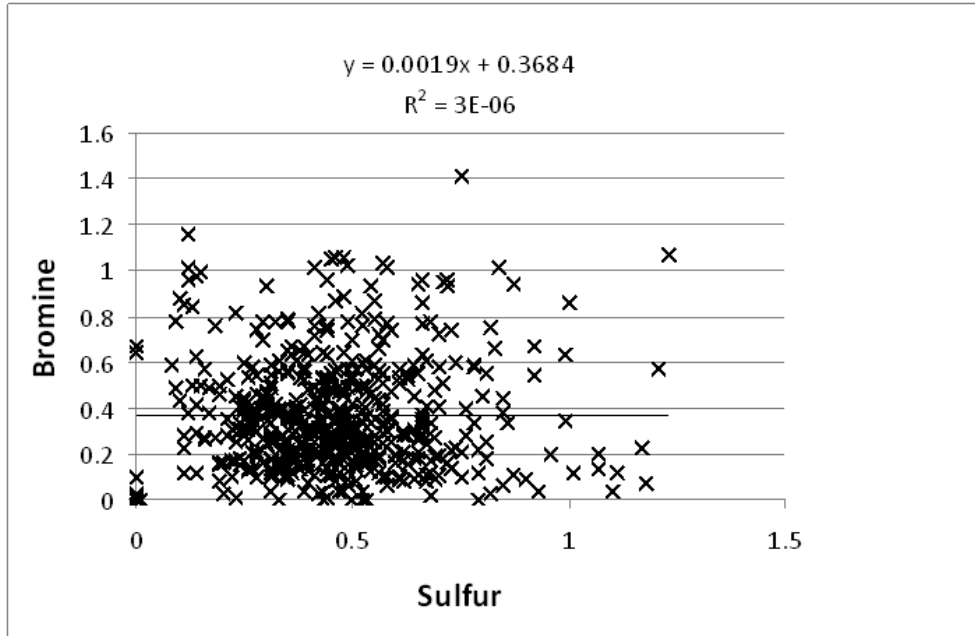
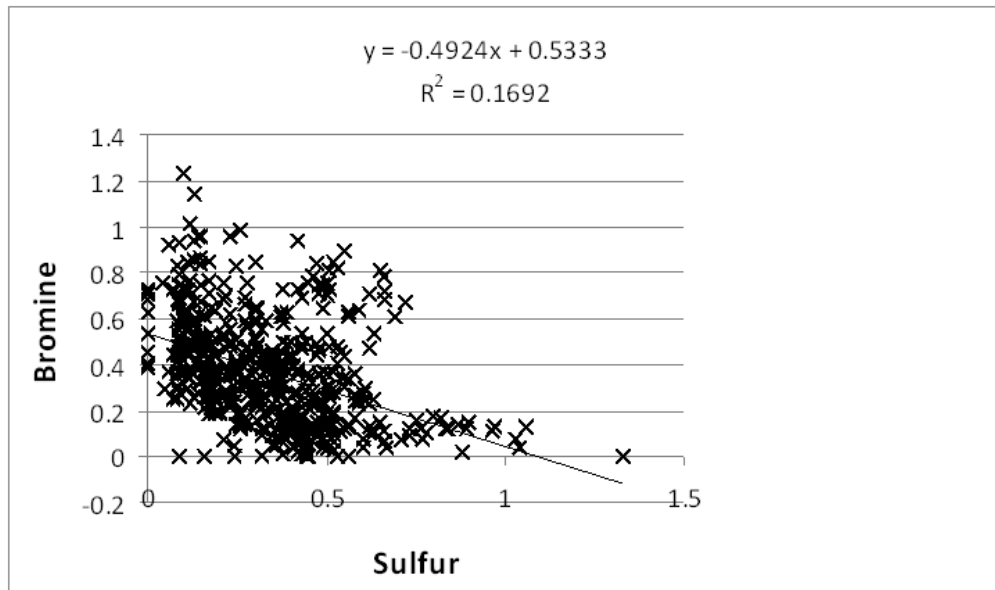


Figure 2.16 Comparison of sulfur and phosphorus in incident filters



**Figure 2.17 Comparison of bromine and sulfur in used filters**



**Figure 2.18 Comparison of bromine and sulfur in incident filters**

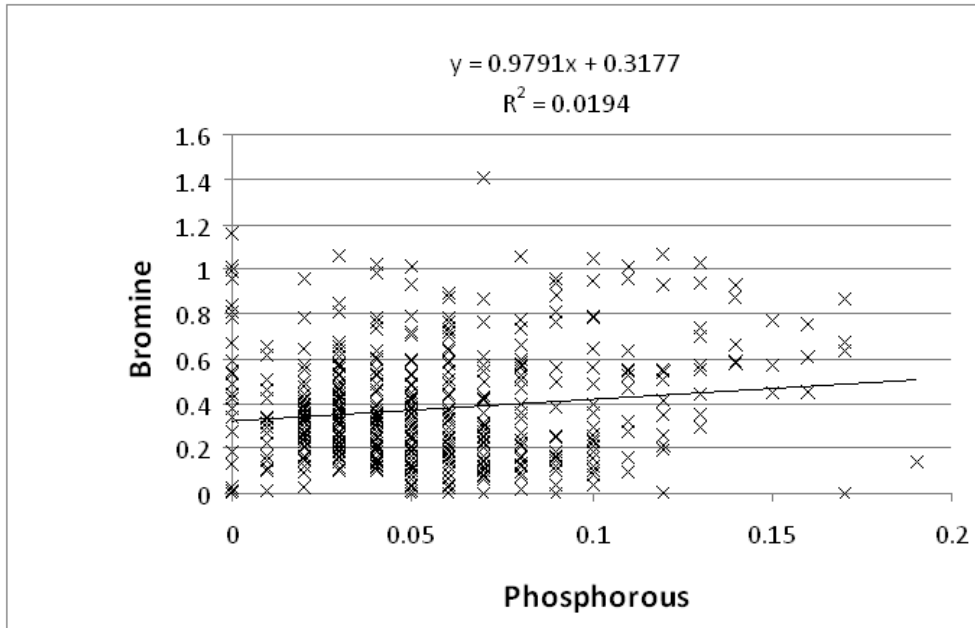


**Figure 2.19 Comparison of bromine and phosphorus in used filters**

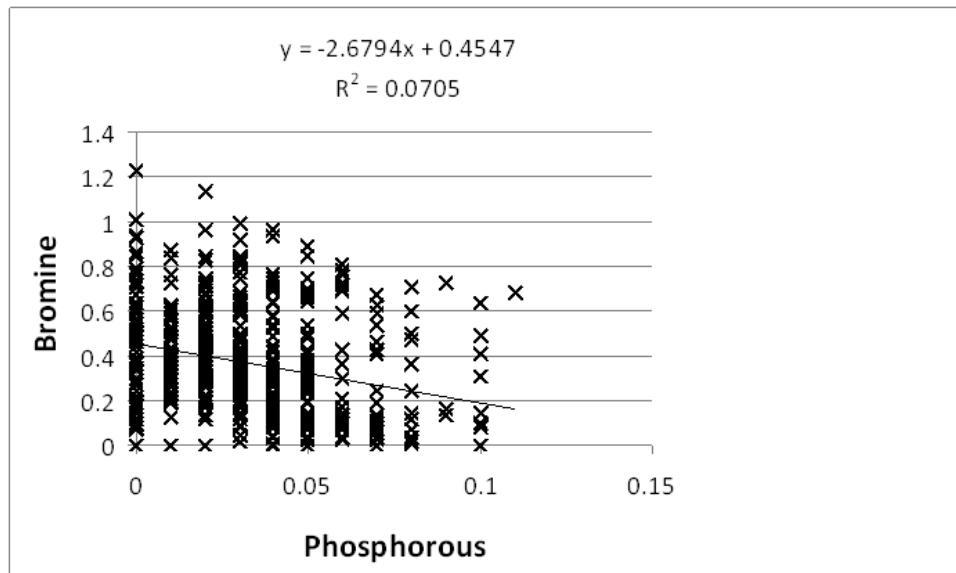


**Figure 2.20 Comparison of bromine and phosphorus in incident filters**

In examining the data, it is important to note that FESEM/EDS results were provided in percent of elements measured. The data are not absolute values. Since the FESEM/EDS method only examines the surface, these numbers are roughly a percent of the surface area, ignoring the fact that FESEM/EDS technique does not detect all elements. It is also important to remember

that FESEM/EDS looks at an area that is small compared to the surface texture of filter media. Thus, some measurement locations may look deeper into the filter than others.

Carbon was not expected to be a useful indicator of oil because it is present on filters in other forms. However, it is useful to look at the nature of carbon deposits on filters to understand how other results may be affected. Since results are in percent of total “atomic weight,” a large amount of carbon will necessarily decrease the amount of the other elements seen. Figures 2.21 and 2.22 show how carbon deposits relate to silicon and oxygen. The clusters of points in the scatter plots roughly appear to form a straight line, suggesting that a linear relationship exists between carbon and silicon, and oxygen respectively. For brevity, only the used filter results are presented, but the results for the incident filters are nearly identical. The very strong negative correlations seem quite surprising. However, the filter media may be composed primarily of silicon oxide (glass). The strong negative correlation results from the carbon deposits covering up the media, the silicon oxide. Finally, the relationships of P, S, and Br to carbon on the filters are shown in Figures 2.23 through 2.25. P and S occur pretty much randomly with carbon, but Br has a clear negative correlation with carbon. These results indicate that P and S are deposited along with the carbon on the filter. That is, carbon does not simply cover up the P and S when it is deposited. Bromine, on the other hand, tends to be covered up by the carbon deposits. Bromine deposits are thus different from the S and P deposits, indicating that much of the Br comes from sources other than those for P and S.

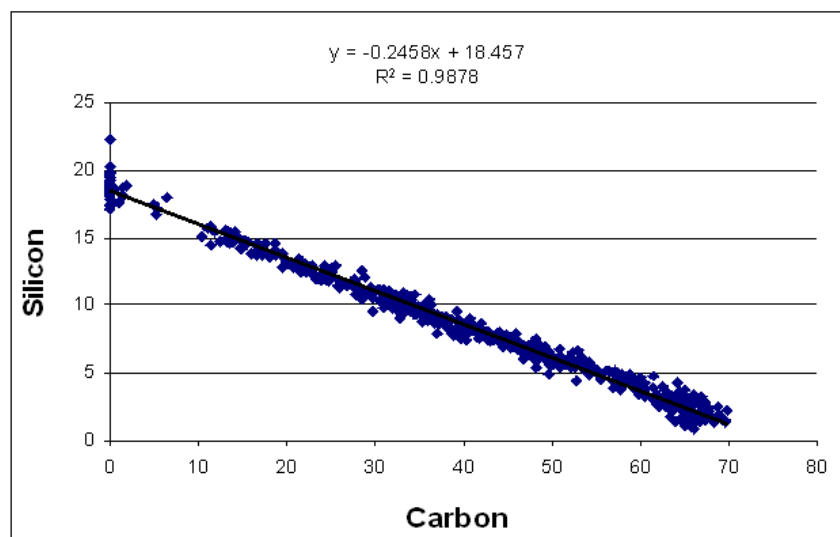


**Figure 2.21 Decrease in silicon with increasing carbon in used filters**

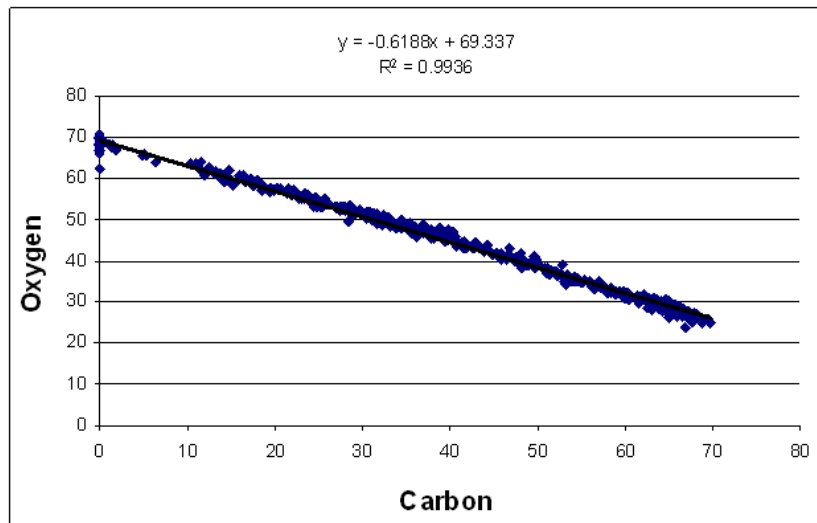


**Figure 2.22 Decrease in oxygen with increasing carbon in used filters**

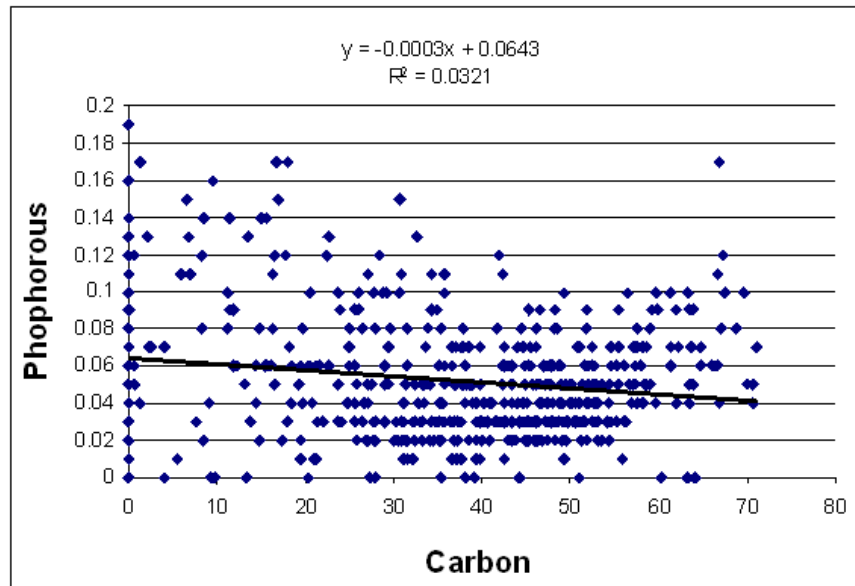


**Figure 2.23 Relationship of phosphorus with carbon in used filters**

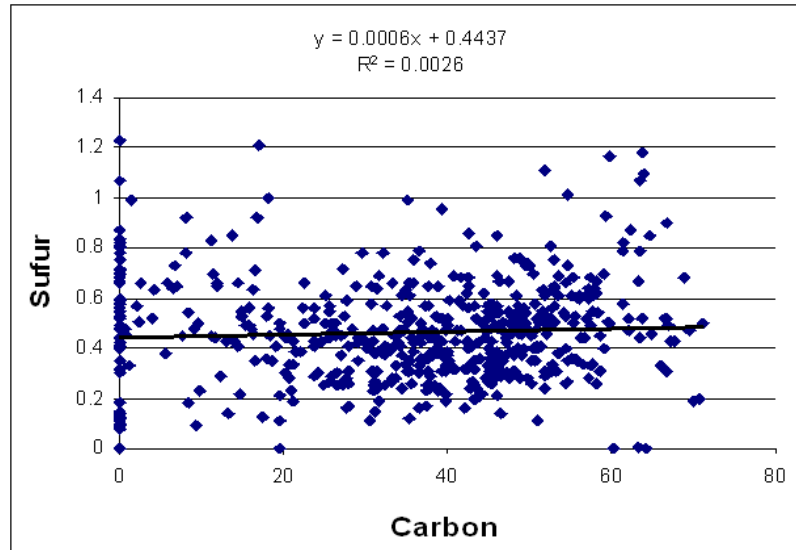


**Figure 2.24 Relationship of sulfur with carbon in used filters**

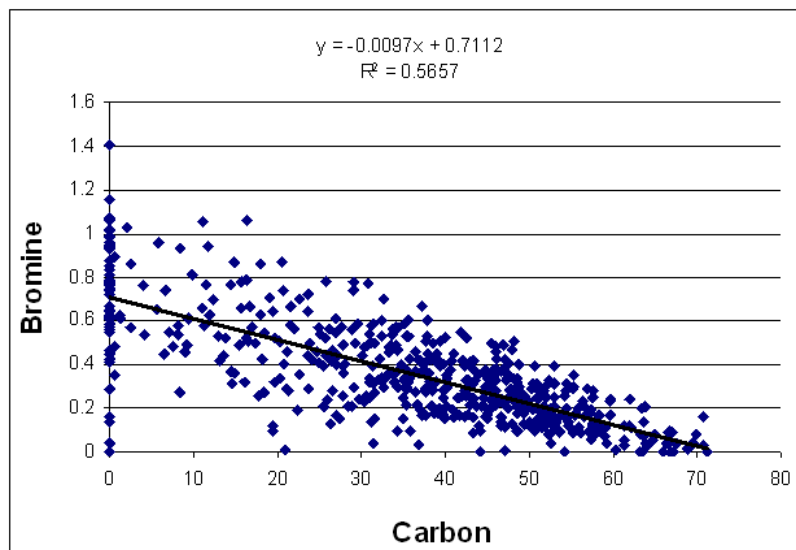


**Figure 2.25 Relationship of bromine with carbon in used filters**

Flame retardants, which are included in many cabin materials, including carpets, upholstery, and plastics, contain Br and generally do not contain S or P. Gerecke (2007) found high concentrations of polybrominated diphenyl ethers (PBDEs) in a sample of settled airplane dust. It should be no surprise then that bromine is present on most, if not all, filters and, that its presence would be different than P and S. Exactly why it tends to be covered up by carbon, while P and S do not, is unknown at this point but is not a factor in excluding it as an effective marker for oil using FESEM/EDS.

#### 2.4.2.2.1 *Microscopic analysis of clean, used and incident filters*

In addition to clean filter elemental composition, the morphology of the clean fibers was also of interest, because these elements fuse to form non-crystalline fibers due to high temperature exposure during the molding and extrusion of glass fibers and subsequent rapid cooling. Figure 2.32 shows a scanning electron micrograph of a sample from a clean filter manufactured by Keddeg Company.

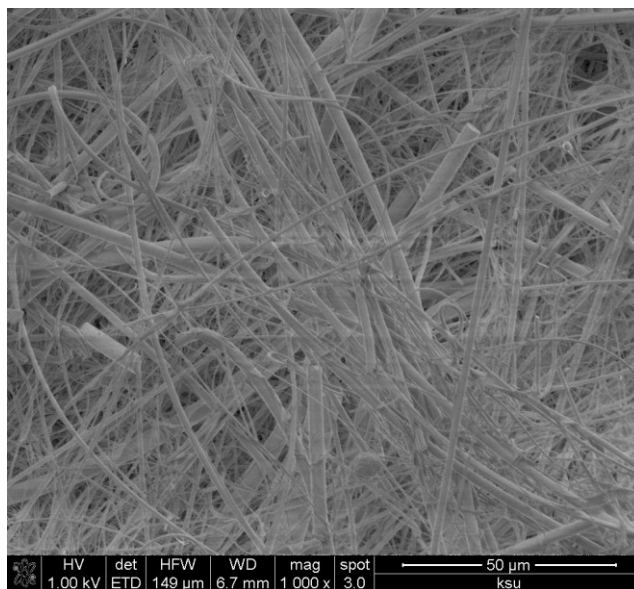


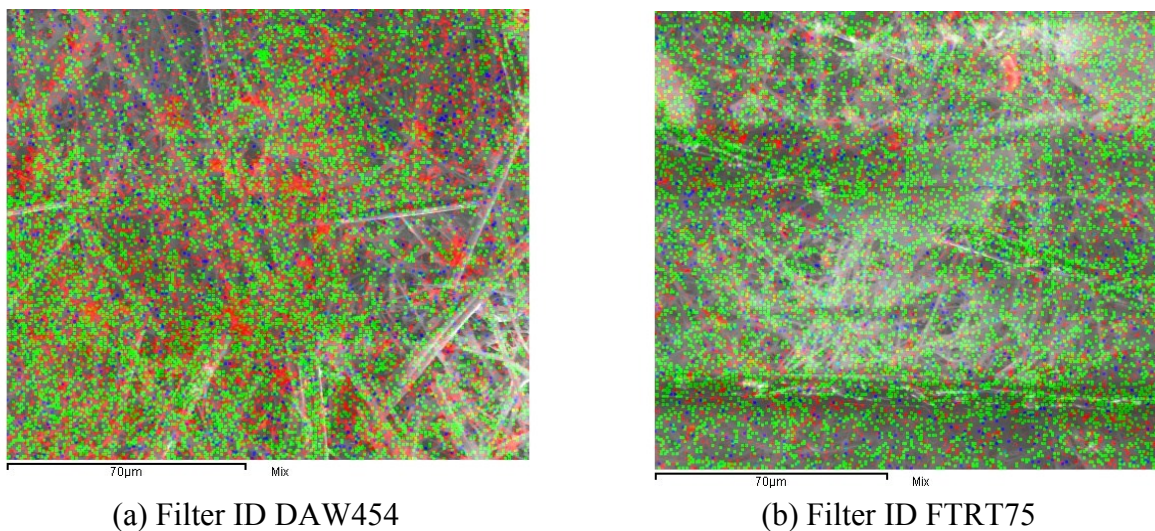
**Figure 2.26 Electron micrograph of clean HEPA filter manufactured by Keddeg Co.**

Microscopic examination of the clean filter samples from three filter manufacturers showed that fibers consisted of high-purity, ultra-long intertwined glass fibers. The filter fibers were very clearly preserved and show precise long string like structures. As shown in Figure 2.32, the micrographs indicate that each clean filter fiber had a uniform diameter along its entire length and most glass fibers had smooth surfaces. The high magnification observations also showed that the glass fibers exhibited a single crystalline nature without apparent lattice defects. The binder, a blue coating, is clearly visible between the glass fibers.

#### 2.4.2.2.2 *Mixed maps*

Mixed maps were obtained from photos taken by FESEM as it skimmed over the filter surface; voltages ranged from 1 to 18 kV during the analysis. This study mapped the surface of the aircraft cabin air filters to a resolution fine enough to determine particulates deposited on the

surface. The mixed maps in Figure 2.33 show the morphological features of elements deposited on used filter surfaces. Only three elements could be represented at a time. Under the experimental conditions, no clear differences between used and incident filters could be found. However, when used and incident filters were compared to clean filters, there was evidence of P, S, and Br pigmentation in the used and incident filters.



Key: Green = Phosphorous, Red = Sulfur and Blue = Bromine

**Figure 2.27 Mixed elemental maps for P, S and Br in used filter samples**

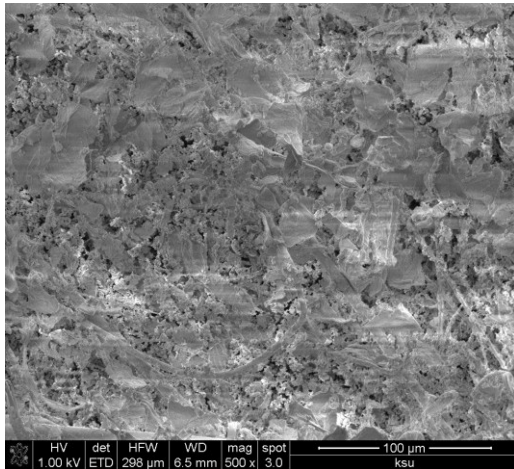
Carbon was abundant in both the used and incident filters. Some possible sources of carbon could be soot and dead skin cells from human bodies. The elemental maps produced in the FESEM/EDS study provide important information on micro-textural and structural characteristics of contaminants deposited on used filter materials.

#### 2.4.2.2.3 *Photomicrographs of used and incident filters*

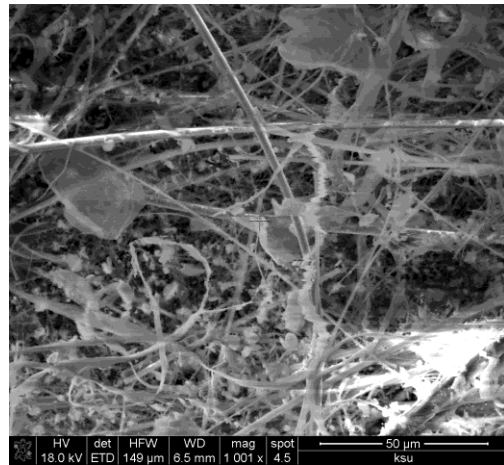
Irregularly-shaped particles were deposited on the surface of the fiber material. An analysis of the dispersed particles indicated new elements not present in clean filters. The thickness of the fibers in both used and incident filters increased because of the particulate deposition on the fibers. In some photomicrographs, the fibers are barely visible and have significant amorphous outer layers. However, the particles could not be described by their origin or formation mechanism, chemical composition, and physical properties. Figures 2.34 (a) and (b)



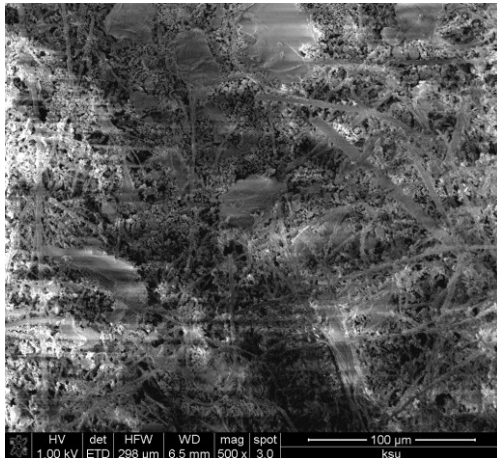
show high-magnification FESEM images of used filters. Figures 2.34 (c) and (d) show the same images for incident filters. Images produced from different filters and at different points during the analysis can be placed side by side. As seen under FESEM in Figure 2.34, the filter depositions vary from small particulates to large irregularly shaped particulates, with images ranging from fibers to spongy amorphous structures with no distinctive shape.



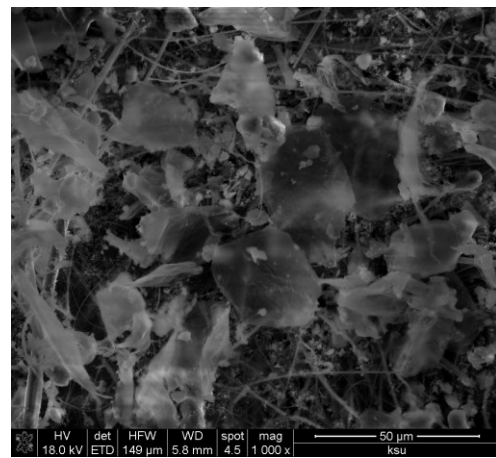
(a) Filter ID 3Q5J9L



(b) Filter ID 9RZMC2



(c) Filter ID 163B4J



(d) Filter ID 23937

**Figure 2.28 Composite image of electron micrographs for (a) used filters ID 3Q5J9L and 9RZMC2 and (b) incident filters ID 163B4J and 23937**

To a casual observer, both used and incident filters look the same with a few variations suggesting gradations of dirtiness in used filters. With FESEM, more information can be derived,

and the used and incident filters can be compared. These filter deposits could also be important indicators of jet engine oil contamination. The microphotographs are representative images of the filter deposition, and their varying natures indicate the wide range of deposits in the cabin filters. The images essentially physically characterize the deposits on the filter surface. However, the chemical nature of these deposits remains unknown to scientists seeking clues about cumulative aircraft cabin air quality from filter analysis.

This study has provided a glimpse into the nature of filter deposition, a reflection of the composition of cumulative air passing through the aircraft cabin. When used and incident filters were compared, used filters had more contaminants with higher mean concentrations than the incident filters. This result is likely because used filters were used longer and were removed during routine maintenance at the end of their expected service life. Incident filters may have been removed much sooner. Each analysis produced slightly different results. In both groups of filters, the first batch of analyses showed more consistent results than the second. The presence of all three contaminants indicates the presence of jet engine oil on filters. While it was hoped that P, S, or Br or some combination of these elements could be used as a clear marker for jet engine oil, the ubiquitous presence of these elements on nearly all filters, the lack of strong correlations between the elements, and other known sources of Br inevitably led to the conclusion that these elements alone or in combination cannot be used to identify the presence of jet engine oil on filters. This result is nevertheless important because the objective of the study was to determine whether or not FESEM/EDS can be used to identify the presence of jet engine lubricating oil on filters and, thus, identify the contaminant source for an air quality incident. Apparently, it is not a suitable technique. Even so, this study provides new information about the concentrations of elements in used filters.

#### ***2.4.2.3 Possible sources of contaminant elements deposited on used filters from aircraft cabins***

Many sources may contribute to the wide range of elements found in used filters. According to Winder and Balouet (2001), jet engine oils and hydraulic fluids used in aviation industry contain a range of ingredients: organophosphate compounds, including tricresyl phosphates (TCP), tributylphosphates (TBP), triphenyl phosphates (TPP) and their derivatives, from 3 to 25 percent in content; toxic inorganic molecules, such as naphthylamines, amines and esters; organometallic additives; zinc dialkyl dithiophosphates, calcium alkyl phenates, magnesium sulphonates, molybdenum, and barium containing additives. If these materials leak

into the bleed air system, then they could contribute significantly to cabin air supply contamination. Such contamination could be a source of S, Ba, Ca, Mg, Zn, and P. Sulfur dioxide (SO<sub>2</sub>) is a well-known component of diesel emissions from trucks often used at airports. Other vehicles at airports also emit such pollutants. Therefore, when an aircraft sits at the airport terminal, the composition of the air being supplied to the cabin differs from the air supplied to the cabin during flight; that may as well influence filter elemental deposition.

In-cabin emission processes include products of metabolic processes from cabin occupants, dust carried into the cabin by passengers. Every aircraft model is unique, and the cumulative cabin air quality may be determined even by passenger seating arrangements. Some aircrafts have a single aisle, others two or three aisles and business and first class compartments. All these arrangements can determine the intensity of metabolic processes in the aircraft cabin. Differences in jet engine characteristics could also influence the quantity of bleed air and type of pollutants deposited on the filters (De Nola et al. 2008). Although aircraft usually fly at high altitudes where the air is considered pristine, events like volcanic eruptions can pollute air even at these altitudes. The ever-changing aircraft routes or flight paths of aircraft can also affect filter deposition levels. More information is needed on the effects of the size of the aircraft, routes, and different cabin and engine maintenance practices unique to airlines.

Traces of a few toxic elements like arsenic (As), lead (Pb), chromium (Cr), and cerium (Ce) have been detected in both used and incident filters. Identifying the source of these elements in the aircraft cabin was outside the scope of this study. The most likely source of these trace elements is the air supplied to the aircraft cabin. The medical ramifications of the presence of these toxic trace elements in aircraft cabin air are not known. After being replaced during scheduled maintenance checks (C-checks), used aircraft cabin air recirculation filters should not be dumped but used for enhanced data mining as part of an emerging air quality management model that views used cabin filters not as the last stop but as temporary storage for recoverable cabin air quality information. This study has demonstrated how the FESEM/EDS system can obtain information from used cabin air recirculation filter samples. These findings have added new knowledge about aircraft cabin air quality. While falling short of being able to fully and accurately detect smoke/fume incidents, the study results should spur scientific debate about the origin of the P and S detected on the filters. The P could possibly be from TCPs in jet engine oils additives or from hydraulic fluids but could very well be from some other unknown source.

No scientific evidence currently establishes a definite link between the elements present in jet engine oil and those deposited in air filters. No studies have shown conclusively how jet engine oils contaminate cabin air filters. FESEM/EDS, however, offers insight in characterizing cabin air quality because all airborne particulates from the cabin environment pass through the cabin air recirculation filters. The FESEM/EDS technique in aircraft filter analysis has the potential to help the airline industry improve air quality. FESEM/EDS is non-destructive and requires very little sample preparation; it can be configured to handle any sample size from large surfaces to ones as small as a few microns. Its multi-element capability means that the FESEM/EDS technique is well suited to analyze elements deposited on cabin air filters.

This study presents, for the first time, using the FESEM/EDS technique, a benchmark for evaluating elemental species on used filters. The FESEM/EDS technique can offer a wide variety of micro-contamination solutions and provides an excellent source of technical information on aircraft cabin air quality. This study's new test protocol for inspecting aircraft's incident filters will enable scientists to recreate a vivid and detailed picture of deposits on cabin air recirculation filters and correlate the elemental deposits to past cumulative cabin air quality.

## **2.5 Conclusions**

In this study, the FESEM/EDS technique was used to identify P, S, and Br as potential markers for jet engine oil contamination of aircraft filters. These contaminants are present in both used and incident filters in a wide range of atomic weight percentages. This study also provided a new methodology to support analysis and characterization of elements deposited on used aircraft cabin air filters. However, P, S, and Br were present on nearly every filter evaluated, whether used or incident, so the lack of strong correlation between these potential markers on the filters and a known non-oil source for Br result in the conclusion that P, S, or Br either singularly or in any combination cannot provide an indication of oil contamination. It appears that FESEM/EDS methods may not be used to identify a unique marker for jet engine oil contamination on aircraft cabin filters.

Nevertheless, this research has provided researchers with new information about used HEPA filter deposition, which reflects the cumulative air quality passing through the aircraft cabin during flight. The study has shown how used filters can be used to assess aircraft cabin air quality. Finally, the study suggests that routine filter screening for P would be a viable option for

detecting cabin air quality incidents. Such screening might help airlines make informed decisions about whether an incident occurred. Nonetheless, this study did not identify the reason for variability of identified contaminant elements from jet engine oil, and how they affect cabin air supply has not been answered by this study.

## 2.6 References

- Abou-Donia, M., (2005). Proceedings of the Contaminated Air Protection Conference Proceedings of the BALPA Air Safety and Cabin Air Quality International Aero Industry Conference. Held at Imperial College, London, 20–21 April 2005.
- Australian Civil Aviation Safety Authority (CASA). Expert Panel on Aircraft Air Quality (EPAAQ), Contamination of aircraft cabin air by bleed air – a review of the evidence. September 2009. [http://www.casa.gov.au/wcmswr/\\_assets/main/cabin/epaaq/epaaq-entire-report.pdf](http://www.casa.gov.au/wcmswr/_assets/main/cabin/epaaq/epaaq-entire-report.pdf)
- ASHRAE (1999). ANSI/ASHRAE Standard 52.2-1999. Method of Testing General Ventilation Air-Cleaning Devices for Removal Efficiency by Particle Size. Atlanta, GA: American Society of Heating, Refrigerating and Air-conditioning Engineers, Inc.
- ANSI/ASHRAE (2007). ANSI/ASHRAE Standard 161-2007, Air Quality within Commercial Aircrafts. 20 pp. Product code: 86493. ISBN: 1041-2336. Atlanta, GA: American Society of Heating, Refrigerating and Air-conditioning Engineers, Inc.
- British Airline Pilot Association (BALPA) Report (2006). U.K. Civil Aviation Authority (CAA) <http://cot.food.gov.uk/pdfs/cot-laystatementbalpa200706.pdf> (Cited: November 20<sup>th</sup>, 2011).
- Bull, K., (2008). Cabin air filtration: Helping protect occupants from infectious diseases. *Travel Medicine and Infectious Disease* (2008). Vol. 6, Issue 3, May 2008, pp. 142–144.
- CEN EN-1822-1: (2009). European Standard for High Efficiency Air Filters (HEPA and ULPA) Part 1: Classification, Performance Testing, Markings. CEN Central Secretariat: rue de Strassart, 36, B-1050 Brussels.
- Cooper, C. D. and Alley, F. C., (2002). *Air Pollution Control: A Design Approach*. 2<sup>nd</sup> ed., pp. 696. Prospect Heights: Illinois, Waveland Press, Inc.
- De Nola, G., Hanhela, P. J. Mazurek, W., (2011). Determination of Tricresyl Phosphate Air Contamination in Aircraft. *Ann. Occup. Hyg.* Vol. 55. No. 7, pp. 710–722, 2011. Oxford University Press on behalf of the British Occupational Hygiene Society doi:10.109/annhyg/mer040.
- Gerecke, A. C., (2007). Brominated flame retardants in settled dust of a commercial aircraft. <http://www.bfr2010.com/abstract-download/2007/P074.pdf> (cited March 15<sup>th</sup>, 2012).

- Harding, R., (1994). Cabin air quality in aircraft. *BMJ British Medical Journal*. Volume: 308, Issue: 6926, Publisher: BMJ Group, Pages: 427 – 428.
- Hinds, C. W., (1999). *Aerosol Technology, Properties Behavior and Measurements of Airborne Particles*. 2<sup>nd</sup> ed. ISBN 0-471-19410-7.
- Hunt, E. H. and Space, D. R., (1994). *The Airplane Cabin Environment: Issues Pertaining to Flight Attendant Comfort*. International In-flight Service Management Organization Conference, Montreal, Canada, November 1994.
- IEST-RP-CC001.5: Institute of Environmental Science and Technology, Recommended Practice for Efficiency Test Method for HEPA and ULPA Filters, 940 East North-west Highway, Mt. Prospect, IL 60056.
- Inflight Safety Professionals (ISP), CWA, AFL-CIO, (2011). [http://msnbcmedia.msn.com/i/MSNBC/Sections/NEWS/z\\_Personal/Gold/AFA%20letter%20to%20FAA%20re.%20SDR%20violations%20and%20need%20for%20regs%20August%202011.pdf](http://msnbcmedia.msn.com/i/MSNBC/Sections/NEWS/z_Personal/Gold/AFA%20letter%20to%20FAA%20re.%20SDR%20violations%20and%20need%20for%20regs%20August%202011.pdf) (Cited: Jan. 20, 2012).
- Korves, T. M., Johnson, D., Jones, B. W., Watson, J., Wolk, D. M. Hwang, G. M., (2011). Detection of respiratory viruses on air filters from aircraft. *Letters in Applied Microbiology* 53, 306 – 312. The Society for Applied Microbiology. doi:10.1111/j.1472-765X.2011.03107.x.
- Michaelis, S., (2003). A survey of health symptoms in BALPA Boeing 757 pilots. *J. Occup Health Safety – Aust. NZ* 2003, 19(3): 253 – 261.
- Michaelis, S., (2007). Frequency of events and underreporting in Aviation Contaminated Air Reference Manual, pp. 211 – 248, ISBN 9780955567209, London, England.
- Michaelis, S., and Loraine, T. (2005). Aircraft Cabin Air Filtration and Related Technologies: Requirements, Present and Prospects. *Handbook of Environmental Chemistry Vol. 4, Part H* (2005): 267 – 289. Copyright Springer-Verlag Berlin Heidelberg 2005.
- MIL-STD-282 Method 102.9.1. (1956). US Government Printing Office Washington, DC pp. 33 – 38.
- Molhave, L., (1991). Volatile organic compounds. Indoor air quality and health. *Indoor Air*. 1991; 4: 357 – 376.
- Murawski, J. T. L., Supplee, D. S., (2008). An Attempt to Characterize the Frequency, Health Impact, and Operational Costs of Oil in the Cabin and Flight Deck Supply Air on U.S. Commercial Aircraft. *Journal of ASTM International*, Vol. 5, No. 5. Paper ID JAI101640. Available online at [www.astm.org](http://www.astm.org)

- Nadeau, G., Herguth, W. R., (2004). Applying SEM/EDS to Practical Tribology Problems. Practical Oil Analysis, July 2004.
- National Research Council (NRC) Report, (2002). The Airliner Cabin Environment and the Health of Passengers and Crew Committee on Air Quality in Passenger Cabins of Commercial Aircraft. Washington DC: National Academy Press.
- Pall Corporation, (2012). <http://www.pall.com/main/Aerospace-Defense-Marine/Literature-Library-Details.page?id=46181> (Cited: June 20<sup>th</sup>, 2012).
- Solbu, K., Thorud, S., Hersson, M., Øvrebø, S., Ellingsen, D. G., Lundanes, E., Molander, P., (2007). Determination of airborne trialkyl and triaryl organophosphates originating from hydraulic fluids by gas chromatography–mass spectrometry Development of methodology for combined aerosol and vapor sampling. *Journal of Chromatography A*, 1161 (2007) 275 – 283.
- Spengler, J., Burge, H., Dumyahn, T., Muilenberg, M., Forester, D., (1997). Environmental Survey on Aircraft and Ground-Based Commercial Transportation Vehicles. Prepared by Department of Environmental Health, Harvard University School of Public Health, Boston, MA, for Commercial Airplane Group, The Boeing Company, Seattle, WA. May 31, 1997.
- Stellmack, M., (2010). Microanalytical Techniques for Identifying Nonprotein Contaminants in Biologics. *BioProcess International*, Vol. 8, No. 2, February 2010, pp. 36 – 39.
- U.S. DOT FAA InFO 10019 (2010). U.S. Department of Transportation. [http://www.faa.gov/other\\_visit/aviation\\_industry/airline\\_operators/airline\\_safety/info/all\\_infos/media/2010/Info10019.pdf](http://www.faa.gov/other_visit/aviation_industry/airline_operators/airline_safety/info/all_infos/media/2010/Info10019.pdf) (Cited: 01/4/2012).
- Winder, C. and Balouet, J. C., (2001). Aircrew Exposure to Chemicals in Aircraft: Symptoms of Irritation and Toxicity. *Journal of Occupational Health and Safety – Australia and New Zealand* 17: 471 – 483, 2001.
- Winder, C. and Michaelis, S., (2005). Aircraft Air Quality Malfunction Incidents: Causation, Regulatory, Reporting and Rates. In: Hocking, M. B., (ed.). *Air Quality in Airplane Cabins and Similar Enclosed Spaces. Handbook of Environmental Chemistry Vol. 4, Part H* (2005): 211-228. DOI 10.1007/b107245. Springer-Verlag Berlin Heidelberg, 2005.

# **CHAPTER 3 - USING GAS CHROMATOGRAPHY AND MASS SPECTROMETRY TO DETERMINE JET ENGINE OIL MARKERS IN AIRCRAFT CABIN AIR FILTERS**

## **3.1 Abstract**

The air that is used to pressurize and ventilate an aircraft cabin is the bleed air that comes from the propulsion engine compressor. Under certain conditions, lubricating oil from the compressor bearings can contaminate the bleed air. When this contamination occurs, it has the potential for creating serious air quality issues for the cabin. Of particular concern is tricresyl phosphate (TCP) compound, an additive in synthetic jet engine lubricating oils. The potential for TCP contamination in aircraft engine bleed air has spurred concerns about the risks smoke/fume incidents pose to aircraft cabin occupants. Unfortunately, there are no onboard sensors that can determine the source air quality problems and it is particularly difficult to identify sources after the fact, especially when the problem is intermittent. However, most commercial aircraft are equipped with high efficiency particulate air (HEPA) filters that clean the air that is recirculated in the cabin. These filters capture liquid droplets and solid particulate matter that may be in the cabin air. It is believed that, in the case of oil contamination of the bleed air, this contamination will be present on the cabin filters. The objective of this research was to determine if gas chromatography interfaced with mass spectrometry (GC/MS) can be used to detect the presence of oil or markers of oil in commercial aircraft cabin air recirculation filters when an incident occurs. The actual chemical analysis was conducted by the Environmental and Occupational Health Sciences Institute (EOHSI) at the University of Medicine and Dentistry of New Jersey (UMDNJ). An Agilent series 6890 GC with a 5973 MSD was used to analyze 184 filters removed from a variety of commercial aircraft divided into two groups. The first group consisted of 110 filters that were collected from the aircraft during routine servicing at the end of the normal filter life and are referred to as “used” filters. The second group consisted of 74 filters that were collected from aircraft that were identified as having air quality problems or complaints. They are referred to as “incident” filters. In addition to being a contaminant of health concern, the study hypothesized that TCP in jet engine lubricating oil would be deposited as a contaminant on used aircraft cabin filters and serve as a unique marker of engine oil



contamination. The jet engine oil signatures were identified by matching retention times in chromatograms of the analyzed samples to retention times in mass spectra against standard mass spectra of jet engine oil. The TCP isomers: tri-*m*-cresyl phosphate (TmCP) and tri-*p*-cresyl phosphate (TpCP) were characterized by an  $m/z = 368$  base peak with corresponding retention times of 21.9 and 23.4 minutes. Using retention times,  $m/z$ , and hydrocarbon peak pattern as jet oil fingerprints, five out of 110 used filters tested had oil markers. Meanwhile, 22 out of 74 incident filters tested positive for oil markers. It is concluded that the method can detect and quantify TCP isomers present on aircraft cabin air recirculation filters and use this information to identify lubricating oil as the source of the contamination in some cases. The study demonstrates a new experimental methodology that could have a positive impact on aircraft cabin air quality. Identifying the source of aircraft cabin air quality problems by analyzing recirculation filters could help airlines maintain air quality in line with the needs and goals of the business.

### 3.2 Introduction

Studies by Brown et al. (2001) found that much is already known about many aspects of aircraft cabin air quality however, there are concerns about the potential contamination of aircraft cabin air with engine lubricating oils. The introduction of contaminants such as tricresyl phosphates (TCPs) into aircraft cabin air supply can have damaging in-cabin repercussions and negative consequences for cabin occupants' health. That is why it is critically important that contamination levels of TCPs in aircraft cabin air be correctly identified and controlled. But because of the complexity of the nature of TCPs, detecting them can be a difficult analysis without the proper tools. Most jet engine lubricating oils used in the aviation industry contain TCPs, which are used as a high temperature vapor phase lubricant. Thus, TCP use involves the delivery of lubricant in a gaseous carrier, e.g., air, to the contacting surfaces (Harrison et al. 2008).

TCPs can be absorbed cutaneously, ingested, inhaled, or injected (Yurumez, et al. 2007). The TCP cresols also known as toluols can exhibit up to ten structural isomers. But it usually occurs mainly in the form of three structural isomers: tri-*o*-cresyl phosphate (ToCP), tri-*m*-cresyl phosphate (TmCP), and tri-*p*-cresyl phosphate (TpCP). Figure 3.1 shows the chemical structure of TCP and its three isomers. Many published scientific reports have demonstrated the risks associated with exposure to TCPs. Studies conducted by Abou-Donia (2005) on animals have

shown that dermal exposure to each of the three TCP isomers; ToCP, TmCP, and TpCP, can cause sensorimotor deficits in rats and neuropathological lesions in the brain.

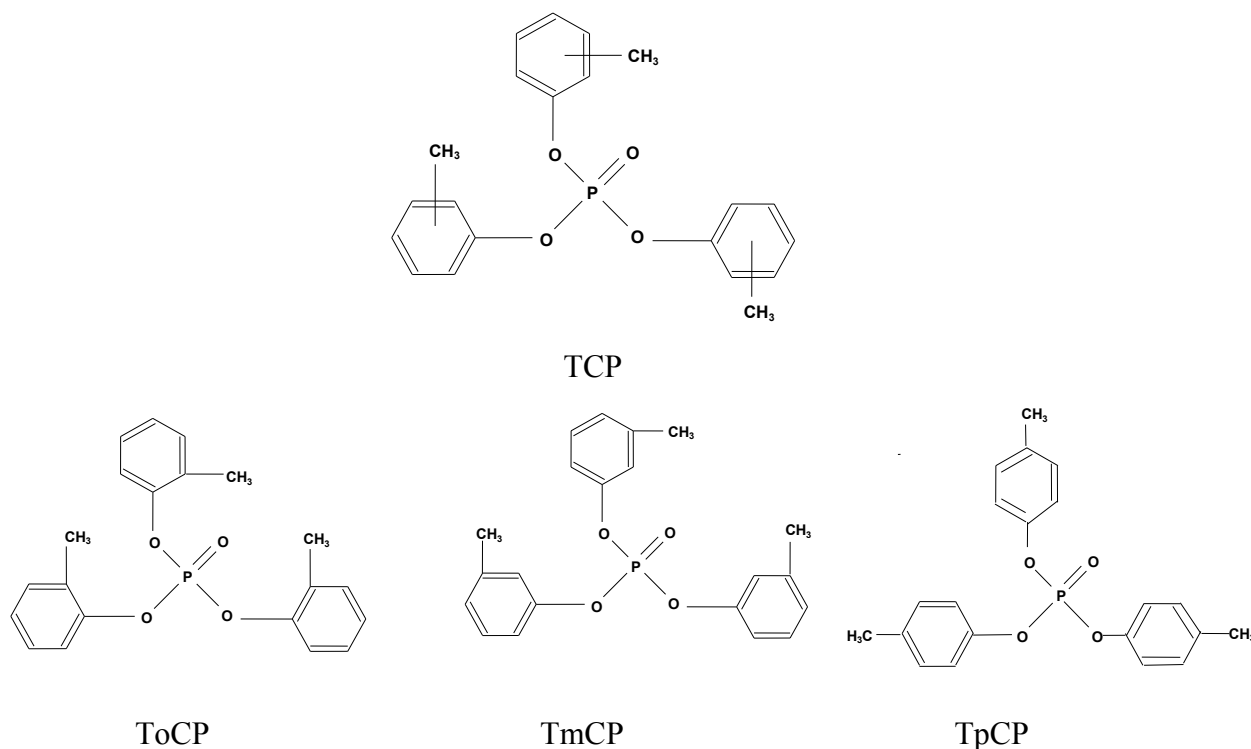


**Figure 3.1 The chemical structure of TCP and its three main isomers**

According to Yurumez et al. (2007), humans exposed to organophosphates (OPs), including TCPs, may rapidly become symptomatic; the onset and severity of symptoms depend on the specific compound, amount, route of exposure, and rate of metabolic degradation. A concentration of TCP isomers of  $100 \mu\text{g}/\text{m}^3$  is currently considered as the standard safe limit but some isomers will cause enzyme damage and limit the production of dopamine in the brain at  $10 \mu\text{g}/\text{m}^3$  (Holt, 2011). The main route by which the general population takes in TCPs is inhalation, i.e. ingestion through the lungs is the easiest method to absorb quantities of OPs. The liver then metabolizes the various isomers in TCP to a cyclic phosphate, which is a known neurotoxin more potent than the most potent TCP isomers. This then binds to the enzyme that enables the production of various neurotransmitters in the brain (Holt, 2011). Studies by Mars et al. (1994) and Somkuti et al. (1988) demonstrated that OP compounds can cause delayed polyneuropathy,

whereas ToCP has weak or absent anticholinesterase effects but can be powerfully neuropathic. A study by Mackenzie et al. (2006) on the possible health implications for pilots breathing contaminated aircraft cabin air has linked certain neurological and respiratory ill health to exposure of contaminated bleed air on commercial and military aircrafts.

TCPs belong to OP triesters, which comprise a broad class of chemical neurotoxins targeting important enzymes such as cholinesterases and various neurotoxic esterases (Viveros et al. 2006). In general, OPs, including TCP irreversibly inhibit the activity of enzymes such as carboxyl ester hydrolases and acetylcholinesterase (AChE) (Pope 1999; Karalliedde 1999). In an attempt to find a bio-marker, Liyasova et al. (2011), analyzed blood from 12 jet airplane passengers and found that butyrylcholinesterase (BChE), an enzyme found in human plasma cholinesterase (primarily in the liver), reacts with ToCP to form phosphorylated BChE. According to Expert Panel on Aircraft Air Quality (EPAAQ) (CASA Report, 2009), tests based on measuring TCP metabolites in blood and/or urine may not be sufficiently sensitive, or able to discriminate exposures to the more neurotoxic compounds (TOCP, DOCP, MOCP and TMPP). The CASA report also noted that that exposure to other potentially toxic components of contaminated cabin air (e.g. O<sub>3</sub>, CO, CO<sub>2</sub>, hydrocarbons) or hypoxia (lack of sufficient O<sub>2</sub>) might be overlooked if the focus was solely on bio-monitoring of OPs. TPC also induces an organophosphorous-induced delayed neuropathy (OPIDN) (Abou-Donia et al. 1990; Hatch 1988; Rosenstock et al. 1991). The constituent product within TCP family that appears to cause most concern is the ToCP isomer, a neurotoxicant that is ten times more toxic than the para- and meta-isomers (Henschler, 1958, Winder and Balouet 2002).

According to an International Programme on Chemical Safety (IPCS) report, the ToCP has significant toxicity and therefore subject to control by regulation (IPCS report, 1990). Thus concerns about TCP toxicity largely focus on the ToCP isomer content (De Nola et al. 2008, Select Committee on Science and Technology, 2000, Craig and Barth, 1999). That is because health problems related to ToCP are more severe than other isomers or esters present in jet engine oils. In spite of the health risks related to TCP, quantitative data on its application in aircraft operations is sparse (Denola et al. 2011). Moreover, in a study intended to present a method to assess exposure to airborne trialkyl and triaryl OPs, Solbu et al. (2007) found that the neurotoxin trimethylolpropane phosphate (TMPP) is also present in jet engine lubricant formulations containing TCP and trimethylolpropane ester (TMPE).

During the past decade, studies have confirmed the presence of TCP in aircraft cabin air. Van Netten and Leung (2002) conducted pyrolysis experiments on jet engine lubricating oil and reported the release of TCPs. They recommended that cabin filters be analyzed for TCP derivatives released during pyrolysis of jet engine oil and hydraulic fluids to determine air quality after incidents. Using thermal-desorption gas chromatography-mass spectrometry (TD/GC/MS), a research group at Cranfield University, UK, has analyzed bleed air samples collected by a portable pump onto sorbent tubes from five different aircraft types in operation and found ToCP, other TCPs, and TBP (Crump et al. 2011). Denola et al. (2011) have also detected ToCP in aircraft cabin air. Solbu et al. (2011) have found OPs in aircraft cabin and cockpit air. The presence of TCPs in the aircraft cabin air supply represents a significant and growing part of the problem of aircraft cabin air quality. Past scientific studies have also detected other VOCs in aircraft cabins. Vapors from organic compounds accumulate in the cabin atmosphere by evaporation from parent substances like oils, paints, adhesives, furnishings, pesticides, disinfectants, cleaning agents, foods, and alcoholic drinks. These VOCs are distributed throughout the aircraft cabin via ECS and in cabin sources. Typical VOCs found in aircrafts cabins include isopropanol, ethanol, propylene glycol, acetone, acetonitrile and insecticides. (Spengler et al. 1997). However, measured concentrations of VOCs in aircraft cabins are generally low (Nagda and Rector, 2003).

When smoke/fume incidents occur they disrupt the performance of critical applications of an aircraft's ECS. As a result, cabin air quality may change, and cabin occupant safety may be at risk. Airborne pollutant emissions during smoke/fume incidents are widely perceived as a main culprit in cabin air contamination and have been implicated in a range of health problems in immune, endocrine, nervous, and reproductive systems of animals and humans. These problems are generally associated with TCP in jet engine oils or hydraulic fluids. The health complications associated with smoke/fume incidents tend to vary. The possible critical health effects of human exposure have been classified as short-term or long-term depending on the length of exposure and the intensity of the smoke/fume incident. Table 3-1 lists some of the reported health symptoms of exposure to smoke/fume incidents (Winder and Balouet, 2001; Michaelis, 2003; Abou-Donia, 1990; Nisse et al. 1998).

**Table 3-1 Health symptoms of long and short-term exposure to smoke/fume incidents**

<b>A. Symptoms from short-term exposure</b>
1. Neurotoxic symptoms: blurred or tunnel vision, nystagmus, disorientation, shaking and tremors, loss of balance and vertigo, seizures, loss of consciousness, parathesias;
2. Neuropsychological symptoms: memory impairment, headache, light-headedness, dizziness, confusion and feeling intoxicated;
3. Gastro-intestinal symptoms: nausea, vomiting;
4. Respiratory symptoms: cough, breathing difficulties (shortness of breath), tightness in chest, respiratory failure requiring oxygen;
5. Cardiovascular symptoms: increased heart rate and palpitations;
6. Irritation of eyes, nose, and upper airways.
<b>B. Symptoms from long-term exposure</b>
1. Neurotoxic symptoms: numbness (fingers, lips, limbs), parathesias;
2. Neuropsychological symptoms: memory impairment, forgetfulness, lack of co-ordination, severe headaches, dizziness, sleep disorders;
3. Gastro-intestinal symptoms: salivation, nausea, vomiting, diarrhea;
4. Respiratory symptoms: breathing difficulties (shortness of breath), tightness in chest, respiratory failure, susceptibility to upper respiratory tract infections;
5. Cardiovascular symptoms: chest pain, increased heart rate, and palpitations;
6. Skin symptoms: skin itching and rashes, skin blisters (on uncovered body parts), hair loss;
7. Irritation of eyes, nose, and upper airways;
8. Sensitivity: signs of immuno-supression, chemical sensitivity leading to acquired or multiple chemical sensitivity.

(Source: Winder and Balouet, 2001; Michaelis, 2003; Abou-Donia, 1990; Nisse et al. 1998; Holt, 2011).

There has been consistent evidence that aircrew experience a variety of specific medical conditions both acute and chronic associated with work in the airline industry. However, according to CASA report (2009), the evidence for the existence of an ‘Aerotoxic Syndrome’ related to smoke/fume events is still based almost entirely on case-series reviews, remains self-reported and should be categorized epidemiologically as inadequate or insufficient evidence to determine whether an association exists. The panel that compiled the CASA report further noted

that “this view is based on the lack of adequately designed studies and the difficulties inherent in undertaking such studies rather than on the presence of evidence of no association.” In spite of the advanced science and technology that supports the civil aviation industry smoke/fume incidents are still not fully understood. Much uncertainty revolves around how much harm can be done by smoke/fume generated during incidents. While it is not clear exactly how much can cause adverse reactions, it is known that smoke/fumes from incidents contain TCPs, which can affect human health adversely. Human health effects related to exposure to TCP and its isomers in workplaces have been investigated. The standards that specify the emission limit of exposure to TCPs emitted from industrial processes have been specified. However, how airborne particulates and TCPs formed in aircraft bleed air system during smoke/fume incidents affect cabin air quality still needs to be understood. In short, the threshold at which TCP aerosols in cabin air will cause undesirable effects on human health still needs to be determined. The risks related to smoke/fume incidents need to be identified, managed, and communicated. Consequently, the ability to monitor cabin air quality needs to be improved.

Even though the potential safety issues of exposure to smoke/fumes from jet engine oils are generally known, airlines still use jet engine oils with TCP additives because of their wide spectrum of activity and ready availability at a low cost. Moreover, no other additive has been found to match TCP's anti-wear and load carrying performance (Select Committee on Science and Technology, 2000), making it still appealing even though a study by Winder and Balouet (2002) confirmed that it contains at least two ingredients hazardous to human health: TCPs and *N*-phenyl-1-naphthylamine. Mobil Jet Oil II, the most popular jet engine oil used in commercial and military airplanes was used as representative jet engine oil for this study. The purpose of this study was to provide a method for determining jet engine oil markers or signatures on aircraft cabin air recirculation filters using GC/MS analysis. This part of study focused on identifying three TCP structural isomers (ortho-, para-, and meta-) and their concentrations in used and incident aircraft filters using GC/MS.

### **3.3 Materials and Methods**

#### **3.3.1 Filter sampling**

For filter sample preparation, the general procedure described in Chapter 2 was adopted for preparing filter samples for analysis using GC/MS. The clean room at the IER is about 97%

efficient at collecting airborne particulate matter. The air circulation system to the room is fitted with both HEPA and electrostatic filters that keep airborne particulates down to 2648 counts/m<sup>3</sup>. The air-circulation system in the room was turned on and ran for about 10 minutes to reach a steady state. The boxes containing the filters were moved one at a time from the closet to the clean room and sampled. Once the boxes were cut open, they were immediately removed from the clean room. The filters, wrapped in a plastic bag, were placed on a table covered with aluminum foil. At this point, the person performing the sampling put on sterilized plastic gloves and a dust mask. All the tools used in disassembling filters and cutting out specimens were wiped with isopropyl alcohol. A sheet metal snip was used to cut the outer aluminum casing and separate it from the filter. A whole panel of filter, as shown in Figure 3.2 (b), was cut and placed in an 18 × 24 in. zip-locked plastic bag and shipped for GC/MS analysis.

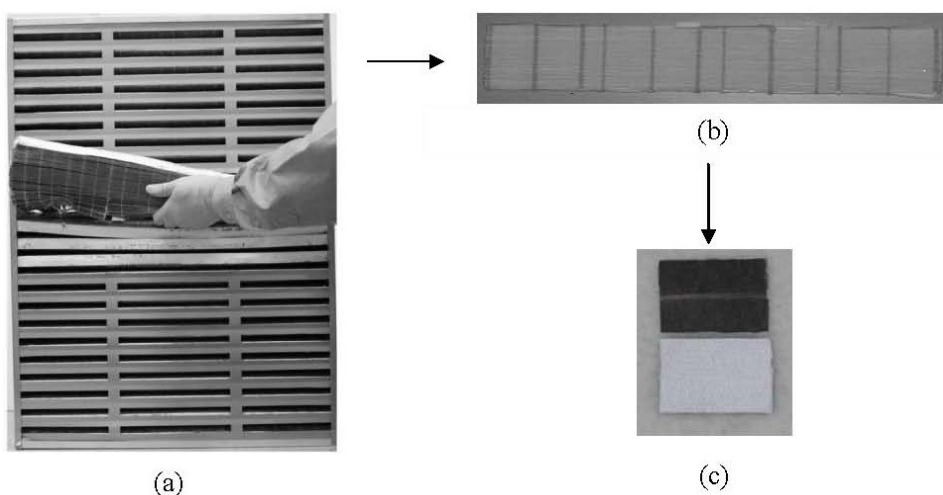


**Figure 3.2 (a) Filter sampling process (b) Filter panel (c) Filter sample for GC/MS analysis**

The filter was then returned to a plastic bag which it came from and shut, taped and returned to the storage cabinet. Samples of Mobil Jet Oil II aviation jet turbine lubricating oil were also analyzed using the GC/MS method and the spectra examined. Clean filters used in the study were acquired from three well-known major aircraft cabin air recirculation filter manufacturers: Keddeg Company, Pall Aerospace Incorporation, and Donaldson Company Incorporation. A total of 90 incident filters were analyzed. All tested filters were supplied anonymously by four U.S. airline companies.

### 3.3.1 Principle operation of GC/MS

The GC/MS instrument separates chemical mixtures and identifies the components at a molecular level. The GC works on the principle that a mixture will separate into individual chemical compounds when heated. The heated gases are carried through a column with an inert gas (such as helium). As the separated substances emerge from the column opening, they flow into the MS where the chemical compounds in the mixture are identified by the mass of the analyte molecule. A library of known mass spectra, covering several thousand chemical compounds stored on a computer is used for comparison with spectral information against the unknowns using retention times and mass ion ratio to achieve accurate identification.

### 3.3.1 Analysis of used aircraft filters by Agilent Series 6890 GC with 5973 MSD

An Agilent series 6890 GC with a 5973 MSD was used to investigate used and incident filter samples extracted from cabin air recirculation filters. Figure 3.3 below shows the picture of 6890 GC/MS model with 5973 MSD.



**Figure 3.3 Hewlett Packard (HP) Agilent series 6890 GC/MS system with 5973 MSD**

Source: American Laboratory and Trading (AHT, 2012).

The Agilent GC/MS has an Agilent 6890 network gas chromatography system with split/splitless inlet is configurable with; Agilent 5973 inert mass selective detector with electron



impact (EI) Source; Agilent 7683 series autosampler; and Agilent 7683 series injector; Agilent 59864B ionization gauge controller; Edwards 1.5 vacuum pump, and cables, mouse, keyboard, monitor, computer preloaded with software (AHT, 2012). The 6890 Plus delivers high levels of performance with electronic pneumatic controls of all gas flow and pressures. Built-in sensors automatically compensate for ambient changes in temperature and barometric pressure differences to reach more accurate and reproducible results. (AHT, 2012).

### **3.3.2 Procedures for preparation of standard solution for GC/MS analysis**

The GC/MS is a qualitative chemical analysis of VOCs on filters. GC/MS successfully focused on analyzing multiple chemical compounds on used filters to detect concentrations ranges of jet engine oil footprints. With GC/MS analysis, the investigation focused on the concentration of well-known ingredients from Mobil Jet Oil II. Therefore, an entire panel of filter was placed in a solvent, and the extract analyzed. In GC/MS analysis, selecting appropriate sample preparation techniques allows reproducibility, accuracy, and simplicity.

Concentration of standard was injected in the low nanogram per microliter range. Recovery was determined by spiking clean filters with 2.0  $\mu\text{g}/\text{mL}$  of each standard analyte. The standard was then used to identify and quantify the peaks of the compounds present in the spiked clean filters. The recovery levels were as follows: Pure samples were injected in amounts of 1.0  $\mu\text{L}$  to the GC/MS. The column was 30 m long, 0.25 mm (0.01 in.) in diameter and was filled with helium carrier gas. The carrier gas flow rate was set at 1.5  $\text{mL min}^{-1}$ , and the temperature was regulated to 100°C for 10 minutes and then to -20°C to 250°C for 10 minutes.

First, a 50  $\text{cm}^2$  sample was cut out from the filter. Specimens were placed in 40 mL vials, and 10 mL methylene chloride ( $\text{CH}_2\text{Cl}_2$ ) solvent was added to each vial. The mixture was then sonicated for 20 minutes. During sonication, the solvent extracted the organic substances deposited on the filter sample. The extract was filtered using a 13/25 mm (0.2/0.45  $\mu\text{L}$ ) syringe filter. The extract was then evaporated to 0.5 mL. A 1.0  $\mu\text{L}$  aliquot was injected into the gas chromatograph port of the GC/MS instrument operated in the electron impaction mode and run in the SIM mode at 368 amu, which is sensitive to TCP. The chromatography used was a 30 m  $\times$  0.25 mm  $\times$  250  $\mu\text{m}$  column with helium as the carrier gas flowing at 1.5 mL/min. The second injection was done with the GC/MS instrument operated in the SCAN mode to confirm the peak identification of the TCP and the synthetic hydrocarbon analysis, key constituents of the Mobil

Jet Oil II. Quantitation was performed with a calibration curve made from standards of target compounds (1-20 ng/ $\mu$ L) run under similar conditions. The compounds of interest (jet engine oil signatures) were identified by matching of retention times in chromatograms of the analyzed samples to retention times in mass spectra against a standard. Quantitation used a calibration curve made using standards of target compounds (1-20 ng/ $\mu$ L) run under similar conditions. Co-elution of other congeners could not be excluded, so identification and quantification, especially of congeners present in small amounts, remains to be confirmed. Microsoft Excel was used to compute descriptive statistics and concentrations of identified TCPs in used and exposed filters.

### **3.4 Analysis, Results and Discussion**

#### **3.4.1 Data analysis**

The concentration levels of known ingredients used in formulating Mobil Jet Oil II were investigated by analyzing concentrations levels of TCP and its isomers in incident filters. Comparisons of incident filter data and spectra were made with data and spectra obtained from Mobil Jet Oil II and clean filter samples. Mass spectral libraries (databases) of validated chemical compounds were used to compare spectra and compound identification information against the unknowns to achieve accurate results. GC/MS is a relative technique; measured sample values are compared to a previously conducted calibration. Therefore, the quality of GC/MS measurements depends upon the reference materials and the stability of the entire system. To ensure that stability, the procedure management software delivers quality control and qualification of the GC/MS analyses with the highest levels of stability, accuracy, and user-friendliness. Positive identifications were made by matching retention times as well as mass spectra against a library. Quantification was done using a calibration curve made from standards of target compounds run under similar conditions. A pattern of key peaks similar to Mobil Jet Oil II were observed. The compounds are TMP phosphate, TmCP, TpCP, and unknown isomers. Microsoft Excel was used to calculate descriptive statistics for TmCP concentrations (ng/cm<sup>2</sup>) in used and incident filters.

### 3.4.2 Results and discussion

Good separations of the standards were obtained. The match of mass spectra to library mass spectra was quite evident. From the standard, the peak identification codes and retention times of 22.4, 21.9 and 23.4 min. for o-TCP, m-TCP and p-TCP respectively were observed. Blank filters (clean filter recovery study): The unused filters had no detectable levels of cresyl phosphate and no other forms of TCP or jet oil related compounds were found. The peaks and background present were hydrocarbons expected from glue used to hold filter paper together.

The TCP peaks and the hydrocarbon were evaluated as potential markers for jet engine lubricating oil on the filter as follows: TCP was first examined in the jet engine oil sample. Four peaks were present at nominal retention times of 21.5, 22.4 and 23.4 min. for the GC conditions used in the study. These peaks correspond to hydrocarbon TMP, m-TCP, p-TCP. Peaks were identified by matching retention times and ion fragment pattern, particularly the presence of ions at 107, 165, 184 and 198. Other compounds do co-elute with these peaks, including the 368 amu ion, so a spectrum subtraction was done to confirm each peak and each mass spectrum reviewed. Synthetic hydrocarbons were present in the jet engine oil sample with 8 peaks present in jet oil from KSU starting at retention times in 20.5-minute range for the conditions used. The mass spectra pattern for the hydrocarbons typically had a base peak at 85amu and strong ion fragments at 113 and 91, as well as additional ions at 127 and 156, without the classic fragmentation patterns associated with the cleavage of CH<sub>2</sub> groups.

To mark a filter as having TCP present, (marked as “yes”) at least two of the three TCP isomers had to be identified in the chromatogram. If two or all three were present in relatively high concentrations then clearly they were from jet engine oil and. The TmCP isomer was present in most samples (but not in the blanks), but that isomer can come from sources other than jet engine oil. Thus, even a high concentration was not sufficient to conclude that jet engine oil was the source. If two isomers were present at very different concentrations the filter was marked ‘maybe’. A peak at 22.4 minute was considered likely to be from jet engine oil when it was very large and accompanied by later eluting peaks with mass spectra consistent with TCPs. The GC runs were stopped at 30 minutes, so evaluating the data for the presence of later eluting compounds was not possible. Some chromatograms were obtained from used filters; tables showing TCP isomers’ concentrations in used and some incident are shown in Appendix B: Tables B.1 and B.2 respectively.

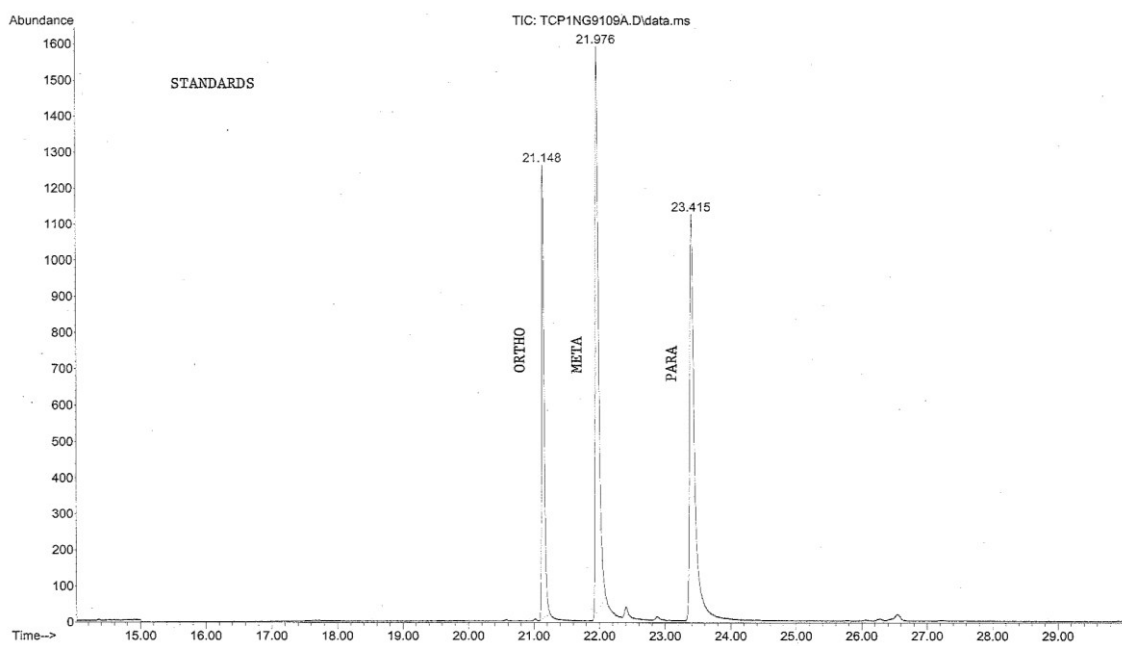
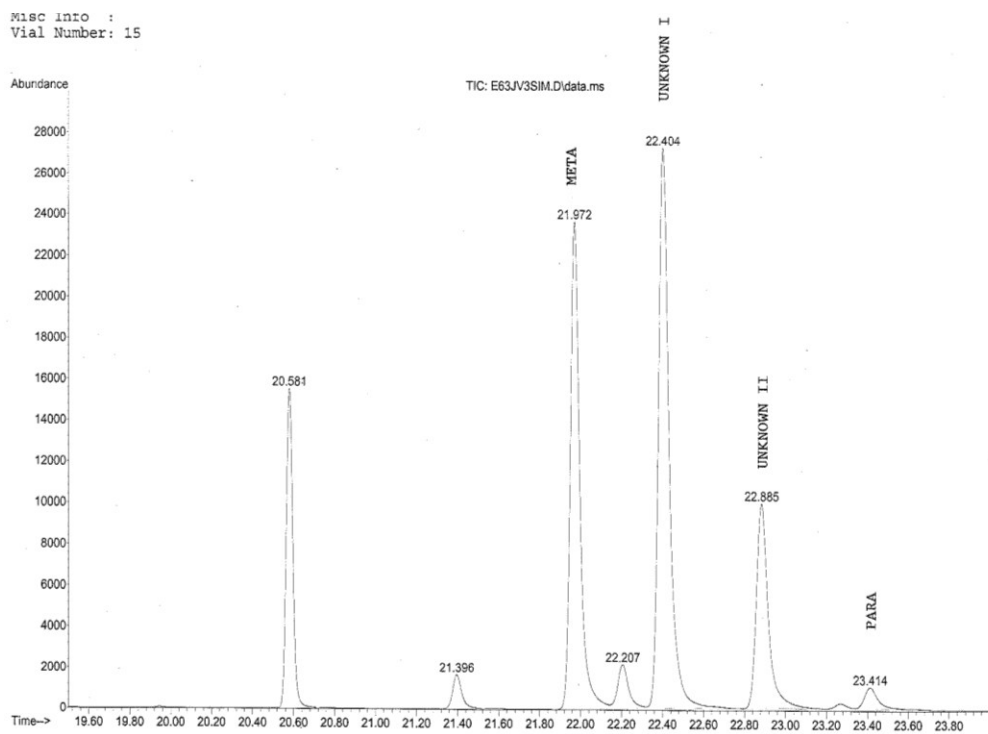
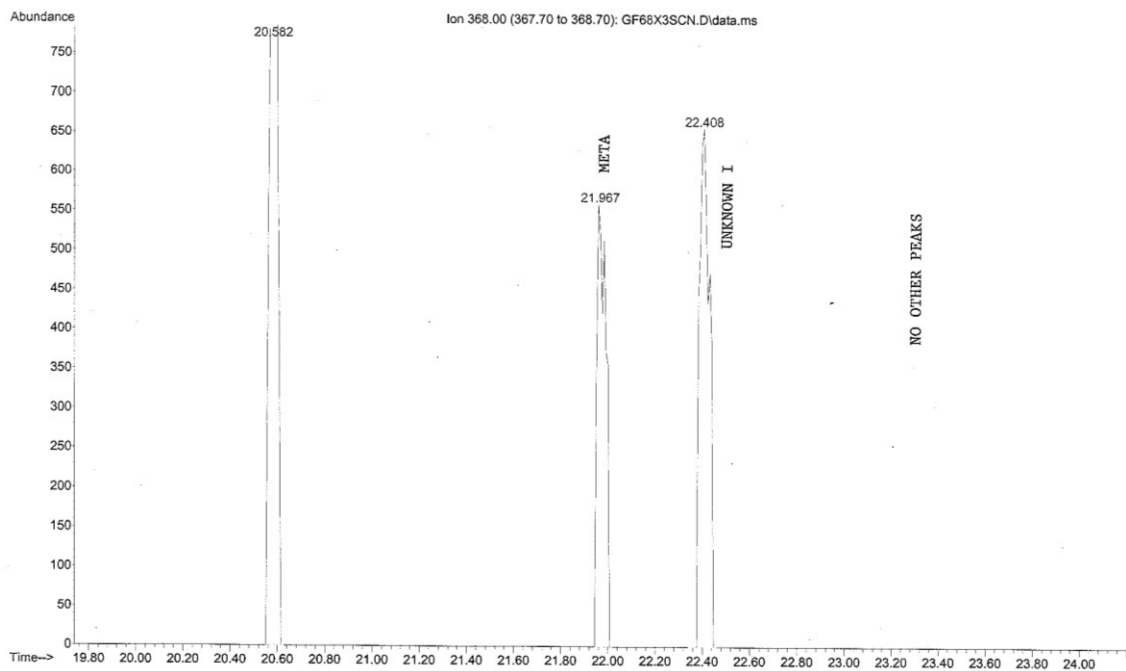


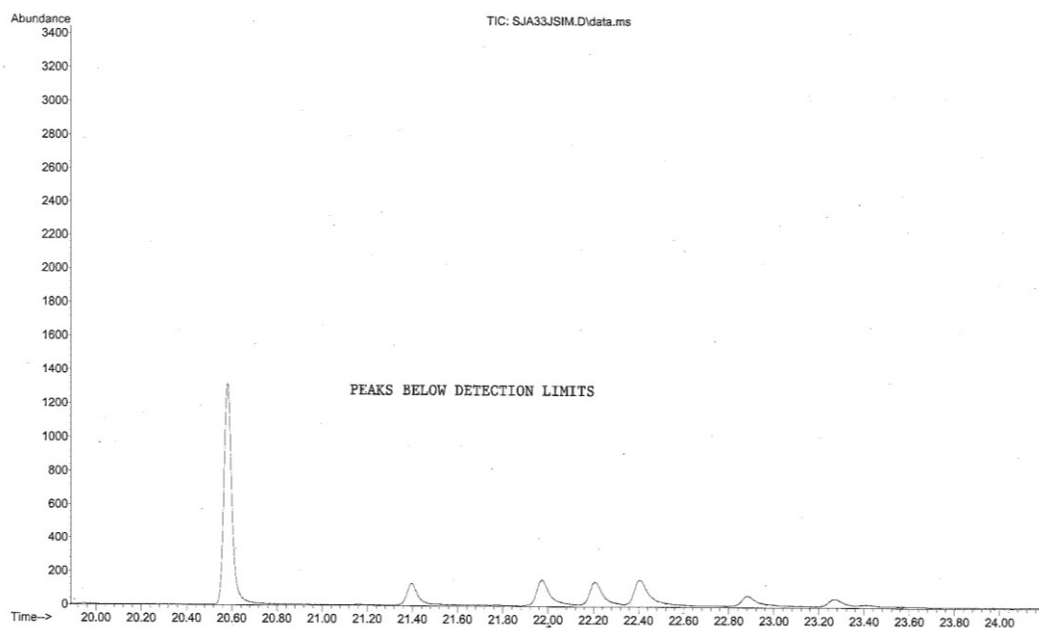
**Figure 3.4 GC/MS spectrum of standard solution**



**(a) Used filter ID E63JV3**

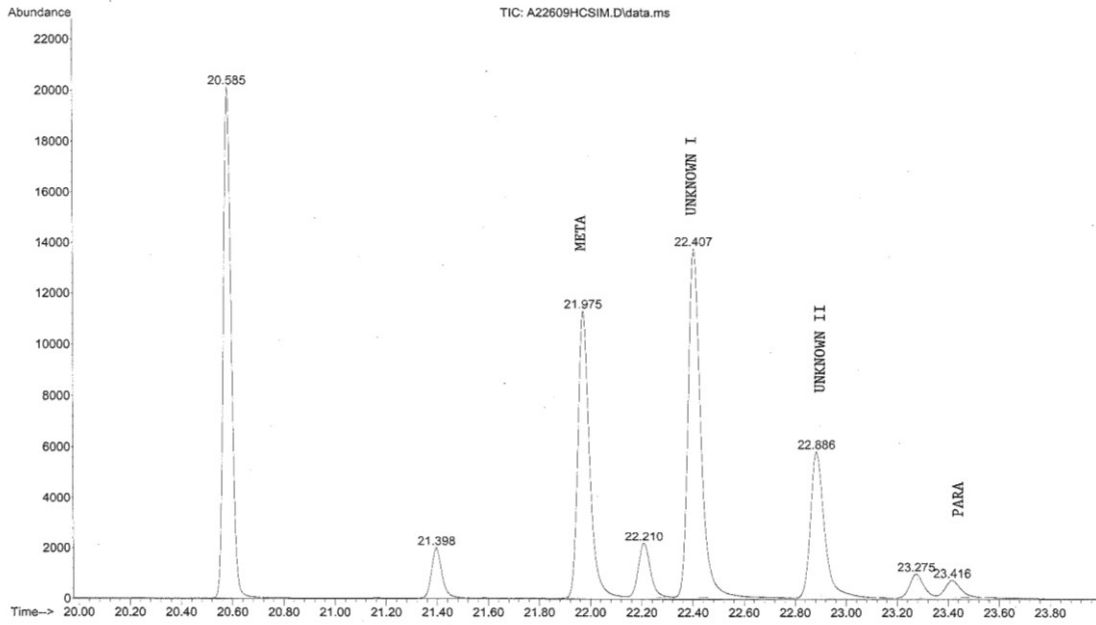


(b) Used filter ID GF68X3

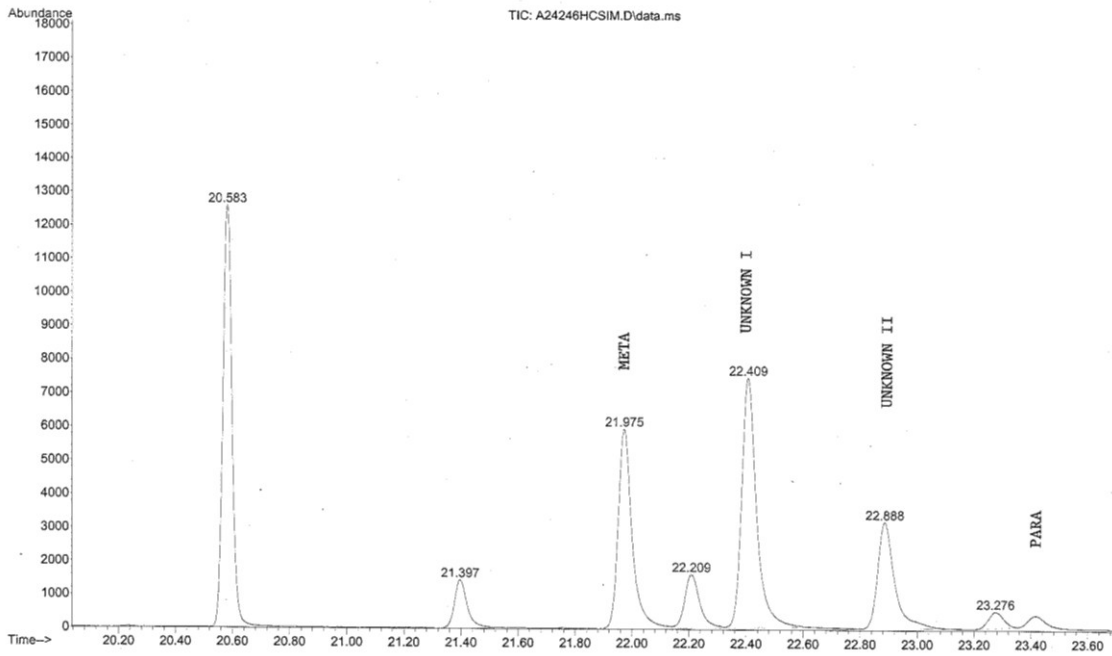


(c) Used filter ID SJA33J

Figure 3.5 Spectra of used filters: (a) ID E63JVE (b) ID GF68X3 and (c) ID SJA33J with peaks below detection levels



(a) Incident Filter ID A22609HC



(b) Incident filter ID A24246HC

**Figure 3.6 Spectra of incident filters (a) ID A22609HC and (b) A24246HC**

**Table 3-2 Descriptive statistics for TmCP and TpCP in used and incident filters**

Filter Category	TCP Isomer	Sample Size (N)	Arith. mean	Geom. Mean	Median	Range	Std. Deviation	Coeff. of variation	Std. error of mean	95% conf. inter.	Upper 95% conf. limit	Lower 95% conf. limit.
Used	TmCP	108	10.82	14.50	5.86	251.70	26.33	2.43	2.52	5.02	15.85	5.80
	TpCP	108	0.69	0.00	0.00	26.80	2.87	4.17	0.28	0.55	1.24	0.14
Incident	TmCP	66	25.82	19.60	11.20	366.40	52.26	2.02	6.43	12.85	38.67	12.97
	TpCP	66	1.61	0.00	0.00	25.20	3.96	2.46	0.49	0.97	2.8	0.63

Descriptive statistics parameters for TmCP and TpCP in both categories of filters are different.

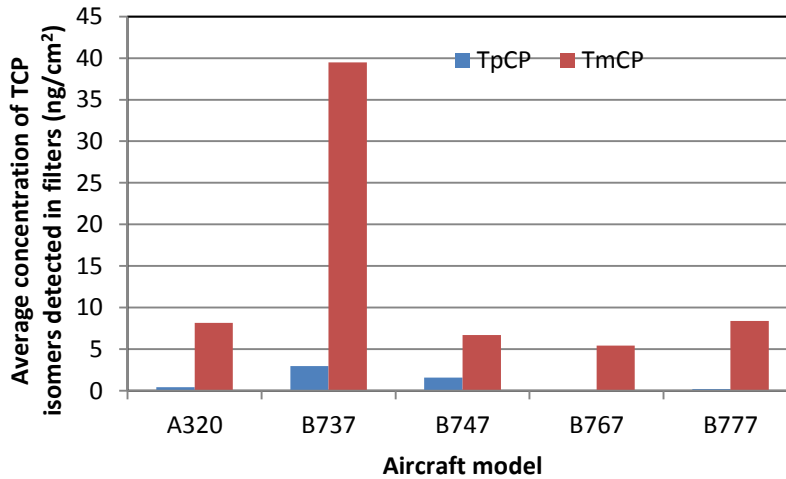


**Figure 3.7 Histograms of mean concentration of TCP isomers detected in used filters**

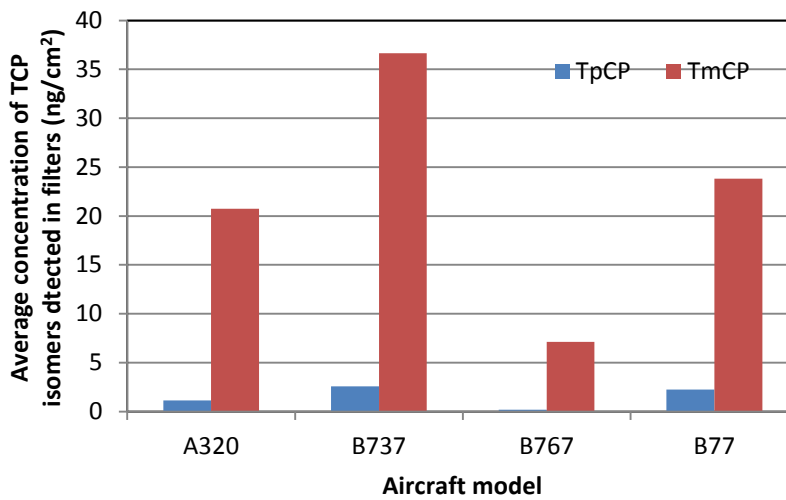


**Figure 3.8 Histograms of mean concentrations of TCP isomers detected in incident filters**

### ***3.4.2.1 Discussion***

Comparing of chromatograms and data obtained from Mobil Jet Oil II with those from incidents and used filters indicate that GC/MS is an effective technique for detecting TCP isomers on airline cabin air filters. Overall, GC/MS analysis results suggest that not all analyzed used filters showed the presence of TCP isomers. Without doubt, jet engine oils with additives ensure that the jet engines function efficiently, but those additives are not friendly to human health. The economics of using jet engine lubricating oil are significant: the consequences are catastrophic if engine failure occurs. However, all known facts about TCP toxicity, means the use of jet engine lubricating oil in aircraft operations must be reinvented; the status quo is unsustainable. The study has established a firm link between incident-occurrences and detection method: GC/MS. The investigation has offered a riveting demonstration of the presence of TCP isomers on used aircraft filters which implies that these compounds are airborne and can only reach the filters through cabin air supply originating from the bleed air. Currently, the performance of aircraft engine types cannot be linked to concentration of TCPs. The identifying, managing and communicating any performance factor linked to cabin air quality incidents could help establish if correlations exist between aircraft engine operation conditions and smoke/fume incidents.

Specifically identifying each isomer of TCP using GC-MS is difficult as it is necessary to have a standard specimen of each pure isomer to properly calibrate the instrument used for the measurements. In practical applications, these standard specimens are not likely to be readily available (B. W Jones, personal communication). Additionally, the exact formulation of TCP in jet oil may vary over time and amongst oil brands. Thus, the characteristic composition for jet oil used in this study is not necessarily accurate for a future application. For these reasons in future applications of this method, a specimen of jet oil from the potential source should always be analyzed along with filter specimens if TCP is to be used as a marker for oil. This oil then effectively becomes a “standard.” That is, it is not necessary to associate each TCP peak in the chromatograph with a specific isomer. Rather, the important consideration is that the TCP peaks seen on the filter correspond to the peaks seen for the jet oil and that the concentration ratios seen on the filters correspond to the concentration ratios seen in the oil. The peaks and concentration ratios identified in this study are not necessarily the ones that would apply in a given application.



### **3.4.3 Recommendations**

Since the TCPs detected on the filters must have been airborne and carried by the cabin air supply to the filters, further studies are recommended to create a database that would help in developing TCPs standards for aircraft cabin environment. With such a database, airlines can reliably assess air quality parameters associated with incidents. Further studies should screen for the presence of other isomers not identified by this study.

### **3.5 Conclusions**

The GC/MS procedure has been developed to determine the presence of jet oil markers in used aircraft filters. Of those 177 filters analyzed, 32 incident and 14 used filters showed the presence of TCPs and hydrocarbon compounds. The findings do support the possible use of cabin air recirculation filter analysis to determine a jet engine oil marker for air contamination by airborne particulates generated during smoke/fume events. The method can be used to monitor incidents by analyzing filters that have been exposed to smoke/fume incidents. The technique could also be useful in investigating oil contamination in a variety of aircraft components. This study will also help increase the understanding of the nature of other volatile hazardous chemical compounds that exist in the bleed air system so that appropriate regulations governing air quality in aircraft cabins can be enacted.

### **3.6 References**

- Abou-Donia, M., (2005). Proceedings of the Contaminated Air Protection Conference Proceedings of the BALPA Air Safety and Cabin Air Quality International Aero Industry Conference. Held at Imperial College, London, 20-21 April 2005.
- Abou-Donia, M. B., Lapadula, D. M., (1990). *Ann. Rev. Pharmacol. Toxicol.*, 30, 405 (1990).
- American Laboratory and Trading. ALT Inc © 2011 (2012).  
[http://www.usedlabequipment.com/lab\\_equipment/HP+Agilent+6890+GC+MS+System+w+5973+MSD\\_17953.php](http://www.usedlabequipment.com/lab_equipment/HP+Agilent+6890+GC+MS+System+w+5973+MSD_17953.php). (Cited: 4<sup>th</sup> May, 2012).
- Brown, T. P., Shuker, L. K., Rushton, L., Warren, F. and Stevens, J., (2001). The possible effects on health, comfort and safety of aircraft cabin environments. *The Journal of The Royal Society for the Promotion of Health*. September 2001, 121 (3), pp. 177–184.  
<http://rsh.sagepub.com/content/121/3/177.full.pdf> (Cited: April 15<sup>th</sup>, 2012)

- Bull, K., and Roux, P., (2010). Cabin Air Filtration Systems – Novel technological solutions for commercial aircraft. 40<sup>th</sup> International Conference on Environmental Systems. American Institute of Aeronautics and Astronautics. AIAA 2010-6291.
- Australian Civil Aviation Safety Authority (CASA). Expert Panel on Aircraft Air Quality (EPAAQ) (2009). Contamination of aircraft cabin air by bleed air – a review of the evidence. [http://www.casa.gov.au/wcmswr/\\_assets/main/cabin/epaaq/epaaq-entire-report.pdf](http://www.casa.gov.au/wcmswr/_assets/main/cabin/epaaq/epaaq-entire-report.pdf)
- Craig, P. H., and Barth, M. L., (1999). Evaluation of the hazards of industrial exposure to tricresyl phosphates: A review and interpretation of the literature. *Journal of toxicology and Environmental Health, Part B, Critical reviews*. Vol. 2 (4) pp. 281-300.
- Crump, D., Harrison, P. and Walton, C., (2011). Aircraft Cabin Air Sampling Study; Part 2 of the Final Report, Institute of Environment and Health, Cranfield University, April 2011. <https://dspace.lib.cranfield.ac.uk/handle/1826/5306> (Cited: November 24<sup>th</sup>, 2011).
- De Nola, G., Kibby, J. and Mazurek, W., (2008). Determination of *ortho*-cresyl phosphate isomers of tri-cresyl phosphate used in aircraft turbine engine oils by gas chromatography and mass spectrometry. *Journal of Chromatography A*, 1200 (2008) 211 – 216.
- De Nola, G., Hanhela, P. J. and Mazurek, W., (2011). Determination of Tricresyl phosphate Air Contamination in Aircraft. *Ann. Occup. Hyg.* Vol. 55. No. 7, pp. 710-722, 2011. Oxford University Press on behalf of the British Occupational Hygiene Society. doi:10.109/annhyg/mer040.
- Hanhela, P. J., Kibby, J., DeNola, G., and Mazurek, W., (2005). Organophosphate and Amine Contamination of Cockpit Air in the Hawk, F-111 and Hercules C-130 Aircraft. Australian Government Department of Defence. Published by DSTO Defence Science and Technology Organisation, Victoria 3207 Australia.
- Hatch R. C. (1988). Poisons causing nervous stimulation or depression. In N.H. Booth and L.E. McDonald (Eds.), *Veterinary Pharmacology and Therapeutics*, Iowa State University Press, Ames, IA, pp. 1053 (1988).
- Henschler, D., (1958). Tricresylphosphate poisoning; experimental clarification of problems of etiology and pathogenesis. *Klin Wochenschr* 1958; 36:663-74.
- Holt, G. C. (2011). A conference most revealing: aircraft cabin air quality. *Journal of Biological Physics and Chemistry* 11 (2011) 216–220 © 2011 Collegium Basilea & AMSI doi: 10.4024/22HO11A.jbpc.11.04.
- International Programme on Chemical Safety (IPCS) Report on Environmental Health Criteria 110:Tricresyl Phosphate. (1990). <http://www.inchem.org/documents/ehc/ehc/ehc110.htm#PartNumber:2>. (Cited: August 20<sup>th</sup>, 2010).

- Karalliedde, L., (1999). Organophosphorus poisoning and anaesthesia. 54: 1073 – 1088.
- Liyasova, M., Li, B., Schopfer, L. M., Florian Nacho, F., Masson, P., Furlong, C. E., Lockridge, O., (2011). Exposure to tri-o-cresyl phosphate detected in jet airplane passengers. *Toxicology and Applied Pharmacology*. 256 (2011) 337-347.
- Michaelis, S. (2003). A survey of health symptoms in BALPA Boeing 757 pilots. *Journal of Occupational Health and Safety - Australia and New Zealand* 19(3): 253 – 261.
- Nagda, N. L. and Rector, H. E., (2003). A critical review of reported air concentrations of organic compounds in aircraft cabins. *Indoor Air* 2003; 13: 292 – 301. ISSN 0905-6947.
- Nisse, P., Forceville, X., Cezard, C. C., Ameri, A., Mathieu-Nolf, M., (1998). Intermediate syndrome with delayed distal polyneuropathy from ethyl parathiol poisoning. *Veterinary and Human Toxicology*, 40: 349 – 52.
- Pope, C. N., (1999). Organophosphorous pesticide: do they have the same mechanism of toxicology? *J. Toxicol. Environ. Health*, 2:161 – 181.
- Rosenstock, L., Keifer, M., Daniell, W. E., McConnell, R. and Claypoole, K., (1991). *Lancet*, 338, 223 (1991).
- Spengler, J., Burge, H., Dumyahn, T., Muilenberg, M. and Forester, D., (1997). Environmental Survey on Aircraft and Ground-Based Commercial Transportation Vehicles. Prepared by Department of Environmental Health, Harvard University School of Public Health, Boston, MA, for Commercial Airplane Group, The Boeing Company, Seattle, WA. May 31, 1997.
- Solbu, K., Thorud, S., Hersson, M., Ovrebø, S., Ellingsen, D. G., Lundanes, E. and Molander, P., (2007). Determination of airborne trialkyl and triaryl organophosphates originating from hydraulic fluids by gas chromatography-mass spectrometry. Development of methodology for combined aerosol and vapor sampling. *J. Chromatogr A*, 1161 (1-2): 275 – 83. Epub 2007 Jun 2.
- Solbu, K., Daae, H. L., Olsen, R., Thorud, S., Ellingsen, D. G., Lindgren, T., Bakke, B., Lundanes, E. and Molander, P., (2011). Organophosphates in aircraft cabin and cockpit air – method development and measurements of contaminants. *J. of Environ. Monit.*, 2011, 13, 1393 – 1403. [www.rsc.org/jem](http://www.rsc.org/jem)
- Select Committee on Science and Technology (2000). Science and Technology - Fifth Report. House of Lords, UK.  
<http://www.publications.parliament.uk/pa/ld199900/ldselect/ldsctech/121/12107.htm>.  
 (Cited 01/07/2012).

- Van Netten, C. and Leung, V., (2000). Comparison of the constituents of two jet engine lubricating oils and their volatile paralytic degradation products *Appl. Occup. Environ. Hyg.* 15(3): 277 – 283.
- Van Netten, C., (1998). Air quality and health effects associated with the operation of BAE 146-200 aircraft. *Applied Occupational & Environmental Hygiene*, 13(10): 733 – 739.
- Viveros, L., Paliwal, S., D. McCrae, D., Wild, J., Simonian, A., (2006). A fluorescence-based biosensor for the detection of organophosphate pesticides and chemical warfare agents. *Sensors and Actuators B* 115 (2006) 150 – 157.
- Winder, C., and Balouet, J. C., (2002). The Toxicity of Commercial Jet Oils. *Environmental Research Section A.* (89): 146 – 164. Dio:1006/enrs.2002.4346.
- Winder, C., and Balouet, J. C., (2001). Aircrew Exposure to Chemicals in Aircraft: Symptoms of Irritation and Toxicity. *Journal of Occupational Health and Safety – Australia and New Zealand* 17: 471 – 483, 2001.
- Yurumez, Y., Durukan, P., Yavuz, Y., (2007). Acute organophosphate poisoning in university hospital emergency room patients. *Intern Med.* 2007; 46(13):965 – 9.

# CHAPTER 4 - NEUTRON ACTIVATION ANALYSIS (NAA) OF COMMERCIAL AIRCRAFT CABIN AIR RECIRCULATION FILTERS

## 4.1 Abstract

The lack of air quality monitoring in the bleed air systems of civil aircraft means unsuspecting cabin occupants may be exposed to a cabin air supply contaminated with smoke/fumes from jet engine lubricating oil. Jet engine lubricating oil, though necessary for aircraft engine operations, poses certain safety hazards if it contaminates the engine bleed air used for pressurizing and ventilating aircraft. The magnitude of the threat posed by smoke/fumes incidents is not known. Furthermore, scientists are unsure of the scope of the problem. This study focuses on using neutron activation analysis (NAA) for monitoring cabin air quality for jet engine oil contamination by analyzing aircraft cabin air recirculation filters. The objective of this part of the research was to analyze used aircraft cabin air filters to determine if elements from jet engine oils contaminating the filters could be detected. Duplicate samples from 200 cabin filters removed from aircraft and from clean – unused filters were analyzed. One hundred and ten of the filters were removed from aircraft during routine servicing at the end of normal filter service life. These filters were designated as “used” filters in this study and were from aircraft not known to have had air quality incidents or related problems. Ninety of the filters were removed from aircraft identified as having air quality issues and are designated as “incident” filters in this study. All of the filter samples were irradiated in a TRIGA MARK II reactor. The high-purity germanium (HPGe) detector coupled with GENIE 2K software was used to analyze gamma-rays emitted from irradiated filters samples. The jet engine oil was also irradiated, and the results of that investigation compared to used, incident, and clean filters. Data obtained from irradiated used, incident, and clean filters and jet engine oil samples were analyzed by SAS software to determine the elements from jet engine oil that might be considered as contaminants in used and incident filters. The analysis also compared the concentration of isotopes of elements in used and incident filters to determine any differences between them. Based on the analysis of the experimental data, the jet engine oil markers in used aircraft filter could not be determined. However, traces of a wide range of elements were detected, including Ag, Ar, As, Au, Ba, Be,

Bi, Cd, Ce, Cr, Cs, Fe, Ga, Gd, Hf, Hg, In, Ir, K, Kr, La, Lu, Mo, Na, Nb, Nd, Ni, Os, Pa, Pb, Pm, Rb, Re, Ru, Sb, Sc, Se, Sn, Sr, Ta, Tb, Tc, Te, Th, W, Xe, Yb, and Zr. Statistical analysis by one way ANOVA using SAS code PROC GML revealed statistically significant differences in the concentrations of some isotopes from the used and incident filters. Therefore, further investigation should verify the findings to ascertain the suitability of this technique for detecting jet engine oil on aircraft cabin filters. Background isotopes must be clearly determined to remove them from the analysis.

## **4.2 Introduction**

Commercial air transportation during the past 50 years has improved in large part because of modern aircraft design. Part of the new technology involves air quality. Civil aviation technology advances and diverse scientific methods have converged in different ways to shape and transform air quality in commercial aircraft. The jetliner's environmental control system (ECS) has been painstakingly designed to meet demanding quality standards for the air supplied to the cabin. Air quality safety standards have always been designed into the aircraft's ECS. But past studies on aircraft cabin air quality have mainly focused on contaminant threats originating from within the cabin, including cigarette smoke (Nagda and Rector, 2003). Meanwhile a modern aircraft's infrastructure has changed significantly; consequently, it has not kept pace with the demands for quality air supply for the cabin. Disruptions arising from smoke/fume incidents are unusual but can cause dangerous situations in an aircraft cabin. Airborne volatile chemical substances emissions from the aircraft bleed air system during smoke/fume incidents have not been studied even though the fumes raise many health concerns, in particular the impact of TCPs additives in jet engine lubricating oils on aircraft cabin occupants. Continuing cabin air quality incidents drive air quality studies in airplanes, particularly studies of hazardous airborne substances released into aircraft cabins during incidents.

Deterioration in air quality during smoke/fume incidents may also hurt airline commerce in addition to having a negative impact on health, particularly the health of frequent fliers like aircrew. In fact smoke/fume incidents may have unfavorable lingering long-term health effects. Furthermore, incidents can create significant emotional strain for aircraft cabin occupants, and the level of concern is even higher amongst flight attendants and pilots. Air quality needs to be maintained at all times during flight, but the FAA rules and regulations governing air quality

provision in aircraft cabins do not cover smoke/fume incidents (ASHRAE, 2007). Essentially all commercial aircraft already have bleed air systems. Too much remains unknown about smoke/fume incidents, in part because a smoke/fume incident is hard to quantify because commercial aircrafts do not have air quality monitoring systems on board. Additionally, because the air quality during smoke/fume incidents cannot be measured, the quality of the air supply for cabin occupants during incidents cannot be adequately judged, and determining how to handle incidents is nearly impossible. In the interest of stakeholders in airline industry, the effects of these incidents must be explored more fully, so the best remedy can be chosen.

In a modern aircraft's ECS, HEPA cabin air recirculation filters remove airborne particulates from the air and are an integral part of air quality control system. Smoke/fume incidents contaminate the air supply in the cabin. Thus, smoke/fume events in aircraft engine bleed air system cause emissions to enter the ECS; eventually, those contaminants pass through the cabin air recirculation filters, making them a focus of interest among researchers. A study by van Netten (1999), did not find significant concentrations of toxic elements in any of the jet engine lubricating oils and hydraulic fluids analyzed. However, according to Winder and Balouet (2001), toxic metals contaminants in commercial jet engine lubricating oils include; cobalt (Co), Mg, manganese (Mn), vanadium (V) and chromium (Cr). Alemon et al. (2004) have successfully used NAA to characterize airborne suspended particles in air filters. Landsberger et al. (1993) also used NAA to determine concentrations of cadmium in air filter samples. In this study, NAA was used to analyze used and incident cabin air recirculation filters to quantify elemental concentrations of jet engine lubricating oil markers. The study aimed to analyze the concentration levels of isotopes in both irradiated incident and used filter samples on cabin air filters to determine jet engine oil contamination. This study investigated the elements present in Mobil Jet Oil II, clean, used and incident cabin air recirculation filters in an attempt to determine the jet engine oil signature on used and incident filters.

#### **4.2.1 Principles of neutron activation analysis (NAA)**

NAA works by irradiating the sample with neutrons in the reactor to induce nuclei of the atoms in the sample to become radioactive. When a sample is irradiated, the stable elements in the sample are transformed into radioactive isotopes by neutron absorption. Each radioactive nucleus emits gamma rays of different and unique energies or wavelengths, whose intensity is

proportional to the concentration of that element in the sample. Gamma ray detection can discriminate between these gamma ray energies, measure their intensities, and determine the concentrations of different elements in the sample (Shultis and Faw, 2007). Figure 4.1 illustrates the irradiation process converting a target material (specimen) into radioactive isotopes (Glascock, 2011). The isotopes decay at a characteristic rate, in most cases, emitting gamma rays of characteristic energies and intensities. As an example, irradiation of iron (Fe) with neutron particle and the resulting to gamma ray energy produced are shown below by Equations (4.1a) and (4.1b). When either prompt gamma rays or delayed gamma rays emitted from the radioactive nucleus are analyzed, elements in the sample can be identified.

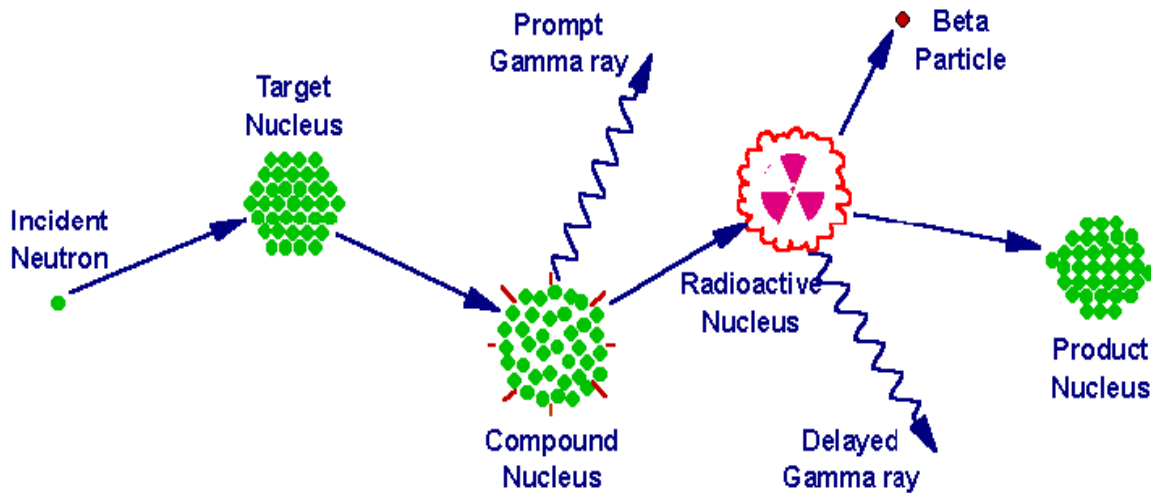


**Figure 4.1 Schematic illustrating neutron activation process and emission of gamma rays**

(Source: Glascock, 2011)



$$\text{Gamma ray energies} = 142.4, 1099.2, 1291.6 \text{ keV} \quad (4.1b)$$

When gamma rays deposit their energy into the crystal, it creates a hole and electron pairs in the crystal and a bias voltage is used to collect the charges. The number of pairs created is proportional to the energy of the gamma ray. The weight of a given element in a sample is



usually determined by comparison. In analysis of filter material by NAA, a sample of filter material is analyzed for its elemental and isotopic composition. The process can be qualitative (determining what elements are present), or quantitative (determining how much of each element are present). The intensity of gamma ray emission by the irradiated sample is measured using a high-purity germanium (HPGe) semiconductor detector. A HPGe detector offers high energy resolution as compared to other types of radiation detectors. A high energy resolution allows one to distinguish more accurately the difference between two similar gamma ray energies. The ability to distinguish between different gamma energies allows one to create a detailed energy spectrum.

The mass of a given element in a sample is usually determined as follows: (a) Counts, (b) Specific activity,  $(\text{Counts}/(\text{time} \times \text{detection efficiency}) \times \text{mass (mg)} = (\mu\text{Ci}/\text{mg})$ , (c) Number of radioactive isotope atoms:  $\text{Activity} = \lambda \times n$ , (d), where  $\lambda$  = decay constant and  $n$  = number of isotope atoms. Based on neutron flux, irradiation time, the number of element atoms is calculated (e) Mass of the element. In the analysis of the filter material with NAA, the elemental and isotopic mass of a sample of the material was determined. Gamma ray detection systems have been developed that can themselves discriminate between the gamma ray energies emitted, measure their intensities and hence determine the concentration of the different elements in the sample. The isotopes decay at a characteristic rate, in most cases emitting gamma rays of characteristic energies and intensities. By analyzing either prompt gamma rays or delayed gamma rays emitted from the radioactive nucleus, elements in the sample can be identified. Therefore, the basic process of NAA consists of three steps: irradiate the sample in a reactor; measure the energy spectrum of gamma radiation emitted by the sample, and identify elements based on the energy level of emitted radiation.

## **4.3 Materials and methods**

### ***4.3.1 Filter Sampling***

Figure 4.2 shows the steps involved in cutting filter specimen once they are received in the laboratory.

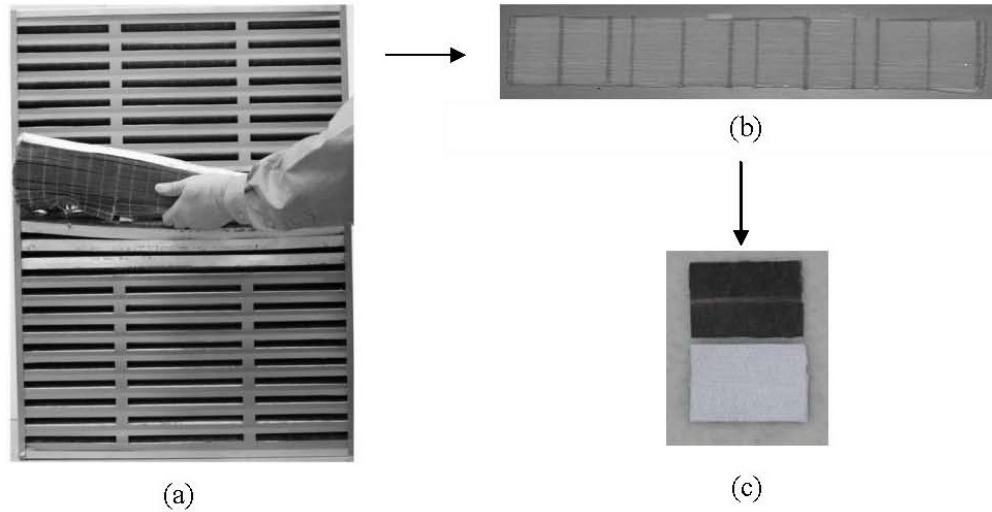


**Figure 4.2 Filter sampling preparation for NAA**

#### ***4.3.2 Preparatory steps for irradiation of filter samples***

In the nuclear laboratory, filter samples were cut into 75-150 mg pieces to provide a more uniform sample size, allowing quick comparative analysis of data. Smaller samples also reduced the amount of radioactive waste for disposal. To prepare for the NAA, samples were weighed in a polyethylene bag. To perform a comparative analysis, samples were placed in a second polyethylene bag to prevent activating any trace elements on labels created by marker pens. A self-sealing plastic sleeve/container (handled with clean gloves to prevent contaminating the sample) was placed on an analytic balance, and the tare weight was set to zero. A sample was placed in the plastic container, and the container weighed on the balance; this weight and sample identification numbers were recorded on a second container. The sample container was then placed into the labeled container. This process was repeated for all samples and for samples of pure iron (used to measure the neutron flux to which the samples were exposed, known as flux monitors). All the samples and flux monitors were placed in a heat resistant polyethylene capsule and sealed in a plastic sleeve. For liquid samples, 5.0 mL was sealed in polyethylene containers to prevent the release of contaminants into the reactor tank and to ensure that cross contamination did not occur. Iron standards were packaged and weighed in the same manner as filter samples. The filter samples were assigned iron standards, one iron standard per polyethylene capsule.

### 4.3.3 Filter irradiation process

Both filter and iron standard samples were placed into sample vials and capped. Sample vials were then placed in 10 specially-machined racks, six samples per vial, and four vials per rack. Therefore, 240 samples could be irradiated at once. Iron wire activation was used to calculate the actual flux. The movable portion of the sample rack was locked in place with aluminum wire. Before irradiation, the sample racks were lowered into the Rotary Specimen Rack (RSR) well, an irradiation site that surrounds the core of the nuclear reactor. The reactor was then operated at a targeted power for a predetermined time and conditions to activate the samples, typically 450-500 kW for eight hours. At the end of a test run, the reactor was shut down.

The target irradiation time and power level was based on an optimization of a number of variables, including trial irradiations, analysis, elements of interest, and the number of samples to be analyzed. Laboratory analysis requires time, and analyzing larger sample sets can cause loss of data from samples counted later in the sequence for radionuclides with short half-lives. Figure 4.3 shows the top view of the research nuclear reactor at Kansas State University.

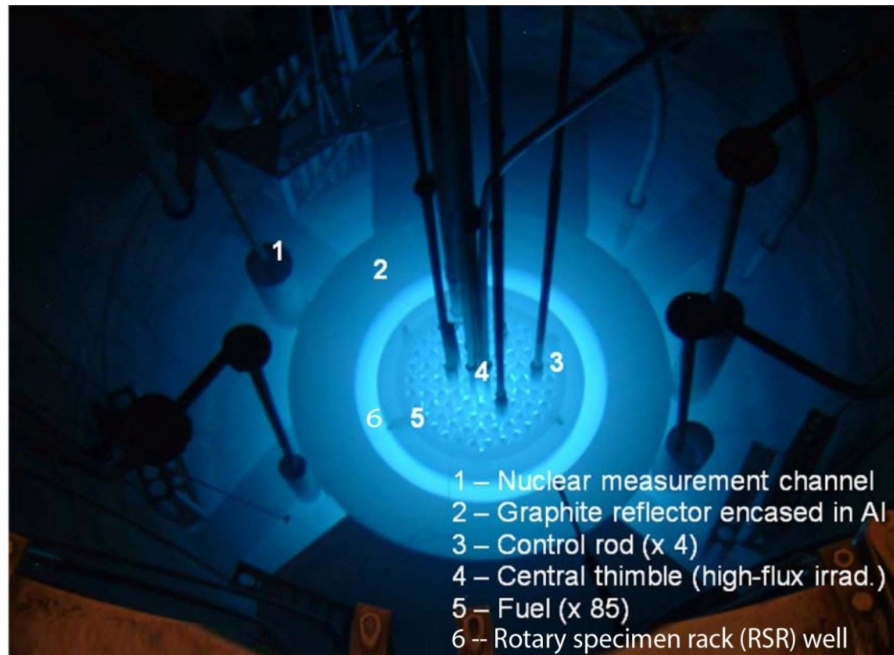


**Figure 4.3 Top view of TRIGA MARK II Reactor at Kansas State University**

The counting sequences for samples with short-lived radionuclides must be tightly controlled, so detecting short-lived radionuclides demands resources. In general, higher power levels and longer operating times increase sensitivity in detecting radionuclides with long half-lives. For all samples analyzed at the Kansas State reactor, irradiation times of 8 hours accommodates the facility's operating schedule, and power levels of 500 kW were selected as a maximum for continued steady state operation over an 8-hour period. At 500 kW the reactor released  $3.0 \times 10^{12}$  fast neutrons at  $\text{cm}^{-2} \text{ s}^{-1}$  and thermal neutron at  $3.6 \times 10^{12} \text{ cm}^{-2} \text{ s}^{-1}$ . These parameters were chosen to produce data for the range of elements identified in the trials. If the samples are highly radioactive, detector dead time limits their usefulness; waiting for a sample to cool enough to reduce activity to a threshold where dead time is acceptable may mean some elements, present in small quantities with a short half-life, fall below detection levels due to the shortness of the radioactive process.

#### ***4.3.4 Handling procedures to minimize or avoid radioactive contamination spread***

Following irradiation, samples were highly radioactive, so they were left in the reactor pool to decay to minimize their radioactivity while they were handled. Meanwhile, the sample racks were removed from the RSR well. Sample vials were removed from racks. Water that leaked into the vials was drained back into the reactor tank. The samples were then removed from the vials and placed in the pit to decay further to acceptable counting levels. A radiation monitor model Victoreen 450 was used to monitor radiation levels before samples were dispatched for counting. A 2-mR/hr radiation level reading was considered safe for counting; otherwise, higher values would saturate the detector and interfere with counting accuracy. New outer bags were prepared and each labeled for sample identification. The bagged samples were weighed, and the sample's iron standards were transferred to the new bags. In case of error or ambiguous results, a portion of the original sample was kept for re-testing. Finally, the samples were transferred to the NAA laboratory, where an analysis was performed using HPGe detector and GENIE 2K software.

To reduce exposure of personnel to radioactivity, the samples were left to decay for a minimum of five to seven days, which would normally be adequate without a significant loss of data due to the shortness of the half-lives. The sample racks were disassembled by cutting the aluminum wire, which was then discarded in accordance to general regulations for radioactive

waste disposal 10CFR20.2001 (1991). At the end of each irradiation, before the samples were removed to new outer bags, they were swiped to verify that they were free from loose surface contamination. The old bags were also disposed of according to 10CFR20.2001 regulations.

#### 4.3.5 Determination of concentration of radioactive atoms within a sample

One method to calculate the concentration of radioactive atoms in a sample is to determine the area under the peak by peak analysis. The peak area refers to the number of photons collected at a specific energy peak. The number of photons collected is proportional to the concentration of the radioactive isotope. The GENIE 2K algorithms calculate the net peak area by subtracting the background continuum (B) from the gross counts (G). The resulting net peak area (S) is displayed in Figure 4.4.

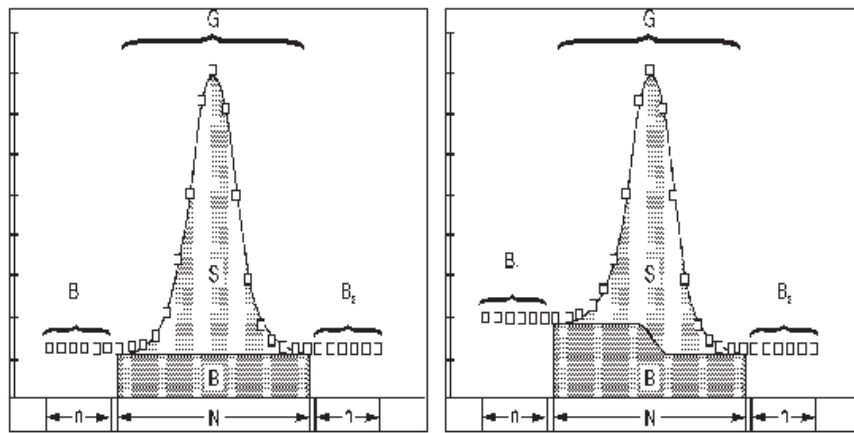


**Figure 4.4 Net peak area calculation for different background continuum counts**

(Source: Canberra Industries, Inc., 2001).

In order to calculate the concentration of radioactive isotope, it is assumed that there are no initial radioactive atoms. Thus, the radioactive atoms are produced only from the irradiation in the reactor. After the irradiation, the activity will decay exponentially. Equation 4.2 is used to calculate the concentration of radioactive isotope (Shultis and Faw, 2007).

$$\mu_x = \frac{C_j(\mu_x)A_x\lambda_i}{N_a\sigma_a\phi m p_i'f_j\eta_j} [1 - e^{-\lambda_i t_o}]^{-1} e^{\lambda_i t_w} [1 - e^{-\lambda_i t_o}]^{-1} \quad (4.2)$$

where:

$C_j(\mu_x)$  = Total number of counts under the peak associated with gamma ray

	energy $E_j$ from radionuclide I (counts)
$N_a$	= Avogadro's number ( $\text{mol}^{-1}$ )
$\bar{\sigma}_a$	= Average thermal absorption cross section of precursor isotope $i$ ( $\text{cm}^2$ )
$\phi$	= Thermal flux density ( $\text{cm}^{-2} \text{s}^{-1}$ )
$m$	= Sample mass (micrograms)
$\mu_x$	= Weight fraction of element $x$ in the sample
$p_{i'}$	= Abundance of precursor isotope $i$ in the element of interest
$f_j$	= Branching ratio of the gamma $j$ in the radioisotope of interest
$\eta_j$	= Overall detection efficiency, including intrinsic efficiency and geometry
$A_x$	= Atomic mass of the element $x$
$\lambda_i$	= Decay constant of the isotope of interest ( $\text{s}^{-1}$ )
$t_o$	= Irradiation time (s)
$t_w$	= Waiting time between the end of irradiation and the start of counting (s)
$t_c$	= Counting time of the detector (s)

#### **4.3.6 Gamma ray counting**

Jet engine oil and clean filters were also irradiated as controls. After irradiation, these samples were left to cool down/decay for 7-10 days, after which gamma rays emitted from the irradiated samples were counted by HPGe detector for one hour. According to Agnello et al. (2009), HPGe detectors have higher energy resolution compared to traditional scintillators like sodium iodide (NaI), and the detectors have enabled significant advances in nuclear spectroscopy. A Canberra multi-channel analyzer (MCA) with Genie 2K software was used to analyze the data from the irradiated samples. The MCA sorted and stored myriad proportional signals coming from the nuclear detector due to gamma ray interaction with the detector. A high energy resolution allowed the difference between two similar gamma ray energies to be distinguished more precisely. This ability to distinguish between different gamma energies facilitated creating a detailed energy spectrum.

#### **4.3.7 Radiation detection and analysis by GENIE 2K software**

The GENIE 2K software has built in algorithms used to calculate the activity of an irradiated sample. By entering the sample mass and irradiation time into the program, the

software calculates the specific activity of a sample. The software program contains a database of isotopic information to be used in the specific activity calculations. Also by using an internal clock, GENIE 2K can account for the irradiation time, waiting time, and counting time of the sample. The software algorithms use equations 4.3, 4.4, and 4.5 to calculate specific activity, thermal flux and concentration of isotope, respectively.

GENIE 2K is a Windows-based software package used to analyze gamma ray spectra obtained from any type of gamma detector. It simultaneously receives data and displays/graphs (spectrum) in real time. Its measurement data can be saved as text for export into standard calculation software like Microsoft Excel. The NAA data analysis involved calculating neutron flux based on the standard or flux monitor (iron). In turn, the flux and peak area were used to calculate the mass of the parent element for each of the daughter isotopes. All counts for the samples were performed for 3600 sec. live time, and the GENIE 2K spectral data acquisition software was used to record the spectrum. A computer program that searched each element present in the sample by energy levels was used to compare the energy peaks in the samples to libraries of known gamma ray energies, and the energy spectrum of the sample was thereby obtained. The instrument also counted total and relative errors ( $-/+ \mu\text{Ci}/\text{mg}$ ). Before counting the samples, the HPGe detector was calibrated for both energy and efficiency.

#### ***4.3.7.1 Energy and efficiency calibration***

The HPGe detector was used in conjunction with the GENIE 2K multi-channel analyzer (MCA) software. The MCA from the HPGe detector output data as counts versus channel number. However, the channel number is not useful unless an energy calibration is performed. Therefore, to perform an energy calibration, a radioactive source that contained isotopes with known energies and activities was used. The calibration source comes with a certificate file that can be used to calibrate energy and efficiency. In this study, the calibration source used had a mixed Europium (Eu) source MGS-1. The Eu source had known quantities of radioisotopes: 152, 154, and 155. With the energy of a photo peak known, the channel number was correlated to energy.

The calibration source was centered above the detector. All subsequent samples were counted at the exact same location as the calibration source. The calibration source and samples had to be on the same location, so any uncertainty due to geometric effects would be minimized. The calibration source was typically counted for three hours to ensure that sufficient counts were

collected under the photo-peak. The GENIE 2K software and the MGS-1 certificate file was used, so a linear relationship could be fitted to the calibration data to relate energy to channel number. Energy calibration, which in essence involves plotting peak energy from certificate file versus observed peak at the channel, was obtained as shown in Figure 4.5. In energy calibration, the GENIE software read the channel number corresponding energy based on equation 4.3a.

An output from GENIE software on energy calibration performed on 7/22/2010 at 9:20:35 is shown below in equations 4.3a through 4.3c and Table 4-1. The software reads the channel and converts it to energy according to equation (4.3). Other related equations produced by GENIE as output are full width at half maximum (FWHM) Equation (4.2b) and low tail Equation (4.3c).

$$\text{Energy (keV)} = -0.678 + 0.262 \times \text{ch} + 0.00\text{E} + 000 \times (\text{ch})^2 + 0.00\text{E} + 000 \times (\text{ch})^3 \quad (4.3a)$$

$$\text{The full width at half maximum (FWHM) equation: } 2.707 + 0.005 \times E^{1/2} \quad (4.3b)$$

$$\text{LOW TAIL} = 0.0\text{E} + 000 + 0.0\text{E} + 0.000\text{E} \quad (4.3c)$$

The energy distribution corresponding to every channel is expected to assume a Gaussian distribution. The full width at half maximum is a parameter used to describe the width of the energy peak corresponding to a channel. For the calibration problem considered the Gaussian distribution obtained had no tails therefore equation (4.3c) shows all zeros. The energy from the certificate file corresponding to each channel and the error  $\pm$  the centroid error was as tabulated in Table (4.1). The centroid error indicates how far off the identified centroid channel is from the actual channel corresponding to energy obtained. The response measured for the test shows a linear regression on the data obtained from calibration.



**Table 4-1 Energy calibration data**

Centroid Channel	Centroid error	Energy (keV)
230.11	0.27	60.00
331.60	0.04	86.50
403.28	0.03	105.30
468.88	0.03	121.80
934.14	0.18	244.70
1315.47	0.03	344.30
2259.51	0.10	591.70
2761.20	0.05	723.30
3333.21	0.03	873.20
3834.59	0.06	1004.80
4863.01	0.06	1274.50
5372.37	0.09	1408.00
6090.67	0.23	1596.5

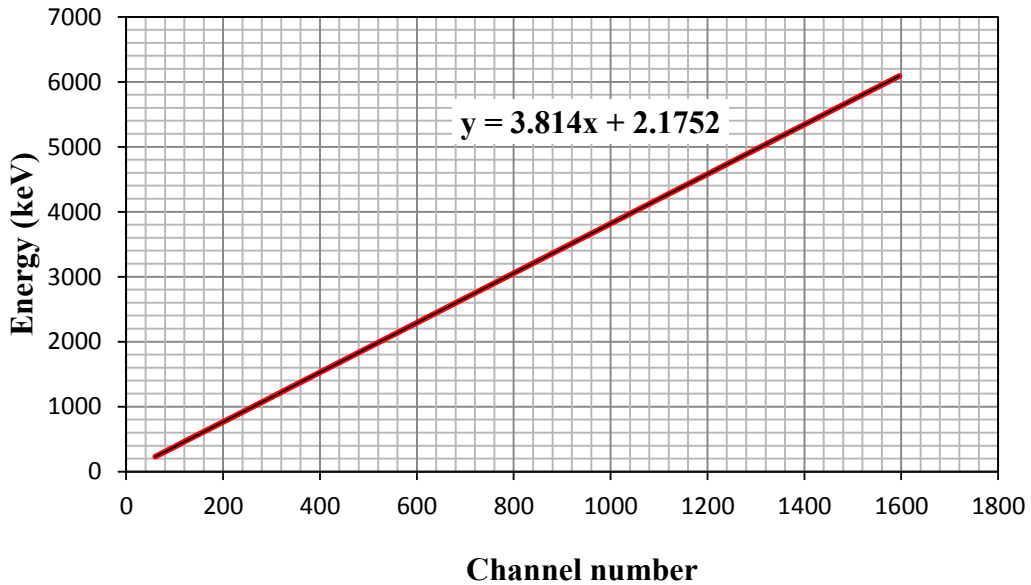


**Figure 4.5 Energy calibration using the MGS-1 certificate file**

The resulting linear line gives a picture of the relationship between channel number and the corresponding energy output. From the efficiency calibration of October 2010 an energy equation 4.4a was obtained and a non-linear fit was performed to calibrate efficiency versus energy (keV), and a relationship of efficiency versus energy was plotted as shown in Figure 4.6.

$$\ln(\text{Eff.}) = A + B \ln(E) + C \ln(E)^2 + D \ln(E)^3 \quad (4.4a)$$

where  $\text{Eff.} = e^{(\ln(\text{Eff.}))}$  and  $E = \text{energy (keV)}$

Constants:  $A = -13.1$ ;  $B = 8.304$ ;  $C = -1.829$  and  $D = 0.119$

Equation 4.4a can be rewritten as follows:

$$\text{Eff} = e^{(A + B \ln(E) + C \ln(E)^2 + D \ln(E)^3)} \quad (4.4b)$$

where  $\text{Eff} = \text{detector calibration efficiency}$

Using Microsoft Excel, equation 4.4b was used to compute the values shown in Table 4.2. The energy and efficiency values tabulated in Table 4-2 were then used to plot for an efficiency curve that starts at zero, peaks at around 26.4 percent which corresponds to 30 keV, and then decreases as shown in as shown in Figure 4.6.

**Table 4-2 Efficiency calibration data**

Energy (keV)	Efficiency
5	0.019
10	0.108
15	0.190
20	0.237
25	0.259
28	0.263
30	0.264
40	0.251
45	0.240
50	0.227
100	0.132
250	0.051
500	0.028
750	0.023
1000	0.023
1500	0.026
2000	0.034

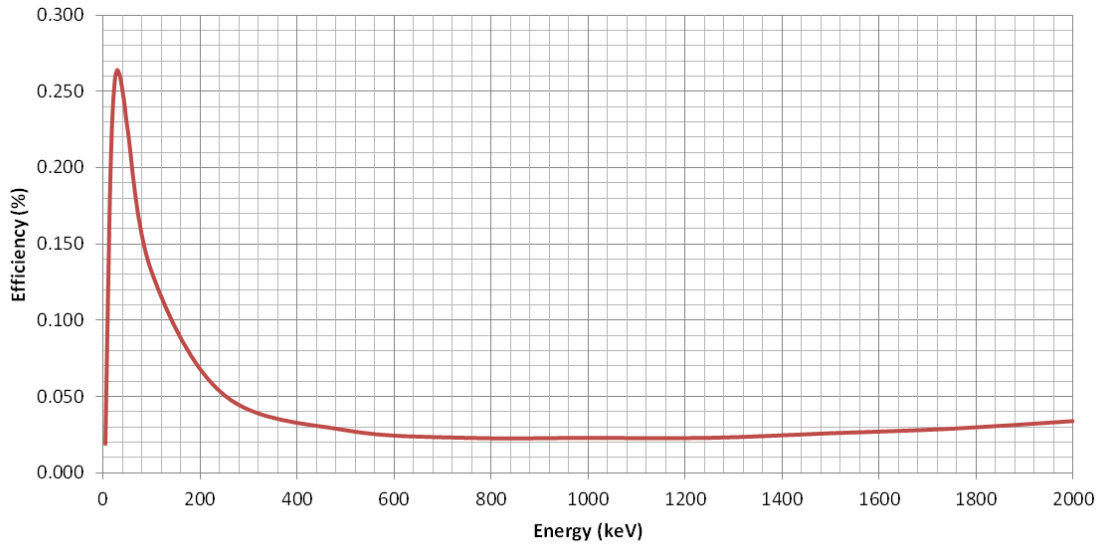


**Figure 4.6 Efficiency calibration curve fitting using MGS-1 certificate file**

From zero efficiency versus energy have a linear relationship up about 27 percent. Thereafter, energy and efficiency are inversely related: as energy increases, efficiency gets smaller. The line's slope flattens out as it moves the right, suggesting that the rate change of efficiency with energy decreases. The flattened slope indicates that changes in efficiency are less and less sensitive to changes in energy increase. At some point, presumably, there is no further decrease in efficiency and the curve is almost parallel to the x-axis, meaning that efficiency is no longer sensitive to increase in energy.

After the energy and efficiency calibration, irradiated samples could be counted. All samples were counted in the same location as the calibration source so that the solid angle remained unchanged. The sample counting time was adjusted to allow sufficient time for enough counts under the photo peak. Ideally, at least 10,000 counts under the photo peak will keep the statistical error low. Once all samples were counted, the GENIE 2K software generated a report. The filter analysis data were used to identify peak regions of interest. The report contained more information than was needed, but the most useful quantities were the specific activities for each identified isotope. The GENIE 2K software also generated an energy spectrum. The energy spectrum was calibrated to show the identified isotopes next to the associated energy peak.

The radiation detector converts electromagnetic radiation (gamma rays) to an electrical signal on a finite time scale. If the rate of gamma incidence on the detector approaches signal

processing time, the signal from individual radiation events can overlap and degrade the signal. The fraction of time that a detector cannot process an individual radiation event is known as dead time. Activity from short-lived radionuclides generated in an 8-hour operation at 500 kW can cause extremely large dead times. Therefore, sample racks were held in storage to allow short-lived radionuclides to decay before analysis. When the samples approached activity levels for which the dead time was acceptable, the sample racks were removed from storage, and the samples were removed from the capsules. The sample identification and weight information were transferred onto fresh, unirradiated containers. The container with the sample was then removed from the container with the label, and the sample container transferred to the unirradiated, newly labeled container. The sample in the fresh container was then placed close to a HPGe detector.

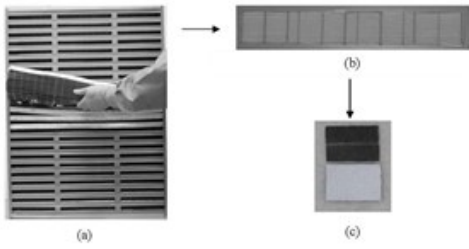
An analysis software routine applied to the spectral data determined the beginning and end of each region of interest for single gamma energy. The criteria used in this analysis were based on a numerical calculation of the second differential of the intensity function versus energy. The software routine summed the number of times radiation was detected within the determined range and removed the value related to the baseline for the function. Another routine performed an efficiency correction to determine the actual radiation emitted from the sample based on detected radiation. The software used the data collection time (automatically recorded) to determine activity. All of the routines performed statistically based error analyses. Analysis software identified the nuclides associated with specific energies of radiation. This analysis used a library of gamma energies that occur from neutron activated elements and half-life information from the library to calculate the maximum value of mass specific radioactivity for each isotope detected, based on times for start and completion of irradiation (user inputs) and the decay interval before data collection. The digital spectrum analyzer (DSA) is a 16K channel integrated MCA paired with the computer to be a complete spectroscopy workstation. Figure 4.7 shows the data acquisition flow chart.

The identification confidence level reported by GENIE 2K software was confidence in the peak identification. Figure 4.7 summarizes the entire process of NAA of used aircraft filters. The SAS code PROC GML was used to calculate the mass concentration for isotopes; thus, mass concentration = concentration ( $\mu\text{Ci}/\text{mg}$ ) multiplied by the mass of the sample. The average mass

concentrations were computed for every filter and the figures obtained were used to analyze differences between used and incident filters. (GENIE 2K Software Manual, 2004)

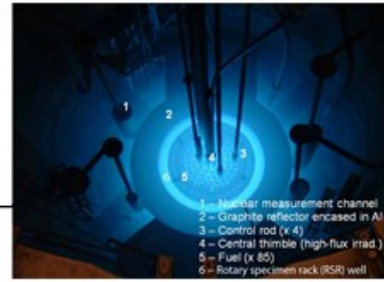
The radiation that enters the crystal caused electrons to be moved into a conduction band, and a bias across the detector collected the electrons to generate the signal. Larger deposits of energy caused more electrons to mobilize, therefore creating a larger signal. Specific signal magnitudes (pulse heights) were correlated to specific energies. A multichannel analyzer recorded the number of pulses that occurred at specific energies during detection. The aggregation of data was therefore an energy spectrum of the radiation intensity. A spectrum for a reference source was used to accurately determine the energy associated with each channel and the absolute efficiency relating detected radiation to radiation emitted from the source.

**Step 1: Filter sampling**



**Step 2: Irradiation of filter samples in nuclear reactor**

Weighing samples



500 kW: Fast neutrons at  $3.0 \times 10^{12} \text{ cm}^{-2} \text{ s}^{-1}$   
Thermal neutrons flux at  $3.6 \times 10^{12} \text{ cm}^{-2} \text{ s}^{-1}$

**Step 3: Gamma ray detection (Measure energy)**

Lead shield to minimize background radiation

HPGe detector is cooled with liquid Nitrogen at 700 K



**Step 4: Data processing (determine elemental concentration)**



Powers the detector. Detector produces pulse then DSA converts signal from analog to digital

GENIE 2K



Spectra + Report file

Figure 4.7 Basic steps in gamma ray data acquisition flow chart

## 4.4 Analysis, Results and Discussion

### 4.4.1 Data analysis

An analysis of variance (ANOVA) was performed by SAS PROC GML to compare the variability in the means of the mass concentrations ( $\mu\text{Ci}$ ) of isotopes in both used and incident filters. The SAS code was used to compare the two categories of mass concentrations calculated for the isotopes detected in the filters; the results are shown below:

```
options nocenter;
data isotopes;
input Filter$ Spot Category AG108m AG110m AS71 AS76 AS77 AU198 AU198m BA131
      BA133 BA133m CD115 CE139 CE141 CE143 CL38 C60 CR51 CS134 Ca47 EU152x
      EU154 FE59 HF175 HF181 HG197 HG203 HO166 IN114m IR192 IR194 LA140 LU177
      LU177x MO99 NB94x ND147 OS185 OS191 PM149 RB86 RE186 RH105 RU103 RU97
      SB122 SB124 SB125 SC46 SE75 SN125x SR85x Si32 TA182 TB160 TE121 TE121x
      TE123m XE127 XE129m XE133m YB169 ZN65 ZR95;
cards;
data on mass concentrations of isotopes ( $\mu\text{Ci}$ )
.
;
proc sort data = Isotopes;
by filter category;
proc means noprint data = isotopes;
by filter category;
var AG108m AG110m AS71 AS76 AS77 AU198 AU198m BA131 BA133 BA133m CD115 CE139
      CE141 CE143 CL38 C60 CR51 CS134 Ca47 EU152x EU154 FE59 HF175 HF181
      HG197 HG203 HO166 IN114m IR192 IR194 LA140 LU177 LU177x MO99 NB94x ND147
      OS185 OS191 PM149 RB86 RE186 RH105 RU103 RU97 SB122 SB124 SB125 SC46
      SE75 SN125x SR85x Si32 TA182 TB160 TE121 TE121x TE123m XE127 XE129m XE133m
      YB169 ZN65 ZR95;
output out = spotavg mean = AG108m AG110m AS71 AS76 AS77 AU198 AU198m BA131 BA133
      BA133m CD115 CE139 CE141 CE143 CL38 C60 CR51 CS134 Ca47 EU152x EU154
      FE59 HF175 HF181 HG197 HG203 HO166 IN114m IR192 IR194 LA140 LU177 LU177x
      MO99 NB94x ND147 OS185 OS191 PM149 RB86 RE186 RH105 RU103 RU97 SB122
      SB124 SB125 SC46 SE75 SN125x SR85x Si32 TA182 TB160 TE121 TE121x TE123m
      XE127 XE129m XE133m YB169 ZN65 ZR95;
proc glm data=spotavg;
class category;
model AG108m AG110m AS71 AS76 AS77 AU198 AU198m BA131 BA133 BA133m CD115 CE139
      CE141 CE143 CL38 C60 CR51 CS134 Ca47 EU152x EU154 FE59 HF175 HF181
      HG197 HG203 HO166 IN114m IR192 IR194 LA140 LU177 LU177x MO99 NB94x ND147
      OS185 OS191 PM149 RB86 RE186 RH105 RU103 RU97 SB122 SB124 SB125 SC46
      SE75 SN125x SR85x Si32 TA182 TB160 TE121 TE121x TE123m XE127 XE129m XE133m
      YB169 ZN65 ZR95 = Category /ss3;
lsmeans Category/stderr pdiff;
run;
quit;
```

This analysis was done with the SAS system for Windows (release 9.2; SAS Institute, Cary, NC). The confidence level for every peak in the spectrum of the isotope detected is reported by GENIE 2K software. The nuclide identification confidence level reported by the software was the confidence level in the peak identification. All the analyses were performed with the elements in the background radiation included. Based on the energy calibration, background counts of identified isotopes vary from time to time, however further work is recommended to identify background isotopes.

#### 4.4.2 Results and discussion

**Table 4-3 Elements detected in background, clean, used, incidents filters and jet engine oil**

Source	Elements detected in the samples	# Elements
Background	Ag, As, Au, Bi, Cd, Ce, Co, Cs, Eu, Fe, Hf, Hg, Ho, In, Ir, K, La, Lu, Os, Pa, Pb, Sb, Sc, Sr, Ta, Te, Th, Xe, Yb, Zn, Zr, U	32
Clean Filters	As, Ba, Ce, Cs, Si, Cr, Co, Cs, Fe, Hf, Hg, La, Lu, Os, Rb, Ru, Sb, Sc, Sn, Ti, Te, Xe, Nd, Os, Th, Bi, Kr, Sm, Yb, Ds Gd	30
Used Filters	Ag, Ar, As, Au, Ba, Be, Bi, Cd, Ce, Cr, Cs, Co, Fe, Ga, Gd, Hf, Hg, In, Ir, K, Kr, La, Lu, Mo, Na, Nb, Nd, Ni, Mn, Os, Pa, Pb, Pm, Rb, Re, Ru, Sb, Sc, Se, Sn, Sr, Ta, Tb, Tc, Tb, Tc, Te, Th, W, Xe, Yb, Zr	50
Incident Filters	Ag, Ar, As, Au, Ba, Bi, Br, Cd, Ce, Cr, Cs, Co, Fe, Gd, Hf, Hg, Ho, In, Ir, K, Kr, La, Lu, Mo, Nb, Nd, Mn, Os, Pa, Pb, Pm, Rb, Re, Ru, Sb, Sc, Se, Sn, Sr, TA, Tb, Tc, Te, Th, Xe, Yb, Zr	55
Mobil Jet Oil II	Na, K, Br, Cd, Co, Fe, Mn, Te, Hf, Os, Sb, Sc, Xe, Pm, Au, Pa, Th, Ru	17

During the experiments, some lower mass isotopes occasionally appeared; these may have come from background radiation. The elements suspected to originate from the background are listed in Table 4-3 and were not eliminated from statistical analysis because FESEM/EDS analysis also showed that some of these elements were present in the filters. For example, Fe, Ba, Zn, Fe, Cl, K, Mn, Ce, Ni, As, Cr, Pb, and Br were detected by FESEM/EDS analysis. To assume that the isotopes from these elements were definitely from background radiation would be inaccurate. Bromine appeared in three filters in the first batch of filters analyzed in 2008. However, Br did not show up in the analysis from 2010. Figures 4.8 through 4.11 show spectra from clean filters from three major filter manufacturers, jet engine oil, and used and incident filters. From these spectra, very few rare earth metals are present in the jet engine oil that are not also in the background.



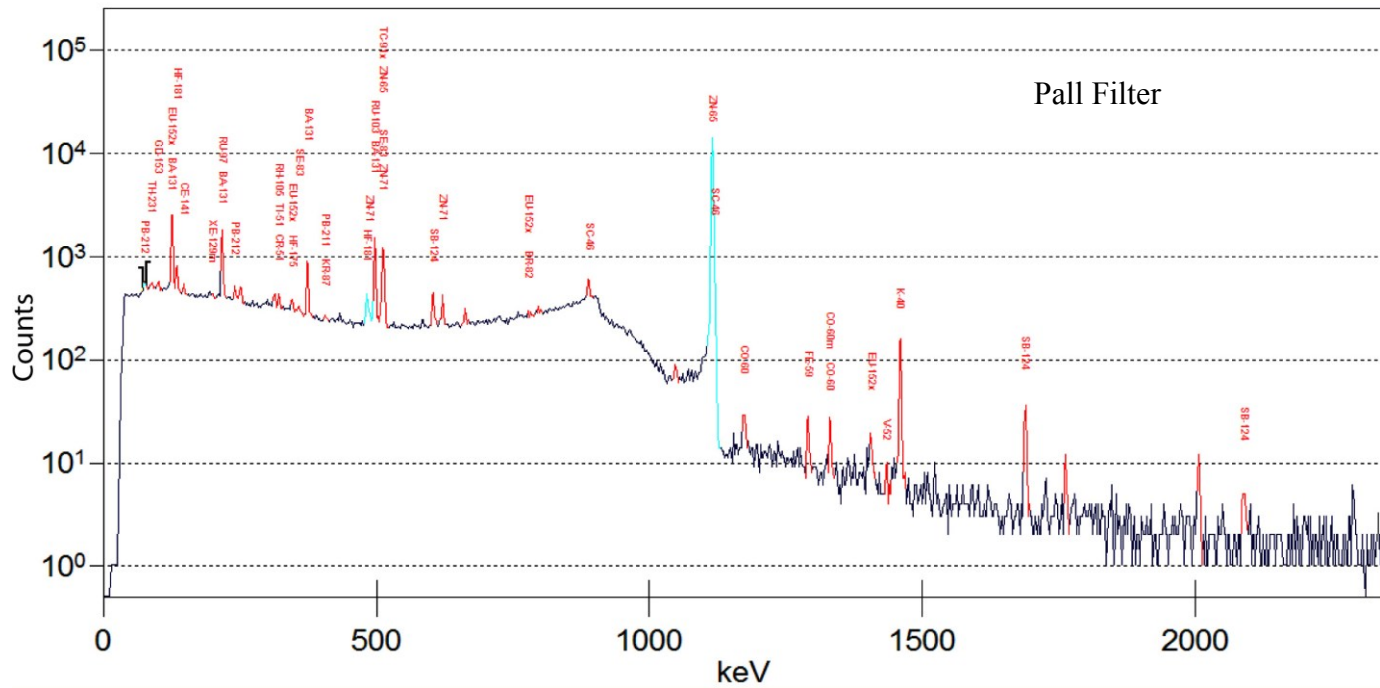
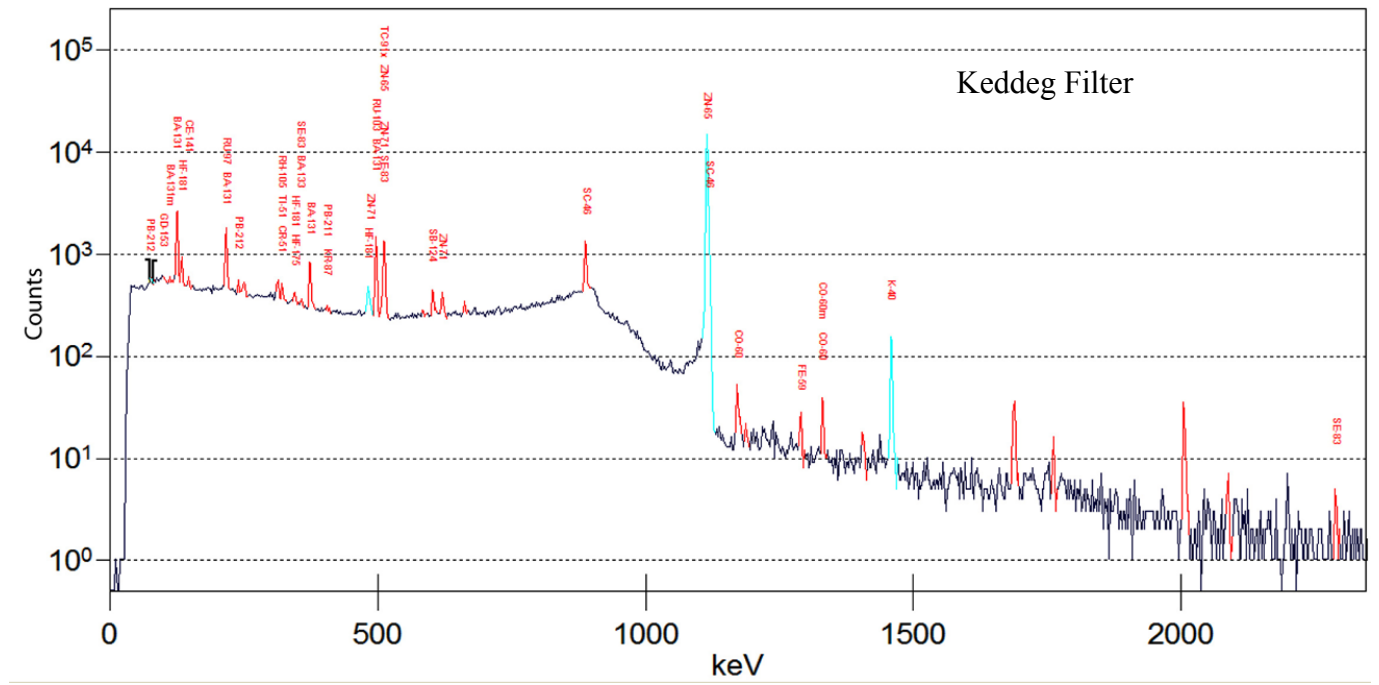
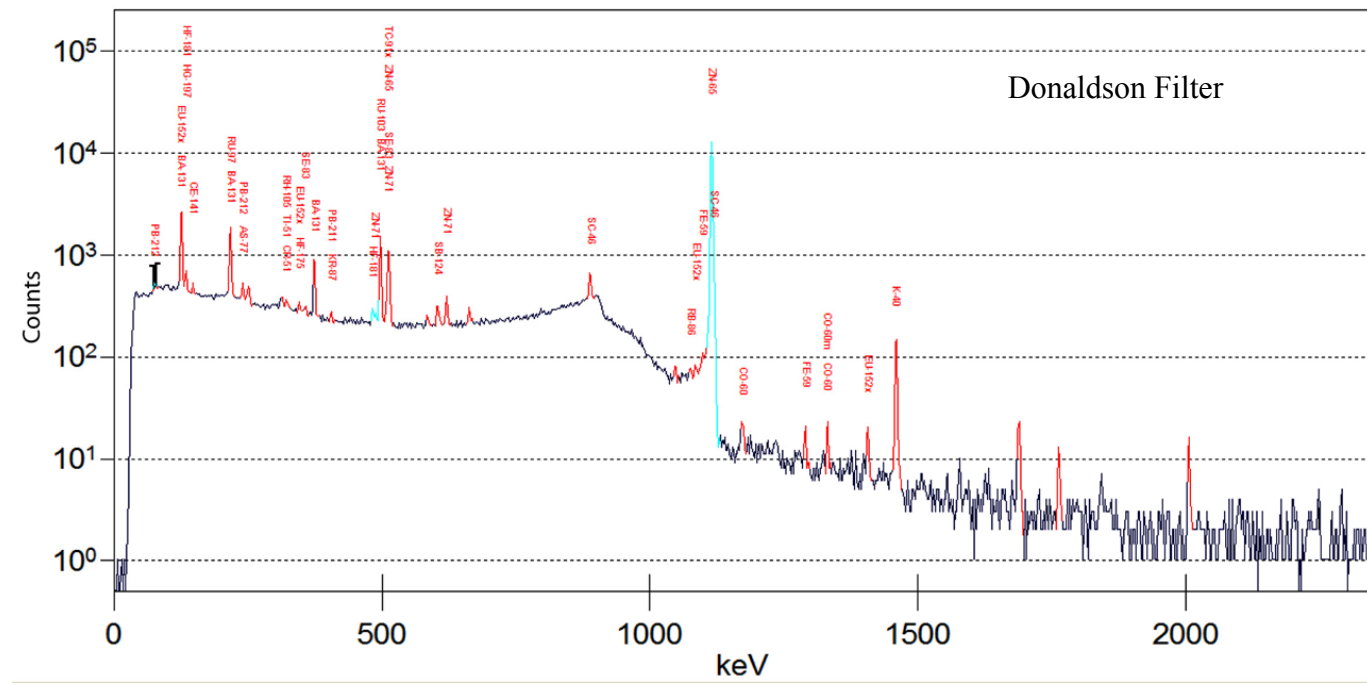


Figure 4.8 Gamma ray spectra showing the elements photo peaks of filter samples from Donaldson, Keddeg and Pall companies irradiated for 8 hours and counted for 1 hour with an HPGe detector after 7-10 days decay time

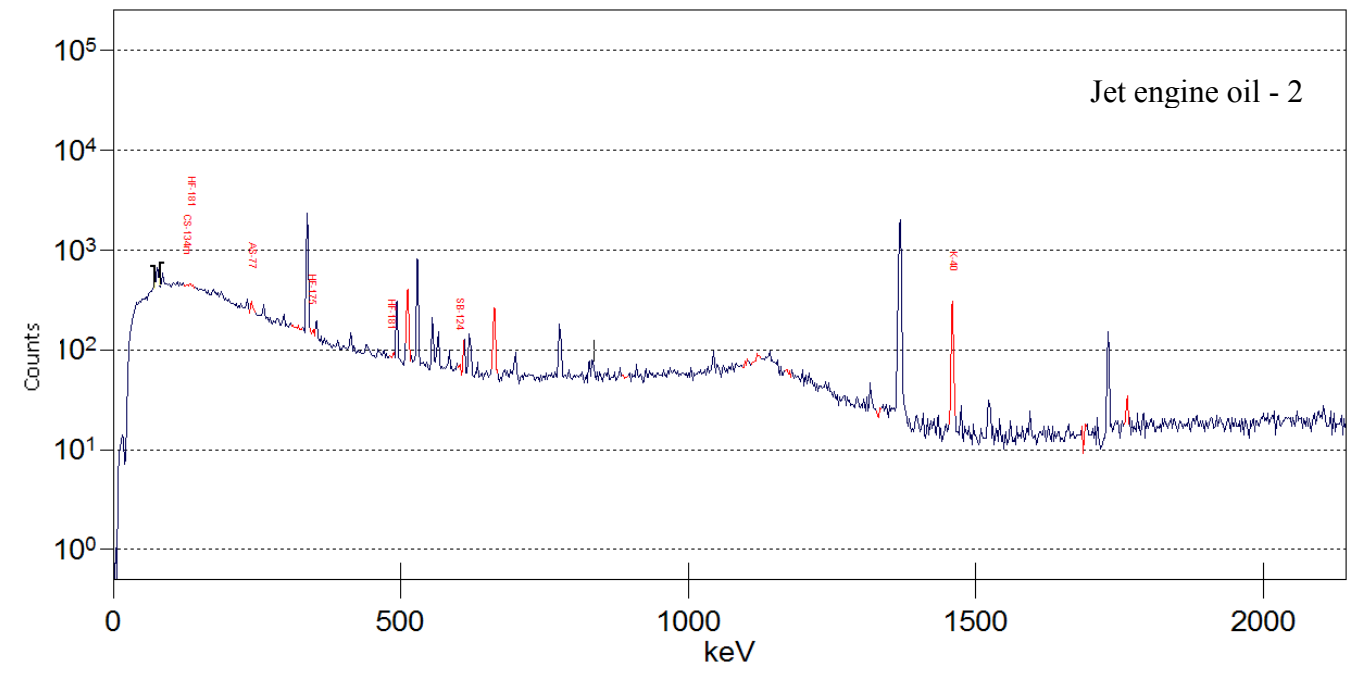
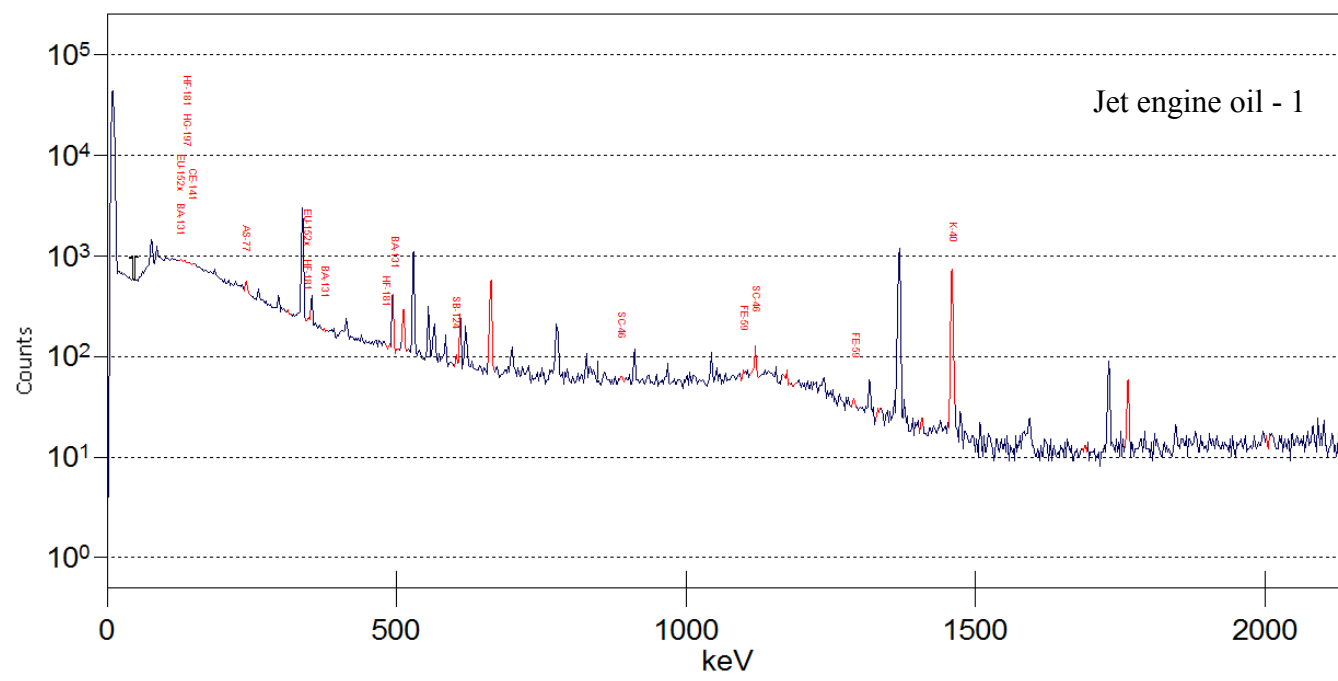


Figure 4.9 Gamma ray spectra showing the elements photo peaks from jet engine oil samples irradiated for 8 hours and counted for 1 hour with an HPGe detector after 7-10 days decay time

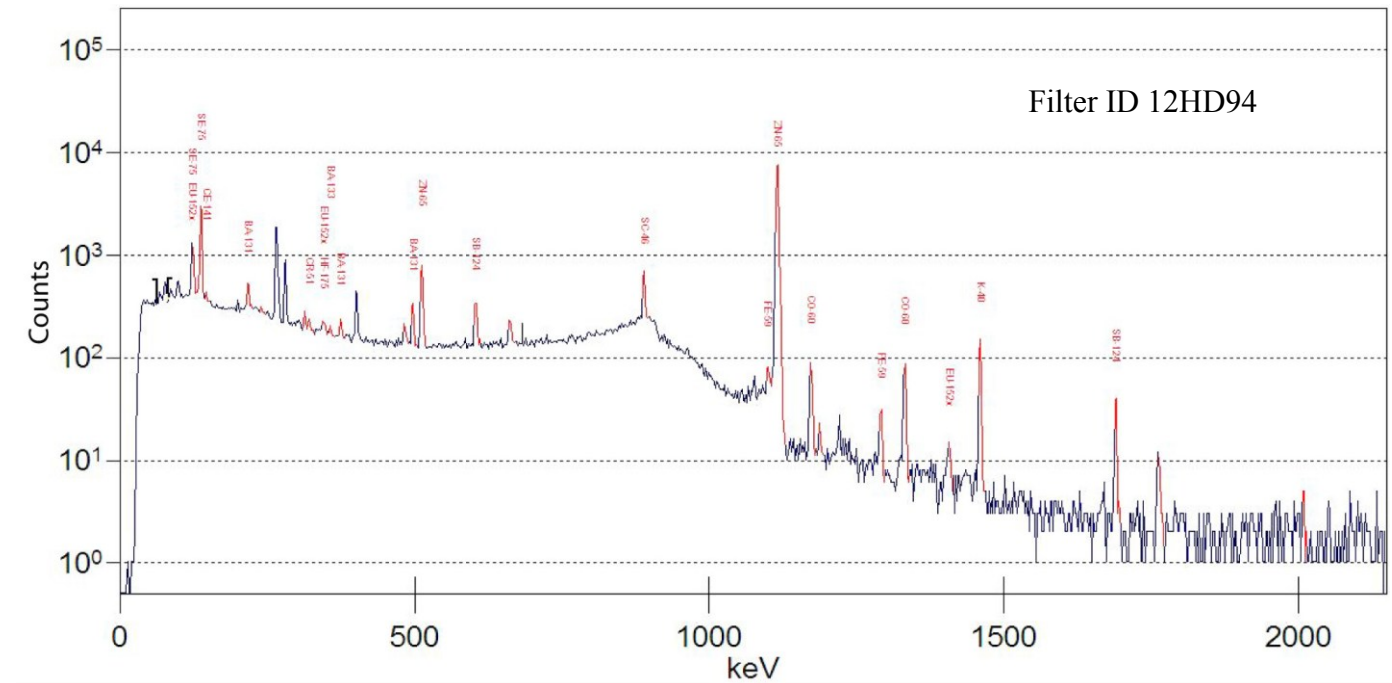
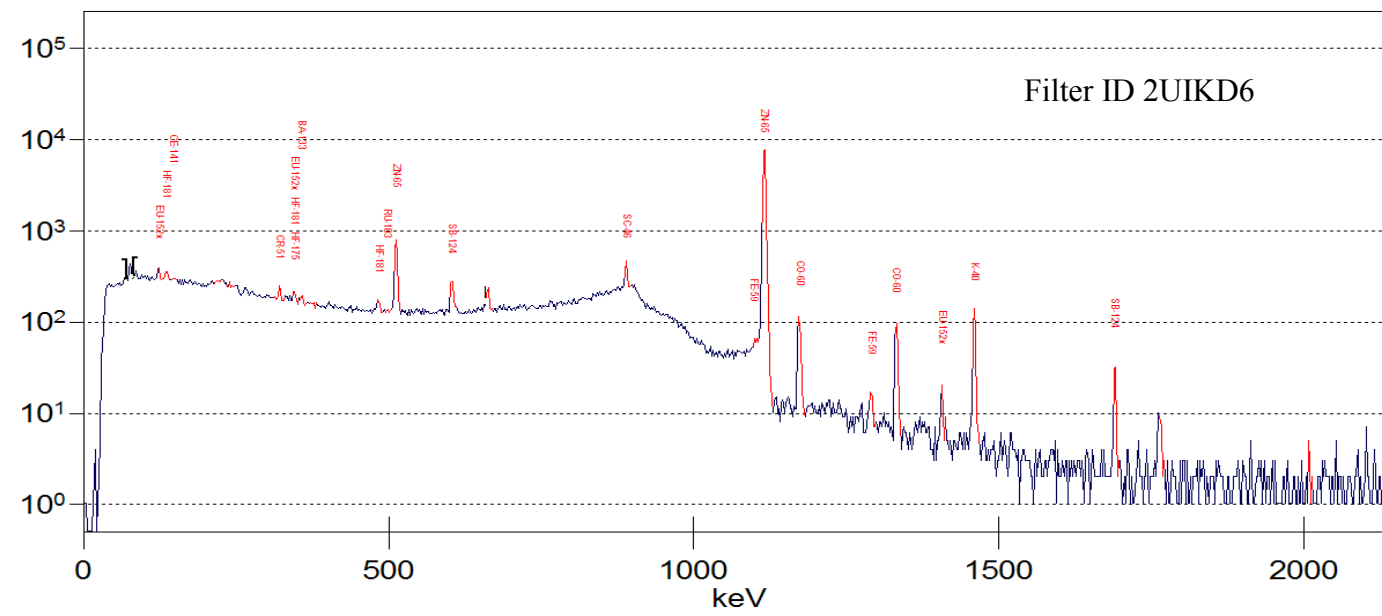
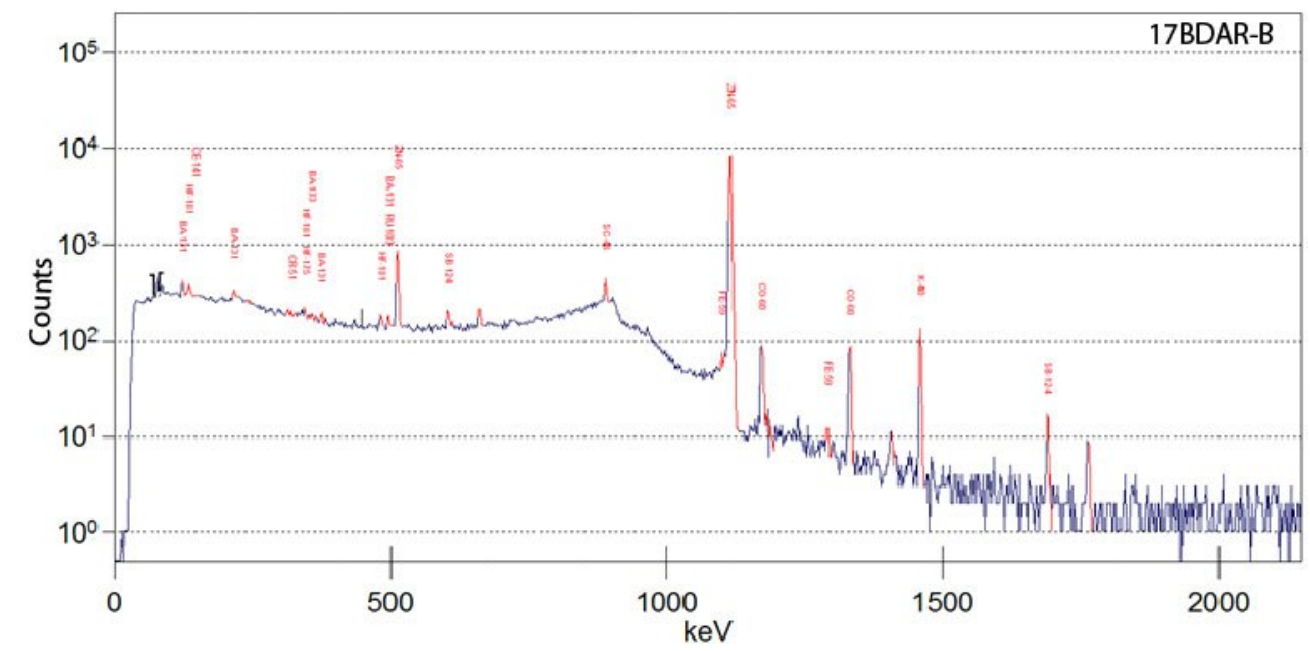
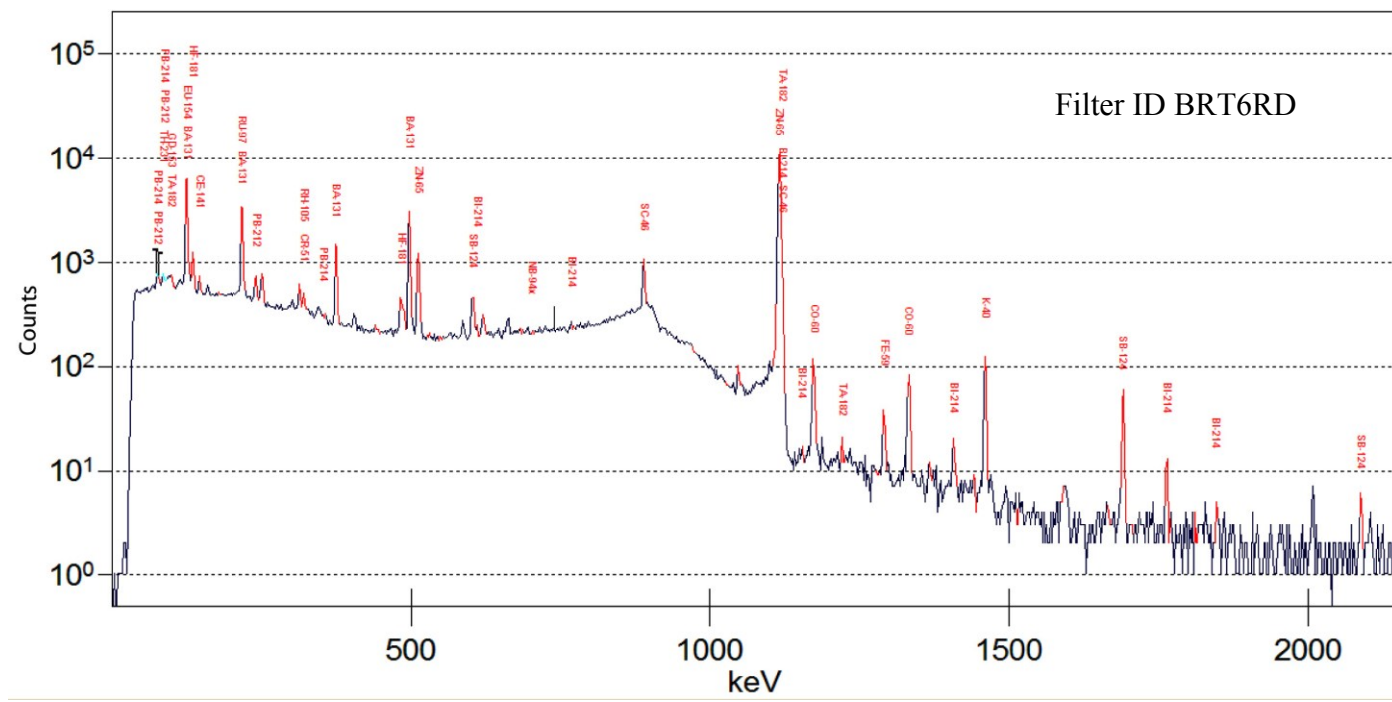


Figure 4.10 Gamma ray spectra showing the elements photo peaks from used filter samples irradiated for 8 hours and counted for 1 hour with an HPGe detector after 7-10 days decay time

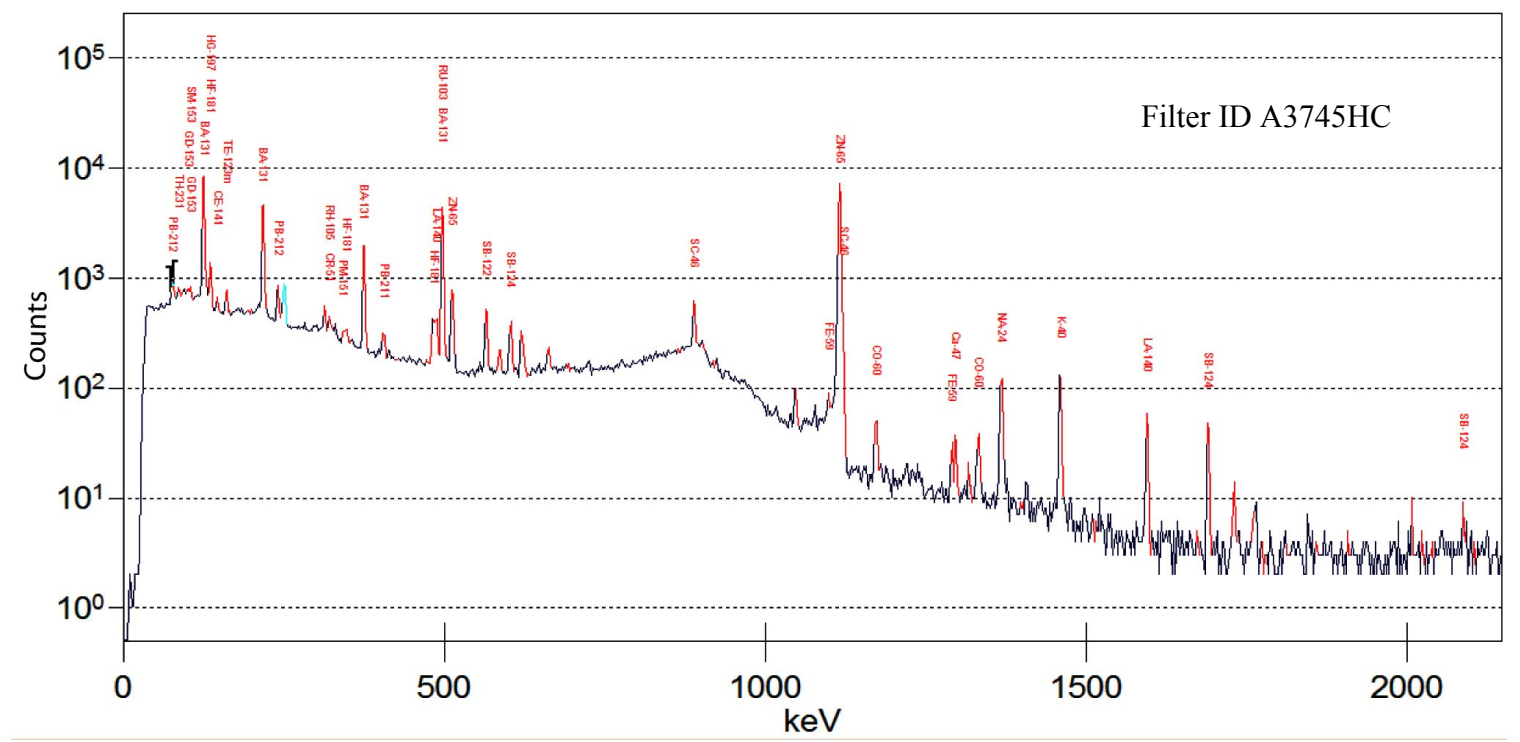
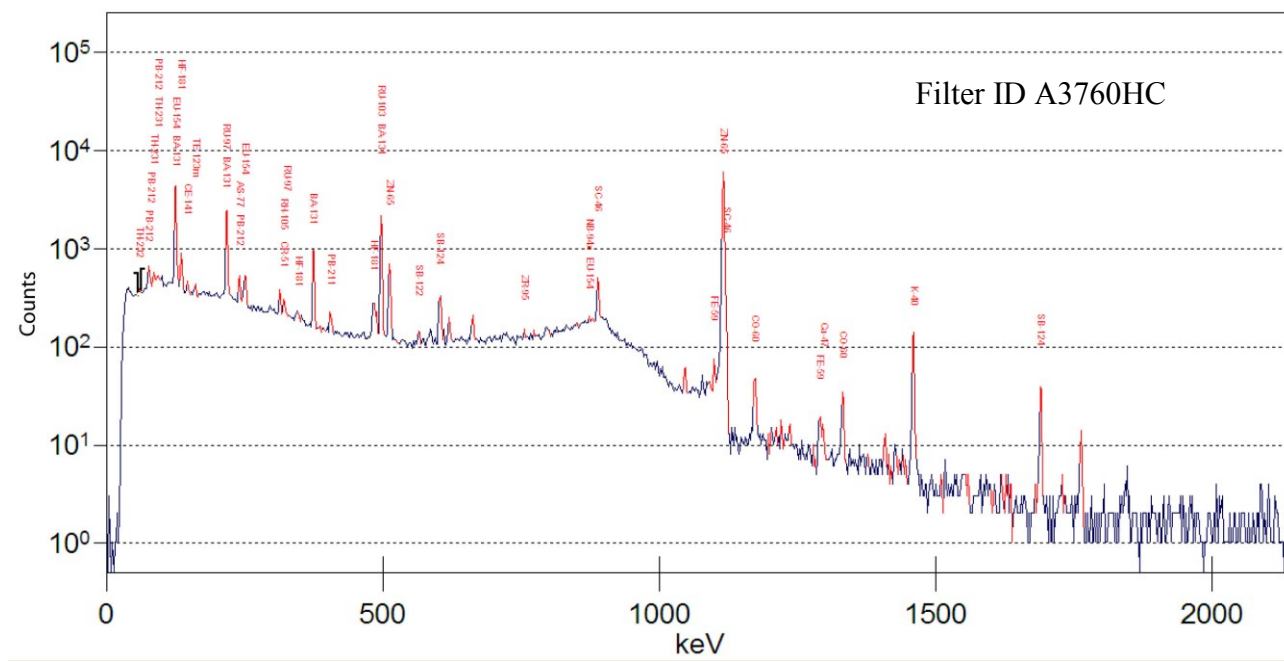
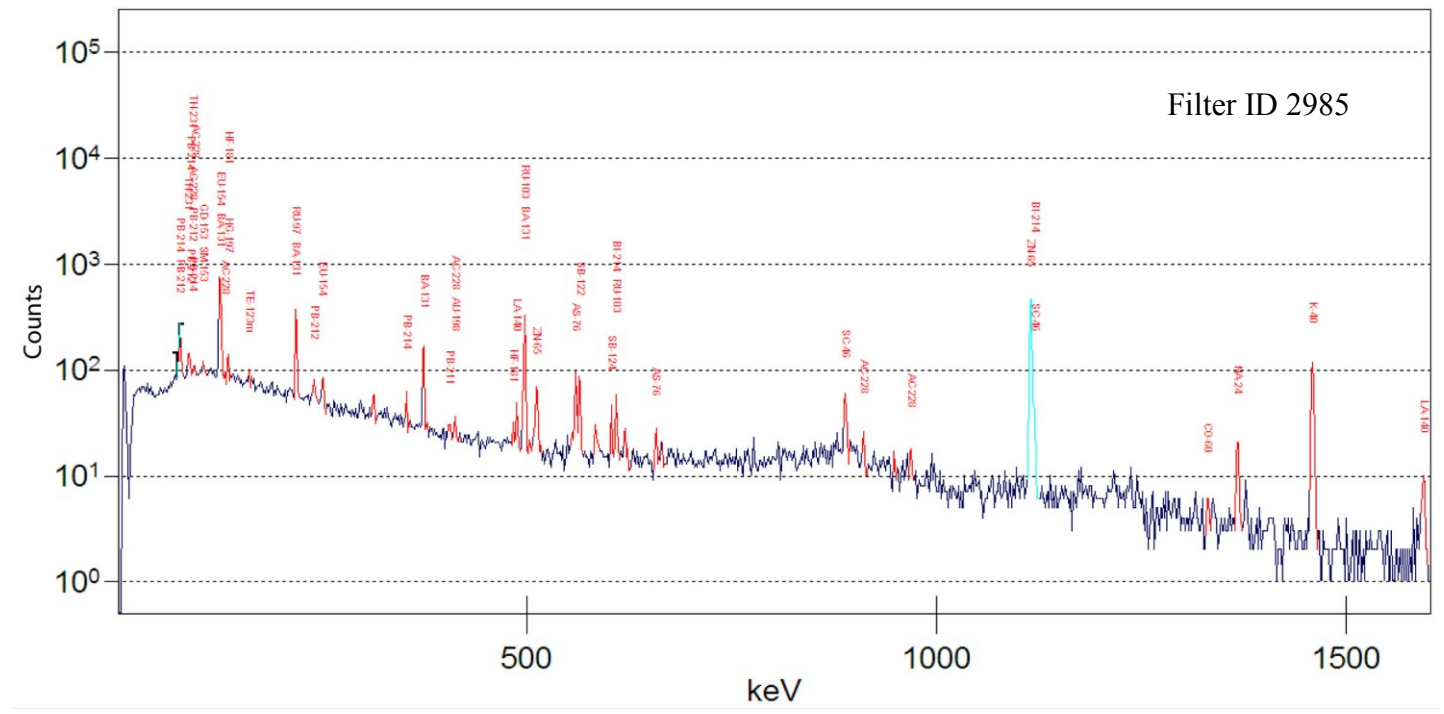
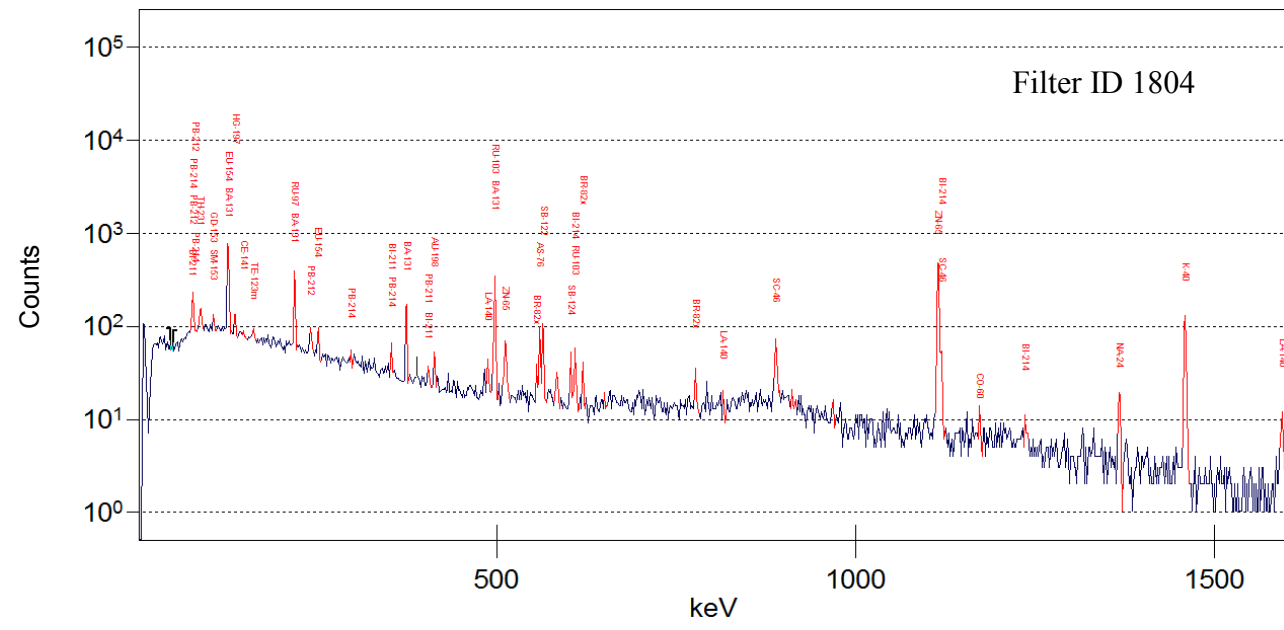


Figure 4.11 Gamma ray spectra showing the elements photo peaks from incident filter samples irradiated for 8 hours and counted for 1 hour with an HPGe detector after 7-10 days decay time

## 4.5 Recommendations

Before further analysis of used aircraft filters by NAA, elemental analysis of jet engine lubricating oil must ascertain the potential markers present in a typical 1.0-mL or 1.0-gm sample matrix. The time the filters remain installed in the aircraft is also critical in assessing the differences in the mean concentrations of isotopes in different types of used filters. Further studies should also determine the exact background isotopes from the reactor and eliminate background isotopes from statistical analysis aimed at determining the variability of mean concentrations of isotopes.

### 4.5.1 Statistical analysis

SAS output:

Dependent Variable: Ba-133

Source	DF	Sum of Squares	Mean Square	F Value	Pr > F
Model	1	482.73680	482.73680	6.15	0.0143
Error	148	11616.16867	78.48763		
Corrected Total	149	12098.90548			

R-Square	Coeff Var	Root MSE	BA133 Mean
0.039899	187.1169	8.859324	4.734646

Source	DF	Type III SS	Mean Square	F Value	Pr > F
Category Least Squares Means	1	482.7368045	482.7368045	6.15	0.0143

Category	BA133 LSMEAN	Standard Error	H0: LSMEAN=0 Pr >  t	H0: LSMEAN1=LSMEAN2 Pr >  t
1	5.94647048	0.87293516	<.0001	0.0143
2	2.07894402	1.29226526	0.1098	

Dependent Variable: Ce-139

Source	DF	Sum of Squares	Mean Square	F Value	Pr > F
Model	1	0.04678894	0.04678894	22.66	0.0010
Error	9	0.01858325	0.00206481		
Corrected Total	10	0.06537219			

R-Square      Coeff Var      Root MSE      CE139 Mean  
 0.715732      68.93147      0.045440      0.065921

Source	DF	Type III SS	Mean Square	F Value	Pr > F
Category	1	0.04678894	0.04678894	22.66	0.0010

Least Squares Means

Category	CE139 LSMEAN	Standard Error	H0: LSMEAN=0 Pr >  t	H0: LSMEAN1=LSMEAN2 Pr >  t
1	0.15219758	0.02272006	<.0001	0.0010
2	0.01661967	0.01717475	0.3585	

**Dependent Variable: Ce-141**

Source	DF	Sum of Squares	Mean Square	F Value	Pr > F
Model	1	0.00347257	0.00347257	11.49	0.0011
Error	79	0.02388188	0.00030230		
Corrected Total	80	0.02735445			

R-Square      Coeff Var      Root MSE      CE141 Mean  
 0.126947      135.3049      0.017387      0.012850

Source	DF	Type III SS	Mean Square	F Value	Pr > F
Category	1	0.00347257	0.00347257	11.49	0.0011

Least Squares Means

Category	CE141 LSMEAN	Standard Error	H0: LSMEAN=0 Pr >  t	H0: LSMEAN1=LSMEAN2 Pr >  t
1	0.01814139	0.00248383	<.0001	0.0011
2	0.00474787	0.00307359	0.1264	

**Dependent Variable: Co-60**

Source	DF	Sum of Squares	Mean Square	F Value	Pr > F
Model	1	0.00018620	0.00018620	9.88	0.0020
Error	160	0.00301442	0.00001884		
Corrected Total	161	0.00320063			

R-Square      Coeff Var      Root MSE      C060 Mean  
 0.058177      201.5161      0.004341      0.002154

Source	DF	Type III SS	Mean Square	F Value	Pr > F
--------	----	-------------	-------------	---------	--------

Category		1	0.00018620	0.00018620	9.88	0.0020
----------	--	---	------------	------------	------	--------

Least Squares Means

Category	C060 LSMEAN	Standard Error	H0: LSMEAN=0 Pr >  t	H0: LSMean1=LSMean2 Pr >  t
1	0.00283932	0.00040476	<.0001	0.0020
2	0.00047692	0.00063313	0.4524	

**Dependent Variable: Eu-152x**

Source	DF	Sum of Squares	Mean Square	F Value	Pr > F
Model	1	2.9401706E-7	2.9401706E-7	8.76	0.0043
Error	63	2.1145187E-6	3.356379E-8		
Corrected Total	64	2.4085358E-6			

R-Square    Coeff Var    Root MSE    EU152x Mean

0.122073    147.8497    0.000183    0.000124

Source	DF	Type III SS	Mean Square	F Value	Pr > F
Category	1	2.9401706E-7	2.9401706E-7	8.76	0.0043

Least Squares Means

Category	EU152x LSMEAN	Standard Error	H0: LSMEAN=0 Pr >  t	H0: LSMean1=LSMean2 Pr >  t
1	0.00016234	0.00002617	<.0001	0.0043
2	0.00000621	0.00004580	0.8925	

**Dependent Variable: Ru-103**

Source	DF	Sum of Squares	Mean Square	F Value	Pr > F
Model	1	0.02343193	0.02343193	10.14	0.0019
Error	105	0.24262258	0.00231069		
Corrected Total	106	0.26605452			

R-Square    Coeff Var    Root MSE    RU103 Mean

0.088072    322.8119    0.048070    0.014891

Source	DF	Type III SS	Mean Square	F Value	Pr > F
Category	1	0.02343193	0.02343193	10.14	0.0019

Least Squares Means

Category	RU103 LSMEAN	Standard Error	H0: LSMEAN=0 Pr >  t	H0: LSMean1=LSMean2 Pr >  t
1	0.00322733	0.00591696	0.5866	0.0019
2	0.03366645	0.00750722	<.0001	

**Dependent Variable: Ru-97**

Source	DF	Sum of Squares	Mean Square	F Value	Pr > F
Model	1	24.07107757	24.07107757	17.24	0.0003
Error	25	34.91580437	1.39663217		
Corrected Total	26	58.98688193			

R-Square	Coeff Var	Root MSE	RU97 Mean
0.408075	124.5422	1.181792	0.948909

Source	DF	Type III SS	Mean Square	F Value	Pr > F
Category	1	24.07107757	24.07107757	17.24	0.0003

Category	RU97 LSMEAN	Standard Error	H0:LSMEAN=0 Pr >  t	H0:LSMean1=LSMean2 Pr >  t
1	2.08766191	0.35632367	<.0001	0.0003
2	0.16601622	0.29544798	0.5792	

**Dependent Variable: Sc-46**

Source	DF	Sum of Squares	Mean Square	F Value	Pr > F
Model	1	0.00016158	0.00016158	28.55	<.0001
Error	53	0.00029997	0.00000566		
Corrected Total	54	0.00046155			

R-Square	Coeff Var	Root MSE	SC46 Mean
0.350073	87.10152	0.002379	0.002731

Source	DF	Type III SS	Mean Square	F Value	Pr > F
Category	1	0.00016158	0.00016158	28.55	<.0001

**Least Squares Means**

Category	SC46 LSMEAN	Standard Error	H0:LSMEAN=0 Pr >  t	H0:LSMean1=LSMean2 Pr >  t
1	0.00423946	0.00042729	<.0001	<.0001
2	0.00078338	0.00048562	0.1127	

**Dependent Variable: Zn-65**

Source	DF	Sum of Squares	Mean Square	F Value	Pr > F
Model	1	310.627973	310.627973	7.90	0.0055
Error	166	6527.566735	39.322691		
Corrected Total	167	6838.194707			



R-Square	Coeff Var	Root MSE	ZN65 Mean
0.045425	183.5421	6.270781	3.416536

Source	DF	Type III SS	Mean Square	F Value	Pr > F
Category	1	310.6279728	310.6279728	7.90	0.0055

Least Squares Means

Category	ZN65 LSMEAN	Standard Error	H0: LSMEAN=0 Pr >  t	H0: LSMEAN1=LSMEAN2 Pr >  t
1	4.32694839	0.58222738	<.0001	0.0055
2	1.38561498	0.86960083	0.1130	

**Table 4-4 Isotopes with statistically significant concentration differences in used and incident filters**

<b>Parent Element</b>	<b>Isotope</b>	<b>Filter type</b>	<b>Mean mass concentration (μCi)</b>	<b>p-value</b>
Barium	Ba-133	Used	5.94647048	0.0143
		Incident	2.07894402	
Cerium	Ce-139	Used	0.15219785	0.001
		Incident	0.01661967	
Cerium	Ce-141	Used	0.01814139	0.0011
		Incident	0.00474787	
Cobalt	Co-60	Used	0.00283932	0.002
		Incident	0.00047692	
Europium	Eu-152x	Used	0.00016234	0.0043
		Incident	0.00000621	
Ruthenium	Ru-97	Used	2.08766191	0.0019
		Incident	0.16601622	
Ruthenium	Ru-103	Used	0.00322733	0.0003
		Incident	0.03366645	
Scandium	Sc-46	Used	0.00423946	0.0001
		Incident	0.00078338	
Zinc	Zn-65	Used	0.58222738	0.0055
		Incident	0.86960083	

The concentrations for isotopes of the elements shown in Table 4-4 display marked differences in both the used and incident filters. For example, for Ba-133, the means for the filter type (category), used (1) and incident (2), are 5.946 and 2.079; these means are significantly different at 5% level with a p-value of 0.0134. The values for Ce, Co, Eu, Tu, Sc, and Zn are listed in Table 4.4; mean concentrations of these isotopes are higher in used filters for all the

elements except Ru-103 and Zn-65, which have higher means in incident filters. The used filters were removed at the end of their normal service life while the incident filters were normally removed much sooner. Clearly, the time the filters remain installed in the aircraft is a critical factor when determining the mean concentrations of isotopes from materials that are deposited on the filters and is the likely reason so many of the isotopes have higher concentrations on the used filters.

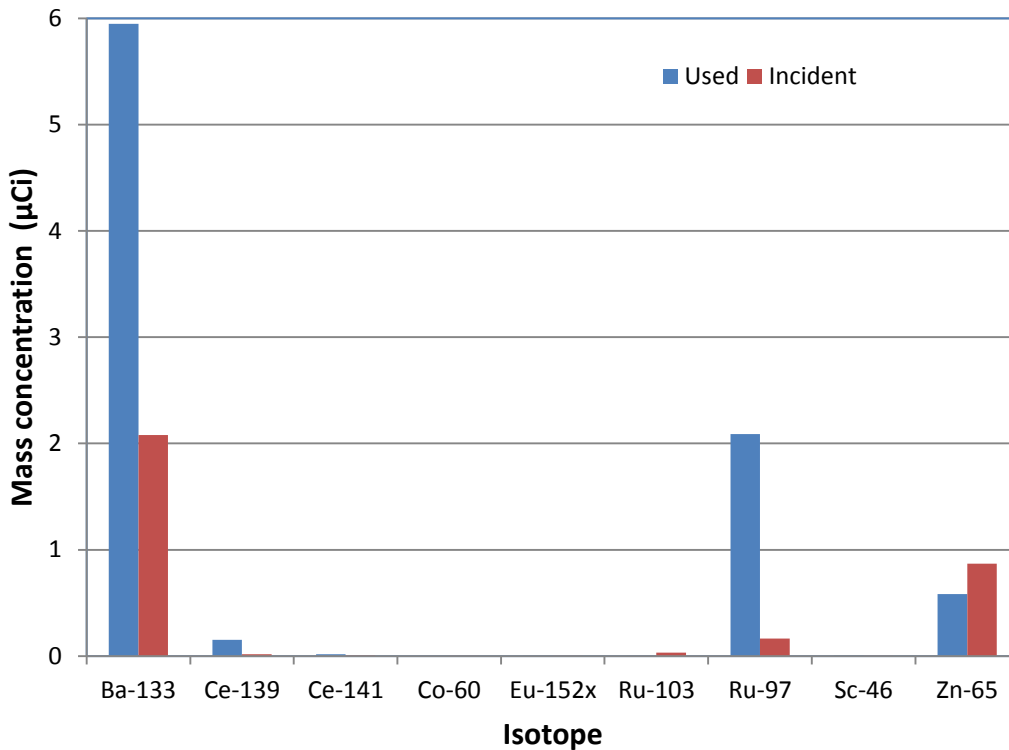


**Figure 4.12 Comparison of isotopes with mean concentrations found to be statistically significantly different in used and incident filters**

Figure 4.12 shows the isotopes with significant differences in mean concentrations. The cause and effect of the differences, however, was not established. Although the statistical analysis has not identified jet engine oil markers, the increases and decreases in the mean concentrations of the identified isotopes could help explain the effect of jet engine oil contamination on filters if the time the filter stayed in aircraft were known. Therefore, further studies should focus on increases and decreases in mean concentrations of identified isotopes and the time filters remain installed in the aircraft, which should help determine whether mean

concentrations are due to long-term accumulation of contaminants or from smoke/fume incidents.

The SAS program averaged the concentration from the two filter categories and calculated the p-value. A wide range of elements were detected on clean, used, and incident filters. Iron was detected in both used and incident filter samples. Dust brought into the cabin by passengers could be a possible source of iron species in the aircraft cabin. The sensitivity of NAA technique depends on the half-life of isotopes being analyzed, number of particles per decay (yield), and the efficiency of the detector.

According to Weaver (1978), the minimum detectable limits of bromine in a sample is 0.009  $\mu\text{g}$  for 1 hr. of radiation using a neutron flux of  $1 \times 10^{13}$   $\text{n/cm}^2\text{-sec}$  instrumental analysis with no interfering elements. Bromine was detected in two incident filters, filters ID 1804 and 2985, with the highest ID confidence level being 60.0% and the lowest being 14.5%. A threshold level of 70.0% is generally acceptable as significant. Bromine could be in the filters, and indeed Gerecke (2007) detected bromine in settled dust from commercial aircrafts. With the current experimental design, bromine could not be detected in many filters because high activity from silicon interfered. In addition, bromine has a short-half life (1.47) days, making it still more difficult to detect. Also, bromine is present in many flame retardants widely used in cabin materials so bromine, if found, could not be uniquely associated with engine oil.

A number of factors make NAA gamma spectroscopy a difficult method, especially looking for markers or determinants of jet engine oil contamination. Among them are: The small amounts of radioactive particles and long decay periods for some elements. Fe 58 which is the parent element of Fe 59 has a small amount of radioactive Fe (about 0.28% of elemental iron is contained in Fe 58). It is this small amount of radioactive Fe which is expected to decay in 44 days. The low cross-section is also a factor. The cross-section, which is essentially the probability of neutron capture, is low in the gamma-ray counting technique for some important isotopes. For Fe the cross section for neutron capture is 1.3 barns (thermal neutrons), 1 barn =  $1 \times 10^{-24}$   $\text{cm}^2$ ). A number of trace elements were found on clean, used, and incident filters. The concentration levels of the isotopes found in the filters are cumulative from many flight hours and may not reflect air quality concerns. Without a doubt, the most useful finding is that elements are present on both used and incident filters. That they can be tested using NAA is

intriguing. For airlines, the findings of this study have implications far beyond health because smoke/fume incidents may also indicate that the aircraft engine is not operating optimally.

One reason smoke/fume incidents have been difficult to understand is that they occur somewhat randomly and there is a low probability of occurrence on any given flight. An incident is difficult to predict. Another reason for the failure to fully grasp the problem is, in part, due to the study approaches that have so far been applied. When it comes to the future of airlines operations nothing is more important than the health and safety of passengers and crew. But, there are different sides to the issues; for the airlines as any other companies they are in business. But they cannot afford to engage in air transportation business and ignore operational consequences which impact negatively on aircraft crew and air travelers. The exploitation of chemical capabilities of Mobil Jet Oil II at the expense of those who are negatively affected is unacceptable. Both of these issues, while mostly different from a technical standpoint, point to the increasing effect of modern society's influence on the environment and often negligence of the cause and effect relationships. It is encouraging that Boeing is currently building a 21<sup>st</sup> century aircraft system that focuses on prevention of fumes events and promotes cleaner air supply to aircraft cabins.

#### ***4.5.1.1 Cost evaluation model for analysis of used aircraft filters by NAA***

This study explored the relationship between safety and the benefits of using NAA to analyze cabin air filters used on commercial aircraft. The costs associated with aircraft filter analysis by NAA are high. As depicted in Figures 4.7 and 4.13, filter testing with NAA is complex and requires time and expertise. Although the method could produce positive results with higher efficiency detectors, using an experimental set up the facilities available at Kansas State is too laborious, costly, and time-consuming to become routine for commercial operations.

4.5.1.2 Cost analysis model for used aircraft filters by NAA

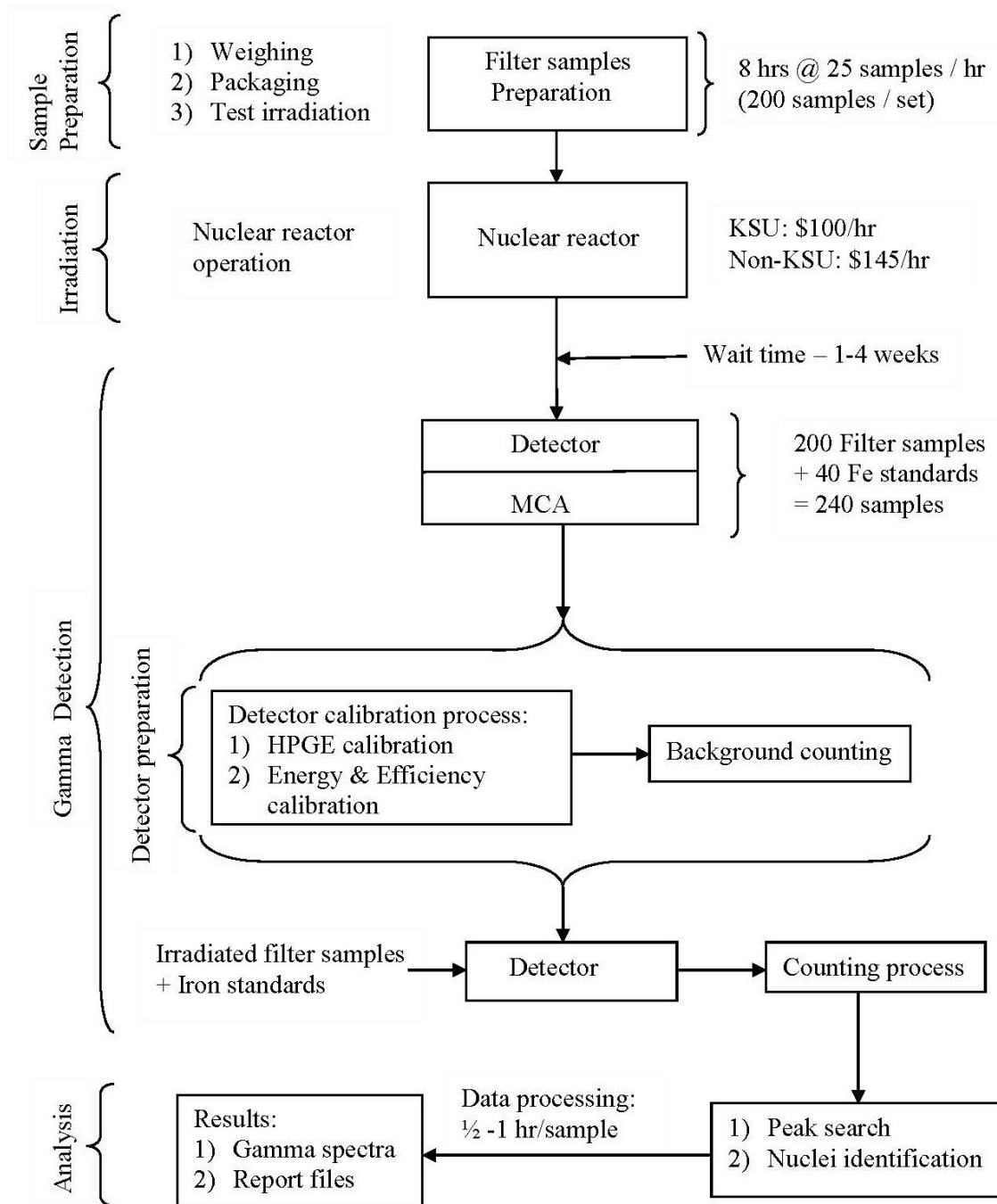


Figure 4.13 Process flow chart of aircraft cabin air filter analysis by NAA

**Table 4-5 Cost evaluation chart and comparison guide for analysis of used aircraft cabin air filters by NAA**

Process	Process description	Filter samples*	KSU rates/hr.	Non-KSU rates/hr.
Sample Preparation	Sample preparation	200	\$25.00	\$25.00
Irradiation	Irradiation	200	\$100.00	\$145.00
Gamma detection	Detector preparation: HPGE calibration Energy and efficiency calibration	240**	\$35.00	\$51.00
Analysis	Peak search Nuclei identification Data processing	240	\$25.00***	\$36.00***
TOTAL COST			\$15,900.00	\$20,190.00
*10 sample sets were analyzed		<b>TOTAL COST</b>	<b>\$ 159,000.00</b>	<b>\$ 201,700.00</b>

\*\* Irradiation of sample set is independent of sample size, but limited to 200 samples.

\*\*\* Sample charge is hourly, averaging 45 minutes per sample.

The rates include staff salary and equipment usage.

## 4.6 Conclusions

This research could not identify unique elements from jet engine oil observable as contaminants on aircraft cabin filters. However, the study gleaned several interesting facts about NAA as a method for analyzing used aircraft cabin filters. The study found a large variety of trace elements deposited on the surface of used and incident filters. The data obtained from the study could be a starting point for explaining the many mysteries of the aircraft cabin air contamination. This suggests that more is going on in an aircraft's ECS than scientists have previously imagined. Never before has the entire catalog of elements deposited on used aircraft cabin filters been revealed. The data produced by this study will be shared among those searching for appropriate detection methods for aircraft cabin air contamination.

Statistical analysis by one way ANOVA using SAS code PROC GML has revealed statistically significant differences in the means of the concentrations of some isotopes from used and incident filters. The isotopes are from parent elements Ba, Ce, Co, Eu, Ru, Sc, and Zn. The

differences in the means of concentrations of the identified isotopes are certainly pointing at where a search should focus on. Future work should focus on determining the differences in mean concentrations of these isotopes after isolating the background isotopes. The length of the time the filters remain installed in aircraft was also critical to determining whether the differences were due to long-term accumulation of contaminants or smoke/fume incidents. A methodology for gathering data from used and incident filters is by itself a positive contribution. Using this method and a different type of reactor or different irradiation conditions with a different detector might produce expected or different results. However, the long-term future of NAA as a method of aircraft filter analysis will depend on its cost.

#### 4.7 References

- Agnello, M., Botta, E., Bressani, T., Bruschi, M., Bufalino, S., DeNapoli, M., Feliciello, A., Fontana, A., Giacobbe, B., Lavezzi, L., Raciti, G., Rapisarda, E., Rotondi, A., Sbarra, C., Sfienti, C., Zoccoli, A., (2009). Study of the performance of HPGe detectors operating in very high magnetic fields. *Nuclear Instruments and Methods in Physics Research A*.606 (2009) 560 – 568.
- Alemon, E., Herrera, L., Ortiz, E., and Longoria, L. C., (2004). Instrumental nuclear activation analysis (INAA) characterization of environmental air filter samples. *Appl. Radiat. Isot.* 2004 June, 60 (6):815-23.
- ANSI/ASHRAE, (2007). ANSI/ASHRAE Standard 161-2007, Air Quality within Commercial Aircrafts. 20 pp. Product code: 86493. ISBN: 1041-2336. Atlanta, GA: American Society of Heating, Refrigerating and Air-conditioning Engineers, Inc.
- Canberra (2001) Canberra. Genie 2000 Spectroscopy System Operations Manual (2001). Canberra Industries Incorporation, Meriden, CT (2001).
- General regulations for radioactive waste disposal 10CFR20.2001 (1991) [http://cfr.regstoday.com/10cfr20.aspx#10\\_CFR\\_20p200120.2001](http://cfr.regstoday.com/10cfr20.aspx#10_CFR_20p200120.2001) Cited: May 20<sup>th</sup> 2011.
- Gerecke, A. C., (2007). Brominated Flame Retardants in Settled Dust of a Commercial Aircraft. <http://www.bfr2010.com/abstract-download/2007/P074.pdf> (Cited: March 15<sup>th</sup>, 2012).
- Glascock, M. D., (2011). Overview of Neutron Activation Analysis. University of Missouri – Columbia. [http://archaeometry.missouri.edu/naa\\_overview.html](http://archaeometry.missouri.edu/naa_overview.html) Cited: March 15<sup>th</sup> 2012.
- Landsberger, S., Larson, S., Wu, D., (1993). Determination of cadmium in environmental tobacco smoke by instrumental neutron activation analysis with compton suppression system. *Anal. Chem.* 1993 June 1: (11) 1506 – 9.



- Nagda, N. L. and Rector, H. E., (2003). A critical review of reported air concentrations of organic compounds in aircraft cabins. *Indoor Air* 2003; 13: 292 – 301. Copyright Blackwell Munksgaard ISSN 0905-6947.
- Shultis, J. K. and Faw, R. E., (2007). *Fundamentals of Nuclear Science and Engineering* 2<sup>nd</sup> edition. CRC Press 2007.
- van Netten, C., (1999). Multi-elemental analysis of jet engine lubricating oils and hydraulic fluids and their implication in aircraft air quality incidents. *Sci. Total Environ.* 1999 May 7: 229 (1-2): 125-9.
- Winder, C. and Balouet, J. C., (2001). Aircrew Exposure to Chemicals in Aircraft: Symptoms of Irritation and Toxicity. *Journal of Occupational Health and Safety – Australia and New Zealand* 17: 471 – 483, 2001.

# **CHAPTER 5 - MONITORING SIMULATED COMMERCIAL AIRCRAFT CABIN AIR QUALITY INCIDENTS USING BLEED AIR SIMULATOR (BAS)**

## **5.1 Abstract**

During smoke/fume incidents, aircraft cabin occupants may be exposed to toxic organophosphorus (OP) compounds emitted from the bleed air. Exposure to OP compounds, including TCP, is associated with increased risks to health. The objective of this study was to design a simplified version of an aircraft engine bleed air simulator (BAS) for the laboratory to simulate the range of bleed air system operations and create smoke/fume incidents. Experiments were conducted to determine what alters aerosol particulate formation during various simulated incidents using Mobil Jet Oil II as a representative jet engine lubricating oil. The BAS system consisted of a modified ASHRAE Standard 52.2 test rig with a tubular reactor where pyrolysis of jet engine oil occurred. Particulate counts were determined with an optical particle counter (OPC). Samples were also collected onto HEPA filters with a high volume isokinetic sampling system; subsequent laboratory analysis included GC/MS, FESEM/EDS and NAA to determine if elements/compounds linked to the jet engine lubricating oil were present. The exposed filters were also analyzed for TCP isomers and hydrocarbons by GC/MS. The six simulated cabin air quality incident results are also described in this study. Probit analysis of jet engine oil aerosols from BAS tests revealed lognormal distributions with the mean (range) of geometric mass mean diameter (GMMD) = 0.41 (0.39, 0.45)  $\mu\text{m}$  and geometric standard deviation (GSD),  $\sigma_g = 1.92$  (1.87, 1.98). The GC/MS analysis found meta- and para- TCP in clean filters exposed in BAS. The results suggest that BAS and the methodology used in this study can provide a practical air quality of bleed air in commercial aircrafts during incidents. Additionally, BAS could provide insights to help airline regulators in drafting guidelines for compliance requirements to minimize threats and risks posed by aircraft cabin air supply contaminant emissions from the bleed air system during incidents caused by jet engine lubricating oil.

## **5.2 Introduction**

Even though commercial aviation technology has become very advanced, modern airplanes still have inherent design challenges in providing quality air through a bleed air system.

For example, smoke/fume incidents occur in aircraft engines when an oil seal is leaky, a joint is cracked, or too much jet oil is added by maintenance staff (van Netten and Leung, 2000; AAIB Bulletin, 2009). During incidents, misty fumes or the gases and/or smoke/fumes generated when the jet engine oil is pyrolyzed may be introduced into the aircraft's environmental control system (ECS) and eventually enter the aircraft cabin where they may cause discomfort and or adversely affect the health of cabin occupants. The negative impact of an incident-occurrence happens when it alters the gaseous and particulate concentration of the cabin air supply. Jet engine lubricating oils and hydraulic fluids have organophosphate additives that can negatively affect aircraft cabin air supply, particularly in those aircrafts with bleed air systems. Moreover, the aircraft cabin is a high-stress environment, and any additional events like smoke/fume incidents will only heighten stress among passengers and crew. Even more troubling, smoke/fume incidents are infrequent and difficult to predict. Yet, although they are rare, cabin occupants are exposed to the airborne constituents of jet engine lubricating oil when such an incident occurs.

At present, incident-occurrences are not monitored in aircraft fitted with bleed air systems. Providing quantitative measurements of airborne aerosols formed in the bleed air system during smoke/fume incidents and accounting for the suspected burden caused by incidents in the aircraft cabin has been a challenge, and airlines are still struggling to deal with the challenge. The uncertainty about the effect of TCP isomers on cabin air quality is a real concern. Scientists have yet to determine the frequency of incidents and ways to combat the events. Currently, what most concerns scientists and stakeholders in civil aviation is whether the smoke/fumes in cabin environments are enough to cause harm to cabin occupants when incidents occur. Additionally, the lack of real-time monitoring of aerosol emissions from the bleed air system has hindered efforts to understand air quality in aircraft cabins during incidents.

As demand for air travel grows, more attention is being paid to aircraft cabin air quality. Airlines are expected to provide superior air quality to passengers at all times during flight. The business of commercial air transport requires providing not only quality air but comfort and safety as well. The safety features of commercial jets include cabin air that meets quality standards of temperature, relative humidity, and odor (Pierce et al. 1999; Lee et al. 1999; Lindgren and Norback, 2002; Haghghat et al. 1999). Previous studies of aircraft cabin environments have helped determine (TLVs) for well-known potential airborne pollutants in aircraft cabins. Table 5-1, below, lists some commercial aircraft in-cabin air quality parameters

and the recommended levels that ensure the safety of the passengers and crew (Hunt and Space, 1994; Hocking, 1998).

**Table 5-1 Air quality parameters measured in commercial airliner cabin environment**

Parameter	Average measurements
Carbon dioxide (CO <sub>2</sub> )	600 –1,500 ppm
Carbon monoxide (CO)	0.6/0.4 ppm
Respirable Suspended Particulate (RSP)	40/175 ppm
Nitrogen dioxide (NO <sub>2</sub> )	Very low
Sulfur dioxide (SO <sub>2</sub> )	Very low
Ozone (O <sub>3</sub> )	0.02 ppm
Formaldehyde (HCHO)	-
Total Volatile Organic Compounds (TVOC)	1.8 – 3.2 ppm
Temperature	24°C

(Source: Hunt and Space 1994; Hocking, 1998).

All human dwellings and recreational environments today, including enclosed spaces like aircraft cabins, face unprecedented demands that air quality be superior. Excessive airborne particulates and gases in any environment inhabited or occupied by humans can cause health problems. That is why accounting for potential sources of all aerosol particulates in an aircraft cabin environment matters. The design of the ECS in commercial aircraft dictates having precise quantification of air quality information. Studies by Ross et al. (2006) have reported findings that suggest that prolonged exposure to contaminated air on commercial aircraft may cause ill health. Currently, standards do not exist to ensure that the passengers and crew are not exposed to undesirable concentrations of aerosols from TCP produced during smoke/fume incidents. The current OSHA standard for ToCP is 0.1 mg/m<sup>3</sup> of air averaged over an eight-hour work shift. Table 5-2 below lists the standards for the exposure limits of ToCP in workplaces. Exposure to TCP and ToCP can occur through inhalation, ingestion, or eye and skin contact (ACGIH, 2001).

**Table 5-2 The OSHA and ACGIH standards for ToCP**

<b>Standards</b>	<b>Tri-ortho cresyl phosphate</b>
OSHA	PEL: 0.1 mg/m <sup>3</sup> TWA
ACGIH	TLV: 0.1 mg/m <sup>3</sup> TWA

(Source: ACGIH 2001; NIOSH 1994; Cone 2005)

Public information such as labels and material safety data sheet (MSDS) for jet engine oils products ironically grossly understate the hazards of oil ingredients especially ToCP according to Winder and Balouet (2002). The approximate concentration range fraction of TCP ingredient in Mobil Jet Oil II is 2 to 3 percent (De Nola et al. 2008; Winder and Balouet, 2000; Kibby et al. 2005). According to an NRC (2002) report, no quantitative measurements of exposure levels for commercial aircraft engine bleed air are available for the ingredients present in jet engine oils. The 2002 NRC report also points out that phosphate esters and aldehydes found in jet engine oils and their pyrolysis products may cause respiratory and neurological effects, particularly at high concentrations (NRC report, 2002).

The aircraft environment is similar to indoor environments although it differs in how air quality is provided (Strøm-Tejsen, 2006). The quality of the air supply is important for the human body to work optimally, which is why air quality provision in aircraft cabins is regulated by FAA rules. While several FAA regulations govern the quantity and quality of the air supplied to cabin occupants during flight, no current government-mandated or even widely accepted industry standards consider the levels of particulate emissions released from jet engine oils during smoke/fume incidents. The bleed air emissions reporting rules that airlines use at the moment are prescriptive. It would be desirable to move from prescriptive standards to performance standards that rely on measurements. Unfortunately, the inability to capture bleed air system data has delayed developing of the necessary scientific information for effective policy interventions. Currently, airlines need reliable methods and interface control solutions for monitoring aircraft bleed air.

### **5.2.1 Trends in development of aircraft engine bleed air monitor**

Bleed air technology dates back to 1963 when it was first incorporated into the jet engines of the Boeing 727, among the first generation of modern commercial aircraft. At the

same time, the synthetic lubricant jet engine oil was introduced into jet turbine engine operations. Since then, no standard has been developed to limit potential airborne solid particulates and gaseous pollutants emitted from the bleed air system during incident-occurrences. Van Netten and Leung (van Netten, 2000; van Netten and Leung, 2001) provided data from GC/MS measurements of what should be monitored, although conditions associated with the emissions of TCPs remain undetermined.

In 1998, Honeywell reported on its bleed air monitor (BAM), which used catalytic oxidation combined with a CO<sub>2</sub> monitor. The device relies on a catalyst to convert VOCs into CO<sub>2</sub> and water and then measures CO<sub>2</sub> concentration in the bleed air as a surrogate measure of exposure to VOCs associated with combustion of organic materials like oil, hydraulic fluid, and exhaust fumes. Initially intended as a unit for ground operations, it was later modified for integration into aircraft systems for continuous monitoring throughout flight (Air Contamination Monitor, Patent No. 5750999, 1998). Magee Scientific offers a compact, portable, sensitive particle monitor for aerosol black carbon called a micro-aethalometer (Magee Scientific, 2009), which could be integrated into aircraft systems. Van Netten has also developed a personal sampler to monitor cabin air for TCPs in a BAe-300 aircraft (van Netten, 2009).

In 2006, with a grant from the US Air Force (USAF), Owlstone Nanotech in Cambridge, designed a prototype sensor to analyze several airborne contaminants concurrently in the bleed air stream. The goal was to provide real-time information on air supply contamination (e.g. jet oil, hydraulic fluid, exhaust fumes, etc.) in-flight (Koehl et al. 2007). A prototype device was developed, but the USAF did not proceed with this project. Boeing has developed an oil detection kit to identify sources of engine oil leaks or aerosol odors. The kit includes a bleed air sampler and portable infrared spectrometer. Ground crews can connect the air sampler to the 3-inch pneumatic ground cart connector and run the engine or APU bleed air through the sampler for 10 minutes. The spectrometer and a laptop computer analyze the sample. The kit's software alerts the user when the sample matches a known contaminant like oil or hydraulic fluid. In other words, the Boeing sniffer device retrieves an oil signature and compares it with the signature in the bleed air (Holley, 2009).

Similarly, collaborative work from Airsense Analytics GmbH and Lufthansa Technik AG resulted in development of an oil smell detection kit called an aerotracer to identify oil contamination in the aircraft air supply system during ground operations. Aerotracers can

monitor for VOCs, but the device has no trigger point (Airsense Analytics, 2008). Although both the Boeing kit and aerotracer can be used for troubleshooting smoke/fume incidents in the cabin, they are portable devices that are not built into aircraft's architecture and can only be used for ground operations. Additionally, even though the data from portable devices might be accurate, real-time monitoring of bleed air during flight cannot be performed today, presenting a major challenge for the airlines. Furthermore, qualitative measurements from jet bleed air operations simply cannot be made. Quality measurements require large equipment like the BAS. ACER members at Auburn University have developed a portable device for measuring airborne TCP in a gaseous phase. The device converts TCP into cresols by acid hydrolysis. The cresols are then quantified using electrochemical detection techniques (Yang et al. 2011). The ACER members, however, have not indicated if this technology can be used for real-time monitoring on aircraft. Additionally, it is not known how sensitive, expensive, durable, or appropriate the electrochemical detection technique is.

Air travel is the quickest and safest mode of transportation; however, incident-occurrences tend to complicate flight experiences for air travelers and cabin crew. During such incidents, the safety and health of air passengers and crew are at risk. For the cockpit crew, incidents may cause pilots to be unable to function at their best. Diverting the aircraft to the nearest airport to avoid further exposure of cabin occupants is usually the first line of action when smoke/fume events occur, but this is costly. Moreover, such frightening experiences raise legitimate concerns about the suitability of bleed air technology in commercial aircraft operations. A smoke/fume incident is actually a crisis of unknown proportion, disrupting cabin air quality in ways that are difficult to predict. Concerns include how long a smoke/fume incident lasts, and most concerns cannot be addressed because of a lack of research.

At present, modern aircrafts do not have smoke/fume incidents monitoring systems on-board (Ross, 2008). Furthermore, no control system is fitted to the ECS to remove airborne particulates from jet engine bleed air during smoke/fume incidents. Technological solutions for particulate and gaseous contamination from the cabin air supply have been recently suggested (Bull and Roux, 2010), but these solutions have not been evaluated for overall effectiveness. The single most critical element of monitoring cabin air quality is figuring out how to measure airborne aerosols in the aircraft bleed air system. To detect smoke/fume incidents, the aircraft cabin occupants remain the on-board sensors, with airlines relying on human smell to detect

smoke/fume incidents caused by oil (AFL-CIO Report, 2003). One obvious problem with this method of detection is smell is subjective and difficult to assess. The smell changes with time and the person doing the sniffing. Also, the nose can take a long time to detect the smell of oil. The reality is that no human odor threshold exists for any known chemical substance, i.e., human reactions to incidents vary greatly. While an aircraft is in flight, whenever aircrew members smell oil or see visible smoke in the cabin, the cockpit crew usually switches off the ventilation feed from the affected engine (Select Committee on Science and Technology Report to the House of Lords, 2000). In severe incidents, the procedures dictate that the crew redirects the aircraft to the nearest airport. This inconveniences passengers and is expensive for the airline. Pilots need an objective way to identify a source of air contamination. Measurement tools developed from scientific studies and procedures for responses to incidents are therefore critical. Airlines can realize significant efficiency gains in cabin air quality assessment by moving from the human-based process (smell) to one that is fully technology-enabled. Scientists have long sought solutions to smoke/fume incidents but simply monitoring the process has been a challenge. The complexity of the pyrolysis of jet engine oils and the sophisticated patterns of aerosol particulate formation associated with the process make measuring jet engine bleed air quality difficult to do.

The aim of this study was to develop a BAS to determine the concentration levels of compounds and elements in a laboratory-simulated jet engine bleed air system to establish detection limits for different exposure levels. To gain insight into the nature of the aerosol particulate emissions and gaseous byproducts emanating from the bleed air system, an aircraft bleed air simulator (BAS) monitored simulated bleed air in real time. The integrated solution included using an ASHRAE Standard 52.2 test rig, a pyrolysis reactor, an air sampling system, and aerosol counting instruments designed to let users continuously monitor smoke/fume incident conditions. The technical challenges of this BAS design are discussed in this study as well. The sampled aerosols were analyzed by FESEM/EDS, GC/MS, and NAA to determine the concentration of compounds and elements deposited on the filter. The overall objective of the study was to facilitate jet engine bleed air monitoring and to aggregate the data to document parameters for aircraft cabin air quality during smoke/fume incidents.



## 5.3 Materials and Methods

### 5.3.1 Experimental setup

The schematic diagram of the BAS shown in Figure 5.1, was used aerosol, sample, and measure various parameters associated with each test run. The experimental rig is 3 feet tall, made of rectangular tubes connected in a line (see Figure 5.1). The main duct consists of a series of ducts (air conditioning chambers) with a square cross section measuring  $610 \times 610$  mm ( $12 \times 12$  in.), except at the test chamber, which is the largest part of the duct system with a square cross-section configuration of  $915 \text{ mm} \times 915 \text{ mm}$  ( $36 \times 36$  in.). The air conditioning chambers were made of galvanized iron sheets with cross-breaking on all four sides to enhance the crushing strength of the sheet metal. The experimental set up (see Figure 5.1) comprises a duct system simulating a bleed air polluting passageway ventilated with clean outside room air. The duct design conforms to ASHRAE Standard 52.2-1999, which delineates appropriate methodology for testing ventilation particulate air filters and other air cleaning devices (ASHRAE, 1999). The set-up was assembled to meet the aerosol generation, transport, and characterization needs of the study.

The general design criteria related to outside air pre-treatment units, terminal units, air devices, and ductwork are in accordance with ASHARE Standard 52.2 to minimize potential air quality effects. The overall design provides air conditioning and ventilation systems to maintain clean room certification. All joints (sheet metal collar joints) in the duct system were air sealed with mastic in addition to being mechanically fastened. The primary function of the duct system was to provide airflow rates required for the experiment by creating uniform and continuous air flow through the system. The elements that produced controlled airflow rates included a blower to move the air; a canvas connector to reduce vibration transmission from the blower; combined orifice and mixing plate, diffusers; and inlet and exhaust filters to clean incoming and exhaust air.

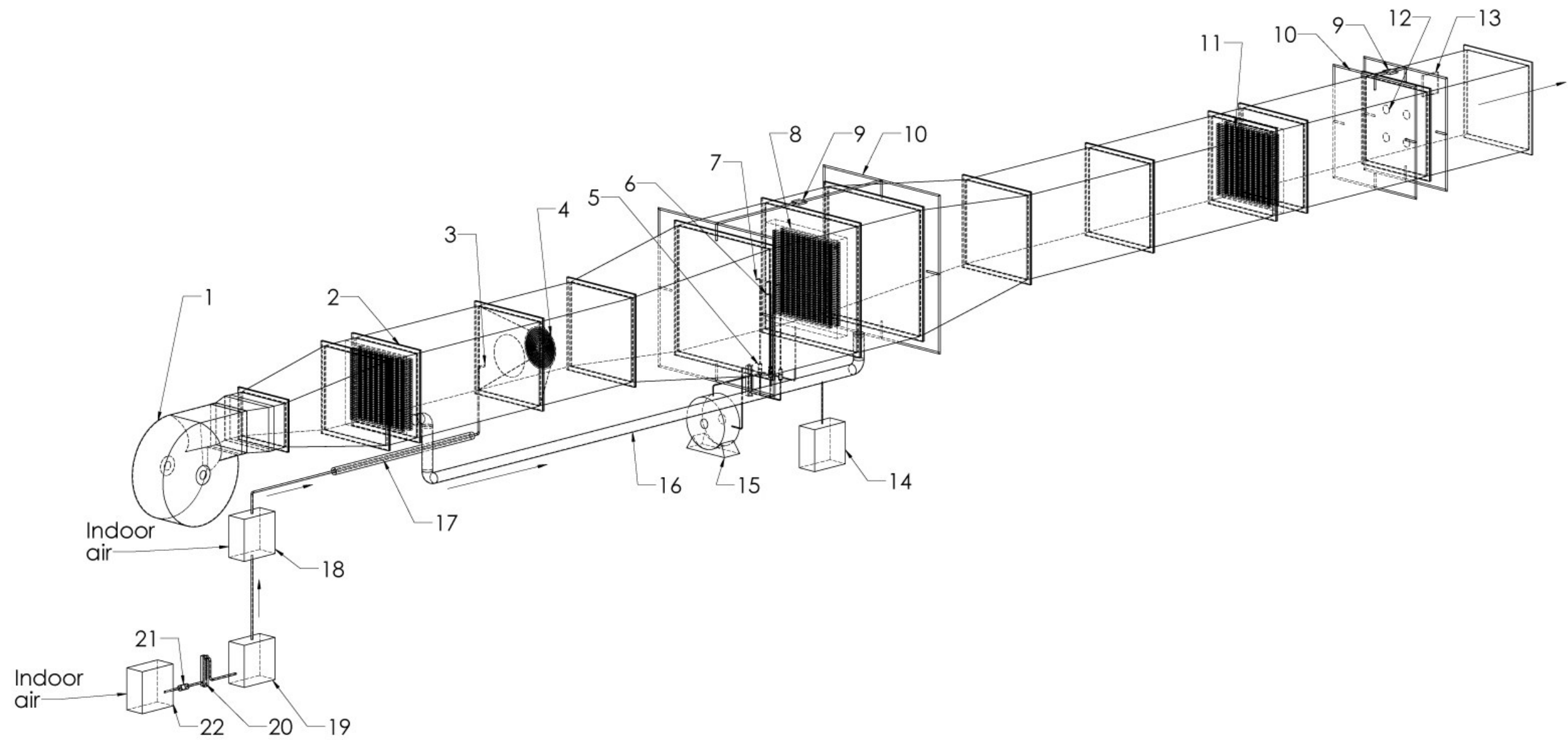


**Figure 5.1 Schematic diagram for aircraft bleed air simulation (BAS) system**

©ASHRAE, www.ashrae.org. (1999) ASHRAE Standard 52.2

- |                             |                              |                              |                          |                     |
|-----------------------------|------------------------------|------------------------------|--------------------------|---------------------|
| 1. Blower                   | 6. Sampling probe to bypass  | 11. Outlet filter bank       | 16. By-pass duct         | 21. Air filter      |
| 2. Inlet filter bank        | 7. Isokinetic sampler probes | 12. ASME nozzle              | 17. Reactor              | 22. Main compressor |
| 3. Aerosol injector         | 8. HEPA filter bank          | 13. CO sensor                | 18. Secondary compressor |                     |
| 4. Mixing orifice and plate | 9. Pressure transmitter      | 14. Optical particle counter | 19. Aerosol generator    |                     |
| 5. Filter cassette          | 10. Pressure ring            | 15. Air sampling pump        | 20. Air flow meter       |                     |

Other features of the BAS included: aerosol generator, pyrolysis reactor, by-pass duct, aerosol sampling lines for the OPC, flow measurement devices, pressure taps, and instrumentation. The ductwork could withstand internal pressures and contain air so that it was distributed to the various sections of the system. The blower was selected to meet the flow rate, pressure rise, and efficiency requirements for aerosol sampling applications. At the inlet, the test equipment unit was fitted with a variable speed fan (blower) to supply and move air across the inlet HEPA cabin air recirculation filter at a constant face velocity of  $0.47 \text{ m}^3/\text{s}$  (1000 CFM). This air flow rate and a pressure rise of 1000 Pa (4.0 in.  $\text{H}_2\text{O}$  column) were the criteria for choosing a blower. Room air was used as the source. The inlet filter bank was fitted after the blower and arranged to discharge along the centerline of the upstream mixing orifice. The inlet filter bank not only cleaned the room air to ensure that the test results.

The primary function of the duct system was to provide airflow rates required for the experiment by creating uniform and continuous air flow through the system. The elements that produced controlled airflow rates included a blower to move the air; a canvas connector to reduce vibration transmission from the blower; combined orifice and mixing plate, diffusers; and inlet and exhaust filters to clean incoming and exhaust air. Figure 5.1 is schematic diagrams of the apparatus were not biased but dampened any flow fluctuations from the fan (i.e., it caused air to flow uniformly downstream at a constant face velocity). At this point, aerosols from the reactor were injected between the inlet filter bank and upstream mixing plate. The mixing plate distributed the aerosol particulates uniformly in the duct system i.e., it controlled and shaped the flow. It created a turbulent jet inside the duct so that the aerosol particulates mixed uniformly with the air. The small flow area on the mixing plate reduced the cross-sectional area for the flow, resulting in higher turbulence. The perforated plate had 30% open area (Mahindra, 2004).

Just ahead of the mixing orifice, the ductwork system assumes a divergent shape (divergent diffuser) to fit into the bigger test chamber. The diverging section increases the cross section of the duct from  $610 \times 610 \text{ mm}$  to  $915 \times 915 \text{ mm}$  ( $24 \times 24 \text{ in.}$  to  $36 \times 36 \text{ in.}$ ) over a length of 1.22 m (4 ft.). The divergent diffuser chamber slowly expands along its length, allowing fluid pressure to increase and decrease fluid velocity. Increasing the cross-sectional area helped create a uniform airflow pattern in the test section. The shape and size of the test section chamber, where measurements were made, was largely determined by testing requirements. The section is  $610 \times 610 \text{ mm}$  ( $36 \times 36 \text{ in.}$ ) in cross section and 1473.2 mm (58 in.)

long and acted as housing for the filter loader. The section has two doors, which allows the user to load the filter and inspect the sampling probes. The aerosol sampling probes and a probe that leads to by-pass duct were installed in the test chamber. The filter in the test section is held in place by a rigid, heavy-duty high strength frame with support members on the entering and exiting sides of the filter. The filter was installed in the chamber to obtain smooth air flow at the outlet of the device section.

Located downstream of the test section is a convergent diffuser, which reduced the cross section of the duct back to  $610 \times 610$  mm ( $24 \times 24$  in.) over a length of 1220 mm (48 in.). The convergent section allows fluid pressure to increase and decrease fluid velocity. The exhaust air was ducted into the room after it passed through the exhaust HEPA filter bank. The inlet and outlet filter banks each consists of a  $610 \times 610 \times 101.6$  mm ( $24 \times 24 \times 4$  in.). Four ASME flow nozzles of 101.6 mm (4.0 in.) diameter designed according to ANSI/ASHRAE Standard 41.2. (1987) were mounted on an aluminum plate inside the last chamber of the ductwork to measure airflow rate through the system. The pressure drop across the ASME nozzles was measured to calculate the flow rate through the test duct. The differential pressure across the nozzles was measured with a pressure transmitter with an accuracy of  $\pm 5$  percent.

### ***5.3.1.1 Reactor design calculations***

The reactor holds air and jet engine oil aerosol mixture securely in a confined space to allow heating to take place. A uniform heat flux was maintained by two electric resistance heaters wrapped around the outer surface of the tube (tube reactor). The tube reactor (pipe) was resistively heated externally to the desired pyrolysis temperature.

Assumptions:

- (i) The flow is considered to be steady-state internal turbulent flow;
- (ii) Constant fluid properties;
- (iii) Uniform heat flux at the surface i.e., tape heater supplying heat at constant heat flux;
- (iv) Adiabatic tube surface;
- (v) The velocity profiles are fully developed;
- (vi) The flow has negligible potential energy (PE) and kinetic energy (KE);
- (vii) There is no work transfer across the boundary of control volume;
- (viii) The rate at which energy is generated is;

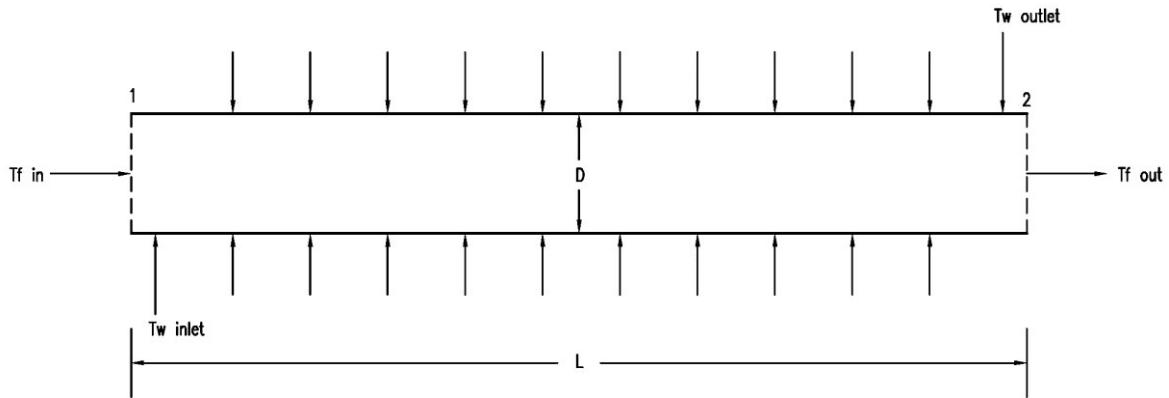


**Figure 5.2 Schematic of pyrolytic reactor for jet engine oil**

From thermo-physical properties of air at 477.59 K (Incropera and Dewitt, 2002), interpolate between 450 and 500 K to find  $\rho_{\text{air}}$ ,  $\mu_{\text{air}}$ ,  $k$  and  $Pr$ .

**Table 5-3 Thermal-physical properties of air at 477.59 K**

$\rho_{\text{oil}}$	$1.1 \text{ kg m}^{-3}$
$\mu_{\text{air}}$	$2.613 \times 10^{-5} \text{ N.s/m}^2$
$k$	$39.176 \times 10^{-3} \text{ W/m}\cdot\text{K}$
$c_{p \text{ air}}$	$1003 \text{ J/(kg}\cdot\text{K)}^{-1}$
$Pr$	0.7
$R$	$8.315 \times 10^3 \text{ kJ(kmol K)}^{-1}$

These thermal properties of air are read from: Table A.6, (Incropera and DeWitt, 2004).

From the law of conservation of energy: Heat flux,  $\dot{q}$  at the internal surface of the tube can be calculated as follows:

$$\dot{q} = h_c A (T_{\text{wall in}} - T_{\text{fluid}}) \quad (5.1)$$

$$\dot{q} = h_c A (593 \text{ K} - 573 \text{ K})$$

Small  $\Delta T$  is considered in order not to burn jet engine lubricating oil.

Nusselt number for turbulent flow in pipes is calculated thus:

$$Nu = (h_c \times D)/k \quad (5.2)$$

$h_c$  = heat transfer coefficient

$$\dot{q} = \frac{Nu k}{D} \pi D L (593 K - 563 K)$$

$$\dot{q} = Nu k \pi D L (593 K - 563 K)$$

Using Dittus-Boelter (1930) and Colburn (1933) equations:  $Nu = 0.023 Re^{0.8} \cdot Pr^n$ , where  $n = 0.4$  for heating,  $0.7 < Pr < 160$  and  $Re > 10^4$ . Since  $Re$  is greater than  $10^4$  and less than  $10^6$ , the flow is turbulent.

$$\dot{q} = 0.023 (Re)^{0.8} \cdot (Pr)^{0.4} k \cdot \pi \cdot D \cdot L (30 K) \quad (5.3)$$

$$Re = \frac{\rho u D}{\mu} \quad \text{and} \quad \dot{m} = \rho u A \quad u = \frac{4 \dot{m}}{\rho \pi D^2} \quad Re = \frac{4 \dot{m}}{\mu \pi D}$$

$$\dot{q} = 0.023 \left( \frac{4 \dot{m}}{\mu \pi D} \right)^{0.8} \cdot (0.7)^{0.4} k \cdot \pi \cdot D \cdot L (593 K - 563 K)$$

In the above equation there are three unknowns;  $\dot{q}$ ,  $D$  and  $L$ . For 1 meter length and reactor diameter of  $9.246 \times 10^{-3} \text{ m}$  (0.5 in.), heat flux,  $\dot{q}$

$$\dot{q} = 329.1 \text{ W}$$

According to Kays and Crawford (2004), heat transfer rate for a tube can be calculated as follows:

$$Q_{conv} = \dot{m} \times c_{pair} (T_{air out} - T_{air in}) \quad (5.4)$$

Mass flow rate of air,  $\dot{m} = 2.596 \times 10^{-3} \text{ kg/s}$

Specific heat capacity of air at 477.59K,  $c_p = 1003 \text{ J/(kg}\cdot\text{K)}^{-1}$

Heat transfer rate,  $Q_s = 2.596 \frac{\text{kg}}{\text{s}} \times 1003 \frac{\text{J}}{\text{kg}\cdot\text{K}} (30\text{K}) = -338.5 \text{ W/m}^2$

The length of the tube reactor is calculated thus:  $L_t = \frac{Q_s}{h_c \times \pi \times D \times (\Delta T_{average})}$

$$L_r = \frac{338.5 \text{ W}}{275.36 \frac{\text{W}}{\text{m}^2\text{K}} \times \pi \times 9.246 \times 10^{-3} \text{ m} \times (30\text{K})} = 1.4 \text{ m} \quad (5.5)$$

The reactor was constructed from stainless steel type 316 smooth bore seamless tubing with wall thickness 0.065 in. Table 5.4 summarizes calculated reactor parameters. The length of

the tube reactor was approximately 4.5ft 6 in. The heater specifications are 120 volts and 2.16 amperes.

**Table 5-4 Calculated reactor parameters**

1.	Pipe size	id = 9.398 mm (0.37in.)
2.	Reynolds Number	Re = $2.461 \times 10^4$
3.	Convective heat transfer coefficient	$h_c = 275.276 \text{ W/m}^2 \text{ K}$
4.	Heat transfer rate	$q = 329.1 \text{ W/m}^2$
5.	Length of reactor tube	$L_r = 1.4 \text{ m (4.55 ft)}$
6.	Residence time	$R_t = 0.07\text{s}$
7.	Pressure drop	$\Delta p = 1.589 \times 10^3 \text{ Pa}$
8.	Heat flux from tape heater	$Q_{tp} = 338.5 \text{ W/m}^2$
9.	Optimum insulation thickness	Optimum insulation = 7/8in.

In the reactor, the sub-micron oil aerosol particles were heated, allowing them to pyrolyze when operated at a sufficiently high temperature. From the reactor, the product of pyrolysis, which in essence is simulated bleed air, was introduced into the duct system as shown in Figure 5.2. This simulated bleed air was injected from the reactor into the duct between inlet filter bank and the mixing orifice. The aerosol concentrations coming from the reactor depend on the compressed air supply, the flow available for consumption by the aerosol generator nozzle, and the temperature and pressure of the reactor. The reactor can be operated at varied temperatures depending on adjustments to the resistance heater.

### ***5.3.1.2 Dilution of sample air***

The initial tests on BAS showed that the concentration of aerosol particles was so high that it exceeded the upper limit that could be counted by the OPC. Finding a design for diluting the air to make the OPC register count measurements was one of the first key technical challenges in aerosol sampling. The design aim for the diluter was to dilute test aerosols with clean air to have an appropriate concentration of test particles to measure. Basically, two options are available for diluting air (B. W. Jones, Personal Communication). In option one, all sampled air passes through the OPC. In addition, dilution is bled into a sample line to get the appropriate dilution for the OPC. The second option is to construct a mixing box for sampled air and clean

air, and the OPC pulls its stream from the mixed air. The total flow in this option is independent of the amount of air pumped through the OPC as long as it is more than the flow through the OPC. The basic equation in both cases is the same:

$$C_d = C_{opc} \frac{(Q_1 + Q_2)}{Q_1} \quad (5.6)$$

- where  $C_d$  = the droplet concentration in the duct  
 $C_{opc}$  = the droplet concentration measured by the OPC  
 $Q_1$  = the flow rate of the air extracted from the duct  
 $Q_2$  = the flow rate of the dilution air

Two critical assumptions are made in the design: the first assumption is that  $Q_1$  in option one is so small that the only useful flow meters are those that would not cause substantial particle drop out. The second assumption is that  $Q_1$  is sufficiently large in option two that using the ASME type flow meter would not result in appreciable drop fall out if the flow is directly measured. If either of these assumptions is incorrect, then option one is probably easier to implement. If both assumptions are correct, then option two should be considered since it offers more accuracy. Equation (5.6) can be used directly used to determine directly the concentration in the duct in option two. Since  $Q_1$  cannot be measured directly in option one, Equation (5.6) can be rewritten as follows to determine the concentration in the duct.

$$C_d = C_{opc} \frac{Q_1}{Q_t - Q_2} \quad (5.7)$$

An uncertainty analysis on determination of  $C_d$  can be performed for each option to assess the accuracy level. Option two has between 5% and 10% uncertainty in determining  $C_d$  whereas option one has between 50% and 100% uncertainty in determining  $C_d$ . However, option one is simpler and cheaper to implement.

In this study, the challenge of sample dilution was addressed by constructing a by-pass duct where air sampling could be carried by OPC: essentially option one. Then a series of tests determined the dilution factor. A by-pass consisting of a PVC pipe schedule 40, 76.2 mm (3.0



in.) i.d. and measuring over 4267 mm (14 ft.) long was fitted below the main duct system. The flow enters the by-pass below the main duct at a 90° elbow as shown in Figure 5.1. The by-pass duct changed the airflow rate from 5.66 m<sup>3</sup>/s (1115 ft<sup>3</sup>/min) in the main duct to 28.2 m<sup>3</sup>/s (5548 ft<sup>3</sup>/min). A series of controlled dilution tests performed over a range of aerosol concentrations ensured that the concentration used in the tests does not overload the OPC. The 400% dilution was found to be optimal.

The jet engine oil aerosol generated from AG was run through the reactor, and the aerosol particulates produced were counted using an OPC, while the gases were measured using an electrochemical sensor. The air running through the duct system was sampled by isokinetic samplers and measured for contaminants in jet engine oil.

**Table 5-5 Calculation of dilution factor**

<b>Table 5.4 (a): A 30-minute average aerosol counts with no dilution</b>																
Particle Size (µm)	0.3	0.4	0.6	0.55	0.7	1.0	1.3	1.6	2.0	2.2	3.0	4.0	5.0	5.5	7.0	10.0
Air only	1724.8062	681.3953	413.1783	374.031	279.845	149.612	85.27132	48.062	23.25581	17.4419	7.751938	2.325581	0.3876	0.387597	0.3876	0
2 million (2M)	458194.96	372134.5	309058.5	291384.9	243936.4	163064	104450.4	68596.1	41937.21	29766.3	5843.798	989.9225	265.891	135.6589	17.8295	1.16279
4 million (4M)	1331414.7	928014	660382.2	595753.9	440072.5	248047	147501.9	90065.5	51658.53	36739.5	6891.085	1113.178	285.659	144.5736	15.1163	0.77519
6 million (6M)	1284055.4	1034595	844682.6	792067.8	647652.3	416222	259212.8	159645	91553.49	64797.3	11034.11	1714.729	375.194	177.5194	22.4806	0.3876
8 million (8M)	1761500.4	1422202	1158413	1084715	885890.7	560955	343436.8	212984	122706.2	85735.3	15210.47	2410.465	522.093	245.7364	29.0698	0
<b>Table 5.4 (b): A 30-minute average aerosol counts with dilution</b>																
Particle Size (µm)	0.3	0.4	0.5	0.55	0.7	1.0	1.3	1.6	2.0	2.2	3.0	4.0	5.0	5.5	7.0	10.0
Air only	1749.2248	516.2791	276.7442	237.5969	156.9767	85.2713	49.22481	30.2326	15.89147	12.4031	4.263566	1.937984	1.16279	0.775194	0.3876	0.3876
2 million (2M)	2575.1938	1644.186	1226.357	1132.171	913.1783	559.302	345.3488	215.504	112.7907	77.5194	18.60465	3.100775	1.93798	1.550388	1.55039	0.77519
4 million (4M)	6537.9845	2945.736	1868.605	1681.008	1256.202	708.915	415.1163	257.364	143.0233	96.124	17.82946	3.875969	1.93798	1.937984	1.55039	1.16279
6 million (6M)	4828.6822	3404.651	2700.388	2534.884	2063.566	1273.26	737.9845	441.86	240.6977	168.217	34.10853	6.20155	2.32558	1.937984	0.77519	0
8 million (8M)	6181.7829	4337.597	3360.465	3120.93	2509.302	1523.64	899.6124	551.55	302.3256	205.814	43.02326	10.07752	3.48837	3.100775	1.93798	1.55039
<b>Table 5.3(c): A 30 minute average dilution factor for different test runs</b>																
Particle Size (µm)	0.3	0.4	0.5	0.55	0.7	1.0	1.3	1.6	2.0	2.2	3.0	4.0	5.0	5.5	7.0	10.0
2 million (2M)	552.64805	329.3296	325.0224	325.3068	322.2112	343.678	352.4372	369.987	432.552	456.857	406.9459	849.3333	342.5	174.5	15	3
4 million (4M)	277.66896	381.7036	414.5897	412.4812	400.0934	397.498	402.8972	396.323	406.1555	438.625	507.4	573.2	368	124	12.6667	1
6 million (6M)	416.41447	357.9572	348.3472	344.6212	339.5448	350.234	376.2234	387.721	407.1517	415.751	369.4545	401.6364	322.333	152.3333	57	-1
8 million (8M)	397.01128	371.9975	375.5202	376.0721	376.4831	389.889	403.7589	408.458	428.3112	443.19	392.23	295.8571	224.333	105.5	18.5	0
Mean	410.93569	360.2469	365.8699	364.6203	359.5831	370.325	383.8292	390.622	418.5426	438.606	419.0076	530.0067	314.292	139.0833	25.7917	0.75
Std dev.	112.64446	22.80051	38.48077	38.15462	35.23678	27.2938	24.52271	16.1742	13.84295	17.0925	60.91318	241.6196	62.8158	30.46993	20.9432	1.70783

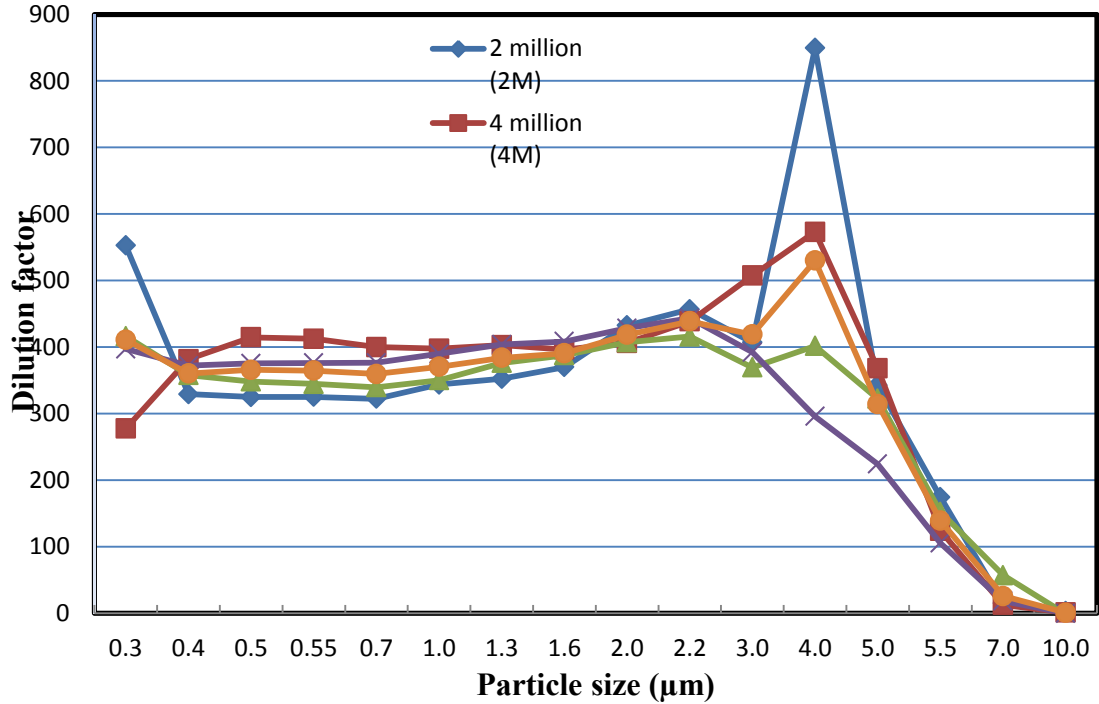


Figure 5.3 Calculation of dilution factor

### 5.3.1.3 Aerosol sampling calculations

An air sample has three basic ingredients: The amount of pollutant collected during the flow of air through the filter medium and the time run in minutes. The volumetric flow rate of aerosol sampling pump  $Q$  in SCFH was calculated according to Equation 5.8 which essentially states the ratio of the flow rates should equal to the ratio of surface which the flow passes:

$$\frac{Q_1}{Q_2} = \frac{A_1}{A_2} \quad (5.8)$$

where  $Q_1$  = Flow rate of air in the duct

$Q_2$  = Flow rate of air in the sampling cassette

$A_1$  = Surface area of the filter in the duct

$A_2$  = Surface area of the small filter in the sampling cassette

Assuming that the volume of an aerosol particle is  $V_p$ , then particle sample volume is calculated thus:

$$V_p = \frac{\pi(D_p)^3}{6} \quad (5.9)$$

where  $D_p$  is the diameter of the particle

$$\text{Particle mass flux: } m_p = \rho_p \times V_p \quad (5.10)$$

Assume that the number of particle counts per cubic feet equals  $n_i$   
 $n_i$  is what the particle counter measures in every sampling period.

Particle mass concentration in the sample is calculated as:

$$m_{ps} = m_p \times n_i \quad (5.11)$$

where  $m_{ps}$  is the mass of particles per volume of air sampled.

Assuming that all particles are accumulated by filter without settling on the cassette, incremental mass flow rate of sampled particles in a given time  $\Delta t$  or total mass of particles in one bin is calculated thus:

$$m_{Fi} = m_{ps} \times Q \times \Delta t \quad (5.1.2)$$

$Q = 1.34$  SCFH (Sample flow rate per filter sampling cassette).

Total mass of particles depositing on the filter media,  $m_T$  is equal to the sum of all the incremental mass in a given test run. The total aerosol loading to the filter media were calculated according to equation:

$$m_T = \sum_{i=1}^{16} m_{Fi} \quad (5.13)$$

Figure 3.3 is a LabVIEW function that shows the various steps in calculation of aerosol mass deposited on the filter.

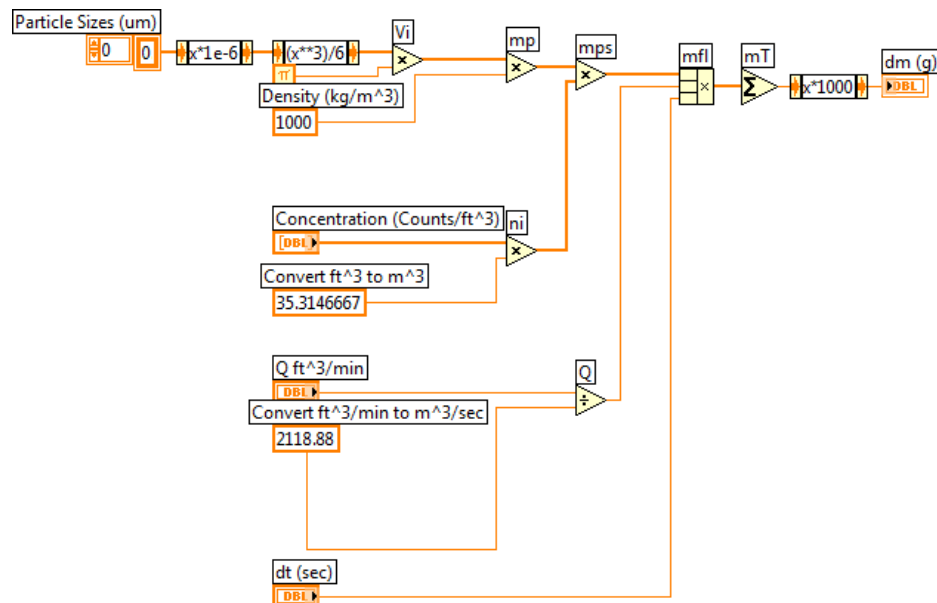


Figure 5.4 LabVIEW function converting counts to mass deposited on filter

The deposition fraction was calculated as the mass deposited on the three small filters divided by the product of the average upstream concentration and the total volume of air passing through the three small filters.

### **5.3.2 Process control and monitoring**

The National Instruments software: Laboratory Virtual Instrumentation Engineering Workbench (LabVIEW) version 8.2 was used to build a control process model to monitor and control the experimental parameters. A program in LabVIEW was designed to communicate with the DAQ system and track different key aerosol production variables at different pyrolysis temperature and pressure ranges. The data acquisition Agilent Model 34970A series and system control were programmed to monitor and capture data from thermocouples, differential pressure transducers, and ASME nozzles. The outputs from the thermocouples and pressure transducers were converted to 0–5 volt electrical signals. The voltages generated at different measurement points of the relays were amplified, and the data transmitted to a microcontroller by an analog to digital converter. A desktop computer with a measurement computing analog-to-digital card was used for data acquisition through a serial cable with an RS-232 communication link. The analog digital data acquisition was programmed to register data points every 7 s. Moreover, special functions of LabVIEW software 8.2 were used to store and synchronically display the obtained data. Appendix D shows the flow chart of LabVIEW program. Figure 5.5 shows a block diagram of the program layout of the control process. The reactor tube was wrapped by two 120 volts, 2.61 ampere heaters and powered by a 1 kW, 120 vdc power supply – variac.

The temperature of the reactor was monitored with K-type thermocouples attached to the outside of the reactor tube. The manufacturer's reported accuracy of the thermocouples is  $\pm 0.15^{\circ}\text{C}$ . The temperature measurement resolution of the DAQ unit was  $0.1^{\circ}\text{C}$  and 0.000 V.

5.3.3 Data acquisition system

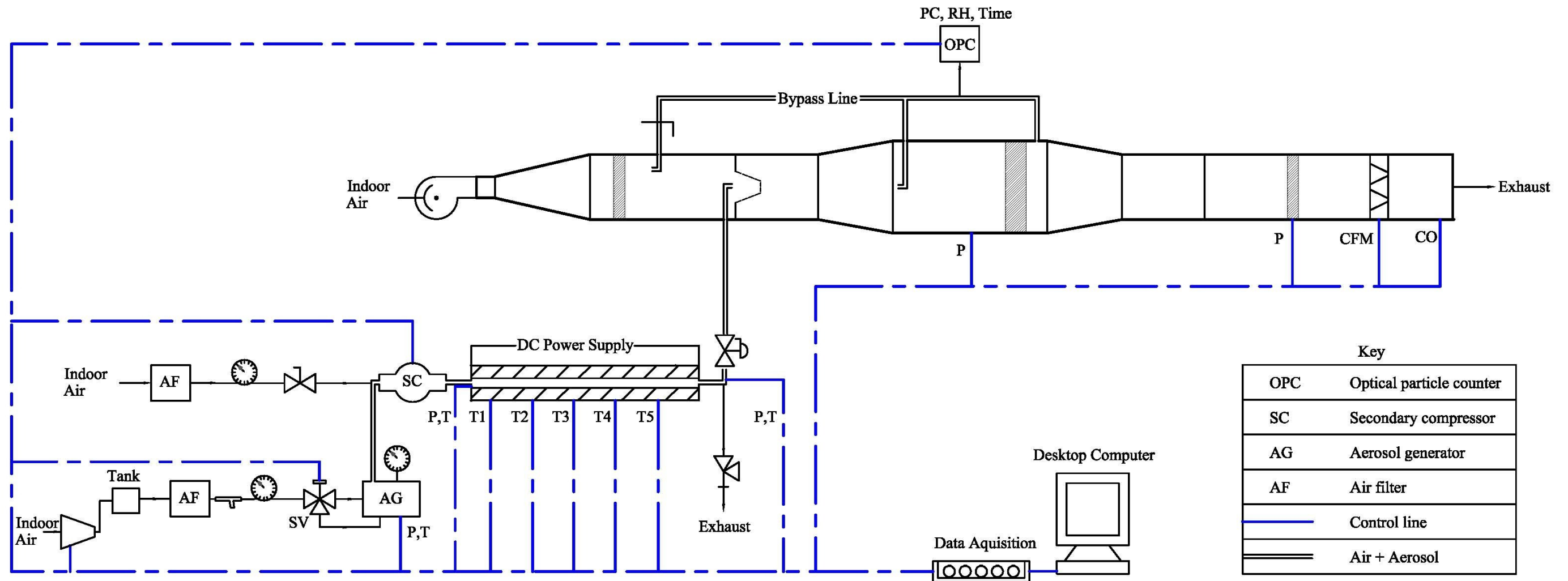


Figure 5.5 Schematic diagram of the BAS and data acquisition system

A pressure transmitter (Omega model PX305-300AI with a 0-300 PSIA range and 0.25 percent full scale accuracy) was fitted at the reactor inlet. The output of this transmitter is a 4-20 mA current loop, which in turn is converted to a 0-5 volts signal to the computer data acquisition system. The On/Off signal from the diaphragm actuated valve sensor interface pressure detector operates a SPDT relay in the control unit. The contact of this relay actuated alarms, indicator lights, or process control equipment. The backpressure regulator at the exit of the reactor tube rated at 350 psig, 350°C. A safety check valve, set to open at 200 PSID, was mounted on a backpressure regulator sitting at the reactor outlet.

During the bleed air simulation experiments, the differential pressure across the filter at the test chamber was measured by the differential pressure gauge. The pressure ring constructed around the duct had a PVC hose connecting the ring to the differential pressure transducers (Model PX653-05D5V, manufactured by OMEGA Engineers Inc., Stamford, CT). The pressure ring opens in the duct through pressure taps, which were built in accordance to the ASHRAE Standard 52.2. The pressure transducers had a measuring range of 0 to 1.25 kPa (0 to 5 in. of H<sub>2</sub>O) and output voltage range of 1-5 vdc. The differential pressure transducers were installed in the sampling chamber, because controlled pressure is necessary to maintain ASHRAE Standard 52.2 certification.

The relative humidity (RH) was measured by OPC. The RH was measured to ensure that tests were performed in an RH range that does not affect aerosol light properties. In a moist environment, aerosol particles experience hygroscopic growth; therefore, their optical properties depend strongly on RH. The response of a particle to RH depends mainly on the size and the solubility of the particle (Zieger et al. 2010). Room air was used as the test air source. The temperature of the air at the test device was kept between 50 and 100°F with an RH between 20% and 65%. Carbon monoxide (CO) was measured using electrochemical gas sensor Model 4101-04 series module 4-20 mA (manufactured by Sierra Monitor Corporation, Milpitas, CA). The CO monitor has a detection range of 0-100 ppm and was attached on the inside of the ceiling in the last chamber of the duct system.

The air flow rate in the duct was measured using ASME nozzles. The manufacturer-reported accuracy of the nozzles is  $\pm 0.11$  m/s or 1.5 percent with starting threshold less than 0.45 m/s. Besides monitoring environmental conditions at the test chamber, the applications also included monitoring reactor temperature profiling, particulate counting, and troubleshooting the

pyrolysis process. The control set-points for temperature, RH, pressure and flow rates were within an acceptable range according to ASHRAE Standard 52.2-1999. Sensor data from connected accessories such as temperature, duct flow rate, pressure, CO concentration, particle diameter, and concentration were displayed on a desktop computer screen. The air distribution in the duct system delivered conditioned air flow and aerosols to the test chamber where sampling occurred. To control the experiment and facilitate data collection, all meters and gauges used in the experiment were set to meet the standards for measurements in clean rooms.

Operational safety procedures: The BAS is a user-friendly system with a series of sensors attached that send real time reports to the system's desktop computer. The system can readjust itself automatically or can be shut down and restarted manually. Alarm and reactor shut down functions are triggered when set temperatures and pressures are exceeded during tests runs. Unusual pressure build up and elevated temperatures in the tube reactor or other unforeseen circumstances are overseen by the electronic control system which kicks in to stop the pyrolysis process; the exhaust by-pass line then opens to vent accumulated gaseous byproducts.

#### ***5.3.4 Experimental measurement conditions and procedure***

The aerosol generator (AG) (model TDA-4Blite, Air Techniques International (ATI), Owing Mills, MD) generated polydisperse sub-micron of Mobil Jet Oil II aerosols. The AG has three Laskin nozzles adjusted by two control knobs. The two knobs permit the unit to be operated with 1 to 3 nozzles, providing a range of aerosol concentrations (i.e., different nozzle flow rates produce different concentrations of aerosol particles). The AG requires only a supply of clean air to function. From compressor 1, air was supplied to the Laskin nozzle, which rests in Mobil Jet Oil II contained in AG. As the air pressure increases, the oil is forced upwards causing it to be aerosolized. With the help of compressor 2, the aerosols and air mixture are sucked into the reactor under pressure. Finally, before running the tests, the operating air pressure of the Laskin nozzle was adjusted to 20 psig (137.90 kPa) to provide required aerosol particle concentration before it was directed to the reactor.

##### ***5.3.4.1 Aerosol sampling procedure***

The sampling system filtered particulates in simulated bleed air flowing through the duct to account for airborne Mobil Jet Oil II aerosols in the simulator. The system had three isokinetic probes, clean 25-mm diameter cut from cabin air recirculation filter, three-piece plastic filter



cassettes to hold the filter media in place, and a vacuum air pump (Model Gast, serial number 0677). The sample was drawn into the isokinetic sampling probe by means of the vacuum pump, which could maintain an isokinetic sampling rate while continuously withdrawing a portion of the air through the sampling train. The pump had separate pressure and vacuum gauges and valves, so vacuum and pressure levels could be independently adjusted. The pump was calibrated before running the tests. An air flow meter (model Dwyer series 2000, Dwyer Equipment, Inc., MI, USA) was connected to the pump to record the sampled air flow rate. Clear, flexible sample transfer lines made of polyvinyl chloride (PVC) hose were used for connections to the various accessories. The PVC hose connected the probes to the three sampling cassettes and the sampling cassettes with the pump, through a rotameter and back to the main duct in a closed loop system where a calibrated sampling pump pulled a known volume of air through cassettes holding filtration media cut from a clean HEPA cabin air recirculation filter.

To ensure that the sample represented the air and aerosol flow in the duct, sampling had to be isokinetic, that is, the particle-laden air was drawn into the sampling probe at a velocity equal to that of the air in the duct at the sampling point. The isokinetic sampling arrangement is schematically shown in Figures 5.6. Isokinetic sampling probes are widely used for air sampling. For this study, three evenly spaced isokinetic samplers were installed in the test section of the duct system. The samples were collected from a highly charged environment: a duct where simulated bleed air had been introduced. The main body of the sampling probe was made of a 13 mm o.d. stainless steel tube to assure rigidity for handling and positioning. Each probe had a sharp edged inlet diameter of 6.4 mm. (0.25 in.) with a 90° gradual bend (radius of curvature = 57 mm (2.25 in.)). The probes were mounted on the floor of the test chamber in an upright position with the nozzle pointed into the airstream; the opening of the isokinetic probe was aligned to the air movement in the duct. Figure 5.6 shows the entire assembly of the sampling system. The filter media trapped the airborne particulates. Captured aerosol particles on HEPA filters were sent to a laboratory for analysis. Such an arrangement permitted gravity to assist the sample pump in keeping the particulate catch in the filter.

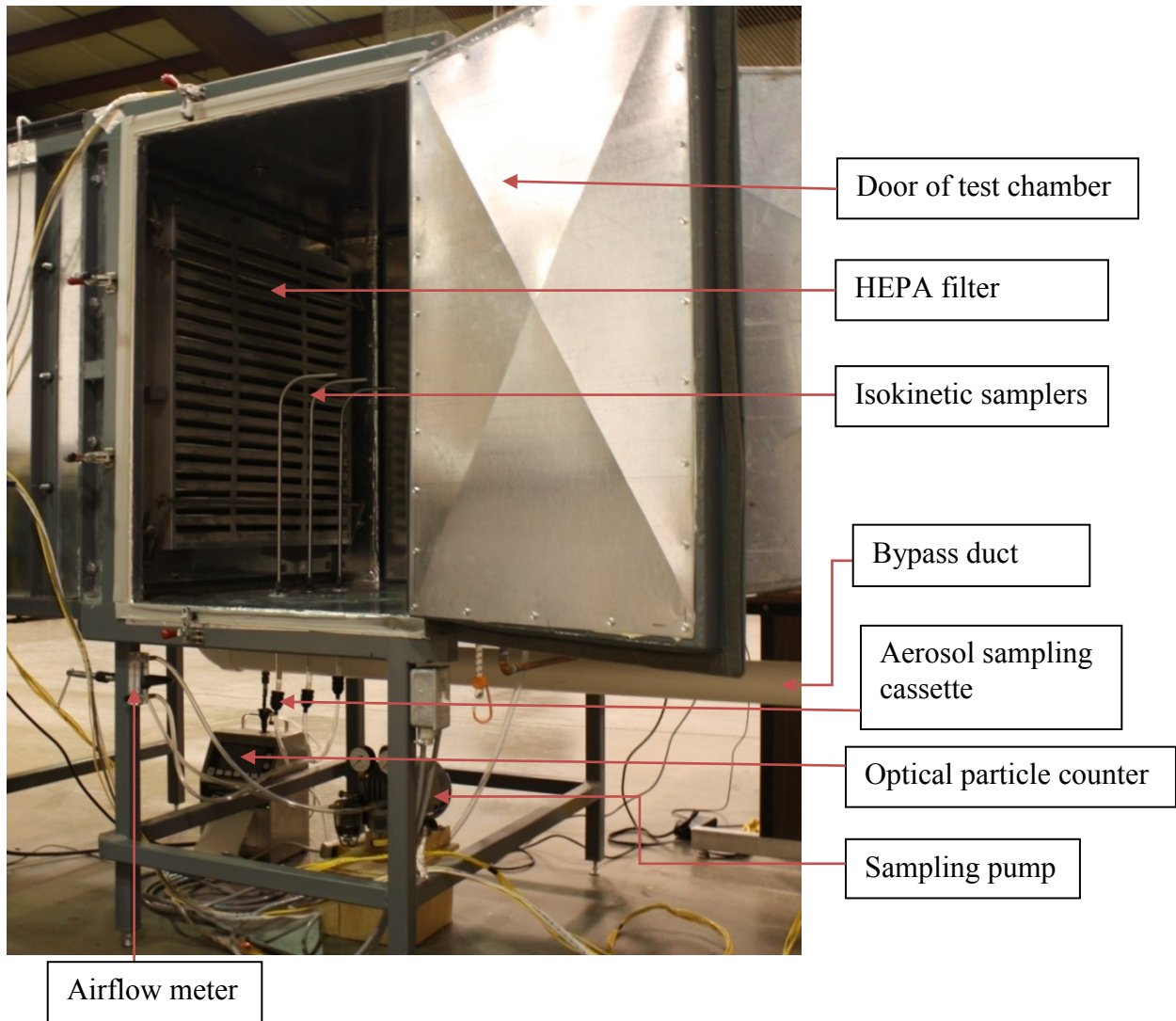


**Figure 5.6 Aerosol sampling device assembly**

The dimensions of the probes were chosen in accordance with ASHRAE Standard 52.2 guidelines, which require sampling in the duct to be isokinetic. This design helps give an accurate measurement of the particulate level in the system. The isokinetic probe helped reduce counting errors in sample flow velocity and the aerodynamics of small particles. The inlet nozzle of the sample probe(s) was sharp edged to maintain isokinetic sampling within 10 percent at 1000 CFM. The sampling rate was adjusted so that the velocity of the sample, at the mouth of the probe, equaled what it would have been in the absence of the probe. The probe distances from the filter were as defined in the standard ASHRAE 52.2. Very similar designs of isokinetic sampling probes have been used by many other researchers (Hewitt, 1978; Ito et al. 1991).

#### 5.3.4.1 Filter cassette holders

A sampling cassette device for separating the particles contained in the airstream is shown in Figure 5.7. An open-face sampling was performed by removing the end plugs from the three-piece cassette filter holder. The inside diameter of cassette holder varies by only  $\pm 5 \text{ mm}^2$  for consistent collection area and minimized error. The filter cassette holders were securely assembled to prevent leakage.

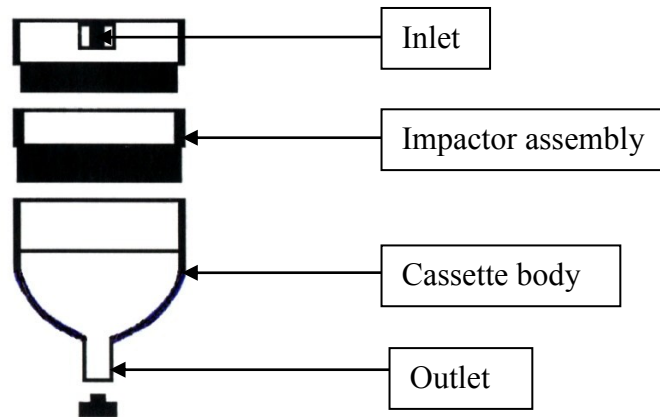


**Figure 5.7 A 25-mm Air sampling filter cassette holder**

The connection of the sample lines starting from the sampler probes down to the cassettes, the vacuum pump, and the rotameter were carefully considered to avoid particle loss in the sample lines. Particle losses associated with sample lines may include inlet losses due to non-isokinetic sampling; losses to the walls of the sample due to diffusion; electrostatic charging and gravitational settling; and losses in bends, resulting from centrifugal force and eddies (Hanley et al., 1995). Before each test run, all sampling equipment was wet-wiped with 70 percent isopropyl alcohol wipes to sterilize them. The end plugs (caps) at the inlet and outlet of the cassettes filter holders were removed and cut circular 25-mm diameter HEPA filter media with a  $0.3 \mu\text{m}$  pore size were then loaded into cassette holders. After loading the filter media, the cassettes were connected to the sample pump with flexible PVC tubing 15.9 mm (5/8 in.) internal diameter.

Special care was taken to prevent contamination of filter media while loading and unloading the cassettes. The cassette samplers were then connected to an air sampling vacuum pump set to draw air through a sampling media (HEPA filter) at a fixed, predetermined air flow rate of  $0.11 \text{ m}^3/\text{min}$  (4.0 SCFH). The cassettes were used in open-face mode to allow the filter to collect particulates from the air which passes through them. The cassettes have 15.9 mm (5/8 in.)

union fittings on inlet and outlet ends for fastening directly between the pump and the probe sheath. The configuration structure of the filter cassette holder is such that it eliminates bypass and infiltration leakage, ensuring maximum sample collection and accurate results. To ensure that all the connections were leak proof and secure, zip ties (tie wraps) were used around the flexible PVC tubing to tighten the connection with probes and the cassettes. This assured that aerosols being sampled originating from the duct.

Collecting particles from the air sample is most commonly achieved by filtration. A fibrous filter cut from aircraft HEPA filters was fitted to sampling cassettes. All plastic cassettes were secured around the seams to prevent leakage past the filter. Open-face sampling was performed by removing the end plugs from the three-piece cassette and the particulate was thus uniformly deposited on the filters. Deposition occurs when particles impact and are intercepted by the fibers (Hinds, 1998). Thus particulates smaller than the pore size may be efficiently collected. The sampling filter media used in this study had pore sizes of  $0.3\mu\text{m}$ . The efficiency of removing particles from the air depends on the face velocity (i.e., the cross sectional air velocity of the filter holder). For particles less than  $1.0\mu\text{m}$ , the overall efficiency decreases with increasing face velocity (Liu et al. 1983; Lippmann, 1995).

The experiment was programmed to sample air for 30 min. for every flight condition. For every test run, the above procedure was repeated two times for jet engine oil at different sampling durations, temperatures, and pressures corresponding to various flight conditions. The sampling flow rate was entered every time the experiment was set to run. At the end of each sampling period, the three-piece cassettes containing filter samples were removed from the sampling train assembly, both ends were locked, and cassettes were placed in appropriately labeled zip-locked plastic bag and shipped along with a blank filter to the analytical laboratory for analysis by FESEM/EDS, GC/MS, and NAA. Blank filter media (clean, unexposed cabin air recirculation filter) were included as part of standard laboratory controls.

#### ***5.3.4.1 Aerosol particle counting***

A laser OPC (Model CI-500 SPECTRO 0.3, Serial number 045455, Climet Instruments Company, Redlands, CA) was fitted to the bypass duct and used to determine particle size distribution. The OPC takes a defined-air sample through a volumetrically controlled pump and measures the airborne particles continuously by scattered light in its laser measuring cell. The

measuring range of particle sizes is from 0.3 – 10  $\mu\text{m}$  in 16 channels. The OPCs 16 channels or bins are set to classify particle size range and counts. The OPC provides single particle count and size classification during sampling period. The sampled air with various size particles is drawn constantly through the flat light beam produced by a focused laser diode. Each scattered signal from a single particle is detected by 90 degree high-speed photo diode so particle color changes can be ignored. Each signal is then counted and classified in 16 different size channels by an integrated pulse height analyzer.

The OPC uses a laser-light illumination source that has a wide collection angle for sensing the scattered light: 50 mW laser diode and wavelength of 780 nm. The OPC determines the size of a sampled particle by the quantity of light scattered by the particle and focused onto a photo detector using a system of mirrors. Since the amount of light scattered from a particle is a strong function of its size, measuring the amplitude of the scattered-light allows the size of the particle to be determined. Particle concentrations are kept low enough within the measuring volume of the counter to ensure only one particle is measured at a time. Particle counters size particles by matching a signal response generated by aerosol particle to an equivalent size of a polystyrene latex sphere. An appropriate optical calibration before installation for use is therefore required for accurate sizing. For this study, the OPC was calibrated by the manufacturer using polystyrene latex spheres. The measured particle size by an OPC depends on a particle's refractive index in addition to its size.

The particle counting by OPC covered the typical ASHRAE 52.2-1999 particle size range of 0.3 – 10.0  $\mu\text{m}$ . This was in accordance with ASHRAE Standard 52.2-1999 procedure which divides the particles in the same size range with each class owning the upper and lower limit and geometric mean size. The OPC unit has an external exhaust system to connect the equipment to the sampled environment. Such an arrangement assures that the pressure is equalized so that the equipment maintains proper flow regulation. During the test, an OPC sampled aerosols from the by-pass. The OPC was operated at volume flow rate specification of 47.20  $\text{cm}^3/\text{s}$  (0.10 CFM). The maximum particle concentration limit for the selected flow rate was  $353.0 \times 10^6$  particles/ $\text{m}^3$  ( $10.0 \times 10^6$  particles/ $\text{ft}^3$ ).

The OPC was also programmed using LabVIEW to provide a contact closure at the end of each sample period, which consisted of 2 s particle counting followed by a 5 s delay before taking the next sampling to count, i.e., 7 s time resolutions. The precision of the OPC varies

according to size range; it is most precise at the smallest size ranges. The sampling inlet system was designed to ensure a representative sampling by OPC. The different particle size ranges measured by each instrument imposed correspondingly different requirements, and these were taken into account in the design. First, there could be no size bias in the size of particles aspirated into the sampling line over the size range from 0.3-10  $\mu\text{m}$ . Secondly, the flow transport line to OPC was designed to minimize losses for the size range covered by the instrument by making it as short as possible. All the measured data from OPC was acquired and transmitted via the RS-232 serial-interface to a logging desktop computer with analog output: 0 ~ +2.9V. That helped to optimize aerosol production and monitoring efficiency while maintaining safe, reliable operations. Each and every component of the experimental system was selected to provide optimal performance and reliable operation using automated data recording. The OPC spectrometer Climet .3 could not measure particles smaller than 0.3  $\mu\text{m}$ .

## **5.4 Analysis, Results and Discussion**

### **5.4.1 Data analysis and results**

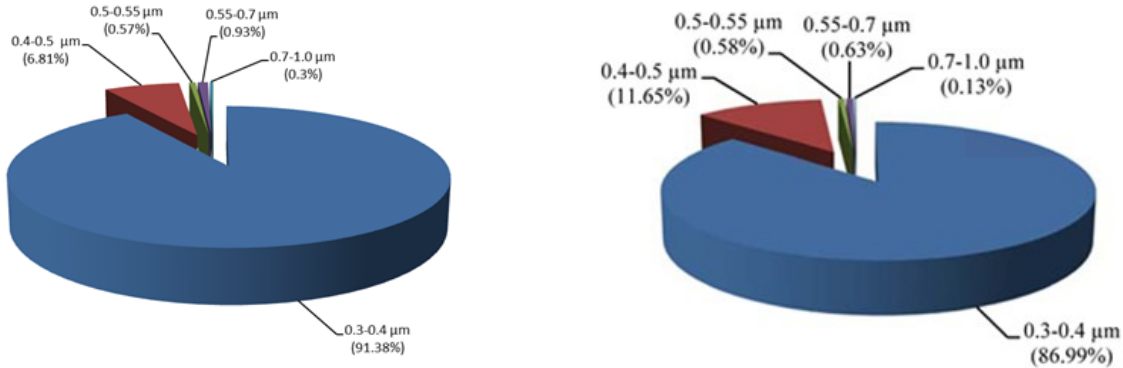
#### ***5.4.1.1 Mobil Jet Oil II aerosol particulate distributions in BAS***

The average background aerosol counts (air only) for each size range were computed and subtracted out from the counts obtained from the OPC during actual test runs. The remaining counts were then computed for parameters needed. Data pertaining to simulated incidents are in Appendix C.1. The average rate of aerosols produced varied dramatically from one simulated condition to another. The total average aerosol particulate counts ranged from a high of 233,555,417 million counts/ $\text{ft}^3$  in ground operations (cold tests) to a low of 163,214,400 million counts/ $\text{ft}^3$  in top climb speed conditions. In terms of percentage, the distribution hit a high of 86.98 percent for 0.3  $\mu\text{m}$  aerosols to a low of 0.002 percent for  $\geq 0.55$   $\mu\text{m}$  size aerosols in top climb (take-off) conditions and 84.1 percent for 0.3  $\mu\text{m}$  aerosols to a low of 16.5 percent in ground operations (cold test). Overall the total test period however, it averaged 37 percent.

Among the six bleed air operations, 0.3 to 0.4  $\mu\text{m}$  size aerosols are predominant. As evident from Table 5-5 the 0.3 to 0.4  $\mu\text{m}$  particulate size range contributes proportionally more aerosols than any other size range. Ground operations (cold tests conditions) have by far the most widespread total particulate size distribution with have the highest 0.3 to 0.4  $\mu\text{m}$  at about 84

percent and the lowest greater than 1.6  $\mu\text{m}$  at 0.01 percent. Figure 5.8 depicts a pie-chart that illustrates particulate size range distribution for simulated cruise speed test one and take-off test one conditions.

**Figure 5.8 Comparison of particulate distribution at cruise test 1 and top climb test 1 conditions**



(a) Cruise speed condition test 1

(b) Top climb (take-off) condition test 1

**Table 5-6 Distribution of aerosol particulates in percentages from various size ranges at different simulated bleed air operations**

Simulated mode of aircraft engine bleed air operation	Test	Percentage distribution in aerosol size range								Total %
		0.3-0.4 $\mu\text{m}$	0.4-0.5 $\mu\text{m}$	0.5-0.55 $\mu\text{m}$	0.55-0.7 $\mu\text{m}$	0.7-1.0 $\mu\text{m}$	1.0-1.3 $\mu\text{m}$	1.3-1.6 $\mu\text{m}$	>1.6 $\mu\text{m}$	
Ground operations (Cold test)	Test 1	84.12	12.33	0.89	1.67	0.88	0.08	0.02	0.01	100
	Test 2	84.07	12.33	0.90	1.67	0.91	0.08	0.03	0.01	100
Top climb (Take-off)	Test 1	86.99	11.65	0.58	0.63	0.13	0.02	0.00	0.00	100
	Test 2	86.54	12.11	0.59	0.63	0.11	0.01	0.00	0.00	100
Cruise	Test 1	91.38	6.81	0.57	0.93	0.30	0.01	0.00	0.00	100
	Test 2	92.00	6.34	0.52	0.85	0.27	0.10	0.00	0.00	100
Initial descent from cruise	Test 1	75.98	19.12	1.59	2.52	0.77	0.02	0.00	0.00	100
	Test 2	76.13	19.04	1.58	2.48	0.75	0.03	0.00	0.00	100
End of descent	Test 1	87.83	9.85	0.76	1.18	0.37	0.01	0.00	0.00	100
	Test 2	87.13	10.62	0.78	1.13	0.33	0.01	0.00	0.00	100
High pressure to low pressure switch-over	Test 1	85.03	12.24	0.93	1.39	0.01	0.00	0.00	0.00	100
	Test 2	86.07	11.42	0.86	1.28	0.37	0.01	0.00	0.00	100

From Table 5-6 and pie charts in Figure 5.8, it is evident that aerosols particulates in the 0.3 to 0.4  $\mu\text{m}$  range are predominant. Suggesting further studies should focus on measuring particulates in less than 0.3  $\mu\text{m}$  size ranges using appropriate equipment.

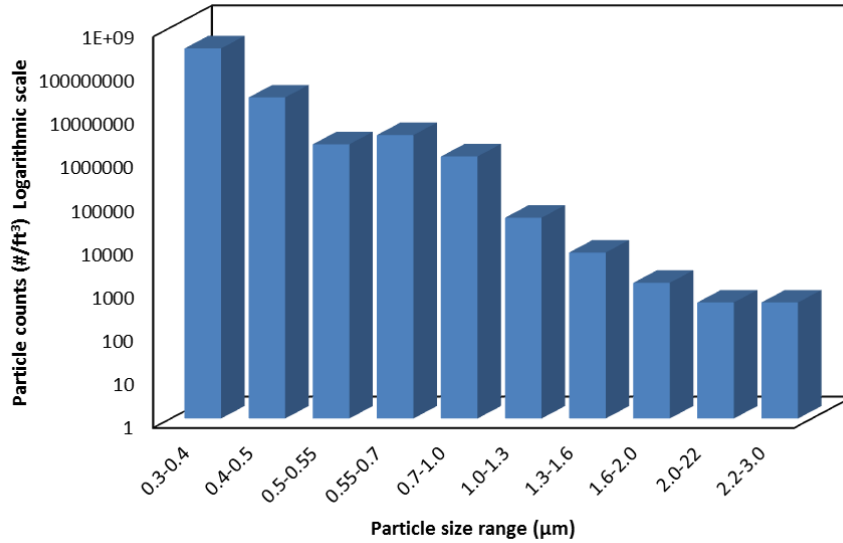


**Figure 5.9 Histogram of particle count distribution at simulated ground operations test 1 (14.1 PSI, 170.4°C)**

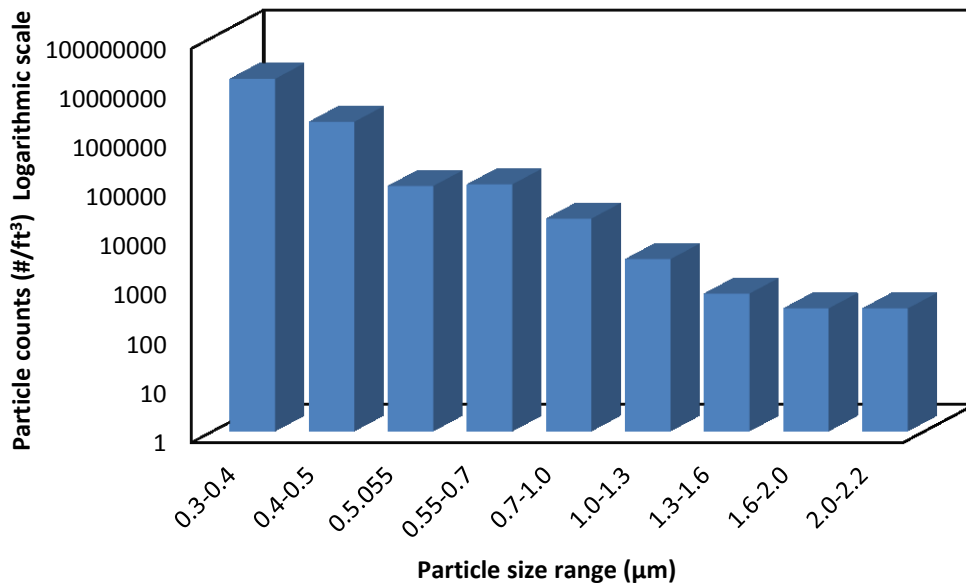


**Figure 5.10 Histogram of particle count distribution at top climb (take-off) condition test 1 (103.2 PSI, 308.0°C)**



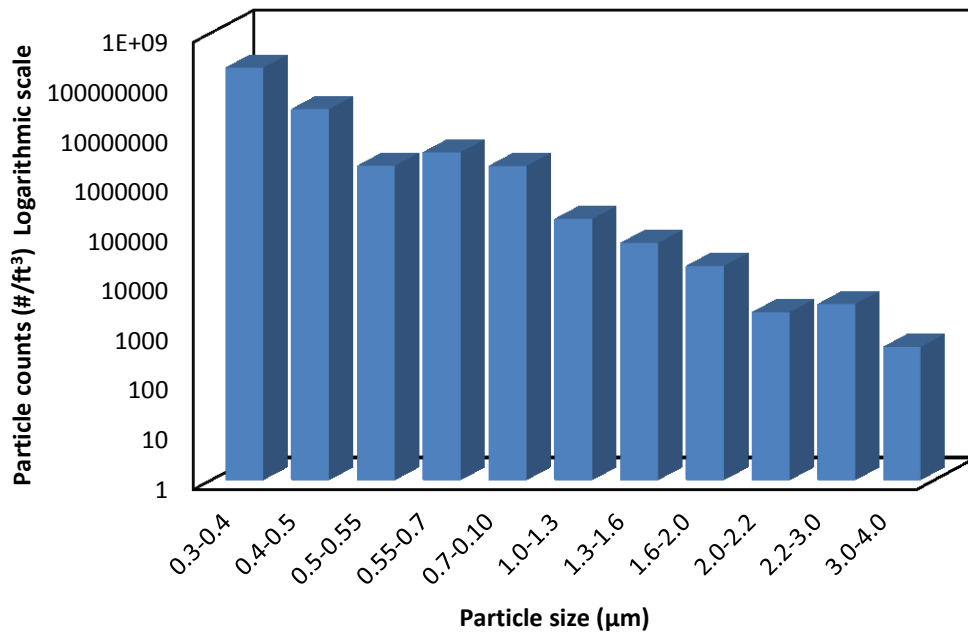


**Figure 5.11 Histogram of particle count distribution at simulate cruise speed test 1: (50.7 PSI, 249.7°C)**

#### 5.4.1.2 Probit analysis

Raw data in the form of particle counts (number concentrations) per cubic foot of air sampled falling within a specified range of sizes were converted to mass concentration in particle size interval. By dividing by the total mass, the mass concentration values were converted to segments of  $dF(d[i])$  of the cumulative distribution in the intervals around  $d(i)$ . The segments  $dF$  were then used to calculate the cumulative function values,  $F(d_p)$ . Each  $F(d_p)$  was plotted against the particle size value which is the upper limit of each particle size-interval counted. A point value was calculated for each of the cumulative function values using an approximation formula developed by Finney (1947):  $\text{Probit} = 4.9[F^{0.14} - (1 - F)^{0.14}]$ . Probit analysis involves fitting a regression model of binomial response variables.

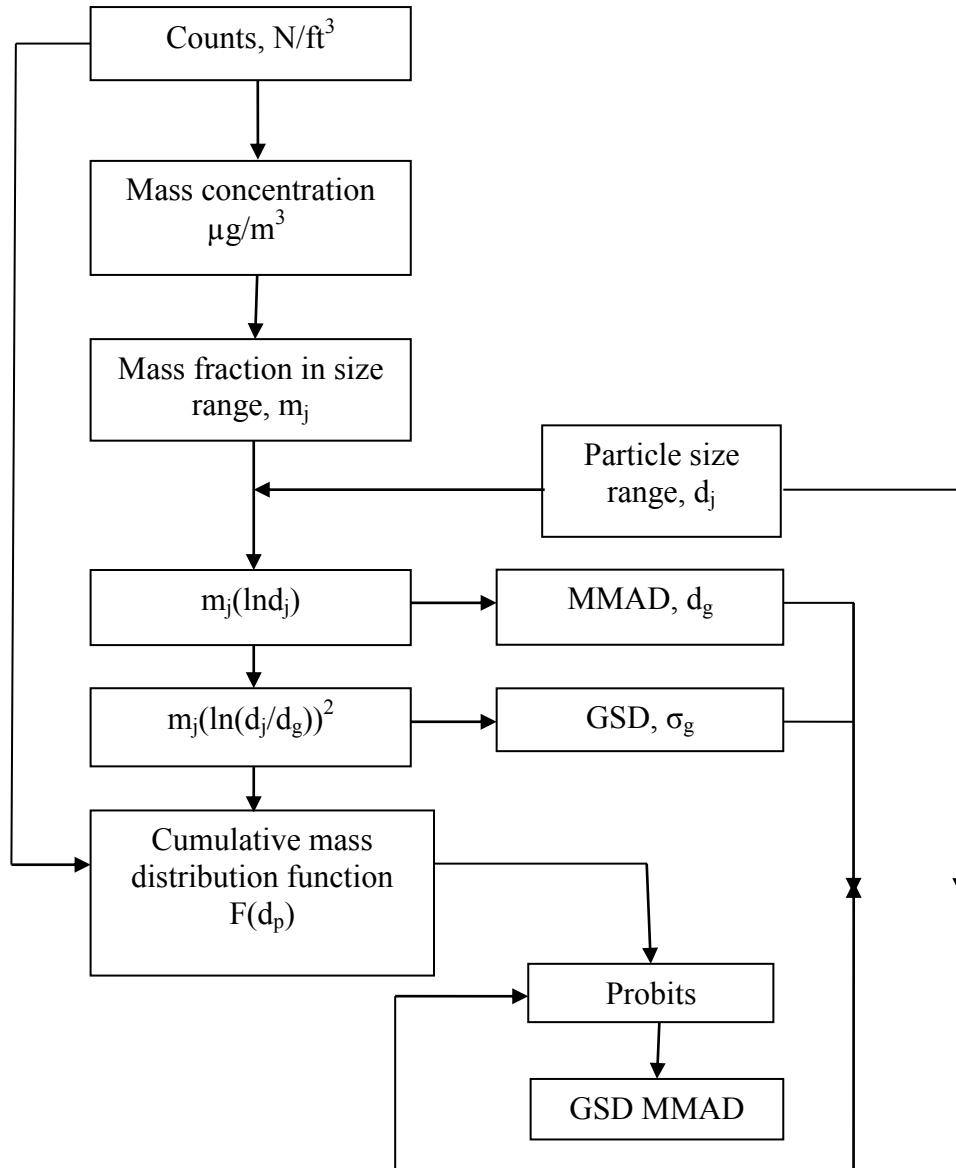


**Figure 5.12 Flowchart for calculation of Mobil Jet Oil II aerosol characteristics: Probit analysis**

From the concentration of aerosols probits are calculated and finally a graph of probits versus the log of particulate size is constructed. Figure 5.12 shows all the necessary steps required to obtain various aerosol parameters for probit analysis. Table 5-7 contains the values of aerosol characteristics obtained in probit analysis. Probit analysis is the transformation of the OPC acquired data into a linear relation of probit vs particle size.

**Table 5-7 Key steps in Probit analysis: Cruise speed (Test 1: 50.7 PSI, 249.7°C)**

	0.3 (µm)	0.4 (µm)	0.5 (µm)	0.55 (µm)	0.7 (µm)	1.0 (µm)	1.3 (µm)	1.6 (µm)	2.0 (µm)	2.2 (µm)
Average	163.717431	29.13471215	4.760637	10.382345	6.999339	0.829193	0.355461	0.118341	0.069340	0.092292
Air only	0.386595	0.110657148	0.013039	0.028075	0.017386	0.001645	0.001057	0.000117	0	0
	163.330836	29.02405501	4.747598	10.354269	6.981954	0.827548	0.354404	0.118223	0.069340	0.092292

Particle size range Lower limit (µm)	Particle size range Upper limit (µm)	Mass conc. (µg/m <sup>3</sup> )	Mass fraction in size range m <sub>j</sub>	Geom. mean particle size d <sub>i</sub> (µm)	m <sub>j</sub> (ln d <sub>j</sub> )	m <sub>j</sub> (ln(d <sub>j</sub> /d <sub>g</sub> )) <sup>2</sup>	Cumulative mass distrib. F(d <sub>p</sub> )	ln(d <sub>p</sub> )	Probits
0.3	0.40	163.3308363	0.756509691	0.35	-0.794200611	0.008893472	0.756509691	-0.916290732	0.691552298
0.4	0.50	29.02405501	0.134432538	0.45	-0.107345416	0.002744771	0.89094223	-0.693147181	1.228331308
0.5	0.55	4.747597923	0.021989747	0.525	-0.014169248	0.001940221	0.912931977	-0.597837001	1.356327033
0.55	0.70	10.35426997	0.047958522	0.625	-0.02254068	0.010656962	0.960890499	-0.356674944	1.760163734
0.7	1.00	6.981954314	0.032338756	0.85	-0.00525566	0.019618359	0.993229256	0	2.460418991
1.0	1.30	0.827548471	0.003833008	1.15	0.000535709	0.004480424	0.997062264	0.262364264	2.731685804
1.3	1.60	0.354403673	0.001641514	1.45	0.000609927	0.00282975	0.998703778	0.470003629	2.967270037
1.6	2.00	0.118223114	0.000547581	1.8	0.000321861	0.001280466	0.999251359	0.693147181	3.110552004
2.0	2.20	0.06934019	0.000321167	2.1	0.000238286	0.000910065	0.999572526	0.78845736	3.245752833
2.2	3.00	0.092291787	0.000427474	2.6	0.000408456	0.001538163	1	1.098612289	4.871387651
3.0	4.00	0	0	3.5	0	0	1	1.386294361	
4.0	5.00	0	0	4.5	0	0	1	1.609437912	
5.0	5.50	0	0	5.25	0	0	1	1.704748092	
5.5	7.00	0	0	6.25	0	0	1	1.945910149	
7.0	10.00	0	0	3.5	0	0	1	2.302585093	
	Total	215.9005208	1		-0.941397377	0.054892654			

Mean mass aerodynamic diameter, MMAD =  $\exp[m_j(\ln d_j)] = 0.39 \mu\text{m}$ . Geometrical size diameter, GSD,  $\sigma_g = \{\exp[m_j(\ln d_j)]\}^{0.5} = 1.8674$ . Figures 5.13 through 5.18 show the distribution of Mobil Jet Oil II aerosol concentrations simulated in BAS for all bleed air operating conditions performed during test 1.

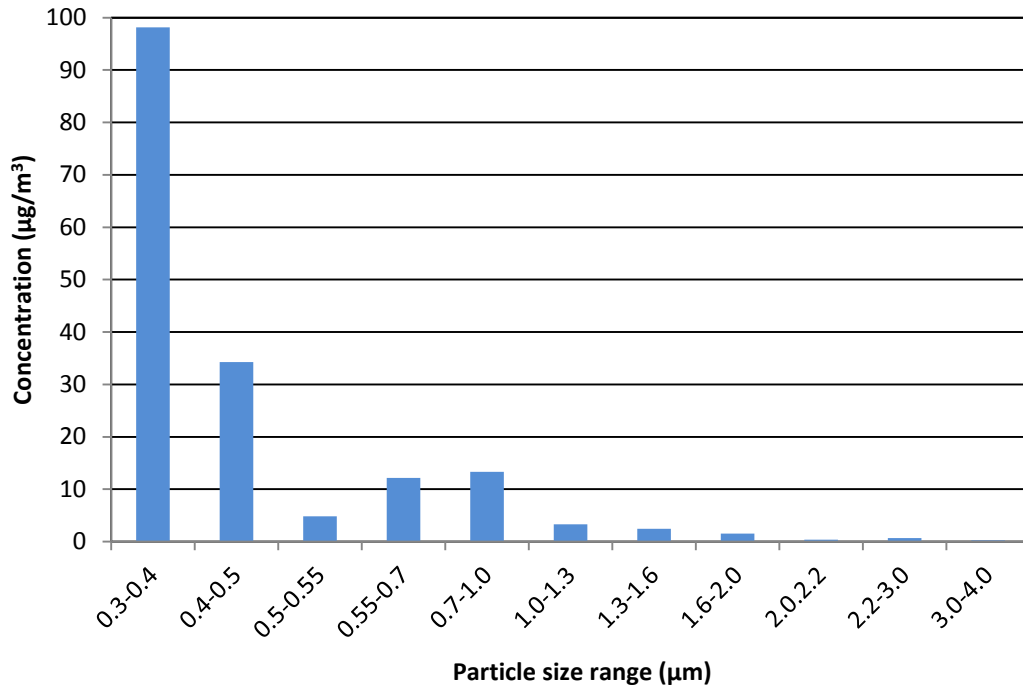


**Figure 5.13 Histogram of aerosol concentration distribution at simulated ground operations test 1 (14.1 PSI, 170.4°C)**

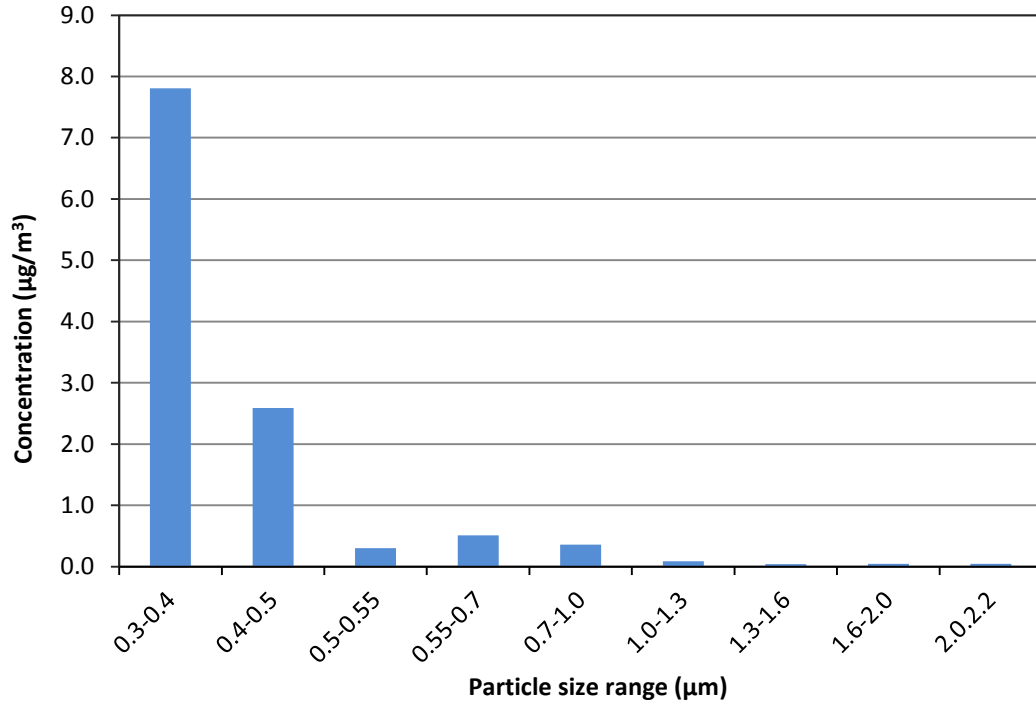


**Figure 5.14 Histogram of aerosol concentration distribution at simulated top climb (Hot test 1: 102.2 PSI, 308.0°C)**

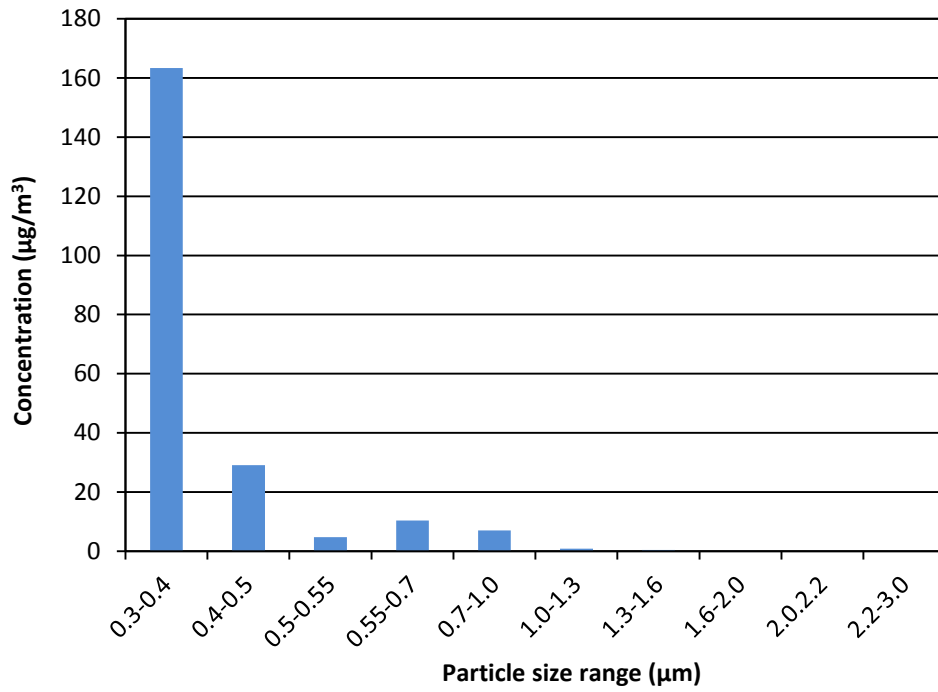


**Figure 5.15 Histogram of aerosol concentration distribution at simulated cruise speed conditions test 1 (50.7 PSI, 149.7°C)**

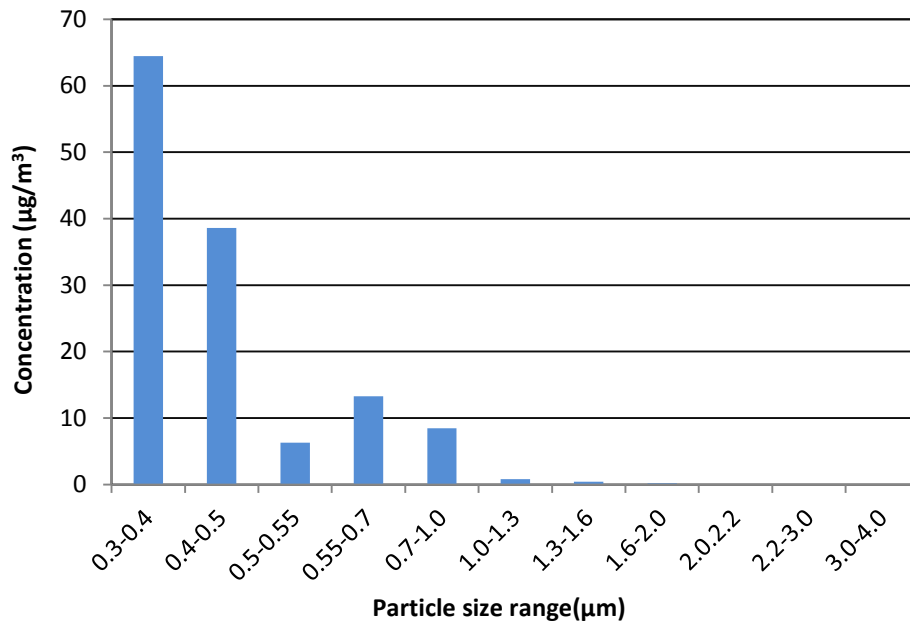


**Figure 5.16 Histogram of aerosol concentration distribution at simulated initial descent from cruise test 1 (29.7 PSI, 185.2°C)**

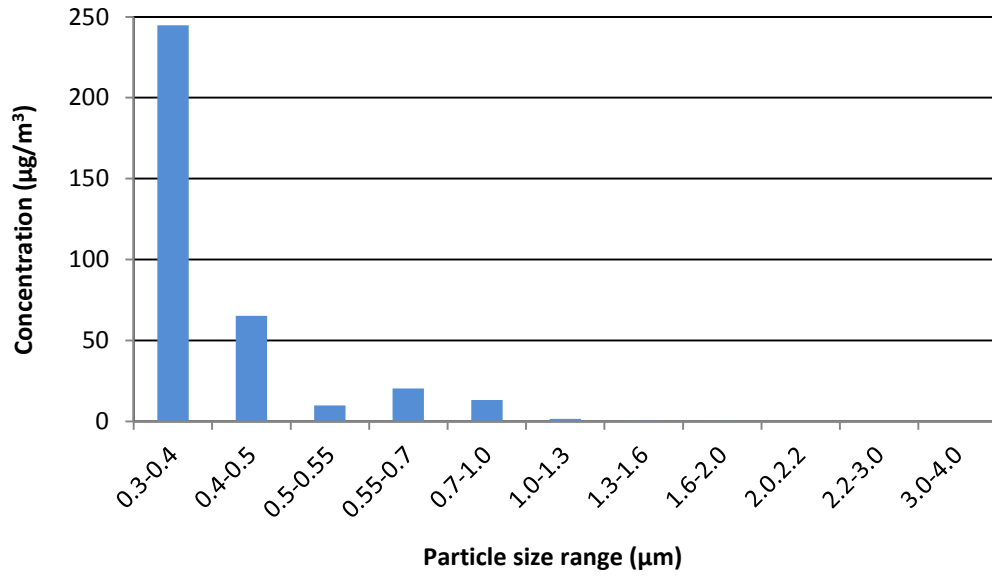


**Figure 5.17 Histogram of aerosol concentration distribution at simulated end of descent test 1 (66.9 PSI, 230.7°C)**

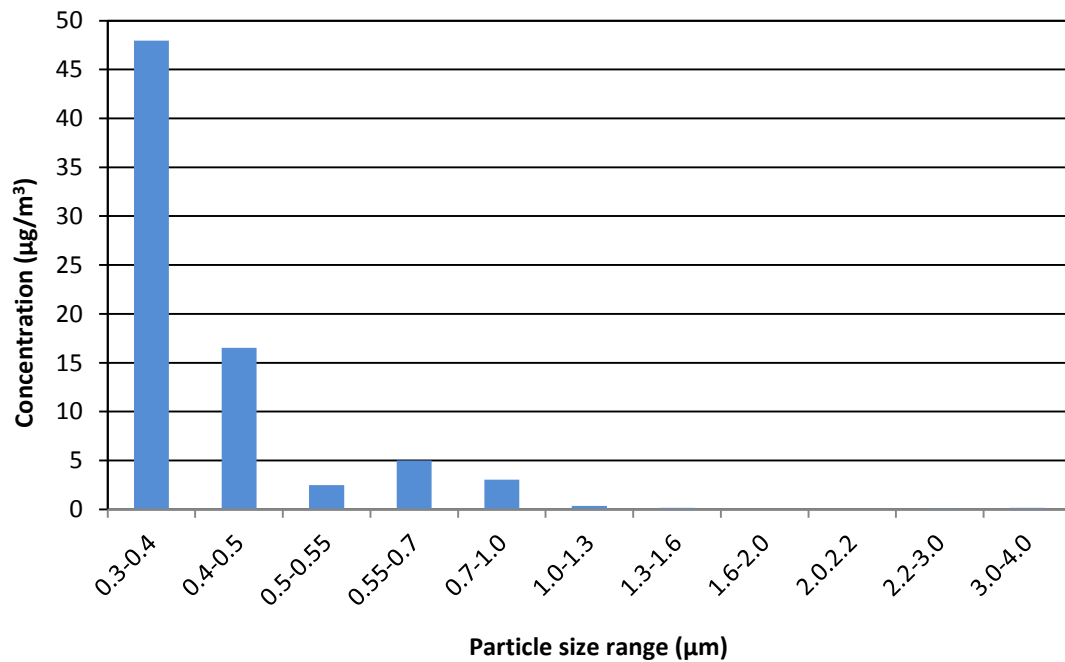


**Figure 5.18 Histogram of aerosol concentration distribution at simulated high pressure to low pressure switch-over (Hot test 1: 70.9 PSI, 280.5°C)**

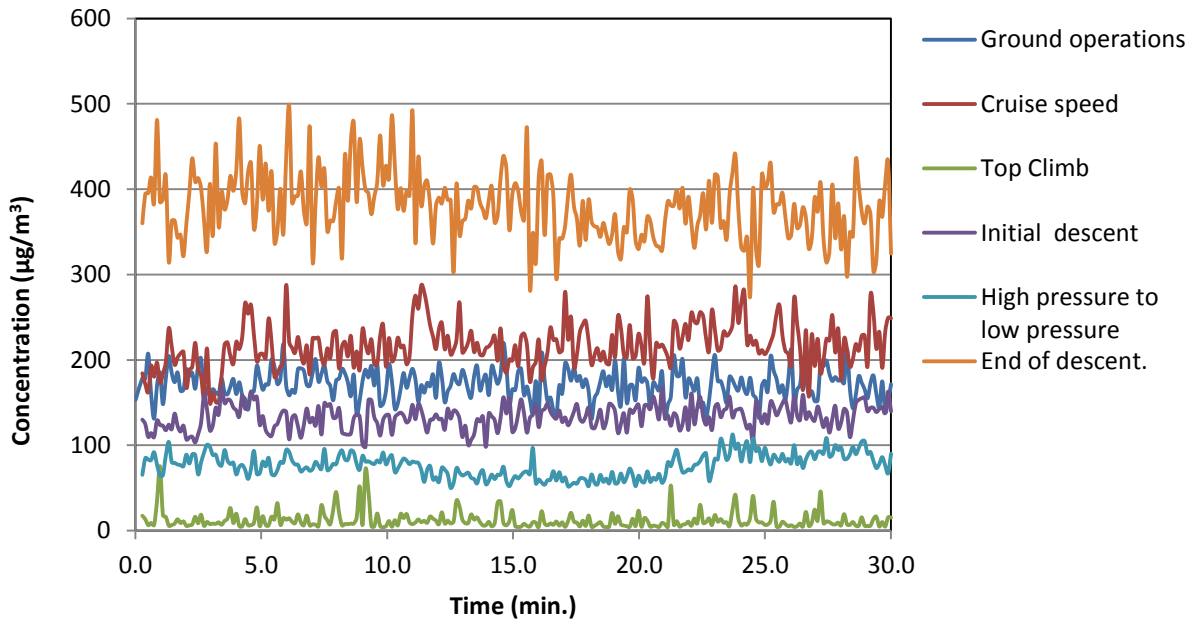


**Figure 5.19 Comparison of Mobil Jet Oil II aerosol concentrations generated from different simulated bleed air conditions**

Figure 5.19 shows the variation of aerosol concentrations in different simulated bleed air conditions. From Figure 5.19, simulated flight conditions for end of descent had the highest aerosol concentrations suggesting that end of descent conditions favor most aerosol formation than any other bleed air condition. The lowest aerosol formation was observed during simulated top climb conditions. Top climb or take-off operations occur at high temperatures and pressures and obviously at such conditions most aerosols have burnt out into gaseous by products.

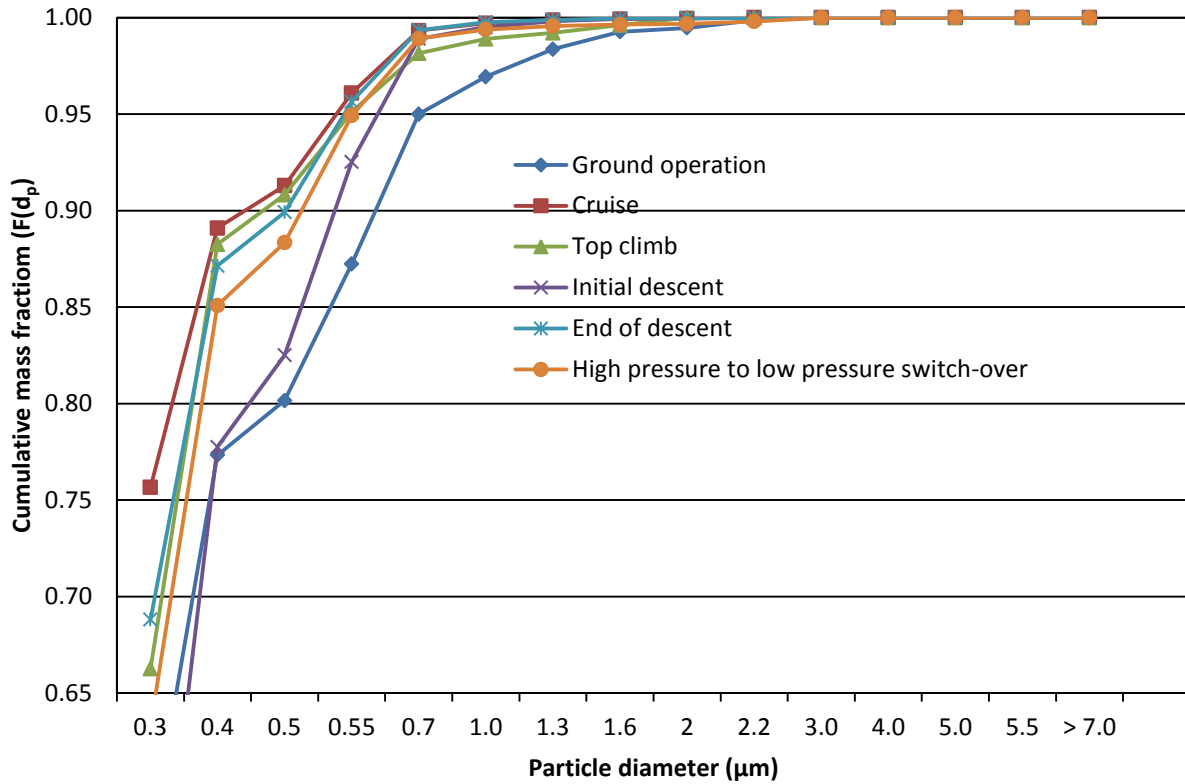


**Figure 5.20 Cumulative mass distribution curves for Mobil Jet Oil II aerosols at different simulated bleed air conditions**

The cumulative distribution enables one to determine readily quantitative information about the particle size distribution (Hinds, 1994). The fraction of particles less than a given size can be read from the graphs. The area under the frequency function curve between two sizes  $a$  and  $b$  equals the fraction of particles whose diameters fall within this interval.



The probit values obtained in Table 5.7 were plotted as the y-axis versus log particle size on the x-axis.

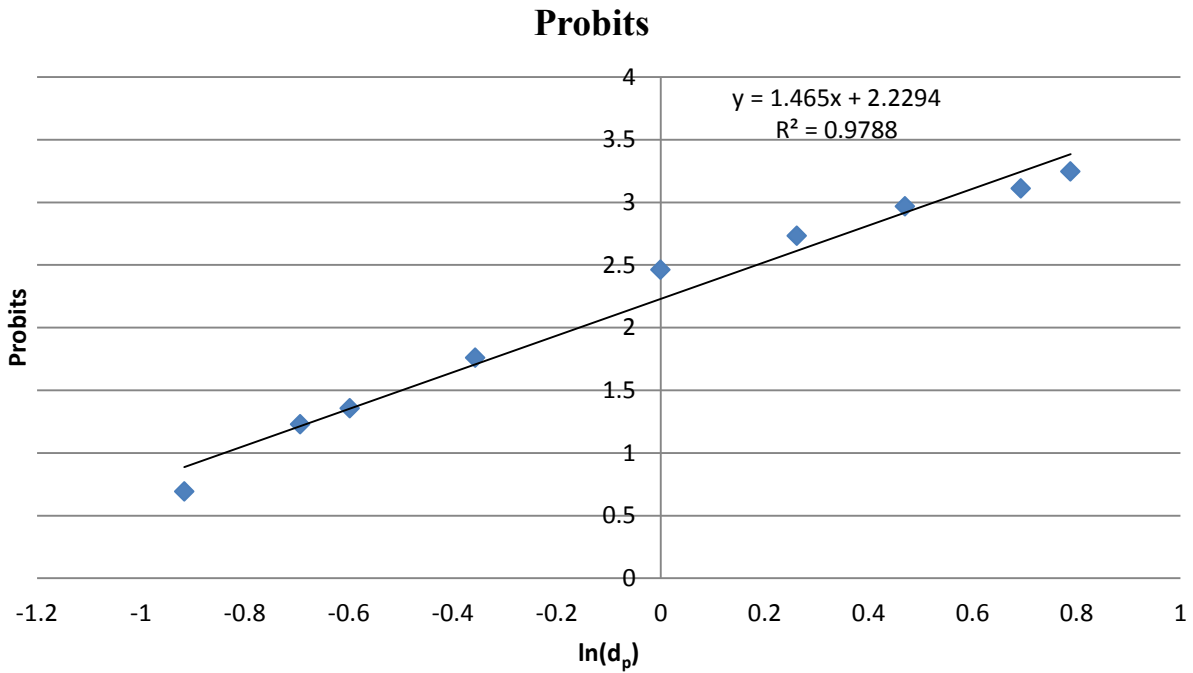


Figure 5.21 Probits versus ln(d<sub>p</sub>) at cruise test 1 (50.7 PSI, 249.7°C)

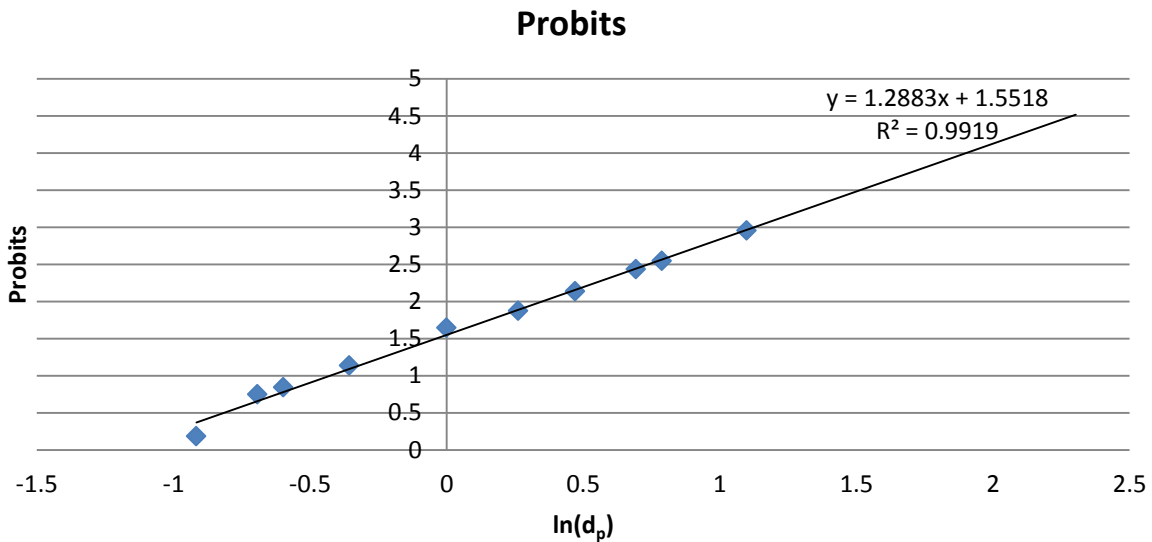
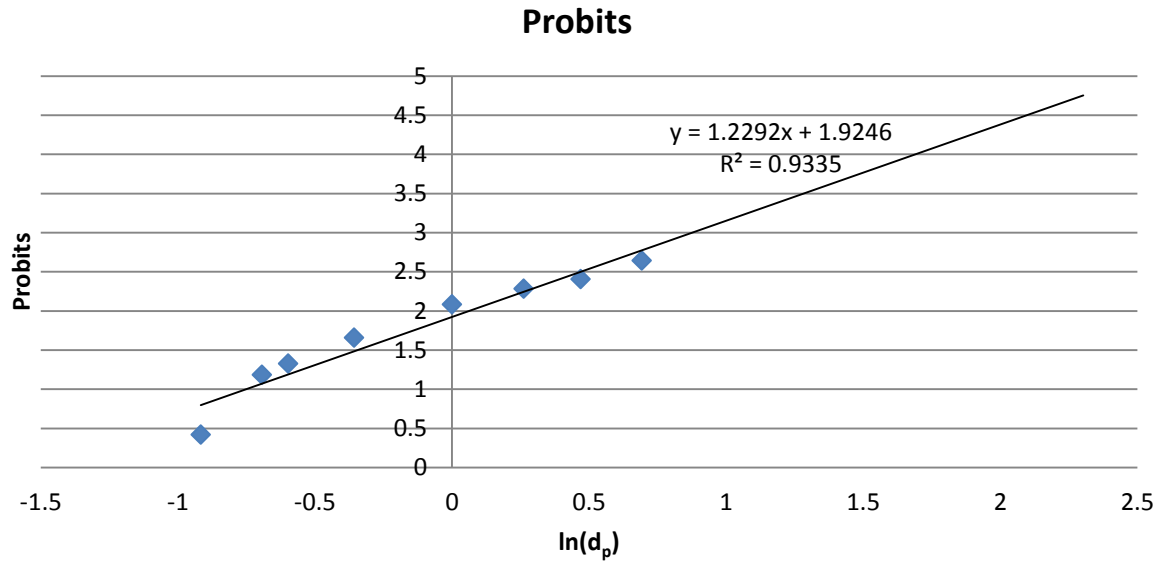


Figure 5.22 Probits versus ln(d<sub>p</sub>) at ground operations test 1 (14.1 PSI, 170.4°C)



**Figure 5.23 Probits versus ln(d<sub>p</sub>) at top climb test 1 (103.2 PSI, 308.0°C)**

**Table 5-8 Summarized results of probit analysis parameters for simulated aircraft bleed air operations**

Simulated mode of aircraft engine bleed air operation	Test	Test conditions	Equation for regression line	R <sup>2</sup>	MMAD μm	GSD σ <sub>g</sub>
Ground operations (Cold test)	Test 1	14.1 PSI, 170.4°C	$y = 1.2883x + 1.5518$	0.9919	0.45	1.9514
	Test 2	14.1 PSI, 170.4°C	$y = 1.377x + 1.5839$	0.9903	0.45	1.9518
Top climb (Take-off)	Test 1	103.2 PSI, 308.0°C	$y = 1.2292x + 1.9246$	0.9335	0.40	1.8887
	Test 2	104.1 PSI, 309.3°C	$y = 1.2236x + 2.0273$	0.9195	0.40	1.8799
Cruise	Test 1	50.7 PSI, 249.7°C	$y = 1.465x + 2.2294$	0.9788	0.39	1.8674
	Test 2	50.0 PSI, 251.1°C	$y = 1.4187x + 2.2382$	0.9777	0.39	1.8635
Initial descent from cruise	Test 1	29.7 PSI, 185.1°C	$y = 1.7012x + 1.9364$	0.9587	0.44	1.9368
	Test 2	29.6 PSI, 185.1°C	$y = 2.357x + 2.2489$	0.9424	0.44	1.9348
End of descent	Test 1	66.1 PSI, 230.9°C	$y = 1.4769x + 2.1693$	0.9564	0.40	1.8814
	Test 2	66.9 PSI, 230.7°C	$y = 1.2729x + 2.0894$	0.9318	0.40	1.8817
High pressure to low pressure switch-over	Test 1	70.9 PSI, 279.5°C	$y = 1.3181x + 1.9352$	0.9225	0.41	1.8974
	Test 2	74.4 PSI, 280.4°C	$y = 1.8444x + 2.2668$	0.9461	0.40	1.8875

According to Finney (1947) analytical model, a linear relationship of probits and  $\ln(d_p)$  with a correlation coefficient of 1.0 ( $R^2 = 1$ ) is a sign of a good fit for lognormal distribution. As is evident from Table 5.8, the  $R^2$  values tend to decrease with increased temperature suggesting that the linearity of the probits decrease with bleed air conditions which are associated with high temperatures. Figures 5.21 through 5.23 support this trend.

#### 5.4.1.3 Trends in experimental conditions: Performance parameters of BAS

Measurements of temperature and pressure variations versus time were plotted to determine the conditions of the experiment. Appendix E.1 shows plots of temperature and pressure variations in the reactor and the duct for various simulated tests conducted (Tables E.1 through E.7). Temperature and pressure profiles for all simulated bleed air conditions suggest that near steady-state conditions were achieved for all experiments conducted. At top climb and high pressure to low pressure switch-over conditions, pressure slightly fluctuated. Table 5-9 summarizes some measured parameters of simulated operational conditions of bleed air at different phases of flight.

**Table 5-9 Results of simulated experimental conditions for aircraft bleed air operations**

Simulated mode of aircraft engine bleed air operation	Test	Simulated bleed air conditions		Average duct flow rate (CFM)	Average aerosol concentration ( $\mu\text{g}/\text{m}^3$ )	MMAD ( $\mu\text{m}$ )	GSD $\sigma_g$	Relative humidity (%)
		Reactor pressure (PSI)	Reactor temperature ( $^{\circ}\text{C}$ )					
Ground operations (Cold test)	Test 1	14.1	170.4	1098.4	171.6	0.45	1.95	44.6
	Test 2	14.1	170.4	1098.6	173.3	0.45	1.95	43.1
Top climb (Take-off)	Test 1	103.2	308.0	1108.6	12.4	0.40	1.89	54.0
	Test 2	104.1	309.3	1107.1	16.4	0.40	1.88	52.7
Cruise	Test 1	50.7	249.7	1115.3	216.8	0.39	1.87	47.5
	Test 2	51.0	251.1	1113.9	231.7	0.39	1.87	45.9
Initial descent from cruise	Test 1	29.7	185.1	1101.9	133.2	0.44	1.94	44.6
	Test 2	29.6	185.1	1100.7	137.8	0.44	1.94	45.0
End of descent	Test 1	66.1	230.9	1108.9	355.9	0.40	1.88	61.5
	Test 2	66.9	230.7	1103.5	380.2	0.40	1.88	48.2
High pressure to low pressure switch-over	Test 1	70.9	280.5	1109.9	76.4	0.41	1.90	40.6
	Test 2	74.4	280.4	1111.4	88.6	0.40	1.89	39.1

**Table 5-10 Mean aerosol characteristics and simulated bleed air conditions**

Simulated mode of aircraft engine bleed air operation	Mean Pressure (PSI)	Mean Temperature (°C)	Mean GMMD nm	Mean GSD $\sigma_g$
Ground operations (Cold test)	14.1	170.4	450	1.95
Top climb	103.7	308.7	400	1.88
Cruise	50.9	250.4	390	1.87
Initial descent from cruise	29.7	185.1	440	1.94
End of descent	66.5	230.8	400	1.98
High pressure to low pressure switch-over	72.7	280.0	405	1.89
Average	-	-	410	1.92
Minimum	14.1	170.4	390	1.87
Maximum	103.7	308.7	450	1.98

From Table 5-10 it is evident that the mean (range) of geometric mass mean diameter (GMMD) = 0.42 (0.39, 0.45)  $\mu\text{m}$  and geometric standard deviation (GSD),  $\sigma_g = 1.92$  (1.87, 1.98). The ranges for both GMMD and GSD are short. Table 5-10 is derived from Table 5.9 to show the variations of GMMD and GSD with simulated bleed air conditions.

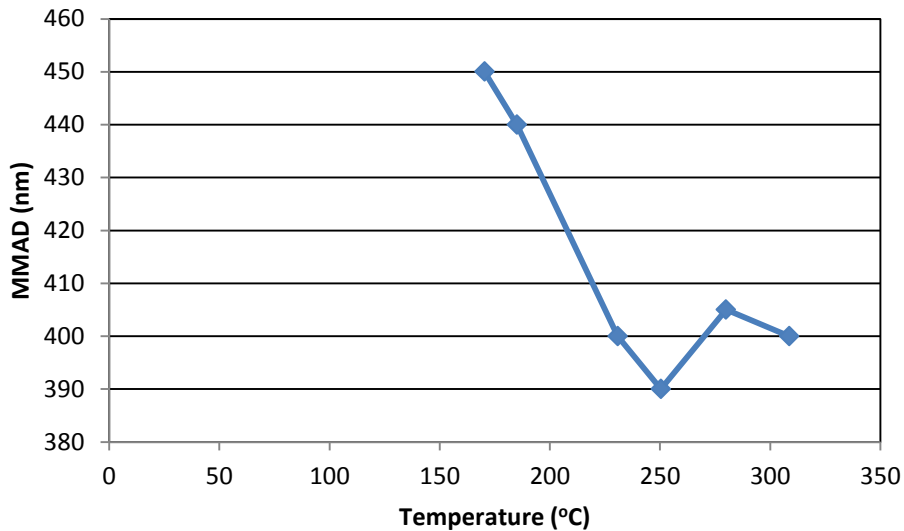


**Figure 5.24 Variability of MMAD of Mobil Jet Oil II aerosols with temperature in bleed air simulator**

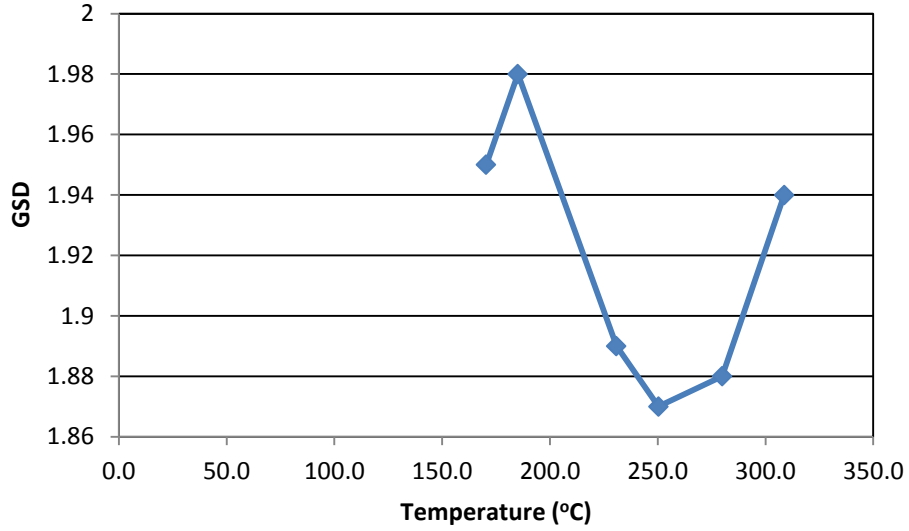


**Figure 5.25 Variability of GSD of Mobil Jet Oil II aerosols with temperature in bleed air simulator**

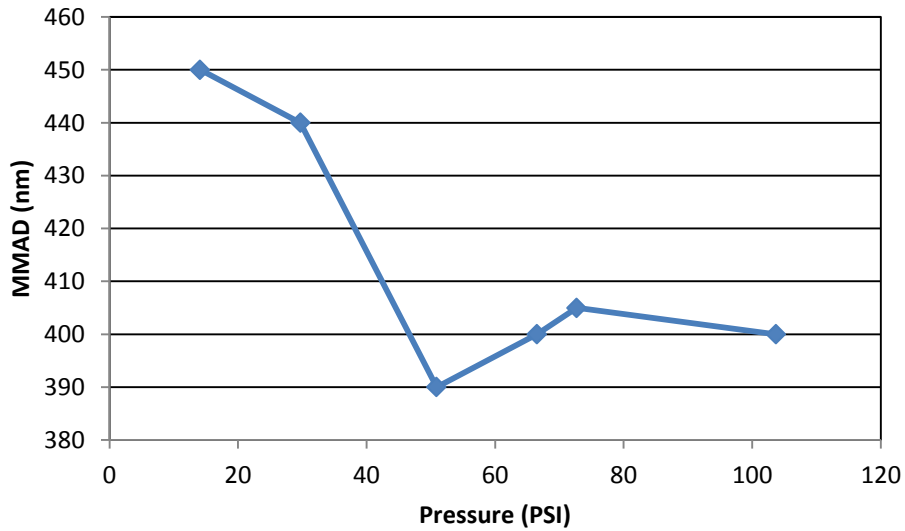


**Figure 5.26 Variability of MMAD of Mobil Jet Oil II aerosols with pressure in bleed air simulator**

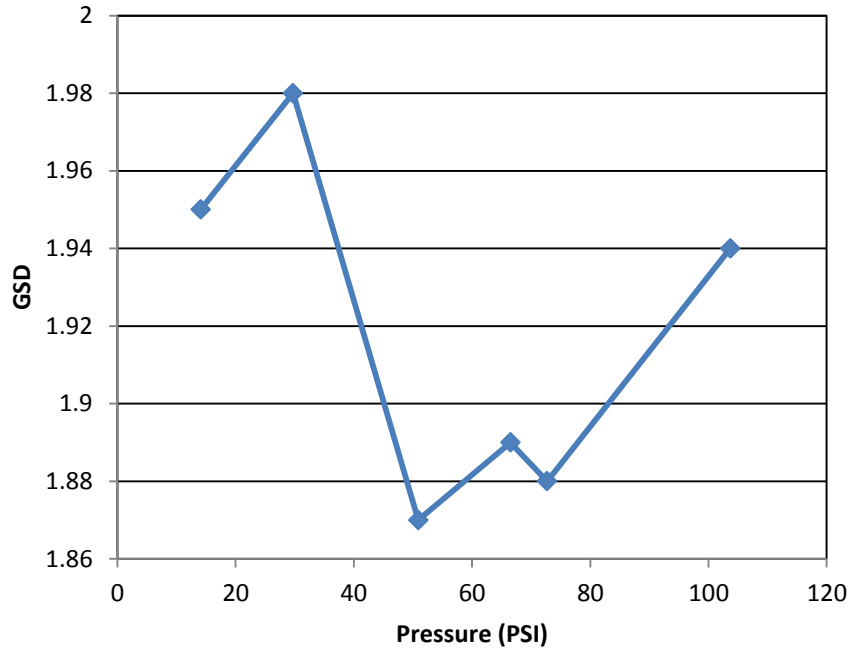


**Figure 5.27 Variability of GSD of Mobil Jet Oil II aerosols with pressure in bleed air simulator**

**Table 5-11 Cumulative mass percentage and aerodynamic diameter for simulated bleed air conditions**

Aerodynamic diameter (µm)	Ground operations	Top climb (Take-off)	Cruise	Initial descent from cruise	End of descent	High pressure to low pressure switchover
0.3	57.31507	66.25928	75.65097	48.63234	68.80793	63.27958
0.4	77.32973	88.24782	89.09422	77.75324	87.13803	85.08403
0.5	80.15243	90.81621	91.29320	82.49988	89.91333	88.34000
0.55	87.23620	95.12292	96.08905	92.52893	95.63952	94.92062
0.7	94.99994	98.14636	99.32293	98.90409	99.34610	98.91057
1.0	96.93986	98.89259	99.70623	99.51118	99.75175	99.38110
1.3	98.36680	99.20687	99.87038	99.81695	99.87994	99.56396
1.6	99.26541	99.60764	99.92512	99.94190	99.95643	99.64187
2.0	99.46794	100.00000	99.95725	99.95934	99.96942	99.67237
2.2	99.86329	100.00000	100.00000	99.97678	99.97807	99.79415
3.0	100.00000	100.00000	100.00000	100.00000	100.00000	100.00000

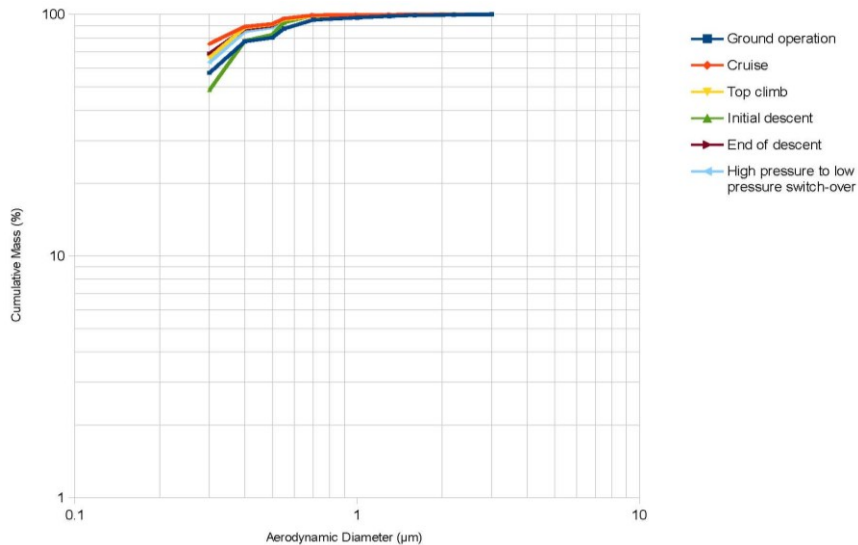


**Figure 5.28 Logarithmic scale for cumulative mass percent curves vs aerodynamic diameter for simulated bleed air conditions**

**5.4.1.4 Carbon monoxide as a marker for pyrolysis of Mobil Jet Oil II**

For this study, the electrochemical sensor which was installed to measure CO seemed to have produced noise other than reasonable data (See column showing CO measurements in Appendix E Tables E-1 through E-6).

**5.4.1.5 Results of exposure tests**

**Table 5-12 Exposure tests**

Sample ID	Amount detected in exposed filter (ng/cm <sup>2</sup> )			m/z 368 peak pattern yes/no	Oil Pattern m/z 57, 85,113 yes/no
	o-tolyl	m-cresyl	p-cresyl		
CT1_20 cold	0.00	<100	<40	Yes, but not quantifiable	NO
CT1_70 cold	0.00	180.00	98.00	Yes, but below quantifiable	NO
CT1_86 cold	0.0	300.00	162.20	YES	YES
CT1-391 cold	N/A	N/A	N/A	-	-
HT1-20 hot	0.00	386.00	238.20	YES	YES
HT1-70 hot	0.00	556.45	291.20	NO	YES
HT1-86 hot	0.00	1318.00	788.00	YES	YES
HT1-391 hot	0.00	3280.28	2176.97	YES	YES

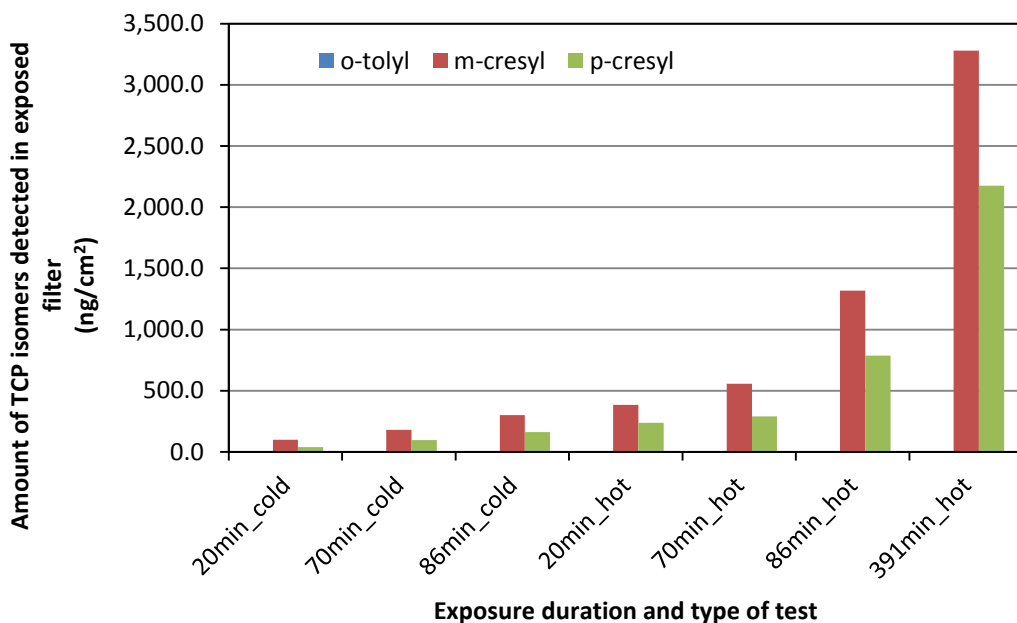


**Figure 5.29 Comparative analysis of the effect of temperature on concentrations of TCP isomers on clean filters exposed in BAS at varied durations**

From the Figure 5.29 it is evident that more TCPs isomers are detected in filters exposed at higher temperature than those exposed to cold suggesting that increase in temperature plays a role in increasing airborne TCPs in the air.

**Table 5-13 Pattern of Mobil Jet Oil II markers on clean filters exposed in BAS**

# of nozzles open	Aerosol loading (µg)	Sampling period in minutes	Test conditions	Cumulative Sample mass (µg)	m/z 368 peak pattern yes/no
<b>1. Cold tests</b>					
1.	0.1	20	146.3 PSI, 168.8°C	12.75	NO
2.	1.0	70	154.5 PSI, 97.2°C	148.12	NO
3.	10.0	86	148.2 PSI, 103.5°C	278.22	YES
4.	100.0	600	NA	NA	NA
<b>1. Hot tests</b>					
1.	0.1	20	33.4 PSI, 297.6°C	10.84	YES
2.	1.0	70	20.6 PSI, 301.7°C	89.90	YES
3.	10.0	86	18.1 PSI, 293.8°C	224.31	YES
4.	100.0	391	14.5 PSI, 298.6°C	1973.55	YES



## 5.4.2 Discussion

Both temperature and pressure plots (Appendix E1: Figures E.3 through E.7) show that BAS conditions were very well simulated and steady state conditions achieved. From the plots, we can conclude that the tests were conducted near steady state conditions. In addition, the results of steady state conditions demonstrate the effectiveness of the BAS. The average repeated measurements over a period of time are the best indicator of how the process varies with time. At present, bleed air emissions in commercial aircrafts are not monitored, in part due to the lack of test methods, rating systems, and real-time sensors. In fact, only limited laboratory performance data exists on bleed air emissions. The study shows that respirable particles from Mobil Jet Oil II that can be measured by the OPC fall between 0.3 to 1.6  $\mu\text{m}$ . The size distribution metrics MMAD and GSD obtained from linear regression analysis of aerosol particulate data had short ranges: (0.39, 0.45) and (1.87, 1.98)  $\mu\text{m}$  respectively.

### 5.4.2.1.1 *The development of BAS*

BAS was designed to simulate jet engine operating conditions and provide users a way to model smoke/fume incidents using a single standardized platform to conduct, monitor, and report cabin air quality incidents. BAS enables real time counting, sizing aerosol particulates in simulated bleed air. As each of the aerosol particulates within the sample are sized irrespective of the others, the experimental design allows users to produce a full and accurate PSD profile. But the real advantage of the BAS system lies in its ability to repeat the performance consistently no matter what flight conditions are to be simulated. The BAS gives airlines the ability to make sense of incidents by offering the data airlines need. The equipment promises to significantly improve smoke/fume incident monitoring.

The development of BAS marks the first platform for aerosol generation and monitoring of jet engine lubricating oil. It is ideal for a wide range of applications, including monitoring aerosol formation from any potential smoke/fume incident causing substance such as hydraulic and deicing fluids. This implies that the system can be tailored to any specific lubricating engine oil and/or hydraulic fluids used in modern aircraft engines. Therefore, BAS could also help airlines distinguish between unique features of different smoke/fume incidents. The BAS provides a tool to airlines to facilitate change and transform air quality. Adopting BAS can

improve data collection and deliver improved accuracy of air quality inventory, which can lead to improvements in cabin occupants' travelling experiences.

The BAS has been designed with one mission in mind: simulate aerosol particles generated from aircraft bleed air system, allowing scientists to better understand the pyrolysis of jet engine lubricating oil. Faced with smoke/fume incidents, airlines need facts based on scientific information so they can act to monitor aerosol particles emissions from aircraft bleed air system. The BAS will allow airlines to objectively compare monitoring methods for the most accurate prediction of aerosol size distribution. BAS can help airlines and scientists combat smoke/fume incidents. BAS will help researchers and airlines understand how jet engine oil and other potential smoke/fume causing substances affect the aircraft cabin environment. With BAS airlines can achieve the following:

- Feedback information on the chemical fingerprint and other cabin environmental impacts on air passing through the cabin
- Learn cabin air quality design practices and how to improve air quality for environmentally-conscious air travelers and crew
- Identify potential cabin air pollutants and compare physical and chemical properties of airborne particles in the cabin environment.

The development of BAS offers an opportunity for researchers to compare models and discuss hypotheses and interpretations of smoke/fume incidents. The data obtained from this study will enable researchers to understand patterns of aerosol size distributions during different phases of simulated aircraft flights. With real-time monitoring, airline operators could also analyze the data for clues on flight conditions associated with smoke/fume incidents. This could lead to the creation of database that could lay groundwork for developing sensors, which would in turn enable accurate measuring and possible control of these aerosols. Since aerosol particulates produced during incidents could cause illnesses, making a universal tool for monitoring air quality in jet engine's bleed air system is a necessity. Without such a tool, there is no independent verification that safety procedures are properly maintained i.e. no monitoring of bleed air is carried out in aircrafts.

The test facility based on ASHRAE 52.2 combined with LabVIEW software control process solutions and other accessories have resulted in a unique system that enables aircraft bleed air system simulation. The BAS is a useful smoke/fume incident handling platform that

can be expanded as the needs and requirements grow. The BAS offers robust, high-performance real-time aerosol particulate monitoring and addition of equipment that can capture aerosols counts below 0.3  $\mu\text{m}$  range can be incorporated. The primary goal for using BAS is to present an accurate representation of smoke/fume incidents. This will strengthen ANSI/ASHRAE Standard 161–2007 which is the authoritative guideline for uniformity in drawing specifications and interpretation of air quality within commercial aircraft.

#### 5.4.2.1.2 *Comparisons of aerosol generator to aircraft bleed air system*

In this study smoke/fumes incidents generated from jet engine oil are modeled in BAS as an example to show what influences the production of aerosol particulates. The BAS system provides a practical framework for monitoring simulated bleed air, delivering and supporting air quality service during smoke/fume incidents. The integrated solution includes air sampling system and aerosol counting instruments designed to continuously monitor smoke/fume incident conditions. The wide range of aerosol particulate counts during the experiment reflects different flight conditions. However, it is important to note that the actual bleed air system as installed in the aircraft is a very complex system not comparable to a simplified BAS developed for laboratory use.

### **5.5 Recommendations**

While this study has revealed some important jet engine oil emission characteristics, significant questions remain on the impact these emissions have on aircraft cabin air supply as it originates from real aircraft bleed operating conditions. Unresolved problems which require additional research efforts include relating these findings to real aircraft cabin. Aircraft cabin occupants may be exposed to jet engine oil emissions and other contaminants over a broad range of concentrations, and temperatures which may affect chemical composition. BAS can help determine the optimum sampling period for establishing detection limits of jet engine oil markers on exposed filters. The normal background range of cabin air contaminants identity and levels of chemicals released into cabin air during a contaminated air event should be determined. In particular, fine particulate aerosols with aerodynamic diameter less than 2.5  $\mu\text{m}$  present significant health risks (Dockery, 1994; Forastiere, 2004; Pope, 2000). Thus, characteristics of fine aerosols from jet engine oil less than 0.3  $\mu\text{m}$  should be investigated. It is recommended that

BAS be used to investigate what could be present in various jet engine lubricating oils and hydraulic fluids subjected to very high temperatures, producing potentially harmful gases like CO and aldehydes that can irritate human airways and various compounds that produce unpleasant odors. Further, tests on faulty engines could help identify compounds that might be released into bleed air systems.

## **5.6 Conclusions**

1. A novel real-time monitoring system for airborne particulates formed during cabin air quality events has been implemented in a laboratory set up that simulates aircraft's bleed air systems. A methodology for assessment of aerosol particulates generated during smoke/fume incidents has been presented.
2. An air sampling methodology for monitoring aerosols in simulated aircraft's bleed air has been developed. A detection method for airborne jet engine oil aerosol formed at various simulated jet engine bleed air operating conditions has been presented. The strategy reflects a potential upgrade in response to perceived types of aerosols generated during smoke/fume incidents from Mobil Jet Oil II. Aerosol particulates from pyrolyzed Mobil Jet Oil II have been characterized. The study also presents best practices for effectively monitoring and reporting airborne contaminants in aircraft bleed air system. Further, it provides a technique for ensuring that bleed air contaminants from jet engine oil is accounted for.
3. Comparisons of analyzed data from hot and cold test runs simulating incidents suggest that both temperature and pressure are the main influencing factors in aerosol formation and PSD.
4. A new opportunity for monitoring smoke/fume incidents has been unveiled. BAS is a practical guide for achieving aerosol particulate size measurements and provides detailed information on how to launch a successful cabin air quality monitoring strategy within an airline company. The study details best practices that can help airlines optimize measurements of cabin air contaminants from bleed air supply, particularly in light of regulatory requirements. The building blocks to best practices are defined as well as procedures to ensure system adoption and successful incorporation into laboratory processes. These findings mark the first definitive evidence that varied aerosol particulates from jet oil could exist in aircraft bleed air.

5. The detection of the presence of TCP isomers in exposed filters confirms that these compounds could exist in aircraft bleed air when an incident occurs. The finding can be a useful part of aircraft cabin air safety; an obvious implication could be that cabin occupants are at greater risk of exposure to volatile TCP compounds in jet engine oil during incidents. Using BAS for monitoring airborne aerosols formed in bleed air system will enlarge the competence in this field in terms of understanding aerosol particulate contamination risks and implementing corrective actions.
6. The study provides a framework for future research in aircraft engine bleed air systems. Deploying BAS technology can advance research that could improve aircraft cabin environment conditions for air passengers' comfort. Resulting compliance standards for detection of bleed air contamination in place for the airlines could improve operating and in-cabin environmental performance, protecting the health and safety of passengers and airline crew. BAS experiments could provide data that might be considered for evaluation of health risk assessments of the air contaminants from commercial aircraft bleed air system and could be useful in improving cabin air quality guidelines and, if warranted, regulations on other products like hydraulic and de-icing fluids that might introduce airborne pollutants into aircraft cabin environment.
7. A bleed air simulator is an essential modeling tool that will enable professionals to create and refine their understanding of aerosols in civil aircraft bleed air systems. The study could provide a foundation for further investigative action on sensor development for VOCs emitted from bleed air system during smoke/fume incidents. Monitoring could provide aerosol production details on emerging trends, highlighting where opportunities lie for sensor development.
8. Finally, the study has provided stakeholders in airline industry with information about what goes on during incidents, knowledge that could enable users to develop new air quality parameters. Temperature and pressure, both of which influence smoke/fume incidents, can now be objectively assessed in the laboratory using BAS. The development of BAS is a significant step that could help airlines manage the problem of smoke/fume incidents.

## 5.7 References

- AAIB. Bulletin 6/2009, (2009). G-BYAO EW/C2006/10/108 [http://www.aaib.gov.uk/cms\\_resources.cfm?file=/Bulletin%206-2009.pdf](http://www.aaib.gov.uk/cms_resources.cfm?file=/Bulletin%206-2009.pdf) (Cited May 5<sup>th</sup>, 2010).
- ACGIH. (2001). Threshold Limit Values and Biological Exposure Indices (TLVs and BEIs), Cincinnati: American Conference of Governmental Industrial Hygienists. ISBN: 1-882417-40-2, pp. 58.
- Air Contamination Monitor, Patent Number 5750999, (1998). <https://www51.honeywell.com/technologylibrary/Technology.do?page=print&techId=17>
- AFL-CIO Report, (2003), Aircraft Air Quality: What is wrong with it and what needs to be done. Association of flight attendants Report submitted to The Aviation Subcommittee of the Transportation & Infrastructure Committee. U.S. House of Representatives, June 4, 2003. [http://www.afanet.org/legislative/aircraft\\_air\\_quality-\\_61303.pdf](http://www.afanet.org/legislative/aircraft_air_quality-_61303.pdf) (Cited: May 15, 2010)
- Airsense Analytics, (2007). <http://www.airsense.com/media///airsense/downloads/airsense-produktdatenblatt-at-engl-14.06.2011.pdf>
- ASHRAE. 1987 (R1992) ANSI/ASHRAE Standard 41.2-1987. Methods for Laboratory Airflow Measurement, Atlanta, GA: American Society of Heating, Refrigerating and Air-Conditioning Engineers, Inc.
- ASHRAE. (1995). 1995 ASHRAE Handbook—HVAC Applications, Chapter 12, Atlanta, GA: American Society of Heating, Refrigerating and Air-Conditioning Engineers, Inc.
- ASHRAE. (1999). ASHRAE Handbook – HVAC Applications, Chapter 9, Aircraft, American Society of Heating, Refrigerating and Air-Conditioning, Atlanta, GA.
- ASHRAE. (1999). ANSI/ASHRAE Standard 52.2-1999. Method of Testing General Ventilation Air-Cleaning Devices for Removal Efficiency by Particle Size, Atlanta, GA: American Society of Heating, Refrigerating and Air-conditioning Engineers, Inc.
- ASHRAE. (2007). ANSI/ASHRAE Standard 161-2007, Air Quality Within Commercial Aircrafts. 20pp; Product code: 86493. ISBN: 1041-2336. Atlanta, GA: American Society of Heating, Refrigerating and Air-conditioning Engineers, Inc.
- Balouet, J. C., and Winder, C., (1999). Aerotoxic syndrome in air crew as a result of exposure to airborne contaminants in aircraft, American Society of Testing and Materials (ASTM) Symposium on Air Quality and Comfort in Airliner Cabins, New Orleans.
- British Airline Pilot Association (BALPA) Report, (2005). [http://www.rsc.org/images/balpa\\_tcm18-99526.pdf](http://www.rsc.org/images/balpa_tcm18-99526.pdf) (Cited: January 5, 2012).

- De Nola, G., Kibby, J., Mazurek, W., (2008). Determination of *ortho*-cresyl phosphate isomers of tri-cresyl phosphate used in aircraft turbine engine oils by gas chromatography and mass spectrometry. *Journal of Chromatography A*, 1200 (2008) 211 – 216.
- Colburn, A. P., (1933). A method for correlating forced convection heat transfer data and a comparison with fluid friction, *Transactions of American Institute of Chemical Engineers*, Vol. 29, pp. 174-210 ISSN 0096-7408.
- Cone, J. E. (2005). Aircraft Cabin Air Quality Trends Relative to Ground Levels Standards, In Hocking, M.B., editor. *Air Quality in Airplane Cabins and Similar Enclosed Spaces. Handbook of Environmental Chemistry Vol. 4, Part H* (2005): 293–315. DOI 10.1007/b107249. Springer-Verlag Berlin Heidelberg, 2005.
- Dittus, F. W. and Boelter, L. M. K., (1930). Heat transfer in automobile radiators of the tubular type. *University of California Publication Eng.* 2 (13) (1930) 443-461.
- Damange, M., Gendre, J. C., Herve-Bazin, B., Carton, B., Peltier, A., (1990). Aerosol evaluation difficulties due to particle deposition on filter holders inner walls. *Ann. occup. Hyg.*, Vol. 34, No. 4, pp. 399 – 403, © 1990 British Occupational Hygiene Society.
- Dockery, D. W. and Pope, C. A., (1994). Acute Respiratory Effects of Particulate Air Pollution; *Ann. Rev. Public Health* 15, 107 – 132.
- Finney, D. J., (1947). *Probit analysis*. Cambridge University Press, London and New York.
- Forastiere, F., (2004). Fine Particle and Lung Cancer; *Occup., Environ. Med.* 2004, 61, 797–798.
- Fox, R. B., (2000). Air quality and comfort measurement aboard a commuter aircraft and solutions to improve perceived occupant comfort levels. In: Nagda, N.L., editor. *Air quality and comfort in airliner cabins*, ASTM STP1393. West Conshohocken, PA: American Society for Testing and Materials.
- Haghighat, F., Allard, F., Shimotakahara, R., (1999). Measurement of thermal comfort and indoor air quality aboard 43 flights on commercial airlines. *Indoor Built Environ.* 8(1): 58 – 66.
- Hanley, J. T., Smith, D. D., Ensor, D. S., (1995). A Fractional Aerosol Filtration Efficiency of In Duct Ventilation Air Cleaners, *Indoor Air*. Vol. 4: 169 –178.
- Harrison, R., Murawski, J., McNeely, E., Guerriero, J., and Milton, D., (2008). Management of exposure to aircraft bleed-air contaminants among airline workers: a guide for health care providers. *The Annual International Aircraft Cabin Safety Symposium*, Torrance, CA.
- Hewitt, G. F., (1978). *Measurement of two phase flow parameters*, London: Academic Press.

- Hinds, W. C., (1998). *Aerosol Technology; properties, behavior and measurements of airborne particles*. Ch. 11. 2<sup>nd</sup> ed., pp. 249. John Wiley and Sons.
- Hocking, M. B., (1998). *Indoor Air Quality: Recommendations Relevant to Aircraft Passenger Cabins*. American Industrial Hygiene Association (AIHA) Journal 59: 446 – 454.
- Holley, J. A., (2009). *Reducing Smoke and Burning Odor (SBO) Events*, Aeromagazine. [http://www.boeing.com/commercial/aeromagazine/articles/qtr\\_01\\_09/pdfs/AERO\\_Q109.pdf](http://www.boeing.com/commercial/aeromagazine/articles/qtr_01_09/pdfs/AERO_Q109.pdf)
- Incropera, F. P. and DeWitt, D. P., (2002). *Fundamentals of Heat and Mass Transfer* 5<sup>th</sup> ed., John Wiley and Sons New York 2002. ISBN 0-471-38650-2.
- Ito, K., Kobashi, S., Tokuda, M., (1991). *Mixing characteristics of a submerged jet measured using an isokinetic sampling probe*. Metallurgical Trans. B. 22B: 439 – 445.
- Kays, W. M. and Crawford, M. E., (2004). *Convective heat transfer and mass transfer*. 4<sup>th</sup> ed. McGraw-Hill Book Company New York 2004. ISBN 0-07-033 457-9.
- Kibby, J., Denola, G., Hanhela, P. J., Mazurek, W., (2005). *Defence Science and Technology Organisation, Department of Defence*. DSTO-RR-0292. Melbourne, 2005.
- Kodilkar, M., (2004). *Development and Verification of a Unique HEPA Filter Test Facility*. M.S. Thesis 2004.
- Koehl, A., Wilks, A., Hart, J., (2007). *Advanced Sensor System to Identify and Quantify Contaminants in Cockpit*. USAF SBIR AF06-023. Contract Number FA8650-06-M6677
- Lee, S. C., Poon, C. S., Li, X. D., Luk, F., (1999). *Indoor Air quality Investigation on Commercial Aircraft*. *Indoor Air* 1999; 9 (3): 180–187. Copyright © Munksgaard 1999. ISSN 0905-6947.
- Lindgren, T., and Norback, D., (2002). *Cabin air quality: indoor pollutants and climate during intercontinental flight with and without tobacco smoking*. *Indoor Air* 2002: 12: 263–272.
- Lippmann, M. (1995). *Filters and Filter Holders*. In: Cohen, B. S., and Hering, S. V., (eds.), *Air Sampling and Instruments for Evaluation of Atmospheric Contaminants*. 247–279. ACGIH. Cincinnati, Ohio.
- Liu, B, Y. H., Pui, D. Y. H., Rubow, K. L., (1983). *Characteristics of air sampling filter media*. In: Marple, V. A. and Liu, B. Y. H. (eds.). *Aerosol in mining and industrial work environments*, Vol. 3. Ann Arbor Science, pp. 989 – 1038.
- Pierce, W. M., Janczewski, J. N., Roethlisberger, B., Janczewski, M. G., (1999). *Air quality on Commercial Aircraft*. ASHRAE Journal, 14, (9) 26 – 34.



- Magee Scientific, (2009). Operating Manual micro-AETHALOMETER®.  
[http://mageesci.com/support/downloads/micro/microAeth\\_AE51\\_Operations\\_Manual\\_Jun-09.pdf](http://mageesci.com/support/downloads/micro/microAeth_AE51_Operations_Manual_Jun-09.pdf)
- Mars, T. C. and Ballantyne, (eds.), (1994). Clinical and Experimental Toxicology of Organophosphates and Carbamates. pp. 394. Butterworth/Heinemann, 1994.
- Material Safety Data Sheet (MSDS) for Tricresyl Phosphate. Issued: 05/18/2008.  
<http://mobiljet2.com/msds.pdf>
- National Research Council (NRC). (2002). The Airliner Cabin Environment and the Health of Passengers and Crew Committee on Air Quality in Passenger Cabins of Commercial Aircraft. Washington DC: National Academy Press.
- OSHA. (1992). Code of Federal Regulations 29, Part 1910, July 1, 1992. Washington, DC: Occupational Safety and Health Administration, U.S. Department of Labor.
- Pope, C. A., (2000). Epidemiology of Fine Particulate Air Pollution and Human Health: Biological Mechanism and Who's at Risk; Environ. Health Perspect. 2000, 108, 6493 – 6502.
- Ross, S. M., Harper, A. C., Burdon, J., (2006). Ill health following reported exposure to contaminated air on commercial aircraft: psychosomatic disorder or neurological injury? Journal of Occupational Health & Safety: Australia & New Zealand 22 (6): 521–528
- Ross, S. M., (2008). Cognitive function following exposure to contaminated air on commercial aircraft: A case series of 27 airline pilots seen for clinical purposes Journal of Nutritional & Environmental Medicine, 17 (2): 111 – 126.
- Select Committee on Science and Technology (2000). Science and Technology - Fifth Report House of Lords.  
<http://www.publications.parliament.uk/pa/ld199900/ldselect/ldsctech/121/12107.htm>.  
(Cited: 01/07/2012).
- Schwartz, J., Dockery, D. W., Neas, L. M., (1996), Is daily mortality associated specifically with fine particles? J. Air Waste Manag. Assoc. 46: 927– 939.
- Somkuti, S. G., Tilson, H. A., Brown, H. R., Campbell, G. A., Lapadula, D. M., Abou-Donia, M. B. (1988). Lack of Delayed Neurotoxic Effect after Tri-o-cresyl Phosphate Treatment in Male Fischer 344 Rats: Biochemical, Neurobehavioral and neuropathological Studies. Toxicological Sciences, 10 (2) 199 – 205.
- Streicher, R. P., (1994). NIOSH/DPPSE. NIOSH Manual of Analytical Methods (NMAM) 4<sup>th</sup> (ed.) 1994.

- Strøm-Tejse, P., Żukowska, D., Fang, L., Space, D. R., Wyon, D. P., (2006). Effects of Gas-Phase Adsorption air purification on passengers and cabin crew in simulated 11-hour flights *Transports: Proceedings of Healthy Buildings*, 2006.
- van Netten, C. and Leung, V., (2000). Comparison of the constituents of two jet engine lubricating oils and their volatile pyrolytic degradation products. *Appl. Occup. Environ. Hyg.* 15 (3) pp. 277 – 283.
- van Netten, C. (2000). Analysis of two jet engine lubricating oil and a hydraulic fluid: their pyrolytic breakdown products and their implication on aircraft air quality. In: Nagda, N.L., (ed.) *Air Quality and Comfort: In Airliner Cabins*. pp. 61-75 ASTM STP 1393, American Society for Testing and Materials, West Conshohocken, PA.
- van Netten, C. and Leung, V. (2001). Hydraulic fluids and jet engine oil: Pyrolysis and aircraft air quality. *Arch. Environ. Health.* 56 (2) 181 – 186.
- van Netten, C. (2009). Design of a small personal air monitor and its application in aircraft. *Science of the total environment* 407 (2009) 1206 – 1210.
- Winder, C. and Balouet, J. C., (2005). Aircrew exposure to chemicals in aircraft: symptoms of irritation and toxicity. *J. Occup. Health Safety Aust. NZ.* 17:471– 483.
- Winder, C. and Balouet, J. C., (2002). The toxicity of commercial jet oils. *Environ. Res.* 89:146 – 164.
- Yang, X., Zitova, A., Kirsch, J., Fergus, J. W., Overfelt, R. A. and Simonian, A. L., (2011). Portable and remote electrochemical sensing system for detection of tri-cresyl phosphate in gas phase. *Sensors and Actuators B:* (2011). Doi: 10.1016/j.snb.2011.10.076
- Zieger, P., Fierz-Schmidhauser, R., Gysel, M., Strom, J., Henne, S., Yttri, K. E., Baltensperger, U., and Weingartner, E., (2010). Effects of relative humidity on aerosol light scattering in the Arctic. *J. Atmospheric Chemistry and Physics (ACP)*. 10: 3659 – 3698.

## **CHAPTER 6 - CONCLUSIONS AND FUTURE WORK**

### **6.1 Conclusions and contributions of the study**

The airline industry is struggling to cope with smoke/fume incidents. In this study technologies that could help airline industry collect data by analyzing used aircraft filters are described. This research has developed both direct and indirect test methods and procedures that could be used to investigate jet engine oil markers on used aircraft cabin air filters. The direct method uses GC/MS whereas the indirect methods employ FESEM/EDS and NAA techniques. All three methods offer different frameworks for investigating and identifying jet engine oil contaminants on the filters. The GC/MS analysis has established that jet engine lubricating oils play a role in the contamination of aircraft cabin air recirculation filters. The method can be used to analyze TCP isomers in used cabin air recirculation filters. However, both FESEM/EDS and NAA techniques allow look at used aircraft cabin air filters and provide new information on elemental deposition on used filters, providing information about past cabin air quality. The three analytical methods for used filters provided by this study are research tools that can be used to establish the past history of aircraft cabin air quality.

Using GC/MS analytical technique, this study has established a link between filter deposition in used aircraft filters and TCP isomers in the Mobil Jet Oil II that was used as representative jet engine oil. Both FESEM/EDS and NAA analyses revealed a wide range of traces of metallic elements present in used and incident filters. These results suggest that airborne particulates in aircraft cabin air contain traces of rare earth elements from outside air, and from processes occurring either in the jet engine or inside the cabin. In fact, the findings suggest that aircraft's ECS involves far more than scientists might expect. The filter analysis techniques vary widely in their ability to detect filter deposits. The NAA technique has delivered new useful data for understanding of cabin air supply. Moreover, both NAA and FESEM/EDS methods in different ways, will build on current expertise in detecting smoke/fume incidents. Both methods underscore the importance of understanding the indirect jet oil footprints on used aircraft filters.

While scientists have long known that jet engine oils have been one potential source of airborne toxic organophosphate compounds to cabin air supply in aircrafts, this research has provided new details on monitoring those pollutants in used cabin air filters. Integrating a

number of technological tools to manage pyrolysis of jet engine lubricating oil has led to the development of BAS, making possible monitoring smoke/fume incidents in a laboratory set up. The BAS development allows bleed air to be simulated and assessed. Aerosol particulates from pyrolysis of Mobil Jet Oil II have been characterized. Detection of the presence of TCP isomers on clean filters exposed to laboratory simulated incidents confirms that BAS works and confirms the fact TCP compounds could exist in aircraft bleed air after an incident. Such findings could be used to define aircraft cabin air safety standards and the risks of exposure to these compounds. The research has provided the fundamentals of a mechanism for detecting aircraft bleed air pollutants, key performance parameters, and some type of data sets that could be obtainable from real jet engine bleed air processes. In fact, the BAS platform can be used to examine any potential substance that can cause smoke/fume incidents to provide airborne particulate information for any substance. Thus, the application of BAS can simulate and sample airborne aerosols, while GC/MS can define aircraft cabin air quality incidents through analysis of exposed filters. The development of BAS is the result of advancing awareness of smoke/fume incidents, and its implementation shows how efforts to manage aircraft cabin air quality are shifting to research laboratories. The BAS protocol could be used to launch new aircraft cabin air quality standards designed to empower airlines to better measure, manage, and report aircraft engine bleed air emissions. The research could transform aircraft cabin air quality solutions, building a scientific case for monitoring incidents, and evaluating risks, and enhancing safety in the aircraft cabin.

The analyses of exposure tests (air sampling of simulated smoke/fume incidents) conducted in BAS using the same analytical methods have also established a firm link between filter deposits on clean filters with jet engine oil. The combined procedures of sampling and analyses of aircraft cabin air filters could significantly improve the process of investigating aircraft cabin air quality. The civil aviation industry could use this new scientific method of filter analysis to monitor cabin air quality incidents. With new methods of filter analysis, valuable cumulative information about air quality can be extracted from used filters. Finally, the study provides a scientific basis for future cabin air quality standards research because the information drawn from experiments in BAS could help in drawing guidelines to establish regulatory standards for TCP emissions from incident-occurrences caused by pyrolysis of jet engine oil during smoke/fume incidents.

### **6.1.1 Significance and impact of the study**

This research has introduced the concept of analyzing used cabin air filters to help satisfy aircraft cabin air quality reporting guidelines. A lot of information can be obtained from analyzing used aircraft cabin by using FESEM/EDS, GC/MS and NAA. The study has shown that cabin filters which are the very heart of the aircraft cabin air filtration undergo a lot of changes while the aircraft is on flight and can provide data critical to understanding cabin air quality. Detecting jet engine oil contaminants in used filters provides a means of identifying bleed air contamination and, more importantly should be of interest to stakeholders in the airline industry. Both cabin air filter analysis and bleed air monitoring are important in improving aircraft cabin air quality.

Because BAS can measure aerosol particle size distribution and sample air it will be a part of a broad scientific effort to improve cabin air quality. Filter analyses support using BAS in detecting airborne pollutants deposited on cabin recirculation filters. Therefore, BAS could help airline operators to understand how to eliminate air quality incidents. Long-term monitoring could lay the groundwork for future research into smoke/fume incidents and facilitate improving safety parameters for aircrafts during incidents. Implementing of BAS will enable airlines to actually see what happens to air quality during incidents through routine analysis of exposed filters. For the airlines, this means mitigating costs and risk while increasing business value. The information derived from the BAS experiments could also help establish detection limits for potential smoke/fume causing substances as well as standards of VOCs emitted during incidents. Finally, the study finding increases options for effective detection of smoke/fume incidents. Given its high simulation performance capabilities, including achievement of steady state conditions at the reactor during its operation, current and future demand for smoke/fume incident simulation in a laboratory set up will provide continued opportunity for expanded use of this critical equipment. The study has identified principal techniques which could support the efficient use of aircraft cabin air supply.

The result of this research has been significant, from essentially operating aircraft bleed air system in the dark, relying on incomplete information, to seeing all facets of smoke/fume incident process. BAS can monitor airborne pollutant emissions that can make air passengers and crew sick and simulates varied conditions of bleed air conditions. In the process, this study has developed methods for analyzing cabin air recirculation filters, which increases the likelihood of

developing air quality standards for aircraft cabins. And overall the study has revealed significant insights into smoke/fume incidents.

To effectively implement regulations requires air quality benchmarks for aircraft bleed air systems to significantly decrease perceived negative impacts from air pollution in aircraft cabins. Increased social corporate responsibility and the push to create a more efficient and less risky cabin environment will allow airlines to show themselves as good stewards and responsible companies, managing not only the contaminants in the cabin air but addressing possible health problems of air passengers and cabin crew. The research findings of this study underscore the importance of understanding cabin air quality incidents as the results confirm that airborne emissions from smoke/fume events disperse into cabin air and migrate to deposit on cabin air recirculation filters. BAS capabilities fit on the continuum of aircraft cabin occupants' health protection and its availability offer best practices involving various technologies including aerosol sampling of particulates and gaseous byproducts from pyrolysis of jet engine oil. The new approach to monitoring aircraft engine bleed air aims to make use of technology to deliver best air quality to the aircraft cabin. It requires certain key technologies, but more broadly it focuses on developing procedures for application of the new analytical techniques for analysis of cabin air recirculation filters.

### **6.1.2 Limitations of the study**

Although simulation of aircraft engine bleed air conditions is possible with BAS, the bleed air arrangement is complex its function in the engine bleed air system cannot be fully simulated by laboratory set up of BAS with an aerosol generator and the reactor. The duct system is a duplicate of the aircraft cabin ECS arrangement. In the BAS the simplified tube reactor is heated from the outside, not recirculating and lubricating the jet engine parts. The study cannot discern how jet engine oil contaminants could affect aircraft cabin air quality. The filter analysis was specific to TCPs in jet engine lubricating oil. However, hydraulic fluids and plasticizers can also cause emissions of organophosphate compounds in aircraft cabin environment. Thus, although the changes in elemental quantities in used filters were used as a basis of screening test for filter contamination, the altered elemental levels may have come from other sources than jet engine oil.

## **6.2 Recommendations and future work**

It is difficult to deliver an appropriate solution with a single study like this one targeting only one type of jet engine oil. Much more research with many more filters, particularly incident filters, and very robust data would validate the findings. Identified markers for filter contamination might come not only from jet engine oil alone but also from other bleed air contaminants, so further monitoring studies should include hydraulic fluids and de-icing fluids. Air quality monitoring of different compounds, varied conditions, and vastly differing aerosol sizes and counts makes the challenge become even more daunting. Further studies should aim at investigating the binding patterns of a group of elements found in used filters. Understanding how the elements exist and bind together on filters could lead to improving the knowledge on how they exist in the cabin air. Additional research should be conducted to determine whether the threshold index or parameters for the elements identified as jet engine oil markers on incident and dirty filters would shift for an incident filter from a smoke/fume incident involving both jet engine oil and hydraulic fluid or de-icing fluids. Unless and until all emissions from smoke/fume incidents are fully disclosed, bleed air emissions will continue to be a daunting task in aircraft cabin air supply.

Because most aircraft cabins are constructed of many materials including plastics, the aircraft cabin environment could also be a source of VOCs. For that reason, further studies would be necessary to identify how these plastics contribute to elements detected by FESEM/EDS. Further studies should also focus on linking airborne pollutant deposits on aircraft filters to specific types of aircraft engines. Additional studies on used filters are recommended to investigate in-cabin pollution levels of different aircraft models and possibly the effect of the routes or regional airspace if aircraft flights remain in a particular region. The decision to monitor bleed air in a specific aircraft model should be based on the perceived risk associated with that aircraft and its engineering and architectural design, as well as the cost involved. Because jet engine oil contaminants found on the surface of used aircraft cabin filters correlate to different commercial aircraft model series or engine types, further studies may offer insight as to whether an engine type or aircraft model is associated with cabin air quality incidents. However, even with the limitations noted here, airlines should begin to use the technologies provided in this study to move toward a better understanding of air quality in aircraft cabins. This need is

reinforced by new threats like the eruption of Iceland's Eyjafjallajökull volcano in April 2010 that caused significant disruption to global aviation industry.



## Appendix A - FESEM/EDS: Raw Data on Distribution of Atomic Weight Percentage of Elements in Aircraft

### Cabin Air Recirculation Filters

**Table A-1 FESEM/EDS Data for Used Filters**

Filter_ID	Sample	Spot	C	O	Na	Mg	Al	Si	P	S	Cl	K	Ca	Ti	Cr	Fe	Ni	Zn	As	Br	Ba	Ce	Total
1F3555	1	1	44.72	43.03	2.22	0.19	0.63	6.42	0.04	0.28	0.25	0.46	0.85	0.00	0.00	0.06	0.00	0.33	0.00	0.30	0.21	0.00	99.99
1F3555	1	2	40.68	45.05	2.46	0.00	0.58	8.04	0.03	0.32	0.26	0.62	0.75	0.00	0.00	0.07	0.00	0.45	0.00	0.38	0.30	0.00	99.99
1F3555	1	3	38.61	44.85	2.38	0.27	1.11	8.98	0.05	0.40	0.33	0.67	1.19	0.00	0.00	0.05	0.00	0.50	0.00	0.28	0.34	0.00	100.01
1F3555	2	1	25.69	52.57	3.04	0.39	1.47	11.09	0.06	0.55	0.58	0.57	2.70	0.00	0.00	0.11	0.00	0.39	0.00	0.44	0.33	0.00	99.98
1F3555	2	2	37.09	44.73	2.28	0.43	1.67	9.00	0.05	0.46	0.42	0.41	2.62	0.00	0.00	0.08	0.00	0.36	0.00	0.19	0.21	0.00	100.00
1F3555	2	3	18.19	56.73	3.76	0.48	1.97	12.82	0.07	0.56	0.41	0.65	2.81	0.00	0.00	0.13	0.00	0.60	0.00	0.43	0.39	0.00	100.00
1S78FS	1	1	39.29	44.05	2.73	0.00	0.68	9.70	0.04	0.52	0.15	0.77	0.53	0.00	0.00	0.06	0.00	0.68	0.00	0.39	0.42	0.00	100.01
1S78FS	1	2	38.51	45.76	2.57	0.00	0.56	9.06	0.07	0.53	0.09	0.75	0.58	0.00	0.00	0.08	0.00	0.56	0.00	0.50	0.37	0.00	99.99
1S78FS	1	3	39.86	45.73	2.53	0.00	0.57	8.41	0.05	0.33	0.13	0.63	0.50	0.00	0.00	0.06	0.00	0.48	0.00	0.40	0.32	0.00	100.00
1S78FS	2	1	50.80	38.64	1.63	0.00	0.50	5.77	0.07	0.35	0.20	0.52	0.53	0.00	0.00	0.08	0.00	0.37	0.00	0.31	0.22	0.00	99.99
1S78FS	2	2	47.24	40.33	2.10	0.00	0.43	7.01	0.05	0.30	0.24	0.62	0.51	0.00	0.00	0.06	0.00	0.45	0.00	0.39	0.28	0.00	100.01
1S78FS	2	3	57.62	33.52	1.11	0.00	0.33	4.79	0.07	0.34	0.24	0.52	0.51	0.00	0.00	0.08	0.00	0.37	0.00	0.28	0.23	0.00	100.01
2D968E	1	1	13.85	61.02	4.54	0.00	1.17	14.95	0.03	0.43	0.00	1.08	1.02	0.00	0.00	0.06	0.00	0.77	0.00	0.52	0.57	0.00	100.01
2D968E	1	2	23.64	56.17	3.66	0.00	0.96	11.89	0.03	0.29	0.09	0.82	0.87	0.00	0.00	0.05	0.00	0.64	0.00	0.44	0.46	0.00	100.01
2D968E	1	3	12.36	63.09	3.76	0.00	1.28	14.61	0.06	0.29	0.00	0.95	1.70	0.00	0.00	0.03	0.00	0.67	0.00	0.70	0.49	0.00	99.99
2D968E	2	1	32.95	50.23	2.64	0.00	1.07	9.67	0.03	0.27	0.08	0.65	1.17	0.00	0.00	0.05	0.00	0.49	0.00	0.34	0.35	0.00	99.99
2D968E	2	2	11.53	61.85	3.89	0.00	1.41	15.35	0.09	0.44	0.11	1.06	2.02	0.00	0.00	0.08	0.00	0.88	0.00	0.76	0.54	0.00	100.01
2D968E	2	3	21.52	55.60	3.67	0.00	0.99	13.55	0.06	0.39	0.00	1.03	1.20	0.00	0.00	0.07	0.00	0.84	0.00	0.58	0.51	0.00	100.01
3C297F	1	1	29.03	47.56	3.20	0.00	0.69	13.43	0.06	0.44	0.34	1.21	1.37	0.00	0.00	0.11	0.00	1.16	0.00	0.74	0.67	0.00	100.01
3C297F	1	2	21.98	55.29	3.85	0.00	1.00	13.15	0.03	0.39	0.28	0.96	1.17	0.00	0.00	0.06	0.00	0.80	0.00	0.56	0.50	0.00	100.02
3C297F	1	3	35.72	47.32	2.83	0.00	0.94	9.41	0.03	0.39	0.24	0.64	1.14	0.00	0.00	0.09	0.00	0.56	0.00	0.34	0.34	0.00	99.99
3C297F	2	1	16.16	58.55	3.86	0.42	1.90	13.35	0.06	0.48	0.32	0.77	2.50	0.00	0.00	0.10	0.00	0.74	0.00	0.32	0.47	0.00	100.00
3C297F	2	2	4.10	65.54	3.63	0.65	2.41	16.03	0.00	0.63	0.47	0.77	4.07	0.00	0.00	0.12	0.00	0.63	0.00	0.54	0.41	0.00	100.00
3C297F	2	3	13.04	61.07	3.18	0.55	1.97	13.93	0.05	0.43	0.34	0.67	3.23	0.00	0.00	0.06	0.00	0.59	0.00	0.53	0.36	0.00	100.00
4S190C	1	1	51.72	37.29	1.63	0.19	0.72	5.41	0.06	0.55	0.22	0.53	0.86	0.00	0.00	0.12	0.00	0.34	0.00	0.17	0.21	0.00	100.02
4S190C	1	2	43.40	42.82	2.10	0.00	0.58	7.46	0.03	0.52	0.19	0.64	0.95	0.00	0.00	0.12	0.00	0.49	0.00	0.42	0.28	0.00	100.00
4S190C	1	3	45.85	41.20	1.98	0.00	0.53	7.07	0.03	0.49	0.19	0.60	0.83	0.00	0.00	0.11	0.00	0.44	0.00	0.38	0.30	0.00	100.00
4S190C	2	1	46.17	41.26	2.21	0.00	0.30	7.01	0.03	0.54	0.12	0.57	0.47	0.00	0.00	0.09	0.00	0.47	0.00	0.46	0.29	0.00	99.99
4S190C	2	2	46.83	40.53	2.27	0.00	0.21	7.14	0.04	0.51	0.10	0.59	0.44	0.00	0.00	0.06	0.00	0.50	0.00	0.49	0.28	0.00	99.99
4S190C	2	3	48.22	40.39	1.93	0.00	0.45	6.49	0.02	0.37	0.12	0.48	0.53	0.00	0.00	0.06	0.00	0.36	0.00	0.34	0.23	0.00	99.99
5H2F01	1	1	48.26	36.22	1.81	0.21	0.62	7.94	0.08	0.61	0.63	0.77	1.32	0.00	0.00	0.12	0.00	0.54	0.00	0.51	0.36	0.00	100.00
5H2F01	1	2	44.69	42.77	1.91	0.20	0.78	6.31	0.07	0.47	0.35	0.59	0.89	0.00	0.00	0.10	0.00	0.38	0.00	0.25	0.25	0.00	100.01
5H2F01	1	3	48.55	38.61	1.56	0.38	1.00	5.98	0.08	0.55	0.44	0.51	1.30	0.00	0.00	0.15	0.08	0.36	0.00	0.22	0.24	0.00	100.01
5H2F01	2	1	31.19	50.97	3.19	0.25	1.29	9.66	0.04	0.38	0.16	0.71	1.02	0.00	0.00	0.10	0.00	0.56	0.00	0.14	0.35	0.00	100.01
5H2F01	2	2	30.94	50.30	2.89	0.33	1.01	10.25	0.03	0.47	0.18	0.75	1.37	0.00	0.00	0.06	0.00	0.55	0.00	0.50	0.36	0.00	99.99
5H2F01	2	3	33.28	49.22	2.52	0.37	1.12	9.48	0.05	0.40	0.23	0.61	1.39	0.00	0.00	0.08	0.00	0.46	0.00	0.48	0.31	0.00	100.00
7WQF45	1	1	45.13	42.54	2.21	0.00	0.61	6.40	0.03	0.58	0.20	0.42	0.89	0.00	0.00	0.08	0.08	0.27	0.00	0.34	0.21	0.00	99.99
7WQF45	1	2	52.04	37.37	2.07	0.00	0.44	5.29	0.04	0.62	0.22	0.39	0.60	0.00	0.00	0.09	0.07	0.26	0.00	0.30	0.20	0.00	100.00
7WQF45	1	3	51.00	38.78	1.88	0.16	0.69	5.22	0.00	0.40	0.19	0.32	0.75	0.00	0.00	0.05	0.05	0.21	0.00	0.13	0.17	0.00	100.00
7WQF45	2	1	35.45	47.34	3.79	0.00	0.81	9.23	0.03	0.66	0.15	0.63	0.71	0.00	0.00	0.04	0.00	0.48	0.00	0.33	0.33	0.00	99.98
7WQF45	2	2	47.95	40.24	2.53	0.00	0.55	6.20	0.04	0.50	0.15	0.42	0.57	0.00	0.00	0.04	0.04	0.27	0.00	0.26	0.24	0.00	100.00
7WQF45	2	3	42.58	43.44	3.07	0.00	0.36	7.39	0.04	0.56	0.17	0.44	0.68	0.00	0.00	0.04	0.04	0.38	0.00	0.52	0.27	0.00	99.98

7ZMK52	1	1	51.79	36.87	1.50	0.16	0.81	5.81	0.04	0.50	0.13	0.53	0.94	0.00	0.00	0.15	0.00	0.34	0.00	0.21	0.23	0.00	100.01
7ZMK52	1	2	52.48	36.80	1.22	0.16	1.04	5.32	0.05	0.52	0.14	0.48	1.12	0.00	0.00	0.12	0.00	0.32	0.00	0.04	0.19	0.00	100.00
7ZMK52	1	3	43.35	42.94	2.05	0.20	0.92	7.11	0.06	0.57	0.13	0.56	1.10	0.00	0.00	0.14	0.00	0.39	0.00	0.24	0.25	0.00	100.01
7ZMK52	2	1	51.49	38.02	1.60	0.15	0.73	5.64	0.03	0.41	0.09	0.46	0.65	0.00	0.00	0.08	0.00	0.32	0.00	0.11	0.22	0.00	100.00
7ZMK52	2	2	47.36	39.51	2.04	0.16	0.81	7.01	0.06	0.55	0.13	0.61	0.69	0.00	0.00	0.13	0.00	0.46	0.00	0.21	0.27	0.00	100.00
7ZMK52	2	3	45.46	41.37	2.06	0.15	0.73	7.05	0.06	0.53	0.13	0.55	0.90	0.00	0.00	0.09	0.00	0.38	0.00	0.27	0.27	0.00	100.00
8P6G4X	1	1	25.78	53.94	3.21	0.00	0.79	11.78	0.02	0.29	0.19	0.80	1.08	0.00	0.00	0.09	0.00	0.80	0.00	0.78	0.45	0.00	100.00
8P6G4X	1	2	33.63	49.61	2.88	0.00	0.56	9.65	0.07	0.28	0.21	0.76	0.76	0.00	0.00	0.06	0.00	0.61	0.00	0.54	0.39	0.00	100.01
8P6G4X	1	3	43.49	43.53	2.08	0.00	0.67	7.46	0.02	0.24	0.17	0.56	0.77	0.00	0.00	0.04	0.00	0.36	0.00	0.33	0.30	0.00	100.02
8P6G4X	2	1	17.92	58.41	4.46	0.00	0.95	13.71	0.03	0.36	0.24	1.02	0.89	0.00	0.00	0.08	0.00	0.78	0.00	0.63	0.52	0.00	100.00
8P6G4X	2	2	20.87	59.08	4.08	0.00	0.97	11.82	0.01	0.23	0.15	0.81	0.91	0.00	0.00	0.06	0.00	0.63	0.00	0.01	0.39	0.00	100.02
8P6G4X	2	3	19.45	57.22	3.75	0.00	1.73	13.64	0.01	0.00	0.00	0.98	1.57	0.00	0.00	0.03	0.00	0.99	0.00	0.10	0.54	0.00	100.01
9E003T	1	1	32.46	49.93	3.42	0.00	0.72	9.40	0.03	0.38	0.51	0.58	1.19	0.00	0.00	0.08	0.00	0.44	0.00	0.53	0.32	0.00	99.99
9E003T	1	2	33.44	49.18	3.40	0.00	0.71	9.00	0.05	0.45	0.67	0.58	1.13	0.00	0.00	0.05	0.00	0.51	0.00	0.49	0.33	0.00	99.99
9E003T	1	3	33.36	49.92	3.11	0.00	0.75	9.22	0.04	0.28	0.30	0.59	1.10	0.00	0.00	0.03	0.00	0.52	0.00	0.46	0.33	0.00	100.01
9E003T	2	1	19.59	56.90	3.77	0.28	1.60	12.62	0.04	0.50	0.36	0.76	2.06	0.00	0.00	0.10	0.00	0.65	0.00	0.32	0.47	0.00	100.02
9E003T	2	2	38.89	45.83	2.69	0.26	1.04	7.75	0.05	0.38	0.31	0.47	1.37	0.00	0.00	0.08	0.00	0.32	0.00	0.32	0.24	0.00	100.00
9E003T	2	3	19.59	56.90	3.77	0.28	1.60	12.62	0.04	0.50	0.36	0.76	2.06	0.00	0.00	0.10	0.00	0.65	0.00	0.32	0.47	0.00	100.02
9RZMC2	1	1	47.97	39.62	2.00	0.00	0.35	6.85	0.03	0.53	0.08	0.55	0.76	0.00	0.00	0.12	0.00	0.41	0.00	0.47	0.27	0.00	100.01
9RZMC2	1	2	48.59	39.64	2.06	0.00	0.40	6.59	0.04	0.48	0.12	0.54	0.49	0.00	0.00	0.07	0.00	0.39	0.00	0.34	0.26	0.00	100.01
9RZMC2	1	3	44.86	40.67	2.34	0.00	0.62	7.99	0.03	0.55	0.14	0.68	0.73	0.00	0.00	0.08	0.00	0.60	0.00	0.35	0.35	0.00	99.99
9RZMC2	2	1	41.42	43.50	2.48	0.20	0.92	8.12	0.03	0.59	0.14	0.65	0.81	0.00	0.00	0.11	0.00	0.49	0.00	0.25	0.29	0.00	100.00
9RZMC2	2	2	47.83	40.21	2.13	0.00	0.58	6.57	0.03	0.47	0.11	0.50	0.61	0.00	0.00	0.07	0.00	0.36	0.00	0.28	0.25	0.00	100.00
9RZMC2	2	3	50.68	38.79	1.92	0.00	0.29	5.75	0.04	0.47	0.11	0.46	0.47	0.00	0.00	0.06	0.00	0.36	0.00	0.39	0.22	0.00	100.01
43RTYZ	1	1	46.00	41.21	2.39	0.00	0.41	6.70	0.02	0.69	0.11	0.50	0.76	0.00	0.00	0.07	0.11	0.32	0.00	0.48	0.22	0.00	99.99
43RTYZ	1	2	47.47	40.43	2.24	0.00	0.39	6.25	0.05	0.67	0.14	0.55	0.58	0.00	0.00	0.10	0.11	0.37	0.00	0.41	0.24	0.00	100.00
43RTYZ	1	3	52.60	36.19	1.87	0.14	0.74	5.28	0.04	0.81	0.16	0.43	0.86	0.00	0.00	0.11	0.11	0.30	0.00	0.18	0.19	0.00	100.01
43RTYZ	2	1	48.19	39.82	2.01	0.18	0.55	6.13	0.03	0.49	0.19	0.45	0.92	0.00	0.00	0.08	0.11	0.32	0.00	0.34	0.20	0.00	100.01
43RTYZ	2	2	49.00	39.22	2.06	0.19	0.74	5.90	0.02	0.46	0.13	0.43	0.92	0.00	0.00	0.06	0.13	0.30	0.00	0.25	0.19	0.00	100.00
43RTYZ	2	3	50.94	38.60	1.66	0.18	0.62	5.44	0.03	0.41	0.14	0.36	0.87	0.00	0.00	0.06	0.06	0.22	0.00	0.25	0.16	0.00	100.00
73J43M	1	1	39.81	47.13	1.87	0.40	1.09	6.59	0.05	0.31	0.38	0.42	1.16	0.00	0.00	0.07	0.00	0.28	0.00	0.25	0.18	0.00	99.99
73J43M	1	2	38.39	46.48	2.56	0.25	1.02	7.96	0.05	0.39	0.36	0.64	0.88	0.00	0.00	0.09	0.00	0.43	0.00	0.21	0.29	0.00	100.00
73J43M	1	3	45.39	41.82	1.93	0.22	0.81	6.52	0.06	0.38	0.41	0.52	1.02	0.00	0.00	0.09	0.00	0.36	0.00	0.24	0.25	0.00	100.02
73J43M	2	1	0.55	69.75	5.46	0.34	1.16	17.25	0.06	0.48	0.14	1.16	1.17	0.00	0.00	0.08	0.00	0.92	0.00	0.89	0.58	0.00	99.99
73J43M	2	2	0.00	69.03	5.90	0.33	1.42	17.57	0.08	0.59	0.19	1.20	1.22	0.00	0.00	0.11	0.00	0.99	0.00	0.74	0.63	0.00	100.00
73J43M	2	3	0.00	69.46	6.16	0.25	1.50	17.39	0.03	0.53	0.16	1.20	1.19	0.00	0.00	0.10	0.00	0.84	0.00	0.61	0.58	0.00	100.00
83MIA9	1	1	64.12	35.53	0.12	0.01	0.00	0.17	0.00	0.00	0.00	0.01	0.00	0.00	0.00	0.00	0.00	0.00	0.00	0.03	0.00	0.00	99.99
83MIA9	1	2	60.29	39.66	0.00	0.00	0.00	0.02	0.00	0.00	0.01	0.00	0.00	0.00	0.00	0.00	0.00	0.00	0.00	0.01	0.00	0.00	99.99
83MIA9	1	3	63.33	36.50	0.04	0.00	0.03	0.07	0.00	0.01	0.01	0.00	0.01	0.00	0.00	0.00	0.00	0.00	0.00	0.00	0.00	0.00	100.00
83MIA9	2	1	32.16	50.09	2.91	0.13	0.97	9.92	0.03	0.78	0.05	0.73	0.92	0.00	0.00	0.10	0.00	0.53	0.00	0.33	0.36	0.00	100.01
83MIA9	2	2	35.15	47.87	2.61	0.09	0.88	9.07	0.03	0.99	0.10	0.76	1.06	0.00	0.00	0.10	0.00	0.59	0.00	0.34	0.35	0.00	99.99
83MIA9	2	3	39.38	45.03	2.19	0.10	1.06	8.50	0.04	0.96	0.67	1.06	0.00	0.00	0.05	0.00	0.46	0.00	0.20	0.31	0.00	100.01	
584C32	1	1	11.17	58.95	4.90	0.00	1.22	17.13	0.08	0.83	0.25	1.42	1.20	0.00	0.00	0.12	0.00	1.34	0.00	0.66	0.74	0.00	100.01
584C32	1	2	0.00	65.72	5.16	0.00	0.76	19.98	0.07	0.75	0.22	1.52	1.97	0.00	0.00	0.15	0.00	1.42	0.00	1.41	0.86	0.00	99.99
584C32	1	3	11.12	63.67	4.43	0.00	0.62	14.87	0.10	0.45	0.19	0.98	1.18	0.00	0.00	0.08	0.00	0.76	0.00	1.05	0.50	0.00	100.00
584C32	2	1	37.69	45.72	2.60	0.30	1.21	8.80	0.05	0.45	0.27	0.68	1.08	0.00	0.00	0.09	0.00	0.54	0.00	0.17	0.34	0.00	99.99
584C32	2	2	25.84	54.15	3.81	0.00	0.82	11.29	0.05	0.50	0.34	0.77	0.81	0.00	0.00	0.10	0.00	0.61	0.00	0.52	0.40	0.00	100.01
584C32	2	3	22.57	55.64	3.67	0.29	0.83	12.06	0.06	0.50	0.28	0.96	1.13	0.00	0.00	0.06	0.00	0.73	0.00	0.70	0.52	0.00	100.00
794TWZ	1	1	42.18	44.64	2.09	0.00	0.54	6.65	0.03	0.32	0.53	0.45	1.43	0.00	0.00	0.06	0.00	0.42	0.00	0.42	0.24	0.00	100.00
794TWZ	1	2	52.70	37.34	1.73	0.14	0.56	4.76	0.03	0.31	0.52	0.33	0.91	0.00	0.00	0.05	0.00	0.26	0.00	0.17	0.18	0.00	99.99

794TWZ	1	3	40.28	46.65	2.40	0.18	0.81	6.53	0.03	0.35	0.43	0.40	1.15	0.00	0.00	0.05	0.00	0.32	0.00	0.21	0.21	0.00	100.00
794TWZ	2	1	20.45	57.16	3.70	0.00	0.76	12.64	0.06	0.46	0.37	0.75	1.64	0.00	0.00	0.08	0.00	0.63	0.00	0.87	0.45	0.00	100.02
794TWZ	2	2	26.92	53.23	3.48	0.00	0.90	10.89	0.02	0.45	0.33	0.68	1.52	0.00	0.00	0.04	0.00	0.58	0.00	0.55	0.39	0.00	99.98
794TWZ	2	3	27.77	53.58	2.20	0.45	1.57	9.94	0.03	0.28	0.32	0.38	2.47	0.00	0.00	0.04	0.00	0.36	0.00	0.39	0.22	0.00	100.00
AI644T	1	1	0.00	67.66	5.06	0.00	1.05	19.38	0.00	0.12	0.16	1.18	2.28	0.00	0.00	0.07	0.00	1.13	0.00	1.16	0.76	0.00	100.01
AI644T	1	2	0.00	67.72	4.99	0.00	1.22	19.40	0.05	0.12	0.00	1.16	2.36	0.00	0.00	0.08	0.00	1.15	0.00	1.01	0.73	0.00	99.99
AI644T	1	3	0.00	70.55	4.77	0.00	1.45	17.58	0.09	0.10	0.00	0.86	2.33	0.00	0.00	0.04	0.00	0.84	0.00	0.88	0.52	0.00	100.01
AI644T	2	1	17.36	57.76	4.42	0.00	1.01	14.67	0.02	0.13	0.48	1.02	0.98	0.00	0.00	0.06	0.00	0.95	0.00	0.50	0.65	0.00	100.01
AI644T	2	2	35.35	48.60	3.10	0.00	0.55	9.13	0.00	0.12	0.44	0.64	0.68	0.00	0.00	0.02	0.00	0.60	0.00	0.38	0.38	0.00	99.99
AI644T	2	3	0.00	70.12	4.95	0.00	1.16	17.43	0.02	0.12	0.36	0.98	2.22	0.00	0.00	0.03	0.00	1.04	0.00	0.96	0.63	0.00	100.02
B014NE	1	1	51.92	38.27	1.69	0.00	0.38	5.57	0.02	0.29	0.09	0.44	0.46	0.00	0.00	0.05	0.00	0.35	0.00	0.26	0.21	0.00	100.00
B014NE	1	2	52.50	38.14	1.45	0.00	0.57	5.05	0.07	0.32	0.12	0.39	0.73	0.00	0.00	0.06	0.00	0.24	0.00	0.20	0.17	0.00	100.01
B014NE	1	3	45.92	41.91	1.94	0.00	0.54	6.93	0.02	0.35	0.11	0.52	0.73	0.00	0.00	0.06	0.00	0.38	0.00	0.35	0.24	0.00	100.00
B014NE	2	1	43.01	43.88	1.40	0.16	1.07	7.31	0.02	0.27	0.09	0.39	1.56	0.00	0.00	0.03	0.00	0.29	0.00	0.31	0.19	0.00	99.98
B014NE	2	2	44.91	42.27	2.07	0.00	0.55	7.36	0.02	0.27	0.11	0.51	0.90	0.00	0.00	0.03	0.00	0.36	0.00	0.37	0.28	0.00	100.01
B014NE	2	3	40.11	45.14	2.52	0.00	0.74	8.39	0.03	0.37	0.11	0.60	0.91	0.00	0.00	0.05	0.00	0.43	0.00	0.30	0.29	0.00	99.99
B92YNB	1	1	49.88	39.28	2.14	0.17	0.62	5.25	0.05	0.48	0.22	0.43	0.64	0.00	0.00	0.11	0.07	0.28	0.00	0.20	0.18	0.00	100.00
B92YNB	1	2	41.63	44.46	2.24	0.22	0.93	7.08	0.03	0.47	0.21	0.45	1.24	0.00	0.00	0.12	0.10	0.34	0.00	0.25	0.24	0.00	100.01
B92YNB	1	3	38.75	46.12	2.50	0.00	0.63	8.27	0.05	0.43	0.18	0.67	0.94	0.00	0.00	0.12	0.10	0.53	0.00	0.42	0.30	0.00	100.01
B92YNB	2	1	50.76	38.47	2.13	0.17	0.95	5.19	0.03	0.58	0.16	0.43	0.50	0.00	0.00	0.09	0.00	0.25	0.00	0.10	0.19	0.00	100.00
B92YNB	2	2	48.85	39.03	2.07	0.00	0.52	6.06	0.04	0.76	0.18	0.50	0.83	0.00	0.00	0.12	0.09	0.30	0.00	0.40	0.22	0.00	99.97
B92YNB	2	3	51.52	38.08	2.06	0.14	0.51	5.07	0.05	0.63	0.16	0.41	0.59	0.00	0.00	0.07	0.07	0.20	0.00	0.28	0.17	0.00	100.01
BRT6RD	1	1	43.34	43.84	1.63	0.00	0.89	7.16	0.04	0.25	0.11	0.41	1.45	0.00	0.00	0.04	0.00	0.33	0.00	0.31	0.21	0.00	100.01
BRT6RD	1	2	36.44	47.59	2.20	0.20	0.86	8.98	0.03	0.30	0.11	0.55	1.51	0.00	0.00	0.04	0.00	0.45	0.00	0.46	0.28	0.00	100.00
BRT6RD	1	3	45.12	41.74	2.01	0.00	0.92	7.42	0.02	0.31	0.12	0.55	0.92	0.00	0.00	0.05	0.00	0.39	0.00	0.17	0.25	0.00	99.99
BRT6RD	2	1	53.05	36.52	1.70	0.00	0.42	5.54	0.03	0.64	0.16	0.49	0.54	0.00	0.00	0.09	0.00	0.31	0.00	0.31	0.22	0.00	100.02
BRT6RD	2	2	52.93	36.42	1.58	0.13	0.60	5.36	0.04	0.75	0.14	0.47	0.80	0.00	0.00	0.08	0.00	0.29	0.00	0.21	0.19	0.00	99.99
BRT6RD	2	3	57.22	33.64	1.30	0.00	0.45	4.66	0.05	0.64	0.18	0.48	0.68	0.00	0.00	0.08	0.00	0.27	0.00	0.18	0.18	0.00	100.01
ESF946	1	1	37.72	46.41	2.92	0.00	0.51	8.59	0.01	0.57	0.31	0.60	0.92	0.00	0.00	0.09	0.00	0.50	0.00	0.51	0.34	0.00	100.00
ESF946	1	2	45.80	41.07	2.56	0.00	0.54	6.55	0.05	0.54	0.39	0.51	0.88	0.00	0.00	0.10	0.00	0.41	0.00	0.33	0.27	0.00	100.00
ESF946	1	3	39.32	45.54	2.68	0.20	0.66	7.97	0.03	0.43	0.22	0.49	1.26	0.00	0.00	0.09	0.00	0.40	0.00	0.41	0.29	0.00	99.99
ESF946	2	1	36.43	48.09	3.34	0.00	0.74	8.57	0.03	0.33	0.22	0.54	0.62	0.00	0.00	0.05	0.00	0.45	0.00	0.27	0.34	0.00	100.02
ESF946	2	2	27.06	53.09	3.97	0.00	0.64	11.26	0.04	0.37	0.23	0.69	0.99	0.00	0.00	0.06	0.00	0.56	0.00	0.61	0.43	0.00	100.00
ESF946	2	3	32.37	50.50	3.46	0.00	0.85	9.47	0.02	0.37	0.23	0.60	0.94	0.00	0.00	0.03	0.00	0.46	0.00	0.34	0.35	0.00	99.99
G48MJ6	1	1	14.42	58.56	4.46	0.34	1.84	14.33	0.04	0.66	0.54	0.95	2.04	0.00	0.00	0.13	0.00	0.76	0.00	0.37	0.55	0.00	99.99
G48MJ6	1	2	24.69	54.38	3.38	0.31	1.38	11.27	0.04	0.43	0.34	0.68	1.72	0.00	0.00	0.07	0.00	0.50	0.00	0.46	0.36	0.00	100.01
G48MJ6	1	3	26.39	52.86	3.41	0.33	1.38	10.64	0.03	0.50	0.55	0.59	1.99	0.00	0.00	0.09	0.00	0.52	0.00	0.42	0.31	0.00	100.01
G48MJ6	2	1	29.32	51.05	3.62	0.00	0.79	10.73	0.07	0.44	0.51	0.79	0.96	0.00	0.00	0.06	0.00	0.70	0.00	0.50	0.47	0.00	100.01
G48MJ6	2	2	35.15	48.37	3.09	0.00	0.72	8.99	0.02	0.31	0.43	0.68	0.88	0.00	0.00	0.07	0.00	0.58	0.00	0.33	0.39	0.00	100.01
G48MJ6	2	3	44.79	41.98	2.24	0.00	0.55	7.06	0.03	0.28	0.37	0.48	1.12	0.00	0.00	0.04	0.00	0.42	0.00	0.37	0.30	0.00	100.03
JD5RT2	1	1	18.37	57.33	4.46	0.23	1.56	12.95	0.06	0.45	0.52	0.81	1.70	0.00	0.00	0.10	0.00	0.71	0.00	0.27	0.48	0.00	100.00
JD5RT2	1	2	35.38	48.20	2.95	0.15	0.92	8.72	0.02	0.31	0.29	0.55	1.29	0.00	0.00	0.07	0.00	0.52	0.00	0.29	0.35	0.00	100.01
JD5RT2	1	3	9.05	63.66	4.84	0.26	1.62	15.17	0.04	0.48	0.33	0.92	1.81	0.00	0.00	0.08	0.00	0.74	0.00	0.46	0.55	0.00	100.01
JD5RT2	2	1	15.45	60.55	4.37	0.26	1.34	12.93	0.06	0.49	0.47	0.78	1.67	0.00	0.00	0.09	0.00	0.62	0.00	0.49	0.43	0.00	100.00
JD5RT2	2	2	21.10	56.60	3.18	0.33	1.71	12.01	0.06	0.43	0.28	0.67	2.35	0.00	0.00	0.02	0.00	0.59	0.00	0.29	0.39	0.00	100.01
JD5RT2	2	3	15.70	60.85	4.20	0.00	0.91	12.97	0.06	0.49	0.47	0.77	1.66	0.00	0.00	0.09	0.00	0.62	0.00	0.78	0.43	0.00	100.00
JR3584	1	1	36.78	47.23	2.60	0.00	0.67	9.23	0.03	0.50	0.00	0.68	0.89	0.00	0.00	0.05	0.00	0.57	0.00	0.42	0.35	0.00	100.00
JR3584	1	2	29.43	51.05	2.91	0.00	0.81	11.17	0.05	0.78	0.00	0.84	1.22	0.00	0.00	0.06	0.00	0.66	0.00	0.59	0.44	0.00	100.01
JR3584	1	3	37.10	47.05	2.77	0.00	0.61	9.07	0.01	0.57	0.00	0.70	0.72	0.00	0.00	0.06	0.00	0.54	0.00	0.42	0.36	0.00	99.98
JR3584	2	1	48.62	40.51	1.86	0.00	0.61	5.90	0.04	0.52	0.09	0.42	0.66	0.00	0.00	0.05	0.00	0.29	0.00	0.21	0.21	0.00	99.99



















2U1KD6	2	1	58.98	32.13	1.06	0.14	0.67	3.96	0.05	0.70	0.17	0.33	1.09	0.03	0.04	0.23	0.00	0.18	0.00	0.11	0.10	0.00	99.97
2U1KD6	2	2	62.23	29.67	1.42	0.22	0.45	3.25	0.07	0.87	0.18	0.35	0.61	0.02	0.03	0.24	0.00	0.18	0.00	0.11	0.12	0.00	100.02
2U1KD6	2	3	58.10	33.27	1.36	0.16	0.55	3.85	0.07	0.67	0.20	0.35	0.74	0.02	0.03	0.24	0.00	0.17	0.00	0.11	0.11	0.00	100.00
ADJ145	1	1	31.62	49.76	3.87	0.20	1.06	10.44	0.01	0.19	0.32	0.66	0.73	0.00	0.00	0.03	0.00	0.58	0.00	0.15	0.40	0.00	100.02
ADJ145	1	2	30.40	52.32	3.58	0.22	0.88	9.73	0.02	0.11	0.27	0.57	0.81	0.00	0.00	0.00	0.00	0.48	0.00	0.23	0.36	0.00	99.98
ADJ145	1	3	19.42	58.84	4.17	0.30	1.42	12.53	0.02	0.11	0.25	0.73	0.99	0.00	0.00	0.05	0.00	0.59	0.00	0.12	0.43	0.00	99.97
ADJ145	2	1	19.42	58.84	4.17	0.30	1.42	12.53	0.02	0.11	0.25	0.73	0.99	0.00	0.00	0.05	0.00	0.59	0.00	0.12	0.43	0.00	99.97
ADJ145	2	2	8.45	64.30	5.15	0.41	1.63	15.66	0.02	0.18	0.30	0.87	1.53	0.00	0.00	0.03	0.00	0.70	0.00	0.27	0.52	0.00	100.02
ADJ145	2	3	0.00	0.00	0.00	0.00	0.00	0.00	0.00	0.00	0.00	0.00	0.00	0.00	0.00	0.00	0.00	0.00	0.00	0.00	0.00	0.00	0.00

**Table A-2 FESEM/EDS Data for Incident Filters**

Filter_ID	Sample	Spot	C	O	Na	Mg	Al	Si	P	S	Cl	K	Ca	Ti	Fe	Zn	Br	Ba	Cu	Ce	Total
198	1	1	66.11	28.49	0.61	0.19	0.51	1.33	0.08	0.49	0.78	0.31	0.77	0.07	0.15	0.06	0.04	0.00	0.00	0.00	99.99
198	1	2	64.38	28.74	0.70	0.33	0.56	2.50	0.00	0.50	0.66	0.39	0.77	0.00	0.15	0.16	0.07	0.10	0.00	0.00	100.01
198	1	3	66.68	27.55	0.67	0.19	0.34	2.12	0.00	0.43	0.55	0.29	0.70	0.00	0.11	0.12	0.17	0.08	0.00	0.00	100.00
198	2	1	65.65	28.60	0.59	0.28	0.43	2.02	0.00	0.71	0.39	0.28	0.68	0.06	0.14	0.09	0.08	0.00	0.00	0.00	100.00
198	2	2	65.95	28.64	0.60	0.18	0.46	1.54	0.06	0.67	0.52	0.29	0.77	0.06	0.18	0.05	0.04	0.00	0.00	0.00	100.01
198	2	3	66.57	27.73	0.62	0.15	0.48	1.77	0.00	0.73	0.48	0.31	0.74	0.07	0.17	0.09	0.09	0.00	0.00	0.00	100.00
199	1	1	67.39	27.88	0.57	0.19	0.52	1.55	0.05	0.56	0.37	0.25	0.42	0.05	0.13	0.06	0.00	0.00	0.00	0.00	99.99
199	1	2	64.50	29.48	0.82	0.10	0.43	2.59	0.06	0.73	0.15	0.30	0.39	0.00	0.12	0.10	0.12	0.10	0.00	0.00	99.99
199	1	3	60.21	31.82	1.12	0.11	0.51	3.86	0.06	0.84	0.10	0.37	0.42	0.00	0.13	0.19	0.12	0.14	0.00	0.00	100.00
199	2	1	63.65	30.40	0.81	0.18	0.43	2.12	0.06	0.50	0.51	0.30	0.57	0.00	0.17	0.13	0.10	0.08	0.00	0.00	100.01
199	2	2	63.09	27.99	0.97	0.15	0.51	3.47	0.07	0.87	0.56	0.57	0.88	0.00	0.22	0.32	0.14	0.20	0.00	0.00	100.01
199	2	3	62.53	28.46	1.00	0.16	0.50	3.09	0.09	0.75	0.80	0.47	1.26	0.00	0.28	0.26	0.16	0.13	0.06	0.00	100.00
951	1	1	40.36	46.97	2.08	0.00	0.62	7.42	0.02	0.18	0.11	0.51	0.73	0.00	0.03	0.40	0.29	0.28	0.00	0.00	100.00
951	1	2	12.44	62.60	4.14	0.00	1.37	14.75	0.02	0.30	0.14	0.99	1.43	0.00	0.06	0.76	0.51	0.51	0.00	0.00	100.02
951	1	3	29.72	52.38	2.97	0.00	0.87	10.61	0.01	0.25	0.11	0.71	1.05	0.00	0.03	0.53	0.39	0.37	0.00	0.00	100.00
951	2	1	0.00	70.33	6.03	0.00	1.53	18.21	0.00	0.19	0.00	1.17	0.62	0.00	0.00	0.94	0.37	0.62	0.00	0.00	100.01
951	2	2	0.00	68.58	4.91	0.00	1.98	18.59	0.03	0.17	0.00	1.18	2.27	0.00	0.04	1.16	0.43	0.66	0.00	0.00	100.00
951	2	3	0.00	69.18	5.12	0.00	1.49	18.62	0.02	0.18	0.00	1.19	1.81	0.00	0.02	1.06	0.65	0.66	0.00	0.00	100.00
2757	1	1	0.00	68.82	5.50	0.00	1.17	19.24	0.02	0.11	0.00	1.15	1.27	0.00	0.01	1.12	0.85	0.75	0.00	0.00	100.01
2757	1	2	53.47	35.71	1.53	0.00	0.46	6.02	0.03	0.51	0.08	0.50	0.72	0.00	0.07	0.32	0.31	0.23	0.05	0.00	100.01
2757	1	3	61.60	29.82	1.16	0.00	0.35	4.76	0.01	0.47	0.10	0.44	0.50	0.00	0.06	0.29	0.23	0.20	0.00	0.00	99.99
2757	2	1	53.55	35.92	1.73	0.00	0.47	5.81	0.01	0.48	0.10	0.54	0.41	0.00	0.06	0.40	0.24	0.25	0.04	0.00	100.01
2757	2	2	64.24	29.04	0.70	0.08	0.54	3.21	0.04	0.40	0.20	0.29	0.82	0.03	0.07	0.13	0.11	0.09	0.00	0.00	99.99
2757	2	3	65.15	28.38	0.80	0.11	0.47	2.80	0.04	0.48	0.24	0.30	0.74	0.08	0.16	0.00	0.10	0.11	0.04	0.00	100.00
2974	1	1	0.00	68.54	5.83	0.00	1.05	19.17	0.04	0.15	0.05	1.16	1.09	0.00	0.06	1.18	0.96	0.74	0.00	0.00	100.02
2974	1	2	0.00	67.07	5.64	0.00	1.26	20.18	0.03	0.17	0.00	1.35	1.17	0.00	0.09	1.33	0.85	0.87	0.00	0.00	100.01
2974	1	3	0.00	69.15	5.75	0.00	0.99	18.89	0.02	0.14	0.00	1.10	1.23	0.00	0.05	1.02	0.96	0.69	0.00	0.00	99.99
2974	2	1	0.00	68.11	5.61	0.00	1.37	19.10	0.03	0.15	0.09	1.24	1.33	0.00	0.00	1.32	0.84	0.81	0.00	0.00	100.00
2974	2	2	0.00	67.57	5.48	0.36	1.76	19.22	0.04	0.09	0.00	1.16	1.77	0.00	0.06	1.19	0.57	0.72	0.00	0.00	99.99
2974	2	3	0.00	68.82	5.50	0.00	1.17	19.24	0.02	0.11	0.00	1.15	1.27	0.00	0.01	1.12	0.85	0.75	0.00	0.00	100.01
6712	1	1	30.24	50.88	3.31	0.00	0.60	11.22	0.01	0.28	0.15	0.79	0.86	0.00	0.03	0.63	0.56	0.44	0.00	0.00	100.00
6712	1	2	25.46	52.94	3.84	0.00	0.81	12.92	0.01	0.31	0.11	0.93	0.82	0.00	0.05	0.79	0.49	0.52	0.00	0.00	100.00
6712	1	3	38.51	46.48	2.55	0.00	0.56	8.95	0.01	0.22	0.11	0.64	0.67	0.00	0.06	0.49	0.39	0.34	0.00	0.00	99.98
6712	2	1	0.00	69.37	4.99	0.00	1.13	18.70	0.02	0.23	0.12	1.19	1.59	0.00	0.05	0.99	0.96	0.65	0.00	0.00	99.99
6712	2	2	0.00	68.64	5.07	0.52	2.31	18.11	0.04	0.24	0.15	1.10	1.98	0.00	0.05	0.91	0.27	0.61	0.00	0.00	100.00
6712	2	3	0.00	69.00	5.03	0.45	1.85	18.37	0.03	0.21	0.12	1.11	1.71	0.00	0.05	0.92	0.54	0.59	0.00	0.00	99.98
7008	1	1	48.29	40.40	1.44	0.29	0.76	5.91	0.03	0.58	0.07	0.43	0.95	0.03	0.07	0.28	0.27	0.17	0.00	0.00	99.97
7008	1	2	49.84	40.11	1.62	0.13	0.51	5.57	0.02	0.49	0.04	0.45	0.46	0.00	0.04	0.28	0.22	0.20	0.00	0.00	99.98

7008	1	3	50.04	39.58	1.52	0.22	0.72	5.60	0.02	0.50	0.06	0.38	0.68	0.03	0.04	0.24	0.20	0.16	0.00	0.00	99.99
7008	2	1	30.76	51.66	3.20	0.00	0.52	10.38	0.03	0.30	0.09	0.73	0.74	0.00	0.04	0.55	0.60	0.39	0.00	0.00	99.99
7008	2	2	30.86	50.93	3.13	0.26	1.00	10.46	0.02	0.27	0.08	0.73	0.95	0.00	0.04	0.58	0.33	0.37	0.00	0.00	100.01
7008	2	3	35.40	48.96	2.64	0.31	0.99	8.85	0.03	0.22	0.10	0.53	0.94	0.00	0.05	0.41	0.29	0.28	0.00	0.00	100.00
7220	1	1	0.00	68.52	4.97	0.00	1.52	19.01	0.03	0.15	0.00	1.26	1.91	0.00	0.04	1.15	0.75	0.69	0.00	0.00	100.00
7220	1	2	0.00	66.77	5.16	0.00	1.49	19.69	0.05	0.22	0.00	1.49	1.96	0.00	0.04	1.57	0.70	0.85	0.00	0.00	99.99
7220	1	3	0.00	62.26	4.72	0.00	1.72	22.28	0.01	0.00	0.00	1.90	2.91	0.00	0.05	2.27	0.73	1.17	0.00	0.00	100.02
7220	2	1	0.00	69.56	6.02	0.00	1.27	18.41	0.02	0.00	0.19	1.21	1.06	0.00	0.03	0.96	0.63	0.64	0.00	0.00	100.00
7220	2	2	0.00	69.24	5.51	0.00	1.52	18.39	0.02	0.13	0.15	1.25	1.43	0.00	0.04	1.12	0.52	0.67	0.00	0.00	99.99
7220	2	3	0.00	69.28	5.21	0.00	1.57	18.57	0.02	0.13	0.00	1.22	1.66	0.00	0.04	1.06	0.58	0.66	0.00	0.00	100.00
22551	1	1	48.08	40.16	1.92	0.00	0.63	6.80	0.03	0.22	0.14	0.56	0.44	0.00	0.03	0.42	0.27	0.30	0.00	0.00	100.00
22551	1	2	49.64	39.36	1.77	0.15	0.88	5.99	0.03	0.24	0.16	0.49	0.52	0.00	0.04	0.42	0.05	0.26	0.00	0.00	100.00
22551	1	3	45.91	41.74	1.81	0.16	0.81	6.87	0.02	0.23	0.15	0.49	0.86	0.00	0.05	0.40	0.23	0.26	0.00	0.00	99.99
22551	2	1	54.33	34.99	1.78	0.13	0.75	5.82	0.04	0.26	0.15	0.48	0.47	0.00	0.06	0.38	0.12	0.25	0.00	0.00	100.01
22551	2	2	22.73	55.76	3.81	0.00	0.70	12.80	0.01	0.28	0.12	0.89	0.89	0.00	0.05	0.70	0.76	0.50	0.00	0.00	100.00
22551	2	3	44.22	43.13	2.20	0.00	0.50	7.30	0.01	0.25	0.11	0.55	0.55	0.00	0.07	0.44	0.38	0.29	0.00	0.00	100.00
23937	1	1	51.01	36.93	1.78	0.00	0.58	6.76	0.02	0.31	0.14	0.55	0.85	0.00	0.07	0.42	0.31	0.27	0.00	0.00	100.00
23937	1	2	58.69	32.41	1.16	0.13	0.57	4.50	0.04	0.30	0.22	0.40	0.83	0.00	0.10	0.25	0.23	0.18	0.00	0.00	100.01
23937	1	3	48.76	39.49	1.71	0.18	0.76	6.44	0.02	0.25	0.15	0.48	0.88	0.00	0.10	0.35	0.19	0.23	0.00	0.00	99.99
23937	2	1	53.55	36.55	1.59	0.14	0.74	5.25	0.03	0.26	0.17	0.44	0.55	0.00	0.11	0.28	0.14	0.19	0.00	0.00	99.99
23937	2	2	56.91	34.17	1.46	0.16	0.62	4.38	0.05	0.36	0.19	0.39	0.67	0.03	0.11	0.21	0.12	0.15	0.00	0.00	99.98
23937	2	3	60.08	30.91	1.38	0.20	0.47	4.61	0.04	0.35	0.19	0.42	0.55	0.03	0.12	0.28	0.20	0.18	0.00	0.00	100.01
24034	1	1	54.76	35.02	1.45	0.23	0.64	5.30	0.00	0.40	0.19	0.53	0.66	0.00	0.14	0.29	0.18	0.22	0.00	0.00	100.01
24034	1	2	52.92	36.36	1.71	0.19	0.69	5.65	0.00	0.40	0.17	0.54	0.56	0.00	0.14	0.29	0.16	0.22	0.00	0.00	100.00
24034	1	3	57.74	33.38	1.21	0.16	0.53	4.48	0.00	0.38	0.22	0.46	0.68	0.00	0.15	0.25	0.20	0.17	0.00	0.00	100.01
24034	2	1	51.74	37.58	1.30	0.14	0.77	5.65	0.00	0.31	0.14	0.44	1.14	0.00	0.11	0.27	0.22	0.19	0.00	0.00	100.00
24034	2	2	58.94	32.46	1.01	0.22	0.69	4.08	0.00	0.39	0.25	0.42	0.91	0.00	0.16	0.23	0.10	0.14	0.00	0.00	100.00
24034	2	3	60.36	32.32	1.07	0.15	0.52	3.48	0.00	0.37	0.22	0.34	0.67	0.00	0.11	0.18	0.08	0.14	0.00	0.00	100.01
24169	1	1	0.00	68.71	5.52	0.00	1.20	18.80	0.00	0.13	0.08	1.12	1.55	0.05	0.05	1.16	0.94	0.68	0.00	0.00	99.99
24169	1	2	0.00	68.23	5.41	0.37	1.80	18.51	0.01	0.15	0.27	1.09	1.79	0.10	0.06	1.04	0.53	0.66	0.00	0.00	100.02
24169	1	3	0.00	67.99	5.63	0.00	1.18	19.46	0.01	0.15	0.06	1.30	1.20	0.00	0.04	1.22	0.87	0.80	0.10	0.00	100.01
24169	2	1	0.00	68.21	5.37	0.37	1.76	18.86	0.01	0.13	0.00	1.12	1.72	0.00	0.06	1.14	0.57	0.67	0.00	0.00	99.99
24169	2	2	0.00	68.58	5.45	0.00	1.28	19.11	0.01	0.12	0.00	1.17	1.54	0.04	0.05	1.10	0.84	0.71	0.00	0.00	100.00
24169	2	3	0.00	68.14	5.28	0.39	1.69	18.72	0.05	0.13	0.10	1.08	1.95	0.06	0.05	1.04	0.67	0.64	0.00	0.00	99.99
26701	1	1	59.16	32.00	1.20	0.16	0.66	4.39	0.07	0.29	0.30	0.40	0.70	0.08	0.10	0.22	0.13	0.13	0.00	0.00	99.99
26701	1	2	58.75	32.02	1.25	0.00	0.53	4.86	0.05	0.26	0.33	0.49	0.64	0.00	0.08	0.32	0.19	0.22	0.00	0.00	99.99
26701	1	3	52.10	36.41	1.78	0.14	0.54	6.08	0.06	0.31	0.31	0.60	0.65	0.00	0.08	0.37	0.30	0.27	0.00	0.00	100.00
26701	2	1	51.07	37.49	1.22	0.00	0.62	6.16	0.07	0.28	0.23	0.47	1.36	0.00	0.08	0.29	0.43	0.21	0.00	0.00	99.98
26701	2	2	47.30	39.81	1.56	0.00	0.83	7.00	0.04	0.23	0.24	0.50	1.48	0.00	0.10	0.33	0.35	0.25	0.00	0.00	100.02
26701	2	3	47.56	40.80	1.71	0.00	0.74	6.32	0.05	0.20	0.24	0.47	1.00	0.00	0.07	0.35	0.27	0.22	0.00	0.00	100.00

27055	1	1	47.87	39.29	1.83	0.00	0.53	7.11	0.04	0.30	0.30	0.59	0.98	0.00	0.11	0.40	0.37	0.27	0.00	0.00	99.99
27055	1	2	42.71	43.10	2.04	0.00	0.66	8.05	0.05	0.24	0.31	0.66	1.04	0.00	0.12	0.44	0.31	0.29	0.00	0.00	100.02
27055	1	3	47.47	39.94	1.66	0.00	0.70	6.95	0.03	0.23	0.27	0.48	1.23	0.00	0.12	0.34	0.36	0.22	0.00	0.00	100.00
27055	2	1	52.92	36.25	1.45	0.00	0.51	5.92	0.05	0.25	0.30	0.48	0.92	0.00	0.09	0.30	0.32	0.23	0.00	0.00	99.99
27055	2	2	48.34	39.01	1.70	0.00	0.63	7.12	0.03	0.19	0.23	0.52	1.10	0.00	0.09	0.42	0.36	0.26	0.00	0.00	100.00
27055	2	3	40.49	45.06	2.10	0.00	0.52	8.48	0.04	0.22	0.12	0.61	1.05	0.00	0.09	0.38	0.58	0.27	0.00	0.00	100.01
27165	1	1	54.17	36.19	1.24	0.00	0.62	4.92	0.04	0.37	0.21	0.43	1.04	0.00	0.11	0.20	0.26	0.19	0.00	0.00	99.99
27165	1	2	49.20	39.40	1.21	0.00	0.75	6.06	0.03	0.33	0.20	0.44	1.47	0.00	0.11	0.25	0.38	0.17	0.00	0.00	100.00
27165	1	3	55.17	34.96	1.12	0.16	0.68	4.95	0.05	0.35	0.23	0.39	1.19	0.00	0.11	0.19	0.28	0.16	0.00	0.00	99.99
27165	2	1	39.87	45.08	2.50	0.00	0.66	8.33	0.05	0.56	0.15	0.84	0.61	0.00	0.12	0.51	0.34	0.36	0.00	0.00	99.98
27165	2	2	45.34	41.80	2.03	0.00	0.49	6.93	0.07	0.55	0.12	0.67	0.77	0.00	0.14	0.39	0.43	0.27	0.00	0.00	100.00
27165	2	3	49.69	38.18	1.79	0.00	0.67	6.52	0.05	0.55	0.13	0.62	0.74	0.00	0.13	0.35	0.31	0.26	0.00	0.00	99.99
27200	1	1	40.25	45.71	2.27	0.00	0.65	8.18	0.00	0.24	0.13	0.53	0.91	0.00	0.06	0.40	0.38	0.30	0.00	0.00	100.01
27200	1	2	39.34	46.08	2.38	0.00	0.80	8.42	0.00	0.24	0.12	0.57	0.93	0.00	0.06	0.49	0.27	0.30	0.00	0.00	100.00
27200	1	3	30.50	51.76	2.46	0.00	1.28	10.27	0.00	0.23	0.10	0.63	1.56	0.00	0.06	0.52	0.27	0.35	0.00	0.00	99.99
27200	2	1	54.07	35.85	1.58	0.12	0.55	5.12	0.00	0.52	0.17	0.46	0.77	0.00	0.10	0.30	0.20	0.19	0.00	0.00	100.00
27200	2	2	58.23	32.85	1.28	0.19	0.50	4.40	0.00	0.49	0.25	0.47	0.64	0.00	0.10	0.25	0.15	0.19	0.00	0.00	99.99
27200	2	3	52.66	37.03	1.74	0.18	0.58	5.38	0.00	0.48	0.22	0.49	0.51	0.00	0.09	0.31	0.12	0.21	0.00	0.00	100.00
27390	1	1	62.09	31.78	0.85	0.15	0.51	2.57	0.04	0.39	0.29	0.31	0.54	0.16	0.11	0.11	0.08	0.00	0.00	0.03	100.01
27390	1	2	57.93	32.54	1.39	0.15	0.63	4.93	0.05	0.44	0.14	0.52	0.54	0.05	0.12	0.26	0.12	0.18	0.00	0.00	99.99
27390	1	3	58.92	31.79	1.32	0.17	0.58	4.66	0.06	0.49	0.18	0.47	0.57	0.08	0.14	0.26	0.14	0.16	0.00	0.00	99.99
27390	2	1	61.90	30.63	0.94	0.14	0.57	3.38	0.05	0.40	0.31	0.38	0.68	0.19	0.13	0.15	0.11	0.00	0.00	0.04	100.00
27390	2	2	59.04	31.75	1.22	0.17	0.56	4.46	0.07	0.49	0.26	0.49	0.68	0.05	0.16	0.26	0.19	0.15	0.00	0.00	100.00
27390	2	3	67.36	25.78	0.84	0.16	0.41	2.85	0.06	0.54	0.40	0.42	0.57	0.06	0.17	0.17	0.11	0.11	0.00	0.00	100.01
27420	1	1	42.89	43.20	2.11	0.00	0.58	7.97	0.05	0.25	0.20	0.61	0.88	0.00	0.09	0.46	0.42	0.29	0.00	0.00	100.00
27420	1	2	46.65	41.38	2.05	0.00	0.62	6.80	0.03	0.19	0.21	0.53	0.66	0.00	0.06	0.35	0.20	0.27	0.00	0.00	100.00
27420	1	3	45.91	41.14	2.01	0.00	0.39	7.50	0.03	0.19	0.27	0.62	0.68	0.00	0.09	0.47	0.39	0.31	0.00	0.00	100.00
27420	2	1	46.80	41.41	1.80	0.00	0.47	6.80	0.03	0.17	0.18	0.54	0.75	0.00	0.05	0.38	0.37	0.26	0.00	0.00	100.01
27420	2	2	49.73	39.63	1.81	0.00	0.52	6.09	0.02	0.18	0.25	0.48	0.44	0.00	0.08	0.32	0.21	0.24	0.00	0.00	100.00
27420	2	3	46.01	41.41	2.32	0.00	0.56	7.26	0.03	0.23	0.13	0.61	0.44	0.00	0.06	0.41	0.24	0.29	0.00	0.00	100.00
27559	1	1	32.35	51.03	2.77	0.00	0.90	9.62	0.04	0.27	0.09	0.71	0.93	0.00	0.04	0.55	0.34	0.36	0.00	0.00	100.00
27559	1	2	33.26	50.14	2.49	0.00	0.73	9.87	0.00	0.25	0.09	0.67	1.10	0.00	0.05	0.52	0.48	0.36	0.00	0.00	100.01
27559	1	3	30.97	52.05	2.54	0.00	1.11	9.77	0.03	0.28	0.13	0.63	1.37	0.00	0.00	0.45	0.33	0.34	0.00	0.00	100.00
27559	2	1	23.86	55.78	3.38	0.00	0.98	11.96	0.05	0.29	0.14	0.87	1.07	0.00	0.04	0.71	0.43	0.45	0.00	0.00	100.01
27559	2	2	28.57	53.62	2.80	0.00	1.10	10.45	0.03	0.28	0.10	0.76	1.00	0.00	0.04	0.58	0.27	0.38	0.00	0.00	99.98
27559	2	3	31.74	51.36	3.00	0.00	1.00	9.96	0.01	0.23	0.08	0.71	0.76	0.00	0.02	0.56	0.21	0.37	0.00	0.00	100.01
27571	1	1	61.42	30.81	1.01	0.00	0.51	3.93	0.04	0.62	0.12	0.37	0.57	0.03	0.09	0.20	0.13	0.15	0.00	0.00	100.00
27571	1	2	64.29	28.63	0.92	0.11	0.51	3.35	0.05	0.66	0.11	0.36	0.52	0.02	0.10	0.19	0.07	0.12	0.00	0.00	100.01
27571	1	3	57.32	33.28	1.15	0.10	0.69	4.77	0.03	0.50	0.09	0.37	1.03	0.04	0.07	0.25	0.15	0.16	0.00	0.00	100.00
27571	2	1	33.15	48.20	3.24	0.00	0.93	10.96	0.02	0.44	0.07	0.87	0.66	0.01	0.06	0.65	0.29	0.45	0.00	0.00	100.00

27571	2	2	40.83	43.40	2.27	0.00	0.86	9.02	0.02	0.38	0.10	0.77	0.92	0.01	0.07	0.62	0.31	0.40	0.00	0.00	99.98
27571	2	3	40.68	44.43	2.46	0.00	0.71	8.66	0.03	0.34	0.09	0.70	0.66	0.02	0.05	0.54	0.30	0.33	0.00	0.00	100.00
27659	1	1	43.10	44.26	2.04	0.00	0.63	7.42	0.00	0.08	0.17	0.50	0.85	0.00	0.05	0.35	0.30	0.26	0.00	0.00	100.01
27659	1	2	42.89	44.42	1.96	0.00	0.74	7.45	0.00	0.07	0.15	0.48	0.96	0.00	0.03	0.35	0.25	0.25	0.00	0.00	100.00
27659	1	3	38.72	45.75	2.02	0.00	0.87	8.96	0.01	0.08	0.16	0.50	1.72	0.00	0.09	0.41	0.44	0.28	0.00	0.00	100.01
27659	2	1	38.93	47.64	2.36	0.00	0.71	7.83	0.00	0.08	0.17	0.51	0.77	0.00	0.03	0.45	0.25	0.27	0.00	0.00	100.00
27659	2	2	39.76	47.24	2.36	0.00	0.46	7.52	0.02	0.07	0.19	0.48	0.83	0.00	0.03	0.37	0.44	0.24	0.00	0.00	100.01
27659	2	3	34.24	49.64	2.48	0.00	1.39	9.37	0.00	0.09	0.14	0.69	1.00	0.00	0.00	0.58	0.00	0.37	0.00	0.00	99.99
27660	1	1	40.61	44.58	2.44	0.00	0.67	8.76	0.00	0.11	0.15	0.67	0.78	0.00	0.04	0.52	0.30	0.36	0.00	0.00	99.99
27660	1	2	24.33	54.52	3.35	0.00	1.01	13.00	0.02	0.10	0.19	1.01	0.79	0.00	0.01	0.73	0.36	0.57	0.00	0.00	99.99
27660	1	3	33.98	47.94	2.73	0.00	0.93	10.64	0.00	0.08	0.12	0.79	1.33	0.00	0.04	0.63	0.35	0.43	0.00	0.00	99.99
27660	2	1	23.51	56.18	3.02	0.00	1.16	11.96	0.04	0.09	0.09	0.79	1.53	0.00	0.05	0.69	0.44	0.43	0.00	0.00	99.98
27660	2	2	37.97	47.29	2.23	0.00	0.98	8.56	0.00	0.09	0.13	0.59	1.11	0.00	0.05	0.41	0.28	0.29	0.00	0.00	99.98
27660	2	3	29.17	52.39	2.71	0.00	1.10	10.78	0.02	0.09	0.13	0.66	1.49	0.00	0.03	0.55	0.55	0.34	0.00	0.00	100.01
27678	1	1	66.61	26.81	0.83	0.19	0.46	2.02	0.07	0.52	0.80	0.38	0.85	0.11	0.15	0.09	0.07	0.00	0.05	0.00	100.01
27678	1	2	65.94	26.88	0.89	0.31	0.49	2.45	0.07	0.52	0.79	0.42	0.70	0.14	0.15	0.13	0.09	0.00	0.03	0.00	100.00
27678	1	3	65.59	27.81	0.90	0.16	0.41	2.27	0.06	0.48	0.69	0.39	0.70	0.14	0.12	0.13	0.11	0.00	0.04	0.00	100.00
27678	2	1	66.94	23.65	0.85	0.14	0.52	3.21	0.07	0.62	0.98	0.62	1.16	0.62	0.19	0.27	0.10	0.00	0.07	0.00	100.01
27678	2	2	66.72	28.11	0.73	0.13	0.33	1.44	0.05	0.42	0.72	0.28	0.59	0.19	0.09	0.07	0.07	0.00	0.04	0.00	99.98
27678	2	3	64.03	30.30	0.80	0.24	0.39	1.43	0.10	0.44	0.82	0.32	0.68	0.10	0.17	0.05	0.08	0.00	0.05	0.00	100.00
27694	1	1	69.65	25.45	0.64	0.12	0.42	1.52	0.03	0.42	0.62	0.28	0.47	0.07	0.13	0.10	0.02	0.05	0.00	0.00	99.99
27694	1	2	69.64	25.75	0.61	0.13	0.39	1.41	0.05	0.44	0.58	0.23	0.49	0.06	0.11	0.06	0.03	0.02	0.00	0.00	100.00
27694	1	3	68.46	26.64	0.55	0.19	0.40	1.44	0.07	0.45	0.53	0.26	0.62	0.05	0.17	0.07	0.06	0.03	0.00	0.00	99.99
27694	2	1	55.17	34.45	1.60	0.25	0.70	5.01	0.06	0.49	0.22	0.43	0.78	0.09	0.15	0.26	0.15	0.16	0.00	0.00	99.97
27694	2	2	56.08	33.59	1.60	0.22	0.49	5.18	0.05	0.46	0.22	0.47	0.66	0.10	0.17	0.28	0.26	0.16	0.00	0.00	99.99
27694	2	3	57.52	33.94	1.19	0.21	0.55	4.00	0.06	0.42	0.31	0.43	0.64	0.09	0.16	0.21	0.13	0.14	0.00	0.00	100.00
28058	1	1	66.03	26.44	0.84	0.19	0.56	3.42	0.05	0.46	0.33	0.43	0.56	0.08	0.17	0.18	0.14	0.12	0.00	0.00	100.00
28058	1	2	66.95	26.68	0.70	0.17	0.40	2.79	0.04	0.42	0.31	0.36	0.57	0.17	0.15	0.14	0.16	0.00	0.00	0.00	100.01
28058	1	3	64.73	28.93	0.70	0.19	0.51	2.45	0.05	0.37	0.37	0.31	0.92	0.13	0.14	0.11	0.10	0.00	0.00	0.00	100.01
28058	2	1	66.17	28.63	0.59	0.19	0.45	1.49	0.06	0.42	0.64	0.30	0.75	0.07	0.17	0.00	0.08	0.00	0.00	0.00	100.01
28058	2	2	66.88	27.52	0.59	0.23	0.62	1.61	0.08	0.44	0.69	0.29	0.76	0.06	0.16	0.05	0.04	0.00	0.00	0.00	100.02
28058	2	3	63.40	30.87	0.56	0.23	0.55	1.80	0.06	0.43	0.63	0.31	0.79	0.06	0.18	0.05	0.07	0.00	0.00	0.00	99.99
28240	1	1	24.29	54.56	3.48	0.00	0.94	12.53	0.02	0.44	0.00	0.92	1.05	0.00	0.06	0.74	0.50	0.46	0.00	0.00	99.99
28240	1	2	26.06	53.93	3.17	0.00	1.09	11.86	0.01	0.30	0.00	0.78	1.30	0.00	0.04	0.60	0.44	0.41	0.00	0.00	99.99
28240	1	3	31.59	50.43	2.83	0.00	1.05	10.61	0.03	0.29	0.00	0.70	1.16	0.00	0.03	0.61	0.31	0.37	0.00	0.00	100.01
28240	2	1	23.94	55.94	2.33	0.00	1.18	11.85	0.04	0.27	0.00	0.65	2.26	0.00	0.03	0.47	0.69	0.35	0.00	0.00	100.00
28240	2	2	17.38	59.04	3.80	0.00	1.41	14.00	0.00	0.45	0.11	0.95	1.18	0.00	0.06	0.76	0.34	0.53	0.00	0.00	100.01
28240	2	3	30.82	50.43	3.20	0.00	1.03	11.04	0.00	0.36	0.00	0.84	0.83	0.00	0.06	0.69	0.25	0.45	0.00	0.00	100.00
28297	1	1	0.00	67.01	5.60	0.00	1.48	20.26	0.03	0.21	0.00	1.50	1.15	0.00	0.01	1.24	0.68	0.84	0.00	0.00	100.01
28297	1	2	0.00	67.01	5.60	0.00	1.48	20.26	0.03	0.21	0.00	1.50	1.15	0.00	0.01	1.24	0.68	0.84	0.00	0.00	100.01



28297	1	3	36.21	46.94	2.85	0.00	0.72	10.23	0.02	0.12	0.00	0.78	0.67	0.00	0.05	0.62	0.34	0.45	0.00	0.00	100.00
28297	2	1	28.97	52.77	2.93	0.00	0.68	10.93	0.02	0.10	0.12	0.71	1.26	0.00	0.02	0.53	0.60	0.36	0.00	0.00	100.00
28297	2	2	21.44	57.12	3.57	0.00	0.91	12.93	0.00	0.10	0.09	0.84	1.25	0.00	0.05	0.66	0.59	0.45	0.00	0.00	100.00
28297	2	3	22.07	56.01	3.32	0.00	0.79	13.07	0.05	0.08	0.00	0.90	1.58	0.00	0.05	0.84	0.68	0.55	0.00	0.00	99.99
28802	1	1	27.54	53.07	3.26	0.00	0.59	11.76	0.01	0.08	0.20	0.83	0.92	0.00	0.04	0.67	0.59	0.45	0.00	0.00	100.01
28802	1	2	24.73	54.79	3.25	0.00	0.74	12.41	0.02	0.09	0.18	0.94	0.98	0.00	0.05	0.75	0.57	0.49	0.00	0.00	99.99
28802	1	3	32.48	50.48	2.68	0.00	1.04	10.07	0.01	0.05	0.16	0.62	1.15	0.00	0.04	0.57	0.30	0.35	0.00	0.00	100.00
28802	2	1	11.53	63.93	3.01	0.00	1.76	14.51	0.04	0.11	0.28	0.85	2.31	0.00	0.05	0.56	0.64	0.41	0.00	0.00	99.99
28802	2	2	0.00	70.06	4.05	0.00	2.09	17.82	0.05	0.09	0.18	1.01	2.55	0.00	0.06	0.85	0.66	0.52	0.00	0.00	99.99
28802	2	3	0.00	69.44	4.26	0.00	1.82	18.29	0.03	0.12	0.27	1.09	2.34	0.00	0.06	0.90	0.77	0.60	0.00	0.00	99.99
28825	1	1	37.14	48.14	2.36	0.00	0.71	8.58	0.03	0.14	0.11	0.46	1.28	0.00	0.02	0.36	0.42	0.25	0.00	0.00	100.00
28825	1	2	5.30	65.65	5.46	0.00	2.16	17.06	0.01	0.24	0.17	1.15	1.12	0.00	0.04	0.96	0.00	0.67	0.00	0.00	99.99
28825	1	3	17.24	59.82	4.13	0.00	0.90	13.71	0.00	0.16	0.19	0.94	1.09	0.00	0.02	0.71	0.61	0.48	0.00	0.00	100.00
28825	2	1	38.71	47.32	2.20	0.00	0.64	7.95	0.03	0.23	0.20	0.55	0.93	0.00	0.06	0.42	0.50	0.27	0.00	0.00	100.01
28825	2	2	52.21	37.54	1.41	0.00	0.84	5.53	0.03	0.21	0.16	0.46	0.91	0.00	0.09	0.31	0.08	0.21	0.00	0.00	99.99
28825	2	3	48.56	38.98	1.79	0.00	0.59	6.87	0.03	0.29	0.27	0.57	0.92	0.00	0.12	0.40	0.36	0.25	0.00	0.00	100.00
28832	1	1	52.29	36.00	1.60	0.00	0.54	6.55	0.03	0.35	0.15	0.58	0.82	0.00	0.07	0.41	0.30	0.27	0.05	0.00	100.01
28832	1	2	48.19	38.36	1.77	0.00	0.52	7.50	0.04	0.33	0.13	0.68	1.11	0.00	0.08	0.49	0.42	0.34	0.03	0.00	99.99
28832	1	3	53.08	34.97	1.65	0.00	0.53	6.72	0.04	0.34	0.13	0.59	0.83	0.00	0.06	0.42	0.32	0.28	0.04	0.00	100.00
28832	2	1	59.35	32.54	1.11	0.15	0.54	3.83	0.05	0.34	0.37	0.43	0.67	0.00	0.12	0.21	0.14	0.14	0.02	0.00	100.01
28832	2	2	60.01	31.40	1.21	0.13	0.65	4.15	0.04	0.36	0.34	0.46	0.71	0.00	0.10	0.22	0.05	0.15	0.03	0.00	100.01
28832	2	3	64.52	28.72	0.97	0.13	0.39	2.78	0.06	0.43	0.44	0.38	0.69	0.00	0.10	0.15	0.11	0.12	0.01	0.00	100.00
28836	1	1	50.42	38.57	1.59	0.15	0.51	5.70	0.02	0.31	0.20	0.49	0.76	0.49	0.11	0.33	0.26	0.00	0.00	0.08	99.99
28836	1	2	52.13	36.85	1.49	0.12	0.75	5.59	0.03	0.32	0.21	0.50	0.92	0.54	0.07	0.29	0.12	0.00	0.00	0.07	100.00
28836	1	3	51.25	38.18	1.52	0.00	0.56	5.74	0.01	0.23	0.17	0.46	0.81	0.35	0.09	0.28	0.27	0.00	0.00	0.07	99.99
28836	2	1	51.36	36.73	1.21	0.00	0.66	5.81	0.03	0.42	0.20	0.50	1.26	1.00	0.14	0.33	0.28	0.00	0.00	0.07	100.00
28836	2	2	53.81	34.79	1.34	0.15	0.67	5.46	0.06	0.43	0.17	0.55	0.85	1.02	0.12	0.34	0.12	0.00	0.05	0.06	99.99
28845	1	1	0.00	67.00	5.74	0.00	0.93	19.68	0.03	0.26	0.18	1.55	1.37	0.00	0.09	1.36	0.99	0.82	0.00	0.00	100.00
28845	1	2	28.45	49.62	3.41	0.00	0.80	12.58	0.02	0.21	0.21	1.05	1.29	0.00	0.08	1.13	0.52	0.63	0.00	0.00	100.00
28845	1	3	24.07	54.40	3.20	0.26	1.25	12.30	0.01	0.19	0.22	0.82	1.62	0.00	0.08	0.70	0.43	0.46	0.00	0.00	100.01
28845	2	1	29.74	51.85	3.07	0.00	0.85	10.83	0.02	0.18	0.17	0.68	1.18	0.00	0.05	0.53	0.48	0.37	0.00	0.00	100.00
28845	2	2	32.04	50.00	3.17	0.00	0.71	10.69	0.01	0.18	0.15	0.76	0.78	0.00	0.06	0.63	0.42	0.41	0.00	0.00	100.01
28845	2	3	30.60	50.39	3.36	0.00	0.61	11.14	0.01	0.19	0.23	0.82	0.94	0.00	0.06	0.71	0.52	0.44	0.00	0.00	100.02
28845	2	3	52.17	36.39	1.35	0.14	0.63	5.46	0.04	0.42	0.16	0.56	0.95	0.99	0.11	0.34	0.20	0.00	0.00	0.07	99.98
28914	1	1	33.05	50.35	2.63	0.00	0.74	9.75	0.00	0.11	0.13	0.64	1.25	0.00	0.02	0.52	0.46	0.35	0.00	0.00	100.00
28914	1	2	24.75	54.16	3.57	0.00	0.98	12.54	0.01	0.11	0.14	0.89	1.17	0.00	0.06	0.71	0.44	0.48	0.00	0.00	100.01
28914	1	3	24.00	55.65	3.33	0.00	0.84	12.11	0.00	0.18	0.14	0.83	1.23	0.00	0.04	0.67	0.54	0.45	0.00	0.00	100.01
28914	2	1	21.92	56.01	4.05	0.00	0.82	13.18	0.00	0.16	0.13	0.92	0.94	0.00	0.04	0.80	0.52	0.51	0.00	0.00	100.00
28914	2	2	27.67	52.46	3.24	0.00	0.79	11.88	0.02	0.13	0.14	0.85	1.04	0.00	0.06	0.74	0.49	0.48	0.00	0.00	99.99
28914	2	3	27.15	52.58	3.18	0.00	1.16	11.73	0.02	0.14	0.19	0.83	1.23	0.00	0.07	0.74	0.51	0.48	0.00	0.00	100.01

28937	1	1	63.13	29.25	0.88	0.17	0.53	3.35	0.05	0.39	0.39	0.40	0.75	0.28	0.11	0.15	0.11	0.00	0.00	0.04	99.98
28937	1	2	65.81	27.12	0.87	0.14	0.58	2.99	0.05	0.42	0.35	0.38	0.69	0.27	0.09	0.14	0.08	0.00	0.00	0.03	100.01
28937	1	3	64.19	28.92	0.89	0.17	0.66	2.88	0.04	0.38	0.36	0.35	0.60	0.27	0.10	0.15	0.01	0.00	0.00	0.03	100.00
28937	2	1	57.95	32.19	1.30	0.13	0.52	4.89	0.03	0.35	0.30	0.45	1.00	0.09	0.11	0.29	0.23	0.17	0.00	0.01	100.01
28937	2	2	60.50	30.80	1.13	0.13	0.41	4.23	0.05	0.38	0.37	0.44	0.77	0.09	0.08	0.26	0.19	0.16	0.00	0.00	99.99
28937	2	3	54.33	35.08	1.33	0.21	0.70	5.48	0.04	0.34	0.26	0.46	0.98	0.10	0.09	0.30	0.14	0.17	0.00	0.00	100.01
28958	1	1	41.89	43.13	2.24	0.19	0.84	8.61	0.01	0.17	0.17	0.62	1.00	0.00	0.07	0.46	0.27	0.33	0.00	0.00	100.00
28958	1	2	40.51	44.57	2.52	0.00	0.46	8.89	0.00	0.15	0.14	0.66	0.73	0.00	0.03	0.53	0.45	0.35	0.00	0.00	99.99
28958	1	3	33.93	48.67	3.15	0.00	0.66	10.35	0.03	0.15	0.14	0.79	0.64	0.00	0.07	0.64	0.40	0.39	0.00	0.00	100.01
28958	2	1	36.45	46.46	2.72	0.00	0.84	10.02	0.02	0.17	0.18	0.72	1.03	0.00	0.04	0.62	0.36	0.38	0.00	0.00	100.01
28958	2	2	33.95	48.24	2.85	0.00	0.76	10.36	0.02	0.16	0.20	0.79	1.08	0.00	0.06	0.66	0.48	0.40	0.00	0.00	100.01
28958	2	3	40.59	44.33	2.44	0.00	0.74	8.68	0.03	0.16	0.20	0.63	0.94	0.00	0.05	0.56	0.30	0.35	0.00	0.00	100.00
29428	1	1	16.63	60.11	3.93	0.00	0.86	14.06	0.00	0.00	0.15	0.95	1.37	0.00	0.04	0.68	0.71	0.51	0.00	0.00	100.00
29428	1	2	0.00	68.75	5.00	0.00	1.45	19.04	0.02	0.09	0.16	1.27	1.77	0.00	0.03	0.97	0.75	0.70	0.00	0.00	100.00
29428	1	3	0.00	70.00	5.00	0.00	1.23	18.30	0.00	0.09	0.16	1.12	1.72	0.00	0.05	0.83	0.93	0.57	0.00	0.00	100.00
29428	2	1	0.00	70.15	4.00	0.42	2.43	17.13	0.01	0.11	0.13	0.88	3.13	0.00	0.02	0.75	0.34	0.51	0.00	0.00	100.01
29428	2	2	0.00	70.88	4.19	0.00	0.99	17.33	0.00	0.10	0.13	0.99	2.57	0.00	0.01	0.99	1.23	0.59	0.00	0.00	100.00
29428	2	3	15.91	60.60	3.55	0.31	1.43	13.80	0.00	0.08	0.00	0.83	1.91	0.00	0.00	0.65	0.48	0.45	0.00	0.00	100.00
29432	1	1	38.88	46.96	2.33	0.19	0.81	8.13	0.01	0.17	0.00	0.48	1.07	0.00	0.05	0.35	0.31	0.26	0.00	0.00	100.00
29432	1	2	44.38	43.80	2.10	0.00	0.47	6.85	0.02	0.25	0.05	0.47	0.62	0.00	0.06	0.32	0.36	0.24	0.00	0.00	99.99
29432	1	3	44.25	43.18	2.28	0.00	0.47	7.26	0.03	0.25	0.05	0.52	0.61	0.00	0.07	0.37	0.37	0.28	0.00	0.00	99.99
29432	2	1	45.36	41.67	2.04	0.00	0.45	7.68	0.03	0.24	0.07	0.59	0.76	0.00	0.03	0.41	0.38	0.29	0.00	0.00	100.00
29432	2	2	46.73	42.93	1.79	0.00	0.29	6.08	0.00	0.14	0.00	0.42	0.63	0.00	0.04	0.35	0.39	0.21	0.00	0.00	100.00
29432	2	3	49.87	39.57	1.49	0.00	0.61	6.06	0.02	0.20	0.07	0.50	0.78	0.00	0.04	0.37	0.19	0.23	0.00	0.00	100.00
29434	1	1	22.76	55.09	3.35	0.00	0.96	12.91	0.00	0.11	0.16	0.92	1.78	0.00	0.05	0.85	0.56	0.50	0.00	0.00	100.00
29434	1	2	20.73	57.51	3.21	0.27	1.27	12.76	0.00	0.12	0.10	0.80	1.68	0.00	0.05	0.58	0.50	0.42	0.00	0.00	100.00
29434	1	3	0.00	69.05	5.66	0.00	1.27	18.20	0.00	0.17	0.12	1.18	1.88	0.00	0.05	1.00	0.77	0.65	0.00	0.00	100.00
29434	2	1	0.00	69.22	4.12	0.44	1.99	18.47	0.00	0.09	0.00	1.12	2.34	0.00	0.04	0.90	0.67	0.60	0.00	0.00	100.00
29434	2	2	21.33	56.45	3.81	0.00	1.07	13.42	0.02	0.13	0.00	0.92	1.17	0.00	0.02	0.69	0.46	0.51	0.00	0.00	100.00
29434	2	3	33.50	49.21	2.89	0.00	0.69	10.42	0.01	0.12	0.12	0.76	0.81	0.00	0.03	0.63	0.39	0.43	0.00	0.00	100.01
29440	1	1	45.46	41.14	2.06	0.18	0.85	6.96	0.04	0.32	0.29	0.53	1.24	0.00	0.09	0.37	0.21	0.24	0.00	0.00	99.98
29440	1	2	49.64	38.91	1.73	0.17	0.80	5.89	0.04	0.26	0.27	0.43	1.10	0.00	0.11	0.32	0.13	0.19	0.00	0.00	99.99
29440	1	3	50.84	38.34	1.72	0.26	0.72	5.41	0.02	0.27	0.27	0.43	0.96	0.00	0.11	0.29	0.17	0.19	0.00	0.00	100.00
29440	2	1	46.37	40.31	2.27	0.00	0.70	7.24	0.01	0.31	0.31	0.62	0.75	0.00	0.10	0.47	0.24	0.31	0.00	0.00	100.01
29440	2	2	36.45	46.72	3.13	0.00	1.28	9.26	0.02	0.32	0.29	0.74	0.76	0.00	0.10	0.57	0.00	0.37	0.00	0.00	100.01
29440	2	3	35.73	46.83	3.09	0.00	0.67	9.92	0.02	0.35	0.19	0.78	0.84	0.00	0.11	0.63	0.43	0.41	0.00	0.00	100.00
29442	1	1	18.67	57.93	3.43	0.00	0.90	14.13	0.02	0.11	0.23	0.93	1.48	0.00	0.04	0.89	0.72	0.51	0.00	0.00	99.99
29442	1	2	1.47	68.06	4.42	0.00	0.91	18.69	0.02	0.13	0.20	1.17	2.10	0.00	0.09	0.97	1.14	0.62	0.00	0.00	99.99
29442	1	3	11.45	62.42	3.87	0.00	0.99	15.86	0.00	0.13	0.17	1.05	1.72	0.00	0.05	0.89	0.86	0.55	0.00	0.00	100.01
29442	2	1	22.19	57.04	3.28	0.00	0.85	12.42	0.04	0.09	0.12	0.80	1.38	0.00	0.01	0.66	0.69	0.43	0.00	0.00	100.00

29442	2	2	0.00	69.66	5.05	0.00	1.85	18.32	0.07	0.10	0.17	1.12	1.69	0.00	0.03	0.90	0.46	0.57	0.00	0.00	99.99
29442	2	3	14.80	61.88	3.89	0.00	0.80	14.17	0.00	0.09	0.14	0.86	1.35	0.00	0.04	0.75	0.79	0.46	0.00	0.00	100.02
29599	1	1	31.84	50.33	3.28	0.00	0.76	10.48	0.00	0.18	0.13	0.77	0.70	0.00	0.02	0.66	0.36	0.44	0.06	0.00	100.01
29599	1	2	0.00	68.68	4.84	0.00	1.58	19.00	0.00	0.10	0.13	1.22	1.93	0.00	0.04	1.00	0.73	0.66	0.08	0.00	99.99
29599	1	3	28.79	51.11	3.49	0.00	0.88	12.09	0.00	0.12	0.11	0.91	0.73	0.00	0.03	0.85	0.37	0.51	0.02	0.00	100.01
29599	2	1	39.58	45.40	2.62	0.00	0.61	8.96	0.00	0.08	0.11	0.63	0.72	0.00	0.04	0.52	0.37	0.34	0.03	0.00	100.01
29599	2	2	31.32	51.38	2.95	0.00	0.71	10.33	0.00	0.09	0.08	0.62	1.14	0.00	0.01	0.51	0.51	0.33	0.02	0.00	100.00
29606	1	1	40.49	45.83	2.45	0.00	0.32	8.15	0.01	0.15	0.10	0.59	0.62	0.00	0.01	0.45	0.52	0.32	0.00	0.00	100.01
29606	1	2	31.36	51.44	3.01	0.00	0.80	10.20	0.01	0.16	0.12	0.72	0.86	0.00	0.04	0.55	0.37	0.37	0.00	0.00	100.01
29606	1	3	37.02	47.52	2.61	0.00	0.70	9.18	0.03	0.16	0.12	0.59	0.88	0.00	0.00	0.47	0.38	0.34	0.00	0.00	100.00
29606	2	1	24.92	54.90	3.88	0.00	1.00	12.09	0.02	0.15	0.00	0.86	0.70	0.00	0.03	0.64	0.32	0.47	0.00	0.00	99.98
29606	2	2	10.99	63.51	4.85	0.00	0.86	15.67	0.02	0.17	0.00	1.06	0.87	0.00	0.03	0.75	0.71	0.53	0.00	0.00	100.02
29606	2	3	18.05	59.64	3.67	0.00	0.96	13.61	0.00	0.14	0.00	0.93	1.24	0.00	0.00	0.68	0.62	0.48	0.00	0.00	100.02
29750	1	1	33.26	49.87	2.83	0.00	0.65	9.86	0.01	0.16	0.13	0.70	1.05	0.00	0.05	0.56	0.51	0.36	0.00	0.00	100.00
29750	1	2	36.54	47.38	2.45	0.00	0.81	9.42	0.04	0.17	0.10	0.60	1.20	0.00	0.04	0.49	0.42	0.33	0.00	0.00	99.99
29750	1	3	34.25	48.65	2.85	0.00	0.71	10.02	0.01	0.18	0.12	0.72	1.00	0.00	0.05	0.56	0.48	0.39	0.00	0.00	99.99
29750	2	1	43.23	43.55	2.16	0.18	0.81	7.49	0.01	0.16	0.14	0.50	0.88	0.00	0.05	0.38	0.21	0.25	0.00	0.00	100.00
29750	2	2	43.49	43.44	2.20	0.15	0.72	7.46	0.01	0.16	0.12	0.51	0.79	0.00	0.05	0.38	0.26	0.25	0.00	0.00	99.99
29750	2	3	41.88	44.18	2.38	0.00	0.51	8.26	0.00	0.18	0.13	0.59	0.66	0.00	0.05	0.46	0.42	0.30	0.00	0.00	100.00
29932	1	1	34.36	49.61	2.45	0.00	0.94	9.45	0.02	0.08	0.11	0.59	1.25	0.00	0.00	0.49	0.31	0.33	0.00	0.00	99.99
29932	1	2	36.96	47.64	2.70	0.00	0.59	9.31	0.02	0.09	0.11	0.64	0.68	0.00	0.02	0.48	0.40	0.35	0.00	0.00	99.99
29932	1	3	33.82	48.96	3.05	0.00	0.76	10.38	0.01	0.08	0.07	0.74	0.71	0.00	0.02	0.63	0.35	0.40	0.00	0.00	99.98
29932	2	1	35.96	48.32	2.71	0.00	0.70	9.44	0.01	0.00	0.11	0.64	0.79	0.00	0.02	0.56	0.39	0.36	0.00	0.00	100.01
29932	2	2	39.73	45.92	2.52	0.00	0.44	8.65	0.01	0.08	0.08	0.63	0.64	0.00	0.00	0.52	0.42	0.35	0.00	0.00	99.99
29932	2	3	29.41	51.91	2.99	0.00	0.80	11.28	0.01	0.08	0.09	0.75	1.13	0.00	0.02	0.62	0.48	0.43	0.00	0.00	100.00
30103	1	1	24.72	55.52	3.25	0.00	0.93	11.78	0.02	0.09	0.14	0.70	1.33	0.00	0.03	0.59	0.53	0.37	0.00	0.00	100.00
30103	1	2	16.58	60.75	4.01	0.00	0.85	13.74	0.02	0.00	0.13	0.86	1.20	0.00	0.02	0.68	0.72	0.45	0.00	0.00	100.01
30103	1	3	25.74	55.18	3.33	0.00	0.94	11.37	0.02	0.00	0.12	0.70	1.13	0.00	0.02	0.58	0.45	0.36	0.06	0.00	100.00
30103	2	1	15.13	58.49	3.52	0.36	2.02	14.77	0.02	0.12	0.21	0.93	2.77	0.00	0.05	0.86	0.23	0.51	0.00	0.00	99.99
30103	2	2	25.14	53.01	3.10	0.00	0.77	12.86	0.02	0.11	0.16	0.89	1.73	0.00	0.05	0.90	0.73	0.52	0.00	0.00	99.99
30103	2	3	17.57	58.10	4.35	0.00	0.87	14.60	0.01	0.10	0.13	1.13	0.93	0.00	0.03	0.92	0.63	0.63	0.00	0.00	100.00
30121	1	1	32.46	49.19	2.64	0.22	0.87	10.49	0.02	0.23	0.18	0.71	1.43	0.00	0.06	0.61	0.48	0.40	0.00	0.00	99.99
30121	1	2	28.10	52.49	2.91	0.00	0.78	11.45	0.06	0.27	0.12	0.82	1.33	0.00	0.05	0.63	0.59	0.42	0.00	0.00	100.02
30121	1	3	31.11	50.56	3.21	0.00	0.83	10.63	0.02	0.19	0.19	0.75	1.01	0.00	0.05	0.61	0.44	0.39	0.00	0.00	99.99
30121	2	1	0.00	69.26	5.36	0.00	1.03	18.73	0.03	0.06	0.00	1.33	1.50	0.00	0.02	1.08	0.92	0.69	0.00	0.00	100.01
30121	2	2	0.00	68.54	4.79	0.00	1.46	19.02	0.00	0.04	0.00	1.32	2.11	0.00	0.03	1.20	0.76	0.75	0.00	0.00	100.02
30121	2	3	0.00	68.96	4.53	0.00	1.63	18.94	0.02	0.07	0.00	1.31	1.96	0.00	0.03	1.10	0.73	0.71	0.00	0.00	99.99
30335	1	1	65.30	28.80	0.62	0.17	0.46	2.12	0.05	0.45	0.42	0.28	0.83	0.08	0.17	0.08	0.12	0.04	0.00	0.00	99.99
30335	1	2	68.90	25.56	0.44	0.17	0.46	1.87	0.07	0.48	0.49	0.26	0.82	0.09	0.19	0.07	0.09	0.04	0.00	0.00	100.00
30335	1	3	63.41	29.09	0.71	0.19	0.68	3.04	0.06	0.44	0.40	0.34	1.11	0.11	0.16	0.14	0.03	0.10	0.00	0.00	100.01

30335	2	1	65.43	27.34	0.62	0.21	0.58	2.65	0.06	0.49	0.58	0.36	1.08	0.15	0.17	0.13	0.08	0.08	0.00	0.00	100.01
30335	2	2	63.93	28.92	0.80	0.24	0.53	2.86	0.08	0.46	0.45	0.31	0.85	0.16	0.13	0.11	0.07	0.11	0.00	0.00	100.01
30335	2	3	61.87	31.52	0.69	0.26	0.31	2.66	0.06	0.40	0.43	0.28	0.94	0.08	0.13	0.09	0.21	0.07	0.00	0.00	100.00
30339	1	1	31.32	50.50	3.00	0.00	0.58	10.99	0.02	0.13	0.14	0.79	0.90	0.00	0.05	0.70	0.46	0.43	0.00	0.00	100.01
30339	1	2	21.33	56.73	3.53	0.00	0.52	13.42	0.02	0.15	0.15	0.94	1.20	0.00	0.06	0.76	0.67	0.51	0.00	0.00	99.99
30339	1	3	1.85	66.75	4.62	0.00	1.31	18.84	0.01	0.21	0.30	1.29	2.17	0.00	0.08	1.11	0.76	0.70	0.00	0.00	100.00
30339	2	1	33.62	48.70	2.94	0.00	0.57	10.47	0.03	0.15	0.16	0.82	0.90	0.00	0.06	0.66	0.49	0.44	0.00	0.00	100.01
30339	2	2	6.47	64.04	4.81	0.00	1.01	17.98	0.03	0.25	0.19	1.28	1.45	0.00	0.08	0.95	0.83	0.65	0.00	0.00	100.02
30339	2	3	35.67	47.03	2.97	0.19	0.69	10.15	0.03	0.19	0.22	0.80	0.69	0.00	0.06	0.60	0.28	0.42	0.00	0.00	99.99
30343	1	1	34.13	48.20	2.67	0.00	0.51	10.48	0.02	0.23	0.13	0.77	1.19	0.00	0.05	0.65	0.55	0.42	0.00	0.00	100.00
30343	1	2	34.45	47.70	2.67	0.00	0.41	10.76	0.01	0.23	0.15	0.79	1.09	0.00	0.06	0.63	0.62	0.42	0.00	0.00	99.99
30343	1	3	39.36	44.62	2.63	0.00	0.40	9.53	0.05	0.25	0.16	0.77	0.75	0.00	0.07	0.60	0.41	0.41	0.00	0.00	100.01
30343	2	1	35.01	47.71	2.77	0.20	0.60	9.97	0.02	0.30	0.17	0.80	0.94	0.00	0.08	0.62	0.41	0.40	0.00	0.00	100.00
30343	2	2	44.03	42.22	2.13	0.00	0.48	8.02	0.03	0.23	0.16	0.62	0.83	0.00	0.06	0.49	0.38	0.32	0.00	0.00	100.00
30343	2	3	42.64	43.01	2.18	0.15	0.78	8.09	0.03	0.24	0.16	0.61	1.07	0.00	0.06	0.45	0.24	0.29	0.00	0.00	100.00
30353	1	1	65.72	27.65	0.91	0.16	0.56	3.08	0.05	0.38	0.20	0.29	0.49	0.17	0.10	0.13	0.11	0.00	0.00	0.00	100.00
30353	1	2	66.70	26.96	0.77	0.26	0.41	2.86	0.05	0.38	0.20	0.29	0.54	0.07	0.08	0.16	0.15	0.12	0.00	0.00	100.00
30353	1	3	67.24	26.79	0.75	0.13	0.37	2.76	0.06	0.39	0.20	0.30	0.47	0.13	0.12	0.14	0.15	0.00	0.00	0.00	100.00
30353	2	1	67.64	26.73	0.72	0.15	0.44	2.13	0.04	0.39	0.45	0.27	0.59	0.13	0.12	0.10	0.08	0.00	0.00	0.00	99.98
30353	2	2	65.03	28.88	0.92	0.13	0.40	2.87	0.03	0.27	0.27	0.25	0.53	0.00	0.08	0.12	0.14	0.09	0.00	0.00	100.01
30353	2	3	64.61	29.25	0.97	0.11	0.36	3.02	0.03	0.25	0.22	0.27	0.43	0.00	0.07	0.13	0.14	0.13	0.00	0.00	99.99
30363	1	1	63.89	29.46	0.84	0.20	0.84	2.44	0.07	0.45	0.49	0.29	0.66	0.00	0.17	0.10	0.00	0.11	0.00	0.00	100.01
30363	1	2	63.82	28.34	0.98	0.21	0.65	3.14	0.07	0.53	0.57	0.40	0.70	0.11	0.18	0.16	0.00	0.12	0.00	0.00	99.98
30363	1	3	67.52	26.85	0.79	0.15	0.44	2.02	0.08	0.43	0.54	0.27	0.54	0.06	0.13	0.10	0.01	0.06	0.00	0.00	99.99
30363	2	1	60.00	30.96	1.33	0.20	0.62	4.26	0.07	0.48	0.29	0.41	0.56	0.12	0.15	0.26	0.11	0.18	0.00	0.00	100.00
30363	2	2	65.05	26.83	0.97	0.17	0.58	3.41	0.07	0.60	0.42	0.45	0.69	0.12	0.15	0.30	0.04	0.16	0.00	0.00	100.01
30363	2	3	60.50	30.60	0.95	0.13	0.55	4.33	0.04	0.46	0.27	0.43	0.83	0.10	0.15	0.29	0.22	0.15	0.00	0.00	100.00
30598	1	1	64.25	27.89	1.05	0.12	0.30	4.22	0.04	0.26	0.17	0.39	0.50	0.08	0.13	0.24	0.20	0.16	0.00	0.00	100.00
30598	1	2	64.83	27.93	1.07	0.12	0.46	3.63	0.03	0.32	0.21	0.32	0.47	0.15	0.12	0.21	0.09	0.00	0.00	0.04	100.00
30598	1	3	64.39	28.01	1.06	0.15	0.32	3.63	0.04	0.33	0.30	0.37	0.51	0.29	0.15	0.21	0.19	0.00	0.00	0.05	100.00
30598	2	1	67.66	26.59	0.96	0.11	0.33	2.36	0.05	0.35	0.43	0.31	0.39	0.10	0.11	0.13	0.09	0.00	0.00	0.03	100.00
30598	2	2	69.79	24.97	0.76	0.11	0.30	2.21	0.03	0.35	0.33	0.28	0.49	0.00	0.12	0.10	0.09	0.09	0.00	0.00	100.02
30598	2	3	68.79	25.03	0.84	0.13	0.46	2.54	0.04	0.41	0.35	0.30	0.54	0.20	0.16	0.14	0.04	0.00	0.00	0.03	100.00
30670	1	1	47.82	40.53	1.82	0.00	0.49	6.72	0.02	0.17	0.17	0.51	0.73	0.00	0.07	0.39	0.30	0.25	0.00	0.00	99.99
30670	1	2	32.36	49.93	2.98	0.00	0.61	10.35	0.04	0.21	0.21	0.77	0.92	0.00	0.09	0.61	0.53	0.39	0.00	0.00	100.00
30670	1	3	32.23	50.48	3.02	0.00	0.61	10.09	0.02	0.18	0.22	0.77	0.83	0.00	0.09	0.59	0.49	0.38	0.00	0.00	100.00
30670	2	1	40.54	44.29	2.38	0.20	0.95	8.30	0.05	0.26	0.33	0.60	1.11	0.00	0.08	0.44	0.20	0.28	0.00	0.00	100.01
30670	2	2	17.38	58.26	3.64	0.00	1.15	13.87	0.05	0.31	0.56	1.10	1.51	0.00	0.12	0.82	0.65	0.58	0.00	0.00	100.00
30670	2	3	39.38	45.77	2.41	0.00	0.36	8.53	0.00	0.14	0.16	0.67	1.00	0.00	0.06	0.65	0.49	0.38	0.00	0.00	100.00
30674	1	1	34.91	48.67	2.47	0.00	0.57	9.88	0.02	0.09	0.14	0.69	1.07	0.00	0.04	0.58	0.48	0.38	0.00	0.00	99.99

30674	1	2	25.04	54.66	3.14	0.00	0.55	12.41	0.00	0.10	0.15	0.81	1.27	0.00	0.04	0.62	0.74	0.47	0.00	0.00	100.00
30674	1	3	13.11	61.20	3.82	0.00	1.24	15.53	0.01	0.10	0.15	1.03	1.69	0.00	0.02	0.93	0.61	0.57	0.00	0.00	100.01
30674	2	1	0.00	69.63	4.48	0.00	1.21	18.48	0.00	0.12	0.00	1.13	2.32	0.00	0.01	0.97	1.01	0.64	0.00	0.00	100.00
30674	2	2	0.00	68.99	4.65	0.44	2.27	18.08	0.00	0.06	0.00	1.08	2.58	0.00	0.04	0.84	0.37	0.58	0.00	0.00	99.98
30674	2	3	0.59	68.83	4.52	0.00	1.54	18.58	0.02	0.08	0.00	1.18	2.23	0.00	0.05	0.92	0.83	0.63	0.00	0.00	100.00
A3861HC	1	1	0.00	68.30	5.30	0.00	1.38	18.32	0.05	0.52	0.27	1.07	2.35	0.00	0.07	0.92	0.85	0.61	0.00	0.00	100.01
A3861HC	1	2	1.11	68.28	5.09	0.00	1.38	17.57	0.03	0.53	0.26	1.00	2.44	0.00	0.10	0.82	0.82	0.57	0.00	0.00	100.00
A3861HC	1	3	13.60	61.13	4.98	0.00	0.60	14.60	0.04	0.50	0.27	0.98	1.15	0.00	0.07	0.78	0.76	0.53	0.00	0.00	99.99
A3861HC	2	1	4.94	65.52	4.73	0.00	0.88	17.43	0.05	0.55	0.31	1.15	1.94	0.00	0.10	0.90	0.89	0.61	0.00	0.00	100.00
A3861HC	2	2	41.60	42.96	2.40	0.22	0.96	8.10	0.04	0.40	0.40	0.64	1.13	0.00	0.07	0.54	0.18	0.35	0.00	0.00	99.99
A3861HC	2	3	25.95	54.29	3.82	0.00	0.53	11.32	0.03	0.39	0.31	0.81	0.84	0.00	0.06	0.61	0.63	0.41	0.00	0.00	100.00
A3869HC	1	1	36.99	47.27	2.66	0.00	0.44	9.20	0.01	0.38	0.16	0.71	0.77	0.00	0.05	0.55	0.41	0.40	0.00	0.00	100.00
A3869HC	1	2	17.01	59.41	4.05	0.00	0.60	14.25	0.06	0.43	0.19	0.95	1.07	0.00	0.09	0.67	0.69	0.52	0.00	0.00	99.99
A3869HC	1	3	16.70	59.24	4.22	0.00	0.85	14.46	0.04	0.43	0.20	0.97	1.04	0.00	0.06	0.77	0.54	0.50	0.00	0.00	100.02
A3869HC	2	1	42.05	43.37	2.15	0.00	0.69	8.10	0.03	0.42	0.23	0.56	1.27	0.00	0.07	0.38	0.38	0.30	0.00	0.00	100.00
A3869HC	2	2	41.42	43.90	2.12	0.00	0.51	8.39	0.01	0.39	0.19	0.58	1.24	0.00	0.07	0.44	0.43	0.31	0.00	0.00	100.00
A3869HC	2	3	29.22	51.36	2.66	0.00	0.57	11.13	0.06	0.50	0.23	0.81	1.64	0.00	0.10	0.58	0.70	0.44	0.00	0.00	100.00
A3871HC	1	1	0.00	68.59	5.90	0.00	1.28	18.19	0.04	0.48	0.23	1.19	1.61	0.00	0.08	1.00	0.75	0.65	0.00	0.00	99.99
A3871HC	1	2	0.00	68.28	5.64	0.00	1.36	18.55	0.01	0.47	0.21	1.26	1.60	0.00	0.07	1.03	0.84	0.69	0.00	0.00	100.01
A3871HC	1	3	0.00	68.27	5.35	0.00	2.09	18.03	0.05	0.49	0.23	1.17	1.84	0.00	0.10	0.94	0.75	0.68	0.00	0.00	99.99
A3871HC	2	1	0.00	67.27	5.26	0.00	1.68	19.21	0.04	0.49	0.26	1.25	1.87	0.00	0.12	1.16	0.65	0.75	0.00	0.00	100.01
A3871HC	2	2	0.00	66.74	5.89	0.00	1.38	19.49	0.07	0.56	0.30	1.45	1.28	0.00	0.10	1.28	0.63	0.85	0.00	0.00	100.02
A3871HC	2	3	0.00	67.44	5.62	0.00	1.29	18.98	0.06	0.46	0.27	1.37	1.63	0.00	0.08	1.21	0.78	0.80	0.00	0.00	99.99
A3873HC	1	1	27.06	53.04	3.44	0.00	0.83	11.53	0.02	0.38	0.24	0.79	1.10	0.00	0.06	0.59	0.45	0.48	0.00	0.00	100.01
A3873HC	1	2	34.47	49.72	2.91	0.00	0.44	9.26	0.02	0.28	0.17	0.62	0.81	0.00	0.04	0.48	0.48	0.32	0.00	0.00	100.02
A3873HC	1	3	13.67	60.34	4.43	0.00	0.59	15.37	0.03	0.51	0.24	1.06	1.44	0.00	0.07	0.85	0.81	0.58	0.00	0.00	99.99
A3873HC	2	1	28.92	52.22	3.46	0.00	0.66	11.07	0.03	0.35	0.16	0.78	0.88	0.00	0.04	0.55	0.44	0.45	0.00	0.00	100.01
A3873HC	2	2	28.14	52.94	3.52	0.00	0.65	10.76	0.08	0.38	0.25	0.78	0.96	0.00	0.06	0.57	0.50	0.42	0.00	0.00	100.01
A3873HC	2	3	10.38	63.71	3.87	0.00	1.45	15.02	0.06	0.42	0.16	0.83	2.25	0.00	0.03	0.63	0.73	0.47	0.00	0.00	100.01
A3875HC	1	1	32.44	49.31	3.21	0.00	0.74	10.73	0.02	0.31	0.22	0.78	0.82	0.00	0.04	0.61	0.33	0.44	0.00	0.00	100.00
A3875HC	1	2	30.90	50.34	3.28	0.00	0.66	11.15	0.02	0.33	0.23	0.76	0.82	0.00	0.05	0.61	0.44	0.42	0.00	0.00	100.01
A3875HC	1	3	37.34	47.29	2.70	0.00	0.47	9.14	0.03	0.28	0.21	0.63	0.69	0.00	0.04	0.46	0.41	0.34	0.00	0.00	100.03
A3875HC	2	1	34.41	49.17	2.54	0.00	0.72	9.56	0.03	0.22	0.17	0.60	1.27	0.00	0.05	0.46	0.47	0.33	0.00	0.00	100.00
A3875HC	2	2	39.53	46.07	1.83	0.00	0.66	8.18	0.02	0.21	0.19	0.43	1.74	0.00	0.05	0.32	0.54	0.24	0.00	0.00	100.01
A3875HC	2	3	27.78	53.23	2.52	0.00	1.40	10.77	0.05	0.22	0.19	0.65	1.93	0.00	0.05	0.50	0.35	0.36	0.00	0.00	100.00
KK3050200	1	1	32.75	49.87	2.89	0.34	1.21	9.10	0.08	0.29	0.22	0.64	1.29	0.00	0.17	0.53	0.25	0.36	0.00	0.00	99.99
KK3050200	1	2	29.69	52.21	3.11	0.36	1.08	9.55	0.07	0.30	0.27	0.67	1.37	0.00	0.17	0.51	0.25	0.38	0.00	0.00	99.99
KK3050200	1	3	0.00	67.77	5.16	0.56	1.60	18.15	0.09	0.38	0.19	1.12	2.25	0.00	0.25	1.08	0.73	0.66	0.00	0.00	99.99
KK3050200	2	1	32.32	48.97	3.04	0.37	0.98	10.13	0.10	0.28	0.28	0.74	1.22	0.00	0.19	0.65	0.31	0.41	0.00	0.00	99.99
KK3050200	2	2	28.39	51.75	3.44	0.27	0.90	11.11	0.08	0.25	0.16	0.77	1.22	0.00	0.12	0.71	0.36	0.48	0.00	0.00	100.01

KK3050200	2	3	0.00	68.08	5.82	0.49	1.68	18.18	0.08	0.28	0.26	1.11	1.76	0.00	0.15	0.99	0.47	0.65	0.00	0.00	100.00
1A2610	1	1	43.83	42.44	2.12	0.19	0.84	7.63	0.03	0.43	0.21	0.63	0.58	0.00	0.12	0.47	0.18	0.31	0.00	0.00	100.01
1A2610	1	2	43.94	42.61	2.14	0.18	0.71	7.49	0.02	0.42	0.21	0.63	0.59	0.00	0.09	0.44	0.23	0.30	0.00	0.00	100.00
1A2610	1	3	41.30	44.35	2.20	0.21	0.82	8.06	0.03	0.39	0.21	0.64	0.72	0.00	0.10	0.44	0.24	0.29	0.00	0.00	100.00
1A2610	2	1	33.41	49.64	2.75	0.22	0.86	9.57	0.03	0.37	0.18	0.67	1.05	0.00	0.08	0.50	0.35	0.32	0.00	0.00	100.00
1A2610	2	2	38.03	46.89	2.24	0.21	0.79	8.41	0.02	0.36	0.16	0.57	1.19	0.00	0.08	0.42	0.38	0.26	0.00	0.00	100.01
1A2610	2	3	35.22	48.37	2.28	0.24	1.13	9.28	0.02	0.35	0.15	0.61	1.30	0.00	0.08	0.44	0.23	0.29	0.00	0.00	99.99
2A2610	1	1	48.77	38.93	1.92	0.15	1.02	6.68	0.02	0.38	0.15	0.55	0.60	0.00	0.06	0.38	0.14	0.25	0.00	0.00	100.00
2A2610	1	2	48.33	39.24	1.97	0.18	0.87	6.75	0.01	0.46	0.11	0.55	0.67	0.00	0.08	0.40	0.13	0.25	0.00	0.00	100.00
2A2610	1	3	49.44	38.67	1.72	0.16	0.65	6.35	0.02	0.41	0.36	0.51	0.80	0.00	0.09	0.38	0.20	0.23	0.00	0.00	99.99
604010-16	1	1	66.36	28.36	0.64	0.20	0.32	1.67	0.06	0.51	0.53	0.31	0.62	0.05	0.15	0.06	0.14	0.01	0.00	0.00	99.99
604010-16	1	2	68.49	26.33	0.56	0.14	0.29	1.79	0.06	0.47	0.58	0.36	0.53	0.05	0.11	0.11	0.09	0.05	0.00	0.00	100.01
604010-16	1	3	68.19	26.96	0.51	0.12	0.31	1.59	0.05	0.48	0.49	0.26	0.66	0.03	0.12	0.08	0.10	0.04	0.00	0.00	99.99
604010-16	2	1	63.12	30.48	0.86	0.20	0.48	2.78	0.06	0.40	0.26	0.29	0.61	0.00	0.14	0.10	0.14	0.08	0.00	0.00	100.00
604010-16	2	2	57.00	35.01	1.31	0.20	0.52	3.85	0.06	0.39	0.20	0.37	0.55	0.00	0.11	0.16	0.15	0.12	0.00	0.00	100.00
604010-16	2	3	62.83	30.76	0.83	0.15	0.49	2.92	0.05	0.40	0.29	0.34	0.47	0.00	0.13	0.12	0.13	0.08	0.00	0.00	99.99
604010-41	1	1	57.79	32.92	1.25	0.21	0.68	4.42	0.05	0.56	0.29	0.46	0.70	0.00	0.19	0.19	0.13	0.16	0.00	0.00	100.00
604010-41	1	2	54.59	34.82	1.65	0.16	0.68	5.32	0.05	0.52	0.21	0.51	0.67	0.00	0.16	0.27	0.19	0.19	0.00	0.00	99.99
604010-41	1	3	59.85	32.61	1.15	0.17	0.49	3.41	0.06	0.47	0.33	0.38	0.53	0.00	0.13	0.17	0.15	0.12	0.00	0.00	100.02
604010-41	2	1	64.96	28.51	0.65	0.24	0.61	2.09	0.07	0.60	0.55	0.32	1.02	0.06	0.24	0.00	0.08	0.00	0.00	0.00	100.00
604010-41	2	2	60.40	31.24	0.72	0.21	0.79	3.23	0.07	0.63	0.40	0.39	1.36	0.10	0.23	0.12	0.10	0.00	0.00	0.00	99.99
604010-41	2	3	57.67	32.96	1.18	0.30	0.81	3.83	0.07	0.77	0.35	0.46	1.04	0.00	0.22	0.15	0.08	0.12	0.00	0.00	100.01
650390-13	1	1	65.13	29.14	0.77	0.20	0.44	2.11	0.05	0.49	0.33	0.29	0.61	0.17	0.13	0.08	0.08	0.00	0.00	0.00	100.02
650390-13	1	2	64.58	30.68	0.71	0.16	0.49	1.63	0.06	0.39	0.32	0.22	0.40	0.11	0.10	0.07	0.08	0.00	0.00	0.00	100.00
650390-13	1	3	67.88	27.22	0.60	0.26	0.46	1.72	0.08	0.44	0.35	0.22	0.51	0.06	0.11	0.05	0.02	0.00	0.00	0.00	99.98
650390-13	2	1	65.07	30.23	0.68	0.17	0.52	1.39	0.00	0.44	0.51	0.23	0.49	0.07	0.14	0.04	0.00	0.00	0.00	0.00	99.98
650390-13	2	2	65.75	29.38	0.71	0.17	0.43	1.45	0.06	0.50	0.50	0.24	0.51	0.07	0.14	0.06	0.04	0.00	0.00	0.00	100.01
650390-13	2	3	65.98	28.82	0.71	0.16	0.40	1.61	0.10	0.48	0.43	0.26	0.64	0.09	0.16	0.07	0.10	0.00	0.00	0.00	100.01
650390-46	1	1	63.62	28.56	0.74	0.25	0.67	3.13	0.08	0.76	0.25	0.41	0.79	0.09	0.30	0.16	0.12	0.07	0.00	0.00	100.00
650390-46	1	2	66.47	26.68	0.70	0.25	0.47	2.85	0.08	0.65	0.21	0.36	0.67	0.07	0.23	0.10	0.15	0.05	0.00	0.00	99.99
650390-46	1	3	65.07	26.02	0.78	0.29	0.74	3.71	0.10	0.90	0.24	0.50	0.86	0.08	0.31	0.17	0.15	0.09	0.00	0.00	100.01
650390-46	2	1	64.39	29.30	0.68	0.21	0.62	2.38	0.07	0.52	0.33	0.32	0.73	0.07	0.23	0.08	0.03	0.05	0.00	0.00	100.01
650390-46	2	2	62.05	31.26	0.81	0.21	0.50	2.74	0.06	0.58	0.28	0.31	0.64	0.08	0.19	0.08	0.17	0.05	0.00	0.00	100.01
650390-46	2	3	62.96	30.75	0.77	0.21	0.48	2.55	0.09	0.56	0.25	0.30	0.52	0.08	0.18	0.09	0.14	0.06	0.00	0.00	99.99
A217994HC	1	1	62.61	29.86	0.90	0.17	0.24	3.97	0.02	0.52	0.10	0.33	0.61	0.00	0.06	0.20	0.28	0.14	0.00	0.00	100.01
A217994HC	1	2	65.60	28.70	0.81	0.11	0.27	2.82	0.02	0.42	0.14	0.28	0.38	0.00	0.06	0.13	0.12	0.11	0.00	0.00	99.97
A217994HC	1	3	62.68	30.04	1.01	0.12	0.39	3.82	0.04	0.45	0.09	0.36	0.48	0.00	0.07	0.20	0.13	0.14	0.00	0.00	100.02
A217994HC	2	1	60.10	32.10	1.11	0.13	0.48	3.63	0.04	0.89	0.12	0.35	0.54	0.00	0.08	0.16	0.12	0.14	0.00	0.00	99.99
A217994HC	2	2	60.32	31.07	1.15	0.14	0.55	4.02	0.05	1.06	0.08	0.36	0.64	0.00	0.10	0.19	0.13	0.15	0.00	0.00	100.01
A217994HC	2	3	64.66	29.19	0.71	0.12	0.39	2.72	0.04	0.83	0.08	0.25	0.58	0.00	0.09	0.12	0.12	0.10	0.00	0.00	100.00

A21803HC	1	1	55.91	34.92	1.53	0.00	0.34	5.01	0.03	0.42	0.13	0.47	0.46	0.00	0.05	0.29	0.23	0.20	0.00	0.00	99.99
A21803HC	1	2	35.25	48.33	2.93	0.00	0.67	9.41	0.04	0.52	0.11	0.68	0.72	0.00	0.08	0.52	0.37	0.36	0.00	0.00	99.99
A21803HC	1	3	40.64	44.17	2.48	0.00	0.57	8.72	0.02	0.47	0.13	0.61	0.92	0.00	0.04	0.49	0.44	0.31	0.00	0.00	100.01
A21803HC	2	1	44.78	41.65	2.19	0.17	0.50	7.49	0.03	0.40	0.12	0.52	1.04	0.00	0.00	0.43	0.44	0.26	0.00	0.00	100.02
A21803HC	2	2	53.28	34.02	1.37	0.00	1.88	6.14	0.04	0.43	0.13	0.57	0.82	0.00	0.06	0.49	0.49	0.29	0.00	0.00	100.01
A21803HC	2	3	48.56	39.36	1.72	0.16	1.00	6.59	0.03	0.35	0.10	0.47	0.94	0.00	0.04	0.37	0.05	0.27	0.00	0.00	100.01
A22023HC	1	1	52.88	38.80	1.57	0.16	0.40	4.37	0.03	0.45	0.09	0.29	0.43	0.00	0.04	0.14	0.21	0.13	0.00	0.00	99.99
A22023HC	1	2	49.64	41.02	1.71	0.13	0.41	4.91	0.04	0.51	0.10	0.33	0.53	0.00	0.05	0.20	0.28	0.14	0.00	0.00	100.00
A22023HC	1	3	48.12	41.81	1.97	0.14	0.57	5.35	0.02	0.52	0.09	0.39	0.43	0.00	0.04	0.23	0.14	0.17	0.00	0.00	99.99
A22023HC	2	1	36.13	45.84	2.55	0.00	0.30	10.47	0.02	0.66	0.14	0.83	1.13	0.00	0.06	0.71	0.68	0.47	0.00	0.00	99.99
A22023HC	2	2	41.75	44.46	2.07	0.19	0.94	7.59	0.03	0.48	0.09	0.57	0.94	0.00	0.05	0.43	0.12	0.29	0.00	0.00	100.00
A22023HC	2	3	47.60	40.83	1.82	0.00	0.30	6.46	0.03	0.49	0.11	0.55	0.67	0.00	0.04	0.44	0.37	0.29	0.00	0.00	100.00
A2258 HC	1	1	36.79	47.42	2.45	0.00	1.02	8.66	0.01	0.36	0.24	0.61	1.25	0.00	0.04	0.53	0.32	0.31	0.00	0.00	100.01
A2258 HC	1	2	36.12	47.16	2.52	0.00	1.10	9.03	0.03	0.46	0.27	0.63	1.50	0.00	0.05	0.52	0.29	0.31	0.00	0.00	99.99
A2258 HC	1	3	31.12	49.92	3.14	0.00	0.85	10.43	0.02	0.53	0.32	0.82	1.27	0.00	0.06	0.70	0.41	0.40	0.00	0.00	99.99
A2258 HC	2	1	31.28	50.62	2.40	0.00	1.27	10.52	0.03	0.09	0.13	0.58	1.84	0.00	0.08	0.46	0.40	0.30	0.00	0.00	100.00
A2258 HC	2	2	48.39	39.93	1.56	0.00	0.65	6.57	0.01	0.17	0.19	0.38	1.27	0.00	0.03	0.32	0.32	0.20	0.00	0.00	99.99
A2258 HC	2	3	45.82	41.78	1.66	0.00	0.85	6.93	0.01	0.13	0.19	0.39	1.41	0.00	0.05	0.33	0.26	0.19	0.00	0.00	100.00
A22607HC	1	1	59.94	32.06	1.30	0.09	0.47	3.65	0.05	0.96	0.08	0.37	0.50	0.00	0.09	0.19	0.11	0.12	0.00	0.00	99.98
A22607HC	1	2	62.48	30.66	1.09	0.10	0.49	2.87	0.05	1.04	0.09	0.34	0.44	0.00	0.08	0.14	0.04	0.10	0.00	0.00	100.01
A22607HC	1	3	61.41	31.42	1.08	0.13	0.48	3.06	0.04	1.03	0.09	0.33	0.48	0.00	0.12	0.14	0.08	0.11	0.00	0.00	100.00
A22607HC	2	1	58.66	32.57	1.46	0.00	0.47	4.39	0.03	0.59	0.12	0.40	0.60	0.00	0.08	0.23	0.23	0.17	0.00	0.00	100.00
A22607HC	2	2	56.42	33.75	1.68	0.00	0.36	5.15	0.03	0.63	0.13	0.50	0.51	0.00	0.08	0.31	0.25	0.21	0.00	0.00	100.01
A22607HC	2	3	55.14	34.90	1.67	0.00	0.44	5.17	0.03	0.62	0.12	0.47	0.66	0.00	0.08	0.28	0.23	0.19	0.00	0.00	100.00
A22609HC	1	1	66.07	29.09	0.65	0.15	0.52	0.91	0.08	0.88	0.53	0.21	0.71	0.06	0.12	0.00	0.02	0.00	0.00	0.00	100.00
A22609HC	1	2	65.08	29.91	0.51	0.18	0.55	1.14	0.07	0.78	0.51	0.20	0.69	0.04	0.19	0.04	0.10	0.00	0.00	0.00	99.99
A22609HC	1	3	67.59	24.82	0.52	0.18	0.73	1.68	0.10	1.33	0.90	0.40	1.22	0.10	0.29	0.13	0.00	0.00	0.00	0.00	99.99
A22609HC	2	1	59.90	30.94	1.47	0.10	0.53	4.29	0.04	0.97	0.14	0.43	0.55	0.00	0.07	0.25	0.13	0.19	0.00	0.00	100.00
A22609HC	2	2	60.54	31.42	1.11	0.10	0.44	3.82	0.04	0.80	0.14	0.36	0.66	0.00	0.06	0.19	0.18	0.13	0.00	0.00	99.99
A22609HC	2	3	59.66	31.63	1.25	0.00	0.50	4.32	0.03	0.82	0.14	0.41	0.67	0.00	0.05	0.21	0.17	0.16	0.00	0.00	100.02
A22623HC	1	1	46.55	40.71	2.48	0.00	0.49	6.53	0.02	0.52	0.37	0.65	0.60	0.00	0.07	0.42	0.28	0.31	0.00	0.00	100.00
A22623HC	1	2	47.58	40.82	2.10	0.00	0.63	6.39	0.04	0.31	0.30	0.51	0.48	0.00	0.06	0.38	0.16	0.25	0.00	0.00	100.01
A22623HC	1	3	36.99	48.84	2.81	0.00	0.48	7.93	0.01	0.36	0.26	0.61	0.56	0.00	0.04	0.41	0.40	0.29	0.00	0.00	99.99
A22623HC	2	1	42.99	43.76	2.31	0.00	0.65	7.49	0.01	0.22	0.29	0.53	0.74	0.00	0.07	0.42	0.29	0.24	0.00	0.00	100.01
A22623HC	2	2	40.45	45.64	2.70	0.00	0.71	7.88	0.03	0.19	0.29	0.57	0.47	0.00	0.08	0.47	0.24	0.29	0.00	0.00	100.01
A22623HC	2	3	32.59	49.41	3.15	0.00	0.98	10.70	0.04	0.17	0.19	0.77	0.68	0.00	0.05	0.59	0.26	0.41	0.00	0.00	99.99
A242337HC	1	1	50.31	38.95	1.81	0.00	0.61	6.08	0.02	0.18	0.16	0.42	0.63	0.00	0.02	0.34	0.23	0.23	0.00	0.00	99.99
A242337HC	1	2	46.71	41.10	2.40	0.00	0.62	7.00	0.00	0.19	0.17	0.55	0.32	0.00	0.03	0.41	0.19	0.30	0.00	0.00	99.99
A242337HC	1	3	44.14	43.55	2.28	0.00	0.48	7.24	0.00	0.16	0.16	0.56	0.34	0.00	0.05	0.41	0.35	0.28	0.00	0.00	100.00
A242337HC	2	1	49.18	38.86	2.01	0.00	0.57	6.89	0.03	0.22	0.19	0.55	0.49	0.00	0.04	0.40	0.28	0.30	0.00	0.00	100.01

A242337HC	2	2	58.69	32.66	1.15	0.00	0.54	4.83	0.01	0.17	0.13	0.36	0.76	0.00	0.03	0.29	0.19	0.19	0.00	0.00	100.00
A242337HC	2	3	58.40	33.52	1.00	0.12	0.80	4.23	0.04	0.16	0.16	0.32	0.79	0.00	0.04	0.26	0.00	0.17	0.00	0.00	100.01
A24237HC	1	1	47.93	40.79	2.08	0.00	0.62	6.34	0.03	0.19	0.16	0.45	0.58	0.00	0.05	0.31	0.26	0.23	0.00	0.00	100.02
A24237HC	1	2	48.18	40.43	2.06	0.00	0.51	6.47	0.02	0.19	0.17	0.48	0.53	0.00	0.05	0.32	0.33	0.26	0.00	0.00	100.00
A24237HC	1	3	51.16	38.22	1.87	0.00	0.63	5.94	0.01	0.20	0.17	0.44	0.54	0.00	0.06	0.33	0.20	0.24	0.00	0.00	100.01
A24237HC	2	1	52.01	37.19	1.80	0.00	0.53	6.18	0.02	0.17	0.19	0.46	0.53	0.00	0.05	0.36	0.27	0.25	0.00	0.00	100.01
A24237HC	2	2	57.11	34.02	1.50	0.00	0.34	5.13	0.01	0.14	0.13	0.39	0.43	0.00	0.02	0.28	0.28	0.20	0.00	0.00	99.98
A24237HC	2	3	51.09	37.89	1.64	0.00	0.77	6.16	0.02	0.19	0.22	0.43	0.75	0.00	0.06	0.35	0.19	0.24	0.00	0.00	100.00
A24246HC	1	1	51.59	37.90	1.92	0.00	0.42	5.67	0.03	0.41	0.17	0.48	0.56	0.00	0.05	0.30	0.28	0.21	0.00	0.00	99.99
A24246HC	1	2	54.51	35.85	1.82	0.00	0.35	5.09	0.04	0.49	0.19	0.45	0.45	0.00	0.06	0.28	0.23	0.20	0.00	0.00	100.01
A24246HC	1	3	52.95	36.20	1.90	0.00	0.47	5.89	0.05	0.46	0.18	0.49	0.54	0.00	0.06	0.32	0.25	0.23	0.00	0.00	99.99
A24246HC	2	1	53.94	34.87	2.09	0.00	0.41	5.84	0.04	0.59	0.24	0.57	0.45	0.00	0.06	0.40	0.24	0.27	0.00	0.00	100.01
A24246HC	2	2	50.94	37.28	2.24	0.00	0.43	6.27	0.04	0.50	0.21	0.53	0.55	0.00	0.08	0.37	0.31	0.25	0.00	0.00	100.00
A24246HC	2	3	53.42	34.72	2.23	0.00	0.39	6.20	0.04	0.61	0.24	0.59	0.49	0.00	0.06	0.42	0.30	0.29	0.00	0.00	100.00
A24665	1	1	51.85	37.11	1.98	0.13	0.69	5.83	0.03	0.55	0.09	0.52	0.48	0.00	0.06	0.36	0.12	0.22	0.00	0.00	100.02
A24665	1	2	48.98	39.19	2.17	0.00	0.48	6.49	0.02	0.60	0.08	0.54	0.46	0.00	0.07	0.35	0.28	0.24	0.05	0.00	100.00
A24665	1	3	49.12	39.47	1.91	0.00	0.44	6.30	0.03	0.55	0.08	0.55	0.54	0.00	0.07	0.37	0.34	0.24	0.00	0.00	100.01
A24665	2	1	49.60	39.59	1.92	0.15	0.57	5.67	0.04	0.58	0.05	0.46	0.58	0.00	0.07	0.28	0.24	0.20	0.00	0.00	100.00
A24665	2	2	47.23	40.43	1.74	0.26	0.77	6.61	0.05	0.61	0.08	0.49	0.85	0.00	0.07	0.35	0.24	0.22	0.00	0.00	100.00
A24665	2	3	50.37	38.41	1.59	0.24	0.90	5.68	0.04	0.66	0.09	0.48	0.83	0.00	0.09	0.29	0.11	0.21	0.00	0.00	99.99
A3195HC	1	1	24.92	53.11	3.38	0.00	1.00	12.34	0.02	0.53	0.29	1.07	1.30	0.00	0.10	0.91	0.48	0.55	0.00	0.00	100.00
A3195HC	1	2	14.14	58.98	4.36	0.00	1.15	15.48	0.05	0.63	0.38	1.36	1.11	0.00	0.12	1.03	0.54	0.67	0.00	0.00	100.00
A3195HC	1	3	28.08	52.27	3.16	0.00	1.14	10.77	0.06	0.45	0.28	0.81	1.51	0.00	0.07	0.64	0.36	0.41	0.00	0.00	100.01
A3195HC	2	1	1.40	67.60	5.26	0.00	1.06	18.07	0.04	0.42	0.18	1.33	1.94	0.00	0.09	1.05	0.94	0.64	0.00	0.00	100.02
A3195HC	2	2	0.00	68.75	5.51	0.00	1.30	18.40	0.06	0.45	0.15	1.31	1.60	0.00	0.10	0.97	0.76	0.63	0.00	0.00	99.99
A3195HC	2	3	32.28	48.70	3.08	0.00	0.87	10.77	0.06	0.40	0.21	0.81	1.28	0.00	0.11	0.61	0.43	0.40	0.00	0.00	100.01
A3740HC	1	1	37.82	47.25	2.28	0.00	0.70	8.54	0.04	0.33	0.15	0.62	1.02	0.00	0.08	0.48	0.37	0.31	0.00	0.00	99.99
A3740HC	1	2	19.55	56.79	3.80	0.00	1.20	13.86	0.01	0.48	0.16	1.02	1.25	0.00	0.03	0.86	0.47	0.54	0.00	0.00	100.02
A3740HC	1	3	22.81	55.65	3.77	0.00	0.97	12.80	0.00	0.35	0.16	0.91	0.90	0.00	0.03	0.72	0.46	0.48	0.00	0.00	100.01
A3740HC	2	1	32.94	50.55	2.59	0.00	0.51	9.41	0.02	0.37	0.22	0.66	1.33	0.00	0.04	0.43	0.61	0.32	0.00	0.00	100.00
A3740HC	2	2	32.04	50.40	2.41	0.00	1.09	9.84	0.04	0.45	0.19	0.67	1.63	0.00	0.09	0.47	0.36	0.31	0.00	0.00	99.99
A3740HC	2	3	20.22	57.30	3.58	0.00	0.79	13.11	0.04	0.51	0.17	0.94	1.42	0.00	0.04	0.70	0.73	0.44	0.00	0.00	99.99
A3745HC	1	1	27.46	52.46	3.61	0.00	0.88	11.37	0.03	0.48	0.17	0.86	1.06	0.00	0.08	0.66	0.46	0.43	0.00	0.00	100.01
A3745HC	1	2	26.84	52.97	3.24	0.00	1.06	11.40	0.03	0.43	0.15	0.80	1.48	0.00	0.09	0.64	0.47	0.42	0.00	0.00	100.02
A3745HC	1	3	17.19	59.69	4.47	0.00	1.09	13.87	0.01	0.27	0.10	0.91	0.73	0.00	0.02	0.74	0.42	0.48	0.00	0.00	99.99
A3745HC	2	1	14.48	60.43	4.76	0.00	0.97	15.01	0.02	0.30	0.12	1.06	0.77	0.00	0.07	0.86	0.58	0.58	0.00	0.00	100.01
A3745HC	2	2	16.68	58.94	4.17	0.00	1.24	14.62	0.02	0.30	0.13	0.99	1.10	0.00	0.04	0.75	0.47	0.54	0.00	0.00	99.99
A3760HC	1	1	41.79	43.56	2.40	0.00	0.57	8.39	0.03	0.35	0.13	0.63	0.84	0.00	0.07	0.48	0.41	0.35	0.00	0.00	100.00
A3760HC	1	2	44.86	41.40	2.49	0.00	0.52	7.73	0.01	0.36	0.11	0.60	0.66	0.00	0.07	0.41	0.44	0.33	0.00	0.00	99.99
A3760HC	1	3	45.91	40.03	2.15	0.00	0.92	7.91	0.03	0.38	0.09	0.66	0.80	0.00	0.07	0.52	0.17	0.38	0.00	0.00	100.02



A3760HC	2	1	55.44	35.31	1.63	0.00	0.29	4.47	0.05	0.37	0.51	0.38	0.59	0.09	0.08	0.26	0.38	0.15	0.00	0.00	100.00
A3760HC	2	2	52.59	36.44	2.00	0.00	0.33	5.67	0.02	0.37	0.28	0.43	0.87	0.00	0.09	0.28	0.38	0.24	0.00	0.00	99.99
A3760HC	2	3	45.64	41.35	2.09	0.00	0.41	7.25	0.04	0.39	0.15	0.57	0.82	0.00	0.12	0.41	0.49	0.29	0.00	0.00	100.02
A3764HC	1	1	13.83	61.28	3.91	0.00	1.37	14.68	0.02	0.28	0.09	0.94	1.70	0.00	0.06	0.76	0.57	0.51	0.00	0.00	100.00
A3764HC	1	2	5.21	65.97	4.54	0.00	1.72	16.75	0.03	0.38	0.00	1.03	2.35	0.00	0.10	0.83	0.58	0.53	0.00	0.00	100.02
A3764HC	1	3	18.61	57.06	4.32	0.00	0.85	14.56	0.03	0.37	0.12	1.06	0.91	0.00	0.03	0.86	0.63	0.57	0.00	0.00	99.98
A3764HC	2	1	37.19	46.89	2.95	0.00	0.64	8.86	0.05	0.42	0.17	0.68	0.80	0.00	0.08	0.54	0.36	0.35	0.00	0.00	99.98
A3764HC	2	2	32.46	49.09	3.33	0.00	0.97	10.32	0.03	0.48	0.12	0.75	1.09	0.00	0.06	0.56	0.36	0.37	0.00	0.00	99.99
A3764HC	2	3	31.74	49.33	3.33	0.00	0.79	10.76	0.03	0.51	0.14	0.86	0.93	0.00	0.06	0.63	0.48	0.42	0.00	0.00	100.01
A3765HC	1	1	0.00	67.34	6.07	0.00	1.35	18.82	0.06	0.66	0.24	1.39	1.50	0.00	0.10	1.01	0.72	0.73	0.00	0.00	99.99
A3765HC	1	2	23.10	55.06	3.86	0.00	1.20	12.31	0.04	0.42	0.18	0.85	1.42	0.00	0.07	0.66	0.38	0.45	0.00	0.00	100.00
A3765HC	1	3	22.63	55.70	4.19	0.00	1.06	12.45	0.03	0.41	0.15	0.88	0.98	0.00	0.07	0.66	0.39	0.42	0.00	0.00	100.02
A3765HC	2	1	33.77	48.15	2.96	0.00	0.77	10.28	0.05	0.40	0.20	0.75	1.07	0.00	0.09	0.59	0.50	0.39	0.05	0.00	100.02
A3765HC	2	2	38.06	45.44	2.79	0.00	0.76	9.12	0.02	0.36	0.21	0.73	1.03	0.00	0.10	0.59	0.35	0.38	0.04	0.00	99.98
A3765HC	2	3	37.57	46.08	2.54	0.00	0.67	9.18	0.05	0.31	0.22	0.69	1.24	0.00	0.06	0.55	0.48	0.33	0.02	0.00	99.99
A3798HC	1	1	23.35	55.07	3.94	0.00	0.97	11.94	0.03	0.62	0.16	0.94	1.27	0.00	0.11	0.69	0.47	0.43	0.00	0.00	99.99
A3798HC	1	2	19.55	57.33	4.56	0.00	0.80	12.84	0.03	0.69	0.19	0.98	1.03	0.00	0.09	0.73	0.61	0.49	0.08	0.00	100.00
A3798HC	1	3	14.88	59.94	4.78	0.00	0.90	14.16	0.07	0.72	0.19	1.10	1.21	0.00	0.10	0.75	0.67	0.50	0.00	0.00	99.97
A3798HC	2	1	34.63	48.07	3.02	0.00	0.72	9.48	0.04	0.54	0.19	0.76	1.01	0.00	0.09	0.56	0.45	0.38	0.07	0.00	100.01
A3798HC	2	2	37.86	45.37	3.17	0.00	0.74	9.07	0.02	0.58	0.21	0.76	0.80	0.00	0.11	0.56	0.36	0.37	0.04	0.00	100.02
A3798HC	2	3	35.99	47.78	3.02	0.00	0.87	8.86	0.01	0.50	0.16	0.64	0.93	0.00	0.09	0.46	0.36	0.31	0.03	0.00	100.01
A3803HC	1	1	0.00	69.35	4.56	0.00	1.61	17.42	0.06	0.66	0.23	1.08	2.75	0.00	0.12	0.84	0.78	0.55	0.00	0.00	100.01
A3803HC	1	2	35.62	48.20	2.45	0.00	0.79	8.97	0.05	0.39	0.19	0.62	1.46	0.00	0.07	0.50	0.37	0.32	0.00	0.00	100.00
A3803HC	1	3	19.97	56.91	4.06	0.00	0.70	13.19	0.10	0.59	0.22	0.97	1.22	0.06	0.16	0.74	0.64	0.46	0.00	0.00	99.99
A3803HC	2	1	33.79	48.94	3.11	0.23	0.61	9.67	0.05	0.51	0.15	0.80	0.77	0.00	0.10	0.61	0.26	0.40	0.00	0.00	100.00
A3803HC	2	2	21.68	56.70	4.14	0.00	0.45	12.47	0.03	0.56	0.15	0.97	0.92	0.02	0.08	0.76	0.61	0.48	0.00	0.00	100.02
A3803HC	2	3	36.37	47.57	2.26	0.00	0.82	9.05	0.02	0.41	0.19	0.63	1.39	0.03	0.10	0.45	0.40	0.31	0.00	0.00	100.00
A3807HC	1	1	36.37	47.57	2.26	0.00	0.82	9.05	0.02	0.41	0.19	0.63	1.39	0.03	0.10	0.45	0.40	0.31	0.00	0.00	100.00
A3807HC	1	2	19.71	56.92	3.85	0.00	0.95	13.49	0.03	0.50	0.23	1.00	1.44	0.02	0.08	0.75	0.54	0.49	0.00	0.00	100.00
A3807HC	1	3	42.61	43.74	2.22	0.18	0.69	7.48	0.03	0.38	0.20	0.64	0.84	0.01	0.08	0.46	0.14	0.30	0.00	0.00	100.00
A3807HC	2	1	0.00	67.91	5.64	0.00	1.12	19.11	0.04	0.62	0.20	1.43	1.44	0.01	0.07	1.01	0.71	0.71	0.00	0.00	100.02
A3807HC	2	2	0.00	68.96	5.35	0.00	0.97	18.36	0.06	0.65	0.17	1.34	1.58	0.02	0.09	0.96	0.81	0.68	0.00	0.00	100.00
A3807HC	2	3	31.66	49.18	3.06	0.00	0.60	11.01	0.04	0.47	0.15	0.85	1.26	0.03	0.07	0.71	0.49	0.43	0.00	0.00	100.01
A3809HC	1	1	36.82	47.29	2.28	0.00	0.84	8.95	0.01	0.25	0.24	0.62	1.35	0.00	0.06	0.52	0.41	0.35	0.00	0.00	99.99
A3809HC	1	2	11.88	60.67	4.51	0.00	1.24	15.48	0.08	0.48	0.39	1.10	1.85	0.00	0.08	0.90	0.71	0.63	0.00	0.00	100.00
A3809HC	1	3	24.38	52.98	3.69	0.32	1.39	12.08	0.05	0.50	0.55	0.84	1.57	0.00	0.08	0.74	0.30	0.54	0.00	0.00	100.01
A3809HC	2	1	37.01	46.75	2.61	0.18	0.73	8.90	0.03	0.35	0.22	0.65	1.29	0.00	0.07	0.50	0.37	0.34	0.00	0.00	100.00
A3809HC	2	2	36.55	46.67	2.90	0.20	0.76	9.28	0.03	0.37	0.25	0.77	0.90	0.00	0.08	0.57	0.28	0.40	0.00	0.00	100.01
A3809HC	2	3	24.55	54.42	3.15	0.00	0.90	11.87	0.01	0.38	0.25	0.82	1.91	0.00	0.00	0.67	0.61	0.46	0.00	0.00	100.00
A3854HC	1	1	21.67	57.30	3.70	0.00	0.48	12.80	0.03	0.19	0.14	0.91	0.92	0.00	0.04	0.71	0.64	0.48	0.00	0.00	100.01

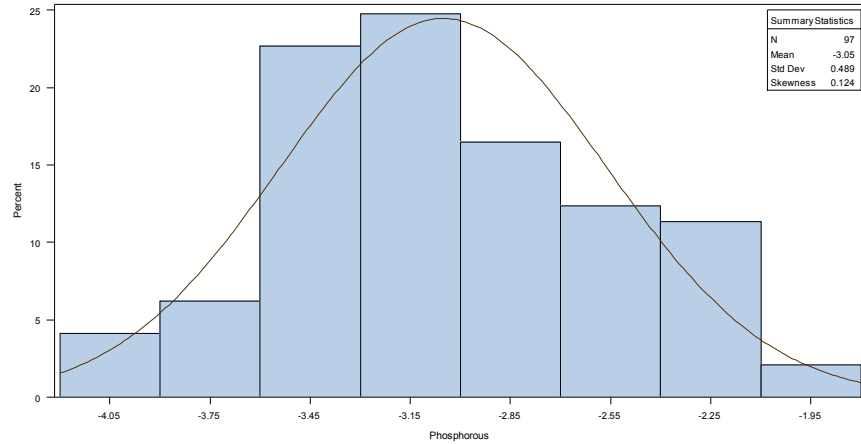
A3854HC	1	2	0.00	68.00	4.93	0.00	1.24	19.60	0.00	0.30	0.21	1.33	1.68	0.00	0.11	1.02	0.85	0.74	0.00	0.00	100.01
A3854HC	1	3	15.66	59.69	3.85	0.00	1.19	14.66	0.00	0.32	0.18	0.97	1.51	0.00	0.05	0.81	0.55	0.56	0.00	0.00	100.00
A3854HC	2	1	30.72	51.18	3.11	0.00	0.43	10.90	0.00	0.25	0.10	0.79	0.84	0.00	0.04	0.66	0.51	0.45	0.00	0.00	99.98
A3854HC	2	2	13.25	61.69	4.16	0.00	0.87	15.01	0.00	0.30	0.16	1.09	1.33	0.00	0.06	0.86	0.64	0.58	0.00	0.00	100.00
A3854HC	2	3	18.65	58.18	3.61	0.00	0.85	13.72	0.03	0.30	0.14	0.92	1.58	0.00	0.08	0.77	0.65	0.50	0.00	0.00	99.98
DM3452216022	1	1	0.00	68.31	6.35	0.49	1.30	18.69	0.10	0.16	0.00	0.95	1.55	0.00	0.00	0.98	0.49	0.62	0.00	0.00	99.99
DM3452216022	1	2	0.00	68.79	6.38	0.51	1.12	18.43	0.08	0.13	0.00	0.92	1.47	0.00	0.00	0.97	0.60	0.60	0.00	0.00	100.00
DM3452216022	1	3	0.00	68.73	6.21	0.50	1.30	18.44	0.07	0.00	0.00	0.92	1.66	0.00	0.00	1.00	0.54	0.62	0.00	0.00	99.99
DM3452216022	2	1	0.00	67.83	6.06	0.52	1.08	19.21	0.11	0.00	0.00	1.01	1.67	0.00	0.00	1.13	0.68	0.71	0.00	0.00	100.01
DM3452216022	2	2	0.00	68.70	5.91	0.57	1.52	18.21	0.10	0.16	0.12	0.91	1.85	0.00	0.00	0.93	0.41	0.61	0.00	0.00	100.00
DM3452216022	2	3	0.00	67.93	6.37	0.50	1.38	19.03	0.07	0.00	0.00	1.02	1.48	0.00	0.00	1.12	0.41	0.69	0.00	0.00	100.00
KK2322123-084	1	1	56.54	33.06	1.70	0.22	0.56	5.02	0.06	0.50	0.22	0.40	0.87	0.04	0.11	0.36	0.14	0.20	0.00	0.00	100.00
KK2322123-084	1	2	55.00	34.39	1.75	0.18	0.87	5.22	0.04	0.43	0.21	0.39	0.72	0.04	0.11	0.32	0.12	0.19	0.00	0.00	99.98
KK2322123-084	1	3	58.43	32.13	1.55	0.19	0.53	4.53	0.06	0.43	0.28	0.37	0.79	0.06	0.10	0.28	0.11	0.17	0.00	0.00	100.01
KK2322123-084	2	1	0.00	66.78	5.86	0.40	1.42	19.64	0.03	0.27	0.00	1.23	1.64	0.05	0.05	1.23	0.66	0.74	0.00	0.00	100.00
KK2322123-084	2	2	0.00	66.02	5.62	0.41	1.57	19.82	0.07	0.33	0.07	1.22	2.12	0.05	0.08	1.27	0.59	0.76	0.00	0.00	100.00
KK2322123-084	2	3	0.00	67.08	5.94	0.48	1.71	18.98	0.02	0.36	0.00	1.16	1.80	0.04	0.09	1.22	0.40	0.70	0.00	0.00	99.98

**Table A-3 SAS OUTPUT**

Distribution of Phosphorus in Used Aircraft filters

Tests for Normality in Used Filters

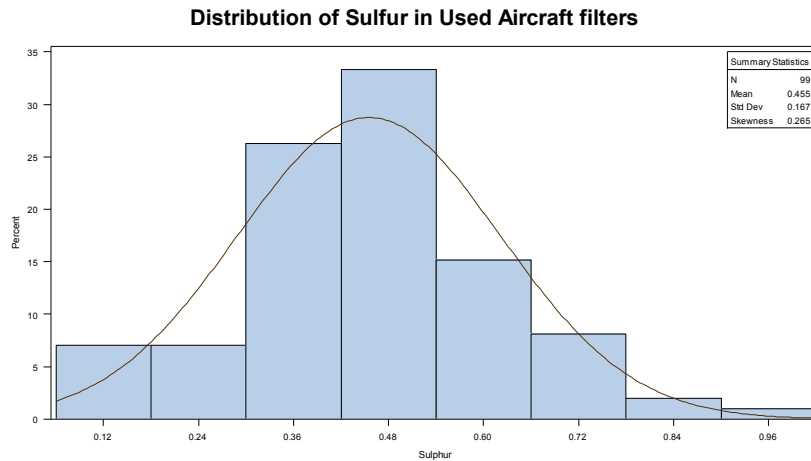
Test		--Statistic---		-----p Value-----
Shapiro-Wilk	W	0.987845	Pr < W	0.5193
Kolmogorov-Smirnov	D	0.066844	Pr > D	>0.1500
Cramer-von Mises	W-Sq	0.069021	Pr > W-Sq	>0.2500
Anderson-Darling	A-Sq	0.404191	Pr > A-Sq	>0.2500



Distribution of Sulfur in Used Aircraft filters

Tests for Normality

Test		--Statistic---		-----p Value-----
Shapiro-Wilk	W	0.984392	Pr < W	0.2933
Kolmogorov-Smirnov	D	0.060424	Pr > D	>0.1500
Cramer-von Mises	W-Sq	0.049581	Pr > W-Sq	>0.2500
Anderson-Darling	A-Sq	0.348491	Pr > A-Sq	>0.2500

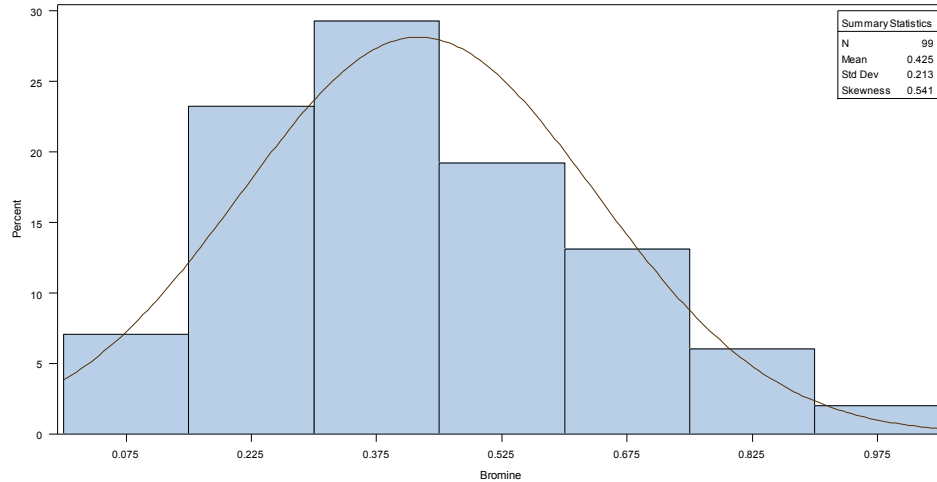


Distribution of Bromine in Used Aircraft filters

Tests for Normality

Test	--Statistic---	-----p Value-----
Shapiro-Wilk	W 0.970355	Pr < W 0.0246
Kolmogorov-Smirnov	D 0.072203	Pr > D >0.1500
Cramer-von Mises	W-Sq 0.112564	Pr > W-Sq 0.0792
Anderson-Darling	A-Sq 0.715408	Pr > A-Sq 0.0628

Distribution of Bromine in Used Aircraft filters



Distribution of Phosphorus in Incident Aircraft filters

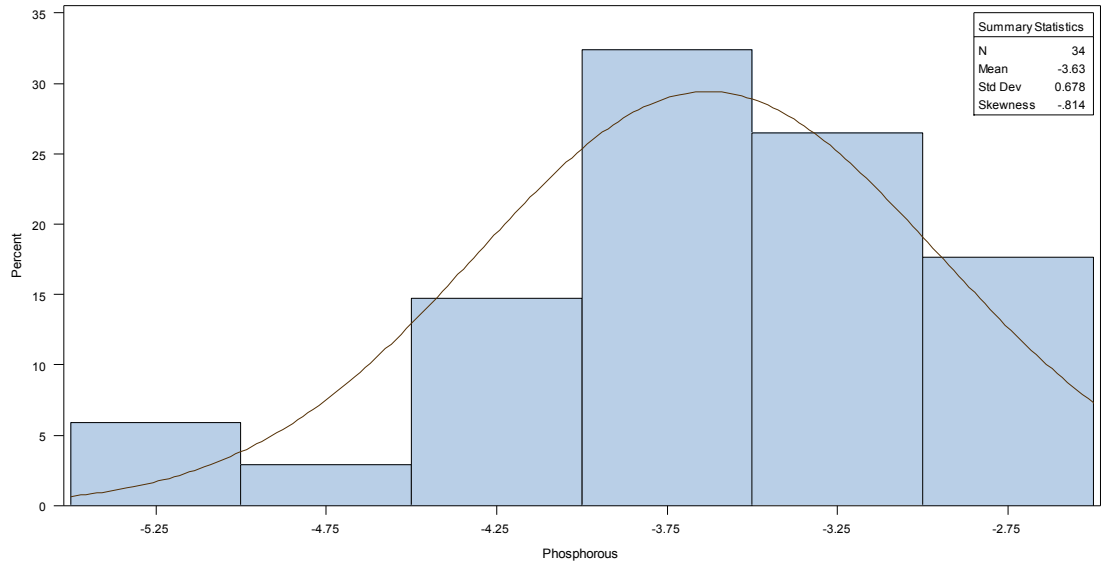
The UNIVARIATE Procedure

Variable: Phosphorus

Tests for Normality

Test	--Statistic---	-----p Value-----
Shapiro-Wilk	W 0.946063	Pr < W 0.0936
Kolmogorov-Smirnov	D 0.112885	Pr > D >0.1500
Cramer-von Mises	W-Sq 0.064399	Pr > W-Sq >0.2500
Anderson-Darling	A-Sq 0.492896	Pr > A-Sq 0.2118

### Distribution of Phosphorous in Incident Filters



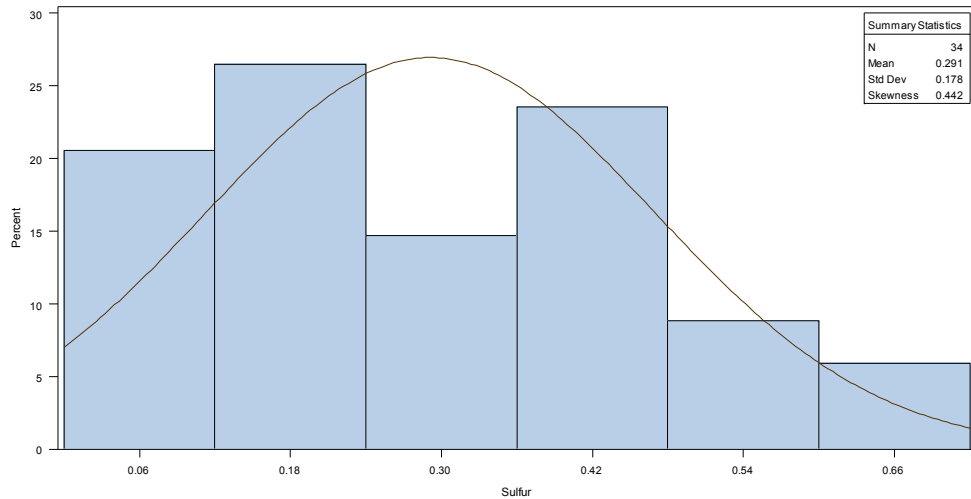
### Distribution of Sulfur in Incident Filter

Variable: Sulfur

#### Tests for Normality

Test		--Statistic--		-----p Value-----
Shapiro-Wilk	W	0.948786	Pr < W	0.1129
Kolmogorov-Smirnov	D	0.11385	Pr > D	>0.1500
Cramer-von Mises	W-Sq	0.103149	Pr > W-Sq	0.0985
Anderson-Darling	A-Sq	0.628608	Pr > A-Sq	0.0948

### Distribution of Sulfur in Incident Aircraft filters

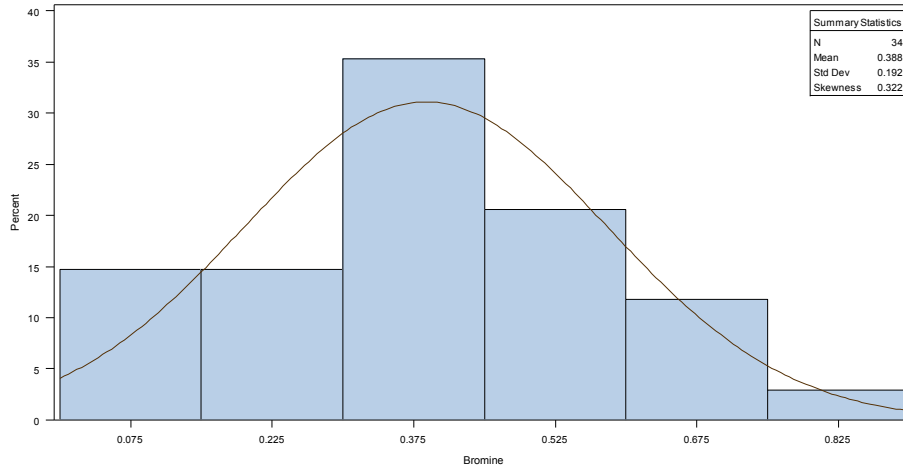


Distribution of Bromine in Incident Aircraft filters

Tests for Normality

Test		--Statistic---		-----p Value-----
Shapiro-Wilk	W	0.972406	Pr < W	0.5309
Kolmogorov-Smirnov	D	0.097589	Pr > D	>0.1500
Cramer-von Mises	W-Sq	0.050127	Pr > W-Sq	>0.2500
Anderson-Darling	A-Sq	0.31333	Pr > A-Sq	>0.2500

Distribution of Bromine in Incident Aircraft filters



Calculation and Test of Correlations, 95% CI for Used Filters

The CORR Procedure

Pearson Correlation Coefficients, N = 99

Prob > |r| under H0: Rho=0

	P	S	Br
P	1.00000	0.58591	0.07262
		<.0001	0.4750
S	0.58591	1.00000	-0.28531
	<.0001		0.0042
Br	0.07262	-0.28531	1.00000
	0.4750	0.0042	

Calculation and Test of Correlations, 95% CI for Incident Filters

The CORR Procedure

Pearson Correlation Coefficients, N = 34

Prob > |r| under H0: Rho=0

	P	S	Br
P	1.00000	0.65239	-0.56459
		<.0001	0.0005
S	0.65239	1.00000	-0.62509
	<.0001		<.0001
Br	-0.56459	-0.62509	1.00000
	0.0005	<.0001	

The TTEST Procedure

Variable: Phosphorus

Category	Method	Mean	95% CL	Mean	Std Dev	95% CL	Std Dev
Incident		0.0320	0.0256	0.0384	0.0184	0.0148	0.0242
Used		0.0524	0.0469	0.0579	0.0278	0.0244	0.0323
Diff (1-2)	Pooled	-0.0204	-0.0305	-0.0103	0.0258	0.0230	0.0293
Diff (1-2)	Satterthwaite	-0.0204	-0.0288	-0.0120			

Method	Variances	DF	t Value	Pr >  t
Pooled	Equal	131	-3.98	0.0001
Satterthwaite	Unequal	87.29	-4.84	<.0001

The TTEST Procedure

Variable: sulfur

Category	Method	Mean	95% CL	Mean	Std Dev	95% CL	Std Dev
Incident		0.2798	0.2161	0.3435	0.1766	0.1415	0.2347
Used		0.4553	0.4220	0.4885	0.1666	0.1462	0.1937
Diff (1-2)	Pooled	-0.1755	-0.2435	-0.1074	0.1691	0.1507	0.1925
Diff (1-2)	Satterthwaite	-0.1755	-0.2466	-0.1043			

Method	Variances	DF	t Value	Pr >  t
Pooled	Equal	129	-5.10	<.0001
Satterthwaite	Unequal	50.101	-4.95	<.0001

Equality of Variances

Method	Num DF	Den DF	F Value	Pr > F
Folded F	31	98	1.12	0.6522

The TTEST Procedure

Variable: Bromine

Category	Method	Mean	95% CL	Mean	Std Dev	95% CL	Std Dev
Incident		0.3878	0.3207	0.4549	0.1924	0.1552	0.2533
Used		0.4252	0.3828	0.4677	0.2127	0.1866	0.2473
Diff (1-2)	Pooled	-0.0374	-0.1191	0.0443	0.2078	0.1854	0.2364
Diff (1-2)	Satterthwaite	-0.0374	-0.1160	0.0411			

Method	Variances	DF	t Value	Pr >  t
Pooled	Equal	131	-0.91	0.3664
Satterthwaite	Unequal	62.778	-0.95	0.3447

Equality of Variances

Method	Num DF	Den DF	F Value	Pr > F
Folded F	98	33	1.22	0.5214

**Table A-4 ANALYSIS OF VARIANCE (ANOVA) USING PROC GML and PROC MIXED PROCEDURES**

SAS OUTPUT

Obs	Filter_ ID	Aircraft	Phosphorus	Sulfur	Bromine	Category
1	1F3555	B777	0.0480	0.4040	0.3160	Used
2	IS78FS	B777	0.0583	0.3950	0.3783	Used
3	2D968E	B777	0.0500	0.3517	0.5567	Used
4	3C297F	B737	0.0400	0.4740	0.4940	Used
5	4S190C	B777	0.0300	0.4860	0.4180	Used
6	5H2F01	B777	0.0583	0.4800	0.3500	Used
7	7WQF45	B777	0.0275	0.5250	0.2575	Used
8	7ZMK52	B777	0.0500	0.5133	0.1800	Used
9	8P6G4X	B737	0.0325	0.2325	0.5125	Used
10	9E003T	B777	0.0425	0.3725	0.4500	Used
11	9RZMC2	B777	0.0333	0.5150	0.3467	Used
12	43RTYZ	B777	0.0317	0.5883	0.3183	Used
13	73J43M	B777	0.0540	0.4600	0.5400	Used
14	83MIA9	B777	0.0167	0.4567	0.1517	Used
15	584C32	B777	0.0683	0.5800	0.7517	Used
16	794TWZ	B777	0.0300	0.3150	0.2975	Used
17	AI644T	B777	0.0320	0.1180	0.7860	Used
18	B014NE	B777	0.0320	0.3200	0.2960	Used
19	B92YNB	B777	0.0420	0.5180	0.2500	Used
20	BRT6RD	B777	0.0360	0.4500	0.2660	Used
21	ESF946	B777	0.0300	0.4560	0.4400	Used
22	G48MJ6	B777	0.0400	0.4680	0.4160	Used
23	JD5RT2	B777	0.0467	0.4583	0.4700	Used
24	JHHCD2	B737	0.0067	0.1233	0.7300	Used
25	JR3584	B777	0.0360	0.5760	0.3980	Used
26	KI9846	B777	0.0475	0.4500	0.6875	Used
27	MSU4TD	B777	0.0200	0.1400	0.6850	Used
28	MTCL37	B777	0.0720	0.4400	0.5640	Used
29	N6D5A7	B777	0.0600	0.5440	0.7220	Used
30	PN38IZ	B777	0.0620	0.5600	0.6080	Used
31	R67R85	B777	0.0340	0.6720	0.3000	Used
32	STJH77	B777	0.0400	0.6960	0.3140	Used
33	TBD533	B777	0.0417	0.5617	0.2817	Used
34	TJ66RG	B777	0.0433	0.5333	0.1200	Used
35	UGA145	B777	0.0300	0.3375	0.5850	Used
36	VT23AC	B777	0.0080	0.1140	0.6620	Used
37	WH3JMZ	B777	0.0400	0.3700	0.6083	Used
38	CRH8ES	B777	0.0980	0.6540	0.6280	Used
39	DAW454	B777	0.1233	0.7550	0.5433	Used



40	DSF6UE	B777	0.0600	0.5580	0.4860	Used
41	12HD94	A320	0.0580	0.5160	0.3600	Used
42	LF4EQ2	B767	0.0550	0.2583	0.1117	Used
43	SJA33J	A320	0.0150	0.1717	0.3617	Used
44	YEK752	A320	0.0300	0.2900	0.4200	Used
45	LR8C66	B777	0.0933	0.3617	0.5050	Used
46	I89VFS	B777	0.0667	0.4700	0.8483	Used
47	E63JV3	B737	0.0700	0.4200	0.2040	Used
48	7YS36N	B777	0.0400	0.4160	0.1760	Used
49	W9E578	B747	0.0225	0.3875	0.5225	Used
50	8835TV	A320	0.0300	0.3933	0.1367	Used
51	WR2F6B	B767	0.0375	0.4225	0.3025	Used
52	HME4A8	B777	0.0375	0.2800	0.7100	Used
53	163B4J	B747	0.0325	0.6250	0.3425	Used
54	46NKJF	B777	0.0800	0.6880	0.6260	Used
55	R5BH23	B777	0.0483	0.3100	0.7533	Used
56	GF68X3	B777	0.0750	0.8717	0.2267	Used
57	7GH325	B777	0.0575	0.3150	0.4675	Used
58	K76GHR	A320	0.0400	0.3420	0.2740	Used
59	QOX417	B737	0.0460	0.3220	0.6920	Used
60	WBH9G4	B777	0.0920	0.3240	0.4480	Used
61	907BVA	B777	0.0860	0.9840	0.1160	Used
62	MA7ET5	B777	0.1440	0.8000	0.5880	Used
63	TT15A5	B737	0.0225	0.4400	0.3625	Used
64	NZ2T7W	B777	0.0360	0.3040	1.0000	Used
65	11S754	B777	0.1000	0.4280	0.4280	Used
66	17BDAR	B777	0.0980	0.6540	0.3760	Used
67	TC66HR	B767	0.0350	0.4850	0.2725	Used
68	F1JH39	B737	0.0740	0.4620	0.1660	Used
69	G09JVE	B747	0.0333	0.5167	0.2283	Used
70	HIDE4H	B777	0.0933	0.6967	0.2100	Used
71	HGD63H	A320	0.0440	0.3960	0.3780	Used
72	RP14DE	B737	0.1150	0.4800	0.7167	Used
73	77G4CJ	B777	0.0940	0.6280	0.8640	Used
74	2965CL	A320	0.0580	0.5160	0.2440	Used
75	B322IJ	B737	0.0700	0.2720	1.0120	Used
76	HFU84F	B777	0.0725	0.6025	0.1625	Used
77	FWX130	B777	0.1167	0.7000	0.5600	Used
78	M6AAM6	B747	0.0425	0.4725	0.4325	Used
79	L6159B	B747	0.0367	0.4267	0.4600	Used
80	CE9B19	A320	0.0500	0.3920	0.3020	Used
81	27QR6F	B777	0.0183	0.1317	0.4883	Used
82	JGFDGG	B747	0.0433	0.6350	0.1633	Used
83	FTRT75	B737	0.0560	0.3680	0.0940	Used
84	WAQE67	B777	0.0583	0.5083	0.3917	Used
85	75G8FW	B777	0.1080	0.7580	0.5860	Used

86	U44MXV	A320	0.0433	0.3933	0.1683	Used
87	G8UX4V	B777	0.0860	0.5960	0.5700	Used
88	MB6LV1	B747	0.0467	0.4733	0.3400	Used
89	NM81X7	A320	0.0260	0.3300	0.4080	Used
90	85HXNS	B747	0.0217	0.2217	0.3217	Used
91	ZD152A	B747	0.0280	0.2880	0.3900	Used
92	BHU548	B737	0.0760	0.6680	0.1140	Used
93	CP163W	B747	0.0267	0.5033	0.3483	Used
94	PL2IX1	B747	0.0250	0.4100	0.2883	Used
95	T007ML	A320	0.0417	0.3217	0.6483	Used
96	DR87FE	B777	0.1220	0.4940	0.1560	Used
97	IUY3T4	B767	0.0280	0.1220	0.8180	Used
98	HFD9LM	B767	0.0480	0.5260	0.2240	Used
99	3Q5J9L	B767	0.0840	0.5740	0.0480	Used
100	2974	B737	0.0433	0.0000	0.6000	Incident
101	22551	A320	0.0233	0.2467	0.3017	Incident
102	26701	A320	0.0567	0.2617	0.2783	Incident
103	27055	A320	0.0400	0.2383	0.3833	Incident
104	27165	A320	0.0483	0.4517	0.3333	Incident
105	27420	A320	0.0317	0.2017	0.3050	Incident
106	27559	B737	0.0267	0.2667	0.3433	Incident
107	27659	A320	0.0075	0.0800	0.2825	Incident
108	27660	A320	0.0133	0.0933	0.3800	Incident
109	27694	A320	0.0533	0.4467	0.1083	Incident
110	28240	B737	0.0167	0.3517	0.4217	Incident
111	28297	B737	0.0250	0.1367	0.5950	Incident
112	28802	A320	0.0200	0.0825	0.5250	Incident
113	28825	A320	0.0200	0.2260	0.3100	Incident
114	29428	B737	0.0050	0.0783	0.7400	Incident
115	29434	B737	0.0050	0.1233	0.5583	Incident
116	29442	B737	0.0200	0.1150	0.8525	Incident
117	29606	B737	0.0150	0.1550	0.4867	Incident
118	30121	B737	0.0300	0.1640	0.6320	Incident
119	30335	B737	0.0633	0.4533	0.1000	Incident
120	30363	B737	0.0667	0.4917	0.0633	Incident
121	30670	B737	0.0360	0.2260	0.4340	Incident
122	30674	B737	0.0167	0.0900	0.6400	Incident
123	60401016	A320	0.0567	0.4417	0.1250	Incident
124	65039046	A320	0.0800	0.6617	0.1267	Incident
125	A3795HC	B767	0.0460	0.4860	0.5500	Incident
126	A3740HC	B767	0.0250	0.4150	0.5000	Incident
127	A3760HC	B767	0.0300	0.3700	0.3783	Incident
128	A3869HC	B767	0.0350	0.4250	0.5250	Incident
129	A21803HC	B737	0.0317	0.4317	0.3367	Incident
130	A22023HC	B737	0.0283	0.5183	0.3000	Incident
131	A217994H	B737	0.0350	0.6950	0.1500	Incident

132	A22623HC	B737	0.0250	0.2950	0.2717	Incident
133	A242337H	B737	0.0120	0.1840	0.2480	Incident

The GLM Procedure  
Class Level Information

Class	Levels	Values
Category	2	Incident Used
Number of Observations Read		133
Number of Observations Used		133

The GLM Procedure  
Dependent Variable: Phosphorus

Source	DF	Sum of Squares	Mean Square	F Value	Pr > F
Model	1	0.01052622	0.01052622	15.86	0.0001
Error	131	0.08693870	0.00066365		
Corrected Total	132	0.09746492			

R-Square	Coeff Var	Root MSE	Phosphorus Mean
0.108000	54.59507	0.025761	0.047186

Source	DF	Type III SS	Mean Square	F Value	Pr > F
Category	1	0.01052622	0.01052622	15.86	0.0001

Parameter	Estimate	Standard Error	t Value	Pr >  t
Intercept	0.0524000000 B	0.00258913	20.24	<.0001
Category Incident	-.0203941176 B	0.00512082	-3.98	0.0001
Category Used	0.0000000000 B	.	.	.

The GLM Procedure  
Dependent Variable: Sulfur

Source	DF	Sum of Squares	Mean Square	F Value	Pr > F
Model	1	0.69011107	0.69011107	24.10	<.0001
Error	131	3.75130778	0.02863594		
Corrected Total	132	4.44141885			

R-Square	Coeff Var	Root MSE	Sulfur Mean
0.155381	40.85481	0.169222	0.414202

Source	DF	Type III SS	Mean Square	F Value	Pr > F
Category	1	0.69011107	0.69011107	24.10	<.0001

Parameter	Estimate	Standard Error	t Value	Pr >  t
Intercept	0.4564161616 B	0.01700741	26.84	<.0001

Category	Incident	-.1651308675 B	0.03363756	-4.91	<.0001
Category	Used	0.0000000000 B	.	.	.

NOTE: The X'X matrix has been found to be singular, and a generalized inverse was used to solve the normal equations. Terms whose estimates are followed by the letter 'B' are not uniquely estimable.

The GLM Procedure  
Dependent Variable: Bromine

Source	DF	Sum of Squares	Mean Square	F Value	Pr > F
Model	1	0.03546400	0.03546400	0.82	0.3664
Error	131	5.65414144	0.04316139		
Corrected Total	132	5.68960544			

R-Square	Coeff Var	Root MSE	Bromine Mean
0.006233	49.97960	0.207753	0.415676

Source	DF	Type III SS	Mean Square	F Value	Pr > F
Category	1	0.03546400	0.03546400	0.82	0.3664

Parameter	Estimate	Standard Error	t Value	Pr >  t
Intercept	0.4252454545 B	0.02087998	20.37	<.0001
Category Incident	-.0374336898 B	0.04129680	-0.91	0.3664
Category Used	0.0000000000 B	.	.	.

NOTE: The X'X matrix has been found to be singular, and a generalized inverse was used to solve the normal equations. Terms whose estimates are followed by the letter 'B' are not uniquely estimable.

The GLM Procedure  
Least Squares Means

Adjustment for Multiple Comparisons: Bonferroni

Category	Phosphorus		H0:LSMEAN=0	H0:LSMean1=LSMean2
	LSMEAN	Standard Error	Pr >  t	Pr >  t
Incident	0.03200588	0.00441806	<.0001	0.0001
Used	0.05240000	0.00258913	<.0001	

Phosphorus			
Category	LSMEAN	95% Confidence Limits	
Incident	0.032006	0.023266	0.040746
Used	0.052400	0.047278	0.057522

Least Squares Means for Effect Category  
Difference Between Simultaneous 95% Confidence Limits for

i	j	Means	LSMean(i)-LSMean(j)
1	2	-0.020394	-0.030524 -0.010264

Category	Sulfur	Standard	H0:LSMEAN=0	H0:LSMean1=LSMean2
	LSMEAN	Error	Pr >  t	Pr >  t
Incident	0.29128529	0.02902126	<.0001	<.0001
Used	0.45641616	0.01700741	<.0001	

Category	Sulfur	95% Confidence Limits	
	LSMEAN		
Incident	0.291285	0.233874	0.348696
Used	0.456416	0.422771	0.490061

Least Squares Means for Effect Category

i	j	Difference	Simultaneous 95% Confidence Limits for	
		Between Means	LSMean(i)-LSMean(j)	
1	2	-0.165131	-0.231674	-0.098588

The GLM Procedure

Least Squares Means

Adjustment for Multiple Comparisons: Bonferroni

Category	Bromine	Standard	H0:LSMEAN=0	H0:LSMean1=LSMean2
	LSMEAN	Error	Pr >  t	Pr >  t
Incident	0.38781176	0.03562938	<.0001	0.3664
Used	0.42524545	0.02087998	<.0001	

Category	Bromine	95% Confidence Limits	
	LSMEAN		
Incident	0.387812	0.317328	0.458295
Used	0.425245	0.383940	0.466551

Least Squares Means for Effect Category

i	j	Difference	Simultaneous 95% Confidence Limits for	
		Between Means	LSMean(i)-LSMean(j)	
1	2	-0.037434	-0.119129	0.044261

----- Category=Incident -----

The GLM Procedure

Class Level Information

Class	Levels	Values
Aircraft	3	A320 B737 B767

Number of Observations Read 34  
 Number of Observations Used 34

----- Category=Incident -----  
 The GLM Procedure

Dependent Variable: Phosphorus

Source	DF	Sum of Squares	Mean Square	F Value	Pr > F
Model	2	0.00069703	0.00034851	1.04	0.3666
Error	31	0.01042177	0.00033619		
Corrected Total	33	0.01111880			

R-Square 0.062689  
 Coeff Var 57.28753  
 Root MSE 0.018335  
 Phosphorus Mean 0.032006

Source	DF	Type III SS	Mean Square	F Value	Pr > F
Aircraft	2	0.00069703	0.00034851	1.04	0.3666

Parameter	Estimate	Standard Error	t Value	Pr >  t
Intercept	0.034000000 B	0.00916769	3.71	0.0008
Aircraft A320	0.003566667 B	0.01058594	0.34	0.7384
Aircraft B737	-.006144444 B	0.01013526	-0.61	0.5488
Aircraft B767	0.000000000 B	.	.	.

NOTE: The X'X matrix has been found to be singular, and a generalized inverse was used to solve the normal equations. Terms whose estimates are followed by the letter 'B' are not uniquely estimable.

----- Category=Incident -----  
 The GLM Procedure

Dependent Variable: Sulfur

Source	DF	Sum of Squares	Mean Square	F Value	Pr > F
Model	2	0.08292664	0.04146332	1.34	0.2765
Error	31	0.95886146	0.03093102		
Corrected Total	33	1.04178810			

R-Square 0.079600  
 Coeff Var 60.37797  
 Root MSE 0.175872  
 Sulfur Mean 0.291285

Source	DF	Type III SS	Mean Square	F Value	Pr > F
Aircraft	2	0.08292664	0.04146332	1.34	0.2765

Parameter	Estimate	Standard Error	t Value	Pr >  t
Intercept	0.424000000 B	0.08793608	4.82	<.0001
Aircraft A320	-.138000000 B	0.10153984	-1.36	0.1839
Aircraft B737	-.158683333 B	0.09721699	-1.63	0.1127

Aircraft B767 0.000000000 B . . .

NOTE: The X'X matrix has been found to be singular, and a generalized inverse was used to solve the normal equations. Terms whose estimates are followed by the letter 'B' are not uniquely estimable.

----- Category=Incident -----

The GLM Procedure

Dependent Variable: Bromine

Source	DF	Sum of Squares	Mean Square	F Value	Pr > F
Model	2	0.19424205	0.09712103	2.93	0.0683
Error	31	1.02752910	0.03314610		
Corrected Total	33	1.22177116			

Source	DF	Type III SS	Mean Square	F Value	Pr > F
Aircraft	2	0.19424205	0.09712103	2.93	0.0683

Parameter	Estimate	Standard Error	t Value	Pr >  t
Intercept	0.4883250000 B	0.09103035	5.36	<.0001
Aircraft A320	-.2000666667 B	0.10511280	-1.90	0.0663
Aircraft B737	-.0564805556 B	0.10063784	-0.56	0.5787
Aircraft B767	0.0000000000 B	.	.	.

NOTE: The X'X matrix has been found to be singular, and a generalized inverse was used to solve the normal equations. Terms whose estimates are followed by the letter 'B' are not uniquely estimable.

----- Category=Incident -----

The GLM Procedure

Levene's Test for Homogeneity of Phosphorus Variance

ANOVA of Absolute Deviations from Group Means

Source	DF	Sum of Squares	Mean Square	F Value	Pr > F
Aircraft	2	0.000489	0.000244	2.17	0.1311
Error	31	0.00349	0.000113		

O'Brien's Test for Homogeneity of Phosphorus Variance

ANOVA of O'Brien's Spread Variable, W = 0.5

Source	DF	Sum of Squares	Mean Square	F Value	Pr > F
Aircraft	2	5.375E-7	2.687E-7	1.12	0.3384
Error	31	7.422E-6	2.394E-7		

Brown and Forsythe's Test for Homogeneity of Phosphorus Variance  
ANOVA of Absolute Deviations from Group Medians

Source	DF	Sum of Squares	Mean Square	F Value	Pr > F
Aircraft	2	0.000495	0.000248	2.10	0.1400
Error	31	0.00366	0.000118		

Bartlett's Test for Homogeneity of Phosphorus Variance

Source	DF	Chi-Square	Pr > ChiSq
Aircraft	2	2.7343	0.2548

----- Category=Incident -----  
The GLM Procedure

O'Brien's Test for Homogeneity of Sulfur Variance  
ANOVA of O'Brien's Spread Variable, W = 0.5

Source	DF	Sum of Squares	Mean Square	F Value	Pr > F
Aircraft	2	0.00361	0.00180	0.94	0.4007
Error	31	0.0593	0.00191		

Brown and Forsythe's Test for Homogeneity of Sulfur Variance  
ANOVA of Absolute Deviations from Group Medians

Source	DF	Sum of Squares	Mean Square	F Value	Pr > F
Aircraft	2	0.0454	0.0227	1.63	0.2132
Error	31	0.4330	0.0140		

Bartlett's Test for Homogeneity of Sulfur Variance

Source	DF	Chi-Square	Pr > ChiSq
Aircraft	2	4.8336	0.0892

Levene's Test for Homogeneity of Bromine Variance  
ANOVA of Absolute Deviations from Group Means

Source	DF	Sum of Squares	Mean Square	F Value	Pr > F
Aircraft	2	0.0959	0.0480	4.67	0.0169
Error	31	0.3187	0.0103		

O'Brien's Test for Homogeneity of Bromine Variance  
ANOVA of O'Brien's Spread Variable, W = 0.5

Source	DF	Sum of Squares	Mean Square	F Value	Pr > F
Aircraft	2	0.0121	0.00605	3.22	0.0535
Error	31	0.0582	0.00188		



----- Category=Incident -----

The GLM Procedure

Brown and Forsythe's Test for Homogeneity of Bromine Variance  
ANOVA of Absolute Deviations from Group Medians

Source	DF	Sum of Squares	Mean Square	F Value	Pr > F
Aircraft	2	0.1023	0.0512	4.79	0.0154
Error	31	0.3311	0.0107		

Bartlett's Test for Homogeneity of Bromine Variance

Source	DF	Chi-Square	Pr > ChiSq
Aircraft	2	6.7115	0.0349

Welch's ANOVA for Phosphorus

Source	DF	F Value	Pr > F
Aircraft	2.0000	0.97	0.4063
Error	12.4849		

Welch's ANOVA for Sulfur

Source	DF	F Value	Pr > F
Aircraft	2.0000	6.43	0.0075
Error	18.6834		

Welch's ANOVA for Bromine

Source	DF	F Value	Pr > F
Aircraft	2.0000	7.50	0.0065
Error	13.3635		

----- Category=Incident -----

The GLM Procedure

Level of	-----Phosphorus-----			----- Sulfur-----		-----Bromine--	
Aircraft	N	Mean	Std Dev	Mean	Std Dev	Mean	Std Dev
A320	12	0.03756667	0.02184538	0.28600000	0.17958848	0.28825833	0.12125487
B737	18	0.02785556	0.01702998	0.26531667	0.18743583	0.43184444	0.22339733
B767	4	0.03400000	0.00898146	0.42400000	0.04775633	0.48832500	0.07613730

----- Category=Incident -----

The GLM Procedure

Least Squares Means

Adjustment for Multiple Comparisons: Bonferroni

Aircraft	Phosphorus LSMEAN	Standard Error	Pr >  t	LSMEAN Number
A320	0.03756667	0.00529297	<.0001	1
B737	0.02785556	0.00432169	<.0001	2

B767            0.0340000    0.00916769    0.0008            3

Least Squares Means for effect Aircraft

Pr > |t| for H0: LSMean(i)=LSMean(j)

Dependent Variable: Phosphorus

i/j	1	2	3
1		0.4958	1.0000
2	0.4958		1.0000
3	1.0000	1.0000	

Phosphorus

Aircraft	LSMEAN	95% Confidence Limits	
A320	0.037567	0.026772	0.048362
B737	0.027856	0.019041	0.036670
B767	0.034000	0.015302	0.052698

Least Squares Means for Effect Aircraft

Difference            Simultaneous 95%  
Between            Confidence Limits for  
i    j            Means            LSMean(i)-LSMean(j)

1	2	0.009711	-0.007583	0.027005
1	3	0.003567	-0.023226	0.030359
2	3	-0.006144	-0.031796	0.019507

Aircraft	Sulfur LSMEAN	Standard Error	Pr >  t	LSMEAN Number
A320	0.2860000	0.05076992	<.0001	1
B737	0.26531667	0.04145346	<.0001	2
B767	0.4240000	0.08793608	<.0001	3

----- Category=Incident -----

The GLM Procedure

Least Squares Means

Adjustment for Multiple Comparisons: Bonferroni

Least Squares Means for effect Aircraft

Pr > |t| for H0: LSMean(i)=LSMean(j)

Dependent Variable: Sulfur

i/j	1	2	3
1		1.0000	0.5518
2	1.0000		0.3382
3	0.5518	0.3382	

Sulfur

Aircraft	LSMEAN	95% Confidence Limits	
A320	0.286000	0.182454	0.389546
B737	0.265317	0.180772	0.349862
B767	0.424000	0.244653	0.603347

Least Squares Means for Effect Aircraft

		Difference	Simultaneous 95%	
		Between	Confidence Limits for	
i	j	Means	LSMean(i)-LSMean(j)	
1	2	0.020683	-0.145203	0.186570
1	3	-0.138000	-0.394990	0.118990
2	3	-0.158683	-0.404732	0.087366

Aircraft	Bromine LSMEAN	Standard Error	Pr >  t	LSMEAN Number
A320	0.28825833	0.05255640	<.0001	1
B737	0.43184444	0.04291212	<.0001	2
B767	0.48832500	0.09103035	<.0001	3

----- Category=Incident -----

The GLM Procedure

Least Squares Means

Adjustment for Multiple Comparisons: Bonferroni

Least Squares Means for effect Aircraft

Pr > |t| for H0: LSMean(i)=LSMean(j)

Dependent Variable: Bromine

i/j	1	2	3
1		0.1274	0.1989
2	0.1274		1.0000
3	0.1989	1.0000	

		Bromine	
Aircraft	LSMEAN	95% Confidence Limits	
A320	0.288258	0.181069	0.395448
B737	0.431844	0.344325	0.519364
B767	0.488325	0.302667	0.673983

Least Squares Means for Effect Aircraft

		Difference	Simultaneous 95%	
		Between	Confidence Limits for	
i	j	Means	LSMean(i)-LSMean(j)	
1	2	-0.143586	-0.315309	0.028137
1	3	-0.200067	-0.466099	0.065966
2	3	-0.056481	-0.311187	0.198226

----- Category=Used -----

The GLM Procedure

Class Level Information

Class	Levels	Values
-------	--------	--------

Aircraft 5 A320 B737 B747 B767 B777  
 Number of Observations Read 99  
 Number of Observations Used 99

----- Category=Used -----

The GLM Procedure

Dependent Variable: Phosphorus

Source	DF	Sum of Squares	Mean Square	F Value	Pr > F
Model	4	0.00837897	0.00209474	2.92	0.0252
Error	94	0.06744093	0.00071746		
Corrected Total	98	0.07581990			

R-Square 0.110511  
 Coeff Var 51.11714  
 Root MSE 0.026785  
 Phosphorus Mean 0.052400

Source	DF	Type III SS	Mean Square	F Value	Pr > F
Aircraft	4	0.00837897	0.00209474	2.92	0.0252

Parameter	Estimate	Standard Error	t Value	Pr >  t
Intercept	0.058275000 B	0.00345798	16.85	<.0001
Aircraft A320	-.0186386364 B	0.00878527	-2.12	0.0365
Aircraft B737	-.0029386364 B	0.00878527	-0.33	0.7388
Aircraft B747	-.0256477273 B	0.00878527	-2.92	0.0044
Aircraft B767	-.0103583333 B	0.01146882	-0.90	0.3687
Aircraft B777	0.000000000 B	.	.	.

NOTE: The X'X matrix has been found to be singular, and a generalized inverse was used to solve the normal equations. Terms whose estimates are followed by the letter 'B' are not uniquely estimable.

----- Category=Used -----

The GLM Procedure

Dependent Variable: Sulfur

Source	DF	Sum of Squares	Mean Square	F Value	Pr > F
Model	4	0.23224815	0.05806204	2.20	0.0745
Error	94	2.47727153	0.02635395		
Corrected Total	98	2.70951967			

R-Square 0.085716  
 Coeff Var 35.56820  
 Root MSE 0.162339  
 Sulfur Mean 0.456416

Source	DF	Type III SS	Mean Square	F Value	Pr > F
Aircraft	4	0.23224815	0.05806204	2.20	0.0745

Parameter	Estimate	Standard Error	t Value	Pr >  t
Intercept	0.456416	0.162339	2.81	0.0062
Aircraft A320	0.000000	0.000000	.	.
Aircraft B737	0.000000	0.000000	.	.
Aircraft B747	0.000000	0.000000	.	.
Aircraft B767	0.000000	0.000000	.	.
Aircraft B777	0.000000	0.000000	.	.

Intercept	0.4918983333 B	0.02095788	23.47	<.0001
Aircraft A320	-.1226256061 B	0.05324515	-2.30	0.0235
Aircraft B737	-.1044619697 B	0.05324515	-1.96	0.0527
Aircraft B747	-.0410165152 B	0.05324515	-0.77	0.4430
Aircraft B767	-.0939316667 B	0.06950941	-1.35	0.1798
Aircraft B777	0.0000000000 B	.	.	.

NOTE: The X'X matrix has been found to be singular, and a generalized inverse was used to solve the normal equations. Terms whose estimates are followed by the letter 'B' are not uniquely estimable.

----- Category=Used -----

The GLM Procedure

Dependent Variable: Bromine

Source	DF	Sum of Squares	Mean Square	F Value	Pr > F
Model	4	0.34560513	0.08640128	1.99	0.1027
Error	94	4.08676515	0.04347623		
Corrected Total	98	4.43237029			

Source	R-Square	Coeff Var	Root MSE	Bromine Mean
	0.077973	49.03275	0.208510	0.425245

Source	DF	Type III SS	Mean Square	F Value	Pr > F
Aircraft	4	0.34560513	0.08640128	1.99	0.1027

Parameter	Estimate	Standard Error	t Value	Pr >  t
Intercept	0.4614416667 B	0.02691846	17.14	<.0001
Aircraft A320	-.1249871212 B	0.06838851	-1.83	0.0708
Aircraft B737	0.0019856061 B	0.06838851	0.03	0.9769
Aircraft B747	-.1125871212 B	0.06838851	-1.65	0.1030
Aircraft B767	-.1653250000 B	0.08927845	-1.85	0.0672
Aircraft B777	0.0000000000 B	.	.	.

NOTE: The X'X matrix has been found to be singular, and a generalized inverse was used to solve the normal equations. Terms whose estimates are followed by the letter 'B' are not uniquely estimable.

----- Category=Used -----

The GLM Procedure

Levene's Test for Homogeneity of Phosphorus Variance

ANOVA of Absolute Deviations from Group Means

Source	DF	Sum of Squares	Mean Square	F Value	Pr > F
Aircraft	4	0.00427	0.00107	4.41	0.0026

Error	94	0.0228	0.000242
-------	----	--------	----------

O'Brien's Test for Homogeneity of Phosphorus Variance

ANOVA of O'Brien's Spread Variable, W = 0.5

		Sum of	Mean		
Source	DF	Squares	Square	F Value	Pr > F
Aircraft	4	0.000011	2.733E-6	2.15	0.0810
Error	94	0.000120	1.273E-6		

Brown and Forsythe's Test for Homogeneity of Phosphorus Variance

ANOVA of Absolute Deviations from Group Medians

		Sum of	Mean		
Source	DF	Squares	Square	F Value	Pr > F
Aircraft	4	0.00397	0.000994	3.10	0.0192
Error	94	0.0301	0.000321		

Bartlett's Test for Homogeneity of Phosphorus Variance

Source	DF	Chi-Square	Pr > ChiSq
Aircraft	4	21.7194	0.0002

Levene's Test for Homogeneity of Sulfur Variance

ANOVA of Absolute Deviations from Group Means

		Sum of	Mean		
Source	DF	Squares	Square	F Value	Pr > F
Aircraft	4	0.0503	0.0126	1.22	0.3062
Error	94	0.9665	0.0103		

----- Category=Used -----

The GLM Procedure

O'Brien's Test for Homogeneity of Sulfur Variance

ANOVA of O'Brien's Spread Variable, W = 0.5

		Sum of	Mean		
Source	DF	Squares	Square	F Value	Pr > F
Aircraft	4	0.00626	0.00156	0.90	0.4683
Error	94	0.1637	0.00174		

Brown and Forsythe's Test for Homogeneity of Sulfur Variance

ANOVA of Absolute Deviations from Group Medians

		Sum of	Mean		
Source	DF	Squares	Square	F Value	Pr > F
Aircraft	4	0.0527	0.0132	1.19	0.3214
Error	94	1.0432	0.0111		

Bartlett's Test for Homogeneity of Sulfur Variance

Source	DF	Chi-Square	Pr > ChiSq
Aircraft	4	5.8852	0.2079

Levene's Test for Homogeneity of Bromine Variance

ANOVA of Absolute Deviations from Group Means

Source	DF	Sum of Squares	Mean Square	F Value	Pr > F
Aircraft	4	0.2144	0.0536	3.80	0.0066
Error	94	1.3253	0.0141		

O'Brien's Test for Homogeneity of Bromine Variance

ANOVA of O'Brien's Spread Variable, W = 0.5

Source	DF	Sum of Squares	Mean Square	F Value	Pr > F
Aircraft	4	0.0498	0.0124	3.10	0.0192
Error	94	0.3778	0.00402		

----- Category=Used -----

The GLM Procedure

Brown and Forsythe's Test for Homogeneity of Bromine Variance

ANOVA of Absolute Deviations from Group Medians

Source	DF	Sum of Squares	Mean Square	F Value	Pr > F
Aircraft	4	0.2114	0.0529	3.52	0.0100
Error	94	1.4102	0.0150		

Bartlett's Test for Homogeneity of Bromine Variance

Source	DF	Chi-Square	Pr > ChiSq
Aircraft	4	13.1484	0.0106

Welch's ANOVA for Phosphorus

Source	DF	F Value	Pr > F
Aircraft	4.0000	7.55	0.0006
Error	21.4623		

Welch's ANOVA for Sulfur

Source	DF	F Value	Pr > F
Aircraft	4.0000	2.90	0.0478
Error	20.3635		

Welch's ANOVA for Bromine

Source	DF	F Value	Pr > F
Aircraft	4.0000	2.67	0.0626
Error	19.9063		

----- Category=Used -----

The GLM Procedure

Level of Aircraft	N	-----Phosphorus-----		-----Sulfur-----		-----Bromine-----	
		Mean	Std Dev	Mean	Std Dev	Mean	Std Dev
A320	11	0.03963636	0.01340644	0.36927273	0.09762773	0.33645455	0.13931162
B737	11	0.05533636	0.03008845	0.38743636	0.14694177	0.46342727	0.30269724
B747	11	0.03262727	0.00873591	0.45088182	0.12553661	0.34885455	0.10231460
B767	6	0.04791667	0.02012068	0.39796667	0.17390879	0.29611667	0.27339821
B777	60	0.05827500	0.03019796	0.49189833	0.17742151	0.46144167	0.20576505

----- Category=Used -----

The GLM Procedure

Least Squares Means

Adjustment for Multiple Comparisons: Bonferroni

Aircraft	Phosphorus LSMEAN	Standard Error	Pr >  t	LSMEAN Number
A320	0.03963636	0.00807610	<.0001	1
B737	0.05533636	0.00807610	<.0001	2
B747	0.03262727	0.00807610	0.0001	3
B767	0.04791667	0.01093509	<.0001	4
B777	0.05827500	0.00345798	<.0001	5

Least Squares Means for effect Aircraft

Pr > |t| for H0: LSMean(i)=LSMean(j)

Dependent Variable: Phosphorus

i/j	1	2	3	4	5
1		1.0000	1.0000	1.0000	0.3650
2	1.0000		0.4969	1.0000	1.0000
3	1.0000	0.4969		1.0000	0.0439
4	1.0000	1.0000	1.0000		1.0000
5	0.3650	1.0000	0.0439	1.0000	

Phosphorus

Aircraft	LSMEAN	95% Confidence Limits	
A320	0.039636	0.023601	0.055672
B737	0.055336	0.039301	0.071372
B747	0.032627	0.016592	0.048663
B767	0.047917	0.026205	0.069629
B777	0.058275	0.051409	0.065141

Least Squares Means for Effect Aircraft

Difference Between Means Simultaneous 95% Confidence Limits for

i	j	LSMean(i)-LSMean(j)	Simultaneous 95% Confidence Limits for	
1	2	-0.015700	-0.048534	0.017134
1	3	0.007009	-0.025825	0.039843
1	4	-0.008280	-0.047361	0.030800
1	5	-0.018639	-0.043895	0.006617
2	3	0.022709	-0.010125	0.055543



2	4	0.007420	-0.031661	0.046500
2	5	-0.002939	-0.028195	0.022317

----- Category=Used -----

The GLM Procedure

Least Squares Means

Adjustment for Multiple Comparisons: Bonferroni

Least Squares Means for Effect Aircraft

		Difference	Simultaneous 95%	
		Between	Confidence Limits for	
i	j	Means	LSMean(i)-LSMean(j)	
3	4	-0.015289	-0.054370	0.023791
3	5	-0.025648	-0.050904	-0.000392
4	5	-0.010358	-0.043329	0.022612

Aircraft	Sulfur LSMEAN	Standard Error	Pr >  t	LSMEAN Number
A320	0.36927273	0.04894705	<.0001	1
B737	0.38743636	0.04894705	<.0001	2
B747	0.45088182	0.04894705	<.0001	3
B767	0.39796667	0.06627462	<.0001	4
B777	0.49189833	0.02095788	<.0001	5

Least Squares Means for effect Aircraft

Pr > |t| for H0: LSMean(i)=LSMean(j)

Dependent Variable: Sulfur					
i/j	1	2	3	4	5
1		1.0000	1.0000	1.0000	0.2348
2	1.0000		1.0000	1.0000	0.5273
3	1.0000	1.0000		1.0000	1.0000
4	1.0000	1.0000	1.0000		1.0000
5	0.2348	0.5273	1.0000	1.0000	

Sulfur			
Aircraft	LSMEAN	95% Confidence Limits	
A320	0.369273	0.272087	0.466458
B737	0.387436	0.290251	0.484622
B747	0.450882	0.353696	0.548067
B767	0.397967	0.266377	0.529556
B777	0.491898	0.450286	0.533511

----- Category=Used -----

The GLM Procedure  
Least Squares Means  
Adjustment for Multiple Comparisons: Bonferroni  
Least Squares Means for Effect Aircraft

		Difference	Simultaneous 95%	
		Between	Confidence Limits for	
i	j	Means	LSMean(i)-LSMean(j)	
1	2	-0.018164	-0.217162	0.180835
1	3	-0.081609	-0.280607	0.117389
1	4	-0.028694	-0.265549	0.208162
1	5	-0.122626	-0.275695	0.030444
2	3	-0.063445	-0.262444	0.135553
2	4	-0.010530	-0.247386	0.226325
2	5	-0.104462	-0.257531	0.048607
3	4	0.052915	-0.183940	0.289771
3	5	-0.041017	-0.194086	0.112053
4	5	-0.093932	-0.293757	0.105894

Aircraft	Bromine LSMEAN	Standard Error	Pr >  t	LSMEAN Number
A320	0.33645455	0.06286799	<.0001	1
B737	0.46342727	0.06286799	<.0001	2
B747	0.34885455	0.06286799	<.0001	3
B767	0.29611667	0.08512366	0.0008	4
B777	0.46144167	0.02691846	<.0001	5

Least Squares Means for effect Aircraft  
Pr > |t| for H0: LSMean(i)=LSMean(j)

Dependent Variable: Bromine

i/j	1	2	3	4	5
1		1.0000	1.0000	1.0000	0.7078
2	1.0000		1.0000	1.0000	1.0000
3	1.0000	1.0000		1.0000	1.0000
4	1.0000	1.0000	1.0000		0.6719
5	0.7078	1.0000	1.0000	0.6719	

		Bromine	95% Confidence Limits	
Aircraft	LSMEAN			
A320	0.336455	0.211629	0.461280	
B737	0.463427	0.338601	0.588253	

----- Category=Used -----

The GLM Procedure  
Least Squares Means  
Bromine

Aircraft	LSMEAN	95% Confidence Limits	
B747	0.348855	0.224029	0.473680
B767	0.296117	0.127102	0.465132
B777	0.461442	0.407994	0.514889

Least Squares Means for Effect Aircraft

		Difference	Simultaneous 95%	
		Between	Confidence Limits for	
i	j	Means	LSMean(i)-LSMean(j)	
1	2	-0.126973	-0.382568	0.128622
1	3	-0.012400	-0.267995	0.243195
1	4	0.040338	-0.263881	0.344557
1	5	-0.124987	-0.321591	0.071616
2	3	0.114573	-0.141022	0.370168
2	4	0.167311	-0.136908	0.471530
2	5	0.001986	-0.194618	0.198589
3	4	0.052738	-0.251481	0.356957
3	5	-0.112587	-0.309191	0.084016
4	5	-0.165325	-0.421983	0.091333

----- Category=Incident -----

The Mixed Procedure

Model Information

Data Set	WORK.FILTER
Dependent Variable	Phosphorus
Covariance Structure	Variance Components
Group Effect	Aircraft
Estimation Method	REML
Residual Variance Method	None
Fixed Effects SE Method	Model-Based
Degrees of Freedom Method	Satterthwaite

Class Level Information

Class	Levels	Values
Aircraft	3	A320 B737 B767

Dimensions

Covariance Parameters	3
Columns in X	4
Columns in Z	0
Subjects	34
Max Obs Per Subject	1

Number of Observations

Number of Observations Read	34
Number of Observations Used	34
Number of Observations Not Used	0

Iteration History			
Iteration	Evaluations	-2 Res Log Like	Criterion
0	1	-153.19744834	
1	1	-156.13715819	0.00000000

Convergence criteria met.

----- Category=Incident -----

The Mixed Procedure

Covariance Parameter Estimates

Cov Parm	Group	Estimate
Residual	Aircraft A320	0.000477
Residual	Aircraft B737	0.000290
Residual	Aircraft B767	0.000081

Fit Statistics

-2 Res Log Likelihood	-156.1
AIC (smaller is better)	-150.1
AICC (smaller is better)	-149.2
BIC (smaller is better)	-145.6

Null Model Likelihood Ratio Test

DF	Chi-Square	Pr > ChiSq
2	2.94	0.2300

Type 3 Tests of Fixed Effects

Effect	Num		Den	F Value	Pr > F
	DF	DF			
Aircraft	2	13.6	1.02	0.3865	

Least Squares Means

Standard

Effect	Aircraft	Estimate	Error	DF	t Value	Pr >  t	Alpha	Lower	Upper
Aircraft	A320	0.03757	0.006306	11	5.96	<.0001	0.05	0.02369	0.05145
Aircraft	B737	0.02786	0.004014	17	6.94	<.0001	0.05	0.01939	0.03632
Aircraft	B767	0.03400	0.004491	3	7.57	0.0048	0.05	0.01971	0.04829

Differences of Least Squares Means

Standard

Effect	Aircraft_Aircraft	Estimate	Error	DF	t Value	Pr >  t	Adjustment	Adj P
Aircraft	A320 B737	0.009711	0.007475	19.6	1.30	0.2090	Bonferroni	0.6467
Aircraft	A320 B767	0.003567	0.007742	12.9	0.46	0.6527	Bonferroni	1.0000

----- Category=Incident -----

The Mixed Procedure

Differences of Least Squares Means

Standard

Effect	Aircraft_Aircraft	Estimate	Error	DF	t Value	Pr >  t	Adjustment	Adj P
Aircraft	B737 B767	-0.00614	0.006023	8.73	-1.02	0.3351	Bonferroni	0.9766

Differences of Least Squares Means

Effect	Aircraft_Aircraft	Alpha	Adj			
			Lower	Upper	Lower	Upper
Aircraft	A320 B737	0.05	-0.00590	0.02532	-0.01069	0.03012
Aircraft	A320 B767	0.05	-0.01318	0.02031	-0.01757	0.02470
Aircraft	B737 B767	0.05	-0.01984	0.007547	\-0.02259	0.01030

----- Category=Used -----

The Mixed Procedure

Model Information

Data Set	WORK.FILTER
Dependent Variable	Phosphorus
Covariance Structure	Variance Components
Group Effect	Aircraft
Estimation Method	REML
Residual Variance Method	None
Fixed Effects SE Method	Model-Based
Degrees of Freedom Method	Satterthwaite

Class Level Information

Class	Levels	Values
Aircraft	5	A320 B737 B747 B767 B777

Dimensions

Covariance Parameters	5
Columns in X	6
Columns in Z	0
Subjects	99
Max Obs Per Subject	1

Number of Observations

Number of Observations Read	99
Number of Observations Used	99
Number of Observations Not Used	0

Iteration History

Iteration	Evaluations	-2 Res Log Like	Criterion
0	1	-400.70076896	
1	1	-423.33652668	0.00000000

Convergence criteria met.

----- Category=Used -----

The Mixed Procedure

Covariance Parameter Estimates

Cov Parm	Group	Estimate
Residual	Aircraft A320	0.000180
Residual	Aircraft B737	0.000905
Residual	Aircraft B747	0.000076
Residual	Aircraft B767	0.000405
Residual	Aircraft B777	0.000912

Fit Statistics

-2 Res Log Likelihood	-423.3
AIC (smaller is better)	-413.3
AICC (smaller is better)	-412.7
BIC (smaller is better)	-400.4

Null Model Likelihood Ratio Test

DF	Chi-Square	Pr > ChiSq
4	22.64	0.0001

Type 3 Tests of Fixed Effects

Effect	Num		Den	F Value	Pr > F
	DF	DF			
Aircraft	4	23.1	8.25	0.0003	

Least Squares Means

Effect	Aircraft	Standard		DF	t Value	Pr >  t	Alpha	Lower	Upper
		Estimate	Error						
Aircraft	A320	0.03964	0.004042	10	9.81	<.0001	0.05	0.03063	0.04864
Aircraft	B737	0.05534	0.009072	10	6.10	0.0001	0.05	0.03512	0.07555
Aircraft	B747	0.03263	0.002634	10	12.39	<.0001	0.05	0.02676	0.03850
Aircraft	B767	0.04792	0.008214	5	5.83	0.0021	0.05	0.02680	0.06903
Aircraft	B777	0.05828	0.003899	59	14.95	<.0001	0.05	0.05047	0.06608

----- Category=Used -----

The Mixed Procedure

Differences of Least Squares Means

Effect	Aircraft_Aircraft		Estimate	Error	DF	t Value	Pr >  t	Adjustment	Adj P
	Standard	Standard							
Aircraft	A320	B737	-0.01570	0.009932	13.8	-1.58	0.1365	Bonferroni	1.0000
Aircraft	A320	B747	0.007009	0.004825	17.2	1.45	0.1643	Bonferroni	1.0000
Aircraft	A320	B767	-0.00828	0.009155	7.5	-0.90	0.3939	Bonferroni	1.0000
Aircraft	A320	B777	-0.01864	0.005616	32.5	-3.32	0.0022	Bonferroni	0.0298
Aircraft	B737	B747	0.02271	0.009447	11.7	2.40	0.0338	Bonferroni	0.2465
Aircraft	B737	B767	0.007420	0.01224	14.1	0.61	0.5540	Bonferroni	1.0000

Aircraft	B737	B777	-0.00294	0.009874	14	-0.30	0.7704	Bonferroni	1.0000
Aircraft	B747	B767	-0.01529	0.008626	6.05	-1.77	0.1263	Bonferroni	0.8953
Aircraft	B747	B777	-0.02565	0.004705	56.1	-5.45	<.0001	Bonferroni	0.0002
Aircraft	B767	B777	-0.01036	0.009092	7.47	-1.14	0.2898	Bonferroni	1.0000

Differences of Least Squares Means

Effect	Aircraft_Aircraft	Alpha	Adj			
			Lower	Upper	Lower	Upper
Aircraft	A320 B737	0.05	-0.03703	0.005628	-0.04652	0.01512
Aircraft	A320 B747	0.05	-0.00316	0.01718	-0.00796	0.02198
Aircraft	A320 B767	0.05	-0.02964	0.01308	-0.03669	0.02013
Aircraft	A320 B777	0.05	-0.03007	-0.00721	-0.03606	-0.00121
Aircraft	B737 B747	0.05	0.002063	0.04336	-0.00660	0.05202
Aircraft	B737 B767	0.05	-0.01881	0.03365	-0.03056	0.04540
Aircraft	B737 B777	0.05	-0.02412	0.01825	-0.03358	0.02770
Aircraft	B747 B767	0.05	-0.03636	0.005777	-0.04206	0.01148
Aircraft	B747 B777	0.05	-0.03507	-0.01622	-0.04025	-0.01105
Aircraft	B767 B777	0.05	-0.03159	0.01087	-0.03857	0.01786

----- Category=Incident -----

The Mixed Procedure

Model Information

Data Set WORK.FILTER  
 Dependent Variable Sulfur  
 Covariance Structure Variance Components  
 Group Effect Aircraft  
 Estimation Method REML  
 Residual Variance Method None  
 Fixed Effects SE Method Model-Based  
 Degrees of Freedom Method Satterthwaite

Class Level Information

Class	Levels	Values
Aircraft	3	A320 B737 B767

Dimensions

Covariance Parameters	3
Columns in X	4
Columns in Z	0
Subjects	34
Max Obs Per Subject	1

Number of Observations

Number of Observations Read	34
Number of Observations Used	34

Number of Observations Not Used 0

Iteration History

Iteration	Evaluations	-2 Res Log Like	Criterion
0	1	-13.02011035	
1	1	-18.21685778	0.00000000

Convergence criteria met.

----- Category=Incident -----

The Mixed Procedure

Covariance Parameter Estimates

Cov Parm	Group	Estimate
Residual	Aircraft A320	0.03225
Residual	Aircraft B737	0.03513
Residual	Aircraft B767	0.002281

Fit Statistics

-2 Res Log Likelihood	-18.2
AIC (smaller is better)	-12.2
AICC (smaller is better)	-11.3
BIC (smaller is better)	-7.6

Null Model Likelihood Ratio Test

DF	Chi-Square	Pr > ChiSq
2	5.20	0.0744

Type 3 Tests of Fixed Effects

Effect	Num	Den	F Value	Pr > F
	DF	DF		
Aircraft	2	20.8	6.66	0.0058

Least Squares Means

Effect	Aircraft	Estimate	Standard Error	DF	t Value	Pr >  t	Alpha	Standard	
								Lower	Upper
Aircraft	A320	0.2860	0.05184	11	5.52	0.0002	0.05	0.1719	0.4001
Aircraft	B737	0.2653	0.04418	17	6.01	<.0001	0.05	0.1721	0.3585
Aircraft	B767	0.4240	0.02388	3	17.76	0.0004	0.05	0.3480	0.5000

Differences of Least Squares Means

Effect	Aircraft_Aircraft	Estimate	Standard Error	DF	t Value	Pr >  t	Adjustment	Standard	
								Adj P	
Aircraft	A320 B737	0.02068	0.06811	24.4	0.30	0.7640	Bonferroni	1.0000	
Aircraft	A320 B767	-0.1380	0.05708	13.9	-2.42	0.0300	Bonferroni	0.0746	

----- Category=Incident -----



The Mixed Procedure  
Differences of Least Squares Means  
Standard

Effect	Aircraft_Aircraft	Estimate	Error	DF	t Value	Pr >  t	Adjustment	Adj P
Aircraft	B737 B767	-0.1587	0.05022	19.1	-3.16	0.0051	Bonferroni	0.0143

Differences of Least Squares Means

Effect	Aircraft_Aircraft	Alpha			Adj	Adj
			Lower	Upper	Lower	Upper
Aircraft	A320 B737	0.05	-0.1198	0.1611	-0.1566	0.1980
Aircraft	A320 B767	0.05	-0.2605	-0.01548	-0.2866	0.01058
Aircraft	B737 B767	0.05	-0.2637	-0.05362	-0.2894	-0.02796

----- Category=Used -----

The Mixed Procedure

Model Information

Data Set	WORK.FILTER
Dependent Variable	Sulfur
Covariance Structure	Variance Components
Group Effect	Aircraft
Estimation Method	REML
Residual Variance Method	None
Fixed Effects SE Method	Model-Based
Degrees of Freedom Method	Satterthwaite

Class Level Information

Class	Levels	Values
Aircraft	5	A320 B737 B747 B767 B777

Dimensions

Covariance Parameters	5
Columns in X	6
Columns in Z	0
Subjects	99
Max Obs Per Subject	1

Number of Observations

Number of Observations Read	99
Number of Observations Used	99
Number of Observations Not Used	0

Iteration History

Iteration	Evaluations	-2 Res Log Like	Criterion
0	1	-61.95664565	
1	1	-68.09019741	0.00000000

Convergence criteria met.

----- Category=Used -----

The Mixed Procedure

Covariance Parameter Estimates

Cov Parm	Group	Estimate
Residual	Aircraft A320	0.009531
Residual	Aircraft B737	0.02159
Residual	Aircraft B747	0.01576
Residual	Aircraft B767	0.03024
Residual	Aircraft B777	0.03148

Fit Statistics

-2 Res Log Likelihood	-68.1
AIC (smaller is better)	-58.1
AICC (smaller is better)	-57.4
BIC (smaller is better)	-45.1

Null Model Likelihood Ratio Test

DF	Chi-Square	Pr > ChiSq
4	6.13	0.1894

Type 3 Tests of Fixed Effects

Effect	Num		F Value	Pr > F
	DF	Den		
Aircraft	4	15.8	3.18	0.0426

Least Squares Means

Effect	Aircraft	Standard							
		Estimate	Error	DF	t Value	Pr >  t	Alpha	Lower	Upper
Aircraft	A320	0.3693	0.02944	10	12.54	<.0001	0.05	0.3037	0.4349
Aircraft	B737	0.3874	0.04430	10	8.74	<.0001	0.05	0.2887	0.4862
Aircraft	B747	0.4509	0.03785	10	11.91	<.0001	0.05	0.3665	0.5352
Aircraft	B767	0.3980	0.07100	5	5.61	0.0025	0.05	0.2155	0.5805
Aircraft	B777	0.4919	0.02291	59	21.48	<.0001	0.05	0.4461	0.5377

----- Category=Used -----

The Mixed Procedure

Differences of Least Squares Means

Effect	Aircraft_Aircraft		Standard						
	Estimate	Error	DF	t Value	Pr >  t	Adjustment	Adj P		
Aircraft	A320 B737	-0.01816	0.05319	17.4	-0.34	0.7368	Bonferroni	1.0000	
Aircraft	A320 B747	-0.08161	0.04795	18.9	-1.70	0.1052	Bonferroni	1.0000	
Aircraft	A320 B767	-0.02869	0.07686	6.77	-0.37	0.7203	Bonferroni	1.0000	
Aircraft	A320 B777	-0.1226	0.03730	24.3	-3.29	0.0031	Bonferroni	0.0472	
Aircraft	B737 B747	-0.06345	0.05827	19.5	-1.09	0.2895	Bonferroni	1.0000	
Aircraft	B737 B767	-0.01053	0.08369	8.97	-0.13	0.9026	Bonferroni	1.0000	

Aircraft	B737	B777	-0.1045	0.04988	15.9	-2.09	0.0526	Bonferroni	0.5275
Aircraft	B747	B767	0.05292	0.08046	7.93	0.66	0.5294	Bonferroni	1.0000
Aircraft	B747	B777	-0.04102	0.04424	18.3	-0.93	0.3660	Bonferroni	1.0000
Aircraft	B767	B777	-0.09393	0.07460	6.09	-1.26	0.2541	Bonferroni	1.0000

Differences of Least Squares Means

Effect	Aircraft_Aircraft	Alpha			Adj		Adj	
			Lower	Upper	Lower	Upper		
Aircraft	A320 B737	0.05	-0.1302	0.09387	-0.1916	0.1552		
Aircraft	A320 B747	0.05	-0.1820	0.01880	-0.2379	0.07470		
Aircraft	A320 B767	0.05	-0.2117	0.1543	-0.2792	0.2219		
Aircraft	A320 B777	0.05	-0.1996	-0.04569	-0.2442	-0.00104		
Aircraft	B737 B747	0.05	-0.1852	0.05830	-0.2534	0.1265		
Aircraft	B737 B767	0.05	-0.1999	0.1789	-0.2833	0.2623		
Aircraft	B737 B777	0.05	-0.2103	0.001340	-0.2670	0.05812		
Aircraft	B747 B767	0.05	-0.1329	0.2388	-0.2094	0.3152		
Aircraft	B747 B777	0.05	-0.1339	0.05184	-0.1852	0.1032		
Aircraft	B767 B777	0.05	-0.2758	0.08796	-0.3371	0.1493		

----- Category=Incident -----

The Mixed Procedure

Model Information

Data Set	WORK.FILTER
Dependent Variable	Bromine
Covariance Structure	Variance Components
Group Effect	Aircraft
Estimation Method	REML
Residual Variance Method	None
Fixed Effects SE Method	Model-Based
Degrees of Freedom Method	Satterthwaite

Class Level Information

Class	Levels	Values
Aircraft	3	A320 B737 B767

Dimensions

Covariance Parameters	3
Columns in X	4
Columns in Z	0
Subjects	34
Max Obs Per Subject	1

Number of Observations

Number of Observations Read	34
Number of Observations Used	34
Number of Observations Not Used	0

Iteration History

Iteration	Evaluations	-2 Res Log Like	Criterion
0	1	-10.87597485	
1	1	-18.09178549	0.00000000

Convergence criteria met.

----- Category=Incident -----

The Mixed Procedure

Covariance Parameter Estimates

Cov Parm	Group	Estimate
Residual	Aircraft A320	0.01470
Residual	Aircraft B737	0.04991
Residual	Aircraft B767	0.005797

Fit Statistics

-2 Res Log Likelihood	-18.1
AIC (smaller is better)	-12.1
AICC (smaller is better)	-11.2
BIC (smaller is better)	-7.5

Null Model Likelihood Ratio Test

DF	Chi-Square	Pr > ChiSq
2	7.22	0.0271

Type 3 Tests of Fixed Effects

Effect	Num Den		F Value	Pr > F
	DF	DF		
Aircraft	2	13.6	7.88	0.0053

Least Squares Means

Effect	Aircraft	Estimate	Standard		t Value	Pr >  t	Alpha	Lower	Upper
			Error	DF					
Aircraft	A320	0.2883	0.03500	11	8.24	<.0001	0.05	0.2112	0.3653
Aircraft	B737	0.4318	0.05266	17	8.20	<.0001	0.05	0.3208	0.5429
Aircraft	B767	0.4883	0.03807	3	12.83	0.0010	0.05	0.3672	0.6095

Differences of Least Squares Means

Effect	Aircraft_Aircraft	Estimate	Standard		t Value	Pr >  t	Adjustment	Adj P
			Error	DF				
Aircraft	A320 B737	-0.1436	0.06323	27.2	-2.27	0.0313	Bonferroni	0.1197
Aircraft	A320 B767	-0.2001	0.05172	8.55	-3.87	0.0042	Bonferroni	0.0053

----- Category=Incident -----

The Mixed Procedure

Differences of Least Squares Means								
Standard								
Effect	Aircraft_Aircraft	Estimate	Error	DF	t Value	Pr >  t	Adjustment	Adj P
Aircraft	B737 B767	-0.05648	0.06498	15.5	-0.87	0.3980	Bonferroni	1.0000

Differences of Least Squares Means						
Alpha						
Effect	Aircraft	_Aircraft	Alpha	Lower	Upper	Adj
				Lower	Upper	Adj
Aircraft	A320	B737	0.05	-0.2733	-0.01389	0.02885
Aircraft	A320	B767	0.05	-0.3180	-0.08213	-0.05903
Aircraft	B737	B767	0.05	-0.1946	0.08165	0.1207

----- Category=Used -----

The Mixed Procedure

Model Information

Data Set	WORK.FILTER
Dependent Variable	Bromine
Covariance Structure	Variance Components
Group Effect	Aircraft
Estimation Method	REML
Residual Variance Method	None
Fixed Effects SE Method	Model-Based
Degrees of Freedom Method	Satterthwaite

Class Level Information

Class	Levels	Values
Aircraft	5	A320 B737 B747 B767 B777

Dimensions

Covariance Parameters	5
Columns in X	6
Columns in Z	0
Subjects	99
Max Obs Per Subject	1

Number of Observations

Number of Observations Read	99
Number of Observations Used	99
Number of Observations Not Used	0

Iteration History

Iteration	Evaluations	-2 Res Log Like	Criterion
0	1	-14.90062385	
1	1	-28.60376311	0.00000000

Convergence criteria met.

----- Category=Used -----

The Mixed Procedure

Covariance Parameter Estimates

Cov Parm	Group	Estimate
Residual	Aircraft A320	0.01941
Residual	Aircraft B737	0.09163
Residual	Aircraft B747	0.01047
Residual	Aircraft B767	0.07475
Residual	Aircraft B777	0.04234

Fit Statistics

-2 Res Log Likelihood	-28.6
AIC (smaller is better)	-18.6
AICC (smaller is better)	-17.9
BIC (smaller is better)	-5.6

Null Model Likelihood Ratio Test

DF	Chi-Square	Pr > ChiSq
4	13.70	0.0083

Type 3 Tests of Fixed Effects

Effect	Num		Den		F Value	Pr > F
	DF	DF	DF	DF		
Aircraft	4	12			2.93	0.0665

Least Squares Means

Effect	Aircraft	Standard							
		Estimate	Error	DF	t Value	Pr >  t	Alpha	Lower	Upper
Aircraft	A320	0.3365	0.04200	10	8.01	<.0001	0.05	0.2429	0.4300
Aircraft	B737	0.4634	0.09127	10	5.08	0.0005	0.05	0.2601	0.6668
Aircraft	B747	0.3489	0.03085	10	11.31	<.0001	0.05	0.2801	0.4176
Aircraft	B767	0.2961	0.1116	5	2.65	0.0453	0.05	0.009203	0.5830
Aircraft	B777	0.4614	0.02656	59	17.37	<.0001	0.05	0.4083	0.5146

----- Category=Used -----

The Mixed Procedure

Differences of Least Squares Means

Effect	Aircraft_Aircraft		Standard						
	Estimate	Error	DF	t Value	Pr >  t	Adjustment	AdjP		
Aircraft	A320	B737	-0.1270	0.1005	14.1	-1.26	0.2269	Bonferroni	1.0000
Aircraft	A320	B747	-0.01240	0.05212	18.4	-0.24	0.8146	Bonferroni	1.0000
Aircraft	A320	B767	0.04034	0.1193	6.45	0.34	0.7459	Bonferroni	1.0000
Aircraft	A320	B777	-0.1250	0.04970	19.1	-2.51	0.0210	Bonferroni	0.2723
Aircraft	B737	B747	0.1146	0.09634	12.3	1.19	0.2569	Bonferroni	1.0000
Aircraft	B737	B767	0.1673	0.1442	11.4	1.16	0.2696	Bonferroni	1.0000

Aircraft	B737	B777	0.001986	0.09505	11.8	0.02	0.9837	Bonferroni	1.0000
Aircraft	B747	B767	0.05274	0.1158	5.78	0.46	0.6654	Bonferroni	1.0000
Aircraft	B747	B777	-0.1126	0.04071	27.7	-2.77	0.0100	Bonferroni	0.1716
Aircraft	B767	B777	-0.1653	0.1147	5.58	-1.44	0.2033	Bonferroni	1.0000

Differences of Least Squares Means

Effect	Aircraft_Aircraft	Alpha	Lower	Upper	Adj	
					Lower	Upper
Aircraft	A320 B737	0.05	-0.3424	0.08843	-0.4717	0.2178
Aircraft	A320 B747	0.05	-0.1217	0.09694	-0.1912	0.1664
Aircraft	A320 B767	0.05	-0.2466	0.3273	-0.3689	0.4496
Aircraft	A320 B777	0.05	-0.2290	-0.02100	-0.2955	0.04556
Aircraft	B737 B747	0.05	-0.09485	0.3240	-0.2160	0.4452
Aircraft	B737 B767	0.05	-0.1487	0.4834	-0.3274	0.6621
Aircraft	B737 B777	0.05	-0.2056	0.2096	-0.3242	0.3282
Aircraft	B747 B767	0.05	-0.2333	0.3388	-0.3446	0.4501
Aircraft	B747 B777	0.05	-0.1960	-0.02916	-0.2523	0.02711
Aircraft	B767 B777	0.05	-0.4513	0.1206	-0.5590	0.2284

## Appendix B - Summarized GC/MS Analytical Report on Used Aircraft Cabin Air Recirculation Filters

**Table B-1: GC/MS results for used filters**

Filter Serial No.	Filter ID	m-TCP	Unk Isomer1	Unk Isomer2	p-TCP	Ratio of meta- to isomer1	Ratio of unk isomer1 unk isomer2	TCP Peak pattern of m/z 368	Filter Type	Aircraft Model
		RT=21.9 minutes	RT=22.4 minutes	RT=22.4 minutes	RT=23.4 minutes			Synthetic hydrocarbon 113, 85amu		
		ng/cm <sup>2</sup> in filter	ng/cm <sup>2</sup> in filter	ng/cm <sup>2</sup> in filter	ng/cm <sup>2</sup> in filter					
1.	11S754	25.9	32.3	14.8	0.6	0.80	0.46	YES/no	Keddeg	B777
2.	12HD94	N/A	N/A	N/A	N/A	N/A	N/A	N/A	Keddeg	A320
3.	163B4J	7.6	9.4	2.3	0.0	0.81	0.24	No/no	Donaldson	B747
4.	17BDAR	14.5	5.2	0.0	0.0	0.86	0.0	No/no	Keddeg	B777
5.	1F3555	2.8	3.3	0.8	0.0	0.83	0.24	No/no	Pall	B777
6.	27QR6F	14.0	19.0	5.7	2.5	0.73	0.30	Maybe/no	Donaldson	B777
7.	2965CL	5.1	6.0	0.1	0.0	0.85	0.01	No/no	Keddeg	A320
8.	2D968E	4.1	5.0	0.8	0.0	0.83	0.15	No/no	Puralator	B777
9.	2U1KD6	25.8	31.6	7.4	4.1	0.82	0.23	Maybe/yes	Keddeg	A320
10.	3C297F	22.3	27.4	12.7	1.3	0.81	0.46	YES/YES	Pall	B737
11.	3Q5J9L	6.4	6.7	0.8	0.0	0.96	0.12	No/no	Pall	B767
12.	43RTYZ	4.4	5.1	0.8	0.0	0.86	0.16	No/no	Pall	B777
13.	46NKJF	4.4	4.2	0.5	0.0	1.04	0.11	No/no	Keddeg	B777
14.	4S190C	5.5	7.2	2.2	0.0	0.77	0.31	No/no	Puralator	B777
15.	584C32	7.8	8.9	2.7	0.0	0.88	0.31	No/no	Pall	B777
16.	5H2F01	6.8	7.5	1.9	0.0	0.91	0.25	No/no	Pall	B777
17.	6025ES	5.0	5.7	0.0	0.0	0.88	0.00	No/no	Keddeg	B777
18.	73J43M	4.0	5.4	1.9	0.0	0.75	0.35	No/no	Pall	B777
19.	75G8FW	3.2	4.0	0.0	0.0	0.81	0.00	No/no	Donaldson	B777
20.	77G4CJ	0.0	0.0	0.0	0.0	0.0	0.0	No/no	Donaldson	B777
21.	794TWZ	17.9	21.2	9.1	1.1	0.85	0.43	Yes/YES	Pall	B777
22.	7GH325	9.6	11.5	2.0	0.0	0.83	0.17	No/no	Donaldson	B777
23.	7WQF45	6.2	8.0	3.1	0.0	0.77	0.39	No/no	Pall	B777
24.	7YSE6N	4.0	4.3	0.0	0.0	0.94	0.00	No/no	Keddeg	B777
25.	7ZMK52	18.1	21.4	9.1	0.8	0.85	0.42	Yes/YES	Puralator	B777
26.	83MIA9	6.2	7.4	2.4	0.0	0.84	0.32	No/no	Puralator	B777
27.	85HXNS	7.4	10.4	2.4	4.8	0.71	0.23	No/no	Pall	B747
28.	883STV	11.1	11.6	2.5	0.4	0.96	0.21	Maybe/maybe	Keddeg	A320
29.	8P6G4X	5.7	7.3	2.2	0.0	0.78	0.30	No/no	Pall	B737
30.	907BVA	10.8	12.9	3.2	0.6	0.84	0.25	Maybe/	Donaldson	B777



31.	9E003T	3.6	3.9	0.0	0.0	0.91	0.00	No/no	Pall	B777
32.	9RZMC2	10.6	14.2	6.8	1.2	0.75	0.48	YES/no	Puralator	B777
33.	AA61L3	8.9	10.9	3.0	9.8	0.82	0.28	No/no	Donaldson	B747
34.	ADJ145	14.1	19.7	6.3	0.0	0.72	0.32	No/no	Donaldson	B777
35.	AO354G	2.9	3.3	0.0	0.0	0.89	0.00	No/no	Donaldson	B777
36.	AI644T	0.0	0.0	0.0	0.0	0.00	0.00	No/no	Pall	B777
37.	B322IJ	5.1	7.5	1.0	0.0	0.68	0.13	No/no	Keddeg	B737
38.	B92YNB	4.3	4.9	0.7	0.0	0.87	0.13	No/no	Pall	B777
39.	BHU548	251.7	357.4	183.8	26.8	0.70	0.51	YES/YES	Keddeg	B737
40.	BO14NE	35.6	42.1	19.7	1.0	0.85	0.47	Yes/maybe	Puralator	B777
41.	BRT6RD	8.1	10.4	4.0	0.0	0.77	0.38	No/no	Puralator	B777
42.	CE9B16	9.2	10.4	2.6	0.3	0.88	0.25	No/no	Keddeg	A320
43.	CP163W	0.0	2.5	0.0	0.0	0.00	0.00	No/no	Donaldson	B747
44.	CRH8ES	6.6	7.3	1.3	0.0	0.90	0.18	No/no	Keddeg	B777
45.	DAW454	3.1	3.8	0.0	0.0	0.83	0.00	No/no	Keddeg	B777
46.	DR87FE	10.0	10.9	2.2	0.1	0.92	0.20	Maybe/no	Keddeg	B777
47.	DSF6UE	6.9	8.6	1.7	0.0	0.80	0.20	no	Keddeg	B777
48.	E63JV3	116.3	155.8	69.9	7.5	0.75	0.45	YES/YES	Keddeg	B737
49.	ESF946	4.4	5.7	1.4	0.0	0.77	0.24	No/no	Pall	B777
50.	F1JH39	3.7	4.7	0.0	0.0	0.78	0.00	No/no	Keddeg	B737
51.	FTR175	7.2	8.8	1.8	0.0	0.81	0.20	No/no	Keddeg	B737
52.	FWX130	16.0	25.1	10.8	1.2	0.64	0.43	Maybe/no	Keddeg	B777
53.	G48MJ6	15.4	19.5	8.1	0.0	0.79	0.41	No/no	Pall	B777
54.	G8UX4V	2.8	3.2	0.0	0.0	0.88	0.0	No/no	Donaldson	B777
55.	GF68X3	4.3	5.8	0.6	0.0	0.75	0.10	No/no	Puralator	B777
56.	GO9JVE	4.6	6.2	0.0	1.2	0.75	0.00	No/no	Keddeg	B747
57.	HFU84F	2.9	3.0	0.0	0.0	0.95	0.00	No/no	Pall	B767
58.	HGD63H	27.0	30.6	9.8	0.3	0.88	0.32	Maybe/no	Keddeg	B777
59.	HIDE4H	3.6	4.4	0.0	0.0	0.82	0.00	No/no	Keddeg	A320
60.	HFD9LM	4.2	4.2	0.0	0.0	1.01	0.00	No/no	Keddeg	B777
61.	HME4A8	3.7	4.8	0.0	0.0	0.77	0.00	No/no	Pall	B777
62.	I89VFS	3.7	5.3	0.5	0.0	0.69	0.08	No/no	Keddeg	B777
63.	IS78FS	11.1	13.7	5.9	0.6	0.81	0.43	YES/no	Puralator	B777
64.	IU74E2	8.5	10.3	3.3	0.0	0.82	0.32	No/no	Pall	B737
65.	IUY3T4	0.0	0.0	0.0	0.0	0.0	0.00	No/no	Pall	B767
66.	J9GF37	10.0	9.8	1.5	0.0	1.02	0.15	No/no	Pall	B767
67.	JD5RT2	10.2	12.8	5.3	0.5	0.80	0.41	YES/no	Pall	B777
68.	JGFD6G	13.1	18.1	6.5	1.5	0.72	0.36	YES/no	Pall	B747
69.	JHHCD2	5.2	6.1	1.1	0.0	0.86	0.18	No/no	Pall	B737
70.	JR3584	10.3	14.4	6.1	0.8	0.71	0.42	YES/no	Puralator	B777
71.	K76GHR	3.1	3.5	0.0	0.0	0.90	0.00	No/no	Keddeg	A320

72.	KI9846	4.4	4.9	0.5	0.0	0.90	0.09	No/no	Pall	B777
73.	L6159B	5.8	7.2	1.5	1.0	0.80	0.20	No/no	Donaldson	B747
74.	LF4EQ2	0.0	2.6	0.0	0.0	0.0	0.0	No/no	Keddeg	B767
75.	LM6524	9.7	12.1	3.5	0.6	0.80	0.29	No/no	Donaldson	B747
76.	LR8C66	6.9	7.9	1.5	0.0	0.87	0.19	No/no	Keddeg	B777
77.	M6AAM6	7.8	9.8	2.6	1.2	0.80	0.27	No/no	Donaldson	B747
78.	MA7ET3	16.0	25.0	11.7	1.0	0.64	0.47	Maybe/no	Keddeg	B777
79.	MB6LV1	5.8	7.3	1.1	0.0	0.79	0.14	No/no	Keddeg	B747
80.	MH64SL	8.1	10.2	1.8	0.0	0.79	0.18	No/no	Donaldson	B777
81.	MSU4TD	2.7	2.9	0.0	0.0	0.91	0.00	No/no	Puralator	B777
82.	MTCL37	4.5	5.5	1.2	0.0	0.82	0.22	No/no	Puralator	B777
83.	N6D5A7	3.4	4.3	0.6	0.0	0.79	0.13	No/no	Pall	B777
84.	NZ2T7W	7.5	8.5	1.5	0.0	0.89	0.18	No/no	Keddeg	A320
85.	NM81X7	6.8	7.7	1.2	0.0	0.88	0.15	No/no	Pall	B777
86.	PL2IX1	3.6	3.8	0.0	0.0	0.93	0.00	No/no	Donaldson	B747
87.	PN38IZ	3.6	4.3	0.4	0.0	0.85	0.08	No/no	Pall	B777
88.	QOX417	4.0	5.3	0.0	0.0	0.75	0.00	No/no	Keddeg	B737
89.	R5BH23	4.5	5.8	1.2	0.0	0.78	0.21	No/no	Pall	B777
90.	R67R85	3.9	4.3	0.0	0.0	0.90	0.00	No/no	Pall	B777
91.	RP14D3	4.7	6.4	0.6	0.0	0.73	0.09	No/no	Keddeg	B737
92.	SJA33J	0.0	0.0	0.0	0.0	0.0	0.0	No/no	Keddeg	A320
93.	STJH77	5.8	3.4	0.0	0.0	1.69	0.00	No/no	Puralator	B777
94.	T007ML	2.9	3.4	0.0	0.0	0.84	0.00	No/no	Keddeg	A320
95.	TBD533	8.0	10.6	4.2	0.0	0.76	0.39	No/no	Pall	B777
96.	TC66HR	7.3	7.6	1.9	0.0	0.97	0.25	No/no	Pall	B767
97.	TJ66RG	5.9	7.5	2.4	0.0	0.79	0.31	No/no	Puralator	B777
98.	TT15A5	0.7	0.0	0.0	0.0	0.0	0.00	No/no	Keddeg	B737
99.	U44MXV	8.8	8.4	2.4	0.0	1.04	0.28	No/no	Keddeg	A320
100.	U5D8UN	7.6	9.1	2.0	0.0	0.84	0.22	No/no	Pall	B767
101.	UGA145	21.0	25.9	11.9	0.5	0.81	0.46	YES/maybe	Puralator	B777
102.	VDSA46	9.2	10.4	2.5	0.0	0.89	0.24	No/no	Donaldson	B777
103.	VT23AC	2.2	2.2	0.0	0.0	1.02	0.00	No/no	Puralator	B777
104.	W9E578	10.0	12.2	3.8	0.7	0.82	0.31	Maybe/no	Donaldson	B747
105.	WAQE67	5.5	6.0	0.6	0.0	0.92	0.10	No/no	Keddeg	B777
106.	WBH9G4	N/A	N/A	N/A	N/A	N/A	N/A	N/A	Keddeg	B777
107.	WH3JMZ	10.2	12.8	5.0	0.5	0.80	0.39	YES/no	Puralator	B777
108.	WR2F6B	4.0	4.3	0.0	0.0	0.92	0.00	No/no	Pall	B767
109.	YEK752	4.5	5.5	0.4	0.0	0.81	0.07	No/no	Keddeg	A320
110.	ZD15ZA	2.9	3.3	0.0	0.0	0.89	0.0	No/no	Donaldson	B747
111.	Blank	0.0	0.0	0.0	0.0	0.00	0.00	No/no	-	-

**Table B-2: GC/MS results for incident filters**

Filter Serial No.	Filter ID	m-TCP	Unk Isomer1	Unk Isomer2	p-TCP	Ratio of meta- to isomer1	Ratio of unk isomer1 unk isomer2	TCP Peak pattern of m/z 368	Filter Type	Aircraft Model
		RT=21.9 minutes	RT=22.4 minutes	RT=22.4 minutes	RT=23.4 minutes			Synthetic hydrocarbon 113, 85amu		
		ng/cm <sup>2</sup> in filter	ng/cm <sup>2</sup> in filter	ng/cm <sup>2</sup> in filter	ng/cm <sup>2</sup> in filter					
1.	23937	5.1	0.0	1.4	0.0	0.84	0.23	No/no	Keddeg	A320
2.	24034	5.4	6.9	2.1	0.0	0.78	0.30	No/no	Keddeg	A320
3.	26701	19.6	18.5	6.5	0.0	1.06	0.35	No/no	Keddeg	A320
4.	27055	10.0	12.7	4.7	0.0	0.79	0.37	No/no	Keddeg	A320
5.	27165	42.4	42.0	19.5	2.2	1.01	0.46	YES/yes	Keddeg	A320
6.	27200	38.3	48.8	25.0	2.0	0.78	0.51	YES/Maybe	Keddeg	A320
7.	27390	17.7	21.3	9.7	1.0	0.83	0.45	YES/no	Keddeg	A320
8.	27420	7.3	9.4	3.5	0.0	0.78	0.37	No/no	Keddeg	A320
9.	27428	35.7	46.1	23.4	1.7	0.77	0.51	YES/yes	Keddeg	A320
10.	27559	5.3	6.5	1.1	0.0	0.82	0.16	No/no	Keddeg	B737
11.	27571	14.1	17.7	6.7	1.0	0.80	0.38	YES/YES	Keddeg	B737
12.	27659	0.0	0.0	0.0	0.0	0.0	0.00	No/no	Keddeg	A320
13.	27660	0.0	0.0	0.0	0.0	0.0	0.00	No/no	Keddeg	A320
14.	27678	6.5	8.4	3.0	0.0	0.77	0.35	No/no	Keddeg	A320
15.	27694	6.4	8.5	3.2	0.0	0.76	0.37	No/no	Keddeg	A320
16.	28058	16.8	20.8	9.4	0.3	0.81	0.45	YES/no	Keddeg	A320
17.	28240	11.3	13.9	4.6	0.3	0.81	0.33	Maybe/yes	Keddeg	B737
18.	28297	4.5	5.3	0.9	0.0	0.86	0.16	No/no	Keddeg	B737
19.	28802	4.7	5.8	1.0	0.0	0.82	0.17	No/no	Keddeg	A320
20.	28825	9.0	10.2	3.5	0.0	0.88	0.34	No/no	Keddeg	A320
21.	28832	11.1	13.3	5.4	0.0	0.83	0.41	No/no	Keddeg	A320
22.	28936	12.8	15.8	6.3	0.0	0.81	0.40	No/no	Keddeg	A320
23.	28937	20.4	23.7	10.4	2.9	0.86	0.44	YES/No	Keddeg	A320
24.	28958	14.6	18.3	7.2	0.7	0.80	0.39	YES/maybe	Keddeg	A320
25.	29428	0.0	0.0	0.0	0.0	0.0	0.00	No/no	Keddeg	B737
26.	29432	59.8	76.4	33.1	4.4	0.78	0.43	YES/no	Keddeg	A320
27.	29434	5.4	6.5	1.3	0.0	0.83	0.19	No/no	Keddeg	B737
28.	29440	8.8	11.5	4.1	0.0	0.76	0.35	No/no	Pall	B737
29.	29442	2.3	0.0	0.0	0.0	0.0	0.00	No/no	Keddeg	B737
30.	29559	0.0	0.0	0.0	0.0	0.0	0.00	No/no	Keddeg	B737
31.	29606	0.0	0.0	0.0	0.0	0.0	0.00	No/no	Keddeg	B737
32.	29750	3.2	3.9	1.6	0.5	0.83	0.40	No/no	Keddeg	A320
33.	30103	0.0	2.5	0.0	0.0	0.00	0.00	No/no	Keddeg	B737
34.	30121	4.1	5.1	1.8	0.0	0.79	0.34	No/no	Keddeg	B737
35.	30335	16.8	21.7	11.3	2.0	0.77	0.52	YES/yes	Pall	B737

36.	30339	0.0	0.0	0.0	0.0	0.00	0.0	No/no	Keddeg	A320
37.	30343	4.4	5.6	0.4	0.0	0.79	0.07	No/no	Keddeg	A320
38.	30363	31.4	40.2	21.7	3.5	0.78	0.54	YES/yes	Pall	B777
39.	30598	16.2	20.8	7.6	1.0	0.78	0.37	YES/maybe	Pall	B777
40.	30670	6.5	7.6	1.8	0.0	0.86	0.23	No/no	Keddeg	B737
41.	30674	0.0	0.0	0.0	0.0	0.00	0.00	No/no	Keddeg	B737
42.	5100224	32.0	40.7	17.9	1.5	0.79	0.44	YES/YES	Pall	A320
43.	5100242	33.8	42.6	19.0	1.1	0.79	0.45	YES/YES	Pall	A320
44.	49372054	51.8	60.1	26.8	3.5	0.86	0.45	YES/yes	Pall	A320
45.	50131042	75.5	92.8	43.9	4.6	0.81	0.47	YES/maybe	Pall	A320
46.	60401016	12.0	15.5	6.1	0.7	0.77	0.39	YES/YES	Pall	A320
47.	60401041	10.5	13.5	5.3	0.5	0.78	0.39	YES/yes	Pall	A320
48.	650390-13	75.8	105.1	56.5	7.6	0.72	0.54	YES/YES	Keddeg	A320
49.	A21794HC	205.8	250.8	129.6	18.2	0.82	0.52	YES/YES	Pall	B737
50.	A21803HC	86.2	105.9	51.0	5.4	0.81	0.48	YES/YES	Pall	B737
51.	A22023HC	366.4	428.7	206.9	25.2	0.85	0.48	YES/YES	Pall	B737
52.	A22589HC	16.2	21.7	8.5	1.3	0.75	0.39	YES/YES	Pall	B737
53.	A22607HC	40.3	54.1	28.0	4.1	0.75	0.52	YES/YES	Pall	B737
54.	A22609HC	56.7	74.4	38.8	4.2	0.76	0.52	YES/YES	Pall	B737
55.	A22623HC	37.9	52.1	24.6	2.0	0.73	0.47	YES/yes	Pall	B737
56.	A24233HC	18.1	24.6	10.4	1.6	0.74	0.42	YES/YES	Pall	B737
57.	A24237HC	18.8	25.6	12.5	2.0	0.73	0.49	YES/no	Pall	B737
58.	A24246HC	31.4	42.1	20.7	1.0	0.75	0.49	YES/YES	Pall	B737
59.	A3740HC	9.8	10.0	2.4	0.0	0.98	0.24	No/no	Pall	B767
60.	A3745HC	11.5	13.2	4.8	0.3	0.87	0.36	YES/maybe	Pall	B767
61.	A3760HC	14.4	17.4	7.1	1.2	0.83	0.41	YES/YES	Pall	B767
62.	A3790HC	11.7	55.7	0.0	0.0	0.21	0.00	No/no	Pall	B767
63.	A3795HC	4.4	4.9	0.4	0.0	0.90	0.08	No/no	Pall	B767
64.	A3798HC	8.9	11.2	3.0	0.0	0.79	0.26	No/no	Pall	B767
65.	A3801HC	4.1	4.6	0.3	0.0	0.89	0.05	No/no	Pall	B767
66.	A3803HC	7.0	8.7	1.9	0.0	0.80	0.21	No/no	Pall	B767
67.	A3807HC	10.3	11.0	2.6	1.0	0.94	0.24	Maybe/no	Pall	B767
68.	A3809HC	3.9	4.9	0.0	0.0	0.80	0.00	No/no	Pall	B767
69.	A3854HC	0.0	2.4	0.0	0.0	0.00	0.00	No/no	Pall	B767
70.	A3861HC	5.1	6.0	0.0	0.0	0.00	0.00	No/no	Pall	B767
71.	A3871HC	4.0	4.6	0.0	0.0	0.86	0.00	No/no	Pall	B767
72.	A3873HC	4.8	5.7	2.2	0.0	0.83	0.39	No/no	Pall	B767
73.	AB0469685	26.2	34.5	15.2	1.0	0.76	0.44	YES/YES	Donaldson	B737
74.	S21070121	6.6	7.9	1.5	0.0	0.84	0.18	No/no	Donaldson	B737
75.	Blank	0.0	0.0	0.0	0.0	0.0	0.0	0.0	-	-

## Appendix C - Summarized NAA Data on Used HEPA Cabin Air Recirculation Filters

**Table C-1: NAA data on used filters**

Sample	Group	Sample Mass (mg)	Daughter Nuclide	Nuclide ID Confidence	Concentration	Nuclide Mass (micrograms)	Combined Uncertainty
27QR6F	B	74.2	CO-60	0.98	2.66E-06	0.197	0.012
27QR6F	B	74.2	ZN-65	0.99	7.75E-03	574.775	23.007
27QR6F	B	74.2	SE-75	0.75	1.44E-05	1.067	0.046
27QR6F	B	74.2	RU-103	0.82	2.54E-05	1.881	0.106
27QR6F	B	74.2	SB-124	0.78	2.03E-07	0.015	0.002
27QR6F	B	74.2	BA-131	0.92	8.92E-04	66.154	4.226
27QR6F	B	74.2	BA-133	0.41	7.79E-03	578.194	217.035
27QR6F	B	74.2	CE-141	0.97	4.05E-06	0.300	0.101
27QR6F	B	74.2	HG-203	0.98	4.06E-06	0.301	0.068
163B4J	A	69.9	CR-51	0.99	2.60E-05	1.816	0.323
163B4J	A	69.9	FE-59	0.96	6.26E-04	43.727	7.509
163B4J	A	69.9	CO-60	0.98	5.39E-06	0.377	0.020
163B4J	A	69.9	ZN-65	0.99	7.25E-03	507.086	20.313
163B4J	A	69.9	RU-103	0.82	2.15E-05	1.500	0.091
163B4J	A	69.9	SB-124	0.77	4.82E-07	0.034	0.002
163B4J	A	69.9	BA-131	0.93	8.23E-04	57.523	3.509
163B4J	A	69.9	BA-133	0.41	6.46E-04	45.163	219.072
163B4J	A	69.9	CE-141	0.99	5.35E-06	0.374	0.091
163B4J	A	69.9	HF-175	0.86	9.00E-06	0.629	0.110
163B4J	A	69.9	HG-203	0.99	2.66E-06	0.186	0.056
907BVA	B	101.3	FE-59	0.98	5.02E-04	50.864	8.785
907BVA	B	101.3	CO-60	0.98	1.77E-06	0.179	0.012
907BVA	B	101.3	ZN-65	0.98	7.23E-03	732.750	29.260
907BVA	B	101.3	RU-103	0.82	1.84E-05	1.861	0.112
907BVA	B	101.3	SB-124	0.78	2.04E-07	0.021	0.002
907BVA	B	101.3	BA-131	0.92	8.59E-04	86.987	5.598
907BVA	B	101.3	BA-133	0.41	8.78E-03	889.544	241.661
907BVA	B	101.3	HF-181	0.76	1.03E-06	0.105	0.008
27559	A	84.3	CR-51	0.99	1.60E-05	1.345	0.372
27559	A	84.3	FE-59	0.98	9.24E-04	77.885	9.102
27559	A	84.3	CO-60	0.98	2.08E-06	0.175	0.012
27559	A	84.3	ZN-65	0.98	6.33E-03	533.430	21.344
27559	A	84.3	RU-103	0.81	1.69E-05	1.421	0.091
27559	A	84.3	SB-124	0.95	1.12E-06	0.094	0.005
27559	A	84.3	BA-131	0.92	7.47E-04	62.948	4.057
27559	A	84.3	BA-133	0.40	5.56E-03	468.978	226.834
27559	A	84.3	CE-141	0.99	7.17E-06	0.604	0.104
27559	A	84.3	HF-181	0.76	1.27E-06	0.107	0.008
27559	A	84.3	OS-185	0.78	3.53E-06	0.298	0.441
27559	B	70.8	FE-59	0.96	6.86E-04	48.552	8.045

27559	B	70.8	CO-60	0.96	2.28E-06	0.161	0.011
27559	B	70.8	ZN-65	0.97	5.87E-03	415.593	16.669
27559	B	70.8	RU-103	0.80	1.56E-05	1.107	0.077
27559	B	70.8	SB-124	0.94	1.47E-06	0.104	0.005
27559	B	70.8	BA-131	0.91	7.47E-04	52.911	3.533
27559	B	70.8	CE-141	0.98	4.48E-06	0.317	0.092
27559	B	70.8	HF-181	0.76	1.17E-06	0.083	0.007
27559	B	70.8	OS-185	0.80	2.59E-06	0.183	0.391
27571	A	82.2	CR-51	0.98	1.76E-05	1.444	0.341
27571	A	82.2	FE-59	0.97	6.84E-04	56.248	7.999
27571	A	82.2	CO-60	0.96	3.74E-06	0.307	0.016
27571	A	82.2	ZN-65	0.97	5.53E-03	454.488	18.206
27571	A	82.2	RU-103	0.80	1.45E-05	1.191	0.082
27571	A	82.2	SB-124	0.76	4.24E-07	0.035	0.002
27571	A	82.2	BA-131	0.91	7.45E-04	61.208	4.054
27571	A	82.2	CE-141	0.98	6.73E-06	0.553	0.100
27571	A	82.2	HF-175	0.90	9.09E-06	0.748	0.117
27571	A	82.2	HF-181	0.76	1.11E-06	0.091	0.007
28958	A	82.9	CR-51	0.99	2.70E-05	2.242	0.344
28958	A	82.9	CO-60	0.98	2.84E-06	0.235	0.014
28958	A	82.9	ZN-65	0.98	6.26E-03	518.730	20.760
28958	A	82.9	RU-103	0.81	1.73E-05	1.437	0.090
28958	A	82.9	SB-124	0.77	5.83E-07	0.048	0.003
28958	A	82.9	BA-131	0.92	7.11E-04	58.908	3.742
28958	A	82.9	CE-141	0.98	8.41E-06	0.697	0.102
28958	A	82.9	HF-181	0.76	1.27E-06	0.105	0.007
30121	B	98.9	SC-46	0.95	3.40E-06	0.336	0.014
30121	B	98.9	CR-51	0.98	1.92E-05	1.895	0.373
30121	B	98.9	FE-59	0.96	4.54E-04	44.936	7.898
30121	B	98.9	CO-60	0.95	1.29E-06	0.127	0.011
30121	B	98.9	ZN-65	0.97	5.48E-03	541.532	21.647
30121	B	98.9	RU-103	0.80	1.33E-05	1.312	0.088
30121	B	98.9	SB-124	0.76	3.56E-07	0.035	0.002
30121	B	98.9	BA-131	0.91	6.30E-04	62.259	4.145
30121	B	98.9	BA-133	0.41	5.76E-03	569.699	210.848
30121	B	98.9	CE-141	0.99	3.40E-06	0.336	0.099
30121	B	98.9	HF-181	0.76	8.85E-07	0.088	0.007
604010-41	B	70.1	CR-51	0.98	4.66E-05	3.266	0.443
604010-41	B	70.1	FE-59	0.97	1.55E-03	108.721	12.087
604010-41	B	70.1	CO-60	0.96	7.55E-06	0.529	0.027
604010-41	B	70.1	ZN-65	0.97	6.26E-03	438.764	17.597
604010-41	B	70.1	RU-103	0.79	1.33E-05	0.936	0.079
604010-41	B	70.1	SB-124	0.94	1.09E-05	0.764	0.031
604010-41	B	70.1	BA-131	0.91	7.45E-04	52.255	3.536
604010-41	B	70.1	HF-181	0.76	1.32E-06	0.093	0.007
A3854H	A	111.5	SC-46	0.97	3.04E-06	0.339	0.016
A3854H	A	111.5	CR-51	0.98	2.46E-05	2.746	0.439
A3854H	A	111.5	CO-60	0.98	2.02E-06	0.226	0.014
A3854H	A	111.5	ZN-65	0.98	6.49E-03	723.183	28.881
A3854H	A	111.5	RU-103	0.81	1.87E-05	2.084	0.121

A3854H	A	111.5	SB-124	0.80	4.29E-07	0.048	0.003
A3854H	A	111.5	BA-131	0.92	8.14E-04	90.770	5.849
A3854H	A	111.5	BA-133	0.41	8.98E-03	1001.778	264.265
A3854H	A	111.5	CE-141	0.99	5.23E-06	0.583	0.112
A3854H	A	111.5	HF-175	0.86	8.96E-06	1.000	0.148
A3854H	A	111.5	HF-181	0.76	1.22E-06	0.136	0.009
A3854H	B	87.1	SC-46	0.97	3.11E-06	0.271	0.013
A3854H	B	87.1	CR-51	0.99	2.39E-05	2.079	0.397
A3854H	B	87.1	FE-59	0.95	7.40E-04	64.424	8.907
A3854H	B	87.1	CO-60	0.96	2.28E-06	0.198	0.013
A3854H	B	87.1	ZN-65	0.98	7.08E-03	616.983	24.674
A3854H	B	87.1	RU-103	0.81	1.83E-05	1.590	0.101
A3854H	B	87.1	SB-124	0.76	3.61E-07	0.031	0.002
A3854H	B	87.1	BA-131	0.92	8.54E-04	74.374	4.769
A3854H	B	87.1	CE-141	0.99	6.39E-06	0.557	0.106
A3854H	B	87.1	HF-181	0.76	1.42E-06	0.124	0.008
CP163W	A	104	CO-60	0.96	1.41E-06	0.147	0.011
CP163W	A	104	ZN-65	0.98	6.39E-03	664.589	26.550
CP163W	A	104	RU-103	0.81	1.57E-05	1.635	0.103
CP163W	A	104	SB-124	0.76	1.78E-07	0.018	0.002
CP163W	A	104	BA-131	0.92	7.49E-04	77.878	5.049
CP163W	A	104	BA-133	0.40	6.35E-03	660.518	238.371
CP163W	A	104	CE-141	0.99	4.79E-06	0.498	0.107
CP163W	A	104	HF-181	0.76	8.75E-07	0.091	0.007
GF68X3	A	76	CR-51	0.99	1.78E-05	1.349	0.390
GF68X3	A	76	FE-59	0.98	9.56E-04	72.628	8.691
GF68X3	A	76	CO-60	0.97	2.43E-06	0.184	0.012
GF68X3	A	76	ZN-65	0.98	8.34E-03	633.473	25.339
GF68X3	A	76	RU-103	0.82	2.23E-05	1.696	0.104
GF68X3	A	76	SB-124	0.76	4.15E-07	0.032	0.002
GF68X3	A	76	BA-131	0.92	1.07E-03	81.255	5.252
GF68X3	A	76	BA-133	0.41	7.81E-03	593.822	223.859
GF68X3	A	76	CE-141	0.99	3.15E-06	0.239	0.106
GF68X3	A	76	HF-181	0.76	1.04E-06	0.079	0.007
GFG8X3	B	83.2	CR-51	0.98	2.66E-05	2.212	0.392
GFG8X3	B	83.2	FE-59	0.97	6.99E-04	58.153	8.219
GFG8X3	B	83.2	CO-60	0.98	2.43E-06	0.202	0.013
GFG8X3	B	83.2	ZN-65	0.99	7.71E-03	641.327	25.641
GFG8X3	B	83.2	RU-103	0.82	2.29E-05	1.908	0.111
GFG8X3	B	83.2	SB-124	0.77	5.27E-07	0.044	0.003
GFG8X3	B	83.2	BA-131	0.92	9.44E-04	78.528	4.945
GFG8X3	B	83.2	CE-141	0.99	5.82E-06	0.484	0.104
GFG8X3	B	83.2	HF-181	0.76	9.94E-07	0.083	0.007
SJA33J	B	70	CR-51	0.98	2.48E-05	1.736	0.359
SJA33J	B	70	FE-59	0.97	1.03E-03	72.242	8.729
SJA33J	B	70	CO-60	0.99	3.59E-06	0.251	0.015
SJA33J	B	70	ZN-65	0.99	7.86E-03	550.060	22.031
SJA33J	B	70	RU-103	0.82	2.39E-05	1.674	0.100
SJA33J	B	70	SB-124	0.77	7.12E-07	0.050	0.003
SJA33J	B	70	BA-131	0.92	1.01E-03	71.037	4.479

SJA33J	B	70	BA-133	0.41	1.07E-02	750.763	226.892
SJA33J	B	70	CE-141	0.98	8.32E-06	0.582	0.099
SJA33J	B	70	HF-181	0.76	1.50E-06	0.105	0.008
TC66HR	A	72.2	CR-51	0.99	2.77E-05	2.002	0.328
TC66HR	A	72.2	CO-60	0.99	2.35E-06	0.170	0.011
TC66HR	A	72.2	ZN-65	0.99	7.73E-03	557.953	22.329
TC66HR	A	72.2	RU-103	0.81	2.24E-05	1.618	0.096
TC66HR	A	72.2	SB-124	0.77	6.99E-07	0.050	0.003
TC66HR	A	72.2	BA-131	0.94	8.49E-04	61.287	3.688
TC66HR	A	72.2	BA-133	0.41	8.80E-03	635.130	226.513
TC66HR	A	72.2	CE-141	0.98	7.71E-06	0.556	0.095
TC66HR	A	72.2	HF-181	0.76	2.03E-06	0.147	0.008
WAQE67	A	89.9	CR-51	0.98	4.31E-06	0.388	0.367
WAQE67	A	89.9	CO-60	0.97	1.30E-06	0.117	0.010
WAQE67	A	89.9	ZN-65	0.97	6.55E-03	588.942	23.547
WAQE67	A	89.9	RU-103	0.80	1.73E-05	1.553	0.097
WAQE67	A	89.9	SB-124	0.76	1.84E-07	0.017	0.002
WAQE67	A	89.9	BA-131	0.92	8.09E-04	72.747	4.730
WAQE67	A	89.9	BA-133	0.41	3.21E-03	288.623	224.334
WAQE67	A	89.9	CE-141	0.99	3.67E-06	0.330	0.101
WAQE67	A	89.9	HF-181	0.76	8.94E-07	0.080	0.007
WAQE67	B	100.4	CO-60	0.96	1.23E-06	0.123	0.010
WAQE67	B	100.4	ZN-65	0.98	6.42E-03	644.958	25.766
WAQE67	B	100.4	RU-103	0.80	1.74E-05	1.746	0.105
WAQE67	B	100.4	SB-124	0.77	2.06E-07	0.021	0.002
WAQE67	B	100.4	BA-131	0.92	8.11E-04	81.452	5.266
WAQE67	B	100.4	BA-133	0.41	9.74E-03	977.665	227.561
WAQE67	B	100.4	CE-141	0.99	3.60E-06	0.361	0.107
WAQE67	B	100.4	HF-181	0.76	7.08E-07	0.071	0.007
12HD94	A	85.4	SC-46	0.96	1.99E-06	0.170	0.009
12HD94	A	85.4	CR-51	0.97	2.92E-05	2.495	0.488
12HD94	A	85.4	FE-59	0.91	1.04E-03	88.809	10.691
12HD94	A	85.4	CO-60	0.92	3.92E-06	0.335	0.018
12HD94	A	85.4	ZN-65	0.95	5.13E-03	437.954	17.635
12HD94	A	85.4	SE-75	1.00	2.05E-05	1.752	0.072
12HD94	A	85.4	RU-103	0.79	6.77E-06	0.579	0.076
12HD94	A	85.4	SB-124	0.74	7.30E-07	0.062	0.004
12HD94	A	85.4	BA-131	0.86	7.05E-04	60.205	4.788
12HD94	A	85.4	CE-141	0.97	8.50E-06	0.726	0.148
12HD94	A	85.4	YB-169	0.36	5.70E-07	0.049	0.012
12HD94	A	85.4	TA-182	0.55	7.64E-08	0.007	0.001
12HD94	A	85.4	HG-203	0.98	1.75E-05	1.492	0.108
46NKJF	B	93.6	CR-51	0.97	1.76E-05	1.649	0.550
46NKJF	B	93.6	CO-60	0.92	2.41E-06	0.226	0.014
46NKJF	B	93.6	ZN-65	0.95	6.92E-03	648.078	26.018
46NKJF	B	93.6	RU-103	0.78	8.45E-06	0.791	0.090
46NKJF	B	93.6	SB-124	0.74	2.59E-07	0.024	0.002
46NKJF	B	93.6	BA-131	0.86	9.61E-04	89.971	7.309
46NKJF	B	93.6	BA-133	0.41	7.14E-03	667.856	231.706
46NKJF	B	93.6	HF-181	0.75	1.06E-06	0.099	0.009



77G4CJ	A	105.3	CO-60	0.97	2.83E-06	0.298	0.017
77G4CJ	A	105.3	ZN-65	0.98	7.92E-03	833.658	33.418
77G4CJ	A	105.3	RU-103	0.81	1.25E-05	1.318	0.111
77G4CJ	A	105.3	SB-124	0.76	2.96E-07	0.031	0.003
77G4CJ	A	105.3	BA-131	0.87	1.02E-03	107.669	8.448
77G4CJ	A	105.3	BA-133	0.41	4.19E-03	441.219	252.825
77G4CJ	A	105.3	CE-141	0.97	7.55E-06	0.795	0.158
77G4CJ	A	105.3	HF-181	0.75	8.26E-07	0.087	0.009
907BVA	A	95	CO-60	0.98	1.85E-06	0.176	0.012
907BVA	A	95	ZN-65	0.99	7.08E-03	672.292	26.976
907BVA	A	95	RU-103	0.83	9.84E-06	0.934	0.092
907BVA	A	95	SB-124	0.76	2.36E-07	0.022	0.002
907BVA	A	95	BA-131	0.88	9.04E-04	85.911	6.599
907BVA	A	95	BA-133	0.41	4.91E-03	466.092	227.324
907BVA	A	95	HF-181	0.76	8.13E-07	0.077	0.008
604010-16	B	56.3	CR-51	0.97	5.62E-05	3.165	0.501
604010-16	B	56.3	CO-60	0.97	6.76E-06	0.381	0.022
604010-16	B	56.3	ZN-65	0.98	6.81E-03	383.658	15.499
604010-16	B	56.3	RU-103	0.80	8.51E-06	0.479	0.075
604010-16	B	56.3	SB-124	0.98	1.32E-05	0.745	0.031
604010-16	B	56.3	BA-131	0.87	9.02E-04	50.783	4.196
604010-16	B	56.3	HF-175	0.86	1.15E-05	0.648	0.136
604010-16	B	56.3	HF-181	0.76	1.54E-06	0.087	0.008
604010-16	B	56.3	OS-185	0.79	6.45E-06	0.363	0.479
604010-41	A	68.9	CR-51	0.97	5.22E-05	3.594	0.549
604010-41	A	68.9	FE-59	0.33	1.15E-03	79.146	20.936
604010-41	A	68.9	CO-60	0.97	7.90E-06	0.545	0.027
604010-41	A	68.9	ZN-65	0.97	6.24E-03	429.656	17.319
604010-41	A	68.9	RU-103	0.79	1.01E-05	0.698	0.082
604010-41	A	68.9	SB-124	0.97	1.21E-05	0.831	0.034
604010-41	A	68.9	BA-131	0.86	8.03E-04	55.324	4.668
604010-41	A	68.9	HF-175	0.91	1.04E-05	0.717	0.144
604010-41	A	68.9	HF-181	0.76	1.35E-06	0.093	0.009
604010-41	A	68.9	OS-185	0.79	3.18E-06	0.219	0.516
A3871H	B	95.5	SC-46	0.97	2.44E-06	0.233	0.012
A3871H	B	95.5	CR-51	0.97	1.71E-05	1.633	0.489
A3871H	B	95.5	CO-60	0.95	1.83E-06	0.175	0.012
A3871H	B	95.5	ZN-65	0.94	5.08E-03	484.748	19.485
A3871H	B	95.5	RU-103	0.78	5.52E-06	0.527	0.078
A3871H	B	95.5	SB-124	0.45	5.69E-07	0.054	0.004
A3871H	B	95.5	BA-131	0.86	7.24E-04	69.130	5.801
A3871H	B	95.5	BA-133	0.41	1.99E-03	190.236	212.030
A3871H	B	95.5	HF-181	0.75	8.07E-07	0.077	0.008
A22589HC	B	80.1	CO-60	0.98	2.66E-06	0.213	0.014
A22589HC	B	80.1	ZN-65	0.98	6.96E-03	557.195	22.392
A22589HC	B	80.1	RU-103	0.81	9.26E-06	0.742	0.083
A22589HC	B	80.1	SB-124	0.76	9.77E-07	0.078	0.004
A22589HC	B	80.1	BA-131	0.87	9.42E-04	75.492	5.858
A22589HC	B	80.1	BA-133	0.41	7.14E-03	572.003	208.797
A22589HC	B	80.1	CE-141	0.97	8.87E-06	0.711	0.136

A22589HC	B	80.1	HF-175	0.94	6.06E-06	0.486	0.135
A22589HC	B	80.1	HF-181	0.76	8.65E-07	0.069	0.008
A22623HC	B	76.1	CR-51	0.97	1.74E-05	1.324	0.494
A22623HC	B	76.1	CO-60	0.93	3.73E-06	0.284	0.016
A22623HC	B	76.1	ZN-65	0.95	7.04E-03	536.006	21.553
A22623HC	B	76.1	RU-103	0.78	1.03E-05	0.783	0.084
A22623HC	B	76.1	SB-124	0.76	1.01E-06	0.077	0.004
A22623HC	B	76.1	BA-131	0.86	8.63E-04	65.680	5.487
A22623HC	B	76.1	BA-133	0.41	7.60E-03	578.024	215.311
A22623HC	B	76.1	CE-141	0.96	5.33E-06	0.405	0.139
A22623HC	B	76.1	HF-181	0.75	1.05E-06	0.080	0.008
A24246HC	A	83.2	CR-51	0.97	3.28E-05	2.726	0.475
A24246HC	A	83.2	FE-59	0.90	6.27E-04	52.161	9.918
A24246HC	A	83.2	CO-60	0.93	4.91E-06	0.409	0.021
A24246HC	A	83.2	ZN-65	0.95	5.41E-03	450.080	18.113
A24246HC	A	83.2	SB-124	0.74	8.32E-07	0.069	0.004
A24246HC	A	83.2	BA-131	0.86	7.60E-04	63.210	5.464
A24246HC	A	83.2	CE-141	0.95	8.49E-06	0.706	0.130
A24246HC	A	83.2	HF-181	0.75	1.22E-06	0.101	0.008
A24246HC	A	83.2	TA-182	0.32	5.84E-08	0.005	0.001
CRH8ES	A	80.1	CO-60	0.98	2.85E-06	0.228	0.013
CRH8ES	A	80.1	ZN-65	0.99	7.30E-03	584.587	23.493
CRH8ES	A	80.1	RU-103	0.82	1.34E-05	1.070	0.090
CRH8ES	A	80.1	SB-124	0.77	3.30E-07	0.026	0.002
CRH8ES	A	80.1	BA-131	0.87	9.21E-04	73.747	5.852
CRH8ES	A	80.1	CE-141	0.98	6.91E-06	0.553	0.136
CRH8ES	A	80.1	HF-181	0.76	9.56E-07	0.077	0.008
CRH8ES	B	96.2	CO-60	0.96	2.27E-06	0.219	0.014
CRH8ES	B	96.2	ZN-65	0.97	7.34E-03	706.399	28.351
CRH8ES	B	96.2	RU-103	0.79	1.23E-05	1.183	0.101
CRH8ES	B	96.2	SB-124	0.77	3.09E-07	0.030	0.003
CRH8ES	B	96.2	BA-131	0.87	9.37E-04	90.187	7.167
CRH8ES	B	96.2	BA-133	0.41	6.20E-03	596.073	242.853
CRH8ES	B	96.2	HF-181	0.75	1.00E-06	0.096	0.009
HIDE4H	A	96.1	CO-60	0.92	1.91E-06	0.183	0.012
HIDE4H	A	96.1	ZN-65	0.94	3.80E-03	365.376	14.718
HIDE4H	A	96.1	SB-124	0.75	1.57E-07	0.015	0.002
HIDE4H	A	96.1	BA-131	0.85	5.33E-04	51.239	4.565
HIDE4H	A	96.1	HF-181	0.75	3.96E-07	0.038	0.006
IUY3T4	B	67.8	SC-46	0.97	2.40E-06	0.163	0.009
IUY3T4	B	67.8	CR-51	0.98	1.72E-05	1.168	0.415
IUY3T4	B	67.8	FE-59	0.96	1.07E-03	72.421	9.455
IUY3T4	B	67.8	CO-60	0.97	2.06E-06	0.140	0.011
IUY3T4	B	67.8	ZN-65	0.98	5.18E-03	351.196	14.173
IUY3T4	B	67.8	RU-103	0.80	8.63E-06	0.585	0.068
IUY3T4	B	67.8	SB-124	0.77	4.18E-07	0.028	0.002
IUY3T4	B	67.8	BA-131	0.86	7.25E-04	49.152	4.156
IUY3T4	B	67.8	HF-175	0.94	3.84E-06	0.260	0.115
IUY3T4	B	67.8	HF-181	0.76	8.59E-07	0.058	0.007
MA7ET5	B	64.9	CO-60	0.94	3.52E-06	0.228	0.014

MA7ET5	B	64.9	ZN-65	0.96	8.04E-03	521.511	20.986
MA7ET5	B	64.9	RU-103	0.78	1.00E-05	0.652	0.077
MA7ET5	B	64.9	SB-124	0.76	2.33E-07	0.015	0.002
MA7ET5	B	64.9	BA-131	0.86	9.05E-04	58.735	4.967
MA7ET5	B	64.9	BA-133	0.41	9.69E-03	628.637	205.514
MA7ET5	B	64.9	HF-181	0.75	1.07E-06	0.069	0.008
NM81X7	A	104.5	CR-51	0.97	2.82E-05	2.946	0.585
NM81X7	A	104.5	CO-60	0.96	2.92E-06	0.305	0.017
NM81X7	A	104.5	ZN-65	0.97	7.25E-03	757.790	30.383
NM81X7	A	104.5	RU-103	0.79	9.43E-06	0.986	0.102
NM81X7	A	104.5	SB-124	0.77	3.16E-07	0.033	0.003
NM81X7	A	104.5	BA-131	0.87	8.62E-04	90.124	7.199
NM81X7	A	104.5	BA-133	0.41	6.07E-03	634.579	245.399
NM81X7	A	104.5	HF-181	0.76	1.33E-06	0.139	0.010
7GH325	A	88.1	CO-60	0.99	1.20E-06	0.106	0.009
7GH325	A	88.1	ZN-65	0.99	7.20E-03	633.923	25.451
7GH325	A	88.1	RU-103	0.80	7.43E-06	0.655	0.092
7GH325	A	88.1	SB-124	0.77	2.17E-07	0.019	0.002
7GH325	A	88.1	BA-131	0.84	8.99E-04	79.162	7.196
7GH325	A	88.1	BA-133	0.40	3.57E-03	314.115	222.804
7GH325	A	88.1	HF-181	0.75	7.26E-07	0.064	0.008
27QR6F	A	63.7	CO-60	0.97	1.56E-06	0.099	0.009
27QR6F	A	63.7	ZN-65	0.99	7.38E-03	470.404	18.938
27QR6F	A	63.7	SE-75	0.99	1.54E-05	0.982	0.042
27QR6F	A	63.7	RU-103	0.81	1.66E-05	1.060	0.088
27QR6F	A	63.7	BA-133	0.41	6.38E-03	406.197	189.057
27QR6F	A	63.7	HG-203	0.98	7.17E-06	0.456	0.084
29750	B	75.2	SC-46	0.97	3.39E-06	0.255	0.013
29750	B	75.2	CR-51	0.97	4.31E-05	3.243	0.573
29750	B	75.2	CO-60	0.98	3.55E-06	0.267	0.015
29750	B	75.2	ZN-65	0.99	6.53E-03	490.982	19.756
29750	B	75.2	RU-103	0.81	6.63E-06	0.499	0.085
29750	B	75.2	SB-124	0.77	4.71E-07	0.035	0.003
29750	B	75.2	BA-131	0.83	8.26E-04	62.079	6.054
29750	B	75.2	BA-133	0.41	5.12E-03	385.085	208.154
29750	B	75.2	HF-181	0.76	1.08E-06	0.081	0.009
A0354G	A	79.6	CO-60	0.98	1.81E-06	0.144	0.011
A0354G	A	79.6	ZN-65	0.99	6.79E-03	540.338	21.715
A0354G	A	79.6	RU-103	0.80	7.00E-06	0.557	0.085
A0354G	A	79.6	SB-124	0.45	3.14E-07	0.025	0.003
A0354G	A	79.6	BA-131	0.83	9.19E-04	73.121	6.837
A0354G	A	79.6	HF-181	0.75	7.76E-07	0.062	0.008
A0354G	B	85.9	CO-60	0.99	1.78E-06	0.153	0.011
A0354G	B	85.9	ZN-65	0.99	6.85E-03	588.294	23.630
A0354G	B	85.9	RU-103	0.81	7.39E-06	0.635	0.090
A0354G	B	85.9	SB-124	0.77	2.81E-07	0.024	0.003
A0354G	B	85.9	BA-131	0.84	8.81E-04	75.663	6.942
A0354G	B	85.9	BA-133	0.41	7.10E-03	610.104	219.534
A0354G	B	85.9	HF-181	0.75	1.02E-06	0.088	0.009
A3807H	A	87.3	SC-46	0.96	2.38E-06	0.208	0.011

A3807H	A	87.3	CR-51	0.96	2.02E-05	1.761	0.586
A3807H	A	87.3	CO-60	0.98	2.97E-06	0.259	0.015
A3807H	A	87.3	ZN-65	0.99	6.00E-03	523.693	21.042
A3807H	A	87.3	RU-103	0.81	5.44E-06	0.475	0.087
A3807H	A	87.3	SB-124	0.77	4.61E-07	0.040	0.003
A3807H	A	87.3	BA-131	0.83	7.80E-04	68.078	6.578
A3807H	A	87.3	BA-133	0.41	4.45E-03	388.455	203.654
A3807H	A	87.3	HF-181	0.75	9.04E-07	0.079	0.009
A3871H	A	67	SC-46	0.97	2.69E-06	0.180	0.010
A3871H	A	67	CR-51	0.97	3.25E-05	2.174	0.505
A3871H	A	67	CO-60	0.98	2.65E-06	0.178	0.011
A3871H	A	67	ZN-65	0.98	5.31E-03	355.975	14.367
A3871H	A	67	RU-103	0.81	6.21E-06	0.416	0.074
A3871H	A	67	SB-124	0.77	4.92E-07	0.033	0.003
A3871H	A	67	BA-131	0.82	7.60E-04	50.907	5.283
A3871H	A	67	HF-181	0.75	9.78E-07	0.066	0.008
A22607HC	A	81.8	CR-51	0.97	4.17E-05	3.414	0.557
A22607HC	A	81.8	FE-59	0.98	7.67E-04	62.720	11.039
A22607HC	A	81.8	CO-60	0.99	6.14E-06	0.502	0.024
A22607HC	A	81.8	ZN-65	0.99	6.32E-03	516.758	20.773
A22607HC	A	81.8	SE-75	1.00	4.39E-05	3.590	0.146
A22607HC	A	81.8	RU-103	0.81	1.30E-05	1.065	0.094
A22607HC	A	81.8	SB-124	0.78	8.11E-07	0.066	0.004
A22607HC	A	81.8	YB-169	0.36	1.06E-06	0.087	0.015
A22607HC	A	81.8	HG-203	0.97	4.84E-05	3.956	0.206
CE9B16	B	80.6	SC-46	0.96	3.36E-06	0.271	0.013
CE9B16	B	80.6	CR-51	0.97	4.60E-05	3.712	0.587
CE9B16	B	80.6	CO-60	0.98	5.44E-06	0.438	0.022
CE9B16	B	80.6	ZN-65	0.99	6.40E-03	515.721	20.735
CE9B16	B	80.6	RU-103	0.84	6.82E-06	0.550	0.084
CE9B16	B	80.6	SB-124	0.77	7.27E-07	0.059	0.004
CE9B16	B	80.6	BA-131	0.85	7.81E-04	62.968	5.750
CE9B16	B	80.6	BA-133	0.41	6.61E-03	532.590	217.243
CE9B16	B	80.6	CE-141	0.96	7.61E-06	0.614	0.156
CE9B16	B	80.6	HF-181	0.76	1.15E-06	0.093	0.009
DAW454	A	92.7	CO-60	0.98	3.61E-06	0.335	0.018
DAW454	A	92.7	ZN-65	0.99	7.59E-03	703.447	28.221
DAW454	A	92.7	RU-103	0.81	8.36E-06	0.775	0.099
DAW454	A	92.7	SB-124	0.77	2.94E-07	0.027	0.002
DAW454	A	92.7	BA-131	0.84	8.94E-04	82.854	7.536
DAW454	A	92.7	BA-133	0.39	1.05E-02	970.100	225.777
DAW454	A	92.7	CE-141	0.95	5.05E-06	0.468	0.170
DAW454	A	92.7	HF-175	0.95	7.81E-06	0.724	0.151
DAW454	A	92.7	HF-181	0.76	7.56E-07	0.070	0.009
GO9JVE	A	95.7	CO-60	0.99	2.70E-06	0.259	0.015
GO9JVE	A	95.7	ZN-65	0.99	6.05E-03	578.515	23.230
GO9JVE	A	95.7	RU-103	0.82	5.97E-06	0.571	0.088
GO9JVE	A	95.7	SB-124	0.77	2.21E-07	0.021	0.002
GO9JVE	A	95.7	BA-131	0.84	7.44E-04	71.154	6.454
GO9JVE	A	95.7	HF-181	0.76	6.16E-07	0.059	0.008

HGD63H	A	99.5	CR-51	0.96	3.45E-05	3.432	0.702
HGD63H	A	99.5	CO-60	0.99	4.13E-06	0.411	0.021
HGD63H	A	99.5	ZN-65	0.99	7.45E-03	741.748	29.757
HGD63H	A	99.5	RU-103	0.80	7.62E-06	0.758	0.104
HGD63H	A	99.5	SB-124	0.77	4.11E-07	0.041	0.003
HGD63H	A	99.5	BA-131	0.84	1.02E-03	101.081	8.947
HGD63H	A	99.5	BA-133	0.41	7.24E-03	720.560	250.306
HGD63H	A	99.5	CE-141	0.97	5.57E-06	0.554	0.179
HGD63H	A	99.5	HF-181	0.71	1.60E-06	0.160	0.012
HGD63H	A	99.5	HG-203	0.90	1.59E-06	0.158	0.093
MA7ET5	A	75.3	CR-51	0.97	1.55E-05	1.163	0.585
MA7ET5	A	75.3	CO-60	0.99	5.14E-06	0.387	0.020
MA7ET5	A	75.3	ZN-65	0.99	8.52E-03	641.642	25.767
MA7ET5	A	75.3	RU-103	0.83	6.67E-06	0.502	0.091
MA7ET5	A	75.3	SB-124	0.78	4.04E-07	0.030	0.003
MA7ET5	A	75.3	BA-131	0.84	1.07E-03	80.549	7.190
MA7ET5	A	75.3	BA-133	0.41	7.11E-03	535.719	226.748
MA7ET5	A	75.3	HF-175	0.89	7.79E-06	0.587	0.150
MA7ET5	A	75.3	HF-181	0.76	9.96E-07	0.075	0.009
MB6LV1	A	90.6	CO-60	0.98	2.60E-06	0.236	0.014
MB6LV1	A	90.6	ZN-65	0.99	6.80E-03	616.151	24.738
MB6LV1	A	90.6	RU-103	0.82	7.34E-06	0.665	0.091
MB6LV1	A	90.6	SB-124	0.78	2.04E-07	0.019	0.002
MB6LV1	A	90.6	BA-131	0.83	9.05E-04	81.966	7.538
MB6LV1	A	90.6	BA-133	0.41	7.98E-03	723.180	224.686
MB6LV1	A	90.6	CE-141	0.94	1.62E-06	0.147	0.166
MB6LV1	A	90.6	HF-181	0.75	9.03E-07	0.082	0.009
PL2IXI	A	82.1	CO-60	0.97	2.00E-06	0.164	0.011
PL2IXI	A	82.1	ZN-65	0.99	6.65E-03	545.883	21.944
PL2IXI	A	82.1	RU-103	0.82	6.60E-06	0.542	0.086
PL2IXI	A	82.1	SB-124	0.77	2.16E-07	0.018	0.002
PL2IXI	A	82.1	BA-131	0.83	8.70E-04	71.410	6.849
PL2IXI	A	82.1	BA-133	0.41	5.03E-03	412.934	208.997
PL2IXI	A	82.1	HF-181	0.75	1.01E-06	0.083	0.008
QOX417	B	105.5	CO-60	0.99	1.45E-06	0.153	0.011
QOX417	B	105.5	ZN-65	0.99	6.21E-03	655.138	26.293
QOX417	B	105.5	SE-75	0.67	1.54E-06	0.163	0.017
QOX417	B	105.5	RU-103	0.81	6.06E-06	0.640	0.097
QOX417	B	105.5	SB-124	0.76	2.48E-07	0.026	0.003
QOX417	B	105.5	BA-131	0.83	7.82E-04	82.456	7.866
QOX417	B	105.5	BA-133	0.41	8.20E-03	865.323	221.729
QOX417	B	105.5	HG-203	0.96	4.87E-07	0.051	0.087
RP14DE	A	70.3	CO-60	0.99	1.52E-06	0.107	0.009
RP14DE	A	70.3	ZN-65	0.99	6.57E-03	461.626	18.579
RP14DE	A	70.3	SE-75	0.45	1.53E-06	0.107	0.013
RP14DE	A	70.3	RU-103	0.82	9.26E-06	0.651	0.078
RP14DE	A	70.3	SB-124	0.77	1.83E-07	0.013	0.002
RP14DE	A	70.3	BA-131	0.84	8.15E-04	57.309	5.442
T007ML	A	82.3	CR-51	0.97	2.64E-05	2.176	0.605
T007ML	A	82.3	CO-60	0.96	2.24E-06	0.184	0.012

T007ML	A	82.3	ZN-65	0.98	6.83E-03	561.761	22.572
T007ML	A	82.3	RU-103	0.81	6.41E-06	0.527	0.089
T007ML	A	82.3	SB-124	0.46	3.88E-07	0.032	0.004
T007ML	A	82.3	BA-131	0.83	8.32E-04	68.466	6.583
T007ML	A	82.3	BA-133	0.40	7.87E-03	647.600	212.070
T007ML	A	82.3	HF-181	0.76	1.21E-06	0.100	0.009
TT15A5	B	96.3	CO-60	0.99	1.44E-06	0.138	0.011
TT15A5	B	96.3	ZN-65	0.99	5.31E-03	511.288	20.540
TT15A5	B	96.3	SE-75	0.50	1.47E-06	0.141	0.009
TT15A5	B	96.3	RU-103	0.82	5.58E-06	0.538	0.081
TT15A5	B	96.3	SB-124	0.78	2.04E-07	0.020	0.002
TT15A5	B	96.3	BA-131	0.85	7.18E-04	69.115	6.167
TT15A5	B	96.3	BA-133	0.41	8.06E-03	775.795	194.033
TT15A5	B	96.3	HF-181	0.85	7.31E-07	0.070	0.005
W9E578	A	90.2	CO-60	0.99	4.37E-06	0.394	0.020
W9E578	A	90.2	ZN-65	0.99	7.94E-03	716.521	28.744
W9E578	A	90.2	RU-103	0.81	9.97E-06	0.900	0.101
W9E578	A	90.2	SB-124	0.77	3.07E-07	0.028	0.003
W9E578	A	90.2	BA-131	0.84	9.91E-04	89.386	7.865
W9E578	A	90.2	BA-133	0.41	5.64E-03	508.574	241.168
W9E578	A	90.2	CE-141	0.97	7.33E-06	0.661	0.172
W9E578	A	90.2	HF-175	0.88	1.01E-05	0.912	0.161
W9E578	A	90.2	HF-181	0.76	1.01E-06	0.091	0.010
12HD49	B	98.4	CR-51	0.94	2.47E-05	2.431	0.669
12HD49	B	98.4	FE-59	0.96	1.14E-03	112.498	13.714
12HD49	B	98.4	CO-60	0.98	3.55E-06	0.349	0.018
12HD49	B	98.4	ZN-65	0.98	5.18E-03	509.915	20.452
12HD49	B	98.4	SE-75	0.99	7.93E-06	0.780	0.035
12HD49	B	98.4	RU-103	0.81	9.81E-06	0.965	0.098
12HD49	B	98.4	SB-124	0.88	7.27E-07	0.072	0.004
12HD49	B	98.4	BA-133	0.40	8.61E-03	847.237	211.971
12HD49	B	98.4	CE-141	0.97	8.86E-06	0.872	0.190
12HD49	B	98.4	TA-182	0.30	4.76E-08	0.005	0.001
12HD49	B	98.4	HG-203	0.97	4.82E-06	0.474	0.095
2965CL	B	69.9	FE-59	0.93	8.78E-04	61.390	11.368
2965CL	B	69.9	CO-60	0.98	4.02E-06	0.281	0.016
2965CL	B	69.9	ZN-65	0.99	6.37E-03	445.361	17.897
2965CL	B	69.9	SE-75	0.50	1.47E-06	0.102	0.008
2965CL	B	69.9	RU-103	0.80	3.57E-06	0.250	0.083
2965CL	B	69.9	SB-124	0.77	8.81E-07	0.062	0.004
2965CL	B	69.9	BA-131	0.81	9.43E-04	65.928	7.056
2965CL	B	69.9	HF-181	0.85	1.10E-06	0.077	0.006
LM6524	B	69.4	CO-60	0.98	5.24E-06	0.364	0.019
LM6524	B	69.4	ZN-65	0.98	1.13E-02	783.196	31.390
LM6524	B	69.4	RU-103	0.82	7.34E-06	0.509	0.113
LM6524	B	69.4	SB-124	0.76	3.72E-07	0.026	0.003
LM6524	B	69.4	BA-131	0.81	1.49E-03	103.688	10.270
LM6524	B	69.4	BA-133	0.41	1.42E-02	987.836	240.721
LM6524	B	69.4	HF-181	0.75	1.37E-06	0.095	0.011
PL21X1	B	92.7	CO-60	0.98	1.92E-06	0.178	0.012

PL21X1	B	92.7	ZN-65	0.99	6.69E-03	619.879	24.833
PL21X1	B	92.7	RU-103	0.81	3.25E-06	0.302	0.095
PL21X1	B	92.7	SB-124	0.77	2.60E-07	0.024	0.002
PL21X1	B	92.7	BA-131	0.81	9.00E-04	83.475	8.465
PL21X1	B	92.7	BA-133	0.41	5.45E-03	505.441	222.150
PL21X1	B	92.7	HF-181	0.75	7.83E-07	0.073	0.009
RP140E	B	107.9	CO-60	0.97	1.02E-06	0.110	0.010
RP140E	B	107.9	ZN-65	0.98	4.28E-03	461.609	18.513
RP140E	B	107.9	RU-103	0.78	1.57E-06	0.169	0.083
RP140E	B	107.9	SB-124	0.76	1.89E-07	0.020	0.002
RP140E	B	107.9	BA-131	0.81	6.20E-04	66.896	7.278
RP140E	B	107.9	BA-133	0.41	6.63E-03	715.545	193.944
RP140E	B	107.9	HF-181	0.75	4.39E-07	0.047	0.008
TT15A5	A	104.3	CO-60	0.97	8.79E-07	0.092	0.009
TT15A5	A	104.3	ZN-65	0.98	5.12E-03	534.003	21.395
TT15A5	A	104.3	SE-75	0.50	9.19E-07	0.096	0.008
TT15A5	A	104.3	RU-103	0.80	4.85E-06	0.506	0.086
TT15A5	A	104.3	SB-124	0.45	1.89E-07	0.020	0.004
TT15A5	A	104.3	BA-131	0.82	6.98E-04	72.831	7.488
TT15A5	A	104.3	HF-181	0.85	5.97E-07	0.062	0.005
U5D8UN	A	75	CO-60	0.98	1.99E-06	0.149	0.011
U5D8UN	A	75	ZN-65	0.98	6.09E-03	457.112	18.356
U5D8UN	A	75	RU-103	0.81	3.15E-06	0.237	0.072
U5D8UN	A	75	SB-124	0.76	4.64E-07	0.035	0.003
U5D8UN	A	75	BA-131	0.84	4.59E-04	34.416	3.790
U5D8UN	A	75	BA-133	0.41	6.48E-03	486.320	199.642
U5D8UN	A	75	CE-141	0.98	5.88E-06	0.441	0.138
U5D8UN	A	75	HF-181	0.75	1.54E-06	0.116	0.009
VDSA46	A	108.7	CO-60	0.95	1.31E-06	0.143	0.011
VDSA46	A	108.7	ZN-65	0.98	6.64E-03	722.309	28.909
VDSA46	A	108.7	RU-103	0.80	4.64E-06	0.505	0.105
VDSA46	A	108.7	SB-124	0.77	3.45E-07	0.038	0.003
VDSA46	A	108.7	BA-131	0.81	9.45E-04	102.723	10.269
VDSA46	A	108.7	BA-133	0.41	9.43E-03	1025.256	237.873
VDSA46	A	108.7	HF-175	0.85	5.75E-06	0.625	0.170
VDSA46	A	108.7	HF-181	0.75	6.56E-07	0.071	0.010
85HXNS	B	74	CO-60	1.00	2.70E-06	0.200	0.013
85HXNS	B	74	ZN-65	0.99	6.19E-03	458.267	18.437
85HXNS	B	74	RU-103	0.83	6.63E-06	0.491	0.096
85HXNS	B	74	SB-124	0.91	2.79E-06	0.207	0.009
85HXNS	B	74	BA-133	0.41	3.53E-03	261.106	210.230
85HXNS	B	74	CE-141	0.97	3.27E-05	2.420	0.235
85HXNS	B	74	EU-152x	0.53	1.95E-07	0.014	0.001
85HXNS	B	74	HF-181	0.75	1.08E-06	0.080	0.010
29440	A	94.3	SC-46	0.96	2.79E-06	0.263	0.013
29440	A	94.3	CO-60	1.00	1.86E-06	0.175	0.012
29440	A	94.3	ZN-65	1.00	5.25E-03	495.377	19.901
29440	A	94.3	RU-103	0.79	2.96E-06	0.279	0.098
29440	A	94.3	SB-124	0.77	4.51E-07	0.043	0.003
29440	A	94.3	BA-131	0.65	6.53E-04	61.593	8.930

29440	A	94.3	HF-181	0.75	8.87E-07	0.084	0.010
29440	B	88.9	SC-46	0.95	3.04E-06	0.270	0.013
29440	B	88.9	CO-60	0.99	1.87E-06	0.166	0.012
29440	B	88.9	ZN-65	0.99	6.13E-03	545.178	21.894
29440	B	88.9	RU-103	0.76	3.17E-06	0.282	0.104
29440	B	88.9	SB-124	0.77	4.74E-07	0.042	0.003
29440	B	88.9	BA-131	0.64	9.08E-04	80.677	10.571
29440	B	88.9	BA-133	0.40	3.01E-03	267.225	214.150
29440	B	88.9	HF-181	0.75	8.79E-07	0.078	0.010
29606	B	83.9	SC-46	0.96	2.66E-06	0.223	0.011
29606	B	83.9	CO-60	0.99	1.52E-06	0.128	0.010
29606	B	83.9	ZN-65	0.99	5.12E-03	429.431	17.275
29606	B	83.9	RU-103	0.80	2.31E-06	0.193	0.090
29606	B	83.9	SB-124	0.77	3.58E-07	0.030	0.003
29606	B	83.9	BA-131	0.66	8.02E-04	67.312	8.699
29606	B	83.9	BA-133	0.41	4.88E-03	409.664	192.563
29606	B	83.9	HF-175	0.88	7.04E-06	0.590	0.146
29606	B	83.9	HF-181	0.75	7.94E-07	0.067	0.009
A3798H	A	87.8	CO-60	1.00	3.18E-06	0.279	0.016
A3798H	A	87.8	ZN-65	1.00	5.09E-03	447.288	17.986
A3798H	A	87.8	RU-103	0.80	3.70E-06	0.325	0.090
A3798H	A	87.8	SB-124	0.77	3.12E-07	0.027	0.003
A3798H	A	87.8	BA-131	0.64	8.35E-04	73.297	9.361
A3798H	A	87.8	BA-133	0.40	2.20E-03	193.450	190.578
A3798H	A	87.8	HF-181	0.75	9.85E-07	0.086	0.010
A3798H	B	93.4	CO-60	1.00	2.65E-06	0.248	0.015
A3798H	B	93.4	ZN-65	0.99	5.01E-03	468.205	18.817
A3798H	B	93.4	RU-103	0.87	2.12E-06	0.198	0.093
A3798H	B	93.4	SB-124	0.77	3.05E-07	0.029	0.003
A3798H	B	93.4	BA-131	0.65	7.24E-04	67.578	9.040
A3798H	B	93.4	HF-181	0.75	1.04E-06	0.097	0.010
A3803H	A	77.1	SC-46	0.96	2.89E-06	0.222	0.012
A3803H	A	77.1	CO-60	0.98	6.91E-06	0.533	0.025
A3803H	A	77.1	ZN-65	0.98	6.29E-03	484.646	19.487
A3803H	A	77.1	RU-103	0.77	3.37E-06	0.260	0.097
A3803H	A	77.1	SB-124	0.77	4.44E-07	0.034	0.003
A3803H	A	77.1	BA-131	0.65	8.85E-04	68.245	8.920
A3803H	A	77.1	BA-133	0.41	3.09E-03	238.250	209.750
A3803H	A	77.1	HF-175	0.90	8.21E-06	0.633	0.160
A3803H	A	77.1	HF-181	0.75	1.00E-06	0.077	0.010
A3861H	B	101.7	CR-51	0.95	3.20E-05	3.255	0.981
A3861H	B	101.7	CO-60	0.99	3.08E-06	0.314	0.017
A3861H	B	101.7	ZN-65	0.99	7.27E-03	738.966	29.615
A3861H	B	101.7	RU-103	0.78	3.21E-06	0.326	0.122
A3861H	B	101.7	SB-124	0.77	3.84E-07	0.039	0.003
A3861H	B	101.7	BA-131	0.64	1.14E-03	116.140	13.989
A3861H	B	101.7	BA-133	0.41	5.38E-03	547.606	253.277
A3861H	B	101.7	CE-141	0.97	6.52E-06	0.663	0.228
A3861H	B	101.7	HF-181	0.75	1.12E-06	0.113	0.012
DSF6UE	A	78.4	CR-51	0.95	3.92E-05	3.076	0.869



DSF6UE	A	78.4	CO-60	0.99	2.36E-06	0.185	0.013
DSF6UE	A	78.4	ZN-65	0.99	7.61E-03	596.912	23.971
DSF6UE	A	78.4	SE-75	0.50	9.97E-07	0.078	0.008
DSF6UE	A	78.4	RU-103	0.83	5.69E-06	0.446	0.105
DSF6UE	A	78.4	SB-124	0.77	5.71E-07	0.045	0.003
DSF6UE	A	78.4	BA-133	0.41	7.81E-03	612.577	223.219
DSF6UE	A	78.4	CE-141	0.97	5.47E-06	0.429	0.208
DSF6UE	A	78.4	EU-152x	0.41	1.90E-07	0.015	0.001
DSF6UE	A	78.4	HF-175	0.86	5.24E-06	0.411	0.177
DSF6UE	A	78.4	HF-181	0.85	8.72E-07	0.068	0.006
F1JH39	A	74.9	CO-60	0.99	2.19E-06	0.164	0.012
F1JH39	A	74.9	ZN-65	1.00	7.06E-03	528.982	21.248
F1JH39	A	74.9	RU-103	0.83	2.67E-06	0.200	0.098
F1JH39	A	74.9	SB-124	0.77	2.74E-07	0.021	0.003
F1JH39	A	74.9	BA-131	0.65	1.12E-03	84.113	10.646
F1JH39	A	74.9	HF-181	0.75	6.21E-07	0.046	0.009
G09JVE	B	87	CO-60	0.99	4.05E-06	0.353	0.018
G09JVE	B	87	ZN-65	1.00	7.11E-03	618.998	24.835
G09JVE	B	87	SE-75	0.51	1.41E-06	0.123	0.016
G09JVE	B	87	RU-103	0.82	4.69E-07	0.041	0.106
G09JVE	B	87	SB-124	0.77	3.80E-07	0.033	0.003
G09JVE	B	87	BA-131	0.64	1.06E-03	91.966	11.268
MB6LV1	B	85.6	CO-60	0.99	2.72E-06	0.233	0.014
MB6LV1	B	85.6	ZN-65	0.99	7.02E-03	600.782	24.118
MB6LV1	B	85.6	RU-103	0.78	1.86E-06	0.160	0.103
MB6LV1	B	85.6	SB-124	0.77	2.37E-07	0.020	0.002
MB6LV1	B	85.6	BA-131	0.78	9.51E-04	81.379	10.001
MB6LV1	B	85.6	BA-133	0.41	9.36E-03	801.096	221.225
MB6LV1	B	85.6	HF-181	0.75	8.68E-07	0.074	0.010
SJA33J	A	62.3	CO-60	0.98	1.99E-06	0.124	0.010
SJA33J	A	62.3	ZN-65	0.98	5.61E-03	349.464	14.097
SJA33J	A	62.3	SE-75	0.99	5.22E-06	0.325	0.018
SJA33J	A	62.3	RU-103	0.79	8.26E-06	0.515	0.080
SJA33J	A	62.3	SB-124	0.76	6.22E-07	0.039	0.003
SJA33J	A	62.3	EU-152x	0.43	3.86E-08	0.002	0.001
SJA33J	A	62.3	HF-175	0.87	9.55E-06	0.595	0.141
SJA33J	A	62.3	HG-203	0.98	4.12E-06	0.257	0.082
U44MXB	A	96.1	CO-60	0.99	3.62E-06	0.348	0.018
U44MXB	A	96.1	ZN-65	0.99	5.62E-03	540.522	21.706
U44MXB	A	96.1	RU-103	0.79	7.10E-07	0.068	0.105
U44MXB	A	96.1	SB-124	0.78	5.02E-07	0.048	0.004
U44MXB	A	96.1	BA-131	0.64	7.99E-04	76.790	10.574
U44MXB	A	96.1	BA-133	0.41	6.11E-03	587.590	219.948
U44MXB	A	96.1	CE-141	0.96	7.47E-06	0.718	0.204
U44MXB	A	96.1	HF-181	0.75	1.08E-06	0.104	0.011
U44MXB	B	71	CO-60	0.99	3.83E-06	0.272	0.016
U44MXB	B	71	ZN-65	0.99	5.34E-03	379.190	15.280
U44MXB	B	71	RU-103	0.79	5.54E-06	0.393	0.086
U44MXB	B	71	SB-124	0.77	5.73E-07	0.041	0.003
U44MXB	B	71	HF-175	0.90	7.68E-06	0.545	0.149

U44MXB	B	71	HF-181	0.75	1.10E-06	0.078	0.009
2D152A	A	102	CO-60	0.99	1.25E-06	0.127	0.010
2D152A	A	102	ZN-65	1.00	5.90E-03	602.088	24.155
2D152A	A	102	RU-103	0.80	3.45E-06	0.352	0.103
2D152A	A	102	SB-124	0.45	1.43E-07	0.015	0.004
2D152A	A	102	BA-131	0.66	8.02E-04	81.805	10.274
2D152A	A	102	BA-133	0.41	1.13E-02	1147.950	218.748
2D152A	A	102	HF-175	0.86	8.21E-06	0.838	0.169
2D152A	A	102	HF-181	0.75	5.94E-07	0.061	0.010
17BDAR	B	68.4	CO-60	0.98	5.31E-06	0.363	0.019
17BDAR	B	68.4	ZN-65	0.99	7.99E-03	546.722	21.980
17BDAR	B	68.4	SB-124	0.77	4.43E-07	0.030	0.003
17BDAR	B	68.4	EU-154	0.32	3.42E-07	0.023	0.003
17BDAR	B	68.4	HF-181	0.75	5.63E-07	0.038	0.010
85HXNS	A	102.2	CO-60	0.98	1.83E-06	0.187	0.013
85HXNS	A	102.2	ZN-65	0.99	5.81E-03	593.688	23.835
85HXNS	A	102.2	RU-103	0.85	4.72E-06	0.482	0.113
85HXNS	A	102.2	SB-124	0.98	2.74E-06	0.280	0.012
85HXNS	A	102.2	BA-133	0.41	5.95E-03	608.539	222.016
85HXNS	A	102.2	CE-141	0.96	3.50E-05	3.576	0.296
85HXNS	A	102.2	EU-152x	0.53	1.66E-07	0.017	0.001
85HXNS	A	102.2	HF-175	0.87	9.75E-06	0.997	0.197
85HXNS	A	102.2	HF-181	0.75	1.11E-06	0.113	0.012
163B43	B	81.2	CR-51	0.95	2.05E-05	1.667	1.005
163B43	B	81.2	CO-60	0.99	6.38E-06	0.518	0.025
163B43	B	81.2	ZN-65	0.99	7.86E-03	638.239	25.624
163B43	B	81.2	SB-124	0.77	7.19E-07	0.058	0.004
163B43	B	81.2	BA-131	0.40	1.39E-03	112.485	38.714
163B43	B	81.2	BA-133	0.41	6.11E-03	495.778	226.663
163B43	B	81.2	EU-154	0.32	1.63E-08	0.001	0.009
115754	A	90.7	CO-60	0.99	1.49E-06	0.135	0.011
115754	A	90.7	ZN-65	1.00	7.61E-03	690.644	27.708
115754	A	90.7	RU-103	0.83	3.18E-06	0.289	0.125
115754	A	90.7	SB-124	0.77	2.67E-07	0.024	0.003
115754	A	90.7	BA-131	0.61	1.28E-03	116.232	16.792
115754	A	90.7	BA-133	0.41	8.80E-03	798.539	229.384
115754	A	90.7	HF-175	0.87	1.28E-05	1.163	0.195
115754	A	90.7	HF-181	0.75	1.25E-06	0.113	0.012
A3861H	A	89	SC-46	0.96	2.28E-06	0.203	0.011
A3861H	A	89	CO-60	0.99	2.20E-06	0.196	0.013
A3861H	A	89	ZN-65	0.99	5.55E-03	493.647	19.849
A3861H	A	89	RU-103	0.84	2.37E-06	0.211	0.106
A3861H	A	89	SB-124	0.77	3.13E-07	0.028	0.003
A3861H	A	89	BA-131	0.60	9.52E-04	84.745	12.978
A3861H	A	89	BA-133	0.40	1.01E-02	900.292	196.361
A3861H	A	89	HF-175	0.90	8.32E-06	0.740	0.161
A3861H	A	89	HF-181	0.75	1.12E-06	0.099	0.011
DSF6UE	B	71.1	CO-60	0.99	2.32E-06	0.165	0.011
DSF6UE	B	71.1	ZN-65	1.00	8.04E-03	571.937	22.987
DSF6UE	B	71.1	SB-124	0.77	3.91E-07	0.028	0.003

DSF6UE	B	71.1	BA-133	0.40	8.20E-03	583.226	200.238
DSF6UE	B	71.1	EU-152x	0.39	1.24E-07	0.009	0.001
DSF6UE	B	71.1	HF-175	0.91	1.01E-05	0.721	0.177
DSF6UE	B	71.1	HF-181	0.74	8.64E-07	0.061	0.011
CE9B16	A	68.2	SC-46	0.96	3.66E-06	0.250	0.013
CE9B16	A	68.2	CO-60	0.99	4.27E-06	0.291	0.016
CE9B16	A	68.2	ZN-65	0.99	6.93E-03	472.615	19.034
CE9B16	A	68.2	RU-103	0.80	2.36E-06	0.161	0.107
CE9B16	A	68.2	SB-124	0.76	5.34E-07	0.036	0.003
CE9B16	A	68.2	BA-131	0.62	9.73E-04	66.350	11.042
CE9B16	A	68.2	BA-133	0.41	5.99E-03	408.476	204.494
CE9B16	A	68.2	HF-181	0.75	9.99E-07	0.068	0.010
DR87FE	B	92.5	CO-60	0.99	3.47E-06	0.321	0.017
DR87FE	B	92.5	ZN-65	0.99	8.18E-03	756.425	30.328
DR87FE	B	92.5	RU-103	0.79	4.38E-06	0.406	0.128
DR87FE	B	92.5	SB-124	0.77	2.60E-07	0.024	0.003
DR87FE	B	92.5	BA-131	0.42	1.15E-03	106.753	15.828
DR87FE	B	92.5	BA-133	0.41	1.30E-02	1204.160	230.719
DR87FE	B	92.5	HF-181	0.75	6.92E-07	0.064	0.012
FTRT75	A	94.6	CO-60	0.99	2.83E-06	0.268	0.015
FTRT75	A	94.6	ZN-65	0.99	7.24E-03	684.802	27.473
FTRT75	A	94.6	RU-103	0.78	4.43E-06	0.419	0.111
FTRT75	A	94.6	SB-124	0.77	4.43E-07	0.042	0.003
FTRT75	A	94.6	BA-133	0.41	4.80E-03	453.629	224.311
FTRT75	A	94.6	EU-152x	0.51	1.22E-07	0.012	0.001
FTRT75	A	94.6	HF-181	0.75	9.03E-07	0.085	0.011
HGD63H	B	96.8	CO-60	1.00	3.76E-06	0.364	0.019
HGD63H	B	96.8	ZN-65	1.00	7.85E-03	759.581	30.457
HGD63H	B	96.8	SB-124	0.77	3.69E-07	0.036	0.003
HGD63H	B	96.8	BA-131	0.41	1.04E-03	100.927	42.085
HGD63H	B	96.8	BA-133	0.41	5.55E-03	537.118	247.888
HGD63H	B	96.8	EU-154	0.32	6.73E-08	0.007	0.010
HGD63H	B	96.8	HF-181	0.75	1.29E-06	0.124	0.013
K76G4R	A	62.9	CO-60	0.99	2.46E-06	0.155	0.011
K76G4R	A	62.9	ZN-65	0.99	6.93E-03	436.126	17.570
K76G4R	A	62.9	SE-75	1.00	4.41E-05	2.773	0.113
K76G4R	A	62.9	RU-103	0.81	5.65E-06	0.356	0.092
K76G4R	A	62.9	SB-124	0.77	5.97E-07	0.038	0.003
K76G4R	A	62.9	YB-169	0.35	1.04E-06	0.065	0.019
K76G4R	A	62.9	HF-175	0.89	9.89E-06	0.622	0.150
K76G4R	A	62.9	HG-203	0.97	4.71E-05	2.963	0.182
Q0XU17	A	103.4	CO-60	1.00	1.60E-06	0.166	0.011
Q0XU17	A	103.4	ZN-65	0.99	6.36E-03	658.065	26.404
Q0XU17	A	103.4	RU-103	0.83	1.50E-06	0.155	0.117
Q0XU17	A	103.4	SB-124	0.77	2.67E-07	0.028	0.003
Q0XU17	A	103.4	BA-131	0.41	9.64E-04	99.650	14.210
Q0XU17	A	103.4	BA-133	0.41	6.66E-03	688.701	226.936
Q0XU17	A	103.4	HF-181	0.75	5.08E-07	0.053	0.011
T007ML	B	87.8	CO-60	1.00	2.25E-06	0.198	0.013
T007ML	B	87.8	ZN-65	1.00	7.39E-03	649.269	26.059

T007ML	B	87.8	RU-103	0.80	3.07E-06	0.270	0.122
T007ML	B	87.8	SB-124	0.78	3.45E-07	0.030	0.003
T007ML	B	87.8	BA-131	0.41	1.28E-03	112.251	16.141
T007ML	B	87.8	BA-133	0.41	1.09E-02	954.051	218.186
T007ML	B	87.8	HF-175	0.93	1.15E-05	1.011	0.191
T007ML	B	87.8	HF-181	0.75	1.29E-06	0.113	0.012
WBH9G4	B	73.3	FE-59	0.97	1.17E-03	85.842	14.519
WBH9G4	B	73.3	CO-60	0.99	2.43E-06	0.178	0.012
WBH9G4	B	73.3	ZN-65	0.99	6.53E-03	478.404	19.250
WBH9G4	B	73.3	RU-103	0.79	1.54E-07	0.011	0.104
WBH9G4	B	73.3	SB-124	0.77	2.80E-07	0.021	0.002
WBH9G4	B	73.3	BA-131	0.40	1.02E-03	74.476	12.235
WBH9G4	B	73.3	BA-133	0.41	1.07E-02	783.785	187.681
WBH9G4	B	73.3	HF-181	0.75	7.87E-07	0.058	0.010
2D152A	B	86.3	FE-59	0.98	1.30E-03	111.818	14.360
2D152A	B	86.3	CO-60	0.99	2.79E-06	0.240	0.014
2D152A	B	86.3	ZN-65	0.99	7.49E-03	646.014	25.941
2D152A	B	86.3	RU-103	0.83	3.44E-06	0.297	0.114
2D152A	B	86.3	SB-124	0.77	3.45E-07	0.030	0.003
2D152A	B	86.3	BA-131	0.62	1.21E-03	104.350	14.165
2D152A	B	86.3	BA-133	0.41	8.03E-03	693.179	227.228
2D152A	B	86.3	HF-175	0.89	8.63E-06	0.744	0.176
2D152A	B	86.3	HF-181	0.75	9.19E-07	0.079	0.011
17BDAR	A	64.2	CO-60	0.98	7.10E-06	0.456	0.022
17BDAR	A	64.2	ZN-65	0.98	8.81E-03	565.684	22.720
17BDAR	A	64.2	SE-75	0.99	4.52E-06	0.290	0.019
17BDAR	A	64.2	SB-124	0.77	3.71E-07	0.024	0.003
17BDAR	A	64.2	BA-133	0.41	7.01E-03	450.160	207.542
17BDAR	A	64.2	EU-152x	0.54	6.02E-09	0.000	0.001
17BDAR	A	64.2	HF-175	0.89	9.17E-06	0.589	0.187
17BDAR	A	64.2	HG-203	0.98	2.55E-06	0.164	0.121
6025ES	B	69.7	CO-60	0.97	3.81E-06	0.266	0.015
6025ES	B	69.7	ZN-65	0.98	9.26E-03	645.407	25.893
6025ES	B	69.7	SB-124	0.77	3.90E-07	0.027	0.003
6025ES	B	69.7	BA-133	0.41	9.05E-03	630.476	216.889
6025ES	B	69.7	EU-152x	0.41	1.31E-07	0.009	0.001
6025ES	B	69.7	HF-175	0.89	1.52E-06	0.106	0.191
ADJ145	A	76.8	CO-60	0.99	1.88E-06	0.144	0.011
ADJ145	A	76.8	ZN-65	0.99	8.31E-03	638.089	25.597
ADJ145	A	76.8	RU-103	0.81	6.28E-06	0.482	0.132
ADJ145	A	76.8	SB-124	0.77	2.37E-07	0.018	0.003
ADJ145	A	76.8	BA-133	0.41	5.08E-03	390.443	220.557
ADJ145	A	76.8	EU-154	0.31	2.51E-07	0.019	0.003
ADJ145	A	76.8	HF-181	0.74	7.73E-07	0.059	0.013
ADJ145	B	77.7	CO-60	0.97	2.95E-06	0.229	0.014
ADJ145	B	77.7	ZN-65	0.99	8.86E-03	688.277	27.587
ADJ145	B	77.7	RU-103	0.76	7.41E-06	0.576	0.134
ADJ145	B	77.7	BA-133	0.41	9.44E-03	733.707	224.792
ADJ145	B	77.7	EU-152x	0.41	1.31E-07	0.010	0.001
ADJ145	B	77.7	HF-175	0.99	1.30E-06	0.101	0.197

ADJ145	B	77.7	HF-181	0.73	4.19E-07	0.033	0.013
FDRT75	B	72.5	CO-60	0.99	2.82E-06	0.204	0.013
FDRT75	B	72.5	ZN-65	0.99	8.62E-03	624.907	25.070
FDRT75	B	72.5	SB-124	0.78	4.65E-07	0.034	0.003
FDRT75	B	72.5	BA-133	0.41	5.57E-03	404.003	219.044
FDRT75	B	72.5	EU-152x	0.53	1.23E-07	0.009	0.001
FDRT75	B	72.5	HF-175	0.94	9.94E-06	0.721	0.183
FDRT75	B	72.5	HF-181	0.74	7.74E-07	0.056	0.011
G8UX4V	B	99.7	CO-60	0.97	1.86E-06	0.186	0.012
G8UX4V	B	99.7	ZN-65	0.98	6.56E-03	653.689	26.191
G8UX4V	B	99.7	SB-124	0.77	2.43E-07	0.024	0.003
G8UX4V	B	99.7	BA-133	0.41	6.78E-03	676.083	220.993
G8UX4V	B	99.7	EU-152x	0.40	9.61E-08	0.010	0.001
G8UX4V	B	99.7	HF-175	0.98	1.85E-06	0.184	0.193
LM6524	A	71.4	CO-60	0.98	3.80E-06	0.271	0.015
LM6524	A	71.4	ZN-65	0.98	8.02E-03	572.880	22.990
LM6524	A	71.4	SB-124	0.45	3.34E-07	0.024	0.005
LM6524	A	71.4	BA-133	0.41	5.64E-03	402.401	203.605
LM6524	A	71.4	EU-152x	0.42	1.18E-07	0.008	0.001
LM6524	A	71.4	HF-175	0.92	5.64E-06	0.403	0.184
LM6524	A	71.4	HF-181	0.74	1.04E-06	0.074	0.012
M6AAM6	B	68.3	CO-60	0.98	2.33E-06	0.159	0.012
M6AAM6	B	68.3	ZN-65	0.98	9.27E-03	633.283	25.412
M6AAM6	B	68.3	SB-124	0.77	4.31E-07	0.029	0.003
M6AAM6	B	68.3	BA-133	0.41	6.61E-03	451.183	216.008
M6AAM6	B	68.3	HF-181	0.74	8.35E-07	0.057	0.013
77G4CJ	B	84.4	CO-60	1.00	2.37E-06	0.200	0.013
77G4CJ	B	84.4	ZN-65	1.00	7.16E-03	604.277	24.267
77G4CJ	B	84.4	SB-124	0.77	2.87E-07	0.024	0.003
77G4CJ	B	84.4	BA-133	0.41	3.14E-03	264.937	204.320
2965CL	A	100.1	CO-60	0.99	4.35E-06	0.435	0.022
2965CL	A	100.1	ZN-65	0.99	6.48E-03	648.292	26.005
2965CL	A	100.1	SB-124	0.77	1.13E-06	0.113	0.006
2965CL	A	100.1	BA-133	0.40	8.60E-03	860.536	226.670
2965CL	A	100.1	EU-152x	0.55	9.53E-08	0.010	0.001
2965CL	A	100.1	HF-175	0.87	8.64E-06	0.865	0.215
2965CL	A	100.1	HF-181	0.74	9.42E-07	0.094	0.014
6025ES	A	69.4	CO-60	1.00	3.43E-06	0.238	0.014
6025ES	A	69.4	ZN-65	1.00	7.75E-03	537.702	21.622
6025ES	A	69.4	SB-124	0.45	3.11E-07	0.022	0.005
6025ES	A	69.4	BA-133	0.41	4.38E-03	304.241	204.873
DAW454	B	84.6	CO-60	1.00	3.92E-06	0.332	0.018
DAW454	B	84.6	ZN-65	1.00	7.95E-03	672.705	26.996
DAW454	B	84.6	SB-124	0.77	3.25E-07	0.027	0.003
DAW454	B	84.6	BA-133	0.41	4.47E-03	378.236	223.534
DAW454	B	84.6	EU-154	0.30	2.39E-07	0.020	0.003
DAW454	B	84.6	HF-181	0.74	8.64E-07	0.073	0.014
DR87FE	A	94.8	CO-60	1.00	3.18E-06	0.302	0.017
DR87FE	A	94.8	ZN-65	1.00	7.90E-03	748.553	30.018
DR87FE	A	94.8	SB-124	0.77	2.80E-07	0.027	0.003

DR87FE	A	94.8	BA-133	0.41	9.96E-03	943.971	235.936
DR87FE	A	94.8	EU-152x	0.40	8.80E-08	0.008	0.001
DR87FE	A	94.8	HF-175	0.86	7.27E-06	0.689	0.218
FWX130	B	90.4	CO-60	1.00	2.88E-06	0.260	0.015
FWX130	B	90.4	ZN-65	1.00	8.38E-03	757.334	30.373
FWX130	B	90.4	SB-124	0.76	3.09E-07	0.028	0.003
FWX130	B	90.4	BA-133	0.41	7.97E-03	720.865	236.363
FWX130	B	90.4	EU-152x	0.55	1.10E-07	0.010	0.001
FWX130	B	90.4	HF-175	0.87	3.47E-06	0.314	0.219
FWX130	B	90.4	HF-181	0.74	1.06E-06	0.096	0.015
GO9JVE	B	85	CO-60	1.00	5.57E-06	0.473	0.023
GO9JVE	B	85	ZN-65	1.00	6.90E-03	586.094	23.543
GO9JVE	B	85	SB-124	0.77	4.42E-07	0.038	0.004
GO9JVE	B	85	BA-133	0.41	4.45E-04	37.808	223.062
GO9JVE	B	85	HF-181	0.74	8.06E-07	0.068	0.013
M6AAM6	A	83	CO-60	1.00	3.18E-06	0.264	0.015
M6AAM6	A	83	ZN-65	1.00	9.10E-03	755.592	30.303
M6AAM6	A	83	SB-124	0.77	5.31E-07	0.044	0.004
M6AAM6	A	83	BA-133	0.41	1.09E-02	901.626	226.951
M6AAM6	A	83	EU-154	0.31	2.42E-07	0.020	0.003
M6AAM6	A	83	HF-181	0.74	1.20E-06	0.099	0.015
WAQE67	B	93.7	CO-60	0.99	3.49E-06	0.327	0.018
WAQE67	B	93.7	ZN-65	1.00	8.40E-03	787.409	31.571
WAQE67	B	93.7	SB-124	0.75	3.80E-07	0.036	0.003
WAQE67	B	93.7	BA-133	0.41	8.13E-03	761.522	233.566
WAQE67	B	93.7	EU-152x	0.54	9.24E-08	0.009	0.001
WAQE67	B	93.7	HF-175	0.91	9.38E-06	0.879	0.225
WAQE67	B	93.7	HF-181	0.74	8.21E-07	0.077	0.014
WR2F6B	A	65.5	CO-60	0.99	2.59E-06	0.170	0.012
WR2F6B	A	65.5	ZN-65	1.00	7.65E-03	501.279	20.174
WR2F6B	A	65.5	SB-124	0.77	4.51E-07	0.030	0.003
WR2F6B	A	65.5	BA-133	0.41	4.27E-03	279.863	199.575
WR2F6B	A	65.5	EU-154	0.31	2.53E-07	0.017	0.002
WR2F6B	A	65.5	HF-181	0.74	1.90E-06	0.125	0.014
WR2F6B	B	49.1	CO-60	0.99	3.82E-06	0.187	0.012
WR2F6B	B	49.1	ZN-65	1.00	7.83E-03	384.280	15.531
WR2F6B	B	49.1	SB-124	0.77	5.49E-07	0.027	0.003
WR2F6B	B	49.1	HF-175	0.93	1.64E-05	0.804	0.165
WR2F6B	B	49.1	HF-181	0.74	1.67E-06	0.082	0.012
DM3452216	B	100.7	CO-60	0.98	1.30E-06	0.130	0.010
DM3452216	B	100.7	ZN-65	0.99	4.98E-03	501.326	20.153
DM3452216	B	100.7	BA-133	0.41	5.59E-03	563.011	184.487
7Y536N	B	92.9	CO-60	0.99	3.47E-06	0.322	0.017
7Y536N	B	92.9	ZN-65	0.99	7.06E-03	656.135	26.349
7Y536N	B	92.9	SB-124	0.76	3.02E-07	0.028	0.003
7Y536N	B	92.9	BA-133	0.40	5.61E-03	520.822	208.032
7Y536N	B	92.9	EU-152x	0.42	7.40E-08	0.007	0.001
7Y536N	B	92.9	HF-181	0.74	6.88E-07	0.064	0.016
46NKJF	A	98.7	CO-60	0.98	1.73E-06	0.171	0.012
46NKJF	A	98.7	ZN-65	0.99	4.12E-03	407.058	16.396

46NKJF	A	98.7	SB-124	0.44	1.13E-07	0.011	0.005
46NKJF	A	98.7	BA-133	0.41	6.61E-03	652.094	86.803
29750	A	78	SC-46	0.95	3.19E-06	0.249	0.014
29750	A	78	CO-60	0.98	2.77E-06	0.216	0.013
29750	A	78	ZN-65	0.99	6.59E-03	514.075	20.690
29750	A	78	SB-124	0.76	4.69E-07	0.037	0.004
29750	A	78	BA-133	0.41	3.19E-03	248.541	200.927
29750	A	78	EU-152x	0.43	7.38E-08	0.006	0.001
29750	A	78	HF-175	0.89	7.39E-06	0.577	0.207
30103	A	83.2	SC-46	0.95	2.52E-06	0.210	0.012
30103	A	83.2	CO-60	0.98	1.04E-06	0.087	0.008
30103	A	83.2	ZN-65	0.99	4.89E-03	406.905	16.410
30103	A	83.2	SB-124	0.76	3.20E-07	0.027	0.003
30103	A	83.2	BA-133	0.41	6.22E-03	517.711	82.835
30124	A	63.5	SC-46	0.94	3.65E-06	0.232	0.013
30124	A	63.5	CO-60	1.00	1.96E-06	0.125	0.010
30124	A	63.5	ZN-65	1.00	7.16E-03	454.625	18.325
30124	A	63.5	SB-124	0.77	4.05E-07	0.026	0.004
30124	A	63.5	BA-133	0.41	3.48E-03	220.985	191.662
30334	B	57.6	CO-60	0.99	2.88E-06	0.166	0.012
30334	B	57.6	ZN-65	0.99	8.08E-03	465.486	18.773
30334	B	57.6	SB-124	0.77	3.68E-07	0.021	0.003
30334	B	57.6	BA-133	0.41	9.77E-03	562.510	179.325
30334	B	57.6	HF-181	0.74	1.33E-06	0.077	0.015
5100224	B	55	CO-60	0.99	1.12E-05	0.616	0.029
5100224	B	55	ZN-65	0.99	8.52E-03	468.454	18.903
5100224	B	55	SB-124	0.87	3.41E-06	0.187	0.009
5100224	B	55	BA-133	0.41	5.26E-03	289.486	199.312
5100224	B	55	CE-141	0.93	4.69E-05	2.581	0.412
5100224	B	55	EU-152x	0.54	1.32E-07	0.007	0.001
5100224	B	55	HF-175	0.91	9.68E-06	0.532	0.217
5100224	B	55	HF-181	0.74	2.27E-06	0.125	0.016
5100242	A	49	CO-60	0.99	9.09E-06	0.445	0.022
5100242	A	49	ZN-65	0.99	7.14E-03	349.935	14.164
5100242	A	49	SB-124	0.87	2.89E-06	0.141	0.007
5100242	A	49	CE-141	0.93	2.84E-05	1.392	0.368
5100242	A	49	EU-152x	0.42	1.16E-07	0.006	0.001
5100242	A	49	HF-175	0.93	1.30E-05	0.637	0.189
5100242	A	49	HF-181	0.74	1.02E-06	0.050	0.014
A3873H	A	90.8	CO-60	0.98	2.77E-06	0.252	0.015
A3873H	A	90.8	ZN-65	0.99	5.77E-03	523.860	21.070
A3873H	A	90.8	SB-124	0.76	7.48E-07	0.068	0.005
A3873H	A	90.8	EU-152x	0.42	4.80E-08	0.004	0.001
A3873H	A	90.8	HF-175	0.94	9.14E-06	0.830	0.212
A3873H	A	90.8	HF-181	0.74	7.10E-07	0.064	0.016
AA61L3	A	87.6	CO-60	1.00	3.06E-06	0.268	0.015
AA61L3	A	87.6	ZN-65	1.00	8.20E-03	718.239	28.825
AA61L3	A	87.6	BA-133	0.41	6.09E-03	533.200	214.875
AA61L3	A	87.6	HF-181	0.74	8.33E-07	0.073	0.018
DM3452216-0029	A	102	CO-60	1.00	1.13E-06	0.116	0.010

DM3452216-0029	A	102	ZN-65	1.00	3.92E-03	399.645	16.092
DM3452216	A	102	EU-152x	0.43	4.65E-08	0.005	0.001
DM3452216	A	102	HF-175	0.87	2.58E-06	0.263	0.187
E63JVE	B	74.3	CO-60	1.00	3.67E-06	0.273	0.015
E63JVE	B	74.3	ZN-65	1.00	8.60E-03	639.070	25.684
E63JVE	B	74.3	SB-124	0.44	3.73E-07	0.028	0.006
E63JVE	B	74.3	BA-133	0.41	7.20E-03	535.156	207.536
E63JVE	B	74.3	EU-152x	0.55	8.34E-08	0.006	0.001
E63JVE	B	74.3	HF-175	0.90	6.08E-06	0.452	0.224
E63JVE	B	74.3	HF-181	0.73	6.94E-07	0.052	0.017
HFU84F	B	97.7	CO-60	0.99	3.31E-06	0.323	0.017
HFU84F	B	97.7	ZN-65	0.99	7.49E-03	731.529	29.352
HFU84F	B	97.7	SB-124	0.76	2.98E-07	0.029	0.004
HFU84F	B	97.7	BA-133	0.41	8.82E-03	861.320	226.975
HFU84F	B	97.7	HF-181	0.74	8.46E-07	0.083	0.016
HFU84F	A	106	CO-60	1.00	2.05E-06	0.217	0.013
HFU84F	A	106	ZN-65	1.00	3.87E-03	410.309	16.521
HFU84F	A	106	SB-124	0.42	1.81E-07	0.019	0.005
J9GFE37	A	78.3	CO-60	0.99	3.17E-06	0.248	0.015
J9GFE37	A	78.3	ZN-65	0.99	8.26E-03	646.461	25.965
J9GFE37	A	78.3	BA-133	0.41	7.57E-03	592.524	205.572
J9GFE37	A	78.3	HF-175	0.87	1.28E-05	1.003	0.223
HIDE4H	B	94.1	CO-60	0.99	3.12E-06	0.293	0.016
HIDE4H	B	94.1	ZN-65	1.00	7.42E-03	698.112	28.018
HIDE4H	B	94.1	BA-133	0.40	9.20E-03	865.882	213.693
I89VFS	A	69.6	CO-60	0.99	1.44E-06	0.100	0.009
I89VFS	A	69.6	ZN-65	0.99	5.52E-03	384.417	15.503
I89VFS	A	69.6	HF-175	0.91	4.84E-06	0.337	0.173
I89VFS	B	71.9	CO-60	0.99	1.60E-06	0.115	0.010
I89VFS	B	71.9	ZN-65	0.99	5.36E-03	385.028	15.532
I89VFS	B	71.9	SB-124	0.44	2.14E-07	0.015	0.005
I89VFS	B	71.9	BA-133	0.41	1.87E-03	134.272	164.940
KK3050200	A	102.1	CO-60	0.99	1.82E-06	0.185	0.012
KK3050200	A	102.1	ZN-65	0.99	5.85E-03	597.647	24.007
KK3050200	A	102.1	SB-124	0.77	2.73E-07	0.028	0.004
KK3050200	A	102.1	BA-133	0.41	3.35E-03	341.736	199.451
KK3050200	A	102.1	EU-152x	0.42	5.49E-08	0.006	0.001
KK3050200	A	102.1	HF-175	0.93	5.53E-06	0.564	0.211
MH64SL	A	87.2	CO-60	0.97	1.27E-06	0.111	0.010
MH64SL	A	87.2	ZN-65	0.99	4.76E-03	414.880	16.713
MH64SL	A	87.2	SB-124	0.44	3.68E-07	0.032	0.005
WBH964	A	96	CO-60	0.99	2.31E-06	0.221	0.014
WBH964	A	96	ZN-65	0.99	8.07E-03	774.443	31.063
WBH964	A	96	SB-124	0.43	3.91E-07	0.038	0.007
WBH964	A	96	BA-133	0.41	5.08E-03	487.881	232.549
WBH964	A	96	EU-152x	0.55	7.44E-08	0.007	0.001
WBH964	A	96	HF-175	0.88	3.01E-06	0.289	0.239
WBH964	A	96	HF-181	0.74	5.57E-07	0.053	0.018
A3875H	A	110.9	CO-60	0.99	2.30E-06	0.256	0.015
A3875H	A	110.9	ZN-65	0.99	5.88E-03	652.226	26.199



A3875H	A	110.9	SB-124	0.76	2.96E-07	0.033	0.004
A3875H	A	110.9	BA-133	0.41	8.11E-03	899.923	206.314
A3875H	A	110.9	EU-152x	0.55	6.22E-08	0.007	0.001
A3875H	A	110.9	HF-175	0.84	7.62E-06	0.845	0.241
A3875H	A	110.9	HF-181	0.72	1.01E-06	0.112	0.020
AB0469658	A	50.1	CO-60	1.00	8.13E-06	0.408	0.021
AB0469658	A	50.1	ZN-65	0.99	6.68E-03	334.664	13.559
AB0469658	A	50.1	SB-124	0.44	6.30E-07	0.032	0.005
AB0469658	A	50.1	EU-152x	0.55	1.52E-07	0.008	0.001
AB0469658	A	50.1	HF-175	0.94	1.23E-05	0.615	0.190
AB0469658	A	50.1	HF-181	0.73	2.55E-06	0.128	0.016
CP163W	B	88.9	CO-60	0.99	1.79E-06	0.159	0.011
CP163W	B	88.9	ZN-65	0.99	6.08E-03	540.168	21.726
CP163W	B	88.9	EU-152x	0.42	4.10E-08	0.004	0.001
CP163W	B	88.9	HF-175	0.91	6.28E-06	0.558	0.211
F1JH39	B	78.4	CO-60	0.99	2.76E-06	0.216	0.014
F1JH39	B	78.4	ZN-65	0.99	7.13E-03	559.264	22.506
F1JH39	B	78.4	SE-75	0.75	1.60E-06	0.125	0.016
F1JH39	B	78.4	SB-124	0.75	4.05E-07	0.032	0.003
F1JH39	B	78.4	BA-133	0.41	5.57E-03	436.796	185.193
115754	B	94.3	CO-60	0.99	2.86E-06	0.269	0.016
115754	B	94.3	ZN-65	0.99	7.81E-03	736.352	29.562
115754	B	94.3	BA-133	0.41	5.86E-03	552.410	210.554
115754	B	94.3	HF-181	0.73	1.03E-06	0.098	0.019
A38098	A	68.9	CO-60	0.99	4.31E-06	0.297	0.016
A38098	A	68.9	ZN-65	0.99	5.37E-03	369.876	14.932
A38098	A	68.9	SB-124	0.76	4.67E-07	0.032	0.003
J9GFE37	B	97	CO-60	1.00	3.36E-06	0.326	0.018
J9GFE37	B	97	ZN-65	1.00	7.83E-03	759.951	30.498
J9GFE37	B	97	SB-124	0.76	3.65E-07	0.035	0.004
J9GFE37	B	97	BA-133	0.41	6.73E-03	652.415	212.721
J9GFE37	B	97	EU-152x	0.42	5.66E-08	0.005	0.001
J9GFE37	B	97	HF-175	0.96	9.54E-06	0.925	0.263
J9GFE37	B	97	HF-181	0.73	1.06E-06	0.103	0.020
822589HC	A	64.9	CO-60	0.99	1.87E-06	0.121	0.010
822589HC	A	64.9	ZN-65	0.99	6.69E-03	434.410	17.530
822589HC	A	64.9	SB-124	0.75	9.63E-07	0.062	0.005
A22623HC	A	73.6	CO-60	0.99	2.99E-06	0.220	0.014
A22623HC	A	73.6	ZN-65	0.99	6.43E-03	472.990	19.062
A22623HC	A	73.6	SB-124	0.76	9.46E-07	0.070	0.005
A22623HC	A	73.6	HF-181	0.74	1.04E-06	0.076	0.017
IUY3T4	A	83.3	CO-60	1.00	2.17E-06	0.181	0.012
IUY3T4	A	83.3	ZN-65	0.99	6.13E-03	510.624	20.551
IUY3T4	A	83.3	SB-124	0.75	4.14E-07	0.034	0.004
IUY3T4	A	83.3	BA-133	0.41	3.78E-03	315.193	181.104
IUY3T4	A	83.3	EU-152x	0.43	8.32E-08	0.007	0.001
IUY3T4	A	83.3	HF-175	0.92	4.11E-06	0.342	0.219
KK3050200	B	77.1	CO-60	1.00	1.25E-06	0.096	0.009
KK3050200	B	77.1	ZN-65	0.99	5.10E-03	393.408	15.874
KK3050200	B	77.1	SB-124	0.75	2.29E-07	0.018	0.003

KK3050200-0026	B	77.1	BA-133	0.41	6.01E-03	463.705	165.417
A3875H	B	124	CO-60	0.99	1.67E-06	0.207	0.013
A3875H	B	124	ZN-65	0.99	5.26E-03	651.879	26.177
A3875H	B	124	SB-124	0.76	2.55E-07	0.032	0.004
A3875H	B	124	BA-133	0.41	6.52E-03	808.317	203.538
A3875H	B	124	EU-152x	0.55	5.37E-08	0.007	0.001
A3875H	B	124	HF-181	0.73	9.60E-07	0.119	0.019
MH64SL	B	107	CO-60	0.99	9.36E-07	0.100	0.009
MH64SL	B	107	ZN-65	0.99	3.03E-03	324.410	13.094
MH64SL	B	107	SB-124	0.44	1.73E-07	0.018	0.004
MH64SL	B	107	BA-133	0.41	2.49E-03	266.275	147.797
U5D8UN	B	101.3	CO-60	0.99	2.30E-06	0.233	0.014
U5D8UN	B	101.3	ZN-65	0.99	5.65E-03	572.516	23.018
U5D8UN	B	101.3	SB-124	0.76	5.25E-07	0.053	0.004
U5D8UN	B	101.3	EU-152x	0.55	4.98E-08	0.005	0.001
U5D8UN	B	101.3	HF-175	0.90	8.09E-06	0.819	0.225
U5D8UN	B	101.3	HF-181	0.73	1.60E-06	0.162	0.019
25599	B	74.6	SC-46	0.95	3.45E-06	0.257	0.014
25599	B	74.6	CO-60	1.00	1.87E-06	0.140	0.011
25599	B	74.6	ZN-65	0.99	6.96E-03	518.892	20.892
25599	B	74.6	SB-124	0.76	4.73E-07	0.035	0.004
25599	B	74.6	BA-133	0.40	4.39E-03	327.719	183.760
25599	B	74.6	HF-181	0.73	9.15E-07	0.068	0.018
E63JVE	A	73.3	CO-60	1.00	3.64E-06	0.267	0.015
E63JVE	A	73.3	ZN-65	1.00	8.19E-03	600.284	24.151
E63JVE	A	73.3	SB-124	0.76	4.65E-07	0.034	0.004
E63JVE	A	73.3	BA-133	0.42	4.42E-03	324.253	192.360
3Q5J9L	B	82.9	CO-60	0.99	1.96E-06	0.163	0.011
3Q5J9L	B	82.9	ZN-65	1.00	5.04E-03	418.193	16.813
3Q5J9L	B	82.9	SB-124	0.76	3.25E-07	0.027	0.004
3Q5J9L	B	82.9	BA-133	0.40	2.62E-05	2.171	179.916
3Q5J9L	B	82.9	HF-181	0.73	1.22E-06	0.101	0.019
24IKD6	A	105.2	CR-51	0.88	1.02E-04	10.753	2.988
24IKD6	A	105.2	CO-60	0.98	4.10E-06	0.432	0.022
24IKD6	A	105.2	ZN-65	0.99	5.58E-03	587.337	23.544
24IKD6	A	105.2	SB-124	0.76	9.04E-07	0.095	0.006
24IKD6	A	105.2	BA-133	0.39	3.29E-03	346.534	200.063
24IKD6	A	105.2	EU-152x	0.55	6.38E-08	0.007	0.001
24IKD6	A	105.2	HF-175	0.92	9.59E-06	1.009	0.271
24IKD6	A	105.2	HF-181	0.73	9.51E-07	0.100	0.022
8835TV	A	105.5	CO-60	0.99	2.76E-06	0.291	0.016
8835TV	A	105.5	ZN-65	0.99	4.42E-03	466.716	18.736
8835TV	A	105.5	SB-124	0.76	3.56E-07	0.038	0.005
8835TV	A	105.5	BA-133	0.41	2.04E-03	214.798	189.192
8835TV	A	105.5	HF-175	0.88	7.01E-06	0.740	0.238
29599	A	93.8	CO-60	1.00	2.14E-06	0.201	0.013
29599	A	93.8	ZN-65	0.99	7.77E-03	728.930	29.188
29599	A	93.8	SB-124	0.76	5.61E-07	0.053	0.005
29599	A	93.8	BA-133	0.41	6.54E-03	613.488	228.481
29599	A	93.8	EU-152x	0.43	6.86E-08	0.006	0.001

29599	A	93.8	HF-175	0.84	1.02E-05	0.959	0.275
29599	A	93.8	HF-181	0.73	1.23E-06	0.115	0.023
30339	A	71.3	CO-60	0.99	3.69E-06	0.263	0.015
30339	A	71.3	ZN-65	0.99	8.86E-03	631.630	25.337
30339	A	71.3	SB-124	0.44	4.27E-07	0.030	0.007
30339	A	71.3	BA-133	0.41	1.16E-02	829.473	202.425
30339	A	71.3	HF-181	0.73	1.35E-06	0.096	0.020
30343	A	83.8	CO-60	0.97	3.90E-06	0.327	0.017
30343	A	83.8	ZN-65	0.98	8.41E-03	705.021	28.242
30343	A	83.8	SB-124	0.76	5.19E-07	0.044	0.004
30343	A	83.8	BA-133	0.41	6.02E-03	504.437	221.441
30343	A	83.8	EU-152x	0.42	5.98E-08	0.005	0.001
30343	A	83.8	HF-175	0.92	1.24E-05	1.037	0.276
30343	A	83.8	HF-181	0.72	9.67E-07	0.081	0.022
822607HC	B	95.2	CO-60	0.99	5.76E-06	0.549	0.026
822607HC	B	95.2	ZN-65	0.99	7.39E-03	703.368	28.161
822607HC	B	95.2	SB-124	0.77	7.68E-07	0.073	0.005
822607HC	B	95.2	BA-133	0.39	8.76E-03	833.685	215.694
5100224	A	80.3	CO-60	0.98	8.34E-06	0.669	0.031
5100224	A	80.3	ZN-65	0.98	6.76E-03	542.434	21.771
5100224	A	80.3	SB-124	0.75	2.55E-06	0.205	0.010
5100224	A	80.3	BA-133	0.41	4.46E-03	357.885	196.688
5100224	A	80.3	CE-141	0.91	3.75E-05	3.009	0.600
5100224	A	80.3	EU-152x	0.55	1.23E-07	0.010	0.001
5100224	A	80.3	HF-181	0.73	1.07E-06	0.086	0.022
A3809H	B	58.5	CO-60	0.99	2.46E-06	0.144	0.011
A3809H	B	58.5	ZN-65	0.99	5.03E-03	294.163	11.888
A3873H	B	107	CO-60	0.99	2.16E-06	0.231	0.014
A3873H	B	107	ZN-65	0.99	3.74E-03	400.593	16.098
A3873H	B	107	SB-124	0.76	4.28E-07	0.046	0.004
A3873H	B	107	BA-133	0.39	3.71E-03	397.216	170.425
A22609HC	A	91.1	CO-60	0.99	3.05E-06	0.278	0.016
A22609HC	A	91.1	ZN-65	0.99	4.57E-03	416.697	16.745
A22609HC	A	91.1	SB-124	0.76	5.76E-07	0.052	0.005
A24246HC	B	91.8	CO-60	0.99	5.40E-06	0.496	0.024
A24246HC	B	91.8	ZN-65	0.99	5.83E-03	535.194	21.465
A24246HC	B	91.8	SB-124	0.76	7.53E-07	0.069	0.005
A24246HC	B	91.8	BA-133	0.41	8.95E-03	821.779	188.866
A24246HC	B	91.8	EU-152x	0.54	5.58E-08	0.005	0.001
A24246HC	B	91.8	HF-175	0.97	5.55E-06	0.510	0.240
HFD9LM	A	104.3	CO-60	0.99	1.93E-06	0.201	0.012
HFD9LM	A	104.3	ZN-65	0.98	5.24E-03	546.973	21.928
HFD9LM	A	104.3	SB-124	0.76	4.86E-07	0.051	0.004
HFD9LM	A	104.3	BA-133	0.41	3.51E-03	365.908	198.767
HFE9LN	B	91.5	CO-60	0.98	2.36E-06	0.216	0.013
HFE9LN	B	91.5	ZN-65	0.98	4.58E-03	418.672	16.817
HFE9LN	B	91.5	SB-124	0.75	3.54E-07	0.032	0.004
HFE9LN	B	91.5	BA-133	0.41	4.27E-03	390.538	175.653
LR8C66	A	88.9	CO-60	0.99	1.78E-06	0.159	0.012
LR8C66	A	88.9	ZN-65	0.99	6.52E-03	579.773	23.240

LR8C66	A	88.9	BA-133	0.41	6.89E-03	612.788	194.166
K76GHR	B	88.2	CO-60	0.98	3.15E-06	0.278	0.015
K76GHR	B	88.2	ZN-65	0.99	6.67E-03	588.185	23.586
K76GHR	B	88.2	SB-124	0.76	6.03E-07	0.053	0.005
K76GHR	B	88.2	BA-133	0.41	8.05E-03	709.637	197.439
K76GHR	B	88.2	HF-175	0.90	1.06E-05	0.938	0.242
K76GHR	B	88.2	HF-181	0.72	1.28E-06	0.113	0.021
29606	A	110.2	CO-60	0.99	1.97E-06	0.217	0.014
29606	A	110.2	ZN-65	0.99	7.19E-03	792.025	31.693
29606	A	110.2	SB-124	0.76	4.12E-07	0.045	0.005
29606	A	110.2	BA-133	0.41	7.12E-03	784.222	227.655
29606	A	110.2	EU-152x	0.55	7.61E-08	0.008	0.001
29606	A	110.2	HF-175	0.89	6.21E-06	0.684	0.284
29606	A	110.2	HF-181	0.73	1.08E-06	0.119	0.023
TJ66HR	B	69.6	CO-60	0.98	2.24E-06	0.156	0.011
TJ66HR	B	69.6	ZN-65	0.99	5.24E-03	364.471	14.670
TJ66HR	B	69.6	SB-124	0.76	3.90E-07	0.027	0.003
TJ66HR	B	69.6	HF-175	0.98	1.23E-05	0.858	0.187
TJ66HR	B	69.6	HF-181	0.73	1.38E-06	0.096	0.016
J6FD6G	B	86	CO-60	0.99	1.62E-06	0.139	0.011
J6FD6G	B	86	ZN-65	0.99	4.36E-03	375.062	15.086
J6FD6G	B	86	SB-124	0.76	1.80E-06	0.155	0.008
J6FD6G	B	86	BA-133	0.40	6.52E-03	560.892	165.063
J6FD6G	B	86	CE-141	0.92	1.63E-05	1.405	0.512
J6FD6G	B	86	EU-152x	0.55	1.04E-07	0.009	0.001
J6FD6G	B	86	HF-175	0.89	9.17E-06	0.788	0.218
J6FD6G	B	86	HF-181	0.73	8.67E-07	0.075	0.018
VDSA46	B	95.9	CO-60	0.98	1.63E-06	0.157	0.011
VDSA46	B	95.9	ZN-65	0.99	6.59E-03	632.034	25.322
VDSA46	B	95.9	SB-124	0.76	3.66E-07	0.035	0.004
VDSA46	B	95.9	BA-133	0.41	7.86E-03	754.251	198.852
76H325	B	95.3	CO-60	0.93	1.34E-06	0.128	0.010
76H325	B	95.3	ZN-65	0.95	5.79E-03	551.644	22.167
76H325	B	95.3	BA-133	0.40	7.58E-03	721.990	193.934
76H325	B	95.3	EU-152x	0.42	5.46E-08	0.005	0.001
76H325	B	95.3	HF-175	0.92	3.64E-06	0.347	0.227
27571	B	121.2	CO-60	0.93	3.72E-06	0.451	0.022
27571	B	121.2	ZN-65	0.95	6.37E-03	772.630	30.983
27571	B	121.2	SB-124	0.73	6.52E-07	0.079	0.007
27571	B	121.2	BA-133	0.41	7.57E-03	917.546	239.536
27571	B	121.2	EU-152x	0.54	7.16E-08	0.009	0.001
27571	B	121.2	HF-181	0.72	8.60E-07	0.104	0.024
A3740H	A	87.6	CO-60	0.95	2.47E-06	0.217	0.014
A3740H	A	87.6	ZN-65	0.97	6.30E-03	551.768	22.180
A3740H	A	87.6	SB-124	0.44	5.34E-07	0.047	0.008
A3740H	A	87.6	EU-152x	0.42	5.69E-08	0.005	0.001
A3740H	A	87.6	HF-175	0.84	3.52E-06	0.308	0.271
A3740H	A	87.6	HF-181	0.72	1.16E-06	0.102	0.023
CR8C66	B	95.6	CO-60	0.95	2.16E-06	0.207	0.013
CR8C66	B	95.6	ZN-65	0.95	6.68E-03	638.268	25.631

CR8C66	B	95.6	SB-124	0.44	3.61E-07	0.035	0.008
CR8C66	B	95.6	BA-133	0.41	6.24E-03	596.415	208.483
CR8C66	B	95.6	EU-152x	0.42	4.05E-08	0.004	0.001
CR8C66	B	95.6	HF-175	0.91	4.52E-06	0.432	0.284
3Q5J9L	A	104	CO-60	0.99	1.94E-06	0.202	0.013
3Q5J9L	A	104	ZN-65	0.99	4.39E-03	456.064	18.359
3Q5J9L	A	104	SB-124	0.74	3.86E-07	0.040	0.005
3Q5J9L	A	104	BA-133	0.41	1.85E-03	192.642	176.747
7Y536NA	A	101.4	CO-60	0.99	3.27E-06	0.331	0.017
7Y536NA	A	101.4	ZN-65	0.99	8.17E-03	828.480	33.227
7Y536NA	A	101.4	SB-124	0.43	5.89E-07	0.060	0.012
7Y536NA	A	101.4	BA-133	0.41	8.99E-03	911.141	228.801
75G8FW	A	78.1	CO-60	1.00	3.55E-06	0.277	0.016
75G8FW	A	78.1	ZN-65	1.00	9.53E-03	744.411	29.892
75G8FW	A	78.1	SE-75	0.98	4.74E-06	0.370	0.028
75G8FW	A	78.1	BA-133	0.41	7.76E-03	605.970	217.087
75G8FW	A	78.1	EU-152x	0.42	4.12E-08	0.003	0.001
75G8FW	A	78.1	HF-175	0.85	1.58E-05	1.234	0.368
75G8FW	A	78.1	HG-203	0.90	1.19E-05	0.926	0.333
75G8FW	B	74.5	CO-60	0.99	5.48E-06	0.408	0.021
75G8FW	B	74.5	ZN-65	0.99	9.48E-03	706.005	28.368
75G8FW	B	74.5	BA-133	0.41	4.80E-03	357.229	211.751
75G8FW	B	74.5	EU-152x	0.42	8.64E-08	0.006	0.001
75G8FW	B	74.5	HF-175	0.91	1.05E-05	0.782	0.368
8835TV	B	93.8	CO-60	0.99	4.77E-06	0.447	0.022
8835TV	B	93.8	ZN-65	0.99	7.41E-03	695.393	27.919
8835TV	B	93.8	SB-124	0.74	9.07E-07	0.085	0.008
8835TV	B	93.8	BA-133	0.41	3.79E-03	355.521	212.702
8835TV	B	93.8	EU-152x	0.54	6.74E-08	0.006	0.001
8835TV	B	93.8	HF-175	0.90	1.21E-05	1.139	0.367
28958	B	89.9	CO-60	0.99	3.29E-06	0.296	0.016
28958	B	89.9	ZN-65	0.98	7.47E-03	671.763	26.981
28958	B	89.9	SB-124	0.74	8.79E-07	0.079	0.007
28958	B	89.9	BA-133	0.40	1.13E-02	1014.960	210.278
28958	B	89.9	EU-152x	0.43	5.89E-08	0.005	0.001
30103	B	92.1	CO-60	0.99	1.35E-06	0.124	0.009
30103	B	92.1	ZN-65	0.99	4.34E-03	399.608	16.111
30103	B	92.1	BA-133	0.41	8.30E-03	764.877	89.141
30343	B	74.2	CO-60	1.00	3.72E-06	0.276	0.016
30343	B	74.2	ZN-65	1.00	7.99E-03	593.060	23.856
30343	B	74.2	SB-124	0.75	5.90E-07	0.044	0.005
30343	B	74.2	BA-133	0.40	7.33E-03	543.932	194.874
A3740H	B	76.6	CO-60	0.97	2.79E-06	0.214	0.013
A3740H	B	76.6	ZN-65	0.98	7.16E-03	548.301	22.063
A3740H	B	76.6	SB-124	0.44	8.10E-07	0.062	0.010
A3740H	B	76.6	BA-133	0.41	9.34E-03	715.197	192.777
A3740H	B	76.6	EU-152x	0.54	7.74E-08	0.006	0.001
A3807H	A	70.7	CO-60	0.99	3.32E-06	0.235	0.014
A3807H	A	70.7	ZN-65	0.99	7.51E-03	531.206	21.385
A3807H	A	70.7	SB-124	0.44	6.87E-07	0.049	0.010

A3807H	A	70.7	BA-133	0.40	6.90E-03	487.708	196.484
A22609HC	B	81.2	CO-60	0.99	3.68E-06	0.299	0.017
A22609HC	B	81.2	ZN-65	0.99	3.98E-03	322.907	13.050
A22609HC	B	81.2	SB-124	0.75	7.69E-07	0.062	0.006
A24233HC	B	113.4	CO-60	0.99	1.49E-06	0.170	0.013
A24233HC	B	113.4	ZN-65	1.00	5.30E-03	601.477	24.164
A24233HC	B	113.4	SB-124	0.78	3.58E-06	0.406	0.019
A24233HC	B	113.4	BA-133	0.39	4.12E-03	467.424	206.636
A24233HC	B	113.4	EU-152x	0.42	5.05E-08	0.006	0.001
A242233HC	A	118.7	CO-60	0.98	1.77E-06	0.210	0.013
A242233HC	A	118.7	ZN-65	0.99	6.00E-03	712.309	28.579
A242233HC	A	118.7	SB-124	0.75	6.07E-07	0.072	0.007
A242233HC	A	118.7	BA-133	0.41	5.32E-03	631.745	211.528
AA61L3	B	87.6	CO-60	0.98	3.12E-06	0.274	0.015
AA61L3	B	87.6	ZN-65	0.99	7.45E-03	652.234	26.204
AA61L3	B	87.6	BA-133	0.41	1.16E-02	1020.007	107.598
ABD469658	A	66.4	CO-60	0.98	6.79E-06	0.451	0.022
ABD469658	A	66.4	ZN-65	0.99	5.39E-03	357.872	14.462
ABD469658	A	66.4	SB-124	0.44	4.31E-07	0.029	0.008
ABD469658	A	66.4	BA-133	0.41	4.92E-03	326.945	165.918
ABD469658	A	66.4	EU-152x	0.55	1.21E-07	0.008	0.001
ABD469658	A	66.4	HF-175	0.88	2.07E-05	1.376	0.302
B322IJ	A	86.8	CO-60	0.97	1.47E-06	0.128	0.010
B322IJ	A	86.8	ZN-65	0.98	6.24E-03	541.960	21.798
B322IJ	A	86.8	SB-124	0.38	3.46E-07	0.030	0.009
B322IJ	B	103.1	CO-60	0.98	1.04E-06	0.107	0.009
B322IJ	B	103.1	ZN-65	0.99	3.41E-03	352.082	14.202
FWX130	A	88.8	CO-60	0.98	3.57E-06	0.317	0.017
FWX130	A	88.8	ZN-65	0.99	7.84E-03	695.805	27.938
FWX130	A	88.8	BA-133	0.41	7.35E-03	652.259	207.365
G8UX4V	A	81.1	CO-60	0.99	2.58E-06	0.209	0.013
G8UX4V	A	81.1	ZN-65	0.99	7.43E-03	602.514	24.221
G8UX4V	A	81.1	BA-133	0.41	8.51E-03	690.468	193.390
G8UX4V	A	81.1	EU-152x	0.54	8.73E-08	0.007	0.001
JGFDGG	A	65.7	CO-60	0.97	1.80E-06	0.118	0.010
JGFDGG	A	65.7	ZN-65	0.99	4.16E-03	273.294	11.075
JGFDGG	A	65.7	SB-124	0.75	1.96E-06	0.129	0.008
JGFDGG	A	65.7	EU-152x	0.55	1.04E-07	0.007	0.001
L6159B	B	69.4	CO-60	0.97	3.19E-06	0.221	0.014
L6159B	B	69.4	ZN-65	0.98	8.53E-03	592.038	23.820
L6159B	B	69.4	BA-133	0.41	4.13E-03	286.614	197.547
L6159B	B	69.4	EU-152x	0.42	5.96E-08	0.004	0.001
L6159B	B	69.4	HF-175	0.93	1.19E-05	0.827	0.340
L6159B	A	68.8	CO-60	0.98	2.68E-06	0.184	0.012
L6159B	A	68.8	ZN-65	0.99	8.65E-03	595.325	23.955
L6159B	A	68.8	BA-133	0.41	9.49E-03	652.772	195.269
LF4EQ2	A	104	CO-60	0.98	3.12E-06	0.324	0.017
LF4EQ2	A	104	ZN-65	0.99	8.11E-03	843.451	33.822
LF4EQ2	A	104	BA-133	0.72	1.30E-02	1357.191	217.254
LF4EQ2	A	104	EU-152x	0.54	8.83E-08	0.009	0.001

LF4EQ2	A	104	HF-175	0.87	8.24E-08	0.009	0.406
LF4EQ2	B	70.7	CO-60	0.99	2.78E-06	0.196	0.013
LF4EQ2	B	70.7	ZN-65	0.99	8.03E-03	568.003	22.863
LF4EQ2	B	70.7	BA-133	0.41	1.21E-02	858.235	188.266
NM81X7	B	73.7	CO-60	0.99	2.94E-06	0.217	0.013
NM81X7	B	73.7	ZN-65	0.99	7.73E-03	569.402	22.907
NM81X7	B	73.7	BA-133	0.41	6.29E-03	463.488	193.048
BHU548	A	93.1	CO-60	0.98	3.81E-06	0.355	0.019
BHU548	A	93.1	ZN-65	0.99	8.62E-03	802.644	32.207
BHU548	A	93.1	SB-124	0.73	6.66E-07	0.062	0.007
BHU548	A	93.1	BA-133	0.41	9.28E-03	863.522	225.536
BHU548	A	93.1	EU-152x	0.54	9.49E-08	0.009	0.001
BHU548	A	93.1	HF-175	0.93	2.16E-06	0.201	0.418
BHU548	B	84.9	CO-60	0.99	5.40E-06	0.459	0.023
BHU548	B	84.9	ZN-65	0.99	7.99E-03	678.080	27.232
BHU548	B	84.9	SB-124	0.76	1.35E-06	0.115	0.008
BHU548	B	84.9	BA-133	0.40	9.91E-03	840.952	206.847
BHU548	B	84.9	EU-152x	0.43	8.20E-08	0.007	0.001
BHU548	B	84.9	HF-175	0.87	1.04E-05	0.884	0.359
YEK752	A	96.4	CO-60	0.98	2.36E-06	0.228	0.014
YEK752	A	96.4	ZN-65	0.99	6.52E-03	628.216	25.237
YEK752	A	96.4	SB-124	0.74	6.55E-07	0.063	0.007
YEK752	A	96.4	BA-133	0.41	6.98E-03	672.913	203.057
YEK752	A	96.4	EU-152x	0.54	5.48E-08	0.005	0.001
YEK752	B	83.9	CO-60	0.99	2.31E-06	0.194	0.012
YEK752	B	83.9	ZN-65	0.99	6.43E-03	539.170	21.690
YEK752	B	83.9	SB-124	0.75	4.61E-07	0.039	0.006
YEK752	B	83.9	BA-133	0.41	9.41E-03	789.298	190.292
YEK752	B	83.9	EU-152x	0.55	6.17E-08	0.005	0.001
YEK752	B	83.9	HF-175	0.86	5.84E-06	0.490	0.326
2UIKD6	B	71.4	CO-60	0.98	5.66E-06	0.404	0.020
2UIKD6	B	71.4	ZN-65	0.99	6.62E-03	472.410	19.036
2UIKD6	B	71.4	SE-75	0.74	1.49E-06	0.106	0.022
2UIKD6	B	71.4	SB-124	0.75	1.43E-06	0.102	0.008
2UIKD6	B	71.4	BA-133	0.41	4.07E-03	290.598	184.580
2UIKD6	B	71.4	EU-152x	0.43	4.01E-08	0.003	0.001
2UIKD6	B	71.4	HF-175	0.84	1.19E-05	0.846	0.319
3067	A	106.5	BA-131	0.89	4.45E-03	474.103	24.827
3067	A	106.5	BA-133	0.75	4.32E-02	4605.261	1203.169
3067	A	106.5	CR-51	0.95	9.85E-05	10.492	1.474
3067	A	106.5	CS-134	0.30	4.70E-07	0.050	0.005
3067	A	106.5	HF-175	0.89	2.28E-05	2.425	0.402
3067	A	106.5	HO-166	0.58	1.44E-05	1.529	1.630
3067	A	106.5	RU-103	0.91	1.40E-04	14.866	0.831
3067	A	106.5	RU-97	0.36	3.22E-03	343.447	219.415
3067	A	106.5	SB-122	0.41	1.19E-05	1.264	0.087
3067	A	106.5	SB-124	0.59	2.22E-06	0.237	0.037
3067	A	106.5	TA-182	0.50	7.84E-08	0.008	0.002
3067	A	106.5	ZR-95	1.00	3.87E-04	41.256	14.529
26701	B	172.6	BA-131	0.86	4.04E-03	697.335	42.068

26701	B	172.6	CE-141	0.99	1.67E-05	2.880	0.482
26701	B	172.6	CR-51	0.89	1.35E-04	23.229	2.340
26701	B	172.6	HF-181	0.67	5.10E-06	0.880	0.052
26701	B	172.6	RU-103	0.91	9.48E-05	16.359	0.922
26701	B	172.6	SB-124	0.44	2.49E-06	0.430	0.029
27055	A	126.8	AS-77	0.41	8.17E+00	1035651.153	169132.711
27055	A	126.8	BA-131	0.98	6.19E-03	784.634	33.294
27055	A	126.8	BA-133	0.55	1.29E-02	1641.560	450.481
27055	A	126.8	CE-141	0.99	3.49E-05	4.430	0.472
27055	A	126.8	CO-60	0.99	8.03E-06	1.018	0.077
27055	A	126.8	CR-51	0.99	9.57E-05	12.131	1.087
27055	A	126.8	HF-175	0.91	8.97E-06	1.138	0.436
27055	A	126.8	HF-181	0.76	6.39E-06	0.810	0.042
27055	A	126.8	HO-166	0.33	1.57E-05	1.994	3.135
27055	A	126.8	LU-177	0.89	9.49E-08	0.012	0.014
27055	A	126.8	RU-97	0.65	9.52E-04	120.769	29.637
27055	A	126.8	SB-122	0.74	2.63E-06	0.334	0.043
27055	A	126.8	SB-124	0.77	2.45E-06	0.311	0.015
27055	A	126.8	SC-46	0.99	3.99E-06	0.506	0.024
27055	A	126.8	TA-182	0.41	2.51E-08	0.003	0.003
27055	A	126.8	TE-123m	0.93	1.70E-05	2.156	0.296
27055	A	126.8	XE-127	0.39	7.14E-06	0.905	4.868
27055	A	126.8	ZN-65	1.00	1.66E-02	2104.151	77.437
27165	B	147	BA-131	0.88	5.08E-03	747.367	38.900
27165	B	147	BA-133	0.37	4.00E-02	5877.963	1589.031
27165	B	147	CE-141	0.94	3.65E-05	5.359	0.475
27165	B	147	CR-51	0.94	2.22E-04	32.633	2.375
27165	B	147	HF-181	0.68	7.61E-06	1.119	0.057
27165	B	147	RU-103	0.99	1.80E-04	26.491	1.304
27165	B	147	RU-97	0.36	7.40E-03	1088.208	421.584
27165	B	147	SB-124	0.57	4.65E-06	0.684	0.036
27165	B	147	TA-182	0.50	2.59E-07	0.038	0.007
27165	B	147	TE-123m	0.92	1.21E-06	0.178	0.143
27420	B	96.8	AS-77	0.71	4.74E-01	45897.209	7209.113
27420	B	96.8	BA-131	0.99	7.43E-03	718.740	27.856
27420	B	96.8	BA-133	0.37	4.96E-02	4797.751	745.750
27420	B	96.8	CE-141	1.00	4.47E-05	4.329	0.284
27420	B	96.8	CO-60	0.99	1.09E-05	1.058	0.094
27420	B	96.8	CR-51	1.00	1.49E-04	14.438	1.349
27420	B	96.8	HF-181	0.89	1.24E-05	1.197	0.080
27420	B	96.8	LU-177	0.98	6.33E-07	0.061	0.015
27420	B	96.8	RB-86	0.99	1.63E-05	1.575	0.258
27420	B	96.8	RU-103	0.83	5.34E-04	51.713	2.366
27420	B	96.8	RU-97	0.79	1.22E-05	1.181	2.452
27420	B	96.8	SB-122	0.89	6.35E-06	0.615	0.029
27420	B	96.8	SB-124	0.87	5.63E-06	0.545	0.027
27420	B	96.8	SC-46	1.00	8.24E-06	0.798	0.040
27420	B	96.8	TE-121	0.67	1.44E-03	139.328	139.103
27420	B	96.8	TE-123m	0.99	4.75E-05	4.597	0.295
27420	B	96.8	ZN-65	1.00	3.79E-02	3670.064	137.363



27659	A	148.8	AS-77	0.42	8.09E+00	1204209.333	190537.927
27659	A	148.8	BA-131	0.98	5.65E-03	840.035	35.370
27659	A	148.8	CR-51	0.99	5.38E-05	8.006	1.380
27659	A	148.8	FE-59	0.95	2.08E-03	309.797	33.594
27659	A	148.8	HF-181	0.75	1.04E-05	1.541	0.069
27659	A	148.8	RB-86	0.98	1.61E-05	2.400	0.495
27659	A	148.8	RU-103	0.81	3.10E-04	46.170	2.123
27659	A	148.8	RU-97	0.68	1.03E-04	15.364	13.274
27659	A	148.8	SB-124	0.77	2.59E-06	0.385	0.024
27659	A	148.8	SC-46	1.00	6.11E-06	0.909	0.045
27659	A	148.8	TE-123m	0.99	1.33E-05	1.983	0.173
27659	A	148.8	ZN-65	1.00	2.82E-02	4193.385	155.909
27660	A	205.8	AS-77	0.46	3.20E+00	657878.878	106795.821
27660	B	189.5	AS-77	0.50	2.25E+00	425705.311	68675.257
27660	A	205.8	BA-131	0.98	3.98E-03	819.062	34.105
27660	B	189.5	BA-131	0.98	4.12E-03	781.186	32.093
27660	B	189.5	BA-133	0.38	2.42E-02	4581.842	2449.323
27660	A	205.8	BA-133m	0.46	2.47E-01	50878.394	16777.180
27660	A	205.8	CE-139	0.91	8.42E-05	17.328	29.092
27660	B	189.5	CE-141	0.99	1.74E-05	3.304	0.344
27660	A	205.8	CE-141	1.00	1.67E-05	3.439	0.361
27660	A	205.8	CO-60	0.98	3.73E-06	0.768	0.036
27660	A	205.8	CR-51	0.97	3.85E-05	7.930	1.329
27660	B	189.5	CR-51	1.00	5.32E-05	10.086	1.286
27660	B	189.5	CS-134	0.79	5.45E-07	0.103	0.010
27660	A	205.8	FE-59	0.98	1.55E-03	318.785	41.788
27660	A	205.8	HF-175	0.98	5.86E-06	1.205	0.519
27660	B	189.5	HF-181	0.75	7.00E-06	1.327	0.060
27660	A	205.8	HF-181	0.75	7.11E-06	1.463	0.065
27660	A	205.8	HG-203	0.98	1.00E-06	0.206	0.080
27660	B	189.5	RB-86	0.93	2.69E-06	0.510	0.174
27660	B	189.5	RU-103	0.82	2.62E-04	49.571	2.233
27660	A	205.8	RU-103	0.83	2.28E-04	46.866	2.146
27660	A	205.8	RU-97	0.69	8.20E-05	16.876	11.037
27660	B	189.5	RU-97	0.71	1.10E-04	20.823	8.819
27660	A	205.8	SB-122	0.71	2.37E-06	0.488	0.080
27660	B	189.5	SB-122	0.78	1.76E-06	0.334	0.063
27660	A	205.8	SB-124	0.85	1.69E-06	0.348	0.022
27660	B	189.5	SB-124	0.86	2.87E-06	0.544	0.024
27660	A	205.8	SC-46	0.99	4.16E-06	0.855	0.043
27660	B	189.5	SC-46	0.99	4.84E-06	0.917	0.048
27660	B	189.5	TA-182	0.57	1.87E-08	0.004	0.001
27660	B	189.5	TE-123m	0.97	1.03E-05	1.960	0.234
27660	A	205.8	TE-123m	1.00	1.04E-05	2.141	0.190
27660	A	205.8	ZN-65	1.00	1.97E-02	4046.562	150.358
27660	B	189.5	ZN-65	1.00	1.90E-02	3601.542	134.002
28240	B	136.6	BA-131	0.85	5.46E-03	745.164	44.245
28240	B	136.6	BA-133	0.60	5.06E-02	6912.319	1371.304
28240	B	136.6	CE-139	0.93	3.09E-04	42.146	24.177
28240	B	136.6	CE-141	0.99	2.36E-05	3.225	0.878

28240	B	136.6	CR-51	0.94	6.62E-05	9.044	1.850
28240	B	136.6	HF-181	0.68	8.13E-06	1.110	0.057
28240	B	136.6	IN-114m	0.82	1.48E-06	0.202	1.046
28240	B	136.6	RU-103	0.99	1.52E-04	20.806	0.935
28240	B	136.6	SB-124	0.47	2.76E-06	0.378	0.028
28240	B	136.6	SN-125x	0.89	1.41E-01	19240.105	61402.107
28240	B	136.6	TE-121	0.66	4.36E-04	59.493	316.097
28297	A	166.2	AS-71	0.86	1.18E-07	0.020	0.147
28297	A	166.2	AS-77	0.67	4.37E-01	72643.753	11624.201
28297	B	120.2	BA-131	0.85	6.78E-03	814.427	48.996
28297	A	166.2	BA-131	0.99	4.61E-03	766.416	29.985
28297	A	166.2	BA-133	0.49	4.26E-02	7072.711	514.420
28297	B	120.2	CE-141	0.96	2.86E-05	3.432	0.523
28297	A	166.2	CE-141	0.98	1.64E-05	2.728	0.338
28297	A	166.2	CO-60	0.99	4.52E-06	0.752	0.072
28297	B	120.2	CR-51	0.86	1.76E-04	21.098	2.409
28297	A	166.2	CR-51	1.00	9.35E-05	15.543	1.466
28297	A	166.2	FE-59	0.98	2.19E-03	364.078	41.090
28297	A	166.2	HF-181	0.75	9.33E-06	1.551	0.069
28297	B	120.2	HF-181	0.76	1.05E-05	1.264	0.062
28297	A	166.2	IN-114m	0.70	1.54E-09	0.000	0.067
28297	A	166.2	RU-103	0.83	3.37E-04	55.985	2.524
28297	B	120.2	RU-103	0.91	1.41E-04	16.895	0.989
28297	A	166.2	RU-97	0.78	1.96E-05	3.263	3.278
28297	A	166.2	SB-122	0.87	2.36E-06	0.392	0.032
28297	A	166.2	SB-124	0.52	2.27E-06	0.377	0.024
28297	B	120.2	SB-124	0.52	2.88E-06	0.346	0.029
28297	A	166.2	SC-46	1.00	1.16E-05	1.928	0.078
28297	B	120.2	TE-123m	0.92	3.47E-07	0.042	0.090
28297	A	166.2	TE-123m	1.00	2.69E-05	4.472	0.301
28297	A	166.2	ZN-65	1.00	2.57E-02	4275.790	158.538
28802	A	163	AG-108m	0.51	7.15E-04	116.525	280.976
28802	B	141.8	AS-77	0.46	4.13E+00	586225.080	115242.719
28802	A	163	BA-131	0.87	5.33E-03	868.224	49.030
28802	B	141.8	BA-131	0.98	6.17E-03	874.807	36.341
28802	B	141.8	CE-139	1.00	2.00E-05	2.830	24.697
28802	A	163	CE-141	0.92	2.43E-05	3.954	0.708
28802	B	141.8	CE-141	0.99	3.04E-05	4.309	0.379
28802	B	141.8	CO-60	0.99	1.01E-05	1.434	0.107
28802	B	141.8	CR-51	0.93	4.64E-05	6.581	1.351
28802	A	163	HF-181	0.67	6.81E-06	1.109	0.059
28802	B	141.8	HF-181	0.75	1.15E-05	1.625	0.071
28802	A	163	HG-203	0.91	4.49E-07	0.073	0.182
28802	B	141.8	LU-177x	0.38	1.21E-07	0.017	0.013
28802	B	141.8	MO-99	0.67	5.58E-05	7.910	6.217
28802	B	141.8	OS-185	0.80	2.14E-05	3.028	2.988
28802	A	163	OS-185	0.81	6.80E-06	1.108	3.019
28802	B	141.8	RU-103	0.83	3.41E-04	48.422	2.231
28802	A	163	RU-103	0.99	1.07E-04	17.371	1.006
28802	B	141.8	RU-97	0.69	1.39E-04	19.733	11.344

28802	B	141.8	SB-122	0.77	4.30E-06	0.609	0.067
28802	A	163	SB-124	0.53	2.34E-06	0.381	0.028
28802	B	141.8	SB-124	0.98	2.82E-06	0.399	0.028
28802	B	141.8	SC-46	0.99	5.89E-06	0.835	0.043
28802	B	141.8	TA-182	0.54	2.84E-08	0.004	0.003
28802	A	163	TE-121	0.67	2.28E-03	371.067	616.188
28802	B	141.8	TE-123m	1.00	1.61E-05	2.287	0.242
28802	B	141.8	ZN-65	1.00	2.91E-02	4128.303	153.442
28958	B	167.5	AG-110m	0.40	3.37E-06	0.564	0.068
28958	A	115.5	AS-71	0.31	4.88E-01	56412.801	2945.527
28958	B	167.5	BA-131	0.86	5.87E-03	982.977	55.971
28958	A	115.5	BA-131	0.87	5.25E-03	606.723	33.652
28958	A	115.5	CE-141	0.89	1.76E-05	2.033	0.419
28958	B	167.5	CE-141	0.94	2.23E-05	3.732	0.465
28958	B	167.5	CR-51	0.97	7.57E-05	12.688	1.824
28958	B	167.5	CS-134	0.66	8.41E-07	0.141	0.017
28958	A	115.5	HF-181	0.72	6.99E-06	0.807	0.050
28958	B	167.5	HF-181	0.80	7.62E-06	1.277	0.067
28958	A	115.5	HG-203	0.86	9.06E-07	0.105	0.190
28958	A	115.5	ND-147	0.93	8.38E-05	9.676	9.119
28958	A	115.5	RB-86	0.97	7.57E-07	0.087	1.096
28958	B	167.5	RU-103	0.91	1.40E-04	23.482	1.256
28958	A	115.5	RU-103	0.99	1.33E-04	15.375	0.880
28958	A	115.5	SB-124	0.44	2.49E-06	0.288	0.024
28958	A	115.5	TE-121x	0.99	1.14E-02	1312.444	2086.607
29428	B	90.1	AG-110m	0.38	3.34E-07	0.030	0.041
29428	A	38.4	BA-131	0.85	1.28E-02	491.015	30.160
29428	B	90.1	BA-131	0.87	9.38E-03	845.076	45.688
29428	A	38.4	BA-133	0.46	3.14E-02	1207.439	507.450
29428	B	90.1	CE-141	0.94	2.32E-05	2.088	0.272
29428	A	38.4	CO-60	0.94	1.48E-05	0.570	0.069
29428	B	90.1	CR-51	0.90	1.60E-04	14.398	1.930
29428	A	38.4	CR-51	0.90	2.25E-04	8.656	0.692
29428	B	90.1	HF-175	0.90	1.81E-05	1.633	0.733
29428	B	90.1	HF-181	0.65	1.14E-05	1.025	0.054
29428	A	38.4	RU-103	0.99	2.52E-04	9.663	0.670
29428	B	90.1	RU-103	0.99	2.02E-04	18.221	1.026
29428	A	38.4	SB-124	0.46	5.13E-06	0.197	0.012
29428	A	38.4	Si-32	0.94	1.75E-01	6708.014	3139.624
29428	B	90.1	SN-125x	0.79	2.58E-01	23270.816	43561.388
29428	A	38.4	TA-182	0.42	1.17E-06	0.045	0.009
29428	B	90.1	TA-182	0.70	1.94E-07	0.017	0.003
29428	B	90.1	ZR-95	0.98	9.08E-05	8.178	15.349
29432	A	164.9	AG-108m	0.96	1.29E-03	212.190	245.497
29432	A	164.9	AS-77	0.47	3.35E+00	552721.740	90114.338
29432	B	102.1	AS-77	0.67	7.15E-01	73003.435	11640.623
29432	A	164.9	AU-198	0.73	9.48E-09	0.002	0.002
29432	A	164.9	BA-131	0.98	4.12E-03	680.041	28.322
29432	B	102.1	BA-131	0.99	6.92E-03	707.025	27.703
29432	B	102.1	BA-133	0.38	1.05E-01	10674.524	1152.259

29432	A	164.9	BA-133	0.85	3.27E-02	5388.625	1111.417
29432	B	102.1	CE-139	1.00	1.05E-05	1.077	21.490
29432	A	164.9	CE-141	0.96	1.27E-05	2.092	0.319
29432	B	102.1	CE-141	0.98	2.33E-05	2.377	0.309
29432	A	164.9	CR-51	0.99	9.20E-05	15.176	1.410
29432	B	102.1	CR-51	1.00	1.38E-04	14.100	1.287
29432	A	164.9	HF-175	0.96	1.60E-05	2.645	0.395
29432	B	102.1	HF-181	0.75	1.37E-05	1.397	0.062
29432	A	164.9	HF-181	0.88	7.03E-06	1.159	0.054
29432	A	164.9	LA-140	0.39	1.52E-05	2.514	0.576
29432	B	102.1	LU-177x	0.38	4.61E-07	0.047	0.006
29432	A	164.9	ND-147	0.98	8.44E-06	1.392	2.841
29432	B	102.1	RB-86	1.00	1.67E-05	1.705	0.376
29432	B	102.1	RU-103	0.81	5.05E-04	51.559	2.332
29432	A	164.9	RU-103	0.83	2.37E-04	39.002	1.811
29432	A	164.9	RU-97	0.70	7.50E-05	12.368	9.215
29432	B	102.1	RU-97	0.78	5.73E-05	5.849	3.150
29432	B	102.1	SB-122	0.87	3.34E-06	0.341	0.030
29432	B	102.1	SB-124	0.87	3.37E-06	0.344	0.021
29432	A	164.9	SB-124	0.97	1.91E-06	0.315	0.020
29432	A	164.9	SC-46	1.00	8.94E-06	1.475	0.062
29432	B	102.1	SC-46	1.00	1.40E-05	1.433	0.060
29432	A	164.9	Si-32	1.00	4.88E-02	8054.061	4696.309
29432	A	164.9	TE-123m	0.98	1.34E-05	2.204	0.256
29432	B	102.1	TE-123m	1.00	3.55E-05	3.625	0.265
29432	B	102.1	ZN-65	1.00	3.46E-02	3529.682	131.471
29432	A	164.9	ZN-65	1.00	2.14E-02	3530.196	131.382
29434	B	128.9	BA-131	0.52	7.04E-03	907.185	54.075
29434	A	164.3	BA-131	0.83	4.49E-03	737.484	45.184
29434	A	164.3	CE-141	0.90	1.76E-05	2.890	0.516
29434	B	128.9	CE-141	0.95	2.81E-05	3.623	0.411
29434	B	128.9	CO-60	0.91	1.36E-06	0.175	0.032
29434	B	128.9	CR-51	0.88	1.67E-04	21.509	2.344
29434	B	128.9	HF-181	0.72	7.40E-06	0.954	0.057
29434	A	164.3	LU-177	0.73	-3.94E-07	-0.065	-0.325
29434	A	164.3	RU-103	0.90	8.09E-05	13.297	0.878
29434	B	128.9	RU-103	0.90	3.88E-04	50.000	2.598
29434	B	128.9	SB-124	0.46	3.34E-06	0.431	0.031
29434	B	128.9	TA-182	0.33	5.25E-06	0.676	0.044
29462	A	113.9	BA-131	0.87	5.76E-03	655.604	35.856
29462	A	113.9	BA-133	0.49	2.20E-02	2504.397	624.347
29462	A	113.9	CE-141	0.91	2.32E-05	2.643	0.433
29462	A	113.9	CR-51	0.92	1.13E-04	12.834	1.857
29462	A	113.9	HF-181	0.79	7.82E-06	0.891	0.047
29462	A	113.9	RB-86	0.97	2.20E-06	0.251	0.462
29462	A	113.9	RU-103	0.91	1.54E-04	17.515	0.969
29462	A	113.9	SB-124	0.56	2.79E-06	0.318	0.025
30670	B	161	AS-71	0.88	6.54E-07	0.105	0.061
30670	B	161	AS-77	0.71	2.90E-01	46636.631	7430.477
30670	B	161	BA-131	0.99	4.41E-03	710.809	27.536

30670	B	161	BA-133m	0.65	6.53E-03	1051.350	1727.679
30670	B	161	CD-115	0.43	1.98E-06	0.318	0.250
30670	B	161	CE-141	0.95	1.20E-05	1.936	0.310
30670	B	161	CO-60	0.94	3.82E-06	0.615	0.075
30670	B	161	CR-51	1.00	8.74E-05	14.063	1.344
30670	B	161	HF-175	0.97	1.53E-05	2.464	0.430
30670	B	161	HF-181	0.89	6.32E-06	1.018	0.073
30670	B	161	HG-197	0.34	2.09E-03	336.435	57.832
30670	B	161	ND-147	0.96	2.82E-06	0.454	2.905
30670	B	161	RU-103	0.82	3.53E-04	56.754	2.531
30670	B	161	RU-97	0.79	5.90E-05	9.500	2.720
30670	B	161	SB-122	0.89	3.01E-06	0.485	0.024
30670	B	161	SB-124	0.59	2.70E-06	0.434	0.025
30670	B	161	SC-46	1.00	8.96E-06	1.442	0.061
30670	B	161	TE-123m	0.99	2.98E-05	4.804	0.314
30670	B	161	ZN-65	1.00	2.15E-02	3460.513	128.591
30674	B	150.5	BA-131	0.87	5.10E-03	768.132	41.971
30674	B	150.5	BA-133	0.64	4.59E-02	6909.814	1069.402
30674	B	150.5	CE-141	0.99	5.66E-06	0.852	0.609
30674	B	150.5	CR-51	0.87	1.27E-04	19.159	2.110
30674	B	150.5	HF-181	0.77	7.68E-06	1.155	0.056
30674	B	150.5	HO-166	0.73	1.12E-05	1.683	2.023
30674	B	150.5	RU-103	0.91	1.48E-04	22.226	1.154
30674	B	150.5	SB-124	0.44	2.60E-06	0.392	0.028
30674	B	150.5	TA-182	0.62	1.27E-07	0.019	0.003
271675	A	169.5	BA-131	0.86	4.52E-03	766.216	45.684
271675	A	169.5	CE-141	0.98	2.32E-05	3.924	0.522
271675	A	169.5	CR-51	0.90	1.58E-04	26.729	1.998
271675	A	169.5	HF-175	0.87	1.62E-05	2.748	0.390
271675	A	169.5	RU-103	0.91	9.94E-05	16.840	0.970
271675	A	169.5	SB-124	0.64	3.52E-06	0.596	0.033
271675	A	169.5	SE-75	0.71	5.35E-07	0.091	0.041
271675	A	169.5	XE-127	0.54	4.68E-03	793.424	103.001
422023HC	A	151.8	BA-131	0.89	4.38E-03	665.179	34.098
422023HC	A	151.8	CE-141	0.97	5.40E-05	8.204	0.522
422023HC	A	151.8	CR-51	0.90	1.53E-04	23.201	1.626
422023HC	A	151.8	HF-181	0.68	7.82E-06	1.187	0.058
422023HC	A	151.8	HG-203	0.97	1.26E-07	0.019	0.090
422023HC	A	151.8	RU-103	0.91	1.41E-04	21.404	1.117
422023HC	A	151.8	RU-97	0.43	3.35E-03	508.589	242.999
422023HC	A	151.8	SB-124	0.91	4.50E-06	0.683	0.034
493720-54	B	106.8	BA-131	0.85	7.44E-03	794.881	45.069
493720-54	A	175.6	BA-131	0.87	6.85E-03	1202.181	64.013
493720-54	B	106.8	BA-133	0.32	5.29E-02	5648.561	1364.057
493720-54	B	106.8	CE-141	0.98	1.44E-05	1.539	0.422
493720-54	B	106.8	CR-51	0.89	2.33E-04	24.850	2.095
493720-54	A	175.6	CR-51	0.90	2.88E-04	50.650	3.359
493720-54	B	106.8	HF-175	1.00	4.84E-07	0.052	0.197
493720-54	B	106.8	HF-181	0.66	6.97E-06	0.745	0.043
493720-54	A	175.6	HF-181	0.75	8.63E-06	1.516	0.061

493720-54	B	106.8	HO-166	0.50	2.82E-04	30.101	16.722
493720-54	B	106.8	IN-114m	0.71	5.37E-08	0.006	0.071
493720-54	B	106.8	RU-103	0.91	1.33E-04	14.219	0.840
493720-54	A	175.6	RU-103	0.91	1.37E-04	24.017	1.348
493720-54	B	106.8	SB-124	0.51	4.48E-05	4.784	0.184
493720-54	A	175.6	SB-124	0.65	3.80E-05	6.668	0.255
493720-54	A	175.6	SE-75	0.72	6.97E-07	0.122	0.037
501310-42	B	94.4	BA-131	0.85	6.96E-03	657.284	39.426
501310-42	A	162.9	BA-131	0.86	4.55E-03	741.010	44.380
501310-42	A	162.9	BA-133	0.42	4.73E-02	7700.418	1225.607
501310-42	B	94.4	CE-141	0.88	3.02E-05	2.847	0.565
501310-42	A	162.9	CE-141	0.99	1.45E-05	2.362	0.587
501310-42	B	94.4	CR-51	0.91	4.01E-04	37.895	3.168
501310-42	B	94.4	HF-181	0.73	8.38E-06	0.792	0.055
501310-42	B	94.4	RU-103	0.91	1.46E-04	13.811	0.900
501310-42	A	162.9	RU-103	0.91	9.59E-05	15.616	1.225
501310-42	B	94.4	SB-124	0.52	1.38E-04	13.050	0.491
501310-42	A	162.9	SB-124	0.52	9.15E-05	14.901	0.562
501310-42	B	94.4	SR-85x	0.99	2.99E-03	281.817	15.901
501310-42	B	94.4	TA-182	0.33	4.13E-07	0.039	0.032
650390-13	B	103.4	AG-110m	0.43	7.77E-07	0.080	0.010
650390-13	B	103.4	BA-131	0.85	8.11E-03	838.303	49.977
650390-13	B	103.4	CE-141	0.96	2.06E-05	2.133	0.506
650390-13	B	103.4	CR-51	0.88	4.51E-04	46.678	3.423
650390-13	B	103.4	IN-114m	0.83	1.53E-07	0.016	0.118
650390-13	B	103.4	OS-185	0.76	2.46E-04	25.394	7.346
650390-13	B	103.4	RU-103	0.90	1.69E-04	17.430	1.043
650390-13	B	103.4	SB-124	0.63	9.53E-05	9.851	0.371
650390-13	B	103.4	TB-160	0.34	9.73E-08	0.010	0.002
650390-46	A	99.1	AS-77	0.49	4.01E+00	397154.788	66268.411
650390-46	A	99.1	AU-198	0.77	2.65E-07	0.026	0.005
650390-46	B	193.9	BA-131	0.83	5.79E-03	1122.736	67.689
650390-46	A	99.1	BA-131	0.99	7.72E-03	764.751	31.576
650390-46	B	193.9	BA-133	0.44	5.58E-02	10820.808	2304.073
650390-46	B	193.9	CE-141	0.92	2.27E-05	4.410	0.704
650390-46	A	99.1	CE-141	0.99	2.26E-05	2.242	0.300
650390-46	A	99.1	CO-60	0.99	3.41E-05	3.379	0.203
650390-46	B	193.9	CR-51	0.90	2.01E-04	39.068	3.737
650390-46	A	99.1	CR-51	1.00	3.11E-04	30.803	2.191
650390-46	A	99.1	HF-181	0.89	1.16E-05	1.145	0.057
650390-46	A	99.1	NB-94x	0.88	1.57E-01	15540.349	27934.668
650390-46	B	193.9	ND-147	0.91	2.10E-04	40.701	35.014
650390-46	B	193.9	OS-185	0.90	7.26E-04	140.769	7.924
650390-46	A	99.1	RB-86	0.95	1.52E-06	0.151	0.446
650390-46	A	99.1	RU-103	0.83	4.61E-04	45.721	2.122
650390-46	B	193.9	RU-103	0.90	1.14E-04	22.160	1.301
650390-46	A	99.1	RU-97	0.71	1.82E-04	18.026	9.183
650390-46	A	99.1	SB-122	0.78	9.56E-05	9.474	0.419
650390-46	B	193.9	SB-124	0.44	7.29E-05	14.130	0.539
650390-46	A	99.1	SB-124	1.00	8.90E-05	8.824	0.332

650390-46	B	193.9	SB-125	0.58	1.90E+00	367499.055	126717.727
650390-46	A	99.1	Si-32	1.00	1.13E-01	11213.516	5425.002
650390-46	A	99.1	TE-123m	1.00	1.54E-05	1.530	0.270
650390-46	A	99.1	ZN-65	1.00	4.46E-02	4418.783	164.503
650390-46	B	193.9	ZR-95	0.98	1.59E-02	3087.350	138.645
650390-B	A	133.8	AG-108m	0.34	2.47E-01	33003.189	1796.107
650390-B	A	133.8	BA-131	0.71	6.29E-03	841.373	51.643
650390-B	A	133.8	CR-51	0.87	5.68E-04	75.975	3.667
650390-B	A	133.8	HF-181	0.80	1.19E-05	1.591	0.061
650390-B	A	133.8	HG-203	0.98	3.75E-07	0.050	0.109
650390-B	A	133.8	OS-185	0.73	8.73E-04	116.788	6.727
650390-B	A	133.8	RB-86	0.87	1.23E-05	1.639	0.552
650390-B	A	133.8	RU-103	0.91	1.14E-04	15.194	1.015
650390-B	A	133.8	SB-124	0.43	7.99E-05	10.696	0.410
650390-B	A	133.8	TA-182	0.54	3.43E-08	0.005	0.006
650390-B	A	133.8	TE-121	0.88	5.31E-03	711.038	921.314
A21794HC	A	266.6	BA-131	0.59	1.43E+00	380832.079	47533.547
A21794HC	A	266.6	BA-133	0.78	1.93E-02	5135.195	1512.966
A21794HC	A	266.6	CE-139	0.87	1.12E-04	29.855	53.588
A21794HC	A	266.6	CE-141	0.93	2.92E-04	77.783	4.010
A21794HC	A	266.6	CO-60	0.98	8.32E-06	2.217	0.144
A21794HC	A	266.6	CR-51	0.91	1.19E-03	317.329	24.049
A21794HC	A	266.6	HF-181	0.72	3.15E-05	8.403	0.385
A21794HC	A	266.6	RU-103	0.87	1.30E-03	347.676	15.744
A21794HC	A	266.6	SB-124	0.97	6.95E-06	1.852	0.095
A21794HC	A	266.6	SC-46	0.99	1.30E-05	3.471	0.148
A21794HC	A	266.6	TE-123m	0.99	2.95E-05	7.871	0.454
A21794HC	A	266.6	ZN-65	1.00	2.01E-02	5369.271	199.793
A21803HC	A	93	AG-108m	0.50	5.61E-03	521.327	255.289
A21803HC	A	93	BA-131	0.35	6.63E-03	616.817	40.485
A21803HC	A	93	CE-141	0.99	2.40E-05	2.228	0.642
A21803HC	A	93	HG-203	0.99	2.17E-07	0.020	0.044
A21803HC	A	93	SN-125x	0.85	7.83E-02	7286.383	18206.349
A21803HC	A	93	TE-123m	0.98	1.70E-06	0.158	0.167
A21803HC	B	113.2	BA-131	0.87	5.36E-03	607.286	33.078
A21803HC	B	113.2	BA-133	0.79	2.13E-02	2413.713	1155.317
A21803HC	B	113.2	CE-139	1.00	6.48E-05	7.331	25.301
A21803HC	B	113.2	CE-141	0.96	3.45E-05	3.903	0.432
A21803HC	B	113.2	CR-51	0.97	1.25E-04	14.120	1.772
A21803HC	B	113.2	HF-181	0.81	6.93E-06	0.785	0.046
A21803HC	B	113.2	HG-203	0.98	1.90E-06	0.215	0.199
A21803HC	B	113.2	RU-103	0.91	1.46E-04	16.558	0.928
A21803HC	B	113.2	RU-97	0.31	3.84E-03	434.550	452.749
A21803HC	B	113.2	SB-124	0.55	3.13E-06	0.354	0.025
A21803HL	B	113.2	SN-125x	0.82	2.65E-01	30013.380	52545.927
A220023HC	B	128.2	BA-131	0.89	5.00E-03	641.384	33.267
A220023HC	B	128.2	CE-141	0.96	4.99E-05	6.396	0.471
A220023HC	B	128.2	CR-51	0.91	1.45E-04	18.590	1.786
A220023HC	B	128.2	HF-181	0.82	8.91E-06	1.142	0.055
A220023HC	B	128.2	RU-103	1.00	1.49E-04	19.165	1.018

A220023HC	B	128.2	RU-97	0.36	4.56E-03	584.103	283.551
A220023HC	B	128.2	SB-124	0.58	5.82E-06	0.746	0.036
A220023HC	B	128.2	TA-182	0.34	1.32E-07	0.017	0.004
A2237HC	B	266.6	BA-131	0.60	1.61E+00	429219.990	53524.085
A2237HC	B	266.6	CR-51	0.90	7.33E-04	195.449	19.821
A2237HC	B	266.6	FE-59	0.94	8.03E-03	2140.617	285.254
A2237HC	B	266.6	HF-181	0.72	3.23E-05	8.613	0.387
A2237HC	B	266.6	RB-86	0.70	1.13E-04	30.112	9.084
A2237HC	B	266.6	RU-103	0.78	1.38E-03	368.045	16.834
A2237HC	B	266.6	SB-124	0.76	6.18E-06	1.647	0.091
A2237HC	B	266.6	SC-46	0.97	7.45E-06	1.986	0.112
A2237HC	B	266.6	TE-123m	1.00	2.12E-05	5.648	0.514
A2237HC	B	266.6	ZN-65	1.00	1.86E-02	4968.037	185.109
A24237HC	A	99.9	AS-77	0.50	3.83E+00	383007.268	60322.538
A24237HC	A	99.9	BA-131	0.98	6.60E-03	659.342	27.153
A24237HC	A	99.9	BA-133	0.34	2.83E-02	2825.919	1333.984
A24237HC	A	99.9	CR-51	1.00	1.24E-04	12.430	1.821
A24237HC	A	99.9	RB-86	0.96	4.06E-06	0.405	0.159
A24237HC	A	99.9	RU-103	0.90	3.48E-04	34.803	1.645
A24237HC	A	99.9	RU-97	0.71	7.00E-05	6.998	7.224
A24237HC	A	99.9	SB-122	0.79	4.75E-06	0.475	0.049
A24237HC	A	99.9	SB-124	0.52	4.64E-06	0.463	0.042
A24237HC	A	99.9	SC-46	1.00	8.93E-06	0.892	0.033
A24237HC	A	99.9	TE-123m	0.99	9.43E-06	0.942	0.153
A24237HC	A	99.9	ZN-65	1.00	3.57E-02	3566.875	132.860
A3745H	A	95.4	AS-76	0.49	3.08E-06	0.294	0.211
A3745H	B	90.7	AS-77	0.71	3.55E-01	32226.604	5176.583
A3745H	A	95.4	AS-77	0.78	1.97E-01	18771.021	2999.295
A3745H	A	95.4	AU-198	0.92	1.49E-08	0.001	0.000
A3745H	B	90.7	BA-131	0.99	5.70E-03	516.963	20.071
A3745H	A	95.4	BA-131	0.99	6.56E-03	626.173	23.911
A3745H	A	95.4	BA-133	0.34	3.25E-02	3098.792	1482.838
A3745H	A	95.4	CE-141	0.98	3.22E-05	3.069	0.311
A3745H	B	90.7	CE-141	0.98	2.42E-05	2.196	0.272
A3745H	A	95.4	CE-143	0.63	4.25E-04	40.540	18.320
A3745H	A	95.4	CR-51	0.99	9.88E-05	9.423	1.146
A3745H	B	90.7	CR-51	0.99	7.17E-05	6.506	1.004
A3745H	B	90.7	FE-59	0.99	1.98E-03	179.911	27.056
A3745H	A	95.4	HF-181	0.89	7.14E-06	0.682	0.063
A3745H	B	90.7	HF-181	0.89	8.42E-06	0.763	0.061
A3745H	B	90.7	OS-185	0.79	7.57E-06	0.686	2.212
A3745H	A	95.4	RB-86	0.89	1.49E-05	1.422	0.204
A3745H	B	90.7	RB-86	0.95	7.94E-06	0.720	0.197
A3745H	A	95.4	RU-103	0.82	5.20E-04	49.583	2.260
A3745H	B	90.7	RU-103	0.82	4.38E-04	39.687	1.815
A3745H	B	90.7	RU-97	0.79	2.40E-06	0.218	1.830
A3745H	A	95.4	RU-97	0.81	1.50E-05	1.426	1.530
A3745H	B	90.7	SB-122	0.89	3.73E-06	0.338	0.017
A3745H	A	95.4	SB-122	0.92	3.80E-06	0.362	0.017
A3745H	B	90.7	SB-124	0.59	2.91E-06	0.264	0.018



A3745H	A	95.4	SB-124	0.63	3.93E-06	0.375	0.035
A3745H	B	90.7	SC-46	0.99	5.86E-06	0.532	0.028
A3745H	A	95.4	SC-46	1.00	6.55E-06	0.625	0.034
A3745H	B	90.7	TA-182	0.33	5.42E-08	0.005	0.002
A3745H	B	90.7	TE-121	0.69	2.51E-03	228.057	72.177
A3745H	A	95.4	TE-123m	0.99	4.61E-05	4.402	0.280
A3745H	B	90.7	TE-123m	1.00	2.59E-05	2.350	0.217
A3745H	A	95.4	ZN-65	1.00	3.14E-02	2995.399	111.836
A3745H	B	90.7	ZN-65	1.00	2.65E-02	2402.814	89.965
A3760	A	74.4	AS-77	0.40	1.09E+01	811309.830	135908.614
A3760	A	74.4	AU-198m	0.33	5.98E-09	0.000	0.003
A3760	A	74.4	BA-131	0.98	5.76E-03	428.445	18.409
A3760	A	74.4	CE-139	1.00	2.12E-04	15.771	21.811
A3760	A	74.4	CE-141	0.99	2.38E-05	1.771	0.271
A3760	A	74.4	CR-51	0.94	4.69E-05	3.491	0.561
A3760	A	74.4	HF-175	1.00	1.90E-05	1.413	0.255
A3760	A	74.4	HF-181	0.89	9.57E-06	0.712	0.037
A3760	A	74.4	RB-86	0.97	1.18E-05	0.874	0.292
A3760	A	74.4	RU-103	0.82	3.42E-04	25.422	1.198
A3760	A	74.4	RU-97	0.75	2.70E-04	20.096	9.834
A3760	A	74.4	SB-122	0.72	5.49E-06	0.409	0.074
A3760	A	74.4	SB-124	0.51	4.08E-06	0.303	0.019
A3760	A	74.4	SC-46	0.99	6.42E-06	0.478	0.025
A3760	A	74.4	TA-182	0.54	6.93E-08	0.005	0.003
A3760	A	74.4	TE-121	0.59	2.33E-03	173.533	83.015
A3760	A	74.4	TE-123m	1.00	5.80E-06	0.431	0.089
A3760	A	74.4	ZN-65	1.00	2.85E-02	2117.095	79.436
CFSD	7	365.6	AG-108m	0.53	4.23E-04	154.802	20.086
CFSD	1	306.3	AS-77	0.68	2.33E-01	71297.901	11351.983
CFSD	3	300	BA-131	0.38	2.45E-03	733.686	47.420
CFSD	6	388	BA-131	0.84	2.79E-03	1082.908	65.600
CFSD	7	365.6	BA-131	0.86	2.38E-03	870.662	52.177
CFSD	5	353.8	BA-131	0.86	7.10E-03	2512.412	142.130
CFSD	1	306.3	BA-131	0.99	2.71E-03	830.515	32.390
CFSD	1	306.3	BA-133	0.51	1.20E-02	3681.235	1510.410
CFSD	5	353.8	BA-133	0.67	5.93E-02	20996.050	4079.618
CFSD	6	388	CE-141	0.95	2.56E-06	0.992	1.720
CFSD	1	306.3	CE-141	0.99	7.89E-06	2.415	0.321
CFSD	1	306.3	CR-51	0.98	2.90E-05	8.881	3.553
CFSD	7	365.6	FE-59	0.35	3.81E-05	13.920	55.478
CFSD	1	306.3	HF-175	0.92	8.17E-06	2.503	0.674
CFSD	1	306.3	HF-181	0.68	1.44E-06	0.441	0.069
CFSD	7	365.6	HF-181	0.68	1.39E-06	0.507	0.039
CFSD	5	353.8	HG-203	0.94	1.01E-06	0.356	0.376
CFSD	1	306.3	LA-140	0.48	4.16E-06	1.276	0.068
CFSD	1	306.3	RH-105	0.58	2.69E-04	82.368	70.435
CFSD	1	306.3	RU-103	0.82	1.95E-04	59.806	2.693
CFSD	3	300	RU-103	0.85	9.26E-05	27.773	1.522
CFSD	6	388	RU-103	0.90	5.24E-05	20.326	1.163
CFSD	7	365.6	RU-103	0.91	4.33E-05	15.826	0.882

CFSK	3	97.9	AG-108m	0.37	3.40E-04	33.286	381.424
CFSK	2	100.4	AS-77	0.52	3.45E+00	346635.633	55633.178
CFSK	3	97.9	AS-77	0.68	7.56E-01	73965.366	11787.864
CFSK	2	100.4	AU-198m	0.68	1.50E-09	0.000	0.001
CFSK	4	127.7	BA-131	0.85	7.50E-03	957.752	56.446
CFSK	6	80.8	BA-131	0.85	1.02E-02	824.713	49.143
CFSK	5	135.8	BA-131	0.88	6.19E-03	841.007	45.394
CFSK	2	100.4	BA-131	0.98	8.04E-03	806.940	32.673
CFSK	3	97.9	BA-131	0.99	8.86E-03	867.568	33.627
CFSK	6	80.8	BA-133	0.47	1.03E-01	8314.749	1476.100
CFSK	5	135.8	BA-133	0.50	2.37E-02	3214.185	1663.495
CFSK	5	135.8	CE-139	1.00	2.55E-05	3.464	22.431
CFSK	3	97.9	CE-141	0.98	2.71E-05	2.651	0.583
CFSK	4	127.7	CE-141	0.99	2.24E-05	2.863	0.495
CFSK	5	135.8	CE-141	0.99	6.65E-06	0.903	0.172
CFSK	5	135.8	CO-60	1.00	1.40E-06	0.190	0.036
CFSK	6	80.8	CR-51	0.96	1.47E-05	1.186	1.770
CFSK	6	80.8	CS-134	0.72	1.20E-06	0.097	0.016
CFSK	6	80.8	HF-181	0.70	1.09E-05	0.885	0.055
CFSK	3	97.9	HF-181	0.85	6.49E-06	0.635	0.049
CFSK	2	100.4	HF-181	0.89	1.21E-05	1.214	0.056
CFSK	5	135.8	HF-181	0.90	7.80E-06	1.059	0.051
CFSK	3	97.9	IN-114m	0.67	1.25E-06	0.123	0.099
CFSK	5	135.8	IN-114m	0.83	1.59E-05	2.164	1.810
CFSK	2	100.4	RB-86	0.99	4.72E-06	0.474	0.359
CFSK	3	97.9	RU-103	0.90	3.88E-04	37.966	1.847
CFSK	4	127.7	RU-103	0.91	1.48E-04	18.925	1.309
CFSK	6	80.8	RU-103	0.91	2.13E-04	17.223	0.991
CFSK	2	100.4	RU-103	0.91	5.05E-04	50.693	2.287
CFSK	5	135.8	RU-103	0.91	1.69E-04	22.970	1.205
CFSK	5	135.8	RU-97	0.32	1.43E-03	194.718	508.092
CFSK	3	97.9	SB-122	0.87	2.23E-06	0.218	0.018
CFSK	6	80.8	SB-124	0.59	1.31E-06	0.106	0.017
CFSK	4	127.7	SB-124	0.68	1.29E-06	0.165	0.019
CFSK	3	97.9	SB-124	0.88	1.75E-06	0.172	0.011
CFSK	2	100.4	SC-46	0.99	7.95E-06	0.798	0.046
CFSK	3	97.9	SC-46	0.99	5.86E-06	0.573	0.037
CFSK	6	80.8	TA-182	0.44	8.70E-08	0.007	0.005
CFSK	5	135.8	TA-182	0.64	2.45E-08	0.003	0.010
CFSK	5	135.8	TE-121	0.66	1.01E-03	137.592	489.890
CFSK	3	97.9	TE-123m	0.98	2.53E-05	2.481	0.254

CFSK	2	100.4	ZN-65	1.00	4.44E-02	4459.701	165.750
CFSK	3	97.9	ZN-65	1.00	4.62E-02	4523.862	168.271
CFSP	1	389.8	AG-108m	0.96	1.93E-03	750.878	538.299
CFSP	5	396.9	AG-110m	0.38	1.97E-07	0.078	0.032
CFSP	1a	389.8	AS-71	0.43	3.19E-02	12435.750	618.777
CFSP	6	387.7	BA-131	0.86	2.38E-03	920.893	55.171
CFSP	5	396.9	BA-131	0.86	2.51E-03	997.310	54.841
CFSP	1	389.8	BA-131	0.88	2.11E-03	822.068	40.799
CFSP	1a	389.8	BA-131	0.89	2.08E-03	811.910	40.899
CFSP	3	405.4	BA-131	0.89	1.96E-03	794.580	41.226
CFSP	6	387.7	CE-141	0.95	1.23E-05	4.783	0.565
CFSP	1	389.8	CE-141	0.96	1.52E-05	5.906	0.485
CFSP	5	396.9	CE-141	0.96	1.75E-05	6.935	0.264
CFSP	3	405.4	CE-141	0.98	9.85E-06	3.992	1.302
CFSP	1a	389.8	CE-141	0.99	1.21E-05	4.709	0.473
CFSP	3	405.4	CO-60	0.88	2.41E-06	0.977	0.087
CFSP	5	396.9	CR-51	0.89	6.36E-05	25.239	3.442
CFSP	1a	389.8	CR-51	0.90	5.14E-05	20.040	2.931
CFSP	6	387.7	CR-51	0.91	5.17E-05	20.037	2.492
CFSP	3	405.4	CR-51	0.91	4.76E-05	19.305	2.008
CFSP	1	389.8	CR-51	0.92	5.35E-05	20.847	1.995
CFSP	5	396.9	CS-134	0.73	1.41E-06	0.558	0.037
CFSP	1	389.8	FE-59	0.35	4.28E-04	166.870	111.169
CFSP	6	387.7	HF-181	0.66	2.06E-06	0.799	0.052
CFSP	1	389.8	HF-181	0.72	1.33E-06	0.520	0.048
CFSP	5	396.9	HF-181	0.78	2.31E-06	0.917	0.055
CFSP	1a	389.8	HF-181	0.80	2.21E-06	0.863	0.048
CFSP	3	405.4	HF-181	0.85	2.13E-06	0.865	0.050
CFSP	1a	389.8	HG-203	0.88	4.95E-08	0.019	0.079
CFSP	3	405.4	HO-166	0.39	1.21E-04	49.219	43.640
CFSP	6	387.7	IR-192	0.38	1.64E-09	0.001	0.000
CFSP	1	389.8	LU-177	0.86	3.06E-08	0.012	0.081
CFSP	1a	389.8	LU-177	0.87	7.04E-08	0.027	0.083
CFSP	5	396.9	OS-185	0.88	1.05E-05	4.182	3.672
CFSP	5	396.9	RB-86	0.88	1.20E-06	0.478	1.045
CFSP	3	405.4	RB-86	0.96	2.12E-06	0.858	0.747
CFSP	1a	389.8	RB-86	0.97	6.21E-06	2.420	0.849
CFSP	5	396.9	RU-103	0.91	6.12E-05	24.300	1.293
CFSP	1	389.8	RU-103	0.91	7.25E-05	28.261	1.411
CFSP	1a	389.8	RU-103	0.91	7.25E-05	28.271	1.398
CFSP	3	405.4	RU-103	0.91	6.40E-05	25.954	1.305
CFSP	6	387.7	RU-103	0.99	4.18E-05	16.199	0.977
CFSP	3	405.4	RU-97	0.36	3.08E-03	1249.362	464.746
CFSP	1a	389.8	RU-97	0.38	1.37E-03	532.978	237.627
CFSP	1	389.8	RU-97	0.39	1.46E-03	570.924	217.303
CFSP	6	387.7	SB-124	0.44	1.48E-06	0.575	0.025
CFSP	1	389.8	SB-124	0.56	9.62E-07	0.375	0.029
CFSP	1	389.8	SB-124	0.78	1.17E-06	0.455	0.039
CFSP	3	405.4	SB-124	0.81	1.04E-06	0.421	0.028
CFSP	1	389.8	SN-125x	0.94	5.65E-02	22023.761	31951.804

CFSP	1	389.8	TA-182	0.30	5.69E-08	0.022	0.005
CFSP	1	389.8	TA-182	0.54	8.31E-09	0.003	0.001
CFSP	6	387.7	TE-123m	0.87	2.59E-07	0.101	0.153
JET OIL	1	220.4	CO-60	1.00	1.76E-04	38.894	1.478
JET OIL	1	220.4	CR-51	1.00	8.99E-05	19.807	1.557
JET OIL	1	220.4	FE-59	1.00	4.44E-01	97859.548	4009.518
JET OIL	1	220.4	ND-147	0.96	1.64E-05	3.620	1.200
JET OIL	1	220.4	RU-103	0.88	3.85E-07	0.085	0.215
JET OIL	1	220.4	SB-124	0.95	1.17E-06	0.259	0.021
JET OIL	1	220.4	SR-85x	0.88	1.58E-04	34.916	16.032
JET OIL	1	220.4	ZN-65	0.98	3.04E-06	0.670	2.548
CFSK	2	317.7	BA-131	0.86	2.58E-03	819.400	48.908
CFSK	4	345.5	BA-131	0.87	2.07E-03	714.764	42.714
CFSK	4	345.5	CE-139	0.86	6.36E-05	21.966	1.587
CFSK	2	317.7	CE-141	0.88	6.91E-06	2.196	0.089
CFSK	4	345.5	CE-141	0.95	4.46E-06	1.541	0.422
CFSK	4	345.5	CR-51	0.88	3.09E-05	10.692	1.966
CFSK	2	317.7	CR-51	0.91	5.55E-05	17.628	2.193
CFSK	4	345.5	HF-181	0.76	1.42E-06	0.490	0.035
CFSK	4	345.5	RU-103	0.91	3.43E-05	11.867	0.782
CFSK	2	317.7	RU-103	0.99	5.75E-05	18.277	1.021
CFSK	4	345.5	TA-182	0.37	5.86E-08	0.020	0.003
CFSK	4	345.5	TE-121	0.67	7.88E-04	272.105	712.931
CFSK	2	317.7	TE-123m	0.86	2.59E-07	0.082	0.136
CFSK	7	119.4	BA-131	0.86	8.21E-03	980.086	54.050
CFSK	7	119.4	CE-139	1.00	1.49E-04	17.764	27.404
CFSK	7	119.4	CE-141	0.92	4.46E-06	0.533	0.487
CFSK	7	119.4	HF-181	0.69	7.98E-06	0.953	0.058
CFSK	7	119.4	HG-203	0.98	1.00E-08	0.001	0.118
CFSK	7	119.4	RU-103	0.91	1.97E-04	23.482	1.251
CFSK	7	119.4	SB-122	0.31	1.49E-04	17.770	5.329
CFSK	7	119.4	SB-124	0.43	1.40E-06	0.167	0.025
4S19OC	A	57.5	BA-133	0.38	3.30E-01	18955.740	2832.250
4S19OC	A	57.5	CO-60	0.90	2.18E-04	12.515	0.410
4S19OC	A	57.5	EU-152x	0.48	4.54E-06	0.261	0.027
4S19OC	A	57.5	SB-124	0.50	2.04E-05	1.176	0.183
4S19OC	A	57.5	ZN-65	0.92	3.58E-01	20605.132	454.419
2D968E	A	116.1	CE-139	0.98	1.13E-03	130.976	61.144
2D968E	A	116.1	CE-139	0.98	1.13E-03	130.976	61.144
2D968E	A	116.1	CO-60	0.95	4.51E-05	5.240	0.229
2D968E	A	116.1	CO-60	0.95	4.51E-05	5.240	0.229
2D968E	A	116.1	FE-59	0.94	2.39E-03	277.631	163.916
2D968E	A	116.1	FE-59	0.94	2.39E-03	277.631	163.916
2D968E	A	116.1	SC-46	0.94	9.40E-06	1.092	0.064
2D968E	A	116.1	SC-46	0.94	9.40E-06	1.092	0.064
2D968E	A	116.1	ZN-65	0.95	4.66E-02	5410.438	118.466
2D968E	A	116.1	ZN-65	0.95	4.66E-02	5410.438	118.466
2D968E	B	142	BA-131	0.95	1.27E-02	1809.828	230.163
2D968E	B	142	BA-133	0.40	8.36E-02	11873.568	2656.003
2D968E	B	142	CE-141	0.97	8.30E-05	11.791	1.710

2D968E	B	142	CO-60	0.96	2.99E-05	4.243	0.565
2D968E	B	142	CR-51	0.99	1.54E-04	21.826	3.920
2D968E	B	142	HF-175	0.95	2.90E-05	4.121	0.865
2D968E	B	142	HF-181	0.87	1.54E-05	2.184	0.284
2D968E	B	142	RU-103	0.98	1.24E-06	0.177	1.112
2D968E	B	142	RU-97	0.55	3.50E-03	497.512	146.347
2D968E	B	142	SB-124	0.56	2.58E-06	0.367	0.052
2D968E	B	142	SC-46	0.96	1.04E-05	1.477	0.189
2D968E	B	142	SN-125x	0.89	3.49E-02	4962.503	19630.399
2D968E	B	142	ZN-65	0.99	3.89E-02	5528.304	689.019
3C297F	A	205.4	BA-131	0.93	1.43E-02	2942.754	116.540
3C297F	A	205.4	CE-141	0.98	2.24E-04	46.011	2.221
3C297F	A	205.4	CO-60	0.99	2.33E-05	4.788	0.224
3C297F	A	205.4	CR-51	0.93	2.75E-04	56.548	4.346
3C297F	A	205.4	HF-175	0.93	6.01E-05	12.339	0.319
3C297F	A	205.4	HF-181	0.87	2.04E-05	4.188	0.104
3C297F	A	205.4	RB-86	0.96	1.82E-06	0.374	0.796
3C297F	A	205.4	RU-97	0.40	1.72E-02	3535.796	1197.553
3C297F	A	205.4	SB-124	0.75	7.06E-06	1.450	0.048
3C297F	A	205.4	SC-46	0.98	1.90E-05	3.911	0.105
3C297F	A	205.4	TE-121	0.67	3.72E-04	76.403	373.405
3C297F	A	205.4	TE-123m	0.95	1.51E-05	3.096	0.492
3C297F	A	205.4	XE-129m	0.91	1.31E-04	26.882	39.239
3C297F	A	205.4	ZN-65	0.98	4.36E-02	8963.746	190.409
3C297F	B	207.3	BA-133	0.70	7.34E-02	15220.754	3184.939
3C297F	B	207.3	CO-60	0.99	2.89E-05	5.990	0.319
3C297F	B	207.3	EU-152x	0.67	2.27E-06	0.470	0.031
3C297F	B	207.3	EU-154	0.56	2.49E-06	0.515	0.058
3C297F	B	207.3	HF-175	0.93	3.46E-05	7.173	2.940
3C297F	B	207.3	HF-181	0.89	1.73E-05	3.582	0.212
3C297F	B	207.3	SB-124	0.87	9.39E-06	1.947	0.064
3C297F	B	207.3	SC-46	0.98	2.17E-05	4.507	0.142
3C297F	B	207.3	TE-121	0.54	2.96E-02	6133.995	6844.773
3C297F	B	207.3	TE-121x	0.95	4.59E-03	950.532	3727.825
3C297F	B	207.3	ZN-65	0.99	5.05E-02	10477.506	224.264
43RTY2	A	155.4	BA-131	0.94	2.24E-02	3474.647	120.220
43RTY2	A	155.4	CE-141	0.98	3.27E-04	50.810	1.922
43RTY2	A	155.4	CO-60	0.99	5.25E-05	8.165	0.333
43RTY2	A	155.4	CR-51	0.96	4.23E-04	65.706	4.862
43RTY2	A	155.4	HF-175	0.89	5.24E-05	8.150	1.908
43RTY2	A	155.4	HF-181	0.78	2.66E-05	4.130	0.137
43RTY2	A	155.4	IN-114m	0.55	4.53E-06	0.705	0.448
43RTY2	A	155.4	RE-186	0.75	2.86E-06	0.445	0.142
43RTY2	A	155.4	RU-97	0.50	9.91E-03	1540.725	437.572
43RTY2	A	155.4	SB-124	0.87	1.33E-05	2.061	0.063
43RTY2	A	155.4	SC-46	0.99	2.83E-05	4.400	0.118
43RTY2	A	155.4	SN-125x	0.86	5.24E-02	8139.569	52464.633
43RTY2	A	155.4	TE-123m	0.97	3.49E-06	0.543	0.876
43RTY2	A	155.4	ZN-65	0.99	6.63E-02	10301.644	219.088
43RTY2	A	155.4	ZR-95	0.94	1.39E-04	21.613	30.071

43RTY2	B	140	BA-133	0.41	1.18E-01	16555.616	3263.783
43RTY2	B	140	CE-141	0.96	2.28E-04	31.862	6.418
43RTY2	B	140	CO-60	0.98	5.22E-05	7.303	0.314
43RTY2	B	140	HF-175	0.98	7.41E-05	10.378	2.800
43RTY2	B	140	HF-181	0.74	2.14E-05	2.993	0.284
43RTY2	B	140	SB-124	0.79	1.45E-05	2.029	0.080
43RTY2	B	140	SC-46	0.98	3.42E-05	4.786	0.102
43RTY2	B	140	XE-129m	0.52	5.50E-03	770.677	4191.224
43RTY2	B	140	ZN-65	0.99	6.97E-02	9760.656	209.292
4S19OC	B	16.2	AU-198	0.56	9.97E-07	0.016	0.021
4S19OC	B	16.2	BA-131	0.95	1.15E-01	1865.722	69.024
4S19OC	B	16.2	BA-133	0.64	1.04E-01	1687.629	1447.912
4S19OC	B	16.2	CR-51	0.95	1.03E-03	16.637	2.195
4S19OC	B	16.2	RU-97	0.51	4.04E-02	654.640	211.628
4S19OC	B	16.2	SB-124	0.79	9.53E-06	0.154	0.016
4S19OC	B	16.2	Si-32	0.89	3.44E-01	5572.902	9471.588
4S19OC	B	16.2	TE-121	0.69	3.52E-02	569.933	350.480
4S19OC	B	16.2	XE-127	0.78	8.63E-04	13.987	17.274
4S19OC	B	16.2	YB-169	0.61	4.47E-07	0.007	0.090
4S19OC	B	16.2	ZN-65	1.00	3.51E-01	5687.835	141.803
584C32	B	94.3	BA-131	0.93	2.12E-02	2000.621	81.603
584C32	B	94.3	CE-141	0.97	3.83E-04	36.102	1.853
584C32	B	94.3	CO-60	0.99	5.96E-05	5.620	0.232
584C32	B	94.3	CR-51	0.95	4.12E-04	38.866	3.473
584C32	B	94.3	HF-181	0.71	2.92E-05	2.755	0.111
584C32	B	94.3	RU-97	0.39	3.68E-02	3470.909	1163.409
584C32	B	94.3	SB-124	0.84	7.43E-06	0.700	0.030
584C32	B	94.3	SC-46	0.98	2.94E-05	2.769	0.079
584C32	B	94.3	SN-125x	0.90	5.35E-01	50430.829	54943.446
584C32	B	94.3	XE-127	0.38	2.52E-04	23.735	3.293
584C32	B	94.3	ZN-65	0.98	6.33E-02	5966.740	128.388
5H2F01	A	129.1	BA-131	0.73	1.76E-02	2271.845	254.549
5H2F01	A	129.1	BA-133	0.87	9.37E-02	12100.204	2246.951
5H2F01	A	129.1	CE-141	0.95	3.62E-04	46.771	3.127
5H2F01	A	129.1	CO-60	1.00	5.08E-05	6.565	0.255
5H2F01	A	129.1	EU-154	0.54	2.57E-06	0.332	0.092
5H2F01	A	129.1	SB-124	0.94	5.83E-06	0.752	0.055
5H2F01	A	129.1	SC-46	0.99	2.73E-05	3.526	0.099
5H2F01	A	129.1	SE-75	0.89	4.67E-06	0.603	0.146
5H2F01	A	129.1	XE-127	0.57	1.40E-05	1.812	1.119
5H2F01	A	129.1	ZN-65	1.00	5.61E-02	7236.343	131.730
7ZMK52	B	163.6	BA-133	0.66	1.07E-01	17425.953	1106.906
7ZMK52	B	163.6	CO-60	0.90	1.19E-04	19.446	0.730
7ZMK52	B	163.6	EU-152x	0.61	1.44E-06	0.236	0.015
7ZMK52	B	163.6	HF-181	0.69	3.14E-05	5.143	0.676
7ZMK52	B	163.6	IN-114m	0.61	1.34E-05	2.194	1.318
7ZMK52	B	163.6	SB-124	0.83	2.57E-05	4.207	0.294
7ZMK52	B	163.6	TE-121x	0.88	4.64E-01	75984.080	15267.310
7ZMK52	B	163.6	ZN-65	0.93	2.37E-01	38804.343	839.445
73J43M	A	147.7	CE-141	0.92	3.90E-04	57.593	9.532

73J43M	A	147.7	CO-60	0.95	5.97E-05	8.818	1.137
73J43M	A	147.7	CR-51	0.94	3.27E-04	48.339	16.782
73J43M	A	147.7	HF-181	0.87	2.66E-05	3.932	0.556
73J43M	A	147.7	IN-114m	0.72	3.84E-06	0.568	0.785
73J43M	A	147.7	RU-103	0.83	4.26E-05	6.298	1.818
73J43M	A	147.7	SB-124	0.72	7.02E-06	1.036	0.142
73J43M	A	147.7	SC-46	0.92	2.74E-05	4.042	0.514
73J43M	A	147.7	TA-182	0.49	7.39E-08	0.011	0.012
73J43M	A	147.7	TE-121x	0.99	3.86E-02	5695.369	8123.961
73J43M	A	147.7	TE-123m	1.00	4.10E-06	0.606	0.670
73J43M	A	147.7	ZN-65	0.92	6.54E-02	9665.014	1204.203
73J43M	B	184.7	BA-131	0.91	1.90E-02	3508.243	184.136
73J43M	B	184.7	CE-141	0.96	2.95E-04	54.567	2.864
73J43M	B	184.7	CO-60	0.99	4.91E-05	9.063	0.345
73J43M	B	184.7	CR-51	0.96	3.56E-04	65.773	5.693
73J43M	B	184.7	HF-181	0.72	1.91E-05	3.535	0.091
73J43M	B	184.7	RB-86	0.95	1.96E-05	3.617	1.724
73J43M	B	184.7	SB-124	0.83	6.18E-06	1.141	0.046
73J43M	B	184.7	SC-46	0.98	2.42E-05	4.477	0.120
73J43M	B	184.7	ZN-65	0.97	5.27E-02	9739.229	207.674
794TWZ	A	245.7	AG-108m	0.49	2.35E-03	576.404	235.286
794TWZ	A	245.7	BA-133	0.87	1.40E-01	34378.319	3099.039
794TWZ	A	245.7	CO-60	0.91	7.03E-05	17.274	0.598
794TWZ	A	245.7	CR-51	0.76	-1.00E-05	-2.458	-92.663
794TWZ	A	245.7	EU-152x	0.78	2.54E-06	0.624	0.029
794TWZ	A	245.7	FE-59	0.31	1.31E-02	3223.437	1157.520
794TWZ	A	245.7	HF-175	0.91	1.07E-04	26.181	6.035
794TWZ	A	245.7	SB-124	0.62	1.14E-05	2.802	1.040
794TWZ	A	245.7	SC-46	0.89	6.60E-05	16.224	0.393
794TWZ	A	245.7	TE-121	0.36	6.73E-01	165258.411	210866.146
794TWZ	A	245.7	TE-123m	0.99	3.93E-06	0.966	0.420
794TWZ	A	245.7	ZN-65	0.93	9.00E-02	22119.483	480.990
794TWZ	B	237.3	BA-131	0.32	3.44E-03	815.877	318.379
794TWZ	B	237.3	BA-133	0.53	6.85E-02	16247.523	4905.117
794TWZ	B	237.3	CE-141	0.94	1.63E-04	38.580	6.054
794TWZ	B	237.3	CO-60	0.98	3.35E-05	7.955	1.053
794TWZ	B	237.3	CR-51	0.95	1.55E-04	36.743	8.082
794TWZ	B	237.3	EU-152x	0.39	1.67E-06	0.396	0.064
794TWZ	B	237.3	HF-181	0.68	5.25E-06	1.246	0.258
794TWZ	B	237.3	RU-103	0.85	3.07E-05	7.283	2.021
794TWZ	B	237.3	SB-124	0.84	3.63E-06	0.861	0.118
794TWZ	B	237.3	SC-46	0.99	2.28E-05	5.409	0.681
794TWZ	B	237.3	ZN-65	1.00	4.00E-02	9482.383	1181.377
7WQF45	A	235.3	BA-133	0.40	6.97E-02	16388.840	3124.861
7WQF45	A	235.3	CE-141	0.86	1.76E-04	41.362	10.980
7WQF45	A	235.3	CO-60	0.98	2.96E-05	6.973	0.302
7WQF45	A	235.3	EU-152x	0.38	7.50E-07	0.176	0.043
7WQF45	A	235.3	EU-154	0.34	1.83E-06	0.430	0.092
7WQF45	A	235.3	FE-59	0.31	2.59E-03	609.423	207.368
7WQF45	A	235.3	RU-103	0.85	2.83E-06	0.667	0.172

7WQF45	A	235.3	SB-124	0.74	4.61E-06	1.084	0.073
7WQF45	A	235.3	SC-46	0.95	1.94E-05	4.567	0.147
7WQF45	A	235.3	ZN-65	0.96	3.94E-02	9271.253	198.736
7WQF45	B	202.7	AG-108m	0.48	2.43E-04	49.170	602.180
7WQF45	B	202.7	BA-131	0.93	1.49E-02	3012.507	122.418
7WQF45	B	202.7	CE-141	0.96	1.74E-04	35.221	1.789
7WQF45	B	202.7	CO-60	0.94	3.21E-05	6.498	0.283
7WQF45	B	202.7	CR-51	0.96	2.04E-04	41.374	3.265
7WQF45	B	202.7	HF-181	0.74	1.46E-05	2.964	0.182
7WQF45	B	202.7	LU-177	0.86	2.17E-06	0.441	0.414
7WQF45	B	202.7	RU-97	0.39	2.25E-02	4559.520	1581.302
7WQF45	B	202.7	SB-124	0.86	8.11E-06	1.643	0.057
7WQF45	B	202.7	SC-46	0.98	2.27E-05	4.599	0.121
7WQF45	B	202.7	TE-121	0.68	1.61E-03	326.560	157.051
7WQF45	B	202.7	ZN-65	0.98	4.34E-02	8801.841	187.561
7ZMK52	A	144.9	BA-133	0.70	2.46E-01	35655.030	3572.008
7ZMK52	A	144.9	CE-141	0.87	1.69E-04	24.535	9.757
7ZMK52	A	144.9	CO-60	0.90	1.22E-04	17.655	0.650
7ZMK52	A	144.9	EU-152x	0.71	3.14E-06	0.455	0.052
7ZMK52	A	144.9	FE-59	0.91	1.35E-02	1952.929	1192.106
7ZMK52	A	144.9	HF-175	0.86	1.54E-04	22.308	7.176
7ZMK52	A	144.9	HF-181	0.77	1.37E-05	1.990	0.498
7ZMK52	A	144.9	RU-103	0.82	3.79E-06	0.549	6.091
7ZMK52	A	144.9	SB-124	0.61	2.90E-05	4.201	0.276
7ZMK52	A	144.9	ZN-65	0.92	2.40E-01	34767.357	752.420
83MIA9	A	141.7	BA-133	0.85	4.34E-01	61472.749	8756.189
83MIA9	A	141.7	CO-60	0.92	2.29E-04	32.499	0.884
83MIA9	A	141.7	EU-152x	0.61	2.73E-06	0.387	0.056
83MIA9	A	141.7	HF-175	0.87	3.79E-04	53.760	22.312
83MIA9	A	141.7	HF-181	0.69	4.50E-05	6.380	1.133
83MIA9	A	141.7	Si-32	0.92	1.28E-01	18140.364	16208.755
83MIA9	A	141.7	ZN-65	0.93	3.43E-01	48662.920	1037.348
9RZMC2	A	212.6	BA-131	0.59	9.43E-03	2005.582	444.506
9RZMC2	A	212.6	CO-60	0.96	3.00E-05	6.375	0.275
9RZMC2	A	212.6	EU-154	0.32	7.04E-07	0.150	0.116
9RZMC2	A	212.6	LU-177	0.37	5.60E-04	119.153	59.417
9RZMC2	A	212.6	OS-191	0.82	2.63E-05	5.583	8.735
9RZMC2	A	212.6	RU-103	0.93	2.25E-06	0.478	1.473
9RZMC2	A	212.6	SC-46	0.95	3.20E-06	0.681	0.101
9RZMC2	A	212.6	TA-182	0.40	2.65E-07	0.056	0.029
9RZMC2	A	212.6	XE-127	0.32	2.55E-04	54.205	32.081
9RZMC2	A	212.6	ZN-65	0.98	4.83E-02	10271.791	219.436
9RZMC2	B	85.5	BA-133	0.41	1.44E-01	12289.982	2673.740
9RZMC2	B	85.5	CE-139	0.86	2.64E-03	225.511	137.408
9RZMC2	B	85.5	CO-60	0.92	6.87E-05	5.873	0.257
9RZMC2	B	85.5	IN-114m	0.57	-1.91E-06	-0.163	-0.344
9RZMC2	B	85.5	TE-121x	0.94	5.89E-02	5035.752	8887.018
9RZMC2	B	85.5	TE-123m	0.91	4.31E-06	0.369	0.859
9RZMC2	B	85.5	ZN-65	0.92	1.11E-01	9492.054	203.513
Al644T	A	91.6	BA-133	0.87	3.65E-01	33403.703	3036.419



AI644T	A	91.6	CE-141	0.87	5.37E-04	49.234	25.381
AI644T	A	91.6	CO-60	0.89	4.52E-05	4.139	0.242
AI644T	A	91.6	EU-152x	0.65	4.23E-06	0.388	0.038
AI644T	A	91.6	HF-175	0.86	3.80E-04	34.850	6.653
AI644T	A	91.6	HF-181	0.69	2.29E-05	2.101	0.611
AI644T	A	91.6	SB-124	0.47	9.39E-06	0.860	0.136
AI644T	A	91.6	SC-46	0.89	1.19E-04	10.874	0.311
AI644T	A	91.6	ZN-65	0.93	1.89E-01	17292.624	381.250
AI644T	B	137	BA-133	0.39	4.64E-02	6355.804	241.986
AI644T	B	137	CR-51	0.88	1.25E-04	17.130	15.029
AI644T	B	137	EU-152x	0.70	3.73E-06	0.511	0.025
AI644T	B	137	HF-175	0.99	2.32E-05	3.182	1.286
AI644T	B	137	OS-191	0.77	6.04E-06	0.828	10.655
AI644T	B	137	RU-103	0.85	6.90E-06	0.945	0.794
AI644T	B	137	SB-124	0.48	1.68E-06	0.230	0.027
AI644T	B	137	SB-125	0.51	7.06E-01	96665.270	56171.098
AI644T	B	137	SC-46	0.94	1.36E-05	1.858	0.082
AI644T	B	137	SN-125x	0.58	1.46E+01	2006121.159	6312769.373
AI644T	B	137	TE-123m	0.97	-1.52E-06	-0.209	-0.425
AI644T	B	137	XE-129m	0.53	1.78E-02	2438.366	4434.379
AI644T	B	137	ZN-65	0.93	3.71E-02	5088.920	111.397
BO14NE	A	191.2	BA-133	0.86	1.77E-01	33853.485	5280.111
BO14NE	A	191.2	CE-141	0.85	7.70E-05	14.726	22.274
BO14NE	A	191.2	CO-60	0.90	7.85E-05	15.011	1.913
BO14NE	A	191.2	EU-152x	0.57	2.04E-06	0.390	0.066
BO14NE	A	191.2	HF-175	0.85	5.77E-05	11.027	6.465
BO14NE	A	191.2	HF-181	0.69	1.46E-05	2.795	1.016
BO14NE	A	191.2	SB-124	0.49	1.66E-05	3.165	0.461
BO14NE	A	191.2	SC-46	0.87	8.10E-05	15.496	1.947
BO14NE	A	191.2	Si-32	0.88	8.87E-02	16954.862	43526.207
BO14NE	A	191.2	ZN-65	0.93	1.51E-01	28878.821	3599.339
BO14NE	A	191.2	ZR-95	0.96	1.90E-03	363.279	259.284
BO14NE	B	111.8	AS-77	0.91	8.87E-05	9.914	1.546
BO14NE	B	111.8	AU-198	0.98	6.64E-11	0.000	0.000
BO14NE	B	111.8	BA-131	0.99	3.66E-03	408.653	8.346
BO14NE	B	111.8	BA-133	0.71	1.26E-01	14048.352	1692.090
BO14NE	B	111.8	Ca-47	0.70	2.49E-03	278.910	70.246
BO14NE	B	111.8	CE-139	0.86	1.76E-03	197.057	77.618
BO14NE	B	111.8	CE-141	0.98	4.56E-05	5.103	0.502
BO14NE	B	111.8	CO-60	1.00	3.76E-05	4.205	0.164
BO14NE	B	111.8	CR-51	1.00	1.94E-04	21.633	1.354
BO14NE	B	111.8	FE-59	1.00	3.83E-03	428.684	56.304
BO14NE	B	111.8	HF-175	0.90	4.16E-05	4.646	0.616
BO14NE	B	111.8	HF-181	0.82	1.48E-05	1.653	0.071
BO14NE	B	111.8	HG-197	0.83	3.43E-09	0.000	0.000
BO14NE	B	111.8	IR-194	0.95	5.37E-13	0.000	0.000
BO14NE	B	111.8	LA-140	0.69	1.09E-09	0.000	0.000
BO14NE	B	111.8	LU-177	0.98	4.04E-08	0.005	0.002
BO14NE	B	111.8	OS-185	0.79	1.30E-05	1.449	0.981
BO14NE	B	111.8	RE-186	0.96	4.12E-09	0.000	0.000

BO14NE	B	111.8	RU-103	0.84	1.76E-04	19.671	1.705
BO14NE	B	111.8	SB-122	0.99	2.33E-09	0.000	0.000
BO14NE	B	111.8	SB-124	0.96	3.63E-06	0.406	0.019
BO14NE	B	111.8	SB-125	0.39	5.03E+00	562437.021	128890.771
BO14NE	B	111.8	SC-46	0.99	1.19E-05	1.325	0.036
BO14NE	B	111.8	SN-125x	0.99	1.54E-02	1726.426	4104.777
BO14NE	B	111.8	TE-123m	0.93	3.71E-05	4.147	0.467
BO14NE	B	111.8	XE-127	0.39	2.81E-05	3.137	3.028
BO14NE	B	111.8	XE-133m	0.94	4.52E-07	0.051	0.045
BO14NE	B	111.8	ZN-65	1.00	8.15E-02	9117.053	169.707
B92YNB	A	228.7	CE-141	0.93	2.67E-05	6.115	17.552
B92YNB	A	228.7	CO-60	0.95	3.53E-05	8.066	1.052
B92YNB	A	228.7	FE-59	0.31	5.06E-03	1158.176	196.626
B92YNB	A	228.7	HF-175	0.93	8.72E-05	19.943	6.182
B92YNB	A	228.7	HF-181	0.74	1.65E-05	3.780	0.609
B92YNB	A	228.7	HG-203	0.87	3.18E-06	0.728	1.659
B92YNB	A	228.7	RU-103	0.89	4.50E-05	10.291	2.370
B92YNB	A	228.7	SB-124	0.75	1.23E-05	2.806	0.361
B92YNB	A	228.7	SC-46	0.97	2.43E-05	5.550	0.704
B92YNB	A	228.7	ZN-65	0.98	5.60E-02	12807.931	1595.600
B92YNB	B	261.6	CE-141	0.93	1.63E-04	42.724	6.087
B92YNB	B	261.6	CO-60	0.99	2.85E-05	7.456	0.316
B92YNB	B	261.6	EU-154	0.42	3.63E-06	0.949	0.105
B92YNB	B	261.6	FE-59	0.97	3.67E-03	960.496	173.789
B92YNB	B	261.6	HF-181	0.74	1.45E-05	3.789	0.329
B92YNB	B	261.6	HG-203	0.87	2.23E-06	0.584	1.426
B92YNB	B	261.6	OS-185	0.78	5.87E-05	15.364	8.695
B92YNB	B	261.6	SB-124	0.94	8.47E-06	2.216	0.085
B92YNB	B	261.6	SC-46	0.98	1.87E-05	4.904	0.151
B92YNB	B	261.6	SN-125x	0.64	2.09E+01	5465456.338	4803411.220
B92YNB	B	261.6	TA-182	0.53	5.61E-08	0.015	0.011
B92YNB	B	261.6	ZN-65	1.00	4.32E-02	11299.797	241.278
B9ZYNB	B	261.6	ZR-95	0.93	3.71E-04	97.101	71.844
BRT6RD	A	104.4	BA-133	0.51	1.98E-01	20713.937	2600.843
BRT6RD	A	104.4	CO-60	0.87	1.13E-04	11.763	0.401
BRT6RD	A	104.4	EU-152x	0.61	2.78E-06	0.290	0.030
BRT6RD	A	104.4	HF-181	0.70	3.34E-05	3.488	0.579
BRT6RD	A	104.4	SB-124	0.89	4.93E-05	5.146	0.223
BRT6RD	A	104.4	ZN-65	0.91	1.70E-01	17707.947	386.393
BRT6RD	B	140.7	AU-198	0.63	7.62E-08	0.011	0.014
BRT6RD	B	140.7	BA-131	0.95	1.79E-02	2522.135	320.518
BRT6RD	B	140.7	CE-141	0.98	1.11E-04	15.580	2.498
BRT6RD	B	140.7	CR-51	0.89	2.47E-04	34.757	5.508
BRT6RD	B	140.7	HF-175	0.86	3.69E-05	5.193	1.075
BRT6RD	B	140.7	HF-181	0.88	2.22E-05	3.125	0.407
BRT6RD	B	140.7	ND-147	0.95	6.17E-05	8.679	4.122
BRT6RD	B	140.7	RU-97	0.54	5.50E-03	773.687	226.719
BRT6RD	B	140.7	SB-124	0.74	3.96E-06	0.557	0.074
BRT6RD	B	140.7	SC-46	0.97	1.46E-05	2.060	0.262
BRT6RD	B	140.7	TA-182	0.72	7.30E-08	0.010	0.006

BRT6RD	B	140.7	TE-123m	0.93	3.23E-05	4.548	1.086
BRT6RD	B	140.7	XE-127	0.39	1.28E-04	18.063	8.257
BRT6RD	B	140.7	ZN-65	0.99	5.25E-02	7393.330	921.238
PN38IZ	B	228	BA-133	1.00	2.16E-01	49216.020	4559.791
PN38IZ	B	228	CE-141	0.86	3.87E-05	8.814	38.423
PN38IZ	B	228	CO-60	0.92	2.41E-04	55.023	1.264
PN38IZ	B	228	EU-152x	0.64	4.72E-06	1.075	0.094
PN38IZ	B	228	HF-175	0.90	2.62E-04	59.771	23.572
PN38IZ	B	228	HF-181	0.66	1.59E-05	3.636	1.460
PN38IZ	B	228	SB-124	0.61	2.46E-05	5.613	0.391
PN38IZ	B	228	SC-46	0.89	1.49E-04	33.993	0.846
PN38IZ	B	228	ZN-65	0.94	2.00E-01	45488.021	971.528
PN38IZ	B	228	BA-133	0.38	6.77E-02	15432.040	3207.205
PN38IZ	B	228	CE-141	0.94	1.47E-04	33.510	5.704
PN38IZ	B	228	CO-60	0.98	6.04E-05	13.774	0.442
PN38IZ	B	228	CR-51	0.88	1.58E-04	35.967	15.766
PN38IZ	B	228	EU-152x	0.53	1.83E-06	0.418	0.035
PN38IZ	B	228	EU-154	0.33	4.24E-07	0.097	0.054
PN38IZ	B	228	SB-124	0.53	3.75E-06	0.854	0.068
PN38IZ	B	228	SC-46	0.97	2.03E-05	4.628	0.141
PN38IZ	B	228	ZN-65	0.98	4.48E-02	10209.583	217.917
ESF946	B	70.3	BA-131	0.61	2.41E-02	1695.468	241.225
ESF946	B	70.3	CE-141	0.85	1.41E-04	9.881	3.356
ESF946	B	70.3	CO-60	1.00	3.22E-05	2.262	0.127
ESF946	B	70.3	EU-154	0.40	1.89E-06	0.133	0.064
ESF946	B	70.3	HF-175	0.99	8.38E-05	5.891	1.650
ESF946	B	70.3	OS-185	0.84	6.43E-05	4.522	2.018
ESF946	B	70.3	SB-124	0.61	1.09E-06	0.077	0.027
ESF946	B	70.3	SC-46	0.99	2.39E-05	1.683	0.073
ESF946	B	70.3	TE-123m	0.96	1.56E-05	1.099	0.713
ESF946	B	70.3	ZN-65	1.00	6.58E-02	4626.886	101.818
G48MJ6	A	214.3	BA-131	0.34	1.03E-02	2198.736	513.097
G48MJ6	A	214.3	CE-141	0.96	1.50E-04	32.167	4.453
G48MJ6	A	214.3	CO-60	0.99	3.36E-05	7.202	0.275
G48MJ6	A	214.3	EU-152x	0.56	2.06E-06	0.442	0.030
G48MJ6	A	214.3	EU-154	0.39	9.80E-07	0.210	0.197
G48MJ6	A	214.3	FE-59	0.32	1.82E-03	390.492	144.555
G48MJ6	A	214.3	HF-181	0.88	4.97E-06	1.066	0.184
G48MJ6	A	214.3	IR-192	0.59	2.88E-08	0.006	0.005
G48MJ6	A	214.3	SB-124	0.45	4.04E-06	0.866	0.057
G48MJ6	A	214.3	SC-46	0.98	1.92E-05	4.116	0.110
G48MJ6	A	214.3	TE-123m	0.90	1.61E-06	0.345	0.543
G48MJ6	A	214.3	YB-169	0.72	8.71E-09	0.002	0.085
G48MJ6	A	214.3	ZN-65	0.99	3.79E-02	8116.315	146.880
G48MJ6	B	145.8	BA-133	0.86	2.04E-01	29727.118	4812.979
G48MJ6	B	145.8	CE-141	0.88	2.64E-04	38.563	16.727
G48MJ6	B	145.8	CO-60	0.87	1.02E-04	14.801	0.503
G48MJ6	B	145.8	EU-152x	0.70	3.42E-06	0.499	0.042
G48MJ6	B	145.8	HF-175	0.91	2.42E-04	35.212	6.424
G48MJ6	B	145.8	HF-181	0.66	3.33E-05	4.854	1.096

G48MJ6	B	145.8	RB-86	0.59	2.05E-03	298.874	134.878
G48MJ6	B	145.8	SB-124	0.49	1.78E-05	2.596	0.195
G48MJ6	B	145.8	SC-46	0.88	1.20E-04	17.491	0.386
G48MJ6	B	145.8	TE-123m	0.89	1.86E-06	0.271	0.961
G48MJ6	B	145.8	ZN-65	0.92	1.47E-01	21451.767	396.851
UGA145	A	96.7	BA-131	0.55	3.05E-02	2951.995	402.604
UGA145	A	96.7	BA-133	0.32	5.05E-02	4883.680	2744.330
UGA145	A	96.7	CO-60	0.98	5.61E-05	5.422	0.262
UGA145	A	96.7	CR-51	0.94	4.43E-04	42.849	14.296
UGA145	A	96.7	IN-114m	0.53	9.78E-06	0.946	0.390
UGA145	A	96.7	SB-124	0.45	9.13E-06	0.882	0.067
UGA145	A	96.7	SC-46	0.97	2.48E-05	2.398	0.125
UGA145	A	96.7	Si-32	0.96	6.11E-02	5909.837	14076.824
UGA145	A	96.7	ZN-65	0.98	9.37E-02	9064.825	195.012
IF3555	A	153.8	BA-133	0.71	2.15E-01	33048.770	2985.113
IF3555	A	153.8	CE-141	0.88	4.62E-04	71.044	25.236
IF3555	A	153.8	CO-60	0.89	1.29E-04	19.890	0.634
IF3555	A	153.8	EU-152x	0.86	3.98E-06	0.612	0.026
IF3555	A	153.8	HF-175	0.91	8.09E-05	12.445	5.175
IF3555	A	153.8	HF-181	0.70	2.44E-05	3.751	0.478
IF3555	A	153.8	OS-191	0.52	4.24E-03	652.246	186.210
IF3555	A	153.8	SB-124	0.50	1.92E-05	2.955	0.203
IF3555	A	153.8	SC-46	0.87	9.78E-05	15.044	0.361
IF3555	A	153.8	TE-121x	0.88	1.04E-01	16048.618	6133.482
IF3555	A	153.8	ZN-65	0.92	1.46E-01	22503.206	487.712
IF3555	B	171.2	CE-141	0.95	3.23E-04	55.289	8.664
IF3555	B	171.2	CO-60	1.00	5.29E-05	9.058	1.163
IF3555	B	171.2	CR-51	0.95	4.53E-04	77.483	12.968
IF3555	B	171.2	EU-152x	0.68	2.25E-06	0.384	0.058
IF3555	B	171.2	HF-175	0.91	5.52E-05	9.443	2.781
IF3555	B	171.2	HF-181	0.89	2.52E-05	4.309	0.582
IF3555	B	171.2	OS-185	0.99	5.07E-05	8.674	6.760
IF3555	B	171.2	SB-124	0.81	6.50E-06	1.113	0.154
IF3555	B	171.2	SC-46	0.99	2.69E-05	4.608	0.582
IF3555	B	171.2	ZN-65	1.00	5.94E-02	10164.803	1266.322
IF3555	B	171.2	ZR-95	0.93	4.16E-04	71.297	75.387
IS78FS	A	48.2	AG-110m	0.54	7.76E-07	0.037	0.006
IS78FS	A	48.2	BA-131	0.35	3.66E-02	1761.961	258.717
IS78FS	A	48.2	CO-60	1.00	7.81E-05	3.763	0.200
IS78FS	A	48.2	SB-124	0.44	4.57E-07	0.022	0.026
IS78FS	A	48.2	ZN-65	1.00	1.10E-01	5279.930	116.780
IS78FS	B	67.6	BA-133	0.47	7.34E-02	4962.781	3624.105
IS78FS	B	67.6	CE-141	0.95	4.44E-05	3.000	5.247
IS78FS	B	67.6	CO-60	0.92	1.03E-04	6.996	0.280
IS78FS	B	67.6	CR-51	0.89	5.75E-04	38.868	5.302
IS78FS	B	67.6	HF-181	0.87	8.90E-06	0.601	0.105
IS78FS	B	67.6	RU-103	0.86	8.35E-05	5.642	1.301
IS78FS	B	67.6	SB-124	0.42	1.98E-06	0.134	0.029
IS78FS	B	67.6	TB-160	0.61	3.08E-11	0.000	0.000
IS78FS	B	67.6	TE-123m	0.99	6.77E-06	0.457	0.624

IS78FS	B	67.6	ZN-65	0.93	1.01E-01	6851.387	148.458
JD5RT2	A	210.9	BA-131	0.61	1.79E-02	3772.758	650.136
JD5RT2	A	210.9	BA-133	0.37	6.23E-02	13129.344	3704.710
JD5RT2	A	210.9	CO-60	1.00	3.98E-05	8.390	1.083
JD5RT2	A	210.9	EU-152x	0.42	2.93E-06	0.618	0.092
JD5RT2	A	210.9	HF-175	0.92	5.27E-06	1.111	3.449
JD5RT2	A	210.9	LU-177	0.40	1.30E-05	2.748	47.613
JD5RT2	A	210.9	RU-103	0.82	1.83E-05	3.850	1.873
JD5RT2	A	210.9	SB-124	0.75	4.14E-06	0.872	0.130
JD5RT2	A	210.9	SC-46	0.99	2.37E-05	5.003	0.632
JD5RT2	A	210.9	TA-182	0.65	5.21E-08	0.011	0.010
JD5RT2	A	210.9	TE-121x	0.90	3.78E-02	7964.197	6862.236
JD5RT2	A	210.9	ZN-65	1.00	5.64E-02	11902.422	1482.652
JD5RT2	B	165	BA-133	0.40	5.31E-02	8763.930	1512.832
JD5RT2	B	165	CE-141	0.95	1.62E-04	26.747	4.127
JD5RT2	B	165	CO-60	0.99	3.23E-05	5.333	0.225
JD5RT2	B	165	CR-51	0.93	2.85E-04	46.956	6.495
JD5RT2	B	165	OS-185	0.82	1.31E-06	0.216	2.308
JD5RT2	B	165	SB-124	0.84	3.84E-06	0.634	0.042
JD5RT2	B	165	SC-46	0.99	1.91E-05	3.144	0.098
JD5RT2	B	165	ZN-65	0.99	4.50E-02	7426.650	158.715
JHHCD2	B	104.5	CR-51	0.89	7.32E-06	0.765	7.799
JHHCD2	B	104.5	SB-124	0.48	4.46E-06	0.466	0.065
JHHCD2	B	104.5	Si-32	0.92	2.28E-02	2386.397	17505.484
JHHCD2	B	104.5	TE-123m	1.00	4.02E-06	0.420	0.812
JHHCD2	B	104.5	ZN-65	0.92	8.15E-02	8514.957	184.283
JR3584	B	191.7	BA-133	0.52	2.03E-01	38980.793	3469.392
JR3584	B	191.7	CE-141	0.87	1.78E-04	34.103	10.570
JR3584	B	191.7	CO-60	0.90	9.00E-05	17.253	0.549
JR3584	B	191.7	EU-152x	0.57	2.24E-06	0.429	0.021
JR3584	B	191.7	HF-175	0.93	8.08E-05	15.481	5.965
JR3584	B	191.7	HF-181	0.78	2.06E-05	3.948	0.480
JR3584	B	191.7	OS-191	0.55	3.45E-03	661.194	211.721
JR3584	B	191.7	SB-124	0.49	1.80E-05	3.456	0.249
JR3584	B	191.7	TE-121x	0.99	1.69E-01	32375.713	21319.991
JR3584	B	191.7	ZN-65	0.93	1.51E-01	28856.736	624.162
JR3584	A	161.5	BA-131	0.60	1.55E-02	2502.952	467.491
JR3584	A	161.5	BA-133	0.52	8.14E-02	13145.683	3263.046
JR3584	A	161.5	CO-60	0.97	3.81E-05	6.152	0.803
JR3584	A	161.5	HF-181	0.81	1.55E-05	2.505	0.398
JR3584	A	161.5	IR-192	0.34	2.15E-08	0.003	0.002
JR3584	A	161.5	RB-86	0.88	4.82E-05	7.778	7.940
JR3584	A	161.5	RU-103	0.82	2.03E-06	0.328	1.606
JR3584	A	161.5	SB-124	0.54	4.40E-06	0.711	0.105
JR3584	A	161.5	SC-46	0.99	1.02E-05	1.650	0.222
JR3584	A	161.5	ZN-65	0.99	5.11E-02	8250.794	1028.087
KI9846	A	159.6	BA-131	0.60	1.75E-02	2785.507	684.556
KI9846	A	159.6	BA-133	0.87	9.79E-02	15619.218	3802.887
KI9846	A	159.6	CE-141	0.96	2.10E-04	33.548	5.394
KI9846	A	159.6	CO-60	0.99	8.86E-05	14.146	1.795

KI9846	A	159.6	CR-51	0.92	3.16E-04	50.478	14.994
KI9846	A	159.6	EU-152x	0.51	2.33E-06	0.373	0.054
KI9846	A	159.6	EU-154	0.31	3.10E-06	0.494	0.190
KI9846	A	159.6	HF-175	0.86	6.28E-05	10.023	4.726
KI9846	A	159.6	LU-177	0.44	1.29E-04	20.607	67.630
KI9846	A	159.6	RU-103	0.90	2.72E-05	4.339	2.676
KI9846	A	159.6	SB-124	0.77	5.02E-06	0.802	0.112
KI9846	A	159.6	SC-46	0.99	2.80E-05	4.464	0.565
KI9846	A	159.6	XE-127	0.77	4.87E-05	7.771	39.064
KI9846	A	159.6	ZN-65	1.00	6.80E-02	10855.771	1352.372
KI9846	B	178.3	BA-133	0.68	9.52E-02	16979.047	3698.950
KI9846	B	178.3	CE-141	0.89	1.96E-04	34.997	6.631
KI9846	B	178.3	CO-60	0.90	7.22E-05	12.877	1.638
KI9846	B	178.3	HF-181	0.75	1.10E-05	1.957	0.368
KI9846	B	178.3	NB-94x	0.93	1.16E-01	20674.402	41285.763
KI9846	B	178.3	SB-124	0.82	4.94E-06	0.880	0.124
KI9846	B	178.3	SC-46	0.92	2.57E-05	4.587	0.581
KI9846	B	178.3	ZN-65	0.90	6.07E-02	10814.575	1347.301
MSU4TD	A	140.4	CE-141	0.95	1.37E-04	19.241	4.161
MSU4TD	A	140.4	CO-60	0.98	1.55E-05	2.174	0.310
MSU4TD	A	140.4	CR-51	0.93	2.09E-04	29.378	12.743
MSU4TD	A	140.4	FE-59	0.30	1.16E-03	162.981	298.296
MSU4TD	A	140.4	HF-181	0.82	1.57E-05	2.209	0.320
MSU4TD	A	140.4	LU-177	0.41	1.70E-04	23.896	49.593
MSU4TD	A	140.4	SB-124	0.80	4.00E-06	0.562	0.082
MSU4TD	A	140.4	SC-46	0.98	1.49E-05	2.088	0.271
MSU4TD	A	140.4	TE-121	0.51	1.76E-02	2465.611	4248.082
MSU4TD	A	140.4	ZN-65	1.00	6.08E-02	8532.954	1063.206
MSU4TD	B	225	BA-133	0.53	1.74E-01	39139.129	6056.999
MSU4TD	B	225	CE-141	0.81	8.29E-05	18.648	35.759
MSU4TD	B	225	CO-60	0.91	2.80E-05	6.311	0.876
MSU4TD	B	225	EU-152x	0.78	2.56E-06	0.576	0.082
MSU4TD	B	225	HF-181	0.62	2.80E-05	6.301	0.996
MSU4TD	B	225	IR-192	0.33	5.76E-08	0.013	0.008
MSU4TD	B	225	OS-185	0.79	6.48E-05	14.583	9.591
MSU4TD	B	225	SB-124	0.68	2.03E-05	4.559	0.638
MSU4TD	B	225	ZN-65	0.94	1.71E-01	38552.737	4800.988
MTCL37	A	125.8	AU-198	0.52	1.90E-07	0.024	0.070
MTCL37	A	125.8	BA-131	0.95	8.66E-03	1089.154	41.842
MTCL37	A	125.8	BA-133	0.32	1.96E-01	24663.851	4118.807
MTCL37	A	125.8	CE-141	0.92	1.31E-04	16.514	1.968
MTCL37	A	125.8	CO-60	1.00	1.08E-04	13.648	0.484
MTCL37	A	125.8	CR-51	0.98	2.59E-04	32.541	4.419
MTCL37	A	125.8	HF-181	0.89	2.19E-05	2.753	0.139
MTCL37	A	125.8	RU-97	0.47	5.04E-03	633.805	243.979
MTCL37	A	125.8	SB-124	0.76	5.67E-06	0.713	0.039
MTCL37	A	125.8	SC-46	0.97	1.97E-05	2.482	0.094
MTCL37	A	125.8	YB-169	0.65	1.27E-06	0.159	0.077
MTCL37	A	125.8	ZN-65	1.00	8.57E-02	10776.701	230.993
MTCL37	B	119.9	AU-198	0.67	5.34E-08	0.006	0.009

MTCL37	B	119.9	BA-131	0.98	2.76E-02	3306.305	106.830
MTCL37	B	119.9	BA-133	0.54	2.18E-01	26079.297	3039.181
MTCL37	B	119.9	CE-141	0.99	1.16E-04	13.949	1.358
MTCL37	B	119.9	CO-60	1.00	1.24E-04	14.850	0.506
MTCL37	B	119.9	CR-51	0.99	4.15E-04	49.793	3.278
MTCL37	B	119.9	EU-154	0.50	2.98E-07	0.036	0.058
MTCL37	B	119.9	FE-59	1.00	1.01E-02	1215.425	73.315
MTCL37	B	119.9	HF-175	0.99	5.30E-05	6.351	1.904
MTCL37	B	119.9	HF-181	0.91	8.37E-06	1.004	0.039
MTCL37	B	119.9	LU-177	0.91	4.53E-06	0.544	0.125
MTCL37	B	119.9	RB-86	0.98	2.93E-05	3.509	0.834
MTCL37	B	119.9	RU-97	0.59	7.61E-03	912.272	230.048
MTCL37	B	119.9	SB-122	0.68	1.36E-07	0.016	0.684
MTCL37	B	119.9	SB-124	0.92	8.47E-06	1.016	0.052
MTCL37	B	119.9	SC-46	1.00	4.17E-05	4.996	0.114
MTCL37	B	119.9	TE-123m	1.00	5.79E-05	6.937	0.794
MTCL37	B	119.9	YB-169	0.65	1.70E-06	0.204	0.107
MTCL37	B	119.9	ZN-65	1.00	1.07E-01	12876.439	270.508
N6D5A7	B	131.9	BA-131	0.95	1.74E-02	2293.225	69.615
N6D5A7	B	131.9	BA-133	0.51	6.74E-02	8886.512	4062.865
N6D5A7	B	131.9	CE-141	0.97	1.66E-04	21.848	1.483
N6D5A7	B	131.9	CO-60	0.97	6.62E-05	8.735	0.292
N6D5A7	B	131.9	CR-51	0.96	2.55E-04	33.599	3.049
N6D5A7	B	131.9	FE-59	0.99	5.33E-03	702.798	77.016
N6D5A7	B	131.9	HF-181	0.69	1.19E-05	1.565	0.090
N6D5A7	B	131.9	RB-86	0.96	7.60E-06	1.002	0.412
N6D5A7	B	131.9	RU-97	0.54	5.60E-03	738.974	181.719
N6D5A7	B	131.9	SB-124	0.79	3.70E-06	0.489	0.024
N6D5A7	B	131.9	SC-46	0.98	2.06E-05	2.711	0.071
N6D5A7	B	131.9	TA-182	0.56	1.36E-07	0.018	0.007
N6D5A7	B	131.9	XE-129m	0.83	1.98E-04	26.092	4.819
N6D5A7	B	131.9	ZN-65	0.98	4.99E-02	6578.351	119.614
N6D5A7	A	216.1	AG-108m	0.40	3.03E-04	65.381	460.745
N6D5A7	A	216.1	BA-131	0.74	8.78E-03	1898.239	281.348
N6D5A7	A	216.1	BA-133	0.86	7.81E-02	16874.190	2304.342
N6D5A7	A	216.1	CO-60	1.00	7.27E-05	15.706	0.485
N6D5A7	A	216.1	CR-51	0.85	1.36E-04	29.433	12.090
N6D5A7	A	216.1	EU-154	0.63	4.96E-07	0.107	0.056
N6D5A7	A	216.1	FE-59	0.33	4.02E-03	868.319	422.584
N6D5A7	A	216.1	HF-175	0.91	1.05E-04	22.785	4.590
N6D5A7	A	216.1	RU-103	0.79	1.82E-05	3.939	1.562
N6D5A7	A	216.1	SB-124	0.95	4.31E-06	0.931	0.051
N6D5A7	A	216.1	SC-46	0.99	2.21E-05	4.771	0.143
N6D5A7	A	216.1	TA-182	0.66	3.32E-08	0.007	0.008
N6D5A7	A	216.1	ZN-65	1.00	4.88E-02	10556.342	224.934
PN38IZ	A	149.2	BA-131	0.91	2.26E-02	3371.520	192.505
PN38IZ	A	149.2	BA-133	0.54	1.28E-01	19083.664	3362.101
PN38IZ	A	149.2	CE-141	0.98	1.96E-04	29.194	2.559
PN38IZ	A	149.2	CO-60	0.98	7.11E-05	10.607	0.402
PN38IZ	A	149.2	CR-51	0.95	3.21E-04	47.838	3.807

PN38IZ	A	149.2	SB-124	0.83	6.95E-06	1.037	0.049
PN38IZ	A	149.2	SB-125	0.35	5.89E+00	878941.446	180749.399
PN38IZ	A	149.2	SC-46	0.99	2.58E-05	3.846	0.112
PN38IZ	A	149.2	TA-182	0.51	4.99E-08	0.007	0.012
PN38IZ	A	149.2	ZN-65	1.00	5.79E-02	8643.718	184.786
R67R85	A	278.9	BA-131	0.34	1.31E-02	3657.540	434.080
R67R85	A	278.9	BA-133	0.41	6.78E-02	18910.138	3312.113
R67R85	A	278.9	CE-141	0.95	1.68E-04	46.854	5.259
R67R85	A	278.9	CO-60	0.98	2.59E-05	7.212	0.292
R67R85	A	278.9	CR-51	0.95	2.15E-04	60.060	14.008
R67R85	A	278.9	EU-152x	0.51	1.87E-06	0.521	0.039
R67R85	A	278.9	HF-175	0.99	5.34E-05	14.891	3.067
R67R85	A	278.9	HF-181	0.74	1.30E-05	3.615	0.170
R67R85	A	278.9	OS-185	0.89	4.92E-04	137.181	98.989
R67R85	A	278.9	OS-191	0.80	1.05E-05	2.931	6.566
R67R85	A	278.9	SB-124	0.77	7.89E-06	2.200	0.081
R67R85	A	278.9	SC-46	0.98	1.58E-05	4.393	0.130
R67R85	A	278.9	SN-125x	0.66	2.79E+00	778384.522	2939145.978
R67R85	A	278.9	TB-160	0.47	1.02E-07	0.029	0.021
R67R85	A	278.9	ZN-65	0.99	3.83E-02	10691.078	227.536
SA4132	A	155.3	BA-131	0.95	1.88E-02	2924.394	371.797
SA4132	A	155.3	BA-133	0.83	7.58E-02	11772.888	3138.026
SA4132	A	155.3	Ca-47	0.57	9.27E-03	1439.726	10393.006
SA4132	A	155.3	CE-141	0.98	3.70E-04	57.468	7.471
SA4132	A	155.3	CO-60	0.98	5.07E-05	7.874	1.017
SA4132	A	155.3	CR-51	0.98	2.99E-04	46.470	7.027
SA4132	A	155.3	FE-59	0.92	8.76E-03	1361.117	186.886
SA4132	A	155.3	HF-181	0.72	2.31E-05	3.581	0.459
SA4132	A	155.3	OS-185	0.85	9.41E-04	146.088	320.797
SA4132	A	155.3	RU-97	0.53	5.73E-03	890.568	267.752
SA4132	A	155.3	SB-124	0.93	6.67E-06	1.035	0.133
SA4132	A	155.3	SC-46	0.99	2.73E-05	4.245	0.533
SA4132	A	155.3	TA-182	0.66	1.84E-07	0.029	0.008
SA4132	A	155.3	YB-175	0.82	#N/A	#N/A	#N/A
SA4132	A	155.3	ZN-65	0.99	5.57E-02	8655.955	1078.417
5H2F01	B	184.5	BA-133	0.47	8.41E-02	15513.325	3851.777
5H2F01	B	184.5	CE-141	0.93	2.84E-04	52.347	16.229
5H2F01	B	184.5	CO-60	0.87	5.87E-05	10.828	1.382
5H2F01	B	184.5	CR-51	0.85	2.27E-04	41.816	18.196
5H2F01	B	184.5	HF-181	0.69	2.62E-05	4.838	0.679
5H2F01	B	184.5	IR-192	0.32	6.06E-09	0.001	0.000
5H2F01	B	184.5	ND-147	0.68	1.72E-03	317.598	638.254
5H2F01	B	184.5	RU-103	0.88	6.30E-05	11.622	2.464
5H2F01	B	184.5	SB-124	0.49	7.82E-06	1.444	0.194
5H2F01	B	184.5	SC-46	0.92	3.26E-05	6.007	0.758
5H2F01	B	184.5	TA-182	0.39	1.13E-07	0.021	0.010
5H2F01	B	184.5	YB-169	0.60	1.39E-06	0.256	0.294
5H2F01	B	184.5	ZN-65	0.91	6.99E-02	12896.892	1606.572
TJ66RG	B	170	HF-175	0.90	5.68E-01	96603.821	117085.494
TJ66RG	B	170	IN-114m	0.55	3.44E-02	5847.024	32295.983



TJ66RG	A	136.5	AG-108m	0.41	7.75E-03	1057.822	412.373
TJ66RG	A	136.5	BA-131	0.57	1.37E-02	1870.308	405.213
TJ66RG	A	136.5	CO-60	0.91	4.19E-05	5.724	0.249
TJ66RG	A	136.5	LU-177	0.32	1.58E-04	21.577	166.748
TJ66RG	A	136.5	RU-103	0.92	7.03E-04	95.902	25.583
TJ66RG	A	136.5	SN-125x	0.58	6.76E+01	9227867.540	7227551.366
TJ66RG	A	136.5	ZN-65	0.92	6.68E-02	9111.640	194.689
UGA145	A	96.7	BA-133	0.64	3.09E-01	29875.366	3603.168
UGA145	A	96.7	CO-60	0.89	1.45E-04	13.979	0.508
UGA145	A	96.7	CR-51	0.79	1.51E-03	145.544	70.346
UGA145	A	96.7	EU-152x	0.60	3.56E-06	0.344	0.047
UGA145	A	96.7	HF-175	0.93	1.48E-04	14.292	6.442
UGA145	A	96.7	HF-181	0.70	4.91E-05	4.744	1.202
UGA145	A	96.7	SB-124	0.72	3.49E-05	3.378	0.223
UGA145	A	96.7	SC-46	0.87	1.11E-04	10.771	0.271
UGA145	A	96.7	TE-121x	0.92	5.69E-01	55005.656	10423.685
UGA145	A	96.7	XE-127	0.37	2.45E-03	237.204	146.017
UGA145	A	96.7	ZN-65	0.92	2.69E-01	26003.015	550.126
UGA145	B	70.6	BA-133	0.72	8.43E-02	5951.890	1842.686
UGA145	B	70.6	CE-139	0.96	7.83E-04	55.246	13.316
UGA145	B	70.6	CO-60	0.95	3.60E-05	2.540	0.167
UGA145	B	70.6	CR-51	0.80	5.05E-05	3.565	12.638
UGA145	B	70.6	RU-103	0.94	4.29E-05	3.029	1.124
UGA145	B	70.6	SB-124	0.71	5.59E-06	0.395	0.041
UGA145	B	70.6	TE-121x	0.86	2.30E-05	1.627	1.404
UGA145	B	70.6	ZN-65	0.95	7.82E-02	5521.500	120.945
VT23AC	A	190.9	BA-131	0.93	1.21E-02	2301.921	99.139
VT23AC	A	190.9	CE-141	0.99	7.77E-05	14.828	1.993
VT23AC	A	190.9	CR-51	0.97	1.19E-04	22.732	3.698
VT23AC	A	190.9	CS-134	0.32	1.30E-08	0.002	0.002
VT23AC	A	190.9	HF-181	0.74	5.24E-06	1.001	0.045
VT23AC	A	190.9	IN-114m	0.58	1.33E-07	0.025	0.351
VT23AC	A	190.9	RU-103	0.97	1.64E-05	3.138	0.689
VT23AC	A	190.9	RU-97	0.36	2.90E-02	5528.912	2014.178
VT23AC	A	190.9	SB-124	0.86	3.32E-06	0.635	0.016
VT23AC	A	190.9	SC-46	0.96	7.65E-06	1.461	0.065
VT23AC	A	190.9	ZN-65	0.99	3.68E-02	7018.402	151.894
VT23AC	B	152.7	BA-133	0.40	7.96E-02	12149.789	3505.877
VT23AC	B	152.7	CE-141	0.96	2.00E-04	30.504	6.121
VT23AC	B	152.7	CO-60	0.97	9.83E-06	1.501	0.187
VT23AC	B	152.7	EU-154	0.36	1.01E-05	1.536	0.109
VT23AC	B	152.7	HF-181	0.73	2.64E-05	4.038	0.295
VT23AC	B	152.7	SB-124	0.77	6.91E-06	1.055	0.066
VT23AC	B	152.7	SC-46	0.99	1.94E-05	2.968	0.154
VT23AC	B	152.7	TA-182	0.36	1.84E-07	0.028	0.015
VT23AC	B	152.7	ZN-65	1.00	8.92E-02	13625.740	290.473
WH3JMZ	A	200.3	BA-131	0.32	2.08E-02	4165.474	721.551
WH3JMZ	A	200.3	CE-141	0.96	6.31E-05	12.632	6.245
WH3JMZ	A	200.3	CO-60	0.99	9.63E-06	1.928	0.248
WH3JMZ	A	200.3	CR-51	0.89	7.75E-05	15.514	15.218

WH3JMZ	A	200.3	CS-134	0.87	1.40E-06	0.280	0.066
WH3JMZ	A	200.3	IN-114m	0.56	1.94E-06	0.389	1.020
WH3JMZ	A	200.3	SB-124	0.45	3.98E-06	0.797	0.111
WH3JMZ	A	200.3	SC-46	0.93	1.41E-05	2.814	0.145
WH3JMZ	A	200.3	ZN-65	0.92	5.61E-02	11231.904	239.728
WH3JMZ	B	75.1	BA-133	0.72	1.87E-01	14029.768	2264.993
WH3JMZ	B	75.1	CO-60	0.93	7.08E-05	5.314	0.353
WH3JMZ	B	75.1	EU-152x	0.58	2.88E-06	0.216	0.032
WH3JMZ	B	75.1	HF-175	0.94	6.63E-08	0.005	4.708
WH3JMZ	B	75.1	HF-181	0.67	3.03E-05	2.275	1.147
WH3JMZ	B	75.1	SB-124	0.49	2.49E-05	1.869	0.125
WH3JMZ	B	75.1	ZN-65	0.92	2.37E-01	17776.232	392.639

Table C-2 NAA data on clean filters

Serial Number	Spot	Element	ID Confidence	Specific Activity [ $\mu\text{Ci}/\text{mg}$ ]	Specific Activity Uncertainty [ $\mu\text{Ci}/\text{mg}$ ]	Specific Activity [ $\text{Bq}/\text{mg}$ ]	Sample Mass [mg]	Activity [Bq]	A[g/mol]	Parent Element	Element Mass [g]	Element % Sample Mass	% Uncertainty	
CFSD	1	BA-131	0.99	0.02400919	0.00037959	888.34	306.3	272098.551	137.33	BA	0.004224	1.379187	0.11927405	
CFSD	1	BA-133	0.506	0.01474968	0.0060289	545.7382	306.3	167159.598	137.33	BA	0.01784	5.824437	0.42550112	Low Confidence
CFSD	1	CE-141	0.99	0.0002954	3.7816E-05	10.92972	306.3	3347.77394	140.12	CE	1.13E-05	0.003697	0.1742541	
CFSD	1	CR-51	0.982	0.00320029	0.00127506	118.4107	306.3	36269.1839	52	CR	4.09E-05	0.013366	0.41559102	
CFSD	1	AS-77	0.678	0.8890241	0.1379555	32893.89	306.3	10075399	72.64	GE	0.11681	38.13567	0.19507956	Low Confidence
CFSD	1	HF-181	0.678	0.00075623	0.00011455	27.98064	306.3	8570.47101	178.49	HF	2.16E-06	0.000704	0.19214354	Low Confidence
CFSD	1	HF-175	0.924	0.00039035	0.00010413	14.44299	306.3	4423.88918	178.49	HF	1.3E-05	0.004239	0.29177915	
CFSD	1	HG-197	0.362	0.6758418	0.05806146	25006.15	306.3	7659382.7	200.59	HG	2.33E-26	7.6E-24	0.1461398	Low Confidence
CFSD	1	LA-140	0.477	0.00350823	0.00014083	129.8043	306.3	39759.0647	138.91	LA	6.09E-06	0.001988	0.12485087	Low Confidence
CFSD	1	RH-105	0.581	0.01704906	0.01456644	630.8152	306.3	193218.702	92.90638	RB	0.000178	0.057955	0.86252417	Low Confidence
CFSD	1	RU-97	0.781	0.00023098	0.00023844	8.546423	306.3	2617.7693	92.90638	RU	2.41E-06	0.000785	1.03902468	
CFSD	1	RU-103	0.822	0.02027342	0.00055758	750.1165	306.3	229760.696	92.90638	RU	0.000211	0.068915	0.12137859	
CFSD	1	SB-124	0.786	0.00094171	0.00011464	34.8431	306.3	10672.4426	92.90638	SB	9.81E-06	0.003201	0.16969164	
CFSD	1	SB-122	0.857	0.00137107	0.00025049	50.72941	306.3	15538.4168	92.90638	SB	1.43E-05	0.004661	0.21761038	
CFSD	1	SC-46	0.996	0.00928887	0.00035675	343.688	306.3	105271.647	92.90638	SC	9.67E-05	0.031576	0.1243036	
CFSD	1	TA-182	0.405	0.00047743	0.00019388	17.66495	306.3	5410.77553	92.90638	TA	4.97E-06	0.001623	0.42295184	Low Confidence
CFSD	1	TE-123m	0.987	0.00090061	5.3746E-05	33.32273	306.3	10206.7508	92.90638	TE	9.38E-06	0.003061	0.13242974	
CFSD	1	YB-175	0.876	0.00042256	0.00037615	15.63466	306.3	4788.89547	92.90638	YB	4.4E-06	0.001436	0.89798249	
CFSD	1	ZN-65	0.999	1.301273	0.01366996	48147.1	306.3	14747457	92.90638	ZN	0.013549	4.423413	0.11868739	
CFSD	2	BA-131	0.855	0.02283788	0.00109328	845.0016	317.7	268456.996	137.33	BA	0.004168	1.311902	0.12754607	
CFSD	2	CE-141	0.881	0.0002589	5.0392E-06	9.579378	317.7	3043.3683	140.12	CE	1.03E-05	0.00324	0.11981312	
CFSD	2	CR-51	0.905	0.00612392	0.00072973	226.5851	317.7	71986.0907	52	CR	8.13E-05	0.025576	0.167856	
CFSD	2	RU-103	0.991	0.00597328	0.00025709	221.0113	317.7	70215.2973	92.90638	RU	6.45E-05	0.020305	0.12581226	
CFSD	2	TE-123m	0.855	2.3954E-05	3.9633E-05	0.886287	317.7	281.573466	92.90638	TE	2.59E-07	8.14E-05	1.65880484	
CFSD	2	XE-127	0.505	0.0071934	0.00062806	266.1557	317.7	84557.6624	92.90638	XE	7.77E-05	0.024452	0.14696734	
CFSD	3	BA-131	0.378	0.0216554	0.00116744	801.2498	300	240374.94	137.33	BA	0.003732	1.243975	0.12993315	Low Confidence
CFSD	3	HO-166	0.4	0.1388686	0.07783014	5138.138	300	1541441.46	200.59	HG	4.69E-27	1.56E-24	0.57279184	Low Confidence
CFSD	3	RU-103	0.852	0.0096123	0.00040012	355.6552	300	106696.552	92.90638	RU	9.8E-05	0.032675	0.12533587	
CFSD	3	YB-169	0.641	0.00012884	4.3273E-05	4.767165	300	1430.14953	92.90638	YB	1.31E-06	0.000438	0.35605854	Low Confidence
CFSD	4	BA-131	0.866	0.01831856	0.00087857	677.7867	345.5	234175.312	137.33	BA	0.003636	1.052293	0.12757956	
CFSD	4	CE-139	0.856	3.8158E-05	2.3987E-06	1.411857	345.5	487.796628	140.12	CE	3.35E-07	9.71E-05	0.13389521	
CFSD	4	CE-141	0.952	0.00016706	4.5394E-05	6.18132	345.5	2135.64603	140.12	CE	7.22E-06	0.002091	0.29632202	
CFSD	4	CR-51	0.881	0.00341571	0.00061613	126.3813	345.5	43664.7288	52	CR	4.93E-05	0.014266	0.21566991	
CFSD	4	HF-181	0.763	0.00074603	4.6586E-05	27.60293	345.5	9536.81059	178.49	HF	2.4E-06	0.000695	0.13370052	
CFSD	4	RU-103	0.907	0.00356642	0.00019767	131.9577	345.5	45591.3684	92.90638	RU	4.19E-05	0.012123	0.13056935	
CFSD	4	TA-182	0.372	0.00121482	0.0001973	44.94816	345.5	15529.5876	92.90638	TA	1.43E-05	0.00413	0.20088575	Low Confidence
CFSD	4	TE-121	0.668	6.2978E-05	0.00016499	2.33018	345.5	805.07709	92.90638	TE	7.4E-07	0.000214	2.62248641	Low Confidence
CFSD	5	BA-131	0.861	0.06287964	0.00276192	2326.547	353.8	823132.215	137.33	BA	0.012779	3.612065	0.12611758	

CFSD	5	BA-133	0.669	0.07283092	0.0139111	2694.744	353.8	953400.441	137.33	BA	0.101752	28.75988	0.22463172	Low Confidence
CFSD	5	HG-203	0.944	7.779E-05	8.215E-05	2.878225	353.8	1018.31594	200.59	HG	3.1E-30	8.75E-28	1.06264588	
CFSD	5	RU-103	0.908	0.01656218	0.00068389	612.8007	353.8	216808.874	92.90638	RU	0.000199	0.0563	0.12522541	
CFSD	5	XE-129m	0.849	0.00494356	0.00208313	182.9116	353.8	64714.1404	92.90638	XE	5.95E-05	0.016805	0.43765196	
CFSD	6	BA-131	0.842	0.02471364	0.00121039	914.4047	388	354789.016	137.33	BA	0.005508	1.419653	0.12796498	
CFSD	6	CE-141	0.949	9.5732E-05	0.00016601	3.542067	388	1374.32199	140.12	CE	4.65E-06	0.001198	1.73816829	
CFSD	6	IR-192	0.36	0.00014991	0.00022981	5.546589	388	2152.07638	192.217	IR	5.81E-09	1.5E-06	1.53756865	Low Confidence
CFSD	6	RU-103	0.904	0.00543942	0.00024344	201.2587	388	78088.3566	92.90638	RU	7.17E-05	0.01849	0.12640914	
CFSD	6	YB-175	0.449	0.01069249	0.1032274	395.6221	388	153501.386	92.90638	YB	0.000141	0.036347	9.65492036	Low Confidence
CFSD	7	BA-131	0.855	0.02108726	0.00101577	780.2286	365.6	285251.583	137.33	BA	0.004429	1.211339	0.12765839	
CFSD	7	FE-59	0.346	2.6882E-05	0.00010713	0.994645	365.6	363.642384	55.84	FE	6.55E-05	0.017924	3.98697613	Low Confidence
CFSD	7	HF-181	0.681	0.00072848	4.9898E-05	26.95371	365.6	9854.27572	178.49	HF	2.48E-06	0.000678	0.13663109	Low Confidence
CFSD	7	RU-103	0.907	0.00449475	0.00019256	166.3057	365.6	60801.3687	92.90638	RU	5.59E-05	0.015279	0.12574455	
CFSD	7	SB-124	0.471	0.00071844	0.00014665	26.58234	365.6	9718.50456	92.90638	SB	8.93E-06	0.002442	0.23589095	Low Confidence
CFSD	7	XE-129m	0.844	0.00146652	0.00084873	54.26128	365.6	19837.9229	92.90638	XE	1.82E-05	0.004985	0.59069029	
CFSD	7	AG-108m	0.528	0.01748839	0.00218182	647.0704	365.6	236568.949	107.868	#N/A	0.000763	0.208776	0.17187472	Low Confidence
CFSK	2	AU-198m	0.683	6.4654E-05	0.00034968	2.392193	100.4	240.176196	196.97	AU	7.12E-10	7.09E-07	5.40984981	Low Confidence
CFSK	2	BA-131	0.983	0.07116793	0.00136603	2633.213	100.4	264374.626	137.33	BA	0.004105	4.088179	0.11976965	
CFSK	2	Ca-47	0.704	0.00121882	0.00019096	45.09641	100.4	4527.67997	40.08	CA	0.065489	65.22829	0.19627447	
CFSK	2	AS-77	0.518	13.18631	2.063459	487893.5	100.4	48984504.4	72.64	GE	0.567904	565.6414	0.1961221	Low Confidence
CFSK	2	HF-181	0.893	0.00635344	0.00018811	235.0774	100.4	23601.7701	178.49	HF	5.94E-06	0.005917	0.12187269	
CFSK	2	RB-86	0.994	0.00185624	0.00140474	68.68073	100.4	6895.54549	92.90638	RB	6.34E-06	0.00631	0.76594444	
CFSK	2	RU-103	0.907	0.05242591	0.0014493	1939.759	100.4	194751.77	92.90638	RU	0.000179	0.178211	0.12141074	
CFSK	2	SC-46	0.985	0.0238508	0.00108466	882.4796	100.4	88600.9518	92.90638	SC	8.14E-05	0.081076	0.12666689	
CFSK	2	ZN-65	0.997	4.179958	0.043903	154658.4	100.4	15527708	92.90638	ZN	0.014266	14.20892	0.11868722	
CFSK	3	AG-108m	0.374	0.01404312	0.1609178	519.5954	97.9	50868.3936	107.868	#N/A	0.000164	0.167647	11.4594452	Low Confidence
CFSK	3	BA-131	0.99	0.07846896	0.00119353	2903.352	97.9	284238.114	137.33	BA	0.004413	4.50758	0.11919602	
CFSK	3	Ca-47	0.661	0.00082729	0.00013876	30.60978	97.9	2996.69728	40.08	CA	0.043345	44.27455	0.20520886	Low Confidence
CFSK	3	CE-141	0.983	0.00101435	0.00022026	37.5311	97.9	3674.29449	140.12	CE	1.24E-05	0.012694	0.24724145	
CFSK	3	AS-77	0.683	2.885556	0.4482171	106765.6	97.9	10452349.5	72.64	GE	0.12118	123.7791	0.19520283	Low Confidence
CFSK	3	HF-181	0.849	0.00340997	0.00023448	126.169	97.9	12351.9488	178.49	HF	3.11E-06	0.003176	0.13676554	
CFSK	3	IN-114m	0.665	0.00067197	0.0005406	24.86292	97.9	2434.07983	114.818	IN	6.19E-07	0.000632	0.81313479	Low Confidence
CFSK	3	RU-103	0.903	0.04026613	0.00133335	1489.847	97.9	145856.003	92.90638	RU	0.000134	0.136877	0.12277147	
CFSK	3	SB-124	0.884	0.00454633	0.000229	168.2143	97.9	16468.182	92.90638	SB	1.51E-05	0.015454	0.12850469	
CFSK	3	SB-122	0.873	0.01189185	0.00086139	439.9985	97.9	43075.8483	92.90638	SB	3.96E-05	0.040424	0.13864799	
CFSK	3	SC-46	0.994	0.0175751	0.00093601	650.2787	97.9	63662.2847	92.90638	SC	5.85E-05	0.059743	0.12966394	
CFSK	3	TE-123m	0.982	0.00234572	0.00022532	86.79157	97.9	8496.89431	92.90638	TE	7.81E-06	0.007974	0.1523257	
CFSK	3	YB-169	0.349	0.00010525	0.00015873	3.89425	97.9	381.247075	92.90638	YB	3.5E-07	0.000358	1.51278326	Low Confidence
CFSK	3	ZN-65	0.998	4.348371	0.0461318	160889.7	97.9	15751104.3	92.90638	ZN	0.014471	14.7814	0.11869663	
CFSK	4	BA-131	0.845	0.06641088	0.00311664	2457.203	127.7	313784.767	137.33	BA	0.004872	3.814914	0.12719566	
CFSK	4	CE-141	0.989	0.00083973	0.00014214	31.06986	127.7	3967.62138	140.12	CE	1.34E-05	0.010509	0.20646886	
CFSK	4	HF-181	0.73	0.00318404	0.00017357	117.8093	127.7	15044.2517	178.49	HF	3.79E-06	0.002965	0.13018441	

CFSK	4	RU-103	0.905	0.01538806	0.00091205	569.3582	127.7	72707.0447	92.90638	RU	6.68E-05	0.052309	0.13224713	
CFSK	4	SB-124	0.681	0.00334739	0.00036399	123.8532	127.7	15816.0594	92.90638	SB	1.45E-05	0.011379	0.16062584	Low Confidence
CFSK	5	BA-131	0.876	0.05483739	0.00222232	2028.983	135.8	275535.95	137.33	BA	0.004278	3.150085	0.12497465	
CFSK	5	BA-133	0.503	0.02904739	0.01499771	1074.753	135.8	145951.516	137.33	BA	0.015577	11.4704	0.52968039	Low Confidence
CFSK	5	CE-139	0.998	1.5309E-05	9.9134E-05	0.566451	135.8	76.9240132	140.12	CE	5.29E-08	3.9E-05	6.47641073	
CFSK	5	CE-141	0.991	0.00024905	4.6746E-05	9.214795	135.8	1251.36909	140.12	CE	4.23E-06	0.003117	0.22182771	
CFSK	5	CO-60	0.996	0.0067289	0.00123645	248.9692	135.8	33810.0108	58.93	CO	9.23E-07	0.00068	0.21849769	
CFSK	5	HF-181	0.898	0.00409799	0.00013501	151.6256	135.8	20590.7606	178.49	HF	5.18E-06	0.003817	0.12272614	
CFSK	5	IN-114m	0.828	0.00854914	0.00714677	316.3183	135.8	42956.0289	114.818	IN	1.09E-05	0.008039	0.84428161	
CFSK	5	MO-99	0.332	1.57557	1.478918	58296.09	135.8	7916609.02	95.94	MO	0.01103	8.121932	0.94607143	Low Confidence
CFSK	5	RU-103	0.909	0.01756246	0.00067628	649.811	135.8	88244.3365	92.90638	RU	8.11E-05	0.0597	0.12433475	
CFSK	5	RU-97	0.317	0.03142354	0.08198815	1162.671	135.8	157890.719	92.90638	RU	0.000145	0.106818	2.61180854	Low Confidence
CFSK	5	TA-182	0.635	0.00050698	0.00147872	18.75839	135.8	2547.38879	92.90638	TA	2.34E-06	0.001723	2.91909004	Low Confidence
CFSK	5	TE-121	0.664	8.102E-05	0.00028845	2.997757	135.8	407.095454	92.90638	TE	3.74E-07	0.000275	3.56222428	Low Confidence
CFSK	5	YB-175	0.634	0.03263066	0.03827558	1207.334	135.8	163956.014	92.90638	YB	0.000151	0.110921	1.17893685	Low Confidence
CFSK	6	BA-131	0.852	0.09037917	0.00431522	3344.029	80.8	270197.567	137.33	BA	0.004195	5.191751	0.12749901	
CFSK	6	BA-133	0.471	0.1262914	0.02196351	4672.782	80.8	377560.769	137.33	BA	0.040295	49.87066	0.21028909	Low Confidence
CFSK	6	CR-51	0.96	0.00162016	0.00241705	59.94574	80.8	4843.61539	52	CR	5.47E-06	0.006767	1.49654275	
CFSK	6	CS-134	0.719	0.02073358	0.00330115	767.1425	80.8	61985.1108	132.9055	CS	4.9E-07	0.000606	0.1983092	
CFSK	6	HF-181	0.697	0.00575445	0.00029451	212.9146	80.8	17203.4977	178.49	HF	4.33E-06	0.005359	0.12882436	Low Confidence
CFSK	6	RU-103	0.905	0.02213261	0.00099992	818.9066	80.8	66167.6509	92.90638	RU	6.08E-05	0.075235	0.1265601	
CFSK	6	SB-124	0.593	0.00339948	0.00051766	125.7806	80.8	10163.0705	92.90638	SB	9.34E-06	0.011556	0.19278	Low Confidence
CFSK	6	TA-182	0.443	0.00180216	0.00130545	66.67992	80.8	5387.73754	92.90638	TA	4.95E-06	0.006126	0.73396335	Low Confidence
CFSK	6	XE-129m	0.823	5.5723E-05	0.00589952	2.061739	80.8	166.588524	92.90638	XE	1.53E-07	0.000189	105.872917	
CFSK	6	YB-175	0.535	0.5414399	0.3925143	20033.28	80.8	1618688.73	92.90638	YB	0.001487	1.840515	0.73452161	Low Confidence
CFSK	7	BA-131	0.859	0.07268369	0.00305819	2689.297	119.4	321102.006	137.33	BA	0.004985	4.17525	0.12548575	
CFSK	7	CE-139	1	8.9293E-05	0.00013771	3.303858	119.4	394.480648	140.12	CE	2.71E-07	0.000227	1.54679195	
CFSK	7	CE-141	0.916	0.00016716	0.00015255	6.185005	119.4	738.489609	140.12	CE	2.5E-06	0.002092	0.92022726	
CFSK	7	HF-181	0.687	0.00419435	0.00020642	155.1911	119.4	18529.8127	178.49	HF	4.66E-06	0.003906	0.12805572	Low Confidence
CFSK	7	HG-203	0.984	7.7687E-07	7.6681E-05	0.028744	119.4	3.43204966	200.59	HG	1.04E-32	8.74E-30	98.7059393	
CFSK	7	RU-103	0.907	0.02042066	0.00080878	755.5644	119.4	90214.3917	92.90638	RU	8.29E-05	0.069416	0.12467943	
CFSK	7	SB-124	0.43	0.00362989	0.00052817	134.3058	119.4	16036.1148	92.90638	SB	1.47E-05	0.012339	0.1874791	Low Confidence
CFSK	7	SB-122	0.309	0.7951361	0.2367724	29420.04	119.4	3512752.26	92.90638	SB	0.003227	2.702904	0.32038547	Low Confidence
CFSK	7	YB-169	0.63	0.00013181	8.0339E-05	4.877107	119.4	582.326564	92.90638	YB	5.35E-07	0.000448	0.62084511	Low Confidence
CFSP	1	AG-108m	0.957	0.07956245	0.05696715	2943.811	389.8	1147497.39	107.868	AG	0.003702	0.949817	0.72569979	
CFSP	1	BA-131	0.885	0.01844348	0.00065637	682.4088	389.8	266002.935	137.33	BA	0.00413	1.059469	0.1234619	
CFSP	1	BA-131	0.88	0.01867424	0.00064475	690.9469	389.8	269331.094	137.33	BA	0.004181	1.072725	0.12316003	
CFSP	1	CE-141	0.992	0.00045249	4.2481E-05	16.74222	389.8	6526.11689	140.12	CE	2.21E-05	0.005663	0.15096427	
CFSP	1	CE-141	0.957	0.00056758	4.2E-05	21.00031	389.8	8185.92018	140.12	CE	2.77E-05	0.007103	0.13947111	
CFSP	1	CR-51	0.904	0.00567435	0.00080495	209.9508	389.8	81838.8226	52	CR	9.24E-05	0.023699	0.18466225	
CFSP	1	CR-51	0.919	0.00590277	0.00052425	218.4026	389.8	85133.3483	52	CR	9.61E-05	0.024653	0.14786576	
CFSP	1	FE-59	0.347	0.00030224	0.00020107	11.18299	389.8	4359.12845	55.84	FE	0.000786	0.201521	0.67566775	Low Confidence

CFSP	1	AS-71	0.426	2.560622	0.0888814	94743.01	389.8	36930826.9	72.64	GE	0.898132	230.4084	0.12321195	Low Confidence
CFSP	1	HF-181	0.718	0.00070126	5.9409E-05	25.94648	389.8	10113.9391	178.49	HF	2.55E-06	0.000653	0.14544246	
CFSP	1	HF-181	0.798	0.00116399	4.9794E-05	43.06774	389.8	16787.8054	178.49	HF	4.23E-06	0.001084	0.12572338	
CFSP	1	HG-203	0.879	3.8268E-06	1.5575E-05	0.141593	389.8	55.1928672	200.59	HG	1.68E-31	4.3E-29	4.07165231	
CFSP	1	LU-177	0.859	8.907E-05	0.000601	3.295576	389.8	1284.6155	174.967	LU	5.5E-08	1.41E-05	6.74853603	
CFSP	1	LU-177	0.866	0.00020474	0.00062255	7.575469	389.8	2952.91774	174.967	LU	1.27E-07	3.25E-05	3.04295285	
CFSP	1	RB-86	0.974	0.00244093	0.00085205	90.31423	389.8	35204.4849	92.90638	RB	3.23E-05	0.008297	0.36854363	
CFSP	1	RU-103	0.909	0.00752805	0.00026312	278.5378	389.8	108574.04	92.90638	RU	9.98E-05	0.02559	0.12328019	
CFSP	1	RU-103	0.909	0.0075306	0.00025787	278.6323	389.8	108610.86	92.90638	RU	9.98E-05	0.025599	0.12308096	
CFSP	1	RU-97	0.383	0.02996513	0.01331708	1108.71	389.8	432175.084	92.90638	RU	0.000397	0.10186	0.45987476	Low Confidence
CFSP	1	RU-97	0.394	0.03209853	0.01216351	1187.646	389.8	462944.259	92.90638	RU	0.000425	0.109112	0.39695599	Low Confidence
CFSP	1	SB-124	0.563	0.00249215	0.00016757	92.20959	389.8	35943.297	92.90638	SB	3.3E-05	0.008472	0.13600473	Low Confidence
CFSP	1	SB-124	0.778	0.00302384	0.00023276	111.8819	389.8	43611.5771	92.90638	SB	4.01E-05	0.010279	0.14107209	
CFSP	1	SN-125x	0.935	0.00059385	0.00086129	21.97245	389.8	8564.85957	92.90638	SN	7.87E-06	0.002019	1.45515995	
CFSP	1	TA-182	0.536	0.00017221	4.7033E-05	6.371822	389.8	2483.73614	92.90638	TA	2.28E-06	0.000585	0.29760072	Low Confidence
CFSP	1	TA-182	0.304	0.00117817	0.00028826	43.59233	389.8	16992.2891	92.90638	TA	1.56E-05	0.004005	0.27173203	Low Confidence
CFSP	1	YB-169	0.353	0.00016784	6.6915E-05	6.209925	389.8	2420.62861	92.90638	YB	2.22E-06	0.000571	0.41584942	Low Confidence
CFSP	2	BA-133	0.709	0.02767072	0.00292015	1023.817	337.6	345640.498	137.33	BA	0.036889	10.92677	0.15847189	
CFSP	2	CE-141	0.927	0.000922	0.00017442	34.11414	337.6	11516.9326	140.12	CE	3.9E-05	0.011539	0.22308019	
CFSP	2	CR-51	0.952	0.00686815	0.00091199	254.1215	337.6	85791.4103	52	CR	9.68E-05	0.028685	0.17778709	
CFSP	2	EU-152x	0.599	0.1137739	0.04179981	4209.634	337.6	1421172.54	151.964	EU	1.02E-06	0.000303	0.38594617	Low Confidence
CFSP	2	EU-154	0.364	0.01899172	0.01908276	702.6936	337.6	237229.373	151.964	EU	9.64E-06	0.002855	1.01172459	Low Confidence
CFSP	2	HF-181	0.719	0.00065671	0.00014046	24.29823	337.6	8203.08096	178.49	HF	2.06E-06	0.000612	0.24438748	
CFSP	2	HF-175	0.931	0.0005491	0.00042884	20.31676	337.6	6858.93666	178.49	HF	2.01E-05	0.005962	0.78987639	
CFSP	2	SB-124	0.618	0.00174702	0.00195113	64.63963	337.6	21822.3388	92.90638	SB	2E-05	0.005939	1.12307484	Low Confidence
CFSP	2	ZN-65	0.877	1.799296	0.01708211	66573.95	337.6	22475366.2	92.90638	ZN	0.020649	6.116341	0.11860216	
CFSP	3	BA-131	0.886	0.01735524	0.00065422	642.1439	405.4	260325.129	137.33	BA	0.004042	0.996956	0.12408585	
CFSP	3	CE-141	0.975	0.00036888	0.00011957	13.64868	405.4	5533.17572	140.12	CE	1.87E-05	0.004617	0.34501695	
CFSP	3	CO-60	0.884	0.01159003	0.00094859	428.8311	405.4	173848.132	58.93	CO	4.75E-06	0.001171	0.14378805	
CFSP	3	CR-51	0.911	0.00525587	0.00051367	194.467	405.4	78836.9388	52	CR	8.9E-05	0.021951	0.1533884	
CFSP	3	HF-181	0.845	0.00112099	5.072E-05	41.47656	405.4	16814.5958	178.49	HF	4.23E-06	0.001044	0.12658421	
CFSP	3	HO-166	0.39	2.941324	2.605819	108829	405.4	44119271.7	200.59	HG	1.34E-25	3.31E-23	0.89378713	Low Confidence
CFSP	3	RB-86	0.956	0.0008319	0.00072419	30.78017	405.4	12478.2796	92.90638	RB	1.15E-05	0.002828	0.87851846	
CFSP	3	RU-103	0.91	0.00664745	0.00023582	245.9557	405.4	99710.4355	92.90638	RU	9.16E-05	0.022597	0.12342937	
CFSP	3	RU-97	0.355	0.06753878	0.0250079	2498.935	405.4	1013068.19	92.90638	RU	0.000931	0.229584	0.38868969	Low Confidence
CFSP	3	SB-124	0.814	0.0026924	0.00015081	99.61876	405.4	40385.4465	92.90638	SB	3.71E-05	0.009152	0.13081906	
CFSP	3	YB-175	0.653	0.00182739	0.00756338	67.6135	405.4	27410.5145	92.90638	YB	2.52E-05	0.006212	4.14058274	Low Confidence
CFSP	5	AG-110m	0.378	0.00040288	0.00016272	14.90655	396.9	5916.40926	107.868	AG	1.91E-05	0.00481	0.4208312	Low Confidence
CFSP	5	BA-131	0.858	0.02224979	0.00093153	823.2422	396.9	326744.841	137.33	BA	0.005073	1.278119	0.12541596	
CFSP	5	CE-141	0.957	0.00065455	8.7355E-06	24.21852	396.9	9612.3292	140.12	CE	3.25E-05	0.008192	0.11897248	
CFSP	5	CR-51	0.886	0.00701847	0.00092397	259.6835	396.9	103068.367	52	CR	0.000116	0.029312	0.17693911	
CFSP	5	CS-134	0.727	0.02435808	0.00137001	901.249	396.9	357705.712	132.9055	CS	2.83E-06	0.000712	0.13091907	

CFSP	5	HF-181	0.776	0.0012138	5.8343E-05	44.91067	396.9	17825.0465	178.49	HF	4.49E-06	0.00113	0.12761929	
CFSP	5	HO-166	0.32	0.2546551	1.123612	9422.239	396.9	3739686.54	200.59	HG	1.14E-26	2.86E-24	4.41387292	Low Confidence
CFSP	5	MO-99	0.33	0.5648316	0.341207	20898.77	396.9	8294721.5	95.94	MO	0.011556	2.91166	0.61554572	Low Confidence
CFSP	5	OS-185	0.884	0.00027381	0.00024025	10.13098	396.9	4020.98493	92.90638	OS	3.69E-06	0.000931	0.88536005	
CFSP	5	RB-86	0.879	0.00047378	0.00103547	17.52988	396.9	6957.61025	92.90638	RB	6.39E-06	0.001611	2.18873838	
CFSP	5	RU-103	0.906	0.00635706	0.00025106	235.2113	396.9	93355.3626	92.90638	RU	8.58E-05	0.02161	0.12464385	
CFSP	6	BA-131	0.855	0.02103247	0.00101268	778.2014	387.7	301708.679	137.33	BA	0.004684	1.208192	0.12765038	
CFSP	6	CE-141	0.947	0.00046216	5.2025E-05	17.09992	387.7	6629.64042	140.12	CE	2.24E-05	0.005784	0.16324235	
CFSP	6	CR-51	0.908	0.00570418	0.00067975	211.0546	387.7	81825.863	52	CR	9.24E-05	0.023823	0.16786025	
CFSP	6	HF-181	0.658	0.00108373	5.9397E-05	40.09816	387.7	15546.0559	178.49	HF	3.91E-06	0.001009	0.13030806	Low Confidence
CFSP	6	IR-192	0.383	8.2128E-05	5.6019E-05	3.038727	387.7	1178.11465	192.217	IR	3.18E-09	8.21E-07	0.69226793	Low Confidence
CFSP	6	RU-103	0.993	0.00433841	0.0002112	160.5212	387.7	62234.0576	92.90638	RU	5.72E-05	0.014748	0.12785261	
CFSP	6	SB-124	0.441	0.00384133	9.4626E-05	142.1293	387.7	55103.5234	92.90638	SB	5.06E-05	0.013058	0.12076072	Low Confidence
CFSP	6	TE-123m	0.871	2.4023E-05	3.66E-05	0.888837	387.7	344.602082	92.90638	TE	3.17E-07	8.17E-05	1.52815592	
CFSP	6	XE-127	0.544	2.4044E-05	3.1049E-05	0.889643	387.7	344.914514	92.90638	XE	3.17E-07	8.17E-05	1.29672638	Low Confidence

**Table C-3 NAA data for jet engine lubricating oil (Mobil Jet Oil II)**

Serial Number	Number	FE Letter	FE Flux	Flux Uncertainty	Isotope	ID Confidence	Specific Activity [ $\mu\text{Ci}/\text{mg}$ ]	Specific Activity Uncertainty [ $\mu\text{Ci}/\text{mg}$ ]	Specific Activity [ $\text{Bq}/\text{mg}$ ]	Sample Mass [mg]	Activity [Bq]	A[g/mol]	$\sigma_{\text{th}}$	$\sigma_{\text{ri}}$	$p_i$	$\alpha$	$\sigma_{\text{th}}+\alpha\sigma_{\text{ri}}$	Parent Element	Element Mass [g]	Element % of Sample Mass	% Uncertainty
Jet Engine Oil	1	FEA	7.93E+10	9.38E+09	CE-137x	0.384	0.0160964	0.0910787	595.56754	220.4	131263.0858	140.12	2.6E-24	3.1E-23	0.15	0.8333333	2.843E-23	CE	9.026E-05	0.0409549	5.659555188
Jet Engine Oil	1	FEA	7.93E+10	9.38E+09	CO-60	1	0.8490152	0.01118158	31413.562	220.4	6923549.153	58.93	1.6E-23	3.5E-23	1	0.8333333	4.517E-23	CO	0.0001891	0.0857887	0.118952891
Jet Engine Oil	1	FEA	7.93E+10	9.38E+09	CR-51	0.997	9.92E-03	6.95E-04	3.67E+02	220.4	8.09E+04	52	1.55E-23	8E-24	0.0435	0.8333333	2.217E-23	CR	9.13E-05	0.0414265	0.137432949
Jet Engine Oil	1	FEA	7.93E+10	9.38E+09	EU-152x	0.356	2.77E-03	7.97E-03	1.02E+02	220.4	2.26E+04	151.964	5.9E-21	4E-21	0.4781	0.8333333	9.233E-21	EU	1.63E-08	7.385E-06	2.879538104
Jet Engine Oil	1	FEA	7.93E+10	9.38E+09	FE-59	0.999	3.13E-01	6.33E-03	1.16E+04	220.4	2.56E+06	55.84	1.3E-24	1.2E-24	0.00282	0.8333333	2.3E-24	FE	4.61E-01	209.01415	0.119933527
Jet Engine Oil	1	FEA	7.93E+10	9.38E+09	ND-147	0.962	0.0004576	0.000150854	16.931759	220.4	3731.759617	22.98977	5.3E-25	3.2E-25	1	0.8333333	7.967E-25	ND	2.254E-06	0.0010227	0.350209145
Jet Engine Oil	1	FEA	7.93E+10	9.38E+09	RU-103	0.884	4E-05	0.000101123	1.4800059	220.4	326.1933048	22.98977	5.3E-25	3.2E-25	1	0.8333333	7.967E-25	RU	1.97E-07	8.94E-05	2.530825118
Jet Engine Oil	1	FEA	7.93E+10	9.38E+09	SB-124	0.952	0.0030402	0.000224402	112.48562	220.4	24791.83153	22.98977	5.3E-25	3.2E-25	1	0.8333333	7.967E-25	SB	1.497E-05	0.0067944	0.139372424
Jet Engine Oil	1	FEA	7.93E+10	9.38E+09	SR-85x	0.879	0.0005693	0.000260612	21.063626	220.4	4642.423259	22.98977	5.3E-25	3.2E-25	1	0.8333333	7.967E-25	SR	2.804E-06	0.0012723	0.472805955
Jet Engine Oil	1	FEA	7.93E+10	9.38E+09	ZN-65	0.982	0.0002861	0.00108804	10.585019	220.4	2332.938232	22.98977	5.3E-25	3.2E-25	1	0.8333333	7.967E-25	ZN	1.409E-06	0.0006394	3.805087518



## Appendix D - Operating procedures for BAS

Figure D.1 shows the operating panel for LabVIEW. The panel allows entry of sampling flow rate and starting and stopping the operations. It also displays particulate count versus time in graph format and a digital reading of various parameters as shown in Figure D.1. To start the operation, the desktop computer was switched on and Magoha DAQ folder opened. To start the LabVIEW program, "HEPA Filter" folder was double-clicked. This folder contains icons for the control setup and a folder for the storage of the data from the experimental runs. The HEPA DAQ folder was opened by placing the mouse pointer over the appropriate file, and double-clicking the left mouse button to open LabVIEW program. After opening the HEPA DAQ file, the start button was clicked followed by force CSV format on the screen panel to activate the OPC. After this operation the OPC started counting aerosol particles and register counts. At this point the OPC should register some readings otherwise the previous procedures might have not been correct.

Start button

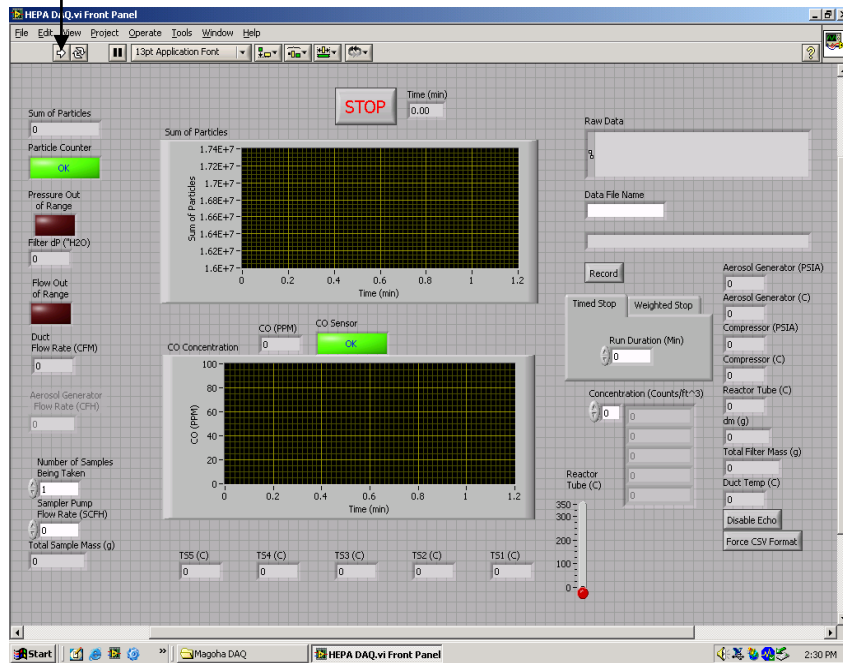
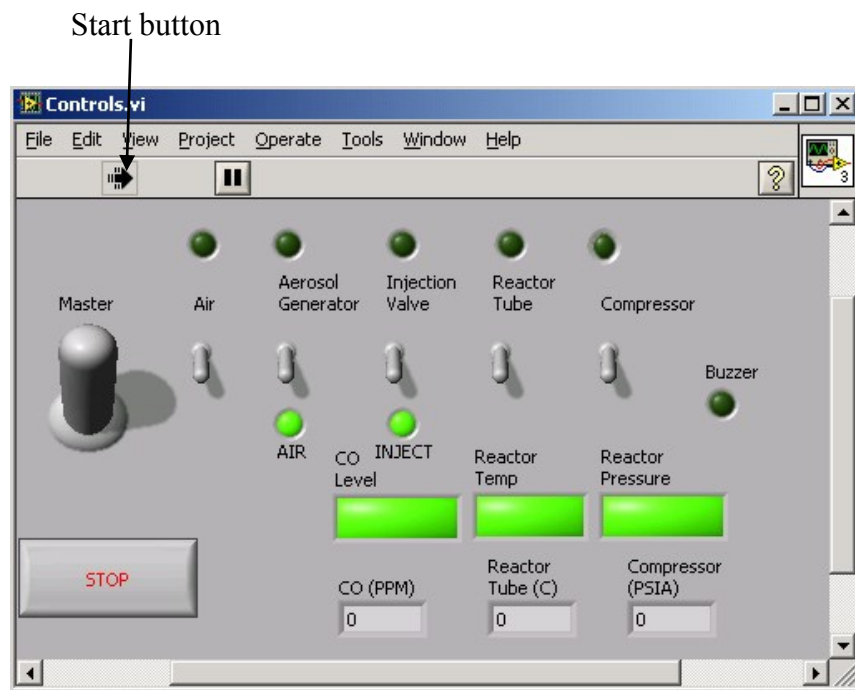


Figure D.1 Pop-up menu from the LabVIEW software at the start of experiment

Agilent, sensor power control system, the OPC, and the blower were switched on. The door cover to the blower reduced noise level. At this point, the yellow hose pipe from aerosol

generator was attached to the speedaire compressor, and the switch knob on the compressor was set to AUTO. From the desktop computer, the control program file was opened by double-clicking on the “control.vi” icon, and the LabVIEW software system started data acquisition and control functions. The control system was switched on by clicking on the control master knob. All lower LED indicators showed GREEN. To initiate control connections the start button located on the left most position of the menu bar (refer to Figure D.1 for details) was clicked using the mouse. The setup produced a display screen with the values for all the sensor outputs on the screen. To stop the data acquisition, the red button with “STOP” sign mark was clicked. The knob labeled AIR was clicked to turn on air. The regulator control knob on top of aerosol generator was adjusted to read to 20 PSIG. The adjustment was locked by pushing down on the control knob. The brass needle valve located just below the control knob was opened to allow air to get into the AG. Click on the knob labeled compressor to switch on compressor number 2. These operations allowed the system to run on air only. The knob labeled “Aerosol Generator” was clicked to activate AG and to start generating polydispersed jet oil aerosols. The system was then run for about 30 minutes to allow the OPC to reach steady-state.



**Figure D.2 Control panel pop-up menu from LabVIEW system software**

From the LabVIEW pop-up menu (see Figure D.1), the program was prepared for the desired test run by inserting on the screen under the heading: Date File Name: the name of the file, desired experimental run time, and number of samples required. Clean circular filters were prepared, fitted into HEPA sampling cassettes, and sample cassettes with clean cut filters installed to the sampling train. The sampler pump was switched on, and with the knob fitted to the rotameter, the pump flow rate was adjusted to read 4.0 SCFH: calibrated pump flow rate. This pump flow rate value was entered on LabVIEW user interface window as shown in Figure D.1. Clicking “RECORD” started data collection on the screen. Before the program began recording data, it automatically requested the user to enter the amount of air going into the reactor. The total airflow rate reading from both rotameters connected to compressors 1 and 2 was entered in a small window that popped up on the LabVIEW menu. The computer did not have this information, which must be manually entered. The system automatically switched off when the sampling time was up. Hot tests required the knob labeled “tape heater” be clicked to switch on the heater. The heater was left to run until steady state was achieved at about 300°C. The rheostat allowed control over temperatures of pyrolysis reaction without any disruptions to the fluid flow. The use of temperature control systems was vital for many applications, including desired aerosol generation and controlled reactions.

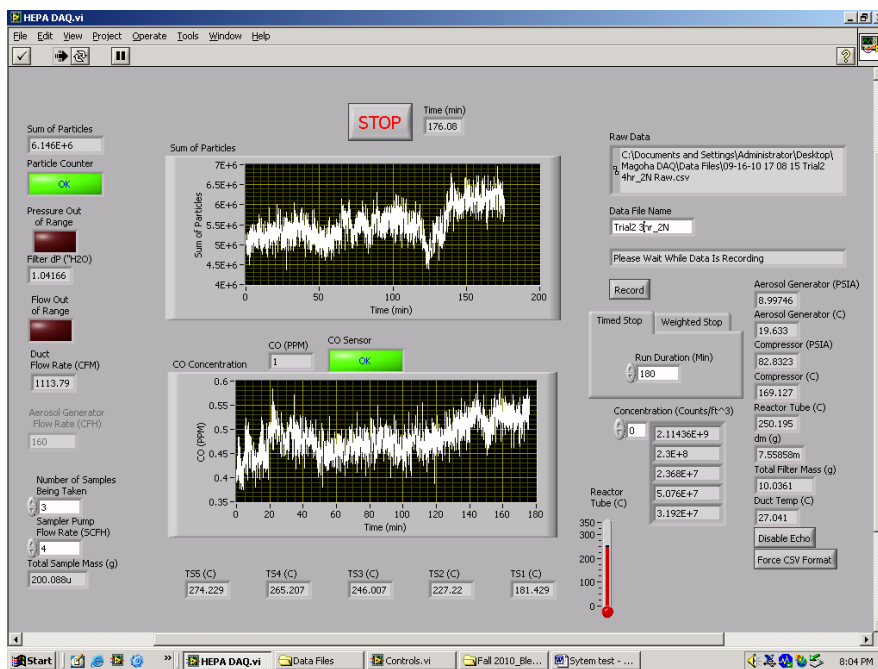


Figure D.3 User interface for aerosol particle counting and CO monitoring

The variac heater enabled the user to heat fluids (aerosol and air mixture) operating over a wide temperature range up to 350°C, the heater had a knob that could be adjusted to maintain the reactor at constant temperatures. Maintaining different temperatures and pressures was important for analytical studies on aerosol production. Whenever the experiment was running, the fan speed, temperature and pressure measurements, and particulate counts were automatically recorded and displayed at 7 second intervals by the desktop computer. All test runs were conducted in duplicate to determine the reproducibility of observations. A new file was generated each time the start button was pressed. When the experiment was running, a file with a csv (comma separated values) extension was generated every time the data acquisition program was invoked. The data written to the file were calculated averages of the values read over the previous 7 seconds. To retrieve these files at the end of the experiment, double-click on the “DATA” file in the "Magotha DAG" folder. The files list was sorted by date with the most recently created file at the top of the list. The files can be recognized by their creation date and time and by the file name assigned in the user interface window.

Shut-down procedures: Switch-off the sampler pump power supply and then disconnect sampling cassettes from the sampling train. From the control panel screen, click on the knob labeled tape heater to switch off heater if a hot test was being conducted. Click on the knob labeled Aerosol Generator to turn off oil. This step stops the oil flow, but air still flows through the reactor. The air will clear the reactor of traces of pyrolysis products that might be present in the reactor. The system is left to run in this mode until the reactor temperature falls below 100°C, then the knob labeled AIR is clicked on to turn off air flow. Click on the knob labeled compressor to switch-off the compressor. Click on the master control knob to switch-off the control system. Close control.vi front panel file to exit control system. From HEPA DAQ File screen, click on STOP key to stop the LabVIEW program from running (OPC should beep). Close HEPA DAQ file to exit LabVIEW program. Close any remaining screen and turn-off the experimental system. Finally, turn the knob on the speedaire compressor to off position. This will switch off the compressor, the blower, the OPC, the sensor power control supply, the DAQ unit – Agilent, the power supply (lambda) and the computer.















1757.390625	1097.93581	0.584557	203360000	29040000	2400000	4160000	2040000	40000	120000	0	0	0	0	0	0	0	0	0	626897800	1.56461E+11	5.378086	24.812	14.151554	95.443	170.244	29.594	90	602900	3165675.969	1.333333	146.405	171.792	176.064	189.334	191.464	0.085462	44.4
1764.390625	1096.496729	0.580622	217280000	31800000	2040000	4080000	1920000	80000	40000	40000	0	0	0	0	0	0	0	0	659010740	1.5712E+11	5.38992	24.727	14.470494	95.355	170.337	29.595	90	643200	3179014.347	1.333333	146.423	171.846	176.16	189.297	191.234	0.063325	44
1771.375	1099.819363	0.584147	173400000	22640000	1400000	2880000	2000000	80000	120000	0	0	80000	0	0	0	0	0	0	579189916.3	1.57699E+11	5.395483	24.786	14.278028	95.677	170.356	29.581	90	506500	3190752.537	1.333333	146.344	172.012	176.185	189.193	191.232	0.046106	44
1778.375	1101.41939	0.586837	167400000	23560000	1840000	3440000	1720000	120000	120000	0	0	0	0	0	0	0	0	0	524276153.1	1.58223E+11	5.404378	24.776	14.024162	95.534	170.234	29.549	90	495500	3201345.714	1.333333	146.454	171.788	176.076	189.34	191.437	0.03955	44
1785.375	1102.616282	0.584229	194280000	28400000	1960000	4280000	2040000	400000	80000	40000	0	0	0	0	0	0	0	0	636457334.7	1.5886E+11	5.392334	24.694	13.91212	95.332	170.398	29.554	90	578700	3214186.869	1.333333	146.468	171.924	176.117	189.309	191.131	0.029706	44
1792.359375	1099.667579	0.58523	161960000	24200000	1560000	3280000	1600000	120000	80000	0	0	0	0	0	0	0	0	0	504504634.5	1.59364E+11	5.370581	24.808	14.261366	95.512	170.294	29.545	90	482000	3224354.698	1.333333	146.363	171.842	176.008	189.278	191.461	0.078087	44
1799.359375	1099.856279	0.585016	180240000	24720000	2000000	3520000	2000000	160000	40000	0	0	0	0	0	0	0	0	0	552048454.4	1.59916E+11	5.38378	24.761	14.627013	95.388	170.316	29.557	90	531700	3235510.563	1.333333	146.411	171.851	176.18	189.283	191.266	0.085462	44















1721.390625	1108.687102	0.594954	6240000	960000	80000	200000	120000	0	0	0	0	0	0	0	0	0	0	21147050.64	11241344204	8.6332	24.983	106.45074	179.55	308.676	30.629	90	19000	225310.6605	1.333333	263.883	301.802	321.496	332.378	340.102	0.612694	53.6
1728.40625	1107.02826	0.592937	20760000	2560000	280000	200000	40000	40000	0	0	0	0	0	0	0	0	0	57448050.91	11298792255	8.581376	24.973	105.26083	179.766	308.654	30.61	90	59700	226462.1336	1.333333	263.873	301.887	321.471	332.353	340.156	0.613512	53.6
1735.421875	1110.27028	0.598086	7120000	960000	120000	120000	80000	0	0	0	0	0	0	0	0	0	0	21422804.95	11320215060	8.645191	24.999	104.57339	179.907	308.707	30.587	90	21000	226892.1699	1.333333	263.87	301.846	321.462	332.378	340.231	0.593013	53.6
1742.40625	1108.66866	0.596742	8240000	920000	40000	80000	0	0	0	0	0	0	0	0	0	0	0	20279017.22	11340494077	8.631993	25.018	106.67246	179.878	308.798	30.584	90	23200	227298.0574	1.333333	263.857	301.726	321.478	332.416	340.221	0.578256	53.6
1749.421875	1104.398368	0.593839	7600000	1120000	80000	120000	40000	0	0	0	0	0	0	0	0	0	0	21758633.34	11362252711	8.582478	25.009	105.36316	179.819	308.789	30.581	90	22400	227734.1888	1.333333	263.963	301.691	321.49	332.363	340.278	0.600394	53.6
1756.390625	1104.821182	0.592921	19160000	2560000	160000	120000	40000	0	0	0	0	0	0	0	0	0	0	49354159.11	11411606870	8.646162	24.976	105.61636	179.806	308.795	30.581	90	55100	228727.2716	1.333333	263.915	301.811	321.503	332.378	340.24	0.588094	53.6
1763.40625	1104.761395	0.595725	22280000	3240000	0	200000	120000	0	0	0	0	0	0	0	0	0	0	59750425.58	11471357295	8.589038	24.976	105.37891	179.927	308.811	30.597	90	64600	229929.0835	1.333333	263.927	301.947	321.5	332.382	340.228	0.544637	53.6
1770.375	1107.314727	0.592806	6440000	920000	80000	40000	40000	0	0	0	0	0	0	0	0	0	0	17678660.88	11489035956	8.661014	25.028	105.455	180.284	308.868	30.603	90	18800	230284.689	1.333333	263.918	301.77	321.474	332.416	340.403	0.628269	53.6
1777.390625	1107.163581	0.598956	14800000	1920000	40000	40000	40000	0	0	0	0	0	0	0	0	0	0	37140730.81	11526176687	8.627716	25.006	106.92303	180.088	308.877	30.607	90	42100	231030.0503	1.333333	264.04	301.736	321.569	332.469	340.397	0.603675	53.6
1784.359375	1108.38325	0.595282	7160000	640000	80000	80000	0	0	0	0	0	0	0	0	0	0	0	17343751.71	11543520439	8.598484	25.028	105.92991	179.97	308.887	30.626	90	19900	231378.1621	1.333333	264.04	301.71	321.562	332.432	340.397	0.60695	53.6
1791.375	1106.502655	0.593593	24280000	1880000	80000	80000	120000	0	0	0	0	0	0	0	0	0	0	57024816.69	11600545255	8.660751	24.96	106.22509	179.727	308.865	30.626	90	66100	232521.4653	1.333333	264.053	301.894	321.6	332.469	340.316	0.572512	53.6
1798.359375	1101.610608	0.594315	19520000	3040000	240000	200000	120000	0	0	0	0	0	0	0	0	0	0	55709060.05	11656254315	8.606645	24.908	106.25527	179.648	308.883	30.626	90	57800	233640.2869	1.333333	264.133	301.992	321.534	332.51	340.312	0.540537	53.6















1786.484375	1115.803189	0.582983	361240000	24200000	21600000	3120000	1320000	40000	0	0	0	0	0	0	0	0	0	857181829	2.0339E+11	6.601974	21.584	51.576021	137.452	249.702	27.016	90	980200	4052375.212	1.333333	208.894	244.4	255.617	275.337	278.757	-0.246613	46.8
1793.484375	1111.353674	0.581409	391600000	26480000	22000000	3600000	1000000	0	0	0	0	0	0	0	0	0	0	919135996.3	2.04309E+11	6.654532	21.62	50.861647	137.536	249.718	27.006	90	1062200	4070680.63	1.333333	208.802	244.439	255.649	275.206	278.549	-0.232675	46.8
1800.46875	1112.154665	0.580294	384360000	25680000	26400000	3840000	1120000	80000	0	0	0	0	0	0	0	0	0	911355192.8	2.05221E+11	6.659963	21.63	50.766529	137.549	249.744	26.98	90	1044300	4088903.756	1.333333	208.887	244.203	255.643	275.298	278.706	-0.249894	47.2













1772.46875	1101.405643	0.581605	140240000	35520000	3000000	4480000	1520000	0	0	0	0	0	0	0	0	0	0	0	516565920.6	1.22509E+11	5.684379	23.513	29.488267	116.741	185.497	28.569	90	461900	2470646.94	1.333333	161.426	186.826	188.797	199.907	201.483	0.146962	44.8
1779.46875	1102.009139	0.583459	136440000	37560000	3200000	5000000	1480000	0	0	0	0	0	0	0	0	0	0	0	526624527.8	1.23035E+11	5.670236	23.509	29.707108	116.829	185.567	28.558	90	459200	2481272.242	1.333333	161.339	186.958	188.743	199.852	201.461	0.097762	44.8
1786.453125	1100.273065	0.584393	136480000	33720000	2880000	4920000	1280000	0	0	0	0	0	0	0	0	0	0	0	501113950.5	1.23536E+11	5.678318	23.506	30.258398	116.867	185.587	28.584	90	448200	2491377.3	1.333333	161.3	186.997	188.782	199.839	201.415	0.150244	44.8
1793.4375	1101.923716	0.587821	156080000	38320000	3160000	5880000	1880000	40000	40000	0	0	0	0	0	0	0	0	0	590992104.1	1.24127E+11	5.687921	23.483	29.634556	116.809	185.617	28.584	90	513500	2503313.571	1.333333	161.349	187.089	188.963	199.855	201.366	0.135481	44.8
1800.4375	1107.168206	0.588214	132640000	31840000	2280000	4600000	1400000	80000	0	0	40000	0	0	0	0	0	0	0	508181523.7	1.24636E+11	5.708782	23.44	29.370583	116.663	185.662	28.624	90	432200	2513561.942	1.333333	161.439	187.167	189.001	199.896	201.355	0.123181	44.4















1780.015625	1106.821274	0.588755	42640000	46440000	4240000	5280000	1920000	120000	0	0	0	0	0	0	0	0	0	0	0	1125001876	3.31867E+11	7.03894	20.375	67.257796	138.267	231.421	25.864	90	1211000	6649684.659	1.333333	192.183	221.493	231.885	247.98	251.041	0.084644	61.2
1787	1105.656507	0.588624	411120000	48800000	3920000	5360000	1440000	40000	0	0	0	0	0	0	0	0	0	0	0	1088760959	3.32956E+11	7.004278	20.411	68.237707	138.335	231.227	25.857	90	1176700	6671544.274	1.333333	192.176	221.32	231.791	248.035	251.147	0.057587	61.2
1794	1104.66391	0.589559	468560000	53400000	4000000	6720000	1960000	80000	0	0	0	0	0	0	0	0	0	0	0	1245385901	3.34201E+11	6.990974	20.408	67.975706	138.458	231.318	25.874	90	1336800	6696574.871	1.333333	192.163	221.199	231.665	247.948	250.97	0.03135	61.2
1801.015625	1107.873827	0.591133	461840000	50160000	3240000	4920000	1560000	0	40000	0	0	0	0	0	0	0	0	0	0	1185325805	3.35386E+11	6.995619	20.408	67.032789	138.383	231.305	25.867	90	1304400	6720419.747	1.333333	192.215	221.193	231.678	247.954	250.918	0.069887	61.6















1780.40625	1107.592211	0.583705	107840000	14600000	1080000	2320000	600000	0	40000	0	0	0	0	0	0	0	0	0	314289549	71111061661	7.19441	23.91	73.170604	148.845	279.465	28.798	90	316200	1423649.788	1.333333	228.503	268.13	282.176	304.989	309.686	-0.138381	40.4
1787.40625	1110.818182	0.586804	97120000	12280000	1280000	1480000	680000	0	40000	0	0	0	0	0	0	0	0	0	279804635.9	71390866296	7.255075	23.941	72.761925	148.978	279.431	28.807	90	282200	1429263.66	1.333333	228.452	267.901	282.198	305.059	309.897	-0.161338	40
1794.40625	1111.272368	0.584623	89760000	10960000	680000	1640000	440000	0	0	0	0	0	0	0	0	0	0	0	246570799.8	71637437096	7.233611	23.952	72.868588	149.15	279.363	28.798	90	258700	1434196.377	1.333333	228.344	268.118	282.268	304.96	309.714	-0.170356	40
1801.390625	1109.271455	0.585722	118160000	15040000	880000	2200000	720000	0	0	0	0	0	0	0	0	0	0	0	330253257.3	71967690354	7.206401	23.942	74.039395	148.982	279.337	28.795	90	342500	1440800.483	1.333333	228.418	267.99	282.23	305.096	309.856	-0.1515	40.4

Figure E.1 Block diagram showing VI in LabVIEW program

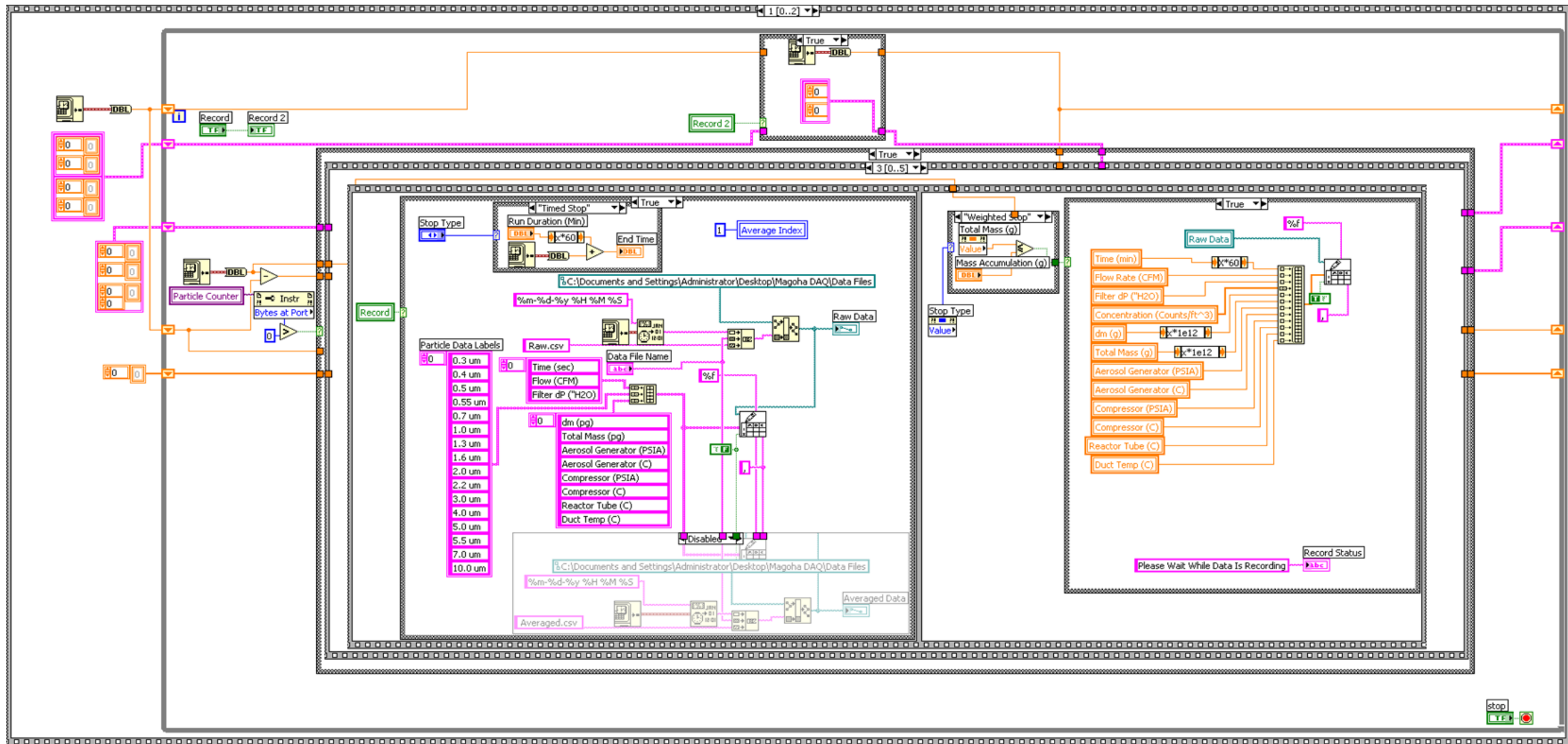


Figure E.2 Block showing VI in LabVIEW Program

### E.1 Temperature and pressure trends in aircraft engine BAS and duct system

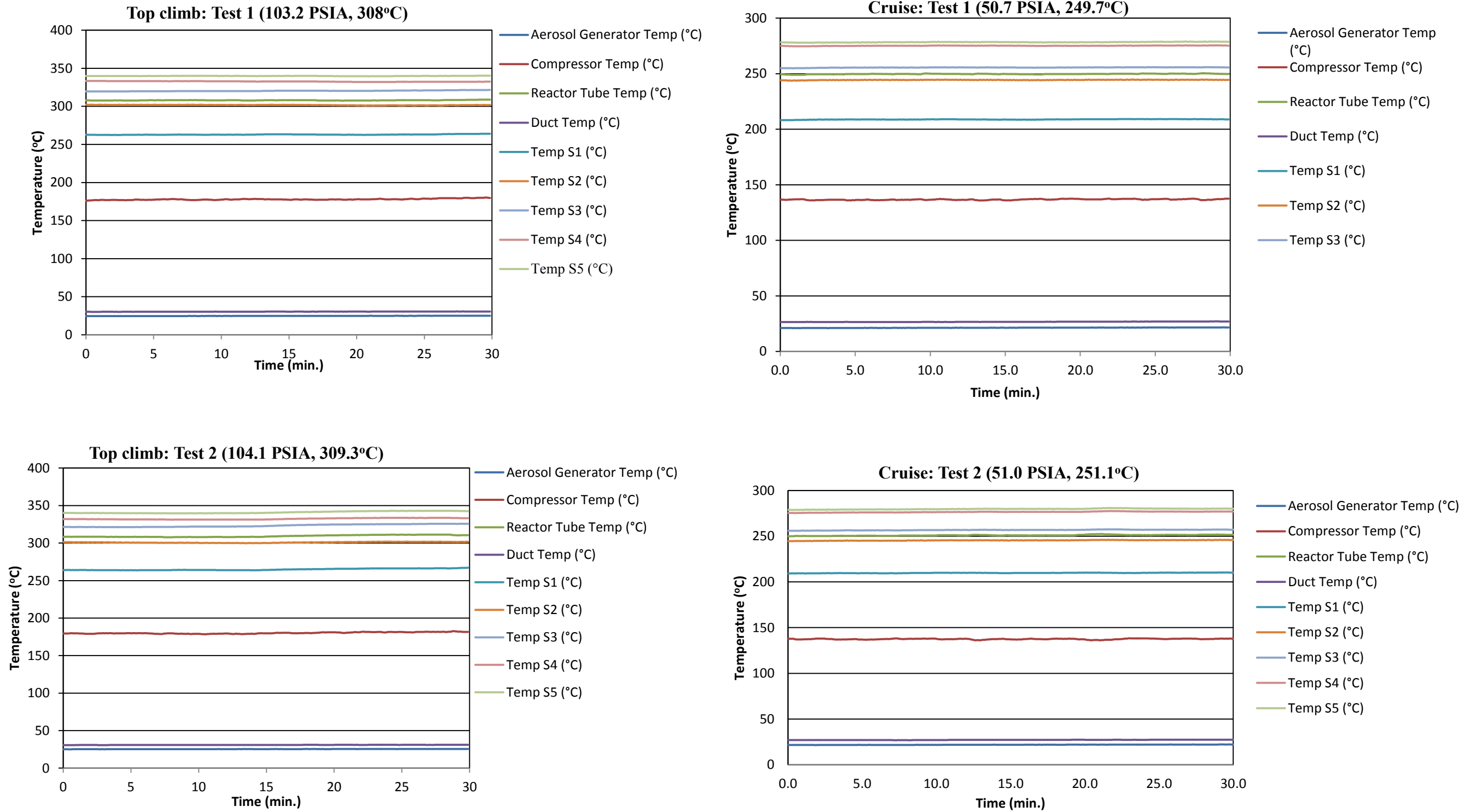
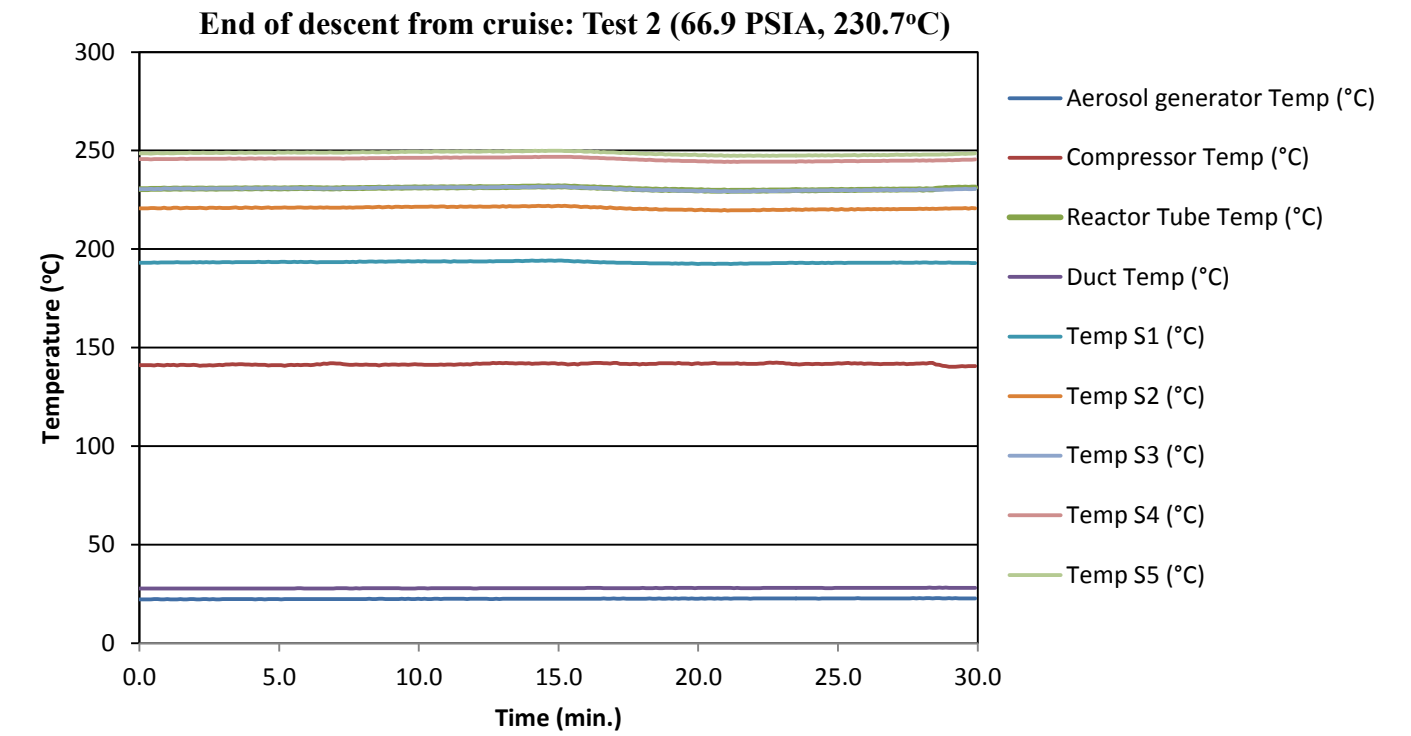
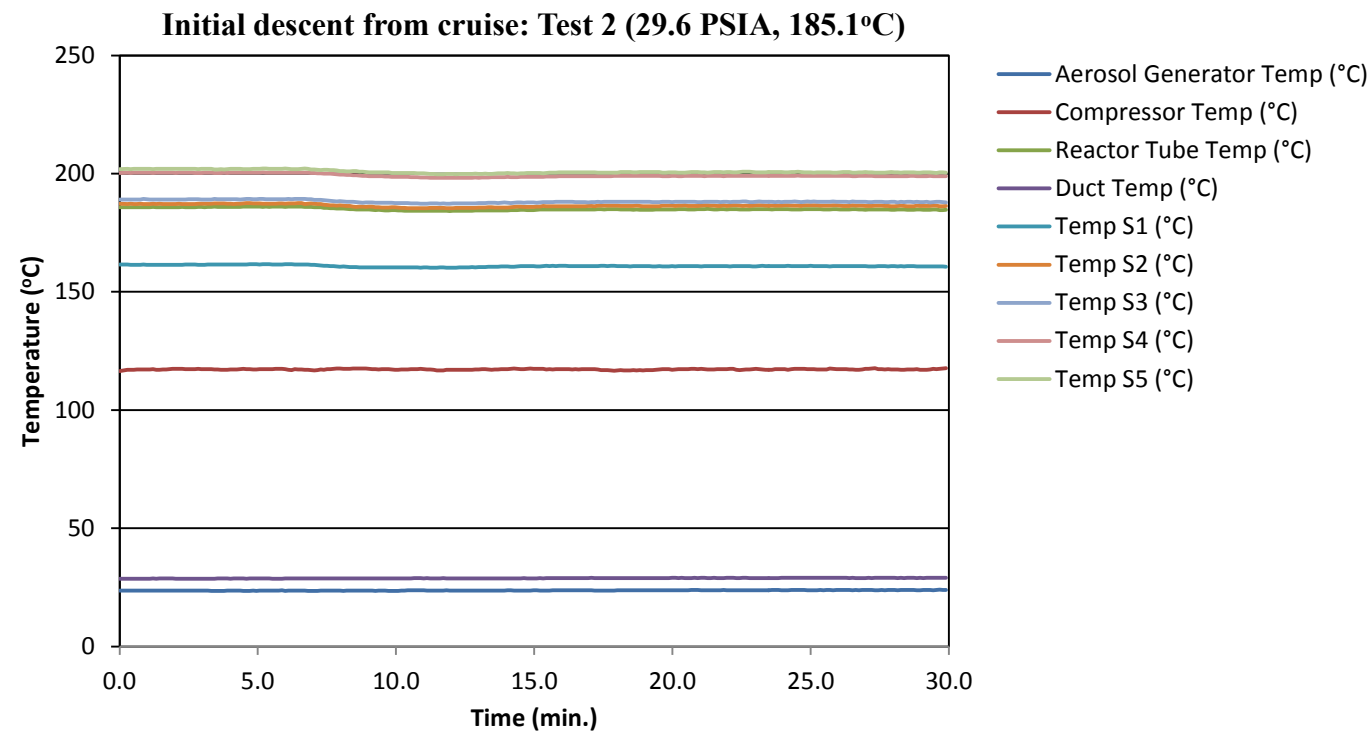
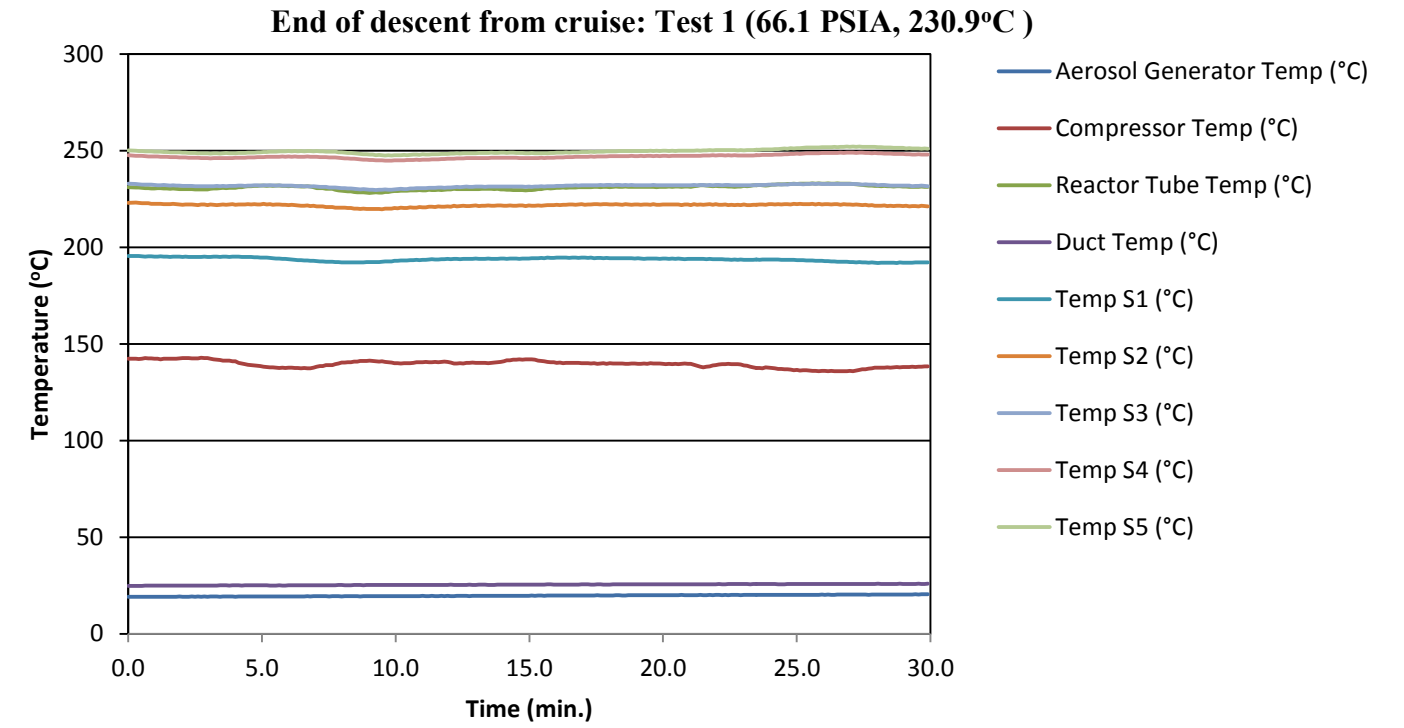
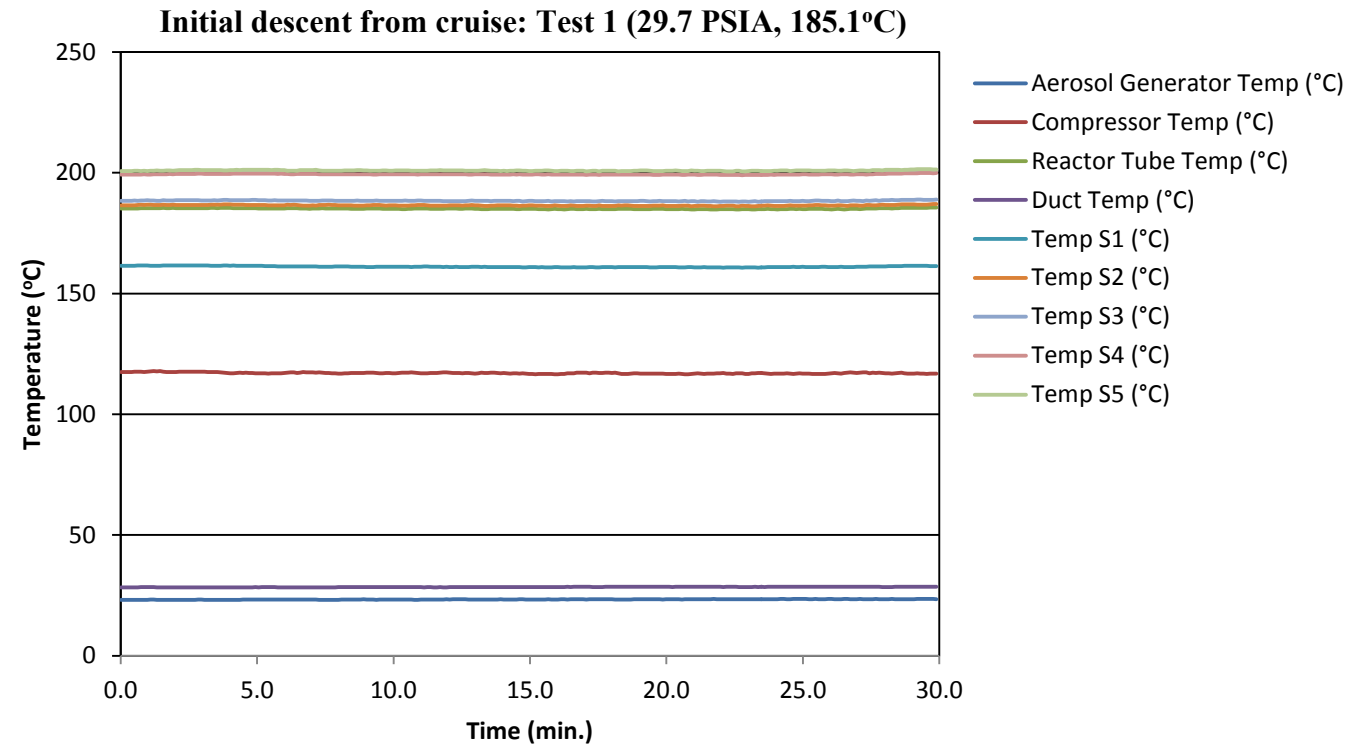
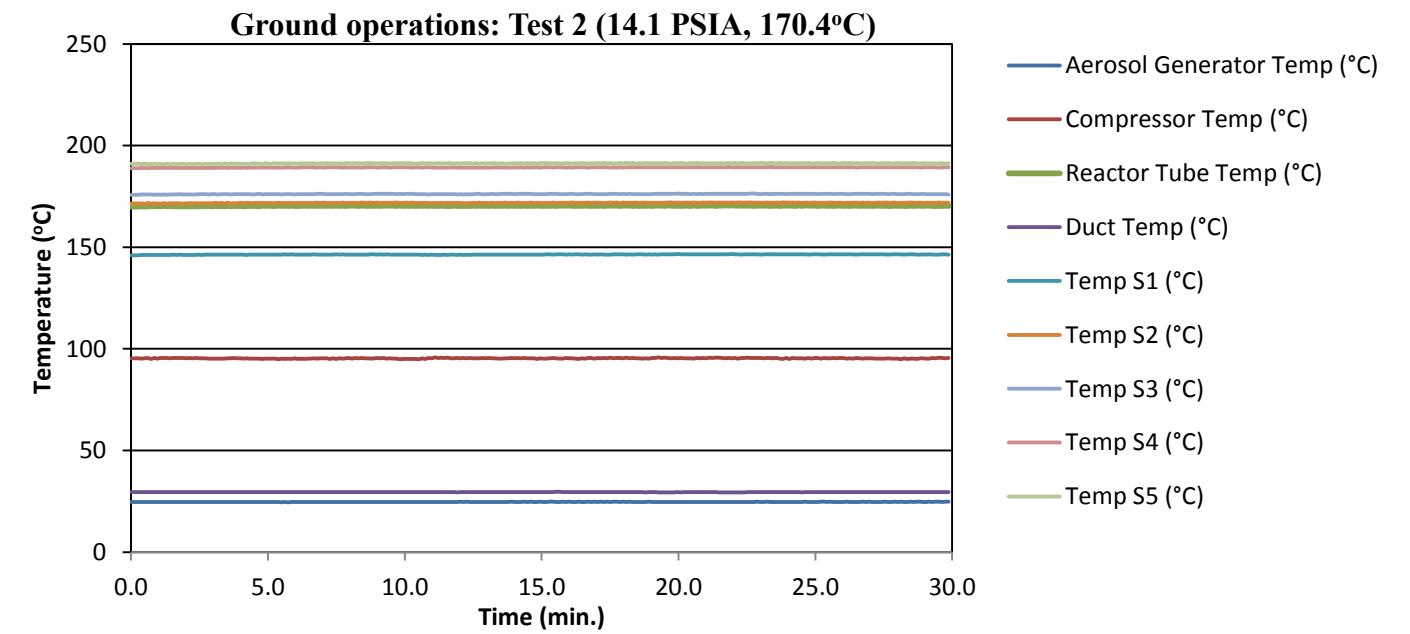
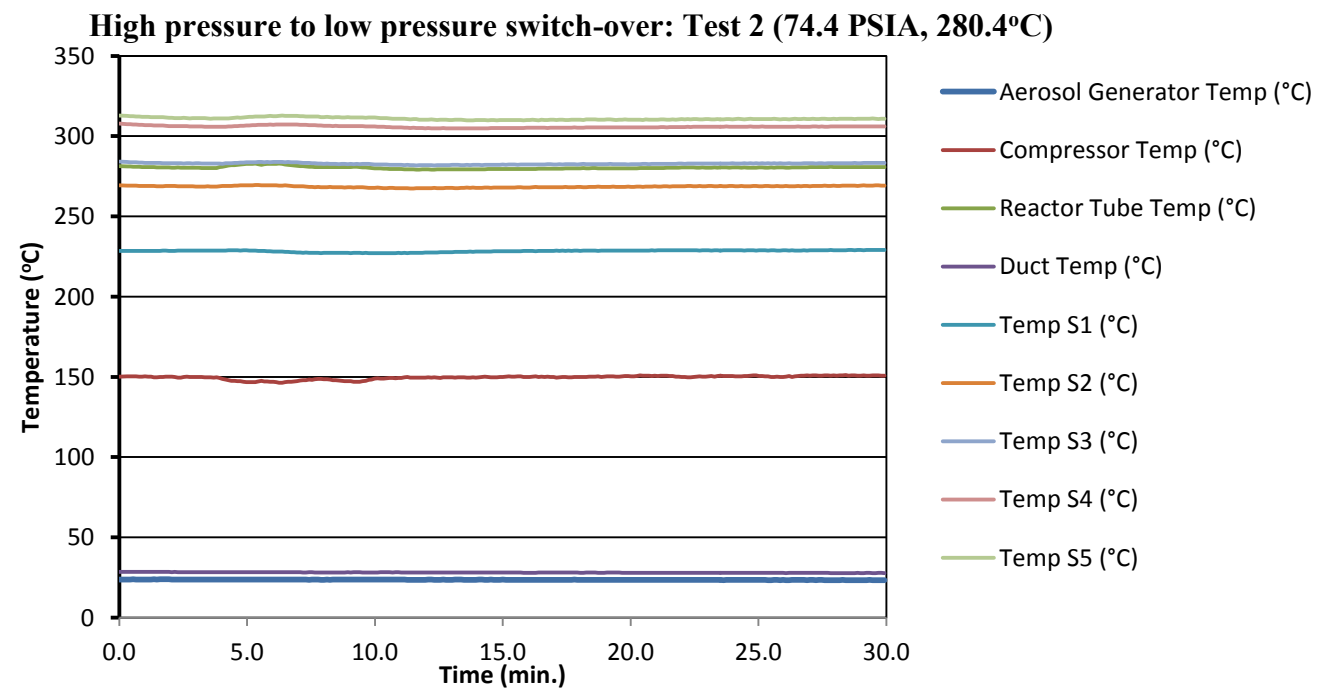
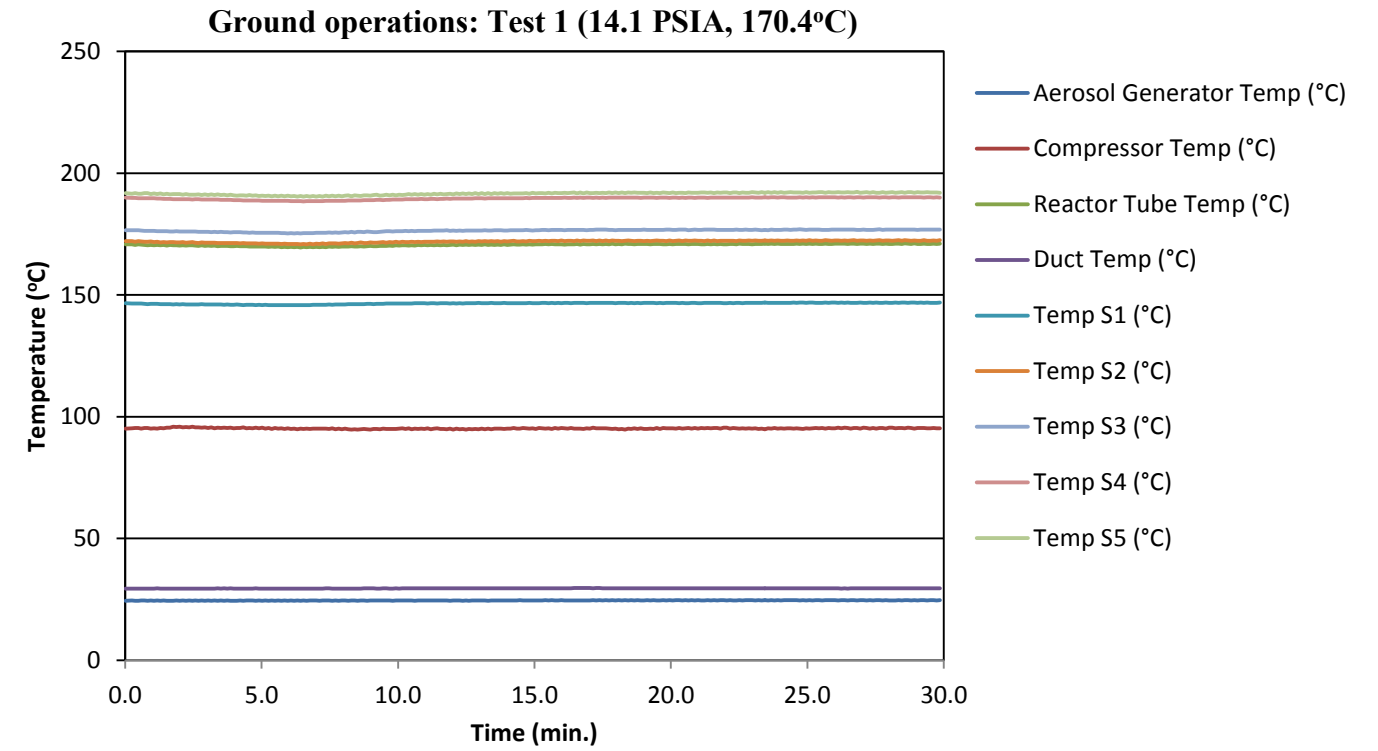
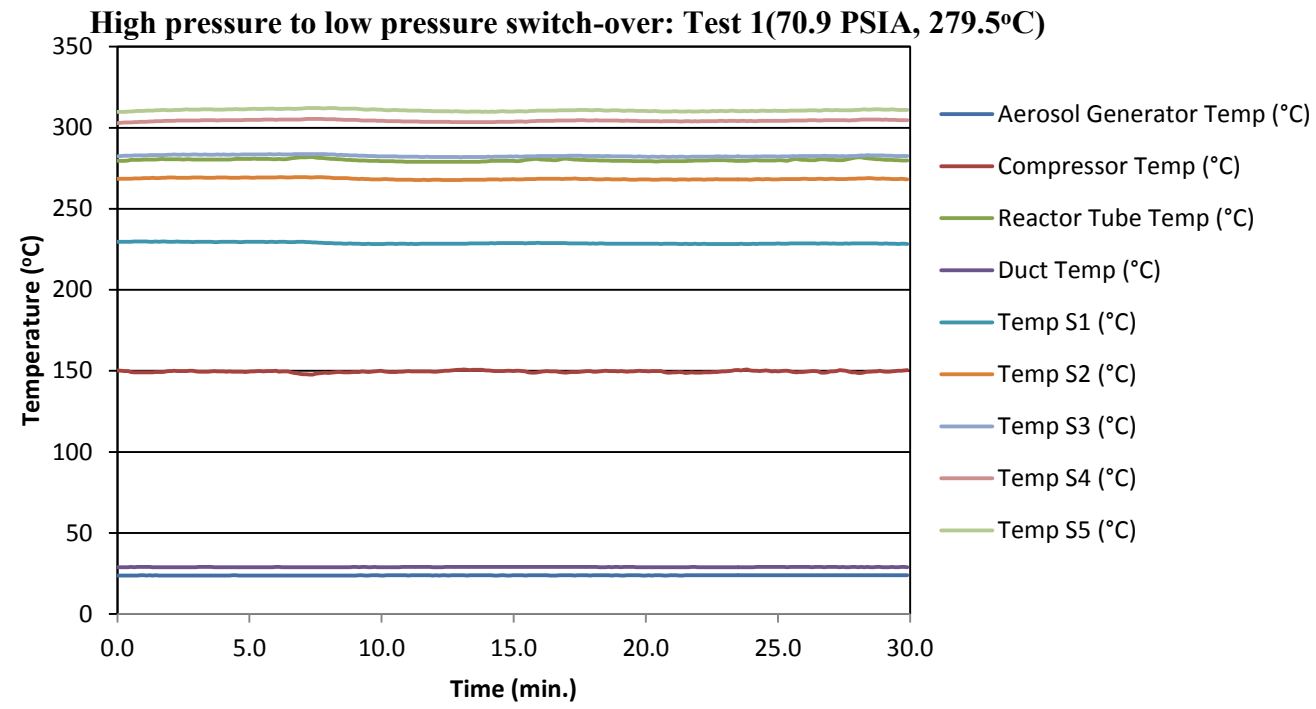


Figure E.3 Temperature profiles in BAS during modeling pyrolysis of Mobil Jet Oil II at top climb and cruise speed conditions (OPC: One nozzle open)





**Figure E.4 BAS temperature profiles during modeling of pyrolysis of Mobil Jet Oil II at initial descent and end of descent from cruise conditions (OPC: One nozzle open)**



**Figure E.5 BAS temperature profiles during modeling of pyrolysis of Mobil Jet Oil II at high pressure to low pressure switch-over and ground operations (OPC: One nozzle open)**

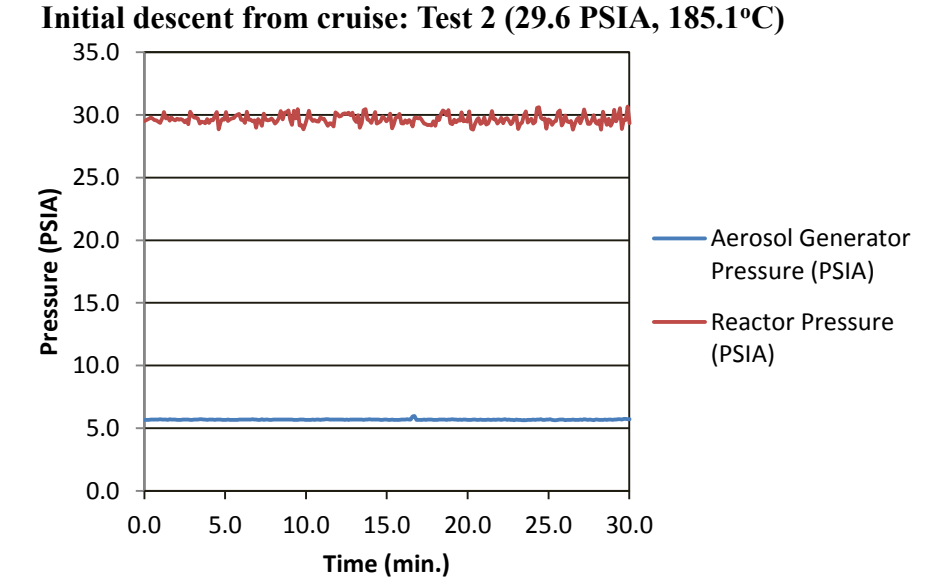
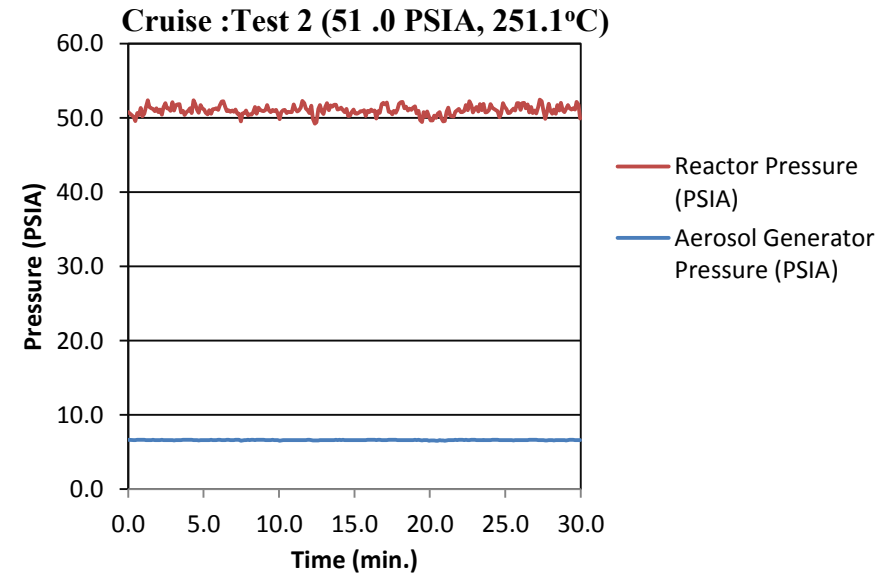
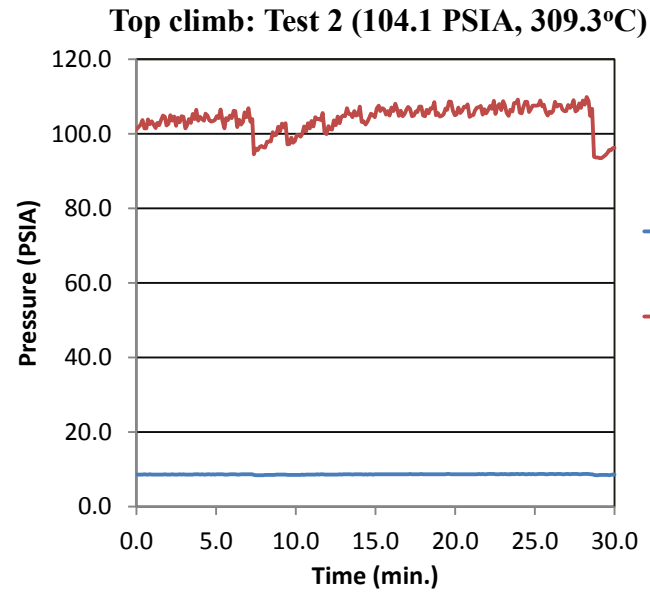
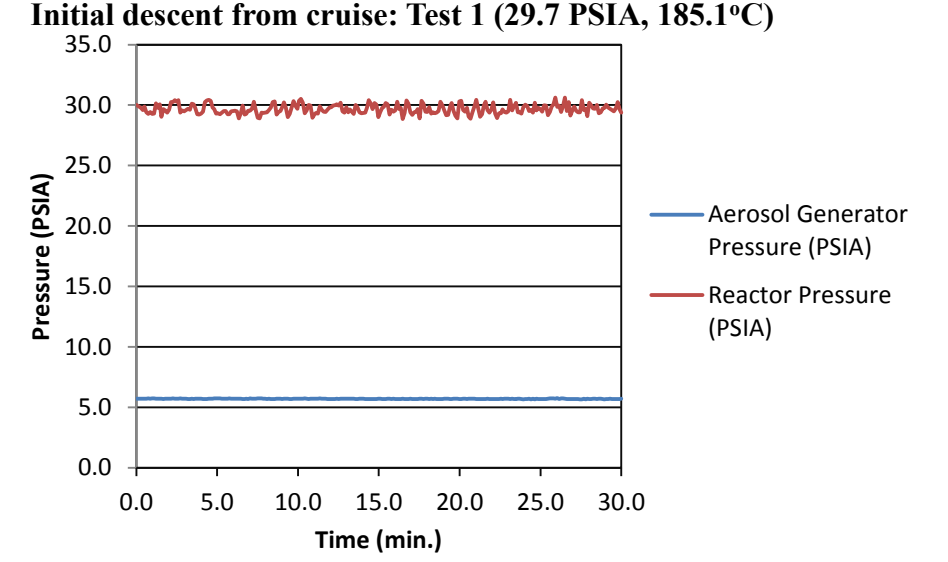
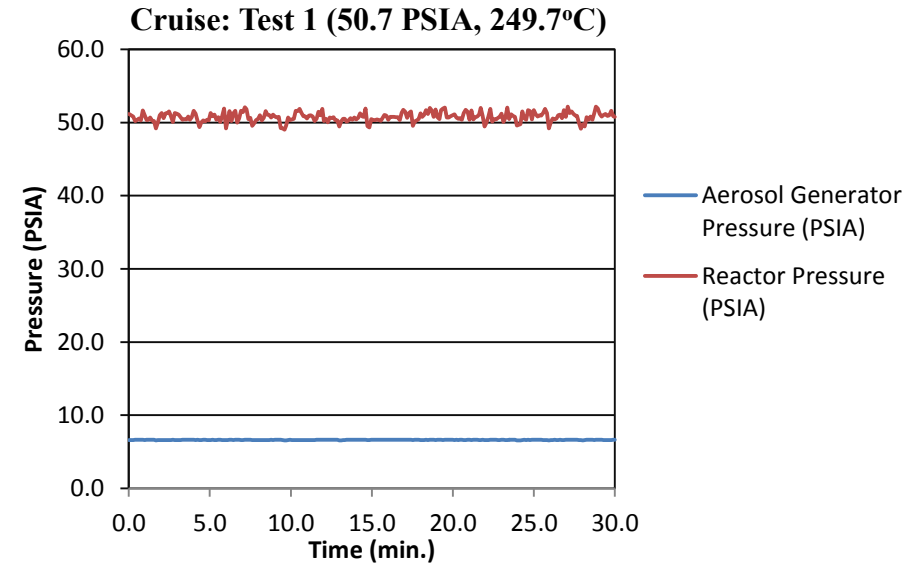
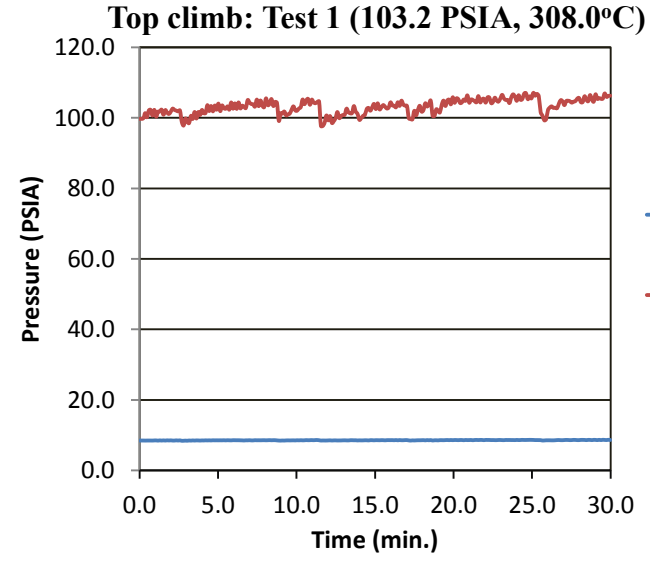
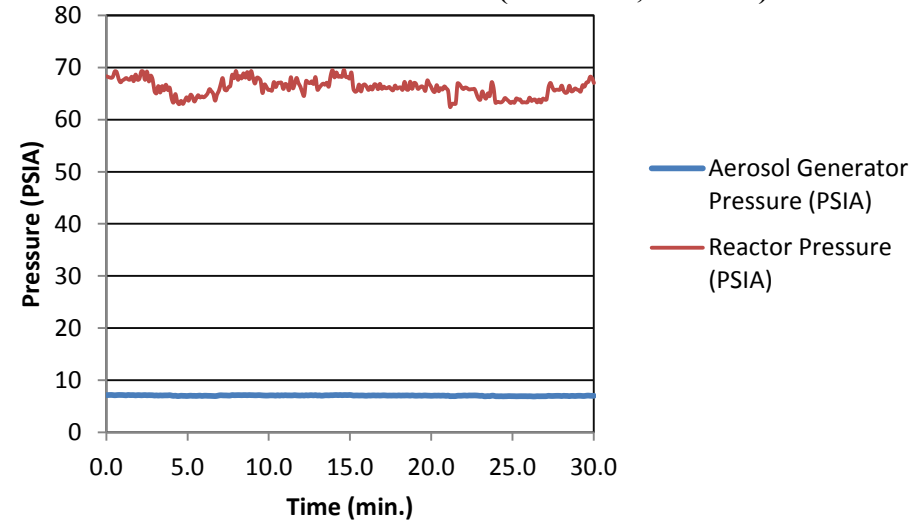
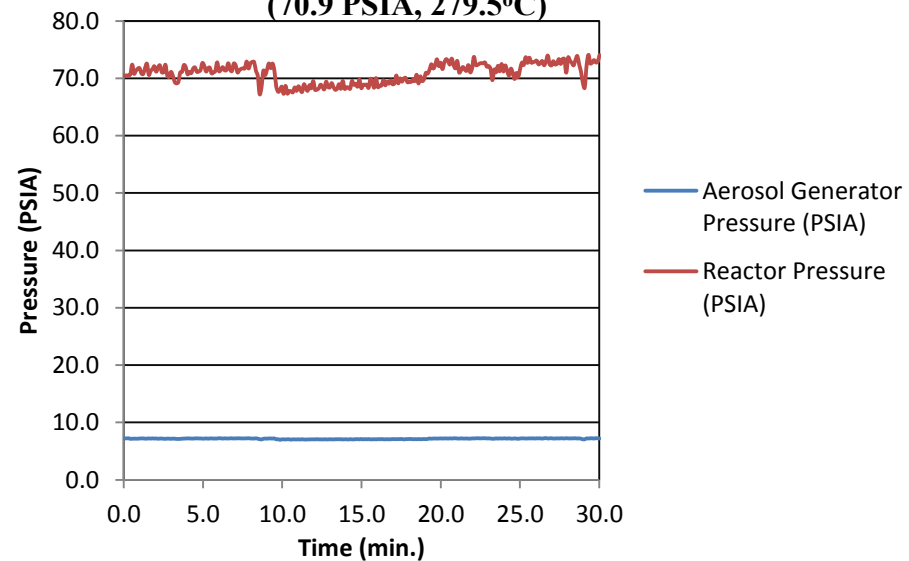


**Figure E.6 Trends in pressure profiles of pyrolysis of Mobil Jet Oil II at simulated top climb, cruise and initial descent from cruise**

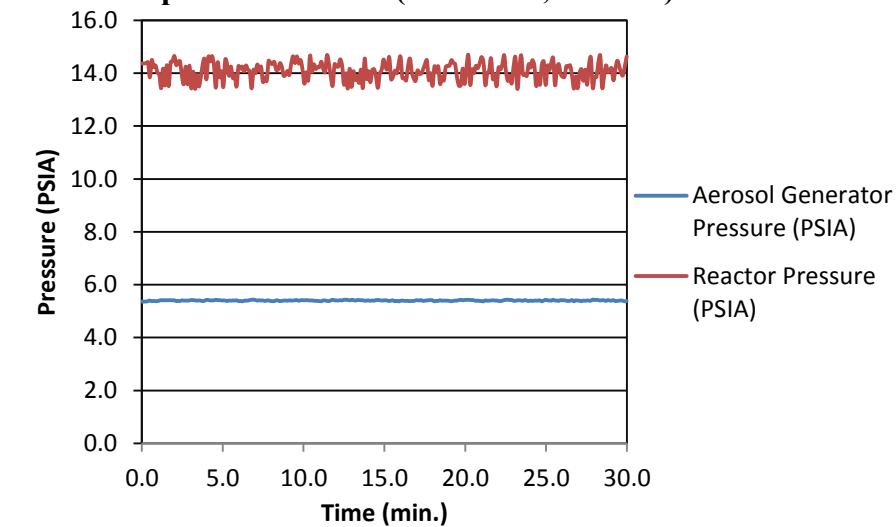
**End of descent from cruise: Test 1 (66.1PSIA, 230.9°C)**



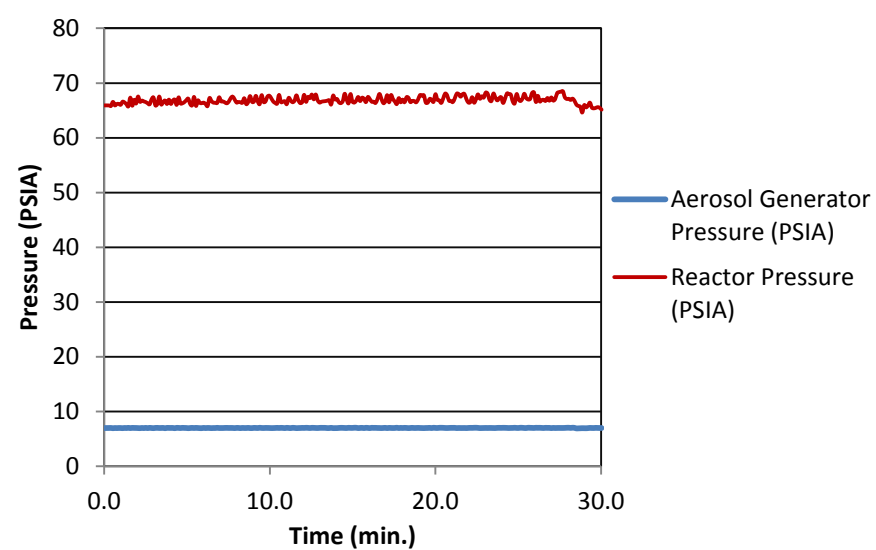
**High pressure to low pressure switch-over: Test 1 (70.9 PSIA, 279.5°C)**



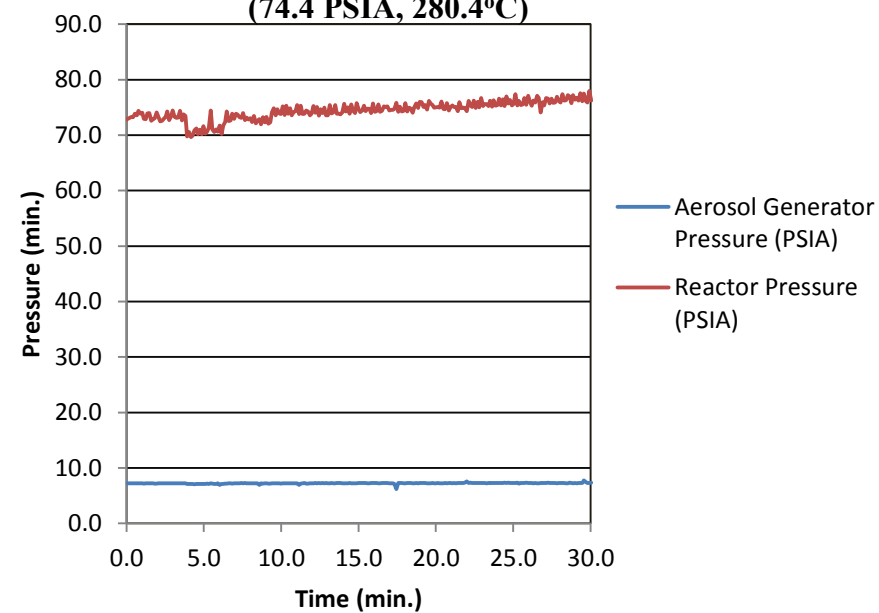
**Ground operations: Test 1 (14.1 PSIA, 170.4°C)**



**End of descent from cruise: Test 2 (66.9 PSIA, 230.7°C)**



**High pressure to low pressure switch-over: Test 2 (74.4 PSIA, 280.4°C)**



**Ground operations: Test 2 (14.1 PSIA 170.4°C)**

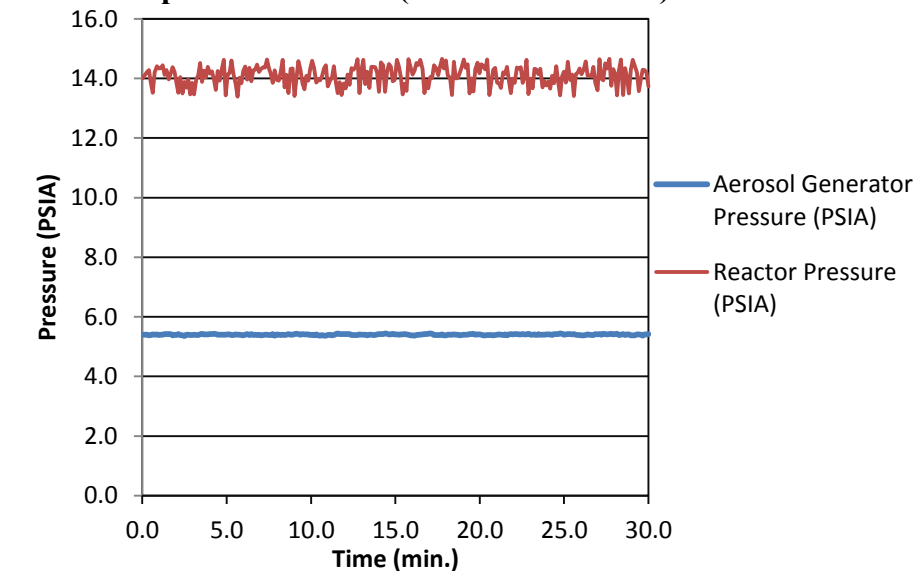


**Figure E.7 Trends in pressure profiles of pyrolysis of Mobil Jet Oil II at simulated high pressure to low pressure switch over and ground operations (cold tests)**